METHODS IN MOLECULAR BIOLOGY™ 462

Lipid Signaling Protocols

Edited by

Banafshé Larijani
Rudiger Woscholski
Colin A. Rosser

Humana Press

Lipid Signaling Protocols

METHODS IN MOLECULAR BIOLOGY™

John M. Walker, SERIES EDITOR

502. Bacteriophages: Methods and Protocols, *Volume 2: Molecular and Applied Aspects*, edited by *Martha R. J. Clokie and Andrew M. Kropinski 2009*

501. Bacteriophages: Methods and Protocols, *Volume 1: Isolation*, Characterization, and Interactions, edited by *Martha R. J. Clokie and Andrew M. Kropinski 2009*

496. DNA and RNA Profiling in Human Blood: Methods and Protocols, edited by *Peter Bugert, 2009*

493. Auditory and Vestibular Research: Methods and Protocols, edited by *Bernd Sokolowski, 2009*

489. Dynamic Brain Imaging: Methods and Protocols, edited by *Fahmeed Hyder, 2009*

485. HIV Protocols: Methods and Protocols, edited by *Vinayaka R. Prasad and Ganjam V. Kalpana, 2009*

484. Functional Proteomics: Methods and Protocols, edited by *Julie D. Thompson, Christine Schaeffer-Reiss, and Marius Ueffing, 2008*

483. Recombinant Proteins From Plants: Methods and Protocols, edited by *Loïc Faye and Veronique Gomord, 2008*

482. Stem Cells in Regenerative Medicine: Methods and Protocols, edited by *Julie Audet and William L. Stanford, 2008*

481. Hepatocyte Transplantation: Methods and Protocols, edited by *Anil Dhawan and Robin D. Hughes, 2008*

480. Macromolecular Drug Delivery: Methods and Protocols, edited by *Mattias Belting, 2008*

479. Plant Signal Transduction: Methods and Protocols, edited by *Thomas Pfannschmidt, 2008*

478. Transgenic Wheat, Barley and Oats: Production and Characterization Protocols, edited by *Huw D. Jones and Peter R. Shewry, 2008*

477. Advanced Protocols in Oxidative Stress I, edited by *Donald Armstrong, 2008*

476. Redox-Mediated Signal Transduction: Methods and Protocols, edited by *John T. Hancock, 2008*

475. Cell Fusion: Overviews and Methods, edited by *Elizabeth H. Chen, 2008*

474. Nanostructure Design: Methods and Protocols, edited by *Ehud Gazit and Ruth Nussinov, 2008*

473. Clinical Epidemiology: Practice and Methods, edited by *Patrick Parfrey and Brendon Barrett, 2008*

472. Cancer Epidemiology, Volume 2: Modifiable Factors, edited by *Mukesh Verma, 2008*

471. Cancer Epidemiology, Volume 1: Host Susceptibility Factors, edited by *Mukesh Verma, 2008*

470. Host-Pathogen Interactions: Methods and Protocols, edited by *Steffen Rupp and Kai Sohn, 2008*

469. Wnt Signaling, Volume 2: Pathway Models, edited by *Elizabeth Vincan, 2008*

468. Wnt Signaling, Volume 1: Pathway Methods and Mammalian Models, edited by *Elizabeth Vincan, 2008*

467. Angiogenesis Protocols: Second Edition, edited by *Stewart Martin and Cliff Murray, 2008*

466. Kidney Research: Experimental Protocols, edited by *Tim D. Hewitson and Gavin J. Becker, 2008*

465. Mycobacteria, Second Edition, edited by *Tanya Parish and Amanda Claire Brown, 2008*

464. The Nucleus, Volume 2: Physical Properties and Imaging Methods, edited by *Ronald Hancock, 2008*

463. The Nucleus, Volume 1: Nuclei and Subnuclear Components, edited by *Ronald Hancock, 2008*

462. Lipid Signaling Protocols, edited by *Banafshé Larijani, Rudiger Woscholski, and Colin A. Rosser, 2009*

Lipid Signaling Protocols

Banafshé Larijani
Editor

Department of Cell Biophysics, Cancer Research UK, London Research Institute London, UK

Rudiger Woscholski
Editor

Division of Cell and Molecular Biology, Imperial College London, London, UK

Colin A. Rosser
Editor

Rye St. Antony School, Oxford, UK

Humana Press

Editors
Ph.D. Banafshé Larijani
Cancer Research UK
Dept. Cell Biophysics
44 Lincoln's Inn Fields
London
United Kingdom WC2A 3PX
banafshe.larijani@cancer.org.uk

Dr. Colin A. Rosser
Rye St. Antony School
Pullens Lane
Oxford
Headington
United Kingdom OX3 0BY
crosser@rye-st-antony.oxon.sch.uk

Dr. Rudiger Woscholski
Imperial College London
Fac. Natural Sciences
Div. Cell & Molecular Biology
London
South Kensington Campus
United Kingdom SW7 2AZ
r.woscholski@imperial.ac.uk

Series Editor
John M. Walker
University of Hertfordshire
Hatfield
Hertz, UK

ISBN: 978-1-58829-727-3
ISSN: 1064-3745
DOI: 10.1007/978-1-60327-115-8
e-ISBN: 978-1-60327-115-8
e-ISSN: 1940-6029

Library of Congress Control Number: 2008937360

Printed on acid-free paper

9 8 7 6 5 4 3 2 1

springer.com

Preface

It has been our endeavor to assemble in a single volume the various tools and methodologies that can be of aide to the interested investigator in unraveling lipid-dependent signaling and cell function. The content of this volume ranges from describing "cutting-edge" lipid analysis and quantification methods to providing a selection of practical approaches to study lipid metabolism and recognition in the cellular context.

Experimental manipulation of lipids requires an understanding of the physical properties of these hydrophobic metabolites as well as the physical methodologies used for their analysis; these are summarized in the first section of this volume. This is complemented, in the second section of this volume, by a selection of biological methods, which are focused around the most relevant lipids, their corresponding metabolizing enzymes, and the recognition proteins.

We have carefully selected authors who have an understanding of the application of physical methodologies in the context of lipid signaling and lipid metabolism in Cell Biology. We hope that this volume will be useful to both researchers in the life sciences who are familiar with the lipid field as well as novice researchers who seek to engage in this area of research. We would like to thank our colleagues who wrote, reviewed, and otherwise contributed to the chapters in this book.

B. Larijani
R. Woscholski
C. A. Rosser

Contents

List of Contributors

Damien Alcor
Cell Biophysics Laboratory, Cancer Research UK, London

Alicia Alonso
CSIC and University of the Basque Country, Bilbao

Facundo D. Batista
Lymphocyte Interaction Laboratory, London Research Institute,
Cancer Research UK, London

Yvette Bultsma
HBO, Division of Cellular Biochemistry, The Netherlands Cancer Institute,
Plesmanlaan, Amsterdam

Tom D. Bunney
Cancer Research UK Centre for Cell and Molecular Biology,
Chester Beatty Laboratories, The Institute of Cancer Research, London

Véronique Calleja
Cell Biophysics Laboratory, Cancer Research UK, London

Rosanna Cazzolli
Phospholipid Biology Group, Garvan Institute of Medical Research, Sydney,
New South Wales

Oscar Ces
Chemical Biology Centre, Imperial College, London

David J. Chitwood
Nematology Laboratory, USDA, ARS, Bldg., BARC-West, Beltsville, USA

Byung-Kwon Choi
Yonsei Proteome Research Center, Biomedical Proteome Research Center
and Department of Biochemistry, Yonsei University, Sudamoon-Ku, Seoul

Shamshad Cockcroft
University College London, London

F.-Xabier Contreras
CSIC and University of the Basque Country, Bilbao

Frank T. Cooke
Department of Biochemistry and Molecular Biology, University College London, Darwin Building, Gower Street, London

Anthony Couvreux
MSCi, CNRS-Université Bordeaux 1, IECB, Pessac

Jan K. Davidson-Moncada
New York Methodist Hospital, Department of Medicine, 506 6th Street, Brooklyn, NY 11215, USA

Lodewijk V. Dekker
School of Pharmacy, Centre for Biomolecular Sciences, University of Nottingham, Nottingham NG7 2RD, UK

Nullin Divecha
The Inositide Laboratory, The Paterson Institute for Cancer Research, Wilmslow Road, Manchester

Stephen K. Dove
School of Biosciences, University of Birmingham, Birmingham

Erick J. Dufourc
UMR5248 CBMN, CNRS–Université Bordeaux 1–ENITAB, IECB, Pessac

Jennifer M. Dyson
Department of Biochemistry and Molecular Biology, Monash University, Clayton, Victoria, Australia

Abdelkader Essafi
Cancer Research-UK Labs, Department of Oncology, Imperial College London, London

Sebastian J. Fleire
Lymphocyte Interaction Laboratory, London Research Institute, Cancer Research UK, London

Michael J. Fry
School of Biological Sciences, University of Reading, Whiteknights, Berkshire, UK

Marie Garnier-Lhomme
Cell Biophysics Laboratory, London Research Institute (LRI), Cancer Research UK (CR-UK), London

Béatrice L.L.E. Gauthé
Chemical Biology Centre, Imperial College, London

Peter Gierschik
Department of Pharmacology and Toxicology, University of Ulm, Ulm

Ana R. Gomes
Cancer Research-UK laboratories, Department of Oncology, MRC Cyclotron Building, Imperial College London, Hammersmith Hospital, Du Cane Road, London W12 0NN, UK

Félix M. Goñi
CSIC and University of the Basque Country, Bilbao

Axelle Grelard
CNRS-Université Bordeaux 1, IECB, Pessac

Jonathon R. Halstead
Division of Cellular Biochemistry, The Netherlands Cancer Institute, Amsterdam

Ka Kei Ho
Division of Cell and Molecular Biology, Imperial College, London

J. Justin Hsuan
Centre for Molecular Cell Biology, Department of Medicine, Royal Free and University College Medical School, Hampstead, London

Ping Huang
Center for Developmental Genetics and Department of Pharmacology, Stony Brook University, Stony Brook, NY

William E. Hughes
Phospholipid Biology Group, Garvan Institute of Medical Research; and Department of Medicine, University of New South Wales, St. Vincent's Hospital, Sydney, New South Wales

Robin Irvine
Department of Pharmacology, University of Cambridge, Cambridge

Pan-Young Jeong
Yonsei Proteome Research Center, Biomedical Proteome Research Center and Department of Biochemistry, Yonsei University, Sudamoon-Ku, Seoul

David R. Jones
Division of Cellular Biochemistry, The Netherlands Cancer Institute, Amsterdam

Michelle B. Josephs
Cancer Research UK Centre for Cell and Molecular Biology, Chester Beatty Laboratories, The Institute of Cancer Research, London

Keiichiro Kami
CR-UK Institute for Cancer Studies, School of Medicine,
University of Birmingham, Birmingham

Matilda Katan
Cancer Research UK Centre for Cell and Molecular Biology, Chester Beatty Laboratories, The Institute of Cancer Research, London

Willem Jan Keune
Division of Cellular Biochemistry, The Netherlands Cancer Institute, Amsterdam

Sun-Young Kim
Yonsei Proteome Research Center, Biomedical Proteome Research Center and Department of Biochemistry, Yonsei University, Sudamoon-Ku, Seoul

Anne M. Kong
Department of Biochemistry and Molecular Biology, Monash University, Clayton, Victoria, Australia

Eric W.-F. Lam
Cancer Research-UK Labs, Department of Oncology, Imperial College London, London

Natalia Lamuño Gandarillas
Cancer Research UK Centre for Cell and Molecular Biology, Chester Beatty Laboratories, The Institute of Cancer Research, London

Jocelyn Laporte
Department of Molecular Pathology, Institut de Génétique et de Biologie Moléculaire et Cellulaire, INSERM U596, CNRS UMR7104,
Université Louis Pasteur de Strasbourg, Illkirch

Banafshé Larijani
Department of Cell Biophysics, Cancer Research UK, London Research Institute, London

Eun-Young Lee
Yonsei Proteome Research Center, Biomedical Proteome Research Center and Department of Biochemistry, Yonsei University, Sudamoon-Ku, Seoul

Cécile Loudet
UMR5144, CNRS-Université Bordeaux 1, IECB, Pessac

Guillermo López-Lluch
Centro Andaluz de Biología del Desarrollo Dpto. Fisiología, Anatomía y Biología Celular Universidad Pablo de Olavide Carretera de Utrera Km. 1, 41013 Sevilla, Spain

Ben Maskrey
Department of Medical Biochemistry and Immunology, Cardiff University, Cardiff

Ursula B. McGovern
Cancer Research-UK Labs, Department of Oncology, Imperial College London, London

Sarah Meeuws
Division of Cellular Biochemistry, The Netherlands Cancer Institute, Amsterdam

Shane Minogue
Centre for Molecular Cell Biology, Department of Medicine, Royal Free and University College Medical School, Hampstead, London

Robert H. Michell
School of Biosciences, University of Birmingham, Birmingham

Christina A. Mitchell
Department of Biochemistry and Molecular Biology, Monash University, Clayton, Victoria

Xavier Mulet
Chemical Biology Centre, Imperial College, London

Valerie B. O'Donnell
Department of Medical Biochemistry and Immunology, Cardiff University, Cardiff

Lisa M. Ooms
Department of Biochemistry and Molecular Biology, Monash University, Clayton, Victoria

Michael Overduin
CR-UK Institute for Cancer Studies, School of Medicine, University of Birmingham, Birmingham

Marie-Hélène
Paclet, GREPI, TIMC-IMAG, CNRS UMR 5525, Laboratoire d'Enzymologie, C.H.U. de Grenoble – B. P. 217, 38043 Grenoble Cedex, FRANCE

Young-Ki Paik
Yonsei Proteome Research Center, Biomedical Proteome Research Center and Department of Biochemistry, Yonsei University, Sudamoon-Ku, Seoul

Bernard Payrastre
Département d'Oncogénèse et Signalisation dans les Cellules Hématopoïétiques, INSERM U563, Hôpital Purpan, Toulouse

Trevor R. Pettitt
Institute for Cancer Studies, Birmingham University Medical School, Birmingham

Dominic Poccia
Department of Biology, Amherst College, Amherst, MA, and Unidade de Investigaçao na Biologia do Desenvolvimento, Universide Lusófona, Lisbon

Karen M. Pomeranz
Cancer Research-UK Labs, Department of Oncology, Imperial College London, London

Sundaresan Rajesh
CR-UK Institute for Cancer Studies, School of Medicine, University of Birmingham, Birmingham

Holger Maria Rohde
Department of Molecular Pathology, Institut de Génétique et de Biologie Moléculaire et Cellulaire, INSERM U596, CNRS UMR7104, Université Louis Pasteur de Strasbourg, Illkirch

Colin A. Rosser
Rye St. Antony School, Oxford

Erika Rosivatz
Division of Cell and Molecular Biology, Imperial College London, London

Dongmin Shao
Division of Surgery, Oncology, Reproductive Biology and Anaesthetics (SORA) Faculty of Medicine Imperial College London MRC Cyclotron, 5th Floor Hammersmith Hospital du Cane Road, London W12 0NN, UK

Yhong-Hee Shim
Department of Bioscience and Biotechnology and Bio/Molecular Informatics Center and Institute of Biomedical Science and Technology, Konkuk University, Kwangjin-Ku, Seoul

Yun-Kyung Shin
Department of Bioscience and Biotechnology and Bio/Molecular Informatics Center and Institute of Biomedical Science and Technology, Konkuk University, Kwangjin-Ku, Seoul

Mireille H. Snel
Division of Cellular Biochemistry, The Netherlands Cancer Institute, Amsterdam

Graham W. Taylor
Centre for Amyloidosis and Acute Phase Proteins, Royal Free and University College Medical School, London

Richard H. Templer
Chemical Biology Centre, Imperial College, London

Shuzhi Teng
Center for Developmental Genetics and Department of Pharmacology, Stony Brook University, Stony Brook, NY

Hélène Tronchère
Département d'Oncogénèse et Signalisation dans les Cellules Hématopoïétiques, INSERM U563, Hôpital Purpan, Toulouse

Rana Varshochi
Cancer Research-UK Labs, Department of Oncology, MRC Cyclotron Building, Imperial College London, Hammersmith Hospital, London

Ana-Victoria Villar
CSIC and University of the Basque Country, Bilbao

Mike Wakelam
The Babraham Institute, Babraham Research Campus, Cambridge

Mark G. Waugh
Centre for Molecular Cell Biology, Department of Medicine, Royal Free and University College Medical School, Hampstead, London

Rudiger Woscholski
Division of Cell and Molecular Biology, Imperial College London, London

Aleksandra K. Zwolinska
Cancer Research-UK Labs, Department of Oncology, Imperial College London, London

List of Color Plates

Chapter 1
Eicosanoids: Generation and Detection in Mammalian Cells

Valerie B. O'Donnell, Ben Maskrey and Graham W. Taylor

Abstract Eicosanoids are 20-carbon lipids generated by the oxidation of arachidonic acid that are involved in physiological signaling in virtually all organ systems. Three primary enzymatic pathways are responsible for their synthesis in mammalian cells: lipoxygenase, cyclooxygenase, and cytochrome P450. They signal through receptor-dependent pathways, and their dysregulation is central to numerous pathological states including cancer and inflammation. Recent advances in their detection and analysis using mass spectrometry have made the study of these molecules more accessible to the research community in general. This review focuses on the available methods for the detection and analysis of eicosanoids and aims to act as a guide for those wishing to approach the analysis of eicosanoids for their own research.

Keywords Eicosanoid · mass spectrometry · lipoxygenase · cyclooxygenase · lipid · detection

1.1 Introduction to Eicosanoids

Eicosanoids are oxidative products of C20 (eicosa-) polyunsaturated fatty acids (arachidonic, eicosapentaenoic). Eicosanoids include prostaglandins/prostanoids, thromboxanes, leukotrienes, epoxides, and hydro(peroxy)-fatty acids (or oxylipins). Many of these products (including the prostaglandins and leukotrienes) exert profound biological effects *in vivo*. Eicosanoids are generated in biological systems by three separate enzyme families, lipoxygenase (LOX), cyclooxygenase (COX), and cytochrome P450 (CYP), which catalyze lipid peroxidation in a highly regulated manner, generating stereo- and regiospecific products (Fig. 1.1). The expression of these enzymes is highly tissue-localized and varies with the inflammatory activation state of the cells. The

V.B. O'Donnell
Department of Medical Biochemistry and Immunology, Cardiff University,
Heath Park, Cardiff, CF14 4XN, UK
e-mail: o-donnellvb@cardiff.ac.uk

B. Larijani et al. (eds.), *Lipid Signaling Protocols*, DOI: 10.1007/978-1-60327-115-8_1,

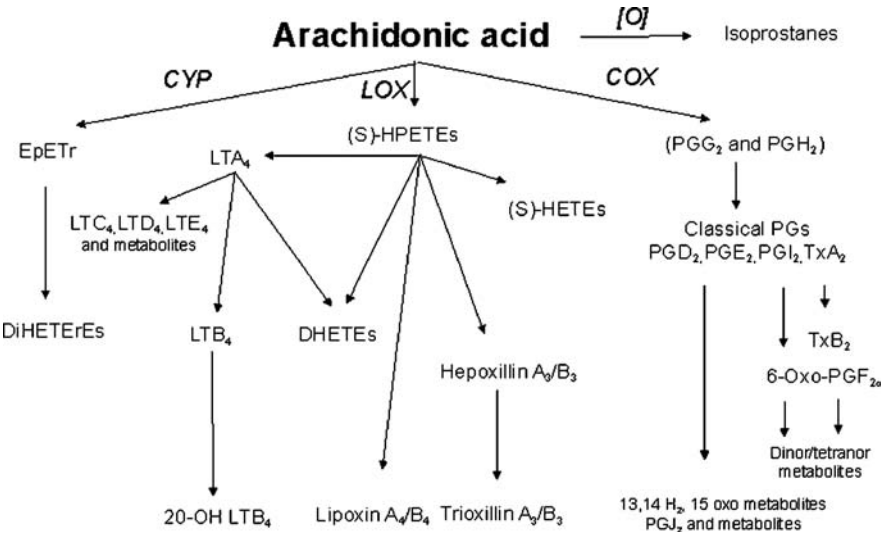

Fig. 1.1 The three families of eicosanoid-generating enzymes. Lipoxygenases (LOX) generate hydro(per)oxyeicosatetraenoic acids (HpETEs, HETEs), hydro(per)oxyoctadecadienoic acids (HpODEs, HODEs, from linoleate), as well as leukotrienes, lipoxins, and hepoxilins. Cyclooxygenases (COX) generate prostaglandin H2 (PGH2), the precursor for all prostaglandins and thromboxane. Cytochrome P450 isoforms generate epoxy fatty acids (EETs) and 20-HETE and metabolize PGH2 to form prostacyclin (PGI2) and thromboxane (TX)

primary products of COX, LOX, and CYP are then transformed in a cell type-specific manner into secondary eicosanoids and their metabolites, some of which may also exhibit potent bioactivity. Prostanoids contain a five-membered cyclopentane ring and derive from the COX pathway. LOX products [leukotrienes, lipoxins, and hydro(peroxy)-fatty acids or oxylipins] differ structurally and are generally straight chain oxidized lipids, while CYP catalyzes epoxidation and ω-terminus hydroxylation.

A wide variety of eicosanoids, including the classical prostanoids and a complex array of isomers (the isoprostanes), can also be generated through a nonenzymatic peroxidative mechanism (e.g., by metal-dependent Fenton chemistry) and, indeed, have been used as markers of oxidative stress *in vivo*.

The formation of eicosanoids normally requires arachidonate release from cell membrane phospholipids. This is mediated by phospholipase A2, acting on phosphatidylcholine or phosphatidylethanolamine to generate arachidonate and lyso-lipids (Fig. 1.2). Arachidonate oxidation generally starts with hydrogen abstraction, followed by delocalization of the radical, then finally oxygen insertion to form an unstable lipid hydroperoxide. The site of hydrogen abstraction and oxygen insertion is governed by the eicosanoid-generating isoform; for example, 5-LOX catalyzes formation of 5(S)-hydroperoxyeicosatetraenoic acid, with oxygen addition occurring at the S-face of C5 in a highly regulated

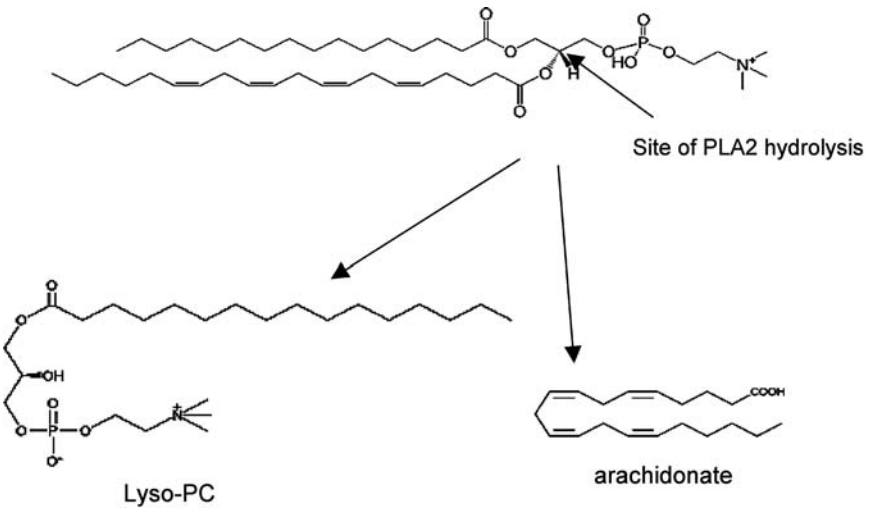

Fig. 1.2 Mechanism of arachidonate release from phosphatidylcholine. Phospholipase A2 isoforms, of which there are several, including cytosolic, secretory, and calcium-independent, hydrolyze the Sn2 bond of phosphatidylcholine (PC), releasing free arachidonate and lyso-PC

manner. This regulation is important since downstream signaling of eicosanoids via receptors is totally dependent on the isomeric structure. For example, prostacyclin from the COX pathway activates IP receptor in response to bradykinin, generating cAMP and lowering blood pressure.

1.1.1 Lipoxygenases

LOXs generate lipid hydroperoxides as their primary products (Fig. 1.3). In this reaction, the resting enzyme is activated (by a small amount of hydroperoxide) by oxidation of the ferrous heme to the active ferric state, which may catalyze hydrogen abstraction from arachidonate. Several LOX isoforms are known in mammalian cells, including 5-LOX (neutrophils), 12-LOX (platelets), and 12/15-LOX (primarily monocytes/macrophages). LOX-dervied hydroperoxides are rapidly reduced to their corresponding hydroxides intracellularly. This reaction is mediated by glutathione peroxidases (GPx), including a phospholipid-specific GPx. Alternatively, LOX-derived hydroperoxides serve as precursors for the generation of secondary mediators including lipoxins (LX) and hepoxilins. These further oxidized products may require additional LOX action for their formation. For example, LXA4 generation is postulated to require the sequential action of 15- and 5-LOX or 5- and 12-LOX. Hence, the formation of lipoxins may be transcellular, with neutrophil-derived 5-HETE being transformed to LXA4 following further oxidation by platelet 12-LOX [1]. Most LOX isoforms

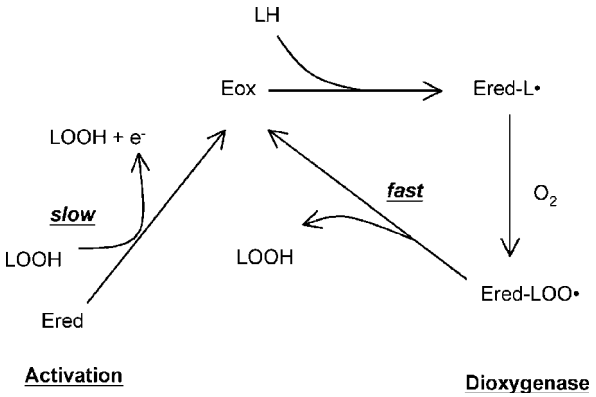

Fig. 1.3 Mechanism of LOX catalysis. Native enzyme is inactive (ferrous) and requires oxidation (e.g., by LOOH) to form the active ferric form (peroxidase cycle). This abstracts a hydrogen from an unsaturated lipid, forming an enzyme-bound alkyl radical (L•). Following oxygen addition, the lipid peroxyl radical (LOO•) is reduced by the nonheme iron to a lipid hydroperoxide (LOOH), which is released from the active site (dioxygenase cycle)

require free arachidonate as their sole substrate; however, the leukocyte-type 12/15-LOX can also oxidize arachidonate that is phospholipid-bound (although at lower rates than free arachidonate) and can also utilize linoleate. However, linoleate-derived products would not be strictly considered eicosanoids, since they contain a C18 carbon chain. Similarly, a new group of bioactive oxygenated derivatives of docosahexaenoic acid (22:6,n-3) have recently been described; they have coined the term *docosanoids* [2]. There are also a wide variety of plant LOXs, often utilizing C18 PUFAs to produce the oxylipins.

1.1.2 Cyclooxygenases

Prostanoids generated by COX include both prostaglandins and thromboxanes. They are generated by two sequential activities of COX that are interdependent but located on opposite sides of the protein: cyclooxygenase and peroxidase. The cyclooxygenase active site abstracts a hydrogen from arachidonate using a tyrosyl radical, and then two molecules of oxygen are stereospecifically inserted, forming an endoperoxide/peroxyl radical that is ultimately reduced to the hydroperoxide PGG2 (Fig. 1.4). The PGG2 is then reduced by the heme peroxidase forming PGH2, which is released and serves as a precursor for the synthesis of downstream eicosanoids, including prostacyclin (PGI2) and thromboxanes. There are two COX isoforms: COX-1 (platelets, gastric, renal) and COX-2 (vessel wall, renal). While COX-1 is primarily constitutively expressed, COX-2 can be induced in many cell types during inflammation (e.g., LPS, IFNγ, IL-1β, TNFα). COX-2 expression in blood vessel walls

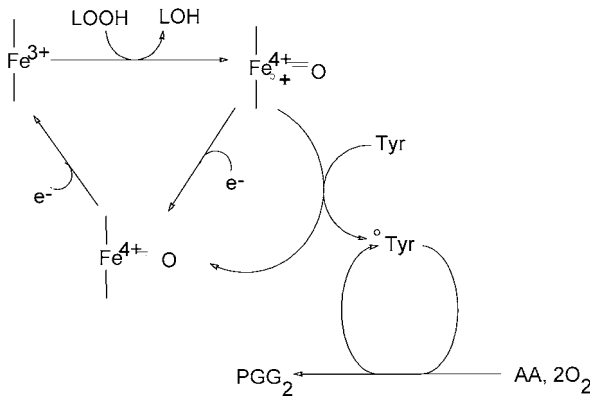

Fig. 1.4 Mechanism of COX catalysis. Cyclooxygenase has two catalytic cycles, cyclooxygenase and peroxidase, which are interdependent. Oxidation of the ferric heme to an oxy-ferryl porphyrin cation radical by LOOH is required for formation of the catalytic tyrosyl radical (Tyr•). This abstracts a hydrogen from arachidonate, forming an alkyl radical. Following the addition of two molecules of oxygen, and reduction by the active site, PGG2 (an endoperoxide, hydroperoxide) is released. PGG2 is then reduced to PGH2 by peroxidase turnover

appears to be maintained by laminar shear [3], where it provides substrate for PGI2 synthesis and regulates blood pressure. Apart from free eicosanoids, recent work by Marnett and coworkers has shown that COX-2 can oxidize 2-arachidonyl glycerol, generating novel esterified prostaglandins. These signal distinctly to their free acid counterparts; for example, PGE2-glyceryl is approximately 10 times more potent at mobilizing calcium than PGE2 [4, 5, 6]. In recent years, the existence of a third COX isoform, COX-3, has been suggested [7]. This enzyme, apparently a splice variant of COX-2, was proposed to be the target for acetaminophen/paracetamol. However, much controversy exists regarding this enzyme. For an interesting discussion of the current thinking, see the Cayman Chemical website (www.caymanchem.com).

1.1.3 Cytochrome P450

CYP enzymes involved in eicosanoid generation include CYP epoxygenases (CYP2C, 2J) that generate epoxyeicosatetraenoic acids (EETs or EpETrEs), CYP ω-oxidases (CYP4A, 4C) that generate 20-HETE, thromboxane synthase, and prostacyclin synthase. EETs signal in diverse ways and have been postulated to account for endothelium-derived hyperpolarizing factors [8]. For example, 11,12-EpETrE plays a role in the recovery of depleted calcium pools in cultures of smooth muscle and 8,9-EpETrE reduces the glomular filtration rate through cyclooxygenase-dependent preglomerular vasoconstriction. Cytochrome P450 is a monooxygenase reaction and transfers one oxygen via a direct

hydroxylation mechanism. They can act on polyunsaturated fatty acids via several different mechanisms of oxygenation, including bisallylic hydroxylation, epoxidation, and hydroxylation of the ω-side chain [9].

1.1.4 Signaling by Eicosanoids

Eicosanoids signal predominantly via activation of 7-transmembrane domain G protein-coupled receptors (GPCRs). This is a diverse family that also includes chemokine and lysophospholipid receptors. Receptors for eicosanoids include EP, IP (prostacyclin), TP (thromboxane), CysLT1/T2 (leukotrienes), and ALX (lipoxin). Separate to this, some eicosanoids can mediate signaling by nuclear receptors/transcription factors; for example, the peroxisomal proliferator activation receptor family (PPARs) is variously activated or inhibited by LOX-derived HETEs either directly through ligand binding or by activation of MAP kinase-dependent PPAR phosphorylation [10–13]. HETEs from 12- or 15-LOX can stimulate numerous signaling pathways in several cell types, including mesangial, smooth muscle, endothelial, and adrenal glomerulosa cells. Pro-inflammatory pathways that are activated by submicromolar concentrations of exogenous 12/15-LOX products [12(S)-HETE] include MAP kinases, Ras translocation, CREB, and protein kinase C [10, 14, 15]. Finally, EETs and 20-HETE can modulate the activity of potassium channels in the vascular smooth muscle, leading to the regulation of vessel tone.

1.2 Measurement of Eicosanoids

1.2.1 General Considerations and Resources

Due to the chemical and biological complexity of eicosanoids, measurements of their concentrations in biological samples must be carefully validated and controlled in the laboratory. While several approaches exist for determining these mediators, there are pitfalls that need to be taken into account and can easily trap the unwary. Ideally, the assay used should be sensitive, specific, and accurate. It is often preferable to measure stable metabolites of eicosanoids rather than unstable precursors, as this will give a more accurate estimate of whole body or tissue generation. For example, 6-oxo-PGF1α and 2,3-dinor-TXB2, excreted at high concentrations into the urine, are used to estimate total systemic PGI2 and TX in humans or mice [16, 17]. In this case, an additional advantage is that samples are obtained noninvasively. Although LTE4 can be used as a marker of cysteinyl leukotriene synthesis *in vivo*, there are currently no other LOX metabolites that are routinely used for the systemic determination of this pathway *in vivo*.

Assays should be applicable to either *in vitro* or *in vivo* situations, although in practice a wider range of products can be determined from isolated cells and

enzyme assays, since samples can be obtained and stabilized more easily from these types of experiments. It would, of course, be preferable for an ideal assay to be economical and of high-throughput, although this can be rather difficult to achieve in practice with eicosanoids.

A number of reviews have been written on the analysis of eicosanoids in biological samples. Several provide far more detail than we include here, in particular regarding long-established methods such as extraction techniques, HPLC, and GC-MS. Instead of replicating the previous information provided by these sources, we will direct the reader to them where relevant. In particular, we recommend the excellent *Prostaglandins and Related Substances: A Practical Approach*, edited by Benedetto, McDonald-Gibson, Nigam, and Slater (IRL Press, Oxford, 1987). Two other excellent books, in particular regarding GC/MS, are *Mass Spectrometry of Lipids. Handbook of Lipid Research*, *Vol. 7,* by Murphy (Plenum Press, New York, 1993), and *Advances in Prostaglandin, Thromboxane, and Leukotriene Research*, *Vol. 18, Mass Spectra of Prostaglandins and Related Products,* by Pace-Asciak (Raven Press, New York,). Finally, for ESI/MS/MS, the excellent review by Murphy et al. [18] provides a comprehensive list of spectra and MRM transitions for all eicosanoid classes and directs the reviewer to articles reporting LC conditions and quantitative analysis throughout. There is also a wealth of information on the fragmentation patterns of specific analytes, giving structures of daughter ions, where known.

We also suggest the following websites:

www.lipidmaps.org is the website of the Lipid Maps Project (NIH glue grant), which is continually updating its database with a wealth of useful information for eicosanoid research, in particular, LC/MS product ion spectra, structures, and links to suppliers. This is an essential resource for those setting up or running assays in eicosanoid LC/MS/MS.

www.cyberlipid.org is an excellent recourse with links throughout the text providing background information on all lipid classes, including eicosanoids.

www.lipidbank.org offers a comprehensive database on lipids. For eicosanoids, information on the structure, biological activities, chemical and physical properties, spectral data (NMR, UV, IR), chemical synthesis, and metabolism is provided.

www.lipidlibrary.co.uk is produced by Bill Christie at the Scottish Crop Research Institute, Dundee. This is an excellent resource on lipids in general, although less information on eicosanoids is here than in the websites listed above.

1.2.2 Stabilization of Samples

Eicosanoids can be unstable and may even be generated artifactually during sample handling and processing. Thus, consideration of how samples are prepared and stored is important. For example, storage of plasma even at 20°C can

be accompanied by nonenzymic oxidation leading to isoprostane generation: Indeed, it was the artifactual increase in "PGF2a" in plasma that led to their discovery [17]. Activation of platelets during venipuncture can cause generation of TXA2 (as measured by its stable hydrolysis product, TxB2). This can be a particular problem when it is remembered that the circulating level of TxA2 is less than 10 pg/ml, but serum (fully activated blood) contains 200 ng/ml of TxA2: Little activation needs to occur to significantly raise the measured level of plasma TxB2. The extraction of eicosanoids from solid tissue may require homogenization, a process that itself can cause activation of eicosanoid generation.

It is important to consider inclusion of inhibitors and other drugs that would minimize artifactual eicosanoid generation. These could include indomethacin (10 μM), EDTA (calcium chelator), dithiopentaacetic acid (DTPA, iron chelator, 100 μM), and butylated hydroxytoluene (BHT, antioxidant, 100 μM), depending on the pathway to be measured.

Eicosanoid breakdown during extraction must also be considered. A number of eicosanoids can be affected by acid treatment. For example, PGE2 can be converted into PGA2, and many epoxides are readily hydrolyzed to their diols by treatment with dilute acids during extractions. Oxidation is also a potential problem and double-bond rearrangements can also occur. Sample losses due to inactivation can be accounted for by the use of suitable internal standards (see below).

1.2.3 Extraction

The determination of eicosanoids in biological samples generally requires extraction. The preferred methods are either organic solvent or reverse-phase solid-phase extraction columns. The chosen method should be fast, simple, and reproducible. It is essential that the extraction procedure does not modify or inactivate the analyte. For example, extremes of pH should be avoided to minimize hydrolysis of labile bonds, isomerization, or elimination of water from alcohols. Solvents should be removed at low temperatures under inert gas when required. In the past, most laboratories utilized solvent extraction, for example, chloroform-methanol or other mixtures such as hexane-isopropanol [19, 20, 21]. Extraction efficiency can be influenced by adding salt to the solution or changing the pH. In fact, with the pKa of carboxylic acids being around 4.5, extraction efficiency is enhanced by acidification. We use low concentrations of acetic acid (1−5%) since this acid is relatively volatile and small amounts can easily be removed under vacuum or when the extract is dried down under inert gas. For the extraction of eicosanoids from primary human and mouse leukocytes and platelets, we routinely use a hexane:isopropanol:acetic acid two-step solvent extraction [19]; details are provided as Appendix 1. For assays of LOX metabolites, we include a reduction step using $SnCl_2$. This converts

hydroperoxyeicosatetraenoic acids (HpETEs) to HETEs, which are more stable. We then measure specific HETE isomers as an index of the total H(p)ETE generated by this pathway (Appendix 1).

Solid-phase extraction is also widely used for eicosanoid extraction and is especially useful when extracting large volumes of biological fluid, since only small amounts of organic solvent are subsequently required for eluting the analytes [22, 23]. Columns used for solid-phase extraction include normal phase (silica), reverse phase (C18), and possibly ion exchange. Analytes elute from reverse phase in order of decreasing polarity, with the solvent's hydrophobicity being increased sequentially. Eicosanoids bind to C18 columns with salts and polar compounds washing off in water and are then eluted with ethyl acetate. A second clean-up, if required, could involve binding to a silica cartridge with removal of neutral lipids and then elution of eicosanoids in methanol. The most specific solid-phase extraction involves antibody binding of the analyte, with the antibody bound to a sepharose matrix [24, 25]. Separate antibodies are required for each analyte, although the cross reactivity of the antibodies can be exploited. This approach was previously used for the extraction of TxB2, 6-oxo-PGF1α, and their 2,3-dinor metabolites from urine before GC/MS analysis [26, 27, 28].

1.2.4 Internal Standards

The extraction of low levels of eicosanoids from complex biological samples is always variable, especially when several steps or extractions are utilized. Typical losses can be up to 50% or more, depending on the analyte and the method. For this reason, the use of internal standards is absolutely essential for quantitative assays using HPLC, GC-MS, or LC-MS. The gold standard is stable isotope-labeled internal standards, for example 12-HETE-d8, where eight deuterium atoms are present, and the m/z shifts by 8 amu. Stable isotope-labeled standards are the optimum since they behave identically to the analyte of interest in terms of extraction and recovery, and standards elute on GC or LC close to the unlabeled analyte, confirming the identity. Of equal importance is the confidence a negative result obtained when using an internal standard; if the analyte is below the detection limit of the assay but the internal standard is recovered, then we are sure that the sample has not simply been lost during extraction and that the level of the analyte is truly below the LOD. Similarly, if the internal standard is not present, then the extraction has failed and a negative cannot be trusted. Deuterated internal standards are available for only a limited number of eicosanoids and, furthermore, are rather costly. As a compromise, for LC/MS/MS determination of eicosanoids, we include a stable isotope-labeled standard for each eicosanoid class (e.g., 12-HETE-d8 for all HETEs, PGE2-d4 for all PGs) in all samples before extraction, and then we separately construct standard curves using mixtures of labeled and unlabeled standards for all analytes of interest. This enables the determination of relative ionization efficiency for all multiple reaction-monitoring (MRM) transitions, as

compared to the stable isotope-labeled standard (e.g., ratio of 12-HETE-d8/12-HETE versus amount of standard used). The use of unlabeled standards for all other analytes is essential since different compounds will give different responses in terms of ionization sensitivity, even within the same class of molecule. In addition, they are required to determine the expected retention time for the analytes in the biological sample. A further important consideration is linearity. For example, in our LC/MS/MS system, the detection of 12-HETE is linear from approximately 1–500 pg on column but above this starts to deviate. It is essential to ensure that concentrations measured in biological samples fall within the linear part of the standard curve, or quantitation accuracy will be lost. Stable isotope-labeled and unlabeled standards for most eicosanoids are available from Cayman Chemical (www.caymanchem.com) or Biomol (www.biomol.com).

1.2.5 Analysis Techniques

1.2.5.1 Immunoassays

There are many choices of analytical technique with which to determine eicosanoid concentrations in biological samples. However, some suffer from significant drawbacks and should be used with caution. For example, immunoassays may hugely (even up to 1,000-fold) overestimate concentrations of analytes. This results from the inevitable cross reactivity of the antibodies with other eicosanoids of similar structure and can be very difficult to eliminate in practice. Early use of RIAs indicated plasma levels of 6-oxo-PGF1a at 10–20 pg/ml [29, 30]. However, the true circulating level is 1–2 pg/ml [31, 32]. In this case, high levels of cross-reactive compounds gave false-positive results. In contrast, when TxB2 is the major prostaglandin in serum, RIAs give accurate results [33]. One way to increase the selectivity of RIAs or ELISAs is to use them following HPLC separation of eicosanoids, where retention time is also used as a diagnostic criterion. Several commercial ELISAs are now available and promise high sensitivity and selective detection of eicosanoids. Lists of non-cross-reacting lipids are included in the specifications provided, but these lists do not tell us what else the eicosanoids react with. Also, if an ELISA is to be used, it should first be validated in the exact biological system of interest using a physicochemical method such as GC/MS or LC/MS/MS. If both assays give the same result, then one could use an ELISA, which for laboratories without routine access to GC or LC/MS would be extremely useful. Care must also be taken when interpreting data from biosynthetic studies, where the initial substrate may well be in vast excess of the products: Arachidonic acid may only have a 0.01% cross reactivity with the analyte of interest, but if it is used as mM concentrations, and the products are present at nM levels, then the dangers of identifying the substrate as product are clear. However, to date, the validation of ELISAs has not been extensively carried out and their use in the biological determination of eicosanoids should be interpreted with much caution.

1.2.5.2 HPLC-UV/Radioactivity

For a limited number of eicosanoids, HPLC with UV detection can be used. In particular, compounds containing conjugated diene-, triene-, or tetraene-chromophores, such as mono-, di-, and tri-hydroxy lipids from the LOX pathway, which absorb at 235, 269, and 301 nm, respectively, possess a distinctive UV profile. These include HETEs, leukotrienes, and lipoxins [22, 34, 35, 36, 37]. However, sensitivity is only in the high-nanograms range. This approach is of very limited use for prostaglandins. In general, HPLC-UV assays are only suitable where relatively large amounts of eicosanoids are present in clean biological matrices such as buffers. Plasma contains too many UV-active materials at vastly higher levels than the eicosanoids for an HPLC-UV method to have any validity. Radiochemical detection following LC separation has been used in the past, where [^{14}C]- or [^{3}H]-arachidonate is provided as the precursor for eicosanoid generation, and LC retention time is used to determine the analyte. However, this approach relies on pretreatment of cells in culture with radiolabeled arachidonate (for incorporation into cellular phospholipids) and so is less useful with primary cells such as neutrophils or platelets that cannot be cultured for significant periods. As mentioned above, HPLC has been combined with RIA, and this can greatly enhance the sensitivity of detection, e.g., for cysteinyl leukotrienes [38, 39, 40].

1.2.5.3 Gas Chromatography

Gas chromatography has long been the method of choice for the routine separation of derivatized fatty acids and their oxidation products. However, the high cost of equipment and the degree of technical expertise required for this approach have limited its use; even now, it is still only utilized in a handful of specialized laboratories worldwide for eicosanoid research. For more details regarding GC/MS of eicosanoids, including derivatization protocols, the reader is directed to Barrow and Taylor [33]. Gas chromatography is based on the partition of the analyte between the stationary and gaseous phases. Therefore, molecules to be analyzed must be volatile and thermally stable at the high GC operating temperatures. For eicosanoids, this requires the derivatization of polar groups, including carboxyl and hydroxyl. Typical methods include N-acylation, methoximine formation, esterification, and trimethylsilyl ether formation (full details are given in Barrow and Taylor [33]). Typical GC capillary columns consist of fused silica to which the stationary phase is bonded [41, 42].

When coupled to mass spectrometry detection, GC/MS provides an unparalled technique in terms of sensitivity and selectivity for eicosanoid detection. Importantly, multiple analytes can be detected in one sample, greatly reducing the cost for routine detection once the equipment is in place and operational.

Following derivatization and chromatography, the sample passes into the mass spectrometer, where it is ionized by either electron impact (EI), chemical ionization (CI, e.g., methane), or electron capture (EC). For example, in EI

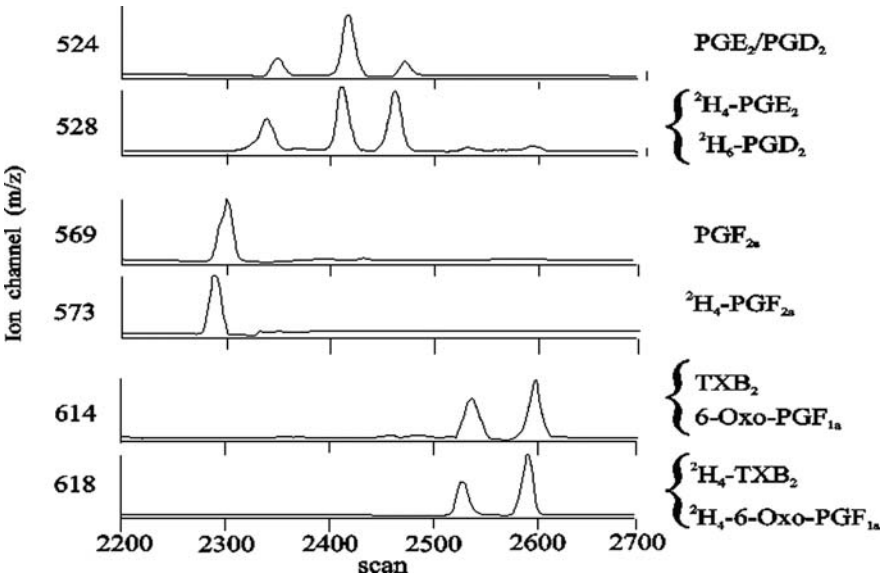

Fig. 1.5 GC/MS analysis of PGs. PGs are analyzed by GC-EXMS as their methoxime-O-trimethylsilylether pentafluorbenzyl ester derivatives. The M-PFB- ion is monitored in the SIM mode for PGE2, PGD2 (m/z 524), PGF2α (m/z 569), 6-oxo-PGF1α, and TxB2 (M/z 614). In each case, the tetradeuterated internal standard has an increased mass (4u) and elutes fractionally before each analyte. Note that PGE2 and PGD2 both form two methoximated isomers, with two isomers overlapping

mode, a beam of high-energy electrons bombards the analyte, causing removal of a low-energy (thermal) electron from the analyte. This is converted to a radical cation (M), which breaks down into a number of fragments. This fragmentation pattern is then used to characterize the analyte. The MS is set to detect a small number of ions in selected ion mode (SIM), and for some analytes down to 1 pg can be detected. An example of PG analysis is shown in Fig. 1.5, where PGE2, PGD2, PGF2α, TxB2, and 6-oxo-PGF1α are quantified in a single assay. For this analysis, the PGs and their internal standards were extracted and derivatized (methoximine O-trimethylsilyl ether, pentafluorobenzyl derivatives) and their chromatography and MS detection are shown (Fig. 1.4).

1.2.5.4 LC/ESI/MS/MS

One of the most important advances in lipid research in the last decade has been the development of high-sensitivity electrospray tandem mass spectrometry and Q-trap instruments. While these instruments were originally designed for proteomic and small metabolite work, lipid biochemists have been quick to realize their potential for both the routine quantitation of eicosanoids and the

structural determination of new molecules. Newer instruments are reaching the sensitivity of GC/MS, with the detection of many eicosanoids being as low as 1 pg. As with GC, multiple analytes can be determined simultaneously, but the major advantage is that derivatization is not required. This saves a significant amount of time and decreases losses due to less sample work-up. This technique uses HPLC on the front end to separate eicosanoids, exactly as has been used for decades, although in recent years, the use of microbore (e.g.,1–2 mm or less with flow rates of 50–100 µl/min) instead of analytical columns has become routine. Following their separation, samples are introduced into the source of the mass spectrometer, where ionization takes place. For most eicosanoids, the formation of a negative ion due to the carboxylate group is facile and gives a strong [M-H]− signal in the negative mode. In the positive ion mode, the protonated [M + H]+ ion is often accompanied by facile dehydration with accompanying signals at −18 amu. Several scanning modes can be utilized for eicosanoid analysis, but, in practice, multiple reaction-monitoring (MRM) transitions and product ion spectra are usually monitored, depending on the application. Routine quantitation of prostaglandins requires stable isotope-labeled internal standards, as described earlier in this chapter. We use one for each PG class, e.g., 12-HETE-d8 for all LOX products and PGE2-d4 for all COX-derived PGs. Following ionization, the analytes are selected by m/z in Q1, then undergo collisionally activated decomposition (CAD) in Q2 using inert gas, before passing into Q3. In MRM mode, they are again selected by m/z in Q3 before being scanned out to the detector. For example, 12-HETE with m/z [M-H]- 319.2 fragments on collision-induced dissociation (CID) in Q2, to give several daughter ions, including one that is diagnostic for the 12-hydroxy isomer, at 179.2. Other positional isomers, e.g., 5-HETE or 15-HETE, do not generate this fragment, instead showing a different pattern of daughter ions, with characteristic ions labeled in each panel (Fig. 1.6). The characteristic fragmentation pattern of each eicosanoid is exploited to ensure selective and specific detection of each individual analyte. Figure 1.7 shows LC/ESI/MS/MS detection of several eicosanoids, including two stable isotope-labeled standards, with each peak representing the 500-pg standard. It can thus be seen how the combination of retention time on LC and unique MRM transition can be exploited to determine the concentration of each lipid present. The specific MRM transitions used are given in Table 1.1. An example of HETE isomer detection in a biological sample is shown in Fig. 1.8.

While retention time and MRM transition are usually considered diagnostic for a particular analyte, one very useful feature of some instruments is the ability to switch modes on a millisecond timescale during a run and obtain a product ion spectrum of an analyte. This then provides definitive proof that the peak of interest is indeed correctly identified. On most triple quadrupole instruments it can be difficult to get good-quality spectra at low concentrations in a biological sample. However, with hybrid instruments, e.g., ESI/Q-Trap, where Q3 can be used as an ion trap, this can be accomplished. In our laboratory using the Applied Biosystems 4000 Q-Trap, good-quality product ion spectra can be

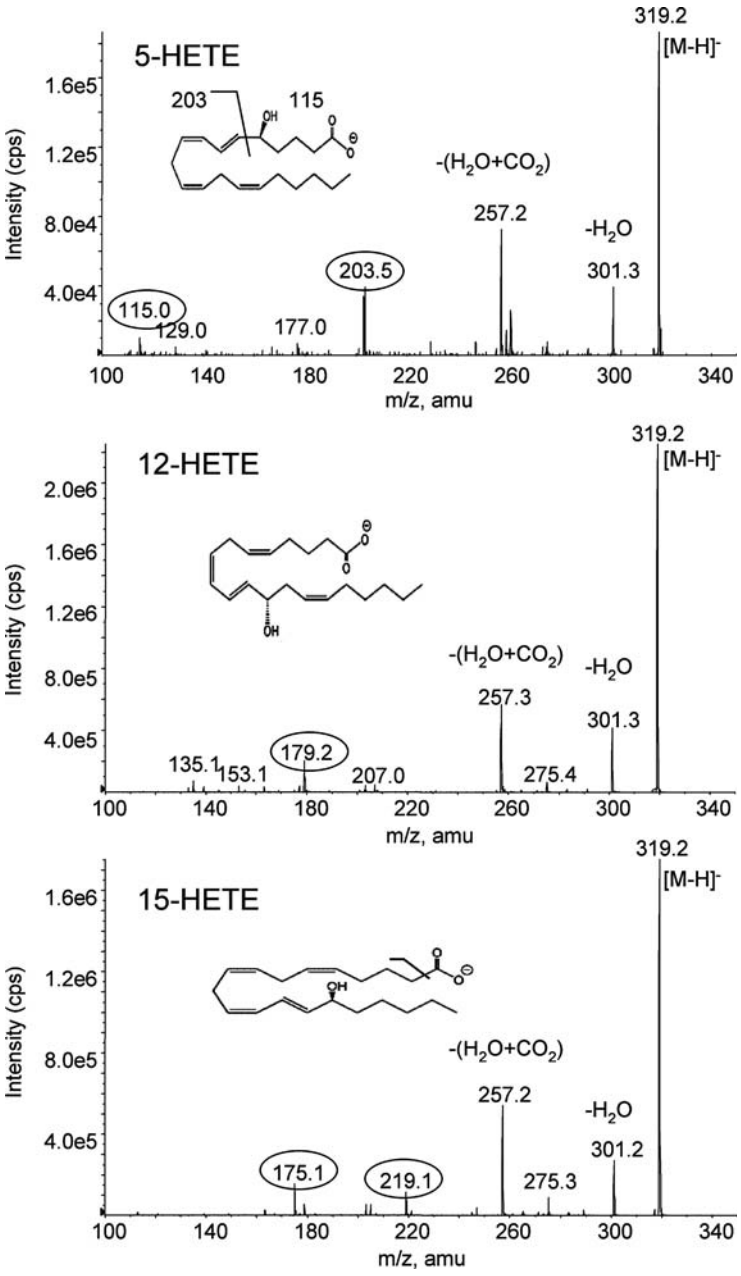

Fig. 1.6 Product ion spectra of 5-, 12-, and 15-HETEs. Methanolic solutions of HETEs (10 ng/ml) were infused at 10 μl/min into the electrospray source of an Applied Biosystems 4000 Q-Trap. Negative product ion spectra were acquired in ion-trap mode. While several ions are identical among different HETE isomers, unique fragments are detected that can be used to selectively monitor each isomer in MRM mode, as shown in the next two figures. We use the following daughter ions for routine quantitation: 5-HETE (m/z 115.0), 12-HETE (m/z 179.2), and 15-HETE (m/z 219.1)

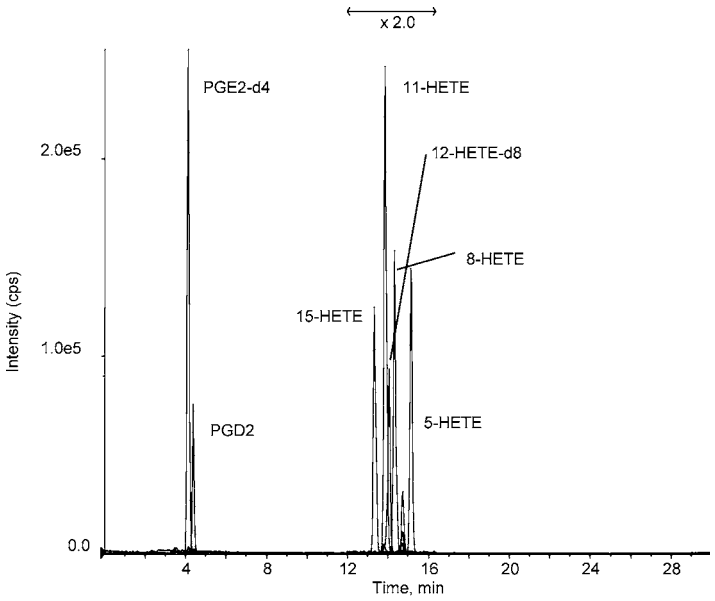

Fig. 1.7 LC/ESI/MS/MS detection of several HETEs and PG standards. 500 pg of each standard was run on LC as described in Appendix 1. Transitions used are as follows: PGE2-d4: 335→275; PGD2: 351→271; 15-HETE: 319→219; 12-HETE-d8: 327→184; 11-HETE: 319→167; 8-HETE: 319→135; 5-HETE: 319→115

obtained at as low as 10X the limit of detection for MRM transitions. For example, PGE2 is detected in MRM mode to 100 fg, but product ion spectra can be obtained during elution of 1 pg from the LC column, during an actual LC run. In fact, one can set up an experiment not only to quantitate specific transitions, but also to generate product ion spectra when elution of an analyte is detected by the instrument. This can greatly increase confidence that one is truly quantitating the correct analyte.

Table 1.1. MRM Transitions Used for Detecting HETE isomers and Some PGs

Compound	MRM Transition
5-HETE	319-115
8-HETE	319-155
11-HETE	319-167
12-HETE	319-179
12-HETE-d8	327-184
15-HETE	319-219
PGE2*	351-271
PGE2-d4	355-275
PGD2*	351-271

*Note that PGD2 and PGE2 have same transitions, however they separate on LC with different retention times.

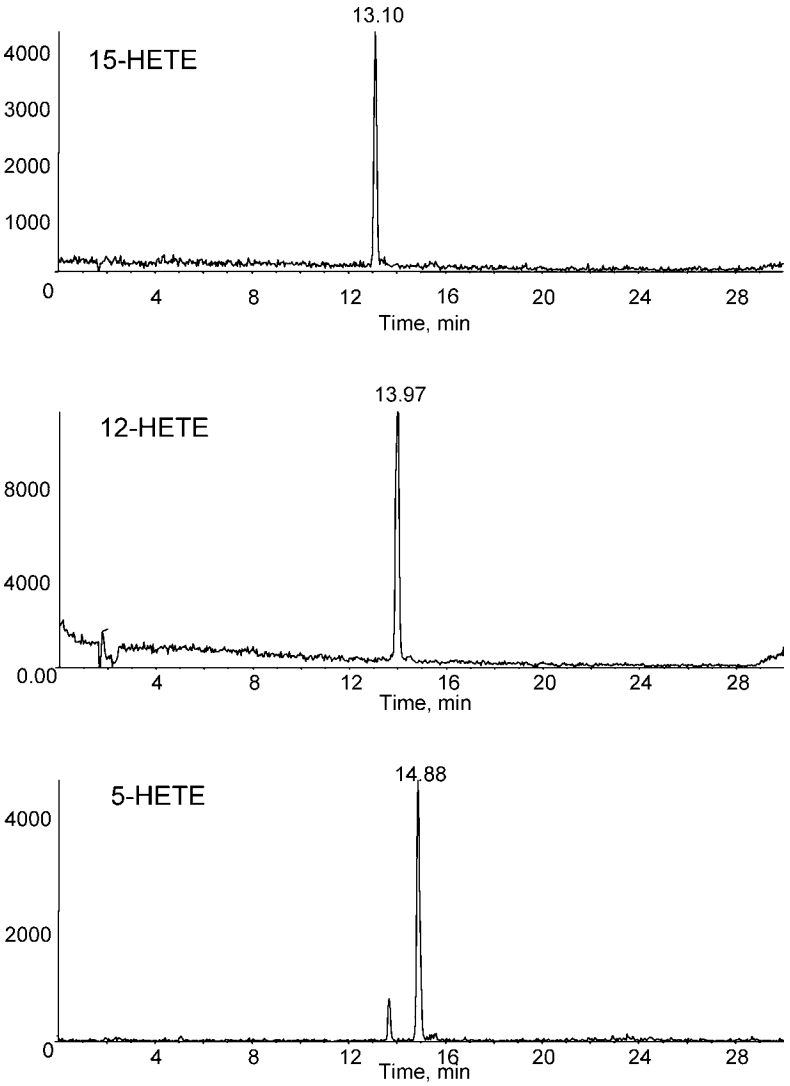

Fig. 1.8 LC/ESI/MS/MS detection of HETE isomers in murine peritoneal lavage from wild-type mice. Peritoneal lavage was spiked with deuterated internal standards and then extracted as in Appendix 1. 10-μl samples were analyzed using LC/ESI/MS/MS as described, and chromatograms for 15-, 12-, and 5-HETE from a single mouse are shown

1.3 Summary

Eicosanoids are a diverse family of lipid mediators that continue to be an active focus of research in many fields of biomedicine. Reliable and cost-effective methodologies for their quantitation are required for their accurate

determination in cell and tissue samples. LC/ESI/MS/MS and GC/MS are the gold-standard methods for quantitating and identifying eicosanoids. However, setting them up represents a significant time and cost investment for laboratories. Unfortunately, this puts them out of the reach of many researchers at least for the time being, although prices are decreasing as instruments are being further developed. Currently, those wishing to quantitate eicosanoids can purchase immunoassays off the shelf and run them locally, or collaborate with others who have routine GC or LC assays set up in their laboratories. Although perhaps more time-consuming, we would advise the use of LC or GC/MS where at all possible, unless the alternative assay has been carefully validated for the particular type of sample being analyzed.

1.4 Appendix 1

1.4.1 Eicosanoid Liquid Extraction

1. Add the appropriate standards to 1 ml of sample (1000 ng for UV detection. 10 ng for MS/MS detection).
2. Reduce hydroperoxides to thier corresponding stable hydroxy form by incubating with 1mM $SnCl_2$ for 10 min at room temperature.
3. Extract eicosanoids by adding a solvent mixture of 1 M acetic acid/2-isopropanol/hexance (2:20:30, v/v/v) to the sample at a ratio of 2.5 ml of solvent mixture: 1 ml of sample.
4. Vortex and then add 2.5 ml of hexane.
5. Vortex again and centrifuge at 1,000 rpm, 4°C for 10 min.
6. Recover the lipids from the hexane (upper) layer.
7. Re-extract by addition of equal volume of hexane, then vortex and centrifuge as before.
8. Combine the hexane layers, dry under N_2 flow, and then resuspend in a small volume (100 µl) of methanol. Store at −70°C under an N_2 atmosphere and analyze within 2 weeks.

NB. All extaction steps must be carried out using clean glassware (new or freshly solvent-rinsed).

1.4.2 RP-HPLC Separation

Eicosanoid samples are separated by reverse-phase high-performance liquid chromatography (RP-HPLC) using a C18 ODS column (e.g., Waters Spherisorb® 5-µm ODS2 4.6 × 150 mm Analytical Column). Products are injected in methanol and eluted over a linear binary gradient changing from 50–90% B over a 20-minute duration at a flow rate of 1 ml/min. (A = water:acetonitrile:acetic acid, 75:25:0.1, B = methanol:acetonitrile:acetic acid, 60:40:0.1.) All solvents are HPLC grade or above.

References

1. Chiang N, Arita M, Serhan CN. Anti-inflammatory circuitry: Lipoxin, aspirin-triggered lipoxins and their receptor ALX. Prostagl Leukot Essent Fatty Acids 2005;73:163–77.
2. Marcheselli VL, Hong S, Lukiw WJ, et al. Novel docosanoids inhibit brain ischemia-reperfusion-mediated leukocyte infiltration and pro-inflammatory gene expression. J Biol Chem 2003;278:43807–17.
3. Topper JN, Cai J, Falb D, Gimbrone MA, Jr. Identification of vascular endothelial genes differentially responsive to fluid mechanical stimuli: Cyclooxygenase-2, manganese superoxide dismutase, and endothelial cell nitric oxide synthase are selectively up-regulated by steady laminar shear stress. Proc Natl Acad Sci USA 1996;93:10417–22.
4. Nirodi CS, Crews BC, Kozak KR, Morrow JD, Marnett LJ. The glyceryl ester of prostaglandin E2 mobilizes calcium and activates signal transduction in RAW264.7 cells. Proc Natl Acad Sci USA 2004;101:1840–5.
5. Rouzer CA, Marnett LJ Glycerylprostaglandin synthesis by resident peritoneal macrophages in response to a zymosan stimulus. J Biol Chem 2005;280:26690–700.
6. Kozak KR, Rowlinson SW, Marnett LJ. Oxygenation of the endocannabinoid, 2-arachidonylglycerol, to glyceryl prostaglandins by cyclooxygenase-2. J Biol Chem 2000;275:33744–9.
7. Simmons DL, Botting RM, Robertson PM, Madsen ML, Vane JR. Induction of an acetaminophen-sensitive cyclooxygenase with reduced sensitivity to nonsteroid antiinflammatory drugs. Proc Natl Acad Sci USA 1999;96:3275–80.
8. Maier KG, Roman RJ. Cytochrome P450 metabolites of arachidonic acid in the control of renal function. Curr Opin Nephrol Hypertens 2001;10:81–7.
9. Oliw EH, Bylund J, Herman C. Bisallylic hydroxylation and epoxidation of polyunsaturated fatty acids by cytochrome P450. Lipids 1996;31:1003–21.
10. Hsi LC, Wilson L, Nixon J, Eling TE. 15-Lipoxygenase-1 metabolites down-regulate peroxisome proliferator-activated receptor gamma via the MAPK signaling pathway. J Biol Chem 2001;276:34545–52.
11. Hsi LC, Wilson LC, Eling TE. Opposing effects of 15-lipoxygenase-1 and -2 metabolites on MAPK signaling in prostate. Alteration in peroxisome proliferator-activated receptor gamma. J Biol Chem 2002;277:40549–56.
12. Nagy L, Tontonoz P, Alvarez JG, Chen H, Evans RM. Oxidized LDL regulates macrophage gene expression through ligand activation of PPARgamma. Cell 1998;93:229–40.
13. Shappell SB, Gupta RA, Manning S, et al. 15S-Hydroxyeicosatetraenoic acid activates peroxisome proliferator-activated receptor gamma and inhibits proliferation in PC3 prostate carcinoma cells. Cancer Res 2001;61:497–503.
14. Willson TM, Lehmann JM, Kliewer SA. Discovery of ligands for the nuclear peroxisome proliferator-activated receptors. Ann NY Acad Sci 1996;804:276–83.
15. Patricia MK, Natarajan R, Dooley AN, et al. Adenoviral delivery of a leukocyte-type 12 lipoxygenase ribozyme inhibits effects of glucose and platelet-derived growth factor in vascular endothelial and smooth muscle cells. Circ Res 2001;88:659–65.
16. Daniel VC, Minton TA, Brown NJ, Nadeau JH, Morrow JD. Simplified assay for the quantification of 2,3-dinor-6-keto-prostaglandin F1 alpha by gas chromatography-mass spectrometry. J Chromatogr B Biomed Appl 1994;653:117–22.
17. Morrow JD, Minton TA. Improved assay for the quantification of 11-dehydrothromboxane B2 by gas chromatography-mass spectrometry. J Chromatogr 1993;612:179–85.
18. Murphy RC, Barkley RM, Zemski Berry K, et al. Electrospray ionization and tandem mass spectrometry of eicosanoids. Anal Biochem 2005;346:1–42.
19. Zhang R, Brennan ML, Shen Z, et al. Myeloperoxidase functions as a major enzymatic catalyst for initiation of lipid peroxidation at sites of inflammation. J Biol Chem 2002;277:46116–22.
20. Lebaron FN, Folch J. The effect of pH and salt concentration on aqueous extraction of brain proteins and lipoproteins. J Neurochem 1959;4:1–8.

21. Bligh EG, Dyer WJ. A rapid method of total lipid extraction and purification. Can J Biochem Physiol 1959;37:911–7.
22. Powell WS. Separation of unlabeled metabolites of arachidonic acid from their deuterium- and tritium-labeled analogs by argentation high-pressure liquid chromatography. Anal Biochem 1983;128:93–103.
23. Metz SA, Hall ME, Harper TW, Murphy RC. Rapid extraction of leukotrienes from biologic fluids and quantitation by high-performance liquid chromatography. J Chromatogr 1982;233:193–201.
24. Vrbanac JJ, Cox JW, Eller TD, Knapp DR. Immunoaffinity purification-chromatographic analysis of arachidonic acid metabolites. In Murphy RC, Fitzpatric FA, eds. Methods in Enzymology, Vol. 187. San Diego: Academic Press; 1990:62–70.
25. Chiabrando C, Benigni A, Piccinelli A, et al. Antibody-mediated extraction/negative-ion chemical ionization mass spectrometric measurement of thromboxane B2 and 2,3-dinorthromboxane B2 in human and rat urine. Anal Biochem 1987;163:255–62.
26. Barrow SE, Ward PS, Sleightholm MA, Ritter JM, Dollery CT. Cigarette smoking: Profiles of thromboxane- and prostacyclin-derived products in human urine. Biochim Biophys Acta 1989;993:121–7.
27. Taylor IK, Ward PS, O'Shaughnessy KM, et al. Thromboxane A2 biosynthesis in acute asthma and after antigen challenge. Am Rev Respir Dis 1991;143:119–25.
28. Moore K, Ward PS, Taylor GW, Williams R. Systemic and renal production of thromboxane A2 and prostacyclin in decompensated liver disease and hepatorenal syndrome. Gastroenterology 1991;100:1069–77.
29. Mitchell MD. A sensitive radioimmunoassay for 6-keto-prostaglandin F1alpha: Preliminary observations on circulating concentrations. Prostaglandins Med 1978;1:13–21.
30. Vermylen J, Defreyn G, Carreras LO, Machin SJ, Van Schaeren J, Verstraete M. Thromboxane synthetase inhibition as antithrombotic strategy. Lancet 1981;1:1073–5.
31. FitzGerald GA, Brash AR, Falardeau P, Oates JA. Estimated rate of prostacyclin secretion into the circulation of normal man. J Clin Invest 1981;68:1272–6.
32. Blair IA, Barrow SE, Waddell KA, Lewis PJ, Dollery CT. Prostacyclin is not a circulating hormone in man. Prostaglandins 1982;23:579–89.
33. Barrow SE, Taylor GW. Gas chromatography and mass spectrometry of eicosanoids. In Benedetto C, McDonald-Gibson RG, Nigam S, Slater TF, eds. Prostaglandins and Related Substances: A Practical Approach. Oxford: IRL Press; 1987:99–142.
34. Powell WS. Reversed-phase high-pressure liquid chromatography of arachidonic acid metabolites formed by cyclooxygenase and lipoxygenases. Anal Biochem 1985;148:59–69.
35. Powell WS. Precolumn extraction and reversed-phase high-pressure liquid chromatography of prostaglandins and leukotrienes. Anal Biochem 1987;164:117–31.
36. Serhan CN. On the relationship between leukotriene and lipoxin production by human neutrophils: Evidence for differential metabolism of 15-HETE and 5-HETE. Biochim Biophys Acta 1989;1004:158–68.
37. Muller M, Sorrell TC. Quantitation of sulfidopeptide leukotrienes by reversed-phase high-performance liquid chromatography. J Chromatogr 1985;343:213–8.
38. Huber M, Kastner S, Scholmerich J, Gerok W, Keppler D. Analysis of cysteinyl leukotrienes in human urine: Enhanced excretion in patients with liver cirrhosis and hepatorenal syndrome. Eur J Clin Invest 1989;19:53–60.
39. Taylor GW, Taylor I, Black P, et al. Urinary leukotriene E4 after antigen challenge and in acute asthma and allergic rhinitis. Lancet 1989;1:584–8.
40. Manning PJ, Rokach J, Malo JL, et al. Urinary leukotriene E4 levels during early and late asthmatic responses. J Allergy Clin Immunol 1990;86:211–20.
41. Ackman RG. Straight chain fatty acids. In Mangold HK, ed. CRC Handbook of Chromatography: Lipids. Vol. 1. Boca Raton, FL: CRC Press; 1984:95–240.
42. Body DR. Branch chain fatty acids. In Mangold HK, ed. CRC Handbook of Chromatography: Lipids. Vol. 1. Boca Raton, FL: CRC Press; 1984:241–75.

Chapter 2
Lipidomic Analysis of Phospholipids and Related Structures by Liquid Chromatography-Mass Spectrometry

Trevor R. Pettitt

Abstract Lipids are highly dynamic molecules with many different roles ranging from structural to signaling. Alterations in particular lipid levels change cellular behavior. In humans, inappropriate changes may manifest as diseases such as Alzheimer's, atherosclerosis, diabetes, obesity, and even cancer. This has led to a great interest in monitoring lipid changes both during normal cellular processes and in disease situations. With the advent of rapid mass spectrometry, it has become possible to analyze many lipids within a single sample with unsurpassed sensitivity and detail. Coupling this with liquid chromatography potentially enables the complete profiling of all the phospholipids, both major and minor, from a single sample within a single analysis run.

Keywords Lipids · phospholipids · lipidomics · HPLC · LCMS · mass spectrometry · phosphoinositides · normal phase

Abbreviations DRG: diradylglycerol; FFA: free fatty acid; lysoPtdOH: lysophosphatidic acid; lysoPtdCho: lysophosphatidylcholine; MRG: monoradylglycerol; PtdOH: phosphatidic acid; PtdCho: phosphatidylcholine; PtdEth: phosphatidylethanolamine; PEtOH: phosphatidylethanol; PtdGly: phosphatidylglycerol; PtdIns: phosphatidylinositol; PtdIns4*P*: phosphatidylinositol 4-phosphate: PtdIns3*P*: phosphatidylinositol 3-phosphate; PtdIns5*P*: phosphatidylinositol 5-phosphate; PtdIns(4,5)P_2: phosphatidylinositol 4,5-bisphosphate; PtdIns(3,4)P_2: phosphatidylinositol 3,4-bisphosphate; PtdIns(3,5)P_2: phosphatidylinositol 3,5-bisphosphate; PtdIns(3,4,5)P_3: phosphatidylinositol 3,4,5-trisphosphate; PtdSer: phosphatidylserine; SM: sphingomyelin; S1P: sphingosine-1-phosphate.

T.R. Pettitt
Institute for Cancer Studies, Birmingham University Medical School, Birmingham, UK
e-mail: t.r.pettitt@bham.ac.uk

B. Larijani et al. (eds.), *Lipid Signaling Protocols*, DOI: 10.1007/978-1-60327-115-8_2,

2.1 Introduction

The traditional view of lipids as primarily structural units is gradually changing. As more is learned, it is becoming apparent that they are highly dynamic, tightly controlled molecules involved in many different cell processes ranging from maintaining membrane integrity to serving as intracellular messengers. Faults in lipid regulation have long been known to be factors in diseases such as atherosclerosis, diabetes, and obesity. However, it is now becoming clear that many other diseases also have a lipid component, including cancer, where PTEN, a phosphoinositide 3-phosphatase, is the second-most deleted/inactivated gene in human tumors [1]. This indicates a crucial role for its substrate, PtdIns(3,4,5)P_3, and/or product, PtdIns(4,5)P_2, in cancer progression. With increasing recognition of the many roles played by lipids, the ability to perform both global and targeted analysis of the constituent lipids in whole cells and within specific intracellular compartments is becoming very important. The development of highly sensitive and discriminating lipid analysis techniques utilizing the latest developments in high-performance liquid chromatography (HPLC) and mass spectrometry (MS) go a long way toward fulfilling these needs. This is increasingly being termed *lipidomics* since it parallels many of the approaches used for proteomics. Infusion-based tandem mass spectrometry using triple quadrupole and hybrid quadrupole–ion-trap mass spectrometers enables the direct analysis of lipid samples [2–4]. However, the bulk, co-infused lipids can cause substantial ion suppression, particularly of minor components. Coupling HPLC to MS (LCMS) significantly reduces complexity and ion suppression at any time point, while enabling isobaric and isomeric discrimination, such as for PtdIns(4,5)P_2, PtdIns(3,4)P_2, and PtdIns(3,5)P_2 [5], structures that cannot be resolved by infusion analyses alone. This makes LCMS particularly suited to the study of signaling and other minor lipids where separation from quantitatively major lipid components, such as PtdCho and PtdEth, greatly improves detection sensitivity.

While various LCMS protocols are present in the literature (e.g., [6–9]), we have achieved good results for a wide range of lipids using the separation conditions described here. Most of the analyses can be achieved using a binary LC system with detection provided by a single quadrupole MS. Since this is now a rather basic form of MS, more capable triple quadrupole and ion-trap instruments can build on these starting points.

2.2 Materials

2.2.1 Equipment and Chemicals

1. Glass syringes (25, 100, 250, and 1000 µl from Hamilton, SGE, etc.).
2. 12-ml screw-capped (with PTFE liners) glass tubes.
3. 1.8-ml screw-capped, silanized glass autosampler vials.

4. 100-µl silanized glass limited-volume vial inserts (e.g., from Alltech Associates).
5. Lipid standards (e.g., from Avanti Polar Lipids, Echelon Biosciences) (*see* Note 1) at 10 µg/ml in chloroform/methanol (2:1 v/v) or in chloroform/methanol/water (25:25:1 v/v/v) for very polar lipids such as PtdInsP_2 and PtdInsP_3 in silanized glass vials. Most lipids are stable at –20°C for months to years (stability decreases with increasing double bonds and/or phosphate groups; light slowly induces photooxidation of double bonds).
6. Solvents (acetonitrile, butan-1-ol, chloroform, dichloromethane, hexane, methanol, water) should be MS or high purity grade.
7. Chemicals (ammonium formate, butylated hydroxytoluene, citric acid, ethylamine, KH_2PO_4, potassium EDTA, tetrabutylammonium hydrogen sulfate) should be analytical grade or better.

2.2.2 HPLC

A modern ternary or quaternary, capillary, biocompatible HPLC system with temperature control and nanoliter autosampler injection capabilities is an ideal front end for LCMS lipid analyses. However, many standard binary analytical HPLC systems can be optimized to provide an effective alternative by removing all unnecessary dead volume so as to minimize solvent delay and peak spreading. Most analytical HPLC systems are designed for columns with 4.6-mm internal diameters (i.d.) using 1-ml/min flow rates and 5–20-µl injection volumes. This is too high for effective electrospray ionization (ESI) MS, where a flow rate of 100–200 µl/min is usually optimal for standard ESI probes. While post-column flow splitting can give 100 µl/min, most of the sample would be directed to waste, hence making it more sensible to optimize the HPLC to work efficiently with smaller bore columns and thus correspondingly lower flow rates. This has the advantage of using less of the potentially harmful and costly solvent. It also means that for a given mass of injected sample, peaks elute in a smaller solvent volume, thus increasing the chromatographic peak height and hence improving the sensitivity.

2.2.2.1 HPLC Optimization

1. Ensure all high-pressure tubing is narrow bore (0.127-mm i.d. or smaller).
2. For biocompatibility, use PEEK, titanium, or fused silica tubing (*see* Note 2).
3. Make high-pressure tubing lengths as short as possible.
4. Ensure all tubing is cut cleanly (or buy precut lengths).
5. Use finger-tight one-piece PEEK fittings for ease of assembly/disassembly.
6. Remove all unnecessary tubing connections.
7. Remove all surplus components (additional check valves, splitters, etc.).
8. Use a low-volume gradient mixer (~50 µl) to minimize gradient delays.
9. Use a low-volume sample injection loop (1–2 µl).

10. Fit bubble traps in each solvent line before the pumps (*see* Note 3).
11. Fit a silica pre-saturator cartridge between the mixer and injector (*see* Note 4).

One-millimeter-inner diameter columns, utilizing a 100-µl/min flow rate and 0.5-µl injection volumes, are generally the smallest that can be used with a standard analytical system following optimization. If the columns are smaller than this, the accuracy and reproducibility of the flow rate, gradient formation, and injection volume will rapidly decline.

2.2.2.2 HPLC Column

Silica (3 µm, 1.0-mm i.d. × 150 mm).

Various column chemistries (e.g., silica, diol, amino, cyano, C18) have been used for lipid analysis, but for lipid class separation, unmodified silica remains the most universally applicable. High-grade, uniformly spherical silicas with low pore size, high surface area, and very low metal content (e.g., Kromasil, Luna silica from Phenomenex) generally give good separation with minimal peak tailing. A 3-µm particle size usually gives better results than 5 µm, although backpressure may be higher, limiting the column length to 150 mm. Currently, 3-µm, 1.0-mm-i.d. × 150-mm columns are optimal since they can be packed to almost as high an efficiency (>80,000 plates/m) as the traditional 4.6-mm analytical columns yet use substantially lower flow rates. At capillary sizes (<1-mm i.d.), packing becomes technically more difficult, often resulting in lower efficiencies. Choose columns with the highest plate count available since this generally indicates the greatest lipid-resolving capability.

Ideally, column walls and the frits at each end should be made from a biocompatible material such as PEEK or titanium (some lipids such as the metal chelating polyphosphoinositides bind to stainless steel, leading to losses). However, the replacement of stainless steel is often not feasible and fortunately is not necessary for most lipids. Binding to new, highly polished stainless steel surfaces is probably minimal although this is likely to increase with aging (*see* Note 5).

2.2.2.3 HPLC Solvents

Warning: Most organic solvents are hazardous, many being flammable and toxic, so efficient vapor extraction is essential. Wear disposable gloves when handling solvents. All dispensing should be performed into glass, in a fume hood, using glass pipettes and/or syringes.

To minimize background noise and contamination on the MS, use fresh solvent batches (manufacturers print an expiration date on their bottle labels) and store the mixtures in brown bottles (with PTFE lids) to reduce photooxidation. Note that many solvents, such as chloroform, contain stabilizers (e.g., amylene, ethanol, methanol) that can subtly alter their chromatographic characteristics. Since different manufacturers may use different stabilizers or different

amounts of stabilizer, chromatographic separations, particularly of low-polarity lipids, may alter depending on the solvent source.

Ethylamine (a volatile alkali) slows the acidic lipids (e.g., PtdOH, PtdGly, PtdIns, PtdSer) by ensuring their deprotonation and, in effect, making them more polar. It also improves peak shape and aids in phospholipid ionization (but not for neutral lipids; *see* Note 11).

1. Solvent A: chloroform/dichloromethane/methanol/water (45:45:9.5:0.5) containing 15 mM ethylamine.
2. Solvent B: acetonitrile/chloroform/methanol/water (30:30:32:8) containing 15 mM ethylamine.
3. Solvent C: chloroform/hexane/propan-2-ol (80:20:1).
4. Solvent D: chloroform/methanol/water (49:49:2).
5. Solvent E: 20 mM ammonium formate in methanol.

2.2.3 Mass Spectrometer

Provided that good HPLC resolution of the lipid classes is achieved, MS detection of pseudomolecular ions for each lipid class will be sufficient for most analyses (see Table 2.1 for possible ions). This can be achieved by electrospray ionization (ESI) on a single quadrupole MS (*see* Note 6). However, this type of instrument cannot provide unambiguous identification of the exact fatty acid composition, only the total number of carbons and double bonds, e.g., C38:4 for a 18:0/20:4 or a 18:2/20:2 structure (an experienced lipid analyst will

Table 2.1 Major lipid ions

Lipid	Detected As
PtdOH	$[M\text{-}H]^-$
PEtOH	$[M\text{-}H]^-$
PtdCho	$[M+H]^+$, $[M+Na]^+$, $[M\text{-}CH_3]^-$
PtdEth	$[M\text{-}H]^-$, $[M+H]^+$
PtdGly	$[M\text{-}H]^-$
PtdIns	$[M\text{-}H]^-$
PtdIns*P*	$[M\text{-}H]^-$, $[M\text{-}H]^{2-}$, $[M\text{-}2\,H+Na]^-$
PtdInsP_2	$[M\text{-}H]^-$, $[M\text{-}H]^{2-}$, $[M\text{-}2\,H+Na]^-$
PtdSer	$[M\text{-}H]^-$
SM	$[M+H]^+$, $[M+Na]^+$, $[M\text{-}CH_3]^-$
LysoPtdOH	$[M\text{-}H]^-$
LysoPtdCho	$[M+H]^+$, $[M+Na]^+$, $[M\text{-}CH_3]^-$
S1P	$[M\text{-}H]^-$
FFA	$[M\text{-}H]^-$
DRG	$[M+Na]^+$, $[M\text{-}OH]^+$
MRG	$[M+Na]^+$, $[M\text{-}OH]^+$
Ceramide	$[M+Na]^+$, $[M\text{-}OH]^+$

often be able to predict the most prevalent structure). Getting exact fatty acid compositions requires fragmentation on a triple quadrupole or ion-trap MS. If HPLC separation cannot resolve different lipid classes with identical molecular ions, then triple quad or ion-trap MS can usually identify the class on the basis of a characteristic fragmentation (e.g., m/z 184 for phosphocholine-containing lipids such as PtdCho or SM; see Table 2.3 for more possibilities). Similarly, the resolution of structural isomers such as PtdIns3*P* and PtdIns4*P* requires the controlled fragmentation capabilities of an ion trap [5]. Attomole LCMS detection limits (signal-to-noise ratio > 5) can be achieved for some lipid structures on certain instruments, but femtomole limits are more usual.

2.3 Methods

2.3.1 Lipid Extraction

To achieve a lipidomic analysis that gives an accurate representation of the lipid content within a sample, care is needed to obtain a quantitative lipid extraction from the starting biological matrix. The widely used Folch extraction procedure [10] described here is a good starting point for the general extraction of lipids from samples containing relatively little water (e.g., cell pellets). This gives 95% or greater recoveries for most lipids when performed closely following the original methodology (*see* Note 7), but lysoPtdOH, S1P, PtdIns(4,5)P_2, PtdIns(3,4,5)P_3, and other very polar lipids still show poor recoveries. Improved recovery of these structures is achieved using an acidified protocol as given in Subheading 2.3.2 (*see* Note 8). Lipid extractions are best performed in glass (although *see* Note 9**)**. All sample transfers should be performed using glass Pasteur pipettes or syringes.

Lipid extracted from 10^6 cells normally provides plenty of material for analysis, although the investigation of very minor structures may require more starting material.

2.3.1.1 Folch Extraction

1. 0.2-ml sample (assume 0.2 g of material contains 0.2 ml of water; add more water if necessary) in a glass screw-capped tube.
2. Add 2 ml ice-cold methanol (this kills cells and denatures protein).
3. Add internal standards if required (*see* Note 1).
4. Vortex mix and stand on ice for 10 min.
5. Add 4 ml of ice-cold chloroform.
6. Vortex and then sonicate in ultrasonic bath for 5 min (keep cool with ice).
7. Stand for 10 min.
8. Add 1.25 ml of 0.88% KCl to split phases.
9. Mix vigorously, and then stand on ice for 10 min.

10. Complete phase split by centrifugation (5 min at 200 × *g*; a higher speed may cause glass tubes to shatter). Alternatively, stand overnight in a cold room.
11. Carefully remove the upper aqueous phase, together with interfacial material, using a glass Pasteur pipette (*see* Note 10).
12. Transfer the lower phase into a clean glass tube.
13. Dry under a stream of nitrogen or on a vacuum dryer (e.g., Maxi-Dry Plus).
14. Resuspend in 50 µl of chloroform/methanol/water (90:9.5:0.5) containing 25 µg/ml of butylated hydroxytoluene (BHT) as antioxidant.
15. Cap tightly and store at –20°C (generally, it is best to analyze as soon as possible to minimize the possibility of sample degradation).

2.3.1.2 Lysolipid/Phosphoinositide Extraction

All glassware in sample contact should be silanized (see Subheading 3.4) to minimize losses (but *see* Note 9).

1. Sample (make to 0.8 ml with water) in a 12-ml silanized glass tube.
2. Add internal standards if required (*see* Note 1).
3. Add 200 µl of 200 mM citric acid/200 mM KH_2PO_4 buffer, pH 3.0, 5 mM tetrabutylammonium hydrogen sulfate.
4. Add 3 ml of water-saturated butan-1-ol (split phases).
5. Vortex vigorously to ensure cell disruption.
6. Sonicate in ice-cooled sonicating bath for 5 min.
7. Stand for 30 min on ice.
8. Complete phase split by centrifugation (200 × *g*, 5 min).
9. Transfer upper, butanol phase into a clean tube using a silanized pipette.
10. Re-extract lower, aqueous phase with a further 3 ml of water-saturated butan-1-ol.
11. Wash combined butanol phases with 1.2 ml of 200 mM potassium EDTA, pH 6.0.
12. Remove and discard lower EDTA phase using a silanized pipette.
13. Add 2.5 ml of methanol to aqueous phase from step 10.
14. Vortex vigorously, and then stand for 10 min on ice.
15. Add 1.25 ml of ice-cold chloroform.
16. Sonicate in ice-cooled sonicating bath for 5 min.
17. Add 1.25 ml of ice-cold chloroform.
18. Add 1.25 ml of 200 mM citric acid/200 mM KH_2PO_4 buffer, pH 3.0.
19. Vortex vigorously, and then stand on ice for 10 min.
20. Complete phase split by centrifugation (200 × *g*, 5 min).
21. Discard upper phase and interfacial material.
22. Wash lower phase with 0.75 ml of 200 mM potassium EDTA, pH 6.0/methanol (1:1).
23. Combine resultant lower phase with the washed butanol phase.
24. Dry on vortex evaporator (e.g., RapidVap from Labconco) (it's possible to dry under a stream of N_2, but that method is much slower).

25. Carefully rinse tube walls with 500 µl of chloroform/methanol/water (5:5:1).
26. Dry again on vortex evaporator.
27. Resuspend in 30 µl of chloroform/methanol/water (25:25:1) containing 25 µg/ml of BHT.
28. Transfer into autosampler vial silanized limited-volume insert.
29. Rinse tube with an additional 30 µl of chloroform/methanol/water (25:25:1) containing 25 µg/ml of BHT. Combine in vial insert.

2.3.2 Lipid Separation

The silica column separates primarily on the basis of polarity, with less polar lipids eluting ahead of more polar structures (Fig. 2.1). Silica allows a partial resolution of individual molecular species within a lipid class, with structures containing longer acyl chains and/or more double bonds eluting slightly ahead of those containing shorter chains and/or fewer double bonds (Fig. 2.2). Similarly, structures containing ether-linked alkyl or alkenyl chains elute slightly ahead of those with the corresponding ester-linked fatty acyl chains.

Always run a set of appropriate lipid standards to check correct chromatographic and MS conditions before running samples. The first one or two runs after a shutdown period often have abnormal retention times.

2.3.2.1 General Phospholipid Separation (Fig. 2.1)

Gradient: 100% solvent A changing to 20% solvent B over 1 min, to 35% solvent B over 9.5 min, to 70% solvent B over 9.5 min, then recycle back to 100% A over 1 min and held for a further 14 min to re-equilibrate (total program time: 35 min).

Flow: 100 µl/min for 20 min, then to 130 µl/min over 5 min, held for 9 min, then back to 100 µl/min over 1 min.

Injection: 1 µl (*see* Note 12).

2.3.2.2 Phosphoinositide Separation (Fig. 2.3)

Gradient: 100% solvent A held for 2 min, then to 45% solvent B over 1 min, then to 50% solvent B over 17 min, then recycle back to solvent A as above.

2.3.2.3 Neutral Lipid Separation (Fig. 2.4)

Gradient: 100% solvent C held for 2 min, then to 100% solvent D over 17 min, held for 2 min, then recycle back to 100% solvent C over 1 min, and held for a further 18 min to re-equilibrate (total program time: 40 min). Flow as above.

Post-column addition of solvent E at 50 µl/min (*see* Note 11).

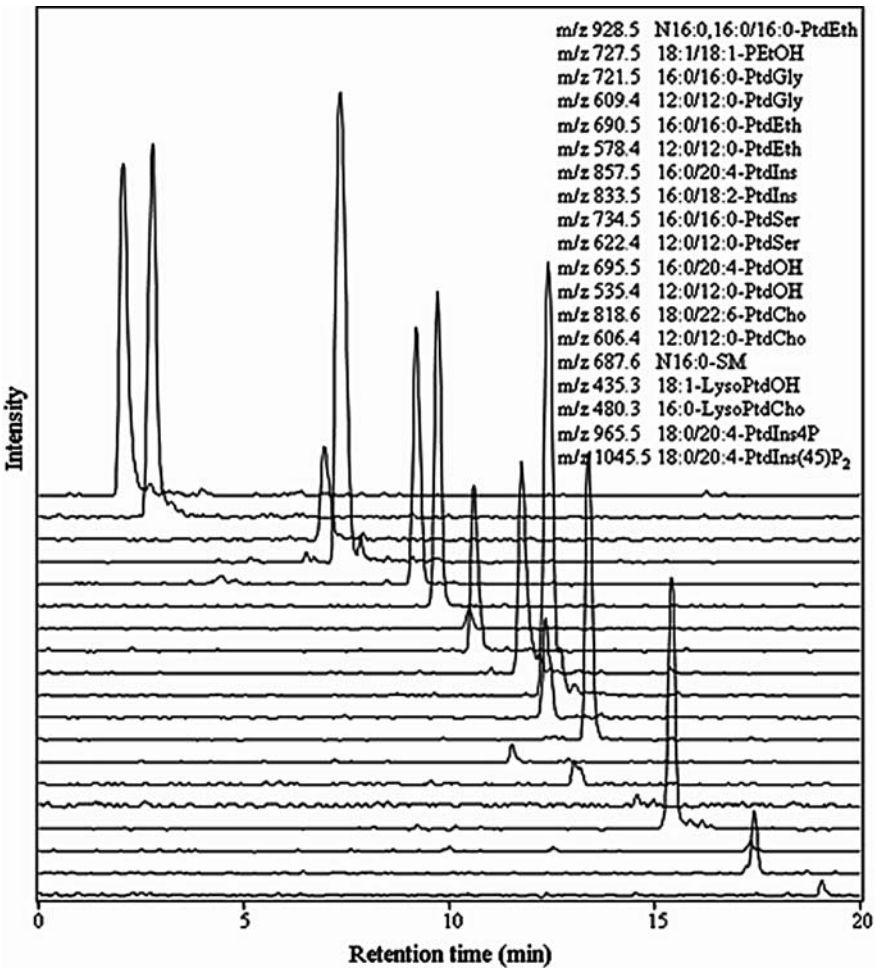

Fig. 2.1 Separation of lipid standards. Detection as $[M\text{-}H]^-$ ions except PtdCho and SM (very small double peak at 14.5–15.0 min), which are detected as $[M\text{-}CH_3]^-$ (these are best detected as $[M + H]^+$). Although not shown, FFA elutes at 4 min and S1P at 17 min. Extracted ion chromatograms (top to bottom) correspond to the listed lipid structures

2.3.3 Mass Spectrometry

The settings for optimal ESI-MS sensitivity vary from instrument to instrument due to design differences in the ionizing interface. Optimum settings for most phospholipids on a Shimadzu QP8000α single quadrupole are a nebulizing (sheath) gas flow of 3.5 l/min, a desolvation temperature of 300°C, and a probe voltage of ±3.5 kV. This produces primarily singly protonated/deprotonated ions, although in positive mode, sodiated adducts, $[M + Na]^+$, may also form at relatively high levels (*see* Note 13). Some lipids, such as the

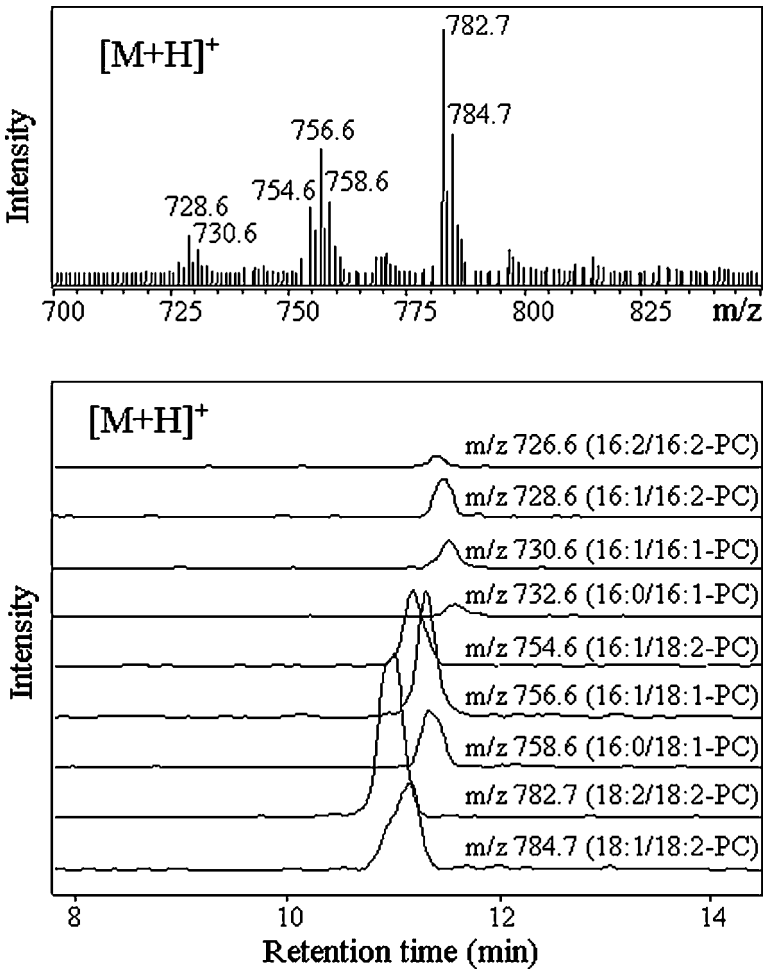

Fig. 2.2 PtdCho molecular species from *Dictyostelium discoideum*. Mass spectra and extracted ion traces showing effect of acyl chain length and double bond number on retention time. Sodium adducts, $[M + Na]^+$, have a mass 22 Da greater than the corresponding $[M + H]^+$

polyphosphoinositides, form doubly deprotonated $[M\text{-}2\,H]^{2-}$ ions. However, these appear relatively unstable at 300°C (where $[M\text{-}H]^-$ predominates) but give a greater signal intensity and become the major ion when analyzed at a lower temperature (150–200°C) [5]. For analysis of DRG and some other neutral lipids, the maximum signal intensity is obtained with a lower probe voltage of 0.75 kV. The maximum sensitivity is achieved by selected ion monitoring for a set of predefined lipid masses. Different masses can be investigated in different time windows to correspond to the elution of different lipid classes.

Settings for polyphosphoinositide analysis with a Bruker Daltonics HCT*plus* Ion Trap are nebulizer gas: 4 l/min N_2; nebulizer pressure: 10 psi; source

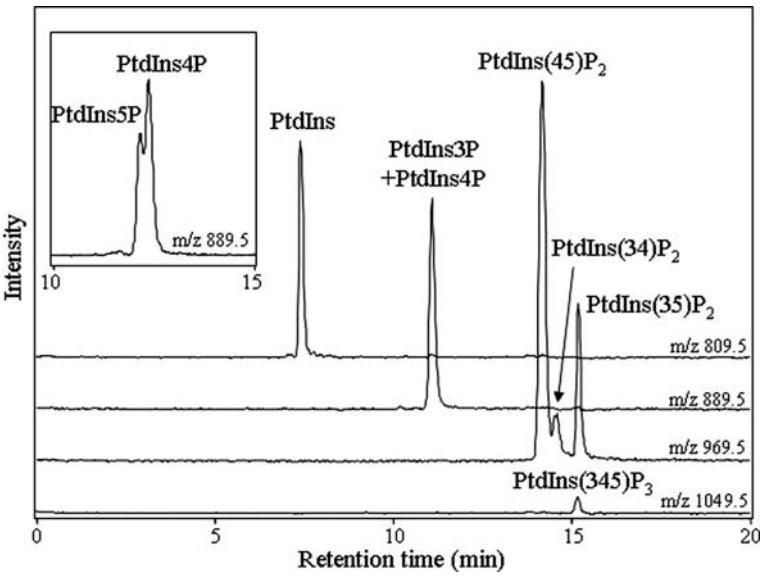

Fig. 2.3 Separation of 16:0/16:0 phosphoinositide standards. Detection as $[M\text{-}H]^-$ ions. $[M\text{-}2\,H]^{2-}$ and sodiated $[M\text{-}2\,H + Na]^-$ detected as minor ions for PtdIns*P*, PtdInsP_2, and PtdInsP_3. Identical molecular species of PtdIns3*P* and PtdIns4*P* coelute, but PtdIns5*P* will partially resolve (inset)

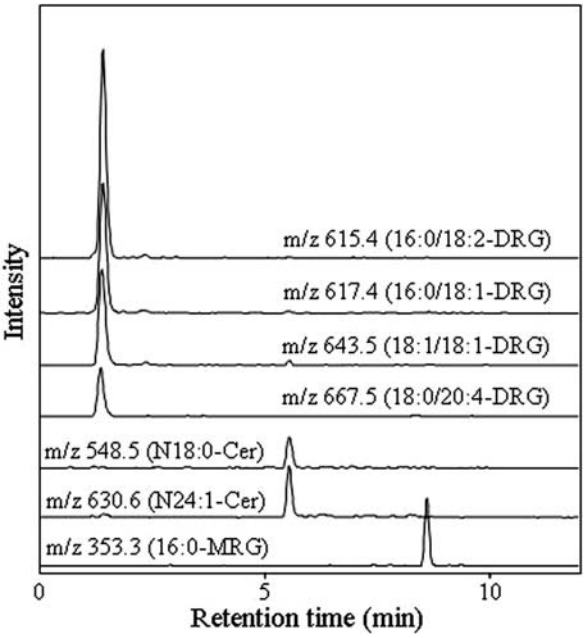

Fig. 2.4 Neutral lipid separation. DRG and MRG detected as $[M + Na]^+$. Ceramide detected as $[M\text{-}OH]^+$ although it also gives a strong $[M + Na]^+$ ion. Very low polarity lipids such as triacylglycerol and sterol esters elute in the solvent front. Phospholipids elute after 10 min but with poor resolution. This part of the gradient is to prevent lipid carryover into subsequent runs

Table 2.2 Monoisotopic ions for diacyl phospholipid species

	PtdOH	PtdCho	PtdEth	PtdGly	PtdIns	PtdSer	PtdIns*P*	PtdInsP_2
Acyl structure	$[M-H]^-$	$[M-H]^+$	$[M-H]^-$	$[M-H]^-$	$[M-H]^-$	$[M-H]^-$	$[M-H]^-$	$[M-H]^-$
14:0/14:0	591.403	678.507	634.445	665.439	753.455	678.435	833.422	913.388
14:0/16:0	619.434	706.539	662.476	693.471	781.487	706.466	861.453	941.419
16:0/16:0	647.465	734.570	690.507	721.502	809.518	734.497	889.484	969.451
16:0/18:2	671.465	758.570	714.507	745.502	833.518	758.497	913.484	993.451
16:0/18:1	673.481	760.586	716.523	747.518	835.534	760.513	915.500	995.466
16:0/18:0	675.496	762.601	718.539	749.533	837.549	762.529	917.516	997.482
16:0/20:4, 18:2/18:2	695.465	782.570	738.507	769.502	857.518	782.497	937.484	1017.451
16:0/20:3, 18:1/18:2	697.481	784.586	740.523	771.518	859.534	784.513	939.500	1019.466
18:0/18:2, 18:1/18:1	699.496	786.601	742.539	773.533	861.549	786.529	941.516	1021.482
18:0/18:1	701.512	788.617	744.554	775.549	863.565	788.544	943.531	1023.498
18:0/18:0	703.528	790.633	746.570	777.565	865.581	790.560	945.547	1025.513
18:0/20:4	723.496	810.601	766.539	797.533	885.549	810.529	965.516	1045.482
18:0/20:3	725.512	812.617	768.554	799.549	887.565	812.544	967.531	1047.498
18:0/20:2	727.528	814.633	770.570	801.565	889.581	814.560	969.547	1049.513
18:0/20:1	729.543	816.648	772.586	803.580	891.596	816.575	971.563	1051.529
18:0/20:0	731.559	818.664	774.601	805.596	893.612	818.591	973.578	1053.545
18:0/22:6	747.496	834.601	790.539	821.533	909.549	834.529	989.516	1069.482
18:0/22:5	749.512	836.617	792.554	823.549	911.565	836.544	991.531	1071.498
18:0/22:4	751.528	838.633	794.570	825.565	913.581	838.560	993.547	1073.513

temperature: 300°C; capillary voltage: −4 kV. Fragmentation of the $[M-2H]^{2-}$ ions provides more phosphoinositide structural information than fragmentation of the $[M-H]^-$ ions [5].

The m/z values for some of the molecular ions derived from mammalian lipids are given in Table 2.2. Diagnostic ions for MS/MS fragmentations are given in Table 2.3.

2.3.3.1 Sample Concentration

The MS signal intensity shows a sigmoidal response to concentration and may even decline at the highest concentrations due to ion suppression effects (Fig. 2.5). For accurate quantification, the sample should be of an appropriate concentration that the response lies on the linear part of the graph. This is best investigated by making serial dilutions (or using smaller injection volumes) and checking that the MS response changes by an appropriate amount. If the response does not lie on the graph's linear part, then the response is being saturated/suppressed, indicating that the sample needs further dilution.

For lipid entering the MS at concentrations above 100 μM (note that with LCMS, the concentration will vary across the run), there are significant effects of acyl chain length and unsaturation on signal intensity [2]. However, at very low concentrations, the signal becomes almost independent of the acyl

Table 2.3 Some diagnostic ions for MS/MS fragmentation

Lipid Class	Precursor Ion	MS/MS	Fragment
Glycerophospholipid	$[M-H]^-$	153.0	Glycerophosphate backbone
Sphingolipids	$[M+H]^+$	264.4	Sphingosine backbone
PtdCho, LysoPtdCho, SM	$[M+H]^+$	184.1	Phosphocholine
PtdEth	$[M-H]^-$	196.0	Glycerophosphoethanolamine
PtdIns	$[M-H]^-$	241.1	Cyclic inositol phosphate
PtdSer	$[M-H]^-$	NL of 87.0	Serine
PtdIns*P*	$[M-H]^-$	321.1	Phosphoinositol phosphate
PtdInsP_2	$[M-H]^-$	401.1	Diphosphoinositol phosphate
PtdInsP_3	$[M-H]^-$	481.1	Triphosphoinositol phosphate
All	$[M-H]^-$	227.2	14:0
All	$[M-H]^-$	255.2	16:0
All	$[M-H]^-$	279.2	18:2
All	$[M-H]^-$	281.2	18:1
All	$[M-H]^-$	283.2	18:0
All	$[M-H]^-$	303.3	20:4
All	$[M-H]^-$	305.3	20:3
All	$[M-H]^-$	307.3	20:2
All	$[M-H]^-$	309.3	20:1
All	$[M-H]^-$	311.3	20:0
All	$[M-H]^-$	327.3	22:6
All	$[M-H]^-$	329.3	22:5
All	$[M-H]^-$	331.3	22:4

NL = neutral loss.

structure. Also, at low concentrations, lipid head-group differences have less effect on signal intensity. As such, it is recommended to use a low sample concentration, under 10 μM (10 pmoles/μl) if possible. For accurate quantification, correction factors may have to be determined and applied to correct for differences between the response (per pmole) for the internal standard and that

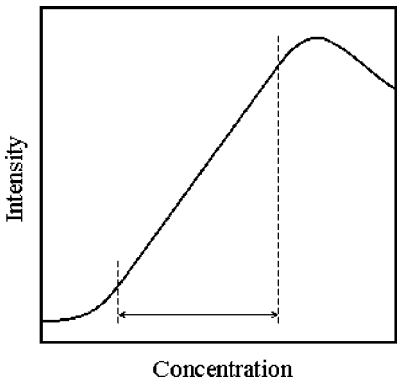

Fig. 2.5 Effect of sample concentration entering the MS on ion signal intensity. To obtain a linear response for quantification, the sample concentrations have to fall between the dashed bars on the linear part of the graph

for the structure(s) being quantified. If possible, always use internal standards of the same lipid class as the class being quantified to minimize response differences.

2.3.3.2 Isotope Correction

When using MS, it is important to be aware that many elements exist naturally as more than one stable isotope (e.g., ^{1}H and ^{2}H; ^{12}C and ^{13}C; ^{16}O, ^{17}O, and ^{18}O). This means that multiple ion masses may be obtained for a single molecular structure. For lipid work, the most important effect of this isotopic distribution is with carbon since 1.1% exists as ^{13}C while the rest is ^{12}C. Thus, every carbon in a structure has a 1.1% probability of being ^{13}C and hence increasing the ion mass by approximately one unit. For example, with 16:0/18:1-PtdOH ($C_{37}H_{71}O_8P$; $[M\text{-}H]^-$; m/z 673.5), there will be a range of masses (M, M + 1, M + 2, M + 3, etc.) containing 0–37 ^{13}C atoms (Fig. 2.6). The presence of deuterium and oxygen isotopes also has a small effect. With this example, 64.5% exists as M, 27.4% as M + 1, 6.7 % as M + 2, 1.2% as M + 3, and 0.2% as M + 4 (*see* Note 14**)**. Abundances of the higher masses are so low that they can be ignored. This means that the $[M\text{-}H]^-$ ion peak at m/z 675.5, which might be expected to be solely 16:0/18:0-PtdOH, may actually contain substantial amounts of the M + 2 isotopic form of 16:0/18:1-PtdOH (assuming the two PtdOH species are not resolved chromatographically). For accurate quantification, this isotopic effect needs to be taken into account, which in this example is done by subtracting the 16:0/18:1 M + 2 contribution from the 16:0/18:0 peak (however, *see* Note 15).

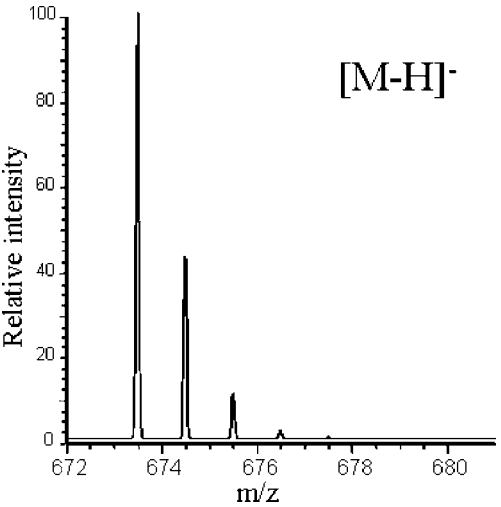

Fig. 2.6 Isotopic $[M\text{-}H]^-$ ion distribution for 16:0/18:1-PtdOH ($C_{37}H_{71}O_8P$; MW = 674.5). Since each of the 37 carbon atoms in 16:0/18:1-PtdOH has a 1.1% probability of being ^{13}C rather than ^{12}C, approximately 40% of the molecules will contain one or more ^{13}C atoms, thus increasing the ion mass correspondingly. The minor 16:0/18:1-PtdOH isotopic ion peak at m/z 675.5 can mask small amounts of 16:0/18:0-PtdOH (also m/z 675.5)

2.3.4 Glassware Silanization

Oven-dry (120°C, 60 min) and then silanize by immersing in 5% dichlorodimethylsilane in toluene (60 min, room temperature) before transfer into 100% methanol for 30 min to deactivate unreacted reagent. Remove and air-dry. Store in a dark, dry atmosphere (silanization is slowly lost).

Acknowledgments The author would like to thank Professor Michael Wakelam for his advice and encouragement. This work was supported by grants from the Wellcome Trust.

Notes

1. 12:0/12:0 structures are useful internal standards since they are not normally found in biological samples at more than trace levels. ^{13}C and deuterated (^{2}H) standards can be used, although the former have limited availability while the latter will undergo hydrogen exchange resulting in deuterium loss and thus generating a range of ion masses (less noticeable with freshly manufactured standards). An ideal internal standard is not present in the endogenous lipid, yet because it has a very similar structure, it behaves almost identically. Use standards of the same class as the lipid being quantified.
2. PEEK (poly ether ether ketone) is probably the most inert surface available for high-pressure tubing and is easy to use. However, it is not fully resistant to halogenated solvents such as chloroform that cause it to soften and eventually burst, which is most likely to occur at tight bends. Fused silica and titanium are generally better than stainless steel, but some binding of phosphoinositides and other polar lipids may still occur.
3. When using volatile solvents, bubbles readily form in the solvent lines, particularly when left standing overnight or longer. Also, some solvent mixtures degas for several hours after preparation. Inline bubble traps (available from Alltech Associates) catch these bubbles before they reach the pumps, minimizing the need for pump-head purging and instrument downtime. Pump-head purging is still required if the flow has been stopped for an extended period (e.g., overnight).
4. Presaturating the solvent stream with silica helps extend the life of the main column. Use a low-volume, cartridge-based guard column as a presaturator to minimize solvent gradient delays.
5. Extended exposure to chlorinated solvents such as chloroform in the presence of methanol and/or water will etch steel surfaces through the slow generation of HCl, thus increasing potential lipid binding sites. Repassivation of the stainless steel with nitric acid can deactivate the surfaces again.
6. For MS detection, a molecule has to become charged in the gas phase. There are several ways to achieve this, but the most widely applicable to lipidomic analysis utilize atmospheric pressure ionization techniques, in particular the relatively mild electrospray ionization (ESI). This causes little fragmentation, so the major structure detected is normally the molecular ion although its exact form depends on both the structure of the molecule and the conditions employed. Atmospheric pressure chemical ionization (APCI) and atmospheric pressure photoionization (APPI) may give better ionization for some lipids, particularly the more difficult-to-ionize neutral lipids such as triacylglycerol and sterols. Probes for these techniques are normally a straight replacement for the standard ESI probe.
7. Both the Folch [10] and Bligh and Dyer [11] lipid extraction methods fail to give quantitative extraction if performed inappropriately. However, the latter is more

sensitive, with small changes often leading to substantially poorer recoveries. For this reason, the Folch procedure is generally recommended unless the sample contains a larger amount of water (>0.5 ml), in which case the Bligh and Dyer procedure may be more appropriate, as it does not require so much organic solvent. A final chloroform/methanol/water ratio of 8:4:3 is required for efficient lipid extraction using the Folch method. Where the maximum sensitivity is critical, extraction recoveries should be checked.

8. Most published phosphoinositide extraction protocols use strongly acidic chloroform/methanol/HCl solutions. We found, however, that the acid causes extensive degradation, particularly of PtdInsP_2 and PtdInsP_3 [5]. It will also hydrolyze all plasmalogens (alkenyl structures). A milder citric acid/KH_2PO_4 acidification coupled with sequential butan-1-ol and chloroform/methanol extractions, followed by a neutralizing EDTA wash, gives >90% recoveries while largely eliminating acid degradation.
9. Most extractions should be performed in glass since lipids such as DRG will penetrate plastic, resulting in nonquantitative recovery. Organic solvents soften plastics and leach plasticizers, leading to greater contaminating noise on the MS. The only time when plastics may be appropriate is when working with highly polar lipids such as lysoPtdOH, S1P, sphingosylphosphorylcholine, PtdInsP_2, and PtdInsP_3 provided that the sample is not left in these vessels for more than a few hours. Polypropylene tubes (e.g., from Sarstedt) give better recovery for these lipids than ordinary glass although this must be set against the loss of low-polarity lipids. Silanized glass tubes give the best recovery, but the silyl groups are slowly lost in the presence of water—this loss is greatly enhanced if combined with acid and elevated temperatures.
10. For improved recovery of polar lipids that may partially partition into the upper aqueous phase, this phase can be re-extracted with 4.5 ml of synthetic lower phase. If necessary (particularly with larger extractions), the lower, organic phase containing the lipids can be washed with 3 ml of the synthetic upper phase to maximize the removal of salts, proteins, and other polar contaminants although this may result in increased losses for very polar lipids such as PtdInsP_2.
11. Neutral lipids (e.g., DRG, MRG, ceramide) show little or no ionization without the post-column addition of ammonium formate. Ethylamine suppresses the signal and thus has to be omitted. If a ternary HPLC system is available, it is possible to combine the neutral lipid and phospholipid separations within a single run by the use of an appropriate intermediary solvent mix miscible with both hexane-rich and methanol/water-rich solvents.
12. If rapidly eluting lipids ($\leq$5 min retention time) are of particular interest, then ensure that the injection solvent is identical to the gradient starting solvent (for sample stability, ethylamine is best omitted if not analyzed immediately) and use a smaller injection volume ($\leq$0.5 µl) to give sharper peaks since very small solvent polarity differences may adversely affect the chromatography. Later peaks are unaffected.
13. Sodium is always present (it is abstracted from the solvent, column, fittings, etc.), but the levels of $[M + Na]^+$ formed can vary substantially depending on factors such as the sample preparation technique, solvents used, sodium content of the silica, and previous samples run.
14. Most MS software now comes with algorithms to calculate isotopic distribution. Alternatively, several freeware/shareware programs are available on the Web, such as IsoPro 3.0.
15. Fourier transformation (FT), time-of-flight (ToF), and similar MS instruments, with their much greater mass accuracy, will often be able to discriminate between potentially overlapping isotopic structures: For example, the M + 2 isotopic form of 16:0/18:1-PtdOH has an exact mass of 676.4951, whereas monoisotopic 16:0/18:0-PtdOH has a mass of 676.5043, a difference of 0.0092. This difference cannot be detected by standard quadrupole and ion-trap instruments.

References

1. Leslie NR, Downes CP. PTEN function: How normal cells control it and tumour cells lose it. Biochem J, 2004;382:1–11.
2. Han X, Gross RW. Shotgun lipidomics: Electrospray ionization mass spectrometric analysis and quantitation of cellular lipidomes directly from crude extracts of biological samples. Mass Spectrom Rev 2005;24:367–412.
3. Pulfer M, Murphy RC. Electrospray mass spectrometry of phospholipids. Mass Spectrom Rev 2003;22:332–64.
4. Taguchi R, Houjou T, Nakanishi H, Yamazaki T, Ishida M, Imagawa M, Shimizu T. Focused lipidomics by tandem mass spectrometry. J Chromatogr B 2005;823:26–36.
5. Pettitt TR, Dove SK, Lubben A, Calaminus SDJ, Wakelam MJO. The analysis of intact phosphoinositides in biological samples. J Lipid Res 2006;47:1588–1596.
6. Merrill AH, Sullards MC, Allegood JC, Kelly S, Wang E. Sphingolipidomics: High-throughput, structure-specific and quantitative analysis of sphingolipids by liquid chromatography tandem mass spectrometry. Methods 2005;36:207–24.
7. Hermansson M, Uphoff A, Kakela R, Somerharju P. Automated quantitative analysis of complex lipidomes by liquid chromatography/mass spectrometry. Anal Chem 2005; 77:2166–75.
8. Sommer U, Herscovitz H, Welty FK, Costello CE. LC-MS-based method for the qualitative and quantitative analysis of complex lipid mixtures. J Lipid Res 2006;47:804–14.
9. Kuksis A, Itabashi Y. Regio- and stereospecific analysis of glycerolipids. Methods 2005;36:172–85.
10. Folch J, Lees M, Stanley GHS. A simple method for the isolation and purification of total lipides from animal tissues. J Biol Chem 1957;226:497–509.
11. Bligh EG, Dyer WJ. A rapid method of total lipid extraction and purification. Can J Biochem Physiol 1959;37: 911–7.

Chapter 3
Measurement of Polyphosphoinositides in Cultured Mammalian Cells

Frank T. Cooke

Abstract The seven phosphorylated derivatives of phosphatidylinositol (PtdIns), often collectively referred to as polyphosphoinositides (PPIn), are a minor component of eukaryotic cell membranes. Nevertheless, their synthesis is needed for an ever-increasing spectrum of cellular processes, including regulation of the actin cytoskeleton, chemotaxis, membrane trafficking, glucose uptake, and organelle acidification. PPIn metabolism is regulated dynamically by a network of kinases and phosphatases. Furthermore, synthesis of PPIn can be provoked by external stimuli; for example, the second messenger phosphatidylinositol 3,4,5-trisphosphate rapidly and transiently accumulates in cells challenged with agonists such as PDGF that activate receptor tyrosine kinases. The measurement of PPIn levels in *in vivo* cultured cells has been vital to our understanding of the metabolism and function of these important signaling molecules; methods are described herein that allow measurement of PPIn levels in culture cells *in vivo*.

Keywords Polyphosphoinositide · HPLC · isotopic labeling

Abbreviations BSA: bovine serum albumin; cpm: counts per minute; dpm: disintegrations per minute; FAF: fatty acid-free; Gro*P*: glycerophospho; HEPES: N-2-hydroxyethylpiperazine-N'-2-ethanesulfonic acid; HBBSS: buffered balanced salts solution; HPLC: high-performance liquid chromatography; Ins: inositol; Ptd: phosphatidyl; PPIn: polyphosphoinositide; P_i: inorganic PO_4: TBAS: tetrabutyl ammonium hydrogen sulfate.

3.1 Introduction

The complex metabolism of the polyphosphoinositides (PPIn) is shown in Fig. 3.1. Metabolism of PPIn is dynamically regulated, and the various PPIn carry out a wide spectrum of cellular functions [1]. Thus, a reliable method for assaying

F.T. Cooke
Department of Structural and Molecular Biology, University College London, Darwin Building, Gower Street, London WC1E 6BT, UK
e-mail: f.cooke@ucl.ac.uk

B. Larijani et al. (eds.), *Lipid Signaling Protocols*, DOI: 10.1007/978-1-60327-115-8_3,

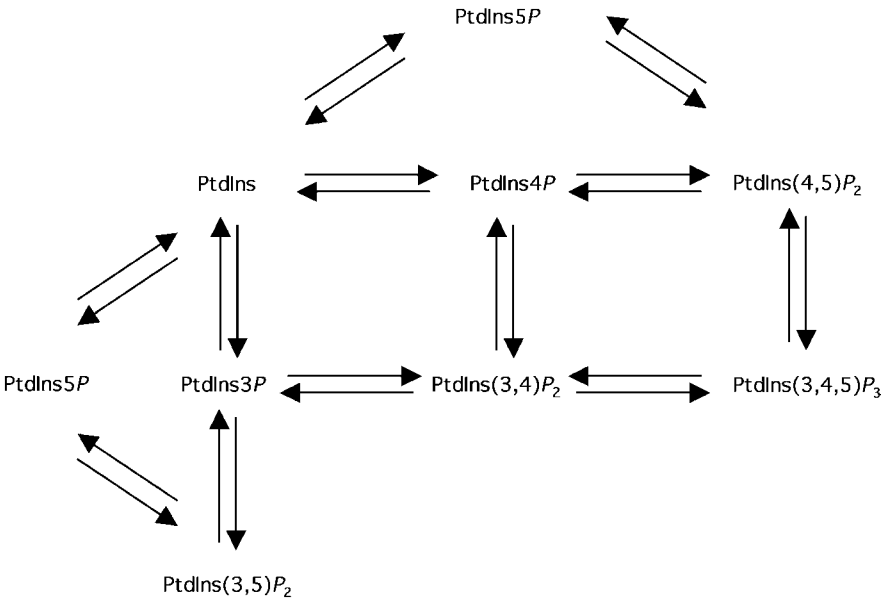

Fig. 3.1 The complex metabolism of the PPIn. Interconversion between the various PPIn is very rapid, so only a brief period of labeling with [^{32}P]-P_i is necessary to reach equilibrium. Inositol incorporates more slowly into PtdIns, but will label all PPIn to the same extent

PPIn levels is a vital tool in studying their metabolism. Although a number of non-isotopic labeling-based methods have been published, such as mass assays for phosphatidylinositol 5-phosphate (PtdIns5*P*) and phosphatidylinositol 3,4,5-trisphosphate [PtdIns(3,4,5)P_3] [2, 3], performing isotopic labeling and subsequent HPLC analysis is still the method of choice for measuring levels of PPIn *in vivo*. While it is likely that advances in other methodologies, such as mass spectrometry, may eventually prevail [4], using the methods described below, PPIn can reproducibly be measured, in a wide variety of cell types.

First, PPIn are isotopically labeled, which can be achieved with either [^{3}H]-inositol or [^{32}P] inorganic PO_4 ([^{32}P]-P_i)—or, indeed, [^{33}P]-P_i (*see* Note 1 and Fig. 3.2). [^{3}H]-inositol incorporates more specifically into inositol-containing lipids, making subsequent analysis easier to interpret; furthermore, PtdIns will be labeled to the same extent as the other PPIn, which can be useful in final data analysis (Fig. 3.2). Additionally, [^{3}H] produces negligible ionizing radiation. However, [^{3}H]-inositol is expensive; incorporating sufficient label into PPIn can be challenging and is dependent on cell type. [^{32}P]-P_i is cheaper and incorporates well in all mammalian cell types. However, as [^{32}P]-P_i incorporates to some extent into the entire cellular phospholipid complement, chromatographic analysis can be harder to interpret. Incorporation of [^{32}P]-P_i into PtdIns is poor. Furthermore, there is the additional problem of hazardous ionizing radiation. Although both [^{3}H]-inositol and [^{32}P]-P_i labeling have been

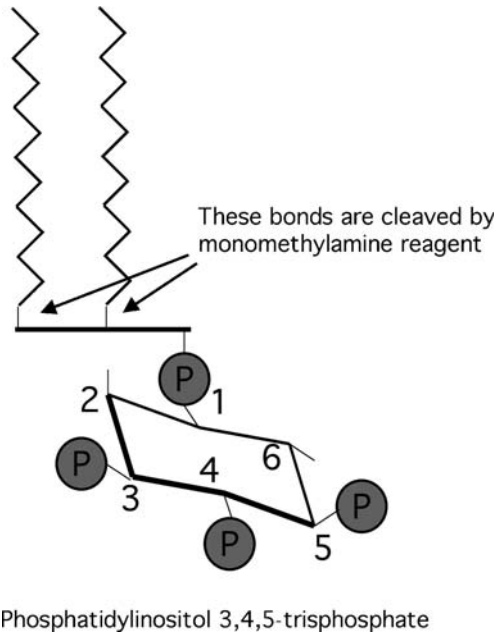

Fig. 3.2 Schematic diagram of PtdIns(3,4,5)P_2. The phosphates in the 3, 4, and 5 positions will label rapidly, whereas the 1 position labels more slowly. [^{32}P]-P_i-labeling will result in varying specific activity between the PPIn: PtdIns will be poorly labeled, whereas PtdIns(3,4,5)P_3 will have approximately three times the label incorporated as PtdInsP_n. The site of cleavage of the monomethylamine reagent is also shown

successfully employed to measure PPIn [5, 6], and methods are presented for both, [^{32}P]-P_i labeling is the preferred method of this author.

Once the cells have been labeled and stimulated/manipulated, they are killed and the lipids recovered using a two-phase organic solvent extraction. Maintaining quantitative recovery in this stage is paramount to the success of the experiment. Due to their charge at neutral pH, PtdInsP_2 isomers and PtdIns(3,4,5)P_3 are quite water-soluble and thus prone to remaining in the upper aqueous phase. Thus, three strategies are employed to encourage them into the organic phase and maximize their recovery [7]: First, the extraction procedure described by Folch et al. is employed [8]. This uses a ratio of 8:4:3 (v/v/v) $CHCl_3$:MeOH:aqueous and was designed specifically for extraction of acidic phospholipids. Many researchers mistakenly use the extraction procedure described by Bligh and Dyer [9], which uses a ratio of 1:1:0.9 (v/v/v) $CHCl_3$:MeOH:aqueous. This ratio gives a poor recovery of PtdInsP_2 isomers and PtdIns(3,4,5)P_3 and should not be used. Second, the aqueous phase is acidified to 1 M HCl, promoting protonation of acidic phospholipids, thus reducing their charge. Third, tetrabutyl ammonium hydrogen sulfate (TBAS) is added to the extraction; TBAS is a quaternary lipophilic ammonium salt and aids neutralization of acidic compounds in the organic phase. In the author's experience, PtdInsP_2 isomers and PtdIns(3,4,5)P_3 cannot be extracted efficiently without the addition of TBAS. Additionally, 20 μg of unlabeled brain phospholipid extract (Sigma Cat. no. P6023; made up to 10 mg/ml in $CHCl_3$ and stored at −70°C) can be added to

each sample before extraction. The author has not found this to be strictly necessary, and so this will be left to the end user to decide.

After extraction, the PPIn are deacylated to remove the fatty acyl chains and the water-soluble glycerophosphoinositol (Gro*P*Ins) head groups (Fig. 3.2) are separated by high-performance liquid chromatography (HPLC) on a strong anion exchange (SAX) column. The Gro*P*Ins head groups are detected by liquid scintillation counting.

The author has obtained acceptable results using a variety of often venerable HPLC systems, so it is difficult to provide a recommendation in this regard. It should be borne in mind that the gradient given in this methodology starts with a ramp from 1% to 7% salt over 30 minutes. With a two-pump HPLC system and a flow rate of 1 ml/min, this would require the pumps to be able to pump reproducible at 10 µl/min. Most modern systems are capable of achieving this.

The convenience of online scintillation detection provides a persuasive argument for use of this method. However, due to the corresponding loss of sensitivity, the author prefers to collect fractions and count them on a static scintillation counter. This method, although laborious, means that the counting accuracy can be improved by simply counting the samples longer. There is discussion on the use of online detection elsewhere in this volume.

Identifying the relevant peaks on the chromatograph, although initially quite daunting, is actually easier than it seems. Example chromatographs are shown in Figs. 3.2 and 3.3. [^{3}H]-inositol labeling gives fewer peaks, and so identifying Gro*P*Ins is relatively easy. With [^{3}H]-inositol and [^{32}P]-P_i, labeling Gro*P*Ins4*P* and Gro*P*Ins(4,5)P_2 are relatively large and can be used to orient oneself. Gro*P*Ins(3,4,5)P_3 is very polar and is usually well separated from any other compounds. Additionally, samples can be prepared from cells treated with 100 nM of the phosphoinositide 3-kinase inhibitor wortmannin, which will reduce significantly all 3-OH phosphorylated lipids [10]. From time to time, it might be useful to run standards. These can be bought, at considerable expense. Alternatively, there is a discussion about their preparation elsewhere in this volume.

Scintillation data can be presented as either counts per minutes (cpm) or disintegrations per minute (dpm). Cpm is the average number of counts acquired per minute by the scintialltion counter, whereas dpm is the average number of radioactive disintegrations in each sample per minute and is calculated from cpm. If counting efficiency is 100%, then cpm and dpm will be equal. This is almost the case for ^{32}P, but the counting efficiency is usually nearer 30% for ^{3}H. Also, in certain scintillation fluids, the high-phosphate content of samples from the later part of the gradient can reduce the counting efficiency of ^{3}H further, an effect called quenching. Modern scintillation fluids designed for high-phosphate samples experience less quenching than older formulas; however, if you want accurate dpm measurements, then you will need to set a quench correction program in your counter. For most applications, data can be adequately presented as cpm, so this is unnecessary. Setting up an online counter for dpm is discussed elsewhere in this volume. The analysis of samples from an experiment can take a few days. As ^{32}P has a half-life of 14.2 days,

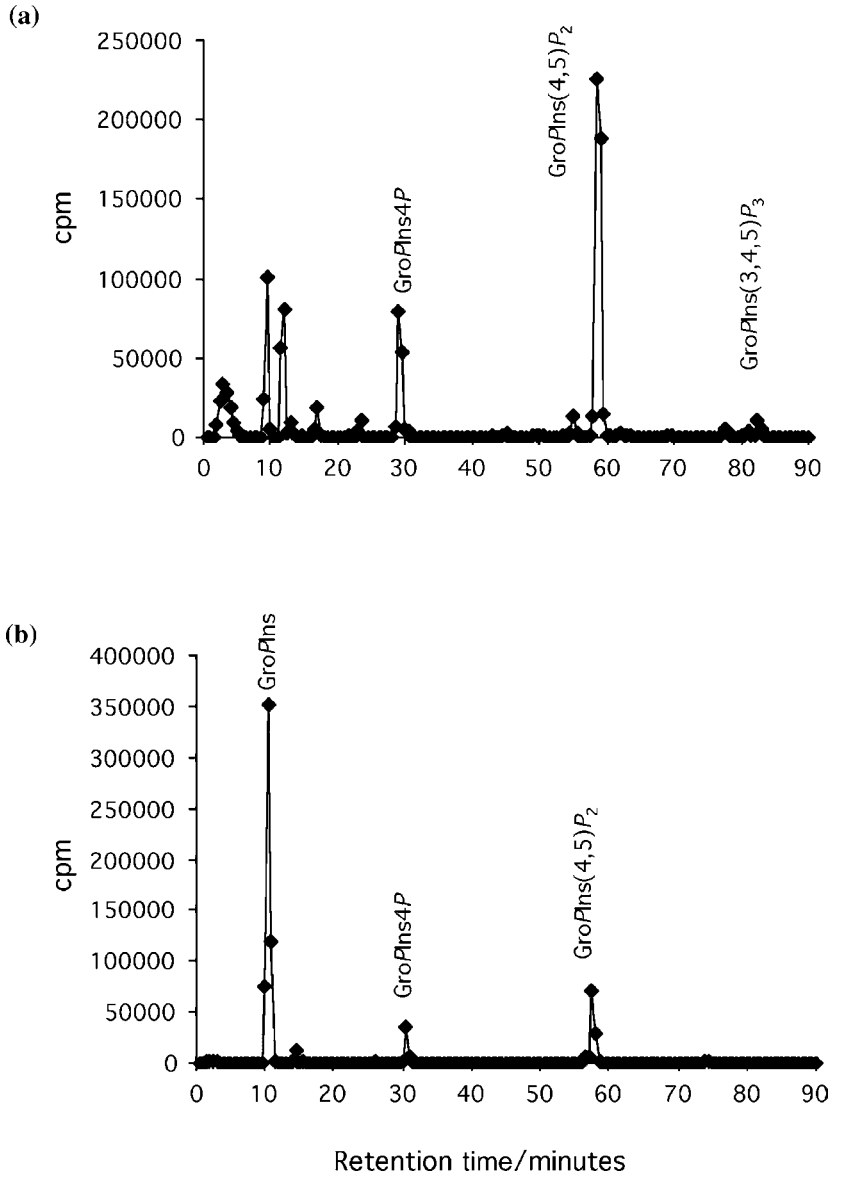

Fig. 3.3 Typical chromatographs of COS-7 cells labeled with [^{32}P]-P_i and Skov-3 cells labeled with [^{3}H]-inositol. Notice that despite eight years having elapsed between these experiments, the retention times are very similar. (a) As expected, [^{32}P]-P_i labeling results in more peaks on the chromatograph, and PtdIns, which by mass is far more abundant than any other PPIn, is poorly labeled. Gro*P*Ins(4,5)P_2 contains the most label, followed by Gro*P*Ins4*P*. It is best to use these peaks to orientate yourself on the chromatograph. (b) [^{3}H]-labeling produces many fewer peaks, especially at the start of the chromatograph, making orientation easier. Gro*P*Ins is the most prominent peak. In this experiment, insufficient label was incorporated to detect the PtdInsP_2 isomers PtdIns(3,5)P_2 and PtdIns(3,4)P_2

significant radioactive decay can occur. Most scintillation counters automatically decay-correct to the start time of the counting program. However, if more than one program is used, decay correction between runs will be necessary.

3.2 Materials

3.2.1 In vivo *$^{32}P_i$ labeling of PPIn of Adherent Cells*

1. [^{32}P]-P_i, Cat. no. PBS13 Amersham/Pharmacia, or equivalent (*see* Note 1).
2. HEPES buffered balanced salts solution (HBBSS): 15 mM HEPES (Sigma), 140 mM NaCl, 5 mM KCl, 2.8 mM $NaHCO_3$, 1.5 mM $CaCl_2$, 1 mM $MgCl_2$, 0.06 mM $MgSO_4$, 5.6 mM glucose, 0.1% (w/v) fatty acid-free bovine serum albumin (FAF BSA); pH 7.4 @ 37°C (*see* Note 2).
3. Glass vials with solvent-resistant stoppers, e.g., 5-ml Chromacol vials (type 5-SV) with PTFE/silicone rubber inserts in lids (type 12-SC-ST2).
4. Rubber policeman, or PTFE scraper.
5. 1 M HCl containing 5 mM TBAS, and MeOH, both ice cold.
6. Aspirator with appropriate shielding.
7. 37°C incubator.

3.2.2 In vivo *[^{32}P]-P_i Labeling of PPIn of Suspension Cells*

1. [^{32}P]-P_i, Cat. no. PBS13 Amersham/Pharmacia (*see* Note 1).
2. HBBSS: 15 mM HEPES (Sigma), 140 mM NaCl, 5 mM KCl, 2.8 mM $NaHCO_3$, 1.5 mM $CaCl_2$, 1 mM $MgCl_2$, 0.06 mM $MgSO_4$, 5.6 mM glucose, 0.1% (w/v) FAF BSA; pH 7.4 @ 37°C (*see* Note 2).
3. Siliconized glass vials with solvent-resistant stoppers, e.g., 5-ml Chromacol vials with PTFE/silicone rubber inserts in lids. Vials should be siliconized with reagents such as Repelcote or Sigmacoat according to the manufacturer's instructions and washed thoroughly before use.
4. Solvents: dH_2O, MeOH, $CHCl_3$.
5. Orbital shaker at 37°C.

3.2.3 In vivo *[^{3}H]-Inositol Labeling of PPIn in Adherent Cells*

1. Inositol-free culture medium (DMEM, etc.), which is available from most media suppliers, buffered appropriately with 20 mM HEPES (*see* Note 3).
2. FAF BSA.
3. Dialysed FBS (*see* Note 4).
4. [^{3}H]-inositol (Amersham, or NEN).
5. Glass vials with solvent-resistant stoppers, e.g., 5-ml Chromacol vials with PTFE/silicone rubber inserts in lids.
6. Rubber policeman, or PTFE scraper.

7. 1 M HCl containing 5 mM TBAS, and MeOH, both ice cold.
8. Aspirator.

3.2.4 In vivo *[^{3}H]-Inositol Labeling of PPIn in Suspension Cells*

1. Inositol-free medium (e.g., RPMI available from Gibco).
2. FAF BSA.
3. Dialysed FBS (*see* Note 4).
4. [^{3}H]-inositol (Amersham, or NEN).
5. Glass vials with solvent-resistant stoppers, e.g., 5-ml Chromacol vials with PTFE/silicone rubber inserts in lids.

3.2.5 *Extraction of Lipids from Suspension Cells*

1. Batch of "clean" upper and lower phases from a Folch solvent mixture prepared freshly for each extraction by mixing $CHCl_3$, MeOH, and aqueous solution (25 mM EDTA, 5 mM TBAS, 1 M HCl) in the ratio of 8:4:3 (*see* Note 5). After mixing, the phases should be separated by centrifugation at 3,000 *g*. The upper and lower phases should be removed and stored in a stoppered glass bottle until use.
2. Glass vials with solvent-resistant stoppers, e.g., 5-ml Chromacol vials with PTFE/silicone rubber inserts in lids.
3. 2.4 M HCl, 5 mM TBAS. $CHCl_3$.
4. Rotary evaporator (*see* Note 6).

3.2.6 *Preparation of Monomethylamine Reagent*

1. Monomethylamine gas (Fluka), 175 g cylinder with tap fitting.
2. Solvents: methanol, *n*-butanol, dH_2O.
3. Dry ice.
4. Fume hood.
5. Glass vials for storage, e.g., 20-ml glass scintillation vials.

3.2.7 *Deacylation of Lipid Samples and Preparation for HPLC Analysis*

1. Monomethylamine reagent, prepared as below (*see* Note 7).
2. Water bath at 53°C.
3. Rotary evaporator (*see* Note 6).
4. Butanol, petroleum-ether (40–60 fraction), ethyl formate, dH_2O.
5. 0.1 mM EDTA.
6. 0.45–μM luer lock filters (Millipore, type HV; Cat. no. SJHV004NS).

3.2.8 HPLC Analysis of Samples

1. HPLC system capable of generating programmable gradients comprising two mobile phases with a manual injector (Rheodyne 7725) and 5-ml sample loop (*see* Note 8). Inline degassing unit is optional but advisable.
2. Whatman Partisphere SAX, 4.6-mm × 125-mm column (*see* Note 9).
3. 2.5 M NaH_2PO_4, 0.22 μm filtered and degassed (*see* Note 10).
4. dH_2O, 0.22 μm filtered and degassed (*see* Note 10).
5. 0.45-μM luer lock filters (Millipore, type HV; Cat. no. SJHV004NS).
6. 2-ml luer lock syringes.
7. Luer lock injection needle.
8. Programmable fraction collector capable of collecting between 170 and 180 samples in 5-ml vials.
9. Scintillation counter.
10. 5-ml scintillation vials, e.g., LIP.
11. Scintillation fluid capable of solubilizing samples containing high levels of phosphate (e.g., Packard UltimaFlow AP) (*see* Note 11).

3.3 Methods

3.3.1 [^{32}P]-P_i Labeling of Adherent Cells

1. Cells should be passaged into an appropriate Petri dish so that they are subconfluent at the time of the experiment. Six-centimeter dishes provide a satisfactory level of labeling for most applications. If the cells are to be deprived of serum, this should be done prior to labeling (*see* Note 12).
2. The cells should be washed twice into HBBSS prewarmed to 37°C and incubated in 0.5 ml of HBBSS containing 0.1% FAF BSA (w/v), 0.3 mCi/ml [^{32}P]-P_i for 1 h at 37°C.
3. After 1 h of labeling, aspirate off the labeling medium and wash the cells twice with HBBSS (*see* Note 13).
4. The cells can now be manipulated according to the experimental protocol employed. For example, cells can be stimulated with an agonist by adding a medium exchanging the HBBSS on the cells with a buffer containing various agonists.
5. The cells are killed by removal of HBBSS with an aspirator and addition of 0.5 ml of ice-cold 1 M HCl and 5 mM TBAS and placed on ice (*see* Note 14).
6. Cells are harvested by scrapping with a PTFE scraper/rubber policeman and decanting into a clean glass vial.
7. The Petri dish and scraper should be washed with 0.667 ml of ice-cold MeOH, and the MeOH combined with the initial 1 M HCl wash (*see* Note 15).
8. As the samples contain 1 M HCl, it is not appropriate to store the cells. Lipid extraction should be undertaken as soon as possible after killing the cells.

3.3.2 [^{32}P]-P_i Labeling of Nonadherent Cells

1. The cells to be labeled were washed twice and resuspended in HBBSS at a density of 2.5×10^7/ml with 0.3 mCi/ml [^{32}P]-P_i in a siliconized glass vial.
2. The cells should be incubated in an orbital shaker, at 37°C for 1 h.
3. The labeled cells should be washed three times in HBBSS and resuspended in HBBSS at a density of 2.5×10^7/ml.
4. 150-µl aliquots of [^{32}P]-P_i-labeled cells (*see* Note 16) can be challenged with agonist in siliconized glass vials. Usually this is done by the addition of agonist in 20 µl of HBBSS. All subsequent procedures for nonadherent cells will assume a final volume of 170 µl of cells.
5. Cells should be killed by the addition of 750 µl of a solution of $CHCl_3$, MeOH, and water to give a final ratio of 1:3.75 (v/v) H_2O:MeOH/$CHCl_3$ (2:1, v/v), which will give a one-phase system. Typically, this meant an addition of 750 µl of a solution of 96.8% (v/v) MeOH/$CHCl_3$ (2:1, v/v), 3.14% (v/v) H_2O.
6. The extracts can be stored at −70°C or processed immediately.

3.3.3 [^{3}H]-Ins Labeling of Nonadherent Cells

1. Cells were washed once with inositol-free medium (*see* Note 17) supplemented with 0.1% (w/v) FAF BSA, and resuspended at 1 × 105/ml in inositol-free medium, supplemented with 5% (v/v) dialysed FBS and containing 1–20 µCi/ml [3 H]-inositol (*see* Note 18).
2. Cells were incubated with [3 H]-inositol for up to 24 h prior to the experiment (*see* Note 19).
3. Cells were washed twice in HBBSS containing 0.1% (w/v) FAF BSA and resuspended at a density of 2.5×10^7/ml.
4. Cells can now be challenged/stimulated and killed as described for [^{32}P]-P_i-labeling from step 5 in Subheading 3.3.2.

3.3.4 Extraction of Lipids from Suspension Cells

1. To cells labeled and killed as described above, add 170 µl of 2.4 M HCl, 5 mM TBAS, and 725 µl of $CHCl_3$.
2. Vortex the samples and centrifuge at 3,000 × *g* for 5 min. The samples will separate into two phases, with approximately 1100 µl of the lower phase and 710 µl of the upper phase. Process all the samples in parallel.
3. Remove the lower phase and place in a second tube containing 710 µl of clean upper phase from a "clean" Folch phase split (*see* Note 20), being careful not to carry over any protein from the interface between the two phases.
4. Add 1100 µl of clean lower phase to the original tube.

5. Both the original set of tubes and the second set of tubes should be vortexed and centrifuged at 3000 × *g* for 5 min.
6. Remove the lower phase from the second tube and place in a clean third tube. Then using the same pipette tip, remove the lower phase from the first tube and place in the second tube. Discard the first tube.
7. Vortex the second set of tubes and centrifuge at 3,000 × *g* for 5 min.
8. Transfer the lower phase from the second tube to the third tube. Discard the second tube.
9. Dry down all samples in a rotary evaporator (*see* Note 6).
10. If necessary, samples can be stored at −70°C overnight before deacylation and subsequent analysis.

3.3.5 Extraction of Phospholipids from Adherent Cells

1. To the samples prepared as described above, add 1.33 ml of $CHCl_3$, vortex, and centifuge at 1,000 × *g* for 5 min. The phases should separate to give approximately 1 ml of the upper phase and 1.5 ml of the lower phase.
2. The extraction procedure is identical to that given for nonadherent cells, except that the volumes of the lower and upper phases are 1 ml and 1.5 ml, respectively.

3.3.6 Preparation of Monomethylamine Reagent

1. Monomethylamine gas (Fluka), from a 175-g cylinder, was slowly bubbled through 268 ml of a mixture of 4:3:1 (v/v/v) methanol/H_2O/*n*-butanol, on dry ice, until the volume of the mixture expanded to 465 ml (*see* Note 21).
2. The methylamine reagent was aliquoted into clean glass scintillation vials, which were closed securely, and stored at −70°C until used (*see* Note 21).

3.3.7 Deacylation of Lipids and Preparation for HPLC Analysis

1. Add 250 µl of monomethylamine reagent to the lipid samples prepared as described above, and vortex vigorously.
2. Incubate the samples at 53°C for 30 min.
3. Let the samples cool to room temperature and centrifuge at 3,000 × *g* for 5 min.
4. Dry the samples *in vacuo* in a rotary evaporator (*see* Note 6).
5. To the dried samples add 0.5 ml of dH_2O and 0.6 ml of butanol/petroleum-ether (40–60 fraction)/ethyl formate (20:4:1, v/v/v).
6. Vortex vigorously and centrifuge at 3000 × *g*.
7. Remove the upper organic phase and discard.
8. Add another 0.6 ml of butanol/petroleum-ether (40–60 fraction)/ethyl formate (20:4:1, v/v/v), and repeat steps 6 and 7.
9. Dry the samples *in vacuo*.

10. Resuspend the samples in 0.5 ml of 0.1 mM EDTA.
11. Remove a 10-µl aliquot from each sample in a scintillation vial, add scintillation fluid, and count radioactivity. This will give a good indication as to whether the labeling and extraction procedure has been reproducible.
12. Store samples at −70°C until analysis.

3.3.8 HPLC Analysis of Lipid Head Groups

1. The HPLC pumps should be primed with the appropriate solvents.
2. If a new column is attached to the HPLC system, then the flow rate should be set to 0.1 ml/min and filtered dH_2O pumped through the column for at least 30 min. New columns are stored in methanol, and pumping salt into the column will cause precipitation.
3. With the column in line, the flow rate should be increased from 0 to 1 ml/min over 10 min.
4. The HPLC system used should be set up to run the gradient shown in Table 3.1. For best reproducibility, a gradient containing no sample should be run prior to loading the first sample in a batch of runs. Each run will be for 120 minutes' duration.
5. The samples to be analyzed should be thawed and filtered through a 0.45-µm PVDF filter. The original tube containing the sample should be washed with 1 ml of dH_2O, which should be filtered into the sample through the same filter.

Table 3.1 HPLC gradient used to separate Gro-InsP head groups

Time (min)	%A	%B
0	100	0
1	99	1
30	93	7
31	85	15
60	71	29
61	67	33
80	40	60
81	0	100
85	0	100
86	100	0
120	100	0

Buffer A is dH_2O and buffer B is 2.5 M NaH_2PO_4. The flow rate is 1 ml/min. The gradient includes a washing step, and a new sample should be loaded immediately after the end of the run. This gradient was developed for use with a 4.6-mm × 125-mm Whatman Partisphere SAX column [7], and the author has used this gradient successfully without modification for more than 10 years. If other columns are used, the gradient might need adjusting, for example, if a 250-mm column is used, then a longer washing step will be required.

6. Samples should be loaded onto into a 5-ml sample loop, injected onto the column, and the gradient and fraction collector started. This can easily be automated from the injector. Fractions should be collected every 30 s for the full duration of the gradient (90 min).
7. After the run has finished, 2 ml of scintillation fluid should be added to the samples and the samples counted in a scintillation counter. The time of counting per sample will be determined by the number of counts in each fraction (*see* Note 22).
8. After 120 min, the next sample should be load onto the column.

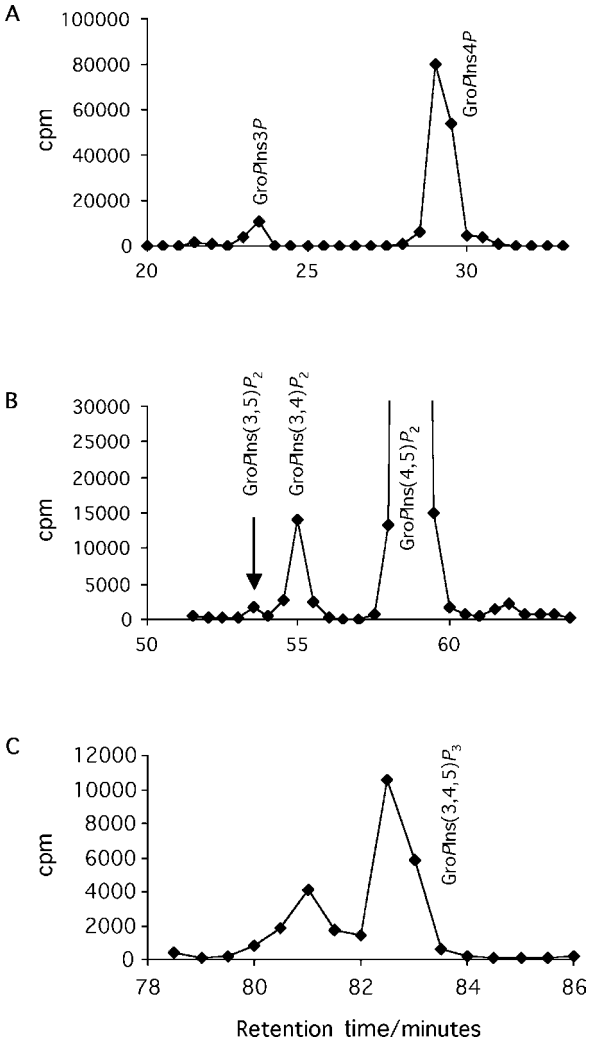

Fig. 3.4 Close-up views of chromatographs from [^{32}P]-P_i labeling showing (a) PtdIns*P*, (b) PtdInsP_2, and (c) PtdInsP_3. Note that PtdIns5*P* cannot be resolved from PtdIns4*P* on this system and is best assayed using a mass assay [2]

Table 3.2 Approximate retention times of various PPIn

PPIn	Retention Time (minutes)
PtdIns	8-12
PtdIns3*P*	22-24
PtdIns4*P*	28-30
PtdIns(3,5)P_2	53
PtdIns(3,4)P_2	55
PtdIns(4,5)P_2	60
PtdIns(3,4,5)P_3	75-80

Times will vary slightly between different batches of column and with aging of the column. Generally, the retention times of PtdInsP_2 isomers are the most consistent. After fitting a new column, the retention times will vary for the first 10 or so runs, after which the column should operate consistently. Toward the end of the column's useful life, retention times can vary and resolution will be lost.

9. After a batch of samples have been analyzed, the HPLC should be turned off by slowly reducing the flow rate from 1 ml/min to 0 over 10 min. This gradual reduction in flow rate avoids cavitation in the column.
10. Typical chromatographs for [^{33}P]-$P_i$and [^{3}H]-inositol labeling are shown in Figs. 3.3 and 3.4, and typical retention times are shown in Table 3.2.

3.3.9 Analysis of Data

1. A background count is estimated from the counts in blank vials, which is subtracted from each vial. Many counters can be set up to do this automatically.

Table 3.3 Typical data from experiment looking at PtdIns(3,4,5)P_3 accumulation in U937 cells

	PtdInsP_3	error
Control	5270	±707
ATP	16846	±280
Insulin	18202	±1268
IL-8	8811	±383
LD4	7916	±182
Bk	5646	±40
IL-6	9645	±476
IGF-1	20299	±1067

U937 cells were serum starved for 16 h, [^{32}P]-P_i labeled and challenged with various agonists or vehicle (HBBSS) as described. Labeled lipids were extracted and PtdIns(3,4,5)P_3measured by HPLC. Error bars represent the range of the data (n = 2). Agonists used were as follows: ATP (100 μM, 40 s); insulin (10 μg/ml, 40 s); interleukin-8 (1 μg/ml, 40 s); leukotriene D_4(LD4, 500 nm, 15 s); bradykinin (Bk, 10 μM, 40 s); interleukin-6 (IL-6, 1,000 U/ml, 40 s); IGF-I (10^{-8} M, 40 s).

2. Once peaks containing the various Gro*P*Ins have been identified, the total counts in those peaks are added together.
3. Data for [^{33}P]-P_i labeling may need decay correcting to a specific time point, as the decay (approximately 5% per day) will be significant while analyzing a number of samples.
4. An example of the type of data that can be produced is shown in Table 3.3.

Notes

1. [^{33}P]-$P_i$can be substituted in this protocol with a corresponding reduction in ionizing radiation hazard and increase in cost.
2. FAF BSA is used to avoid inadvertently stimulating cells with lyso-phosphatidic acid.
3. When handling small volumes of culture medium outside a 5/10% CO_2 environment, it is advisable add buffer to avoid the pH change caused by degassing.
4. FBS contains significant quantities of inositol, which can be removed by dialysis. Most suppliers sell dialysed FBS.
5. The author makes a clean Folch split by adding together (in this order) 7.09 ml of 1 M HCl, 375 µl of 0.5 M EDTA, 37.5 µl of 1 M TBAS, 10 ml of MeOH, and 20 ml of $CHCl_3$ in a 50-ml polypropylene Falcon tube. This mixture should be vortexed and centrifuged at 3,000 × *g*. By adding the organic solvents, the last evaporation is limited. Once the phases have been separated, the upper and lower phases should be immediately transferred to glass stoppered bottles. It is important to add EDTA to the phase split, as a small amount of this will carry over into the lipid extract and chelate metal ions in the deacylation step, thus improving the fidelity of this reaction.
6. Care should be taken when choosing a rotary evaporator, as the protocols described use both aggressive chemicals (HCl and monomethylamine), which can corrode pump bearings, and volatile solvents ($CHCl_3$ and petroleum ether), which will pass through a standard −80°C trap and dissolve in the pump's lubricating oil, thus reducing its effectiveness. Both of these situations will eventually destroy a standard vane pump (e.g., Edwards style). The two options are to have an expensive −120°C condensing trap, or to employ a PTFE diaphragm pump and a −80°C trap. As PTFE diaphragm pumps are resistant to aggressive chemicals, any that pass through the trap will not corrode the pump mechanism. The pump outlet should, of course, be vented into a fume cabinet.
7. The author has always used methylamine reagent prepared as described [11]. Commercial preparations of methylamine reagent are available, but most of them use water as a solvent, which is not ideal for deacylating lipids. If a commercial preparation of methylamine reagent is used, it might be worth adding methanol and butanol to give the same proportions as those given above.
8. As samples are concentrated on an SAX column, there is no need to load the samples in as small a volume as possible. Thus, for better reproducibility, a 1.5-ml sample volume is suggested. However, due to the very small bore of HPLC tubing, there is a significant boundary layer that reduces the effective volume of the sample's loop. Thus, it is best to err on the side of caution and have a sample's loop be at least twice the volume of the sample.
9. The author has used 4.6-mm × 125-mm Whatman Partisphere SAX columns (Cat no. 4621-0505) for over 10 years now and has generally had good results with them. A "good" column will give acceptable performance for well over 100 HPLC runs. Some batches of columns seem to work better (and for longer) than others, so it is worth recording batch numbers for future reference. Of course, it is quite possible that there are better columns than the Whatman on the market. However, if other columns are used, then it is possible that the gradient shown in Table 3.1 will have to be modified.

10. Mobile phases should be degassed prior to use in HPLC. The main reason for doing this is to avoid air bubbles being trapped in the pump heads, which can cause irreproducible gradients. Solvents can be degassed by sparging with helium, which is wasteful; under vacuum; by boiling; or by use of an online degassing unit. The author combines degassing with filtering by using disposable 22-μm bottle filters, and uses a degassing unit inline between the solvent reservoirs and the pump heads.
11. It is important to use a scintillation fluid that is designed to solubilize samples containing high levels of phosphate. Most scintillation fluids are unable to do this. The Packard Ultima Flow AP is designed specifically for this purpose, but, sadly, it is very expensive.
12. Mammalian cells vary considerably in their tolerance to serum starvation. This should be investigated thoroughly prior to embarking on a labeling experiment. It should also be noted that ensuring an equal number of cells in each dish is important for reproducibility, and this is often an area where improvements could be made.
13. Care should be taken to minimize the loss of cells from the Petri dish during washing.
14. A convenient way of keeping the cells ice cold is to have an aluminum tray in an ice bucket and place the cells on the tray. The tray will provide a flat surface for stability, as the samples will still be quite radioactive.
15. It goes without saying that this step presents a great opportunity to cause significant radioactive contamination of the surrounding area. Furthermore, the reproducibility of the experiment replies on a high recovery of material from this stage. Both criteria mean that great care should be exercised in this step of the procedure.
16. 150-μl aliquots of [^{32}P]-P_i-labeled cells labeled in this fashion are usually sufficient for adequate detection of PPIn.
17. Mammalian cells vary in their tolerance to inositol-free medium, especially when combined with serum starvation. A trial of different periods of inositol/serum withdrawal should be done prior to any labeling experiments.
18. The amount of label used in each experiment will depend on the ability of the cells to take up the label and the sensitivity required.
19. The time of incubation with the label might have to be adjusted if the cells being used are not able to tolerate withdrawal of inositol/serum from the medium.
20. When pipetting volatile organic solvents, it is important to equilibrate the pipette with the solvent before use. This prevents evaporating solvent in the pipette ejecting solvent from the tip. To equilibrate the tip, pipette some $CHCl_3$ up and down into each new tip.
21. Monomethylamine reagent prepared in this fashion can be stored for several years at −70°C.
22. The counting error is proportional to the square root of the total counts seen. Thus, improved accuracy can be achieved by increasing the counting time. Most scintillation counters will automatically calculate the counting error. The end user must thus decide what is deemed acceptable.

References

1. Parker PJ. The ubiquitous phosphoinositides. Biochem Soc Trans 2004;32(Pt 6):893–8.
2. Morris JB, Hinchliffe KA, Ciruela A, Letcher AJ, Irvine RF. Thrombin stimulation of platelets causes an increase in phosphatidylinositol 5-phosphate revealed by mass assay. FEBS Lett 2000;475(1):57–60.
3. van der Kaay J, Batty IH, Cross DA, Watt PW, Downes CP. A novel, rapid, and highly sensitive mass assay for phosphatidylinositol 3,4,5-trisphosphate (PtdIns(3,4,5)P_3) and its application to measure insulin-stimulated PtdIns(3,4,5)P_3 production in rat skeletal muscle *in vivo*. J Biol Chem 1997;272(9):5477–81.
4. Pettitt TR, Dove SK, Lubben A, Calaminus SD, Wakelam MJ. Analysis of intact phosphoinositides in biological samples. J Lipid Res 2006;47(7):1588–96.

5. Auger KR, Serunian LA, Soltoff SP, Libby P. Cantley LC. PDGF-dependent tyrosine phosphorylation stimulates production of novel polyphosphoinositides in intact cells. Cell 1989;57(1):167–75.
6. Hawkins PT, Jackson TR, Stephens LR. Platelet-derived growth factor stimulates synthesis of PtdIns(3,4,5)P_3 by activating a PtdIns(4,5)P_2 3-OH kinase. Nature 1992;358(6382):157–9.
7. Stephens LR, Hughes KT, Irvine RF. Pathway of phosphatidylinositol(3,4,5)-trisphosphate synthesis in activated neutrophils. Nature 1991;351(6321):33–9.
8. Folch J, Lees M, Sloane Stanley GH. A simple method for the isolation and purification of total lipides from animal tissues. J Biol Chem 1957;226(1):497–509.
9. Bligh EG, Dyer WJ. A rapid method of total lipid extraction and purification. Can J Biochem Physiol 1959;37(8):911–7.
10. Stephens L, Cooke FT, Walters R, Jackson T, Volinia S, Gout I, Waterfield MD. Hawkins PT. Characterization of a phosphatidylinositol-specific phosphoinositide 3-kinase from mammalian cells. Curr Biol 1994;4(3):203–14.
11. Clarke NG. Dawson RM. Alkaline O leads to N-transacylation. A new method for the quantitative deacylation of phospholipids. Biochem J 1981;195(1):301–6.

Chapter 4
Inositol Lipid-Dependent Functions in *Saccharomyces cerevisiae*: Analysis of Phosphatidylinositol Phosphates

Stephen K. Dove and Robert H. Michell

Abstract Inositol phospholipids regulate many cellular processes, including cell survival, membrane trafficking, and actin polymerization. Quantification of inositol lipids is one of the essential techniques needed for studies that aim to decipher inositol lipid-dependent cellular functions. The study of phosphoinositides in most organisms is hampered by a lack of facile genetic tools. However, the essential elements of most inositol lipid signaling pathways appear to be conserved across eukaryote phylogeny. They can therefore readily be elucidated (both genetically and biochemically) in the budding yeast *Saccharomyces cerevisiae*. Because of the low abundance of polyphosphoinositides in cells, many analytical methods start by radioactively labeling intact cells and then extracting the lipids with chloroform/methanol/water mixtures based on those first devised half a century ago. Yeast present special extraction problems because the cell wall must be broken in order to facilitate solvent access and maximize lipid yield. Once lipids have been extracted, fatty acids are removed and the resulting water-soluble glycerophosphoinositol phosphates are analysed by anion-exchange HPLC. This chapter describes how to extract and quantify the inositol lipids of *S. cerevisiae* cells that have been radiolabeled to isotopic equilibrium with [^{3}H]*myo*-inositol.

Keywords Inositol · phosphoinositide · signaling · membrane trafficking · yeast · HPLC · phosphatidylinositol

S.K. Dove
Phosphoinositide Lab, School of Biosciences, University of Birmingham, Edgbaston, Birmingham B15-2TT, UK
e-mail: s.k.dove@bham.ac.uk

B. Larijani et al. (eds.), *Lipid Signaling Protocols*, DOI: 10.1007/978-1-60327-115-8_4,

4.1 Introduction

Polyphosphoinositides (PPIn) are a class of seven diacylglycerophospholipids based on phosphatidylinositol (PtdIns), in each of which the *myo*-inositol head group of PtdIns is further phosphorylated. All are derived from PtdIns (see Fig. 4.1) by widely conserved phosphorylation pathways: These are catalyzed by ATP-dependent kinases [1–3]. PtdIns is present in all eukaryotic cell membranes, so a balance of kinase, phosphatase, and phospholipase activities can modulate PPIn levels in each membrane compartment within seconds.

Each of the seven PPIn regulates one or more cellular processes [4–10]. PPIn function primarily through interactions with effector proteins, the functions of which are modulated when PPIn bind to them.

The study of inositol lipid function began in the 1950 s with an analysis of the chemical structure and metabolism of these lipids in response to extracellular agonists [11,12]. Studies since then have defined numerous PPIn-dependent signaling and regulatory pathways, several of which are influenced in animal cells by hormones and growth factors. Notably, these are the PPIn 3-kinase/PtdIns(3,4,5)P_3 and phospholipase C/1,2-diacylglycerol/Ins(1,4,5)P_3 signaling systems [1,5,6,13,14] and the involvement of PPIn in various aspects of membrane trafficking. Given the relatively recent identification of phosphatidylinositol 5-phosphate and 3,5-bisphosphate, PPIn species that were not previously recognized and whose functions have yet to be described fully [10,15,16], the accurate identification and quantitation of PPIn from intact radiolabeled cells is even more important today than it was in earlier decades.

The yeast *S. cerevisiae* offers technical advantages to anyone interested in the study of PPIn-dependent cell regulation because its genetics are facile and

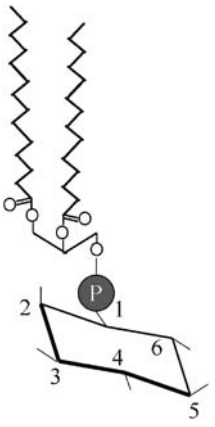

Fig. 4.1 Structure of phosphatidylinositol (also abbreviated as PtdIns), highlighting the five hydroxyl groups that are potentially available to modifications such as phosphorylation. Phosphorylation of one or more of the D-3, D-4, and D-5 hydroxyls produces the seven PPIn. D-6 phosphorylation occurs in GPI anchored proteins. Phosphorylation of the axial D-2 hydroxyl has never been observed in lipids

its genome is annotated to a high degree: Gene knockouts and knock-ins can often be achieved within a single week. We have used this organism extensively in our studies of the "novel" PPIn phosphatidylinositol 3,5-bisphosphate [PtdIns(3,5)P_2] [10,15,17].

The most widespread method for the analysis and quantification of PPIn involves radioactive labeling of cells with [^{3}H]*myo*-inositol. The chemical levels of these lipids are so low that they preclude normal chemical analyses. Once cells have been radiolabeled, the lipids can be extracted by methods based on those devised in the mid-20th century, notably those of Folch [18,19] and of Bligh and Dyer [20]. These extract cells in single-phase mixtures of chloroform, methanol, and water and then add more water and/or chloroform so as to generate a two-phase system. The upper phase, rich in water and methanol, contains the water-soluble contents of the cell while the lower, chloroform-rich, phase contains the lipids. In these methods, phase partition separates lipids from water-soluble materials (including water-soluble radiochemicals) and facilitates concentration of the lipids by vacuum drying.

Both of these methods were developed with relatively nonpolar lipids in mind, but PPIn are very acidic and polar. This can result in significant losses of PPIn into the upper, water-rich, phase if precautions are not taken. Acidification of the upper phase protonates the phosphomonoester groups on PPIn, thereby suppressing their charge and making them partition into the lower phase. This is necessary if PPIn are to be recovered quantitatively. HCl concentrations of 0.6–0.8 M work best, since higher concentrations can degrade PPIn or cause phosphate migration: They can also be difficult to remove before continuing with the analysis. The inclusion of a strong organic counteranion (e.g., tetra-butyl ammonium hydrogen sulphate; TBAHS) aids extraction as it promotes the retention of polar lipids in the lower phase.

4.2 Materials

4.2.1 Preparation of Inositol-Free SC Medium

All individual components listed below can be obtained from Sigma. They should be of tissue-culture or molecular-biology grade if possible. Store reagents for preparation of the vitamin stock solution at 4°C in a foil-wrapped, air-tight box containing dry silica gel.

1. 100 ml of 40% (w/v) D-glucose solution (i.e., 400 mg/ml) in distilled or reverse-osmosis/deionized water (dH_2O), autoclaved for 15 min at 121°C. Store at room temperature for up to one year.
2. 1 L of **5 × Salts and trace elements solution**: 2.5 g each of $MgSO_4.7\,H_2O$, NaCl, and $CaCl_2.6\,H_2O$, 2.5 mg of H_3BO_3, 2.0 mg of $ZnSO_4.7\,H_2O$, 1.0 mg

each of $FeCl_3.6\,H_2O$ and $Na_2MoO_4.2\,H_2O$, 0.5 mg each of KI and $MnCl_2$, and 200 µg of $CuSO_4.5\,H_2O$. Add the powders to 950 ml of dH_2O, with continuous vigorous stirring to prevent precipitation. Make up to 1 L with dH_2O and autoclave for 15 min at 121°C. Store at room temperature for up to one year (or until precipitation occurs).

3. 10 ml of **500 × Vitamin solution**: 10 mg of calcium pantothenate, 2 mg each of niacin, pyridoxine.HCl, and thiamine.HCl, 1 mg each of *p*-aminobenzoic acid and riboflavin, and 0.5 mg each of biotin and folic acid. The above are dissolved in 9 ml of 18.3 MΩ dH_2O, made up to 10 ml with dH_2O and filter-sterilized using a syringe-driven 0.22-µM filter. Store in 1-ml aliquots at −80°C for up to one year. This solution is light-sensitive, so wrap the tubes in foil.
4. 1.75 g of powdered ammonium sulfate, 0.5 g of KH_2PO_4, and 0.75 g of asparagine.
5. 50 mg of each of the following powdered reagents: uracil, histidine, lysine, tryptophan, leucine, and adenine.

4.2.2 Preparation of Monomethylamine Reagent

1. A small (170 g) cylinder of anhydrous monomethylamine, e.g., Aldrich 29,553-1 or Fluka 65572.
2. The correct flow regulator for the above cylinder to control the gas flow rate (Note: These are NOT interchangeable among different manufacturers); e.g., Aldrich Z146951 or Fluka 99112.
3. 1 m of silicone rubber tubing and a rubber bung to fit a 500-ml conical flask. The bung should have two holes bored into it, such that glass Pasteur pipettes can be inserted through the bung to make a gas-tight fit.
4. A mixture of 140 ml of pure methanol and 105 ml of dH_2O (this may be either distilled, or subjected to reverse osmosis, filtration, and ion-exchange polishing, ideally to a resistivity of ∼18 MΩ). Mix these in a 500-ml Duran glass bottle that is new or has only ever been used to prepare this reagent. Only if the bottle is new, prewash it by autoclaving full of 18.3 MΩ dH_2O.
5. 500 g of wet or dry ice.
6. 35 ml of *n*-butanol.
7. A clamp stand.

4.2.3 Radiolabeling of Yeast Cells with [^{3}H]Inositol

1. [^{3}H]*myo*inositol (specific radioactivity 20–30 Ci/mmol, e.g., NET-114 from NEN). Store at −20°C for up to one year.
2. YPD medium (20 g/L of Bactopeptone, 10 g/L of yeast extract, 100 mg/L each of adenine and uracil in 18.3 MΩ dH_2O. Autoclave for 15 min at 121°C, cool to 50°C, and add 50 ml of 40% glucose). Store at room temperature in the dark for up to one year. Open only in a laminar flow hood.

3. Inositol-free SC medium (SC-Ino); *see* Subheading 4.3.1.
4. CH_3OH:12 M HCl 100:1 (v/v). Make fresh the night before and store at 4°C.
5. 50-ml Falcon-type disposable polypropylene centrifuge tubes (e.g., Becton-Dickinson Cat. no. 352098).

4.2.4 Cell Breakage and Lipid Extraction

1. $CHCl_3$ (AR grade), aliquoted the night before and cooled to 4°C.
2. CH_3OH:12 M HCl 100:1 (v/v) made the night before and stored at 4°C.
3. 0.8 M HCl, 5 mM tetrabutylammonium hydrogen sulfate (TBHAS; Sigma), 1 mM EDTA, 1 mM Inositol. Made fresh the night before and stored at 4°C.
4. Acid-washed glass beads (425–600-μm diameter, e.g., Sigma G-8772).
5. PPIn mixture from bovine brain (e.g., Sigma P6023) made up at 1 mg/ml in $CHCl_3$:CH_3OH 2:1 (v/v) and stored at −20°C in a light-tight bottle for up to one year.
6. Glass or polypropylene 20-ml scintillation vials.
7. Centrifugal vacuum evaporator (e.g., Speed-Vap) connected, through a refrigerated trap (preferably cooled to −80°C), to a high-vacuum pump.

4.2.5 Deacylation of PPIn Using Monomethylamine Reagent

1. Monomethylamine reagent (prepared as in Subheading 4.3.2 or from other commercial sources; *see* Note 4).
2. 3 mM HEPES.KOH, pH 7.5. This is prepared in large batches (0.5 L) and stored at −20°C in 20-ml aliquots until needed. It is stable at room temperature, but repeatedly opening the bottle leads to bacterial contamination.
3. *n*-butanol:petroleum ether (bp 40–60°C):ethyl formate (20:4:1, by volume), stored in a Duran bottle and kept at room temperature. Stable for several years provided the bottle is kept well sealed.

4.2.6 HPLC Analysis of Deacylated PPIn

1. Two-pump programmable HPLC system with inert and salt-resistant metal pumps and piping (e.g., Gilson with 10 WTI pump heads and titanium flow lines) and a 5-ml sample injection loop.
2. Flow detector or fraction collector.
3. Scintillation fluid that will tolerate high-salt aqueous solutions (e.g., Perkin-Elmer Ultima Flo AP; Cat. no. 6013599).
4. Partisphere SAX HPLC column (5 μM, 46 mm × 250 mm: Whatman Cat. no. 4621 1505).
5. Guard cartridge holder (Whatman Cat. no. 4631 0003).
6. Guard cartridges (Whatman Cat. no. 4641 0005).

7. Glass filter unit and/or 0.22-μM filters (e.g., Sigma).
8. 1.25 M $(NH_4)_2HPO_4$ in 18.3 MΩ dH_2O, adjusted to pH 3.8 with orthophosphoric acid.

4.3 Methods

4.3.1 Preparation of Inositol-Free SC Medium

1. To prepare 0.5 L of this medium, add 100 ml of the "5 × salts/trace elements solution" from step 2 in Subheading 4.2.1 to 350 ml of dH_2O and stir.
2. Add to the solution above: 1.75 g of ammonium sulfate, 0.5 g of KH_2PO_4, 0.75 g of asparagine, and 50 mg each of one or more of the following: uracil, lysine, leucine, histidine, tryptophan, and adenine (*see* Note 1). Stir until completely dissolved (20 min; under cold conditions it may be necessary to slightly warm the solution in a microwave oven).
3. Adjust this solution to pH 5.7 using 1.0 M NaOH or HCl.
4. Make the medium up to 500 ml with 18.3 ml of dH_2O (*see* Note 2).
5. Either filter-sterilize by passing the medium through a 0.22-μM filter into a sterile container or autoclave for 15 min at 121°C.
6. When cool, add 1 ml of the "500 × vitamin solution" from step 3 of Subheading 4.2.1 and 5 ml of 40% glucose (*see* Note 3) in a laminar flow hood (if medium is to be filter-sterilized, these reagents can be added before filtration). The medium is now ready to use. Store at room temperature for up to one year, in the dark (the medium is light-sensitive). To avoid contamination, open only in a laminar flow hood.

4.3.2 Preparation of Monomethylamine Reagent

Monomethylamine reagent removes the ester-linked fatty acids from phospholipids by transmethylation. This method of deacylation is required for proper HPLC analysis of deacylated PPIn (see Subheading 4.3.5). Commercial preparations of monomethylamine solution are available, but we routinely prepare our own from monomethylamine gas (*see* Note 4).

Monomethylamine gas is corrosive, toxic, and flammable. The following procedure MUST be carried out in a well-vented fume hood.

1. Assemble the equipment as shown in Fig. 4.2. First place the water/methanol mixture and a clean stirrer bar in the clean 500-ml glass Duran bottle (labeled "L" in Fig. 4.2). Put the flask into a polystyrene container packed with dry ice ("K" in Fig. 4.2; wet ice will suffice, but must be renewed often) that is mounted on a stirrer. Stir for 30 min to cool ("J" in Fig. 4.2).
2. Check that the main valve on the monomethylamine cylinder is off ("B" in Fig. 4.2) and then remove the nut masking the side connection. Place this

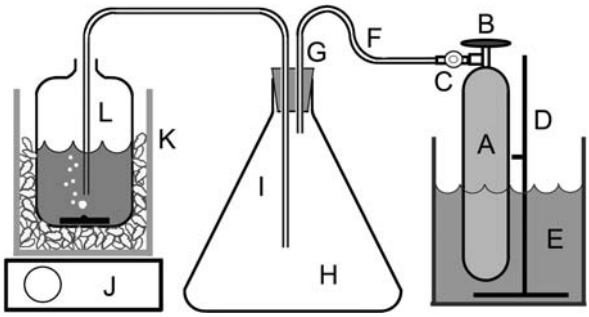

Fig. 4.2 Apparatus for the preparation of monomethylamine reagent from monomethylamine gas. The monomethylamine cylinder (A) is controlled by a main gas valve (B) and a flow regulator valve (C). The cylinder is clamped to a stand (D) and immersed in a water bath set to 30°C (E). The cylinder is connected via silicone rubber tubing (F) to a short Pasteur pipette (G) that passes through a silicone rubber bung into a 500-ml conical flask that acts as a liquid trap (H). A long Pasteur pipette (I) connects the trap via more silicone rubber tubing to a Duran bottle (L) containing a water/methanol mixture. This bottle is immersed in a dry-ice bucket (K) and is stirred by a magnetic stirrer (J)

nut in a safe place, as you will need it when returning the cylinder to the manufacturer.

3. Clamp the cylinder and then screw on the flow regulator valve, checking that it is in the closed position ("C" in Fig. 4.2). Put the cylinder, fixed in the clamp stand, into a 30°C water bath ("E" in Fig. 4.2; *see* Note 5).
4. **Carefully** insert a long and a short disposable Pasteur pipette through the holes in the rubber bung, ensuring that they fit tightly. Using silicone rubber tubing ("F" in Fig. 4.2), connect the **short** pipette ("G" in Fig. 4.2) with the flow regulator on the monomethylamine cylinder ("C" in Fig. 4.2). Connect the **long** pipette to a length of silicone rubber tubing, attach another long Pasteur pipette to the free end, and place this into the methanol/water mixture, taking care that it does not interfere with the stirrer (*see* Note 5).
5. Check that all connections are tight, that the flow regulator valve is CLOSED, that the fume hood is working properly, and that the methanol/water solution is cool. Carefully open the main valve ("B" in Fig. 4.2) on the top of the monomethylamine cylinder; no gas should flow at this point.
6. Slowly open the flow regulator valve ("C" in Fig. 4.2) until gas is heard bubbling into the water/methanol mixture. The gas must first raise the pressure in the flask, so this will take a few seconds. Adjust the valve until there is a rapid flow of bubbles, but not so rapid as to cause splashing or excessive heating of the monomethylamine reagent. Ensure that the stirring is continuous, so as to dissipate the heat of the reaction. Continue the bubbling for 1–3 h, adding extra ice (wet or dry) as necessary. Toward the end of the procedure, open the flow regulator valve fully to ensure the release of all gas. When the cylinder is empty, shut the flow regulator and main valves.

7. Once the cylinder is empty, the volume of the methanol/water plus monomethylamine solution will have increased to ~400 ml.
8. Add 35 ml of *n*-butanol to the monomethylamine solution, cap the bottle tightly, and stir gently for 1 min in the dry-ice bath.
9. Store the bottle containing the monomethylamine reagent at −20°C (or, better, at −80°C) for up to two years. Open the bottle only in a fume hood, and keep it on ice whenever it is in use. NEVER allow it to warm up.
10. Carefully disassemble the apparatus (in the fume hood) while wearing gloves and eye protection. Be careful: Monomethylamine gas will be present in the tubing and the flask used as a trap. To remove all traces of monomethylamine, leave the trap flask, bung, and tubing in the fume hood for one week. Store them safely in a labeled box for the next preparation of the reagent; do not use them for other purposes.

4.3.3 Radiolabeling of Yeast Cells with [^{3}H]Inositol

1. Sterilize an inoculating loop in a "roaring" flame, and use it to pick a yeast colony off a fresh (<1 week old) agar plate. Inoculate it into 10 ml of YPD medium, and incubate for 16 h at 30°C in an orbital shaker at 200 rpm.
2. Using a standard aseptic technique, remove a sample of the yeast suspension and determine the cell number using a hemocytometer.
3. Inoculate inositol-free SC medium in a 50-ml Falcon tube (e.g., Cat. no. 352098) to a density of 6×10^4 cells/ml (*see* Note 6). Add 10 μCi/ml [^{3}H]inositol, and incubate at 30°C for 14–18 h (or to a cell density of $2–3 \times 10^6$ cells/ml; *see* Notes 7 and 8 for details).
4. Once cells have reached the required density, either they can be killed and lipids extracted or they can first be subjected to some chemical, biological, or physical "stress" to induce changes in PPIn turnover. For example, hyperosmotic stress provokes a rapid increase in the quantity of PtdIns(3,5)P_2 in cells; and hypoosmotic stress stimulates the Plc1p-catalyzed hydrolysis of PtdIns(4,5)P_2. Our method for inducing hyperosmotic stress is to take 2 ml of culture radiolabeled as above, add 0.5 ml of 5 M NaCl (made in fresh SC medium lacking inositol), mix, and incubate at 30°C for 10 min.
5. Cells are killed by the addition of 2 volumes of ice-cold CH_3OH:12 M HCl 100:1 (v/v), vortexed, and placed on ice for 5 min (*see* Note 9). In the example given, 2.5 ml of cell suspension would be killed with 5 ml of CH_3OH:12 M HCl 100:1 (v/v).
6. Dead cells are harvested by centrifugation (10 min, 4°C, 6,000 × *g*) and the supernatant completely removed. **CAUTION: This supernatant contains 90–95% of the total radioactivity added to the cells and so should be disposed of appropriately.** The dead cells can now be either processed for lipid extraction immediately or snap-frozen in liquid nitrogen and stored at −80°C overnight (no longer or else lipid degradation takes place; *see* Note 10) before lipid extraction.

4.3.4 Extraction of PPIn from Radiolabeled Yeast Cells

During the following procedure, ensure that all solutions, cells, and lipid extracts are kept cold throughout by working on ice. Precool centrifuges to 4°C and work as quickly as possible.

1. In the same Falcon 352098 tubes in which they were radiolabeled (*see* Note 11) and killed, resuspend the acid methanol-killed yeast cells (Subheading 4.3.3) in 0.3 ml of water:CH_3OH:12 M HCl 66:100:1 (v/v) and add 0.8 g of acid-washed glass beads. Place the cells on ice (*see* Note 12 and Fig. 4.3, part 1).
2. Vortex the yeast 10 times for 30 s, with 30 s of cooling on ice in the intervals. Process two tubes simultaneously (one in each hand), alternating them so that while one set is on ice, the other is being vortexed, and vice versa.
3. Add 1.33 ml of ice-cold $CHCl_3$ and 0.47 ml of ice-cold CH_3OH:12 M HCl 100:1 (v/v) to each sample and vortex for 30 s. The resulting mixture should form a single $CHCl_3$:CH_3OH:water phase (*see* Note 13 and Fig. 4.3, part 2).
4. Incubate the samples on ice for 10 min. During this time, the PPIn are extracted.
5. Add 20 μg of bovine brain PPIn to all samples, to act as a carrier, and vortex the samples for 30 s.
6. Add 0.4 ml of 0.8 M HCl, 5 mM TBAHS, 1 mM EDTA, and 1 mM inositol to all samples, and vortex for 1 min. The extractions should now split into two phases (*see* Fig. 4.3, part 3, and Note 14), with protein collecting at the interface between the two phases.
7. Place a pipette through the upper layer (expel a little air as you go through to ensure that no upper phase adheres to the outside of the pipette tip) and remove the lower layer as completely (Fig. 4.3, part 4) as possible to labeled 20-ml scintillation vials. (Note: Mark the scintillation vials with permanent pen twice on autoclave or similar tape. Labeling applied directly to tubes will be washed off at later states of the procedure!) Try not to transfer any glass

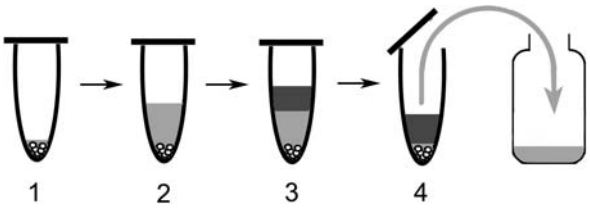

Fig. 4.3 Stages in lipid extraction: (1) Cells and glass beads are in a small volume of acidified methanol after cell disruption. (2) Chloroform and methanol are added to produce a monophasic mixture that extracts the PPIn. (3) Acid is added to form a two-phase system. Lipids are in the lower phase, and water-soluble components in the upper phase. (4) The lower phase is removed to a separate vial and dried to remove all solvent and acid

beads, although a small number will not present a problem. Do not transfer ANY upper phase. Keep the scintillation vials on ice at all times.
8. Dry off the organic solvents by placing the vials in a speed-vap vacuum dryer connected to a vacuum pump. There should be a refrigerated trap (−80°C if possible) between the speed vap and the pump. If not, a trap can simply be rigged using a glass trap suspended in dry ice in methanol in a polystyrene container. Empty the trap after each use. Samples should take 30–60 min to dry.
9. Add 1 ml of methanol and dry again. This removes any residual HCl: HCl evaporates last and can concentrate to high levels that will interfere with deacylation. This step can be extended overnight if desired.

4.3.5 Deacylation of PPIn Using Monomethylamine Reagent

1. Place each lipid extract (e.g., from Subheading 4.3.5) on ice to cool. Add 1 ml of monomethylamine reagent (generated in Subheading 4.3.2) dry lipid extracts and cap the tube quickly.
2. Make sure that the lids of all tubes are fastened tightly, and place the samples in a suitable rack in a water bath at 53°C for 40 min. After the first 5 min, vortex all samples to disperse the lipid into the hot reagent.
3. Remove samples from the water bath and place them on ice to reduce the internal vapor pressure. Leave for 15 min. Label the tube caps, so that they can later be reunited with the correct partners.
4. Remove tube caps and place the samples in a speed-vap. Remove the excess monomethylamine *in vacuo* as before (with the same arrangement of trap). This takes 2 h.
5. Remove the dry samples from the speed-vap and add 1 ml of 3 mM HEPES.KOH, pH 7.5, and 2 ml of butanol:petroleum ether (bp 40–60°C);ethyl formate (20:4:1, by volume) to each sample (*see* Note 15). Recap the tubes and vortex for 1 min. A two-phase system should now form (*see* Note 16).
6. Remove the speed-vap trap and defrost/clean it. Place it back into the refrigerated holder or dry-ice methanol bath ready for the next step.
7. Remove the lower layer from each sample to a 2-ml Eppendorf tube. Take care not to transfer any glass beads.
8. Add another 1 ml of water to each sample and vortex for 1 min. Remove the lower layer and pool it with the previous lower layer from the same sample.
9. Dry the pooled lower phases in the speed-vap. This drying stage should at least reduce the volume by half (to ~1 ml), so as to ensure removal of all organic solvents. If samples are completely dried (this may take overnight), they can be stored at −20°C for many years or shipped in the mail without any need for refrigeration. We routinely store samples after resuspension in

1 ml of dH_2O at −20°C. Some of our standard samples have survived a decade without any hydrolysis in this way.
10. Samples are now ready for HPLC analysis once they are made up to 2 ml with water.
11. Replace the oil in the high-vacuum pump and defrost and clean the glass trap.

4.3.6 HPLC Analysis of Deacylated PPIn

The following is not an exhaustive guide to the principles and methods of HPLC, which are beyond the scope of this work. They are offered as a guide.

1. Ensure that the water and salt reservoirs are full and that the Flo-detector has sufficient scintillation fluid for all experiments.
2. Check the waste container to make sure it will not overflow. Empty if necessary.
3. Place an ion-exchange guard cartridge in the guard cartridge holder, run water through it at 1 ml/min for 10 min (*see* Note 17), and then stop the flow.
4. Connect the Partisphere 5 μM SAX column in the correct orientation (observing the direction of the flow arrow on the cartridge) to the guard cartridge holder and turn the flow to 0.1 ml/min before tightening the connection (*see* Note 18).
5. Connect the column outlet to the Flo-detector or fraction collector and tighten.
6. Increase the flow of water up to 1 ml/min over 10 min (*see* Note 18). The backpressure (for a 250-mm column with a new guard cartridge) should be about 950 psi.
7. Run water through the column for 2 h if this is the first time that it has been used (*see* Note 20).
8. Fill the solvent reservoirs with: (A) 18.3 MΩ dH_2O; (B) 1.25 M $(NH_4)_2HPO_4$ in 18.3 MΩ dH_2O, adjusted to pH 3.8 with orthophosphoric acid.
9. Activate the column by running the following program: 0 min, 0% B; 5 min, 0% B; 50 min, 50% B; 60 min, 50% B; 55 min, 0% B'; 95 min, 0% B (*see* Note 21). The backpressure will rise to about 1,300–1,700 psi during the high-salt part of this gradient. The column is now ready to use.
10. Inject the sample and run the following program: 0 min, 0% B; 5 min, 0% B; 45 min, 12% B; 52 min, 20% B; 64 min, 100% B; 80 min, 100% B; 95 min, 0% B; 120 min, 0% B.
11. Collect (0.5-min) fractions or turn on the Flo-detector (6-s updates) from the injection point. An example of the kind of data you will obtain is shown in Fig. 4.4.
12. After the day's HPLC has finished, run the HPLC with water for 60 min and then reduce the flow rate to 0 over 10 min (*see* Note 18).

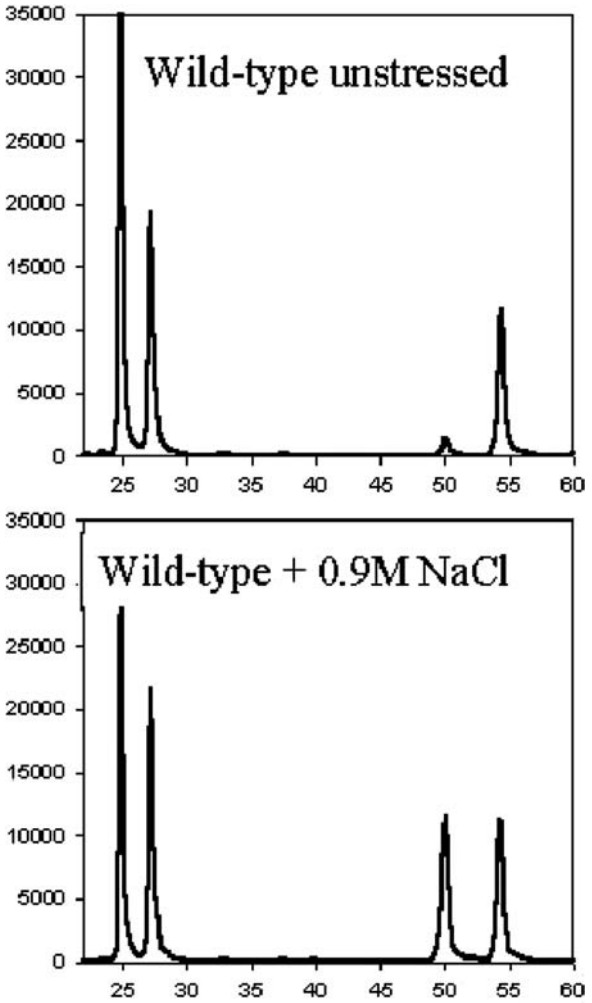

Fig. 4.4 HPLC analysis of PPIn. The *x*-axis shows time while the *y*-axis shows radioactivity eluting from the column. The data were collected on a Packard A525 Flo-detector with a 6-second update time and Ultima Flo AP scintillation fluid. The initial part of the gradient is omitted for clarity. PtdIns elutes at 15–20 min. The other peaks are PtdIns3*P* (25 min), PtdIns4*P* (and also PtdIns5*P*; 27.5 min), PtdIns(3,5)P_2 (50 min), and PtdIns(4,5)P_2 (54 min). This gradient will also resolve PtdIns(3,4)P_2 (53 min) and PtdIns(3,4,5)P_3 (60 min)

Notes

1. Only the amino acids that a particular strain needs to survive should be added to this SC-[^{3}H]inositol radiolabeling medium. For instance, for a strain whose genotype is *ade3 ura3 trp1 his3 leu2*, add only adenine, uracil, tryptophan, histidine, and leucine at 50 mg/L. Do not add the other amino acids or higher concentrations of glucose (the final concentration of glucose in this medium is only 0.4%), because the aim is to obtain

maximal incorporation of [^{3}H]inositol into lipids. Yeast synthesize inositol from glucose, so limitation of the glucose supply tends to divert glucose into amino acid anabolism and maximizes the specific radioactivity of the resulting lipid extract.

2. Medium can be prepared with high supplementary salt concentrations, so that experiments can be performed in which yeast that have been acclimatized to high salt are diluted into normal medium, resulting in a hypotonic stress. This is simply done by adding NaCl to a final concentration of 0.9 M and then sterilizing by filtration (NOT autoclaving).
3. Dilute glucose should NEVER be autoclaved in the yeast medium, as it caramelizes. This inhibits the growth of many strains. The same is true of all media and solutions, including those for bacterial work. Autoclave glucose as a 40% solution in 18.3 MΩ dH_2O.
4. Some commercial preparations of monomethylamine reagent in water are not suitable for the procedure outlined in Subheading 4.3.5: They catalyze extensive side reactions that preclude any meaningful analysis of the lipid samples. Monomethylamine in methanol is reputed to be better and can be used for lipid analysis where the less abundant PPIn are not under scrutiny. However, it also produces more side reactions than the freshly prepared and chilled reagent we describe. Commercial monomethylamine in methanol reagent can be obtained from Sigma (Cat. no. 395048, currently 100 ml and 800 ml). Since this reagent is solely monomethylamine in methanol, it must be adjusted, immediately before use, to the same solvent composition as that used in the described protocol (methanol:water:*n*-butanol: 4:3:1, by volume).
5. The reason for placing the gas cylinder into the water bath is that as gas is released, expansion of the residual gas causes a decrease in the cylinder temperature. Unless care is taken, this decreased pressure in the cylinder can suck monomethylamine reagent back into the cylinder—hence, the use of a flask as a liquid trap between the cylinder and reagent.
6. One milliliter of yeast culture that is labeled with 10 μCi/ml of [^{3}H]inositol through five or six divisions incorporates $\sim 1 \times 10^6$ dpm into inositol lipids: Most is in PtdIns, and 0.1–2% in each of the PPIn. Thus, about 5,000–20,000 dpm is incorporated into each of [^{3}H]PtdIns3*P*, [^{3}H]PtdIns4*P*, and [^{3}H]PtdIns(4,5)P_2 for each milliliter of radiolabeled culture, and ~1,000–4,000 dpm into [^{3}H]PtdIns(3,5)P_2.
7. Many regulatory pathways in yeast change their behavior at different stages of growth. We usually study cells in the early exponential phase, as they respond to the widest range of stresses. However, this is inappropriate for some nutritional signaling studies or for studies of pathways that are activated in the stationary phase: Adjust this appropriately for your study. Another reason to choose the early exponential phase if possible: The higher the cell density, the harder it is to break the cell wall.
8. If an accurate measure of the relative concentration of the various PPIn is important, cells must be radiolabeled to close to isotopic equilibrium. This is easily achieved by growing yeast for five or six generations in a medium that contains [^{3}H]Ins, but is otherwise inositol-free (*see* Note 6). Under these conditions, 95% of the PPIn is made from [^{3}H]PtdIns, and the relative amounts of radioactivity recovered in the various compounds give a true picture of their relative concentrations. Whenever lipid labeling has not reached isotopic equilibrium with the added precursor, changes in the proportion of the radioactivity found in a particular compound are difficult to interpret. They can, for example, be caused by relative changes in turnover rate, in the amount present, or in the metabolic activity of different intracellular pools of the compound.
9. Pipetting organic solvents can present a problem since they vaporize in the pipette to a much greater extent than water. The increased internal vapor pressure then tends to drive solvent out of the pipette. To avoid this, pipette the solvent up and down in the pipette five times, expel all liquid, and then use the vapor-filled pipette normally.
10. We have stored cells successfully for up to three days using this method, but in a few experiments some of the lipids were degraded even after only 16 h. Storage at this stage should only be used as an emergency measure.

11. PPIn are highly charged and very polar, so the use of glassware for extracting and handling them is generally to be avoided. They can adsorb irreversibly to silica or glass and be lost, especially when in the small quantities found in most cell extracts. Whenever possible, we handle intact lipids in polypropylene tubes.
12. Yeast cells cannot be extracted without disruption of their wall. We favor a method where the wall is disrupted with glass beads. The mass of glass beads used to disrupt yeast cells and the time needed for disruption vary greatly with the shape of container, the number of yeast, and their growth stage. The figures we give are based upon no more than 5×10^7 cells in a 0.3-ml volume in the indicated Falcon tubes. Another significant variable is the power of the vortexer and the way the tube is held. For best breakage, the tube should be held lightly enough that it "rides up" into the hand. As this happens, the glass beads make a sound like sand scratching against the walls of the tube. We also wet the suction cup of the vortexer to ensure that the tube adheres but is also free to move.
13. The volumes of solvents given are in the ratios worked out empirically by Folch in the 1940 s. These ratios should be $CHCl_3$:CH_3OH:acidified dH_2O (13.3:6.7:1, by volume). This mixture should be monophasic (i.e., not splitting into two distinct layers; if it does, then add methanol dropwise and vortex until it goes clear). Note that when large amounts of yeast are disrupted, the extraction can be very cloudy because of protein. To distinguish the two, place the sample back on ice for a minute and then look again. If a layer is forming at the top of the extraction, more methanol is needed. It is important for effective extraction that the solution is monophasic because then the hydration shells of the PPIn are effectively removed and they are more likely to be retained in the lower layer during extraction.
14. Once acid is added at this step, a two-phase system is formed. The whole extraction now has the composition $CHCl_3$:CH_3OH:dH_2O (8:4:3, by volume). This is the desired solvent ratio adapting this method to larger or smaller samples. It is essential that after the addition of acid, the extraction is well mixed, or proper partitioning between the phases will not occur. The upper phase is 40% of total volume (in this case, 1 ml) and is of composition $CHCl_3$:CH_3OH:dH_2O (3:48:47, by volume). The lower phase ($\sim$1.5 ml, containing PPIn) is $CHCl_3$:CH_3OH:dH_2O (86:14:1, by volume). Note that this is an unstable two-phase system, unlike that between immiscible hydrocarbons and water. This means that the volumes and compositions of the upper and lower phases are dictated by the proportions of the various solvents: It is important to get all volumes correct.
15. The *n*-butanol:petroleum ether:ethyl formate partition step removes the monomethyl fatty acids created during deacylation. Essentially, during deacylation, fatty acids that are ester-linked to phospholipids are attacked and transacylated to the monomethylamine. The hydrophobic fatty acid methyl esters must be removed. The *n*-butanol provides a medium less dense than water; the petroleum ether makes this upper phase very nonpolar; and the ethyl formate inactivates any residual monomethylamine.
16. The two-phase system formed by water and the above mixture is fairly stable. The lower aqueous phase contains the [^{3}H] glycerophosphoinositol-based phospholipid backbones and also the unlabeled glycerophosphoester head groups of other phospholipids. The upper organic layer contains fatty acid methyl esters and nonsaponifiable lipids (sterols, sphingolipids, and phospholipids with alkyl or alkenyl substituents, etc.).
17. HPLC columns are expensive. There are several precautions that maximize their life and maintain their analytical resolution. First, the silica matrix of the column is slightly soluble in water. Dissolution of the column matrix is minimized by use of a prepacked silica guard cartridge that saturates the incoming mobile phase with silica. The guard cartridge must be flushed through with water to remove residues and fines before connection ahead of the main column. The guard cartridge traps particulates and impurities in the samples, reducing their access to the analytical column. Whatman sells a dedicated inline holder for its Partisphere prepacked guard cartridges that saves

the effort of repacking them. We change the guard cartridge when the backpressure from a guard cartridge plus 250-mm column, equilibrated with 100% water, is greater than 1,300 psi (values from Gilson system); or after two months use; or after 40 runs, whichever is reached first.

18. A second factor that influences the lifetime of the column is the speed with which the flow rate is changed. Rapid changes in flow rate can cause compaction or cavitation of the column matrix, reducing flow rates and column life. We change flow rates at no more than 0.1 ml/min per min: for example, a change in flow rate from 1 ml/min to zero should take $\geq$10 min. If the above precautions are observed, one column can yield over 300 analyses.

References

1. Berridge MJ, Heslop JP, Irvine RF, Brown KD. Inositol trisphosphate formation and calcium mobilization in Swiss 3T3 cells in response to platelet-derived growth factor. Biochem J 1984;222:195–201.
2. Giudici ML, Hinchliffe KA, Irvine RF. Phosphatidylinositol phosphate kinases. J Endocrinol Invest 2004;27:137–42.
3. Gonzales ML, Anderson RA. Nuclear phosphoinositide kinases and inositol phospholipids. J Cell Biochem 2006;97:252–60.
4. Irvine RF. 20 years of Ins(1,4,5)P_3, and 40 years before. Nat Rev Mol Cell Biol 2003;4:586–90.
5. Rebecchi MJ, Pentyala SN. Structure, function, and control of phosphoinositide-specific phospholipase C. Physiol Rev 2000;80:1291–335.
6. Vanhaesebroeck B, Leevers SJ, Ahmadi K, Timms J, Katso R, Driscoll PC, Woscholski R, Parker PJ, Waterfield MD. Synthesis and function of 3-phosphorylated inositol lipids. Ann Rev Biochem 2001;70:535–602.
7. Birkeland HC, Stenmark H. Protein targeting to endosomes and phagosomes via FYVE and PX domains. Curr Top Microbiol Immunol 2004;282:89–115.
8. Komander D, Fairservice A, Deak M, Kular GS, Prescott AR, Downes CP, Safrany ST, Alessi DR, van Aalten DM. Structural insights into the regulation of PDK1 by phosphoinositides and inositol phosphates. EMBO J 2004;23:3918–28.
9. Stephens L, Williams R, Hawkins P. Phosphoinositide 3-kinases as drug targets in cancer. Curr Opin Pharmacol 2005;5:357–65.
10. Michell RH, Heath VL, Lemmon MA, Dove SK. Phosphatidylinositol 3,5-bisphosphate: Metabolism and cellular functions. Trends Biochem Sci 2006;31:52–63.
11. Hokin LE. Dynamic aspects of phospholipids during protein secretion. Int Rev Cytol 1968;23:187–208.
12. Michell RH. Inositol phospholipids and cell surface receptor function. *Biochim Biophys Acta* 1975;415:81–147.
13. Creba JA, Downes CP, Hawkins PT, Brewster G, Michell RH, Kirk CJ. Rapid breakdown of phosphatidylinositol 4-phosphate and phosphatidylinositol 4,5-bisphosphate in rat hepatocytes stimulated by vasopressin and other Ca2 + -mobilizing hormones. Biochem J 1983;212:733–47.
14. Stephens LR, Hughes KT, Irvine RF. Pathway of phosphatidylinositol(3,4,5)-trisphosphate synthesis in activated neutrophils. *Nature* 1991;351:33–9.
15. Dove SK, Cooke FT, Douglas MR, Sayers LG, Parker PJ, Michell RH. Osmotic stress activates phosphatidylinositol-3,5-bisphosphate synthesis. Nature 1997;390:187–92.
16. Pendaries C, Tronchere H, Racaud-Sultan C, Gaits-Iacovoni F, Coronas S, Manenti S, Gratacap MP, Plantavid M, Payrastre B. Emerging roles of phosphatidylinositol monophosphates in cellular signaling and trafficking. Adv Enzyme Regul 2005;45:201–14.

17. Dove SK, Piper RC, McEwen RK, Yu JW, King MC, Hughes DC, Thuring J, Holmes AB, Cooke FT, Michell RH, Parker PJ, Lemmon MA. Svp1p defines a family of phosphatidylinositol 3,5-bisphosphate effectors. EMBO J 2004;23:1922–33.
18. Folch J, Ascoli I, Lees M, Meath JA, Le BN. Preparation of lipide extracts from brain tissue. J Biol Chem 1951;191:833–41.
19. Folch J, Lees M, Sloane Stanley GH. A simple method for the isolation and purification of total lipides from animal tissues. J Biol Chem 1957;226:497–509.
20. Bligh EG, Dyer WJ. A rapid method of total lipid extraction and purification. Can J Biochem Physiol 1959;37:911–7.

Chapter 5
Methods for the Determination of the Mass of Nuclear PtdIns4*P*, PtdIns5*P*, and PtdIns(4,5)P_2

David R. Jones, Yvette Bultsma, Willem Jan Keune and Nullin Divecha

Abstract Phosphatidylinositol (PtdIns) and its phosphorylated derivatives represent less than 5% of total membrane phospholipids in cells. Despite their low abundance, they form a dynamic signaling system that is regulated in response to a variety of extra- and intracellular cues [1]. Protein domains including PH, FYVE, ENTH, PHOX, PHD fingers, and lysine-/arginine-rich patches can bind to specific phosphoinositide isomers, which, in turn, can induce changes in the subcellular localization, posttranslational modification, protein interaction partners, or activity of the protein containing such a domain [2, 3]. Phosphoinositides and the enzymes that synthesize them are found in many different subcellular compartments including the nuclear matrix, heterochromatin, and sites of active RNA splicing, suggesting that phosphoinositides may regulate specific functions within the nuclear compartment [4–6]. The existence of distinct subcellular pools has led to the challenging task of the quantitation of temporal and spatial changes in phosphoinositides. We report methods to measure the mass levels of three different phosphoinositides within the nuclear compartment.

Keywords Neomycin affinity chromatography · phosphatidylinositol-5-phosphate · phosphatidylinositol-4-phosphate · phosphoinositides · nuclear lipid signaling

5.1 Introduction

Historically, short-term radiolabeling of cultured cells with [^{32}P]orthophosphate followed by crude separation of [^{32}P]-labeled phoshoinositides by simple thin-layer chromatography (TLC) or by high-performance liquid chromatography (HPLC) of the deacylated head group has been the method of choice for determining the levels of different phosphoinositides [7]. However, such

N. Divecha
The Inositide Laboratory, The Paterson Institute for Cancer Research, Wilmslow Road, Manchester, m20 4BX
e-mail: ndivecha@picr.man.ac.uk

B. Larijani et al. (eds.), *Lipid Signaling Protocols*, DOI: 10.1007/978-1-60327-115-8_5,

methods are laborious and require dedicated equipment and specialized personnel. Radiolabeling methods also assume that the incorporation of the radiolabel is an indication of the mass of the phosphoinositide, an assumption that is rarely demonstrated. Novel technologies have recently emerged that utilize specific phosphoinositide recognition domains fused to fluorescent proteins to identify the subcellular localization of specific phosphoinositide isomers using microscopy [8,9]. While this has been successful in some instances, it is clear that further characterization of why and how these probes recognize specific membrane compartments is required [9–12].

Subcellular fractionation followed by the use of assays that are relatively simple, robust, and able to measure the mass of a given phosphoinositide isomer would be the preferred method of choice [13,14]. It should be noted, however, that a major drawback of this methodology is the requirement for subcellular fractionation, which may lead to artifactual changes in phosphoinositide levels due to their metabolism or changes in their intracellular location. With these caveats in mind, we describe methods to measure the phosphoinositides PtdIns4*P*, PtdIns5*P*, and PtdIns(4,5)P_2 in isolated nuclear fractions [15]. The PtdIns4*P* and PtdIns5*P* [13] assays are based on the specificity of two enzymes: a phosphatidylinositol-4-phosphate-5-kinase (PIP5 K) that phosphorylates PtdIns4P on the 5' position of the inositol head group [16] and a phosphatidylinositol-5-phosphate-4-kinase (PIP4 K), which phosphorylates PtdIns5*P* on the 4' position [17]. The PH domain from PLCδ1, which specifically interacts with PtdIns(4,5)P_2, is used to develop a dot-blot assay for the measurement of PtdIns(4,5)P_2. Because all the procedures require prior purification of phosphoinositides away from the bulk phospholipids, we describe a rapid and miniaturized method, based on previously established methods [18,19], for the affinity purification of phosphoinositides using neomycin-coated glass beads.

5.2 Materials

5.2.1 Cell Culture and Nuclear Isolation

1. Dulbeco's modified Eagle's medium (DMEM) (Invitrogen) supplemented with 10% fetal bovine serum.
2. Swell buffer: 5 mM Tris-HCl, pH 7.4, 1.5 mM KCl, 2.5 mM $MgCl_2$. This can be made as a 20-times stock and stored at 4°C.
3. 1.8 M sucrose.
4. 1 M $MgCl_2$.
5. 33 mM EGTA.
6. Cushion buffer: 10 mM Tris-HCl, pH 7.4, 1 mM EGTA, 1.5 mM KCl, 5 mM $MgCl_2$, 460 mM sucrose. This can be made as a 20-times stock without the sucrose and stored at 4°C.

7. Final resuspension buffer (FRB): 10 mM Tris-HCl, pH 7.4, 1 mM EGTA, 1.5 mM KCl, 5 mM $MgCl_2$, 290 mM sucrose. This can be made as a 20-times stock without the sucrose and stored at 4°C.
8. Nuclear membrane strip solution: 10 mM Tris-HCl, pH 7.4, 1 mM EGTA, 1.5 mM KCl, 5 mM $MgCl_2$ 290 mM sucrose, 0.3% Triton X-100.
9. Swing out centrifuge (Hereus Megafuge 1.0) cooled to 4°C.
10. 10-ml Polyallomer centrifuge tubes (Beckman Cat. no. 326814).

5.2.2 *Lipid Extraction and Phosphoinositide Purification Using Neomycin-Coated Glass Beads*

1. 2.4 M HCl.
2. Theoretical upper phase (TUP): 235 ml of methanol, 15 ml of chloroform, and 235 ml of 1 M HCl can be prepared and stored in a glass bottle.
3. Ammonium formate buffer (AF): 100 ml of chloroform, 200 ml of methanol, 3.2 ml of 2 M ammonium formate, and 16.2 ml of H_2O can be prepared and stored in a glass bottle.
4. Neomycin-coated glass beads (prepared exactly as described in Schacht [18]). The beads are washed three times with AF buffer and resuspended such that 30 ul yields a packed pellet of 20 ul. The beads are stored at room temperature in AF buffer in a glass bottle.
5. Neomycin elution buffer: 5 ml of chloroform, 10 ml of methanol, 4 ml of 2.4 M HCl.

5.2.3 *PtdIns5*P *and PtdIns4*P *Assay*

1. PtdIns4*P* and PtdIns5*P* lipid standards (Sichem or Echelon) adjusted to 1 μmol/ml. Synthetic commercial phosphoinositides are normally produced as ammonium salts, which are relatively insoluble in chloroform. In order to solubilize the lipids, we routinely convert them to the acidic form (*see* Note 1).
2. Phosphatidylserine (10 mM in chloroform; Sigma Cat. no. p3660).
3. Phosphatidic acid (3 mM in chloroform; Sigma).
4. 2xPIPkin buffer: 100 mM Tris-HCl, pH 7.4, 20 mM $MgCl_2$, 2 mM EGTA, 140 mM KCl.
5. GST-PIP4Kalpha (phosphatidylinositol-5-phosphate 4-kinase alpha) purified after expression in bacteria (*see* Note 2).
6. GST-mPIP5Kalpha (murine phosphatidylinositol-4-phosphate 5-kinase alpha) purified after expression in HEK293 mammalian cells (*see* Note 2).
7. Stop solution: 50 ml of chloroform; 50 ml of methanol; 400 μl of Folch extract [Sigma type I Folch fraction from bovine brain (Cat. no. 030K7063) at a stock concentration of 1 mg/ml in chloroform]. It can be stored at –20°C in a glass bottle.

8. TLC plates: Silica gel TLC plates (Merck Cat. no. 1.05721.0001) are dipped in a solution of 1% potassium oxalate, 1 mM EDTA (*see* Note 3), and then placed in an oven (110°C) for 1 h.
9. TLC developing solution: chloroform:methanol:28% ammonia:H_2O (45:35:2:8) should be prepared fresh, placed into a TLC tank containing two pieces of Whatman 3 MM paper (20 cm × 20 cm), and allowed to equilibrate for 1 h before plate development.

5.2.4 PtdIns(4,5)P_2 Assay

1. Nitrocellulose membranes (Schleicher and Schull, 0.45-μm pore size).
2. GST-$PH^{PLC\delta1}$ purified after expression in bacteria (*see* Note 4).
3. TBS-0.05%Tween-20: 50 mM Tris-HCl, pH 8.0, 140 mM NaCl, 0.05%v/v Tween-20.
4. PtdIns(4,5)P_2 standard (Sichem or Echelon) dissolved and stored in chloroform at 1 μmol/ml after washing the lipid with HCl to bring it to its acidic form (*see* Note 1).

5.2.5 Mass Assay of Phospholipid Phosphate

1. Clean high-temperature-resistant glass tubes.
2. Concentrated perchloric acid.
3. 2.5% ammonium molybdate.
4. 10% ascorbic acid freshly prepared in water (0.5 g in 5 ml).

5.3 Methods

All organic solvents should be of the highest quality available (HPLC grade or better) and high-purity water (Milli-Q) should be used for the preparation of all aqueous solutions. All operations are performed at room temperature unless otherwise stated.

5.3.1 Growth, Differentiation, and Stress Stimulation of MEL Cells

1. MEL cells are routinely maintained at a density of 0.2–1.0 × 10^6 cells/ml in DMEM-10%FBS at 37°C.
2. MEL cell differentiation: MEL cells are diluted to 0.1 × 10^6 cells/ml and then either maintained as control cells or differentiated by the addition of 1.5% DMSO. After four days, 90% of the cells are differentiated as assessed by staining for hemoglobin.

3. UV irradiation or H_2O_2 stimulation of MEL cells: MEL cells are diluted to 0.2×10^6 cells/ml on day 1 and on day 2 are treated with UV irradiation or H_2O_2 (1 mM). For UV irradiation, cells (100 ml) are centrifuged ($352 \times g$) and the cell pellet resuspended in 5 ml of DMEM-FBS and spread on a 10-cm-diameter culture plate. The lid is removed and the cells are irradiated with 500 J/m^2 using a Stratagene DNA cross linker. The cells are diluted to 100 ml and maintained in culture for 1 h [15].

5.3.2 Nuclear Isolation

1. 2×10^6 cells are pelleted by centrifugation ($352 \times g$) and washed once with ice-cold PBS (25 ml). The PBS is decanted and the remaining PBS is removed using a tissue.
2. The cells are resuspended in 5 ml of swell buffer and maintained on ice for 5 min. The cells are then disrupted by two passages through a 22-gauge needle using a 6-ml syringe before being transferred to a 10-ml polyallomer centrifuge tube (*see* Note 5).
3. To stabilize the nuclei, 800 µl of 1.8 M sucrose, 150 µl of 33 mM EGTA, and 25 µl of 1 M $MgCl_2$ are added and the nuclei are pelleted by centrifugation (4 min, $352 \times g$, 4°C) (*see* Note 6).
4. The supernatant is removed (*see* Note 7), the nuclei are resuspended in 1 ml of ice-cold FRB, and 5 ml of ice-cold cushion is layered directly underneath. The nuclei are pelleted through the sucrose cushion by centrifugation (4 min, $352 \times g$, 4°C) and washed once with 5 ml of ice-cold FRB.
5. To remove the nuclear membrane, the nuclear pellet is resuspended in 5 ml of nuclear membrane strip solution and incubated on ice for 5 min. The nuclei are pelleted by centrifugation, washed once with 5 ml of ice-cold FRB, and finally resuspended in 300 µl of ice-cold FRB.
6. The protein concentration is determined using a Bradford assay (Biorad) and compared to BSA standards.

5.3.3 Lipid Extraction and Phosphoinositide Purification Using Neomycin-Coated Glass Beads

1. 200 µg of nuclear protein is made up to 200 µl with FRB in a 1.5-ml Eppendorf tube. 500 µl of methanol and 250 µl of chloroform are sequentially added. The tubes are left at room temperature for 15 min, after which 250 µl of chloroform and 250 µl of 2.4 M HCl are added. After vigorous mixing, centrifugation (maximum speed in an Eppendorf microfuge for 1 min) yields two phases. 800 µl of the upper phase is carefully removed and discarded. The lower organic phase, containing the phosphoinositides, is washed by the addition of 800 µl of TUP. The tube contents are mixed and centrifuged, and the lower organic phase is transferred to a new 1.5-ml Eppendorf tube and

dried by rotary evaporation. All traces of water and methanol must be removed from the total lipid extracts before progressing to subsequent steps (outlined below) or storage at −20°C. Storage at −20°C for more than a few days should be avoided.

2. The dried total phospholipid extract is dissolved in 950 µl of AF buffer and 30 µl of neomycin-coated bead suspension is added to give a final packed bead volume of approximately 20 µl. The beads are kept in suspension by end-over-end tumbling for 15 min at room temperature to allow phosphoinositide interaction with the neomycin-coated beads. The beads are then pelleted by centrifugation (maximum speed in an Eppendorf microfuge for 1 min) and the supernatant is decanted into a high-temperature-resistant glass tube. The supernatant contains all phospholipids except PtdInsPs, $PtdInsP_2$s, and $PtdInsP_3$ and constitutes over 95% of the starting phospholipid phosphate content (see Subheading 5.3.6), which proves extremely useful for normalization of the data obtained with the specific mass assays for phosphoinositides.
3. The neomycin beads are washed twice with 1 ml of AF buffer and the phosphoinositides are eluted by resuspension in 950 µl of neomycin elution buffer. The tubes are tumbled end over end for 15 min at room temperature to aid elution of the phosphoinositides, after which the beads are pelleted by centrifugation. The supernatant is carefully decanted into a new Eppendorf tube into which 250 µl of chloroform and 250 µl of H_2O are added. The tubes are vigorously mixed and centrifuged, and the lower phase is removed into a new Eppendorf tube and dried by rotary evaporation.
4. The neomycin-coated glass beads are allowed to dry, after which they are transferred back into a glass bottle containing AF buffer. When all of the beads have been used, the batch is washed with methanol, then water, and finally three times with 1 mM HCl. The beads are then washed in water, then methanol, and then rewashed three times back into AF buffer. After three cycles of use, the efficiency of the neomycin-coated glass beads to bind phosphoinositides is dampened but may be restored by reduction with sodium borohydride [18].

*5.3.4 PtdIns5***P** *and PtdIns4***P** *Mass Assay*

1. The dried phosphoinositides are resuspended in 500 µl of chloroform, and 50 µl is removed into a new Eppendorf tube for PtdIns4*P* measurement. The remaining 450 µl are used to measure PtdIns5*P* (*see* Note 8).
2. A standard curve for PtdIns4*P* and PtdIns5*P* is generated by placing 2, 5, 10, 20, 50, and 100 pmoles of the standard lipid into Eppendorf tubes.
3. 10 nmoles of phosphatidylserine (1 µl) and 3 nmoles of phosphatidic acid (1 µl) are added to every tube and the lipids are dried by rotary evaporation (*see* Note 9).

4. 50 µl of diethylether is added to each tube followed by 100 µl of 10 mM Tris-HCl, pH 7.4. The Eppendorf tubes are then capped, vortexed, and sonicated in a bath sonicator (20 s each tube). The lipid solution is then gently centrifuged (300 rpm in an Eppendorf microfuge for 30 s) before the diethylether is removed by rotary evaporation for 5 min (*see* Note 10).
5. A master mix is prepared containing 2xPIPkin, 20 µM ATP, 2 µCi [^{32}P]ATP, 0.5 µg GST-PIP4K (for the PtdIns5*P* assay), or GST-PIP5K (for the PtdIns4*P* assay). 100 µl of the master-mix solution is added to each tube to start the reaction and incubated at 30°C for 2 h.
6. The reactions are stopped by the addition of 1 ml of stop solution followed by 250 µl of 2.4 M HCl. The tubes are vigorously shaken and then centrifuged. The lower phase, containing the radiolabeled phosphoinositides, is removed into a new Eppendorf tube and dried by rotary evaporation. The upper phase, which contains the majority of the free [^{32}P]ATP, is discarded.
7. [^{32}P]PtdIns(4,5)P_2 is separated from other phosphoinositides and residual-free ATP by TLC. 0.5-cm pencil lines, 1 cm apart, are marked 1.5 cm above the bottom of the TLC plate. The samples are resuspended in 8 µl of chloroform:methanol (90:10) and spotted onto the pencil marks. The Eppendorf tube is washed with a further 8 µl of chloroform:methanol (90:10), and the wash is spotted on top of the original sample. The spotted samples are allowed to dry for 10 min at room temperature before development in a TLC tank containing 70 ml of TLC developing solution until the solvent front reaches 4 cm from the top (*see* Note 11).
8. Quantitation of the radioactivity in [^{32}P]PtdIns(4,5)P_2 is carried out using a phosphoimager (we routinely use the Fuji BAS reader) or by exposing the dried TLC to X-ray film followed by scraping off the silica containing the [^{32}P]PtdIns(4,5)P_2 and quantitation by Cerenekov counting. Densitometry of the exposed developed X-ray film is not recommended. The absolute number of pmoles of PtdIns4*P* or PtdIns5*P* is defined by comparison with the standard curves (Fig. 5.1a, b). The analysis of both PtdIns5*P* and PtdIns4*P* is linear between 1 and 50 pmoles of phosphoinositide input. It is important that investigators establish the linearity of the assay procedures for any biological sample at the beginning of a new study. Previous data have shown that PIP4K alpha can phosphorylate PtdIns3*P* and in some rare instances phosphorylate PtdIns4*P* to generate [^{32}P]PtdIns(4,5)P_2. We outline two procedures to assess both of these potential problems (*see* Notes 11 and 12).

5.3.5 *PtdIns(4,5)*P_2 *Mass Assay*

1. Phosphoinositides purified by neomycin-coated bead affinity chromatography (*see* Note 13) are dried in 0.5-ml Eppendorf tubes, dissolved in 2 µl of chloroform, and applied to pencil-marked spots on a dry nitrocellulose

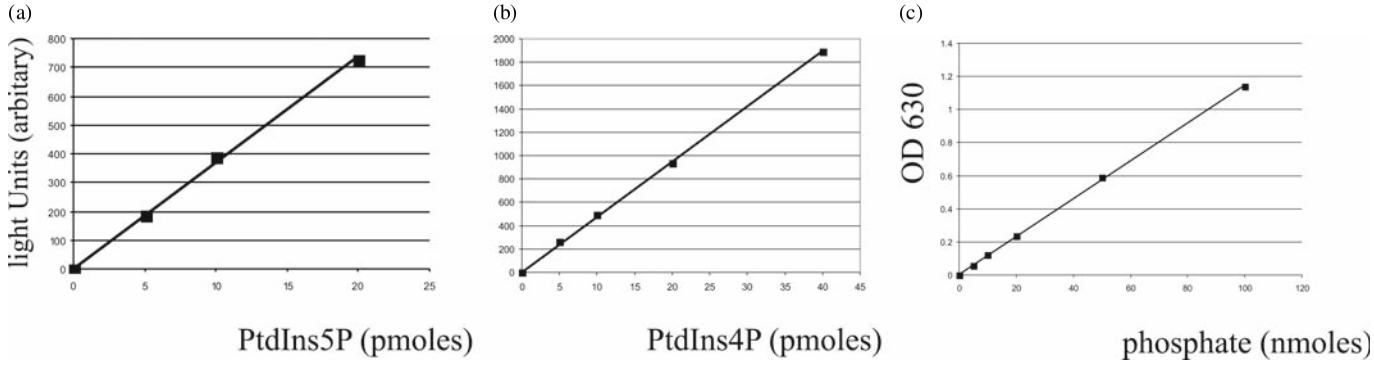

Fig. 5.1 Known amounts of (a) PtdIns5*P* standard and (b) PtdIns4*P* standard were dried and phosphorylated in the presence of [^{32}P]ATP using either (a) GST-PIP4K alpha or (b) GST-PIP5K alpha. The labeled phosphoinositides were separated by TLC and quantitated using a phosphorimager. (c) Standard amounts of phosphate (nmoles) were dried and subjected to phosphate analysis and the reaction was quantitated by measuring the absorbance at 630 nM. The squares show the actual data, while the black line indicates a trend line used to calculate quantities in any sample

membrane. The Eppendorf tube is washed with 2 µl of chloroform which is applied on top of the original spot. Samples are spotted 1 cm apart.

2. A standard curve of PtdIns(4,5)P_2 (0.39, 0.78, 1.56, 3.125, 6.25, 12.5, 25 pmoles) dissolved in 2 µl of chloroform is spotted in duplicate 1 cm apart on the same piece of nitrocellulose membrane as the samples under investigation.
3. The samples and standards are dried at room temperature for 10 min before wetting the nitrocellulose membrane in distilled water and then in TBS-Tween. The membrane is blocked using TBS-Tween, 1% BSA, for 30 min and then incubated overnight with GST-$PH^{PLC\delta1}$ (0.1 µg/ml) diluted in TBS-Tween, 1% BSA, at 4°C.
4. The membrane is washed three times (5 min each) with TBS-Tween and then incubated with a monoclonal antibody directed against GST (clone 2F3) diluted (1:100) in TBS-Tween, 1% BSA, for 1 h.
5. The membrane is washed three times (5 min each) with TBS-Tween and then incubated with an anti-mouse antibody conjugated to horseradish peroxidase (DAKO) diluted (1:20,000) in TBS-Tween, 1% BSA, for 20 min.
6. The membrane is washed three times (5 min each) with TBS-Tween and then once with distilled water. The interaction between the GST-$PH^{PLC\delta1}$ and PtdIns(4,5)P_2 is visualized using chemiluminescent reagent (Super Signal, Pierce). Quantitation is carried out using a CCD camera to capture light output (*see* Note 14). Light is captured at the highest sensitivity and lowest resolution. For high-resolution pictures, the blot is exposed to X-ray film (*see* Note 15). PtdIns(4,5)P_2 levels are quantitated by comparison with the standard curve (Fig. 5.2).

5.3.6 Mass Assay of Phospholipid Phosphate

1. A 1 mM solution of potassium phosphate is used to generate a standard curve (0, 5, 10, 20, 50, 100, 150 nmoles) of phosphate and, together with the samples derived from the supernatants from the neomycin-coated bead column, are dried in ultra clean (phosphate-free) 15-ml glass tubes (*see* Note 16) in an 80°C oven overnight.
2. 50 µl of concentrated perchloric acid is added to each tube followed by incubation at 180°C for 30 min using a heating block in a fume cupboard.
3. After cooling to room temperature, 250 µl of water, 50 µl of 2.5% (w/v) ammonium molybdate, and 50 µl of freshly prepared 10% (w/v) ascorbic acid are sequentially added and incubated at room temperature until color development is complete (at least 2 h). 150 µl is pipetted in duplicate into the wells of a flat-bottomed, transparent 96-well microtiter plate and the absorbance is measured at a wavelength of 630 nm using a spectrophotometer plate reader. Quantitation of phospholipid phosphate in the unknown samples is performed by comparison with the standard curve (Fig. 5.1c).

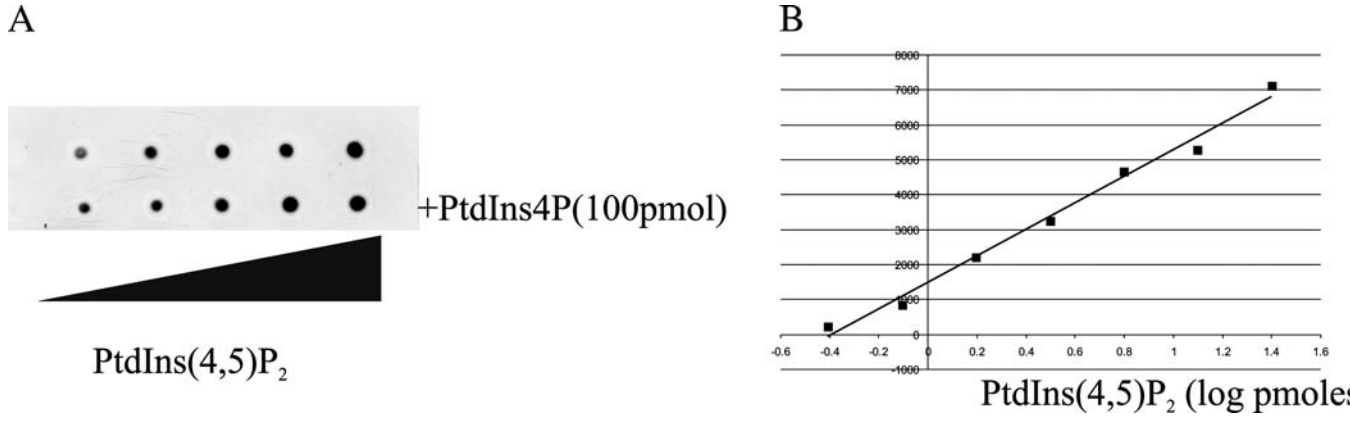

Fig. 5.2 Increasing standard amounts of PtdIns(4,5)P_2 were either spotted alone or in the presence of 100 nmoles of PtdIns4*P* onto a piece of nitrocellulose membrane. The membrane was then subjected to PtdIns(4,5)P_2 analysis. (a) There is little effect on the standard curve of spotting PtdIns(4,5)P_2 in the presence of an excess of PtdIns4*P*. (b) A plot of the log[PtdIns(4,5)P_2] against light captured during chemilluminescent detection of the GST-PH$^{PLC\delta1}$–PtdIns(4,5)P_2 interaction. The squares show the actual data, while the line indicates a trend line used to calculate the level of PtdIns(4,5)P_2 in a biological sample

Notes

1. To convert phosphoinositides into their acidic form, the dried lipid is resuspended in 1 ml of chloroform/methanol (1:1 v/v) transferred into an Eppendorf tube and 200 µl of H_2O and 250 µl of 2.4 M HCl are added. The tube is vigorously shaken and then centrifuged (maximum speed for 1 min in an Eppendorf microfuge), and 750 µl of the upper phase is removed and discarded. The lower phase is washed with 750 µl of TUP. The lower phase is removed into a new Eppendorf tube. 10 µl of the lower phase is dried in a clean glass tube and used to measure the total amount of phospholipid phosphate (*see* Subheading 5.3.6). PtdIns4*P* and PtdIns5*P* each contain two phosphate groups. Therefore, the number of moles obtained in the phosphate assay is twice the number of moles of starting lipid. For PtdIns(4,5)P_2 the amount of phosphate represents three times the number of moles of starting lipid. The remainder of the lower phase is dried and resuspended in chloroform (adjusted to 1 nmole lipid/ml) and stored at −20°C in a clean glass tube closed with a Teflon-coated cap (Supelco).
2. cDNA clones encoding GST-PIP4K and GST-PIP5K and protocols for their isolation are available on request from N. Divecha.
3. Preparation of TLC dipping solution: A 1.5-L solution of 2% potassium oxalate, 2 mM EDTA in water is diluted with 1.5 L of methanol. This solution is then placed in a spare TLC tank and TLC plates are dipped in one direction (the undipped area is designated the top of the plate and should be marked with a pencil) and dried in an oven (110°C). The dipping solution can be stored in the TLC tank at 4°C for at least three months.
4. A cDNA clone used for bacterial expression of GST-$PH^{PLC\delta1}$ and the protocol for its purification is available on request from N. Divecha.
5. Nuclei can be isolated from smaller numbers of cells, in which case the cells are resuspended in 1 ml of swell buffer and disrupted using a 1-ml syringe. The sucrose cushion buffer can be layered carefully directly underneath the disrupted cell solution and centrifuged as stated. For different cell types, different gauge needles may yield cleaner nuclei. For example, passage of HeLa cells through a 25-gauge needle yields much purer nuclei than through a 23-gauge needle. The purity of nuclei can be rapidly assessed microscopically. Clean nuclei display a rounded morphology, whereas contaminated nuclei display an abundance of cytoskeletal material attached to the nuclei. A more thorough assessment of contamination can be carried out by Western blotting analysis using antibodies directed against actin (Chemicon Cat. no. MAB-150-1R) and tubulin (anti-α-tubulin, Sigma Cat. no. T5168). However, care should be taken, as numerous studies have demonstrated the presence of actin in nuclei and in a number of chromatin remodeling complexes.
6. If nuclei are unstable (manifested by an inability to pellet and to resuspend the nuclei during the wash procedures), the addition of spermine (0.15 mM) and spermidine (0.1 mM) immediately after hypotonic lysis should alleviate this problem. We have also found that some batches of sucrose tend to increase nuclear instability. Therefore, we always use molecular biology-grade sucrose (Sigma) that is both RNAse- and DNAse-free.
7. The supernatant contains the light (plasma membranes and endoplasmic reticulum) and the heavy (mitochondria, lysosomes, and rough endoplasmic reticulum) membranes, which can be further fractionated by sucrose gradient centrifugation, or total membranes can be isolated by centrifugation at 100,000 × *g* for 1 h.
8. The assays for PtdIns4*P* and PtdIns5*P* show approximately the same sensitivity and are linear in approximately the same range. In mammalian cells, *C. Elegans* and *Drosophila* PtdIns4*P* constitutes 6 to 10 times the amount of PtdIns5*P* (our unpublished data). Thus, only 10% of the affinity-purified phosphoinositide is used for the PtdIns4*P* assay. However, the amount of material required for a PtdIns4*P* or PtdIns5*P* assay should be empirically determined at the beginning of a new study.
9. If the eluted phosphoinositides are to be used solely for PtdIns4*P* and PtdIns5*P* assays, then the phosphatidylserine and phosphatidic acid may be added directly to the neomycin elution buffer.

10. Samples can be sonicated directly into 10 mM Tris-HCl, pH 7.5, using a bath sonicator. However, for a large number of samples, we have found this to be irreproducible. The use of diethylether is a modification of a previously described method to generate liposomes and in our hands yields very reproducible solubilization of phosphoinositides. Removal of the diethylether should not exceed 5 min.
11. *In vitro* PIP5K can phosphorylate a number of different phosphoinositides including PtdIns3*P*. However, in biological samples we have never observed the formation of [^{32}P]PtdIns(3,5)P_2 [PtdIns(3,5)P_2 is separated from PtdIns(4,5)P_2 using the TLC system described]. *In vitro* PIP4K can phosphorylate both PtdIns5*P* and PtdIns3*P*, but it shows a preference for PtdIns5*P*. If the levels of PtdIns3*P* are higher than PtdIns5*P*, then in some instances we have seen the production of PtdIns(3,4)P_2. In the TLC system described, PtdIns(3,4)P_2 will migrate slightly below PtdIns(4,5)P_2. To separate PtdIns(3,4)P_2 from PtdIns(4,5)P_2, the simplest strategy is to deacylate the lipids and to separate the corresponding glycerophosphoinositol bisphosphates using PEI cellulose TLC plates (Merck). Briefly, the dried lipids are deacylated by the addition of 200 µl of monomethylamine reagent [100 µl of monomethylamine (fluka 41% in H_2O) and 100 µl of methanol] and incubated with continuous mixing for 50 min at 53°C. The monomethylamine is removed by rotary evaporation (this takes approximately 2–3 h) and the glycerophosphoinositol bisphosphates are then dissolved in 200 µl of H_2O. This solution also contains the fatty acids, which are removed by washing with 200 µl of a mixture of *n*-butanol:petroleum ether (bp 40–60°C):ethyl-formate (20:4:1, v/v/v). The tubes are shaken vigorously and centrifuged, and the upper phase is discarded. Another 150 µl of the organic solvent mixture is added, mixed thoroughly, and centrifuged, and the lower aqueous phase is removed into a clean 0.5-ml Eppendorf tube and dried by rotary evaporation. The glycerophosphoinositol bisphosphates are dissolved in 2 µl of 10 mM potassium phosphate and are spotted onto a PEI cellulose TLC plate 1.5 cm from the bottom. The Eppendorf tube is washed with 2 µl of 10 mM potassium phosphate that is then spotted on top of the original spotted sample. The TLC plate is developed in a tank containing 70 ml of 0.48 M HCl. Standards of deacylated PtdIns(3,4)P_2 and PtdIns(4,5)P_2 are easily generated using GST-PIP4K to phosphorylate 1 nmole of either PtdIns3*P* or PtdIns5*P* under the conditions outlined in the PtdIns5*P* assay followed by their deacylation.
12. To demonstrate that GDT-PIP4K phosphorylates only PtdIns5*P*, after TLC the area of silica containing the [^{32}P]PtdIns(4,5)P_2 is scraped into a 1.5-ml Eppendorf tube (this must be carried out within 3–4 h of developing the TLC, as otherwise recovery of the lipid is dramatically reduced). Then 500 µl of methanol, 200 µl of 2.4 M HCl, and 250 µl of chloroform are added; the tube contents are mixed, briefly sonicated, and incubated at room temperature for 30 min. The silica is then pelleted by centrifugation (maximum speed in an Eppendorf microfuge for 1 min) and the supernatant is decanted into a new 1.5-ml Eppendorf tube. 250 µl of chloroform and 250 µl of H_2O are added to the supernatant, and the tube contents are thoroughly mixed and centrifuged to generate two phases. The lower organic phase is removed into a new 1.5-ml Eppendorf tube and dried by rotary evaporation. The PtdIns(4,5)P_2 is resuspended using the diethylether (see 5.3.4 Section 4). After removal of the diethylether, 1 µl of Span-20 (100% stock) detergent is added. The reaction is initiated by the addition of 100 µl of 2xPIPkin buffer and 1 µl of recombinant yeast phosphoinositide-5-phosphatase. After incubation for 1 h at 30°C, the lipids are extracted (as described in the PtdIns4*P* assay) and then separated by TLC (as described for the PtdIns5*P* assay), and the radioactivity present in PtdIns(4,5)P_2 and in PtdIns*P* is assessed by phosphorimaging analysis. Because the phosphatase specifically removes the phosphate group on the 5' position of PtdIns(4,5)P_2, any decrease in radioactivity associated with PtdIns(4,5)P_2 (due to its dephosphorylation) should appear as radiolabeled PtdIns*P*.
13. Elution of phosphoinositides for PtdIns(4,5)P_2 analysis is carried out using 500 µl of neomycin elution buffer. After decanting the eluted phosphoinositides into a clean 1.5-ml

Eppendorf tube, 178 µl of chloroform and 178 µl of H_2O are added to generate two phases. The bottom phase is removed into a clean 0.5-ml Eppendorf tube and dried by rotary evaporation.

14. We have also used a similar methodology to measure PtdIns(3,4,5)P_3 using the PH domain of the general receptor for phosphoinositides (GRP-1), which shows high specificity for PtdIns(3,4,5)P_3 (to be described elsewhere) and a GST-2xFYVE domain from HRS-1 [20] to assess PtdIns3*P* levels. A modification of the procedure can also be used to test the specificity of a potential lipid-interacting domain. Instead of spotting a standard curve of PtdIns(4,5)P_2, 100 nmoles of various phosphoinositides are spotted on the nitrocellulose membrane. The potential lipid-interacting domain can be purified as a bacterial or mammalian GST protein or also as a GFP protein, in which case an antibody directed against GFP is used to visualize the lipid interaction.
15. Quantitation can also be performed by densitometry of the film, although different exposures should be taken to ensure that the film is not saturated (overexposed) at the higher levels of PtdIns(4,5)P_2. The advantage of the CCD camera is the large linear dynamic range of light sensitivity.
16. It is possible to clean tubes after each use. However, to avoid contamination artifacts, we use cheap disposable glass tubes.
17. To measure PtdIns4*P*, PtdIns5*P*, and PtdIns(4,5)P_2 in whole cells, 1×10^6 cells are resuspended in 200 µl of PBS and directly extracted by the addition of chloroform (250 µl) and methanol (500 µl). For cells that are attached to culture dishes, we routinely use a confluent well from a 6-well plate (3-cm well diameter). After specific treatment, the cells are washed with PBS, the supernatant removed by aspiration, and the plate is immediately frozen on a bed of dry ice. The plate can then be stored at −80°C for up to two weeks. The plate is removed from the −80°C freezer and placed on a bed of ice, and 200 µl of 2.4 M HCl is added to each of the wells. The cells are scraped and transferred into a 1.5-ml Eppendorf tube, and the well is washed with 500 µl of cold methanol, which is pooled with the HCl extract. 250 µl of chloroform is then added to the Eppendorf tube to generate a one-phase extraction solution. Following incubation at room temperature for 15 min, 250 µl of chloroform and 250 µl of H_2O are added, mixed, and centrifuged, and the lower phase is treated as outlined in the specific assay procedure.

References

1. Divecha N, Irvine RF. Phospholipid signaling. Cell 1995;80:269–78.
2. Overduin M, Cheever ML, Kutateladze TG. Signaling with phosphoinositides: Better than binary. Mol Interv 2001;1:150–9.
3. Balla T. Inositol-lipid binding motifs: Signal integrators through protein-lipid and protein-protein interactions. J Cell Sci 2005;118:2093–104.
4. Irvine RF. Nuclear lipid signalling. Nat Rev Mol Cell Biol 2003;4:349–60.
5. Hammond G, Thomas CL, Schiavo G. Nuclear phosphoinositides and their functions. Curr Top Microbiol Immunol 2004;282:177–206.
6. Martelli AM, Fala F, Faenza I, et al. Metabolism and signaling activities of nuclear lipids. Cell Mol Life Sci 2004;61:1143–56.
7. Jackson TR, Stephens LR, Hawkins PT. Receptor specificity of growth factor-stimulated synthesis of 3-phosphorylated inositol lipids in Swiss 3T3 cells. J Biol Chem 1992;267: 16627–36.
8. van der Wal J, Habets R, Varnai P, Balla T, Jalink K. Monitoring agonist-induced phospholipase C activation in live cells by fluorescence resonance energy transfer. J Biol Chem 2001;276:15337–44.

9. Lee SB, Varnai P, Balla A, Jalink K, Rhee SG, Balla T. The Pleckstrin homology domain of phosphoinositide-specific phospholipase Cdelta4 is not a critical determinant of the membrane localization of the enzyme. J Biol Chem 2004;279:24362–71.
10. Varnai P, Bondeva T, Tamas P, et al. Selective cellular effects of overexpressed Pleckstrin-homology domains that recognize PtdIns(3,4,5)P_3 suggest their interaction with protein binding partners. J Cell Sci 2005;118:4879–88.
11. Balla A, Tuymetova G, Tsiomenko A, Varnai P, Balla T. A plasma membrane pool of phosphatidylinositol 4-phosphate is generated by phosphatidylinositol 4-kinase type-III alpha: Studies with the PH domains of the oxysterol binding protein and FAPP1. Mol Biol Cell 2005;16:1282–95.
12. Levine TP, Munro S. Targeting of Golgi-specific Pleckstrin homology domains involves both PtdIns 4-kinase-dependent and -independent components. Curr Biol 2002;12: 695–704.
13. Clarke JH, Letcher AJ, D'Santos CS, Halstead JR, Irvine RF, Divecha N. Inositol lipids are regulated during cell cycle progression in the nuclei of murine erythroleukaemia cells. Biochem J 2001;357:905–10.
14. Morris JB, Hinchliffe KA, Ciruela A, Letcher AJ, Irvine RF. Thrombin stimulation of platelets causes an increase in phosphatidylinositol 5-phosphate revealed by mass assay. FEBS Lett 2000;475:57–60.
15. Jones DR, Bultsma Y, Keune WJ, et al. Nuclear PtdIns5*P* as a transducer of stress signaling: An *in vivo* role for PIP4Kbeta. Mol Cell 2006;23:685–95.
16. Loijens JC, Anderson RA. Type I phosphatidylinositol-4-phosphate 5-kinases are distinct members of this novel lipid kinase family. J Biol Chem 1996;271:32937–43.
17. Rameh LE, Tolias KF, Duckworth BC, Cantley LC. A new pathway for synthesis of phosphatidylinositol-4,5-bisphosphate [see comments]. Nature 1997;390:192–6.
18. Schacht J. Purification of polyphosphoinositides by chromatography on immobilized neomycin. J Lipid Res 1978;19:1063–7.
19. Palmer FB. Chromatography of acidic phospholipids on immobilized neomycin. J Lipid Res 1981;22:1296–1300.
20. Itoh F, Divecha N, Brocks L, et al. The FYVE domain in Smad anchor for receptor activation (SARA) is sufficient for localization of SARA in early endosomes and regulates TGF-beta/Smad signalling. Genes Cells 2002;7:321–31.

Chapter 6
Lipid Quantification and Structure Determination of Nuclear Envelope Precursor Membranes in the Sea Urchin

Marie Garnier-Lhomme, Erick J. Dufourc, Banafshé Larijani and Dominic Poccia

Abstract Nuclear envelope assembly is a fundamental cellular process normally taking place once in every cell cycle in eukaryotes. The timing of fusion of nuclear membrane precursors to form the complete double membrane surrounding the chromosomes is tightly controlled, but much remains unclear concerning its regulation. Small amounts of material available and the high background of irrelevant cellular membranes have limited detailed analysis. We have employed several sensitive and high-resolution techniques to analyze the nuclear membrane structure, composition, and dynamics using purified membrane fractions and a cell-free system that results in nuclear envelope formation. We discuss the application of cholesterol and phospholipid colorimetric assays, fluorescent filipin labeling, electrospray ionization tandem mass spectrometry coupled to HPLC (HPLC-ESI/MS/MS), electron microscopy (EM), and solid-state nuclear magnetic resonance (NMR) spectroscopy. Colorimetric assays determine the amounts of inorganic phosphates from phospholipids and cholesterol/cholesteryl esters present in membrane-containing fractions. Filipin staining of natural membranes allows the localization and relative quantification of cholesterol. HPLC-ESI/MS/MS determines the quantitative composition of membrane phospholipid species from small amounts of membranes. Cryosectioning of cryoprotected sperm cells facilitates EM verification of membrane domains existing *in vivo*. Deuterium solid-state NMR provides information about membrane rigidity and lipid-phase behavior. The sensitivity, quantification, and structural determinations provided by these techniques should prove useful in studying membrane dynamics in a variety of systems exhibiting membrane fusion.

D. Poccia
Department of Biology, Amherst College, Amherst, MA 01002;
Unidade de Investigaçao na Biologia do Desenvolvimento, Universide Lusófona, Lisbon, Portugal
e-mail: dlpoccia@amherst.edu

B. Larijani et al. (eds.), *Lipid Signaling Protocols*, DOI: 10.1007/978-1-60327-115-8_6,

Keywords Membrane characterization · nuclear envelope · cholesterol · filipin · HPLC-ESI/MS/MS · cryosectioning · electron microscopy · solid-state NMR

Abbreviations NE: nuclear envelope; LS: lipophilic structure; MV: membrane vesicle; S10: 10,000g supernatant; HPLC: high pressure liquid chromatography.

6.1 Introduction

Membrane fusion and fission are constantly regulated in the life of a cell. Such alterations support activities such as endocytosis, secretion, processing through the endoplasmic reticulum and the Golgi apparatus, and reconstitution of organelles at mitosis. The characterization of membrane dynamics in cells is a formidable challenge benefiting from both *in vivo* and *in vitro* approaches. Accuracy, sensitivity, and reproducibility as well as preservation of changing structures and composition during membrane transitions are important elements that need to be considered prior to analysis. This requires the use of very powerful techniques and their adaptation to natural systems.

This chapter presents a novel application of methods for probing membrane dynamics and structure and for cholesterol and phospholipid localization and quantification. These have been optimized on a sea urchin cell-free system that supports nuclear envelope (NE) assembly [1]. The system consists of permeabilized sperm nuclei and fertilized egg extracts made of membrane vesicles (MVs) and cytosol [1]. Membrane domains in both sperm nuclei and egg MVs that are essential for NE formation led us to apply new approaches to their characterization.

The ability of membranes to interact with each other and fuse is linked to structure and thus lipid composition. Colorimetric assays are used to quantify amounts of phospholipids compared to cholesterol, filipin staining to localize and quantify relative amounts of cholesterol, mass spectrometry to quantify and identify phospholipid species, electron microscopy to reveal membrane domains, and deuterium NMR to probe membrane dynamics.

Protein components of signaling pathways co-localize in specific membrane domains. Cholesterol modifies membrane width as well as membrane rigidity [2–6]. Its location and concentration are often correlated with protein assembly. Filipin is a fluorescent polyene known for its affinity for cholesterol [7–11]. Under specific conditions of temperature and concentration, filipin can lead to either cholesterol extraction [12, 13] or complex formation with cholesterol [11, 14–16]. Later we present optimal conditions for maximum labeling and minimum extraction.

Mass spectrometry (MS) is a general and extremely sensitive method for lipid characterization. MS can detect lipids in the low femtomolar range. When coupled to HPLC, the technique is very powerful for determining types of phospholipids and their fatty acid chain lengths and degrees of unsaturation. We emphasize novel protocols for determination of phosphoinositides, important in many signaling pathways.

Membrane structure can be determined using a variety of techniques, including solid-state NMR, fluorescence spectroscopy, X-ray diffraction, and electron microscopy (EM). Cryo-electron microscopy combines high-resolution imaging with minimum membrane damage resulting from fixation artifacts. Among techniques that probe membrane dynamics [solid-state NMR, electron spin resonance, infrared spectroscopy, fluorescence (FRAP, FCS, FRET)], we chose solid-state NMR to determine the coexistence of different lipid phases and membrane order in a noninvasive manner.

6.2 Materials

6.2.1 Buffers

1. Freezing buffer: 2 ml of 3% bovine serum albumin (BSA) in SXN, 10 ml of SXN, 6 ml of glycerol.
2. K_4EDTA: 5.84 g of EDTA in 100 ml of distilled water and 30 pellets of KOH added progressively, pH 6.
3. LB buffer: 10 mM HEPES, 250 mM NaCl, 5 mM $MgCl_2$, 10 mM glycine, 250 mM glycerol, 1 mM DTT, pH 8.
4. MPSW: Millipore filtered sea water, artificial sea water filtered through a 0.22-μm Stericup from Millipore, Inc.
5. MWB buffer: membrane wash buffer, 250 mM sucrose, 50 mM KCl, 50 mM HEPES, 1 mM DTT, 1 mM ATP, 1 mM PMSF, pH 7.5.
6. PHEM buffer: 60 mM PIPES, 25 mM HEPES, 2 mM $MgCl_2$, 10 mM EGTA, pH 6.9.
7. SXN buffer: 50 mM HEPES, 250 mM sucrose, 150 mM NaCl, 0.5 mM spermidine, 0.15 mM spermine, 0.3 mM glucose, pH 7.2.
8. Sorensen's buffer: 202.5 ml of 0.2 M disodium hydrogen orthophosphate, 47.5 ml of 0.2 M sodium dihydrogen phosphate, and 250 ml of distilled water, pH 7.4.

6.2.2 Determination of Inorganic Phosphate in Phospholipids in Biological Samples

1. Glass test tubes and marbles.
2. 50 mM K_2HPO_4 stock solution.
3. 10 N sulfuric acid.
4. Beakers containing sand.
5. 72% (v/v) perchloric acid.
6. A freshly prepared solution of 14 ml of distilled water, 2 ml of 3 M sulfuric acid, 2 ml of 2.5% (w/v) ammonium molybdate $(NH_4)_6Mo_7O_{24}$,4 H_2O, and 2 ml of 10% (w/v) ascorbic acid. The sulfuric acid and ammonium molybdate

components of this solution can be prepared in advance and stored at room temperature. The ascorbic acid solution is prepared fresh.
7. Oven.
8. 96-well microplates, SpectraMAX Plus Microplate Reader (Molecular Devices, Wokingham, UK).

6.2.3 Cholesteryl Ester and Cholesterol Assay

1. Cholesterol solution (Thermo Electron Corporation). This is obtained as a 7.76 mM stock and stored at −20°C.
2. Chloroform-resistant 2-ml microfuge tubes (Eppendorf UK Ltd., Cambridge, UK).
3. Cholesterol assay kit (Thermo Electron Corporation).
4. Soniprep 150 probe sonicator (Sanyo-Gallenkamp).
5. Incubator (37°C).
6. 96-well microplates, SpectraMAX Plus microplate reader (Molecular Devices).

6.2.4 Cell Membrane Cholesterol Labeling and Imaging Using Filipin

6.2.4.1 Cell Fixation

1. 16% stock solution formaldehyde (TAAB Laboratories Equipment, Ltd., Berkshire, UK).
2. SXN buffer.
3. MPSW.

6.2.4.2 Cell Labeling

1. Filipin III (Sigma-Aldrich, Dorset, UK).
2. DMSO (Sigma-Aldrich).
3. PHEM buffer.
4. Hemocytometer (Hawksley, Sussex, UK).

6.2.4.3 Filipin Imaging

1. PHEM buffer.
2. DABCO [1,4-diazabicyclo(2.2.2)octane] (Sigma-Aldrich).
3. Modified TE 2000 inverted microscope (Nikon Ltd., Japan).
4. Mercury source (Nikon).
5. DAPI excitation filter (Nikon).

6.2.4.4 Filipin Intensity Measurements

1. Quartz cuvette [Photon Technology International (PTI), Inc., Ford, West Sussex, UK].
2. A QM6/2005 Spectrofluorimeter (PTI, Inc.).
3. Felix32 Analysis software V1.0 (PTI, Inc.).

6.2.5 PtdIns Species Analysis by HPLC-Tandem Mass Spectrometry

6.2.5.1 Lipid Extraction

1. Glass universals (20-ml glass tubes with plastic screw caps).
2. Specimen tubes, soda glass with polyethylene stoppers (VWR International, Cat. no. 212-7048).
3. Chromacol screw-top vial, 5 ml (VWR International, Cat. no. 372-1211-04).
4. Glass Pasteur pipettes.
5. Dimethyldichlorosilane (Fisher Scientific, Loughborough, Leicestershire, UK).
6. HPLC-grade toluene, chloroform, methanol, and water (Rathburn Chemicals, Ltd., Walkerburn, Scotland, UK).
7. Phosphoinositides: PI(3)P (diC16, H^+); PI(4)P (diC16, H^+); PI(5)P (diC16, H^+); PI(3,4)P_2 (diC16, H^+); PI(3,5)P_2 (diC16, H^+); PI(4,5)P_2 (diC16, H^+); and PI(3,4,5)P_3 (diC16, H^+) (Cell Signals, Columbus, OH).
8. Phospholipids: 1,2-dilauroyl-sn-glycero-3-phosphocholine (DLPC), 1,2-dilauroyl-sn-glycero-3-phosphoethanolamine (DLPE), 1,2-dilauroyl-sn-glycero-3-[phospho-L-serine] (sodium salt) (DLPS), 1,2-dilauroyl-sn-glycero-3-phosphate (monosodium salt) (DLPA), 1,2-dilauroyl-sn-glycero-3-[phospho-rac-(1-glycerol)] (sodium salt) (DLPG) (Avanti Polar Lipids, Inc., Alabaster, AL).
9. DiC16 PtdIns (monosodium salt) (Echelon Biosciences, Inc., Salt Lake City, UT).
10. Extraction solvent: 1 vol of methanol supplemented with 1 drop of concentrated hydrochloric acid and 2.5 vol of chloroform.
11. Probe sonicator, Soniprep 150 (Integrated Services, TCP Inc., Palisades Park, NJ).
12. 0.22-μm Durapore membranes (Millipore, Cat no. GVW 04700).
13. Membrane filters, holders kit: borosilicate glass funnel, anodized aluminum clamp, sintered glass filter with silicone rubber stopper (Fisher Scientific, Cat. no. FDC-910-010B).
14. Borosilicate flask (Fisher Scientific).
15. Ethylenediaminetetraacetic acid (EDTA) purified grade (Sigma-Aldrich).
16. Potassium hydroxide (KOH) pellets (Sigma-Aldrich).

17. Centra MP4 Benchtop Centrifuge 000720 (International Equipment Company).
18. Nitrogen gas cylinder.
19. Sample concentrator from Techne Inc., Burlington, NJ, USA.
20. 100-µl silanized inserts (Alltech Associates, Carnforth, Lancashire, UK).
21. 100-µl Hamilton gastight syringe (Alltech Associates).
22. Screw-thread standard amber vials, 12 mm × 32 mm (Alltech Associates).

6.2.5.2 Lipid Analyses

1. Series 200 micropumps (Perkin Elmer LAS Ltd., Buckinghamshire, UK).
2. Series 200 autosampler (Perkin Elmer LAS Ltd.).
3. Normal-phase Luna silica (2) 3-µm column (Phenomenex Macclefield, Cheshire, UK).
4. API 3000 mass spectrometer equipped with an ESI source (Sciex/Applied Biosystems Warrington, Cheshire, UK).
5. HPLC and MS/MS are controlled by Analyst software V1.0.1 (Sciex/Applied Biosystems).
6. Ethylamine 70% (Sigma-Aldrich).
7. Phase A: chloroform/methanol/water (90:9.5:0.5) containing 7 mM ethylamine.
8. Phase B_1 for phospholipid analysis: chloroform/acetonitrile/methanol/water (30:30:35:5) containing 10 mM ethylamine.
9. Phase B_2 for phosphoinositide analysis: chloroform/acetonitrile/methanol/water (30:30:32:8) containing 10 mM ethylamine.
10. PEEK tubing, 0.005-in. i.d. (color-coded) red (Alltech Associates).
11. Amber bottles, 500 ml (VWR International).
12. Kontes three-valve mobile phase cap (Alltech Associates, Cat. no. 10140).
13. PEEK tubing loop, 2.5 µl, red.

6.2.5.3 Data Analyses

1. Algorithm: Analyst Classic (Sciex/Applied Biosystems).
2. Microsoft Office Excel software.

6.2.6 Electron Microscopy

6.2.6.1 Transmission Electron Microscopy

1. SXN buffer (*see* Subheading 6.2.1, step 7).
2. PHEM buffer (*see* Subheading 6.2.1, step 6).
3. Sorensen's buffer.
4. 8% stock solution glutaraldehyde (TAAB Laboratories Equipment, Ltd.).
5. 16% stock solution formaldehyde (TAAB Laboratories Equipment, Ltd.).

6. Acrolein (Agar Scientific Ltd., Stansted, UK).
7. Tannic acid (Sigma-Aldrich).
8. Osmium tetroxide (Agar Scientific Ltd.).
9. Uranyl acetate (Agar Scientific Ltd.).
10. Ethanol, normal grade.
11. Resin mixture: 20 ml of Araldite CY212, 20 ml of dodecenylsuccinic anhydride (DDSA), 1 ml of benzyldimethylamine (BDMA), and 0.25 ml of dibutylphthalate (Agar Scientific Ltd.).
12. Sucrose (Sigma-Aldrich).
13. Liquid nitrogen.
14. Methylcellulose (Sigma-Aldrich).
15. JEOL 1010 TEM microscope.

6.2.6.2 Scanning Electron Microscopy

1. 16% stock solution formaldehyde.
2. SXN buffer.
3. Polylysine-coated cover slips.
4. Platinum.
5. Polaron sputter coater SC7640 (Quorum Technologies Ltd., East Sussex, UK).
6. JEOL field emission JSM-6700F microscope.

6.2.7 Solid-State NMR

6.2.7.1 Deuterated Probe Suspensions

1. Freeze-dryer.
2. Deuterium-depleted water (Isotec, branch of Sigma-Aldrich).
3. Deuterated lipids: 1,2-dipalmitoyl-D62-sn-glycero-3-phosphocholine (16:0/16:0 DPPCd62) and 1-palmitoyl(D31)-2-oleoyl-sn-glycero-3-phosphocholine (16:0/18:1 POPCd31) (Avanti Polar Lipids, Inc.).
4. Water bath.
5. Liquid nitrogen.
6. A 3-mm microprobe for ultra-high amplitude (Fisher Scientific, Cat. no. C72403).

6.2.7.2 Vesicle Sizing by Dynamic Light Scattering

1. ALV/CGS-3 Correlator light scattering (ALV-Laser Vertriebsgesellschaft mbH, Langen, Germany).
2. ALV Correlator Software V.3.0 (ALV-Laser Vertriebsgesellschaft mbH).
3. Microsoft Office Excel software.

6.2.7.3 Biological Sample Preparation

1. Protein assay kit (Bio-Rad Laboratories, UK, Ltd.).
2. Improved Neubauer hemocytometer (Jencons Scientific Ltd., Bedfordshire, UK).

6.2.7.4 Probe Incorporation

1. Distilled water.
2. Centrifuge.
3. NMR rotor for a 10-mm coil of 800-µl volume.

6.2.7.5 Instrumentation

6.2.7.5.1 ^{2}H NMR Instrumentation

1. Brüker WB Avance DSX 500.
2. Static triple WB 1 H/X/Y probe equipped with a homemade 10-mm coil (E.J. Dufourc, unpublished).
3. TopSpin software (Brüker, Wissembourg, France).

6.2.7.5.2 ^{31}P NMR Instrumentation

1. Brüker NB Avance 400.
2. QNP NB 5-mm liquid probe.
3. Brüker software.

6.2.7.6 Data Analyses

1. Origin software V7.5 (OriginLab Corp., Northampton, MA).
2. NMR Friend V1.2 to import and treat NMR spectra on Origin developed by Sébastien Buchoux, UMR CRS–University of Bordeaux 1, IECB, Bordeaux, France.

6.3 Methods

The sea urchin cell-free system for nuclear envelope formation consists of isolated sperm nuclei from which lateral nuclear envelopes have been stripped by 0.1% Triton X-100. They will be referred to as 0.1% permeabilized nuclei. These are added to 10,000 × *g* supernatants of homogenized 10-min postfertilization eggs (S10) or to their component parts (cytosol [S150] and total membrane vesicles [MV0] prepared by centrifuging S10 at 150,000 × *g*). Protocols for preparing permeabilized sperm nuclei, egg extracts, cytosol, and MV fractions as well as procedures for forming nuclear envelopes *in vitro* with this system are treated extensively elsewhere [17, 18].

A portion of the sea urchin sperm nuclear membrane, which is not removed by 0.1% detergent or disassembled *in vivo* following fertilization, remains at the tip and base of the conical nucleus. These regions can be stained with lipophilic dyes and are called "lipophilic structures" (LSs). They are required for MV binding *in vitro,* which occurs with ATP present. The addition of GTP and its hydrolysis lead to membrane fusion of MVs and LSs to create the complete nuclear envelope.

6.3.1 Determination of Inorganic Phosphate of Phospholipids in Biological Samples [19]

Cholesterol and phospholipid concentrations are measured for MVs and sperm nuclei using colorimetric assays.

1. Extracted lipid samples [20] (*see* Subheading 6.3.4) are dissolved in 500 µl of TN buffer by hard vortexing and transferred to glass test tubes (*see* Note 1).
2. Standards of 400 µM, 200 µM, 100 µM, 50 µM, 25 µM, 12.5 µM, and 1 µM K_2HPO_4 are prepared in distilled water from the 50 mM stock solution.
3. 500 µl of each standard solution, TN, and water blanks, and samples to be assayed are transferred to rimmed glass test tubes. 100 µl of 10 N sulfuric acid is added to each tube, and the tubes are placed in beakers with sand.
4. Each tube is covered with a marble and heated for 1.5 h at 200°C. Samples will turn brown.
5. The beakers are transferred from the oven to a hood and 100 µl of 72% perchloric acid is added.
6. The beakers are returned to the oven for 60 min, the tubes cooled down under a hood, and the marbles removed.
7. 2 ml of the distilled water/6 N sulfuric acid/2.5% ammonium molybdate/10% ascorbic acid solution is added to the samples, which are transferred to sealed glass tubes and incubated at 50°C for 30 min. After incubation samples are pale blue.
8. The sample absorption is determined in a 96-well plate. Blanks (TN buffer and water), standards, and the samples are all run as duplicates (2× 200 µl) and the absorption read at 820 nm.

6.3.2 Cholesteryl Ester and Cholesterol Assay [21]

1. Cholesterol standard solutions of 7.76 mM, 5.17 mM, 2.59 mM, 1.29 mM, are prepared fresh in TN buffer.
2. 5 µl of the samples to be assayed (*see* Note 2**)**, standards, and a TN blank are transferred to 1.5-ml microfuge tubes and 500 µl of a cholesterol liquid stable reagent (Thermo Electron Corporation) is added.

3. The solutions are probe-sonicated at power 10 for 3 s and incubated for 5 min at 37°C.
4. Sample absorption is determined in a 96-well plate. 200 µl of each sample is read in duplicate at 500 nm (*see* Note 3).

6.3.3 Cell Membrane Cholesterol Labeling and Imaging Using Filipin

To assess the distribution of cholesterol in cells and fractions, cholesterol is imaged. Polyene filipin is used to label cholesterol in whole sperm membranes and in 0.1% permeabilized nuclei. In parallel, filipin labeling is quantified by fluorimetry and compared to the results obtained by colorimetric assays. Similar results are obtained.

1. Sperm cells, 0.1% and 1% permeabilized nuclei (*see* Note 4) are fixed in 4% formaldehyde in MPSW (sperm cells) or SXN buffer (permeabilized nuclei) for 2.5 h at 4°C (*see* Note 5).
2. Cells are then spun at 200 × *g* for 10 min at 4°C, resuspended in 1 ml of 1% formaldehyde in MPSW or SXN buffer, and stored overnight at 4°C.
3. Filipin stock solution (5 mg/ml in DMSO) is diluted 100-fold in PHEM buffer to 50 µg/ml [16].
4. Cells in 1% formaldehyde are spun at 200 × *g* for 10 min at 4°C and resuspended in 30 µl of PHEM. 5×10^5sperm cells or 1×10^6 0.1% nuclei are incubated in 1 ml of filipin solution.
5. Staining is carried out on a roller at 4°C for 4 h (*see* Note 6).
6. Sperm are spun at 200 × *g* for 10 min at 4°C and washed twice in 500 µl of PHEM buffer. Nuclei are resuspended in 60 µl of PHEM buffer and counted using a hemocytometer. Volumes are adjusted to obtain an equivalent concentration of nuclei in all samples.
7. For microscopy, 5 µl of cells are supplemented with 45 µl of PHEM buffer containing the antifade DABCO (1 spatula of DABCO in 1 ml of PHEM buffer) (*see* Note 7). Filipin is excited at 360 nm using a mercury source combined with a DAPI excitation filter (Fig. 6.1).
8. For fluorimetry, 50 µl of cells are transferred to a quartz cuvette. Filipin is excited at 360 nm by an arc lamp at 75 W and the emission intensity is measured between 400 and 700 nm.

6.3.4 PtdIns Species Analysis by HPLC-Tandem Mass Spectrometry

Previous work on MV characterization revealed a highly PtdIns-enriched population, MV1, by liquid NMR [20]. However, PtdIns, PtdIns*P*, PtdInsP_2, and PtdInsP_3 content could not be resolved, so HPLC-ESI/MS/MS procedures

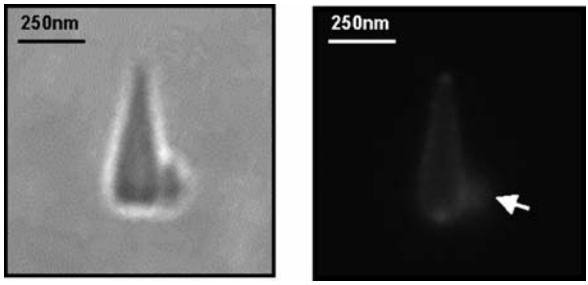

Fig. 6.1 Cholesterol distribution imaging using filipin. *P. lividus* sperm were fixed in 4% PFA for 2.5 h at 4°C, washed twice in MPSW, and labeled with 50 µg/ml filipin for 4 h at 4°C. Labeling at low temperature was to avoid cholesterol extraction by filipin. Cholesterol in the sperm head region is mainly associated with sperm plasma membrane and/or lateral nuclear envelope, the acrosomal vesicle, and/or lipophilic structures at the nuclear tips. Little if any chromatin staining is apparent. The single plasma membrane surrounding the tail is not apparent here. The single large mitochondrion (arrow) of the midpiece is displaced, facilitating visualization of the centriolar fossa LS. Left: bright field image, right: fluorescent image. Bars are 250 nm

were optimized to bypass this problem. Lipid extraction was optimized to prevent loss of charged lipids and more specifically phosphoinositides. Lipid analyses of MV1 confirmed the NMR data and added details about the relative populations of PtdIns*P*, PtdInsP_2, and PtdInsP_3.

1. All glassware (glass universals, specimen tubes, funnel, chromacol screw-top vial, and Pasteur pipettes) is silanated using a 3% solution of dimethyldichlorosilane in HPLC-grade toluene (*see* Note 8). Glassware is left in a fume hood for 1 h and then rinsed twice in methanol and twice in HPLC-grade water.
2. Two mixtures of internal standard (IS) are prepared, one containing the phosphoinositides (IS1): DPPI(4)*P*, DPPI(4,5)P_2, and DPPI(3,4,5)P_3 (*see* Note 9) at 100 µg/ml in chloroform/methanol/water (5:5:1) and the second containing other phospholipids (IS2): DLPC, DLPA, DLPS, DLPG, DLPE, and DPPI at 100 µg/ml in chloroform/methanol/water (5:5:1).
3. Biological samples are extracted according to a modified Folch procedure [18]. 200 µl of sample and 2 µg of IS2 (*see* Note 10) are added to 4 ml of acidified chloroform/methanol (2.5:1) (see Note 11) in a glass universal.
4. The mixture is probe sonicated for 10 s at power 22 and left at room temperature for 1 h.
5. Samples are filtered through a 0.22-µm membrane resistant to chloroform. For vacuum filtration, the membrane is placed on a sintered glass filter with silicone rubber stopper overhung by a borosilicate funnel. The system is sealed with an anodized aluminum clamp and placed on a borosilicate flask (*see* Note 12). Samples are collected in a specimen tube placed inside the flask.

6. The extracted sample is supplemented with 0.2 vol of K_4EDTA (*see* Note 13), transferred to a chromacol screw-top vial using a Pasteur pipette and spun at 800 × *g* for 15 min at 4°C.
7. The organic phase is collected, transferred to a fresh chromacol tube, and dried at 37°C under nitrogen using a sample concentrator.
8. The lipid pellet is resuspended in 100 µl of chloroform/methanol/water (5:5:1) and transferred to a 100-µl silanized insert using a 100-µl gas-tight syringe. The insert is placed in an amber vial and the lipids dried under nitrogen.
9. For phosphoinositide analyses, 3 µg of IS1 and 2 µg of IS2 are added and dried under nitrogen at this step (*see* Note 10).
10. Before use, lipids are resuspended in the HPLC phase A without the modifier.
11. Mass spectrometry lipid analysis is carried out on an API 3000 instrument. Lipids are separated by HPLC prior to detection using a Luna silica column. A gradient elution protocol, adapted from Pettitt et al. [22], from 100% phase A to 70% phase B_1 over 20 min, is used to separate the phospholipids (PC, PG, PE, PI, PS, and PA). The phosphoinositides are separated using a 100% phase A to 55% phase B_2 gradient over 20 min (Fig. 6.2). The stainless steel autosampler loop is replaced by a 2.5-µl red polyetheretherketone (PEEK) tubing loop to increase recovery of phosphoinositides (*see* Note 14). The injection needle is flushed using phase A without ethylamine.
12. Lipid ionization is optimized by direct infusion at 100 µl/min of a synthetic lipid mixture containing at least one saturated and one unsaturated species for each lipid type.
13. Phospholipids are ionized at 4 kV at 300°C. Phosphoinositide ionization is carried out under the same conditions except the temperature is decreased to 150°C (*see* Note 15).
14. Phospholipid species are determined using precursor scans. The fragmentation conditions are adapted from Brügger et al. [23] and are shown in Table 6.1. In a typical lipid analysis, precursor scans and multiple ion scans of PL and phosphoinositides are acquired.
15. Lipid quantification is carried out using the Analyst Classic integration algorithm. Phospholipids are quantified on precursor scan chromatograms after C_{13} correction. Phosphoinositides are quantified on multiple ion scan chromatograms, which is more sensitive than precursor scans (*see* Note 16).
16. Moles of lipids are backcalculated from internal standards and lipid peak areas using an "in-house" macro written in Excel.

6.3.5 Electron Microscopy

Membrane imaging by transmission electron microscopy requires direct (tannic acid, osmium tetroxide) [24] or indirect (formaldehyde, glutaraldehyde) lipid fixation. Two different methods are applied to sperm cells, one using tannic

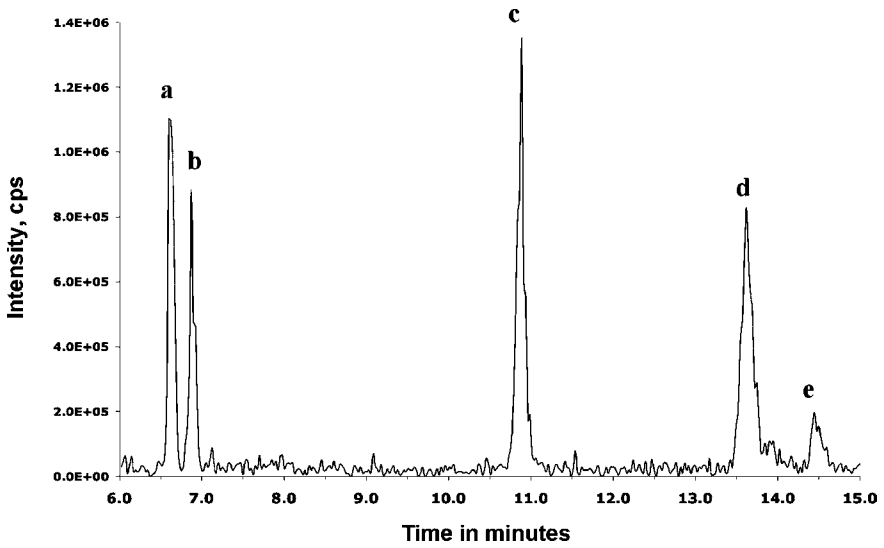

Fig. 6.2 Phosphatidylinositide separation and ionization by HPLC tandem mass spectrometry in the MV2 fraction. MV2 membranes were bound to nuclei by ATP treatment and extracted, and the phosphatidylinositides were analyzed by HPLC-ESI/MS/MS using a 100% chloroform/methanol/water/ethylamine (90:9.5:0.5:7 mM) to 55% chloroform/acetonitrile/methanol/water/ethylamine (30:30:32:8:10 mM) gradient over 20 minutes. Phosphatidylinositides were ionized in the negative mode at 150°C and −4000 V. Phosphatidylionositols eluted first between 6.5 and 7 min (peaks a and b). Peak "a" shows the polyunsaturated ion −885.5 m/z or 18:0/20:4 PtdIns from MV2 and peak "b" is the internal standard ion −809.5 m/z or 16:0/16:0 PtdIns. PIPs eluted at 11 min (peak c). The main MV2 species was the polyunsaturated ion −965.5 m/z or 18:0/20:4 PIP. Peak "c" is the superposition of −965.5 m/z and the internal standard ion −889.5 m/z or 16:0/16:0 PIP. PIP2 s eluted at 13.5 min. Peak "d" represents the most abundant MV2 PIP2 ion, −1055 m/z, the alkyl-acyl 18:0a/22:6 PIP2, and the internal standard ion −969.5 m/z or 16:0/16:0 PIP2. PIP3 s eluted last at 14.5 min, and the main MV2 PIP3 species was the same alkyl-acyl species 18:0a/22:6. Peak "e" is the superposition of the −1135.6 m/z ion or 18:0a/22:6 PIP3 and the internal standard ion −1049.5 m/z or 16:0/16:0 PIP3. All internal standards were added postextraction to preserve PIP3

acid to enhance membrane contrast, the other substituting the dehydration step with cryoprotection and cryosectioning to better preserve membrane structure. In contrast to sectioning embedded cells, cyrosectioning does not require a dehydration step that can be very damaging to membranes. It better protects membrane lipids from extraction. The double bilayer of the NE could be resolved in whole sperm and a bilayer is observed in the acrosomal and centriolar fossae of 0.1% permeabilized nuclei, revealing details of LS region structure. We adapted the method of Möbius et al. [25] to image membranes on sperm-derived cells using chemical fixation, cryoprotection, and cryosectioning.

Table 6.1 Fragmentation conditions for phosphopholipid analysis

Lipid Type	Characteristic Fragment	DP	CE	CXP	RT
PtdCho	+ 184 m/z	+ 120 V	+ 52 V	+ 12 V	9–12 min
PtdGly	−153 m/z	−60 V	−40 V	−13 V	4–5 min
PtdEth	−196 m/z	−60 V	−45 V	−8 V	5–6.5 min
PtdIns	−241 m/z	−120 V	−60 V	−13 V	7–8 min
PtdSer	*NL 87 m/z	−50 V	−35 V	−30 V	7.6–8.8 min
PtdOH	−153 m/z	−60 V	−40 V	−13 V	11–11.5 min
PI(4)*P*	−321 m/z	−120 V	−60 V	−13 V	8.2 min
PI(4,5)P_2	−401 m/z	−120 V	−60 V	−13 V	10.1 min
PIP_3	−481 m/z	−120 V	−60 V	−13 V	10.5 min

Fragmentation conditions for each lipid type were optimized by direct infusion on an ESI-API 3000 MS/MS spectrometer. DP: declustering potential; CE: collision energy; CXP: collision cell exit potential; RT: retention time. The characteristic RT for each phospholipid was measured in biological samples using a 100% chloroform/methanol/water (90:9.5:0.5) to 70% chloroform/acetonitrile/methanol/water (30:30:35:5) gradient. Phosphatidylinositide RTs are measured using a 100% chloroform/methanol/water (90:9.5:0.5) to 60% chloroform/acetonitrile/methanol/water (30:30:32:8) gradient. *NL: Neutral loss in the negative mode.

1. For TEM, sperm and either 0.1% or 1% permeabilized nuclei are washed once in SXN and pelleted at 500 × *g*, 4°C for 10 min and 1,500 × *g*, 4°C for 2 min, respectively.
2. Pellets are fixed for 1 h in 0.1 M Sorensen's buffer containing 2.5% glutaraldehyde/1% tannic acid (*see* Note 17). After the first 30 min, the pellet is gently lifted from the bottom of the microcentrifuge tube to allow homogeneous fixation of the pellet.
3. The pellet is washed in Sorensen's buffer by centrifugation at 500 × *g* for 10 min at 4°C and kept in buffer at 4°C until processing for EM.
4. Samples are postfixed in 1% osmium tetroxide in 0.05 M Sorensen's buffer for 30 min, washed and dehydrated in an ascending ethanol series, and embedded in Araldite over two days.
5. Thin sections of approximately 80 nm are cut and then observed on a JEOL 1010 TEM.
6. For cryosectioning, sperm are fixed in 2% formaldehyde, 0.2% glutaraldehyde, and 1% acrolein in 0.1 M PHEM buffer for 30 min on ice (*see* Note 18).
7. Infiltration is carried out with 1.8 M sucrose in 80 mM PHEM containing 0.5% osmium tetroxide and 0.2% uranyl acetate for 2 h on ice.
8. As an alternative method, sperm cells are fixed in 4% formaldehyde in 0.1 M PHEM for 30 min on ice and infiltrated in 1.7 M sucrose containing 4% formaldehyde.
9. Droplets containing sperm cells are put on cutting pins and frozen in liquid nitrogen.

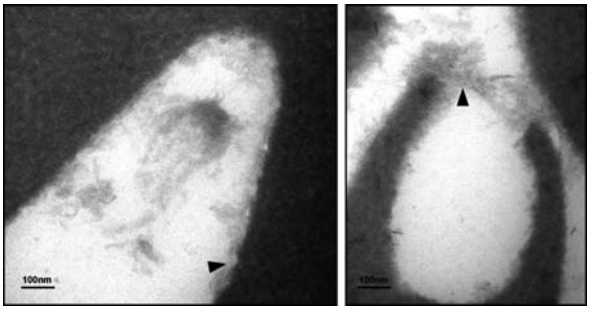

Fig. 6.3 Cryoprotected and cryosectioned 0.1% permeabilized nuclei show membranous structures at both the centriolar and acrosomal fossae. *S. purpuratus* 0.1% permeabilized nuclei were fixed in 2% PFA, 0.2% glutaraldehyde, and 1% acrolein in 0.1 M PHEM buffer. Infiltration was carried out in 1.8 M sucrose in 80 mM PHEM buffer containing 0.5% osmium tetroxide and 0.2% uranyl acetate. (a) Centriolar fossa showing a bilayer structure along the chromatin (arrow). (b) A similar bilayer structure was observed at the acrosomal fossa (arrow) linking the two chromatin extremities. In this method, dehydration by ethanol is avoided and membranes are better protected from lipid extraction

10. After cryosectioning, sections are picked up and thawed according to Liou et al. [26] in a 1:1 mixture of 2.3 M sucrose and 2% methylcellulose (Fig. 6.3).
11. For SEM, pellets are resuspended in 4% formaldehyde by diluting 16% formaldehyde with SXN buffer.
12. Cells in one drop are bound to a polylysine-coated cover slip, dehydrated in a critical point dryer, coated with platinum, and viewed on a field emission JSM-6700F microscope.

6.3.6 Solid-State NMR

Solid-state NMR is a powerful, noninvasive method to study membrane dynamics. ^{31}P and ^{2}H are the most common isotopes used. In this technique, a spectrum profile can be directly related to a lipid-phase or membrane state.

In the case of isolated membranes, ^{31}P ssNMR is the most appropriate method since it does not require the addition of a labeled probe. In the case of organelles like the nucleus where major sources of ^{31}P are DNA or RNA nucleotides, it is necessary to use ^{2}H NMR. Since the natural abundance of deuterium is very low (less than 0.1%), the incorporation of a deuterium labeled probe into the membranes is required.

The principle of incorporation developed here is based on the exchange of lipids by fusion of a donor membrane (deuterated membrane) with an acceptor membrane (membrane of interest). To facilitate this event, the donor membrane properties (vesicle size and lipid phase) are adapted for each type of membrane studied.

Three main parameters were considered in the choice of the probe in suspension: membrane curvature, sample weight, and membrane accessibility. In the case of small acceptors such as MVs, it is helpful to use very small donor vesicles (small unilamellar vesicles or SUVs of 50 nm diameter) in order to avoid probe contamination of acceptors during high-speed washes. When studying membranes of sperm cells, larger donors (multilamellar vesicles or MLVs of 1-μm diameter) are preferred since they have a curvature closer to typical membranes. Under these conditions, only probe vesicles bound to sperm spin down at $500 \times g$. The choice of probe vesicle size may also be determined by membrane accessibility. For instance, lipophilic structures are retained on the acrosomal and centriolar fossae of 0.1% permeabilized nuclei, where access is limited (50-nm gaps between axoneme and membrane). In this case, SUVs of 40-nm diameter are used.

To probe natural membranes, two different donor lipids were tested: 16:0/16:0 PtdCho labeled on both fatty acid chains (62 deuterium nuclei, DPPC $^2H_{62}$) and 16:0/18:1 PtdCho labeled on the saturated chain only (31 deuterium nuclei, POPC $^2H_{31}$). The advantages and drawbacks of each probe are summarized in Table 6.2.

1. To label membranes with MLV deuterium probes, buffers are freeze-dried and the powder resuspended in the corresponding volume of deuterium-depleted water.
2. The deuterated probe is hydrated at 90% calculated as mentioned in Equation (1).

$$\left(\frac{m_{(H_2O)}}{m_{(H_2O)} + m_{(lipid)}}\right) \times 100 = \text{hydration } \% \tag{1}$$

3. The mixture is hydrated by three cycles that consist of freezing the suspension in liquid nitrogen for 10 s and thawing in a water bath heated above the transition temperature for 15 min (Table 6.3).

Table 6.2 Advantages and drawbacks of two different deuterated lipid probes

DPPCd62 16:0/16:0		POPCd31 16:0/18:1	
Advantages	Drawbacks	Advantages	Drawbacks
High sensitivity	Not biologically relevant	Biologically relevant	Low sensitivity
Qualitative results from powder spectra at RT	High-transition *T*: lipid phase not stable around *T* of interest	Low-transition *T*: stable lipid phase at RT	

Table 6.3 Physical characteristics and incorporation conditions of both deuterated lipid probes

Probe	Transition *T*	Hydration *T*	Incubation *T*	^{2}H ssNMR *T*
DPPCd62	35°C	50°C	40°C	20°C and 40°C
DOPCd31	−3°C	40°C	40°C	10°C and 40°C

4. The suspension is homogenized by vortexing and turns milky.
5. To label with SUV probes, the lipid is hydrated at 98% in the deuterium-depleted buffer to a minimum final volume of 1 ml.
6. The suspension is transferred to a 5-ml plastic tube and probe-sonicated above the lipid transition temperature for at least 15 min. The pulse cycles are 4-s sonication with a 6-s break (*see* Note 19). The suspension turns translucent.
7. SUVs are spun at 10,000 × *g* for 10 min in order to pellet any metal residue from the probe that could interfere with NMR measurements.
8. Vesicles are sized by transferring 0.5 ml of SUV to a glass tube for light-scattering measurements. The correlation function is acquired at different angles: 45°, 60°, 75°, 90°, 120°, and 150°.
9. The viscosity, η, and the refractive index, n, are adjusted to $\eta = 1.19$, $n = 1.074$ for SXN and $\eta = 1.25$, $n = 1.3448$ for MWB. An average correlation time, τ_c, is measured for each angle and $1/\tau_c$ is plotted against the scattering vector $\mathbf{q}^2$ according to the equation $1/\tau_c = D\mathbf{q}^2$, where D is the diffusion coefficient. The square root of the scattering vector varies with the scattering angle according to the equation $\mathbf{q} = [4\pi n \sin(\theta/2)]/\lambda$; where θ is the scattering angle and λ the laser wavelength (632.8 nm). D is inversely proportional to the radius of the vesicle: $D = (k_B T)/(6\pi\eta R)$, where k_B is Boltzmann's constant, T the temperature in Kelvin, and R the hydrodynamic radius.
10. The radius of the vesicles is calculated from the slope of the graph ($1/\tau_c = D\mathbf{q}^2$) after linear fitting using Microsoft Excel software.
11. Sperm cells are concentrated by centrifugation at 500 × *g* for 10 min at 4°C. 250 µl of concentrated sperm are added to 10 ml of ice-cold SXN and spun at 2,000 × *g* for 5 min at 4°C. The pellet is resuspended in 500 µl of SXN supplemented with 500 µl of freezing buffer and snap-frozen in liquid nitrogen.
12. Aliquots of 4×10^8 sperm cells are thawed on ice and spun at 500 × *g* for 20 min at 4°C. These correspond to 1.5 mg of phospholipids (PL) (Table 6.4). The pellet is resuspended in 1 ml of deuterium-depleted SXN buffer.

Table 6.4 Conditions for probe incorporation in sperm, permeabilized nuclei and membrane vesicles (MVs)

Sample	Phospholipid Mass Determination	Lipid Probe Suspension	Wash Conditions	
			Centrifugation	Buffer
Sperm	3.78×10^{-9} mg/nucleus	MLV/SUV	500 × *g* for 15 min at room temp (2x)	SXN
0.1% Nuclei	0.50×10^{-9} mg/nucleus	SUV	500 × *g* for 15 min at RT (2x)	SXN
MVs	0.10×10^{-9} mg PL/mg protein	SUV	10,000 × *g* for 15 min at RT (2x)	MWB

13. Membrane vesicles are prepared from fertilized egg cytoplasm (7 ml of S10) spun at 150,000 × *g* for 2 h at 4°C.
14. The pellet containing the egg membrane vesicles (MVs) is resuspended in 700 µl of membrane wash buffer (MWB) and protein content estimated by Bradford assay. From this, the total amount of PL can be estimated (Table 6.4).
15. MVs are snap-frozen in liquid nitrogen.
16. Before use, MVs are thawed on ice and pelleted at 10,000 × *g* for 30 min at 4°C. The pellet is resuspended in 700 µl of deuterium-depleted MWB.
17. Permeabilized nuclei are prepared as described previously [18], resuspended in a 1:1 ratio (SXN/freezing buffer), aliquoted in 1.5 ml, and snap-frozen in liquid nitrogen.
18. Before use, 5×10^9 nuclei are thawed on ice and spun at 500 × *g* for 10 min at 4°C. The pellets are resuspended in a total volume of 1 ml of deuterium-depleted SXN buffer. Nuclei are spun a second time at 500 × *g* for 10 min at 4°C and resuspended in 1 ml of deuterium-depleted SXN buffer to get rid of as much deuterated water as possible.
19. For probe incorporation, membranes are incubated in a 1:1 phospholipid molar ratio with the lipid probe suspension.
20. The mixture is kept in a water bath at 40°C for 30 min and gently agitated every 10 min to avoid precipitation.
21. The sample is washed by centrifugation according to the conditions mentioned in Table 6.3. The pellet is resuspended after every wash by very gentle vortexing (*see* Note 20).
22. The final volume is determined by the NMR rotor volume, which is 800 µl. The rotor is closed by a homemade cork cap sealed with paraffin.
23. The ^{2}H NMR spectra are acquired using a quadrupolar echo-pulse sequence $90°x$-τ-$90°y$-τ-acq [27]. The two 90° pulse durations (p1) are determined in each new experiment (*see* Note 21). For the samples in SXN and MWB, p1 is at 6.5 µs. The sweep width is 500 kHz, the recycle delay is 1 s, and the echo delay between the pulses is 30 µs.
24. The number of scans is dependent on the sample concentration but is usually fixed around 60 k.
25. Samples are allowed to equilibrate for 45 min at a given temperature and are typically analyzed at low temperature (10°C or 20°C depending on the probe; see Table 6.2) for approximately 15 h followed by 10 h at 40°C and finally back to the low temperature (*see* Note 22).
26. ^{31}P NMR experiments are carried out at 162 MHz using a phase-cycled Hahn echo-pulse sequence $90°$-τ-$180°$-τ-acq with gated broadband proton decoupling [28]. The spectral window is 50 kHz and the 90° pulse length is 3.8 µs.
27. 3 K scans are commonly acquired, the recycle delay is 5 s, and the echo delays between pulses are 50 µs.
28. For ^{31}P wide-line NMR, samples are transferred either to a 50-µl rotor (biological membranes) or to a 5-mm NMR tube (model membranes).

29. Spectra are analyzed on Origin using the import software "NMR friend" developed by Sébastien Buchoux (UMR CNRS–University of Bordeaux 1, IECB Bordeaux). Quadrupolar splittings ($\Delta\nu_Q$) are measured for two different C-^{2}H bonds on the 16:0 chain. The most rigid C-$^2H_2$ bond is close to the glycerol backbone (C-$^2H_{plat}$), near the membrane surface, and the most fluid C-^{2}H bond is the methyl group at the extremity of the chain C-$^2H_3$ in the center of the bilayer. $\Delta\nu_Q(C^2H_{plat})$ is measured at the largest peaks of the spectrum (dashed lines in Fig. 6.4), and $\Delta\nu_Q(C^2H_3)$ is measured on the most intense and smallest doublet (arrows in Fig. 6.4).

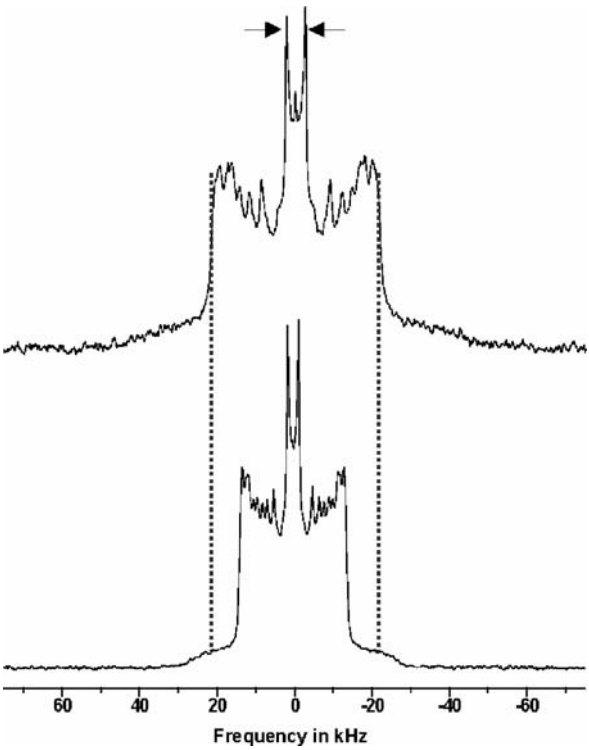

Fig. 6.4 Effect of cholesterol on membrane dynamics probed by deuterium solid-state NMR. Liposomes of deuterium labeled 16:0/18:1PC (POPC) contained 30% (top spectrum) and 0% cholesterol (bottom spectrum). Spectra were acquired at 20°C using a quadrupolar echo-pulse sequence. On the bottom spectrum, the quadrupolar splitting of the methyl group (arrows), $\Delta\nu_Q(C^2H_3)$, is very narrow (3 kHz) due to the large degree of motion of the carbon-deuterium bonds, C^2H_3, at the end of the fatty acid chain. The broadest quadrupolar splitting corresponds to the most static carbon–deuterium bond, C^2H_2, located close to the glycerol backbone of the phospholipid. This plateau quadrupolar splitting is referred to as $\Delta\nu_Q(C^2H_{plat})$ and measures 26.7 kHz. When adding 30% cholesterol (top spectrum), $\Delta\nu_Q(C^2H_3)$ and $\Delta\nu_Q(C^2H_{plat})$ (dashed line) were significantly enlarged (5.1 kHz and 40.7 kHz, respectively)

"NMR friend" calculates the first-order moment (M_1). $\Delta\nu_Q$ and M_1 are directly proportional to the order parameter S that determines the rigidity of the membrane. $\Delta\nu_Q$ and M_1 measurements are used to determine natural membrane dynamics.

Acknowledgments The authors would like to thank Axelle Grélard and Cécile Loudet for their advice on NMR spectroscopy, Sebastien Buchoux for developing "NMR Friend," Stephen Gschmeissner for processing EM samples, and Trevor Pettitt and Michael Wakelam for their advice on HPLC and MS. This work was partially supported by Cancer Research, UK and the Amherst College Faculty Research Award Program Axel H. Schupf '57 Fund for Intellectual Life.

Notes

1. To provide sufficient phospholipids for detection, we recommend lipids extracted from the following to be used: 40 µl of S10, 40 µl of S150, 40 µl of MVs, 10 µl of concentrated sperm, two aliquots of 0.1% nuclei or 1% nuclei, and LSs made from two aliquots of 0.1% nuclei.
2. We have found the following amounts usually give optimal material for cholesterol detection: 6 µl of S10, S150, MVs (resuspended in the same volume as the starting material), <10 µl of concentrated sperm diluted in TN, ≥1 aliquot of 0.1% or 1% nuclei, and LSs derived from the 0.1% nuclei.
3. A pink coloration is observed in the presence of cholesterol and cholesteryl esters.
4. For LS characterization from 0.1% nuclei, whole sperm is used as a positive control, and 1% permeabilized nuclei where LSs have been solubilized are considered the negative control. 1% permeabilized nuclei do not support nuclear envelope formation.
5. Fixation at 4°C decreases nonspecific cholesterol loss from the plasma membrane significantly.
6. Labeling in the cold minimizes nonspecific cholesterol extraction by filipin.
7. Filipin fluorescence intensity is very faint and bleaches very rapidly. The use of an antifade mount is necessary.
8. Care must be taken when handling dimethyldichlorosilane. It is explosive when in contact with water and metal. The 3% solution can be reused once for silanization.
9. Phosphoinositide standards are in the protonated form, not the sodiated form, which is crucial for ionization.
10. For PL analysis (PA, PC, PI, PA, PG, and PS), the internal standard is added prior to extraction. In the case of phosphoinositides, the DPPI(3,4,5)P_3 standard was found to be very unstable when added prior to extraction of the biological sample. For this reason, all lipid internal standards are added postextraction when measuring the phosphoinositide content. It should be verified that the intensity of the internal standards, IS2, remains the same whether they are extracted with biological sample or if they are added postextraction.
11. Solvent acidification allows protonation of negatively charged lipids and improves lipid recovery in the organic phase.
12. To view a diagram of the assembly, see the Fisher Scientific website (http://www.fisher.co.uk) and look for product FDC-910-010B.
13. The addition of a K_4EDTA aqueous phase facilitates the phase separation and the purification of lipids from soluble proteins and salts. K_4EDTA also chelates lipid counterions such as Ca^{2+} that affect lipid ionization.

14. Charged lipids adhere to the stainless steel loop and thus affect phosphoinositide recovery significantly, so the commercial stainless steel loop is replaced by polyetheretherketone (PEEK) tubing.
15. Phosphoinositides are very unstable molecules that need to be ionized under gentle conditions to preserve their structure.
16. Precursor scans on PtdInP, PtdInP_2, and PtdInP_3 have very low sensitivities that can be overcome by multiple ion scans.
17. Tannic acid solution is made fresh each day.
18. Acrolein, as opposed to PFA and glutaraldehyde, is a lipid fixative that preserves cholesterol in the membranes.
19. For very small SUVs (50-nm diameter), it might be necessary to probe-sonicate for as long as 1 h.
20. Repeated resuspension avoids loss of sample. Care is taken not to retain any aggregates in the sample.
21. Salts and carbohydrates in buffers modify dramatically the two 90° pulse, p1, values. It is thus crucial to measure p1 for every new NMR experiment.
22. High temperature is necessary for better probe incorporation. We assume that the long treatment of 10 h at 40°C allows both donor and acceptor membranes to be in the fluid state and so enhances the lipid exchange between them.

References

1. Cameron LA, Poccia DL. *In vitro* development of the sea urchin male pronucleus. Dev Biol 1994;162:568–78.
2. Oldfield E, Chapman D, Derbyshire W. Lipid mobility in Acholeplasma membranes using deuteron magnetic resonance. Chem Phys Lipids 1972;9:69–81.
3. Marsan MP, Muller I, Ramos C, Rodriguez F, Dufourc EJ, Czaplicki J, Milon A. Cholesterol orientation and dynamics in dimyristoylphosphatidylcholine bilayers: A solid state deuterium NMR analysis. Biophys J 1999;76:351–9.
4. Durfourc EJ, Parish E, Chitrakom S, Smith I. Structural and dynamical details of cholesterol-lipid interaction as revealed by deuterium NMR. Biochemistry 1984;23:6062–71.
5. Aussenac F, Tavares M, Dufourc EJ. Cholesterol dynamics in membranes of raft composition: A molecular point of view from 2 H and 31P solid-state NMR. Biochemistry 2003;42:1383–90.
6. Stockton GW, Smith IC. A deuterium nuclear magnetic resonance study of the condensing effect of cholesterol on egg phosphatidylcholine bilayer membranes. I. Perdeuterated fatty acid probes. Chem Phys Lipids 1976;17:251–63.
7. Kinsky SC. Antibiotic interaction with model membranes. Ann Rev Pharmacol 1970;10:119–42.
8. Behnke O, Tranum-Jensen J, van Deurs B. Filipin as a cholesterol probe. II. Filipin-cholesterol interaction in red blood cell membranes. Eur J Cell Biol 1984;35:200–15.
9. Norman AW, Demel RA, de Kruyff B, van Deenen LL. Studies on the biological properties of polyene antibiotics. Evidence for the direct interaction of filipin with cholesterol. J Biol Chem 1972;247:1918–29.
10. Drabikowski W, Lagwinska E, Sarzala MG. Filipin as a fluorescent probe for the location of cholesterol in the membranes of fragmented sarcoplasmic reticulum. Biochim Biophys Acta 1973;291:61–70.
11. Robinson JM, Karnovsky MJ. Evaluation of the polyene antibiotic filipin as a cytochemical probe for membrane cholesterol. J Histochem Cytochem 1980;28:161–8.

12. Schnitzer JE, Oh P, Pinney E, Allard J. Filipin-sensitive caveolae-mediated transport in endothelium: Reduced transcytosis, scavenger endocytosis, and capillary permeability of select macromolecules. J Cell Biol 1994;127:1217–32.
13. Beknke O, Tranum-Jensen J, van Deurs B. Filipin as a cholesterol probe. I. Morphology of filipin-cholesterol interaction in lipid model systems. Eur J Cell Biol 1984;35: 189–99.
14. Pham NA, Gal MR, Bagshaw RD, Mohr AJ, Chue B, Richardson T, Callahan JW. A comparative study of cytoplasmic granules imaged by the real-time microscope, Nile Red and Filipin in fibroblasts from patients with lipid storage diseases. J Inherit Metab Dis 2005;28:991–1004.
15. Tabas I, Zha X, Beatini N, Myers JN, Maxfield FR. The actin cytoskeleton is important for the stimulation of cholesterol esterification by atherogenic lipoproteins in macrophages. J Biol Chem 1994;269:22547–56.
16. Mukherjee S, Zha X, Tabas I, Maxfield FR. Cholesterol distribution in living cells: Fluorescence imaging using dehydroergosterol as a fluorescent cholesterol analog. Biophys J 1998;75:1915–25.
17. Collas P, Poccia D. Methods for studying *in vitro* assembly of male pronuclei using oocyte extracts from marine invertebrates: Sea urchins and surf clams. Methods Cell Biol 1998;53:417–52.
18. Byrne RD, Zhendre V, Larijani B, Poccia DL. Nuclear envelope formation *in vitro*: A sea urchin egg cell-free system. Methods Mol Biol 2009;in press.
19. Rouser G, Fkeischer S, Yamamoto A. Two dimensional thin layer chromatographic separation of polar lipids and determination of phospholipids by phosphorous analysis of spots. Lipids 1970;5:494–6.
20. Larijani B, Poccia DL, Dickinson LC. Phospholipid identification and quantification of membrane vesicle subfractions by 31P-1 H two-dimensional nuclear magnetic resonance. Lipids 2000;35:1289–97.
21. National Committee for Clinical Laboratory Standards. User evaluation of precision performance of clinical laboratory device (NCCLS). NCCLS Publication EP5-T; 1984.
22. Pettitt TR, Dove SK, Lubben A, Calaminus SD, Wakelam MJ. The analysis of intact phosphoinositides in biological samples. J Lipid Res 2006;47:1588–96.
23. Brügger B, Erben G, Sandhoff R, Wieland FT, Lehmann WD. Quantitative analysis of biological membrane lipids at the low picomole level by nano-electrospray ionization tandem mass spectrometry. Proc Natl Acad Sci USA 1997;94:2339–44.
24. Mizuhira V. Futaesaku Y. New fixation method for biological membranes using tannic acids. Acta Histochem Cytochem 1972;5:233–6.
25. Mobius W, Ohno-Iwashita Y, van Donselaar EG, Oorschot VM, Shimada Y, Fujimoto T, Heijnen HF, Geuze HJ, Slot JW. Immunoelectron microscopic localization of cholesterol using biotinylated and non-cytolytic perfringolysin O. J Histochem Cytochem 2002;50:43–55.
26. Liou W, Geuze HJ, Slot JW. Improving structural integrity of cryosections for immunogold labeling. Histochem Cell Biol 1996;106:41–58.
27. Davis J, Jeffrey K, Bloom M, Valic M, Higgs T. Quadrupolar echo deuteron magnetic resonance spectroscopy in ordered hydrocarbon chains. Chem Phys Lett 1976;42:390–4.
28. Rance M, Byrd R. Obtaining high-fidelity spin-1/2 powder spectra in anisotropic media:phase cycled Hahn spectroscopy. J Magn Reson 1983;52:221–40.

Chapter 7
Solution and Solid-State NMR of Lipids

Axelle Grelard, Anthony Couvreux, Cécile Loudet and Erick J. Dufourc

Abstract Lipid structure and dynamics are of first importance for cellular function. Lipids such as phosphatidyl inositol (PtdIns) are essential in signaling pathways, as they are recognition sites at the membrane surface. Their head-group or chain structure appears to be crucial for such a signaling role. Other lipids such as cholesterol and sphingomyelin are key molecules in maintaining membrane integrity and are the building blocks of membrane domains, such as "rafts." It is essential to have techniques that can decipher both the structure and dynamics of various classes of lipids. With its liquid-state and solid-state facets, NMR is a very powerful tool for such a determination. We show that lipids extracted from membranes and dissolved in organic solvents can reveal their molecular structure when observed with multinuclear one-dimensional or two-dimensional NMR. We also show that multinuclear solid-state NMR provides information on the nature of the membrane phase (lamellar, hexagonal, isotropic, etc.), its dynamics (fluid or gel, or liquid ordered with cholesterol), and the molecular structure of embedded lipids when using the magic angle spinning apparatus. Typical examples of relatively simple experiments are shown both with liquid- and solid-state NMR of lipids.

Keywords Liquid- and solid-state ^{1}H-^{13}C-^{31}P-^{2}H-NMR · membranes · gel and fluid phases · hexagonal phases · liquid-ordered state · cholesterol · sphingomyelin · phosphatidylinositol · dipalmitoylphosphatidylcholine · dipalmitoylphosphatidylglycerol · high-resolution and wide-line spectra

E.J. Dufourc
UMR 5248 CBMN, CNRS-Université Bordeaux 1-ENITAB, IECB, 2 rue Robert Escarpit, 33607 Pessac, France
e-mail: e.dufourc@iecb.u-bordeaux.fr

B. Larijani et al. (eds.), *Lipid Signaling Protocols*, DOI: 10.1007/978-1-60327-115-8_7,

7.1 Introduction

One of the building blocks in cell biology, lipids are present in many cellular locations. They may be found in solution at very low concentration or appear in small aggregates that allow their transport in water media; they may also be embedded in cellular membranes where their dynamics are much more reduced. In this case, they constitute the cement of the bilayer membrane and also play many signaling roles. For instance, cholesterol (CH) and sphingomyelin (SM) are key molecules in maintaining membrane integrity and are the building blocks of membrane domains, such as "rafts" [1, 2]. Lipids such as phosphatidyl inositol (PtdIns) are essential in signaling pathways as they are recognition sites at the membrane surface [3]. Their head-group or chain structure appears to be crucial for such a signaling role.

In order to decipher their structure both in solution and in their membrane environment, nuclear magnetic resonance (NMR) is one of the most powerful techniques because it can act both in solution and in media of reduced dynamics such as membranes or aggregates. NMR relies on the presence of active nuclei in atoms that constitute the lipid molecules. A lipid naturally contains protons (^{1}H), carbon (only the ^{13}C is active, but in low natural abundance), phosphorus (^{31}P), oxygen (only the ^{17}O is magnetically active but has a very low natural abundance), and nitrogen (^{14}N). Some lipids may be chemically labeled with the hydrogen isotope, deuterium (^{2}H), with fluorine (^{19}F) or other nuclei of interest for structural biology.

Since lipids are usually not water-soluble, the easiest way to analyze the chemical structure of lipids is to dissolve them in organic solvents such as chloroform ($CHCl_3$) or methanol (MeOH). It is also of great interest to measure both their structure and dynamics in a hydrated membrane state (liposomes, bilayers vesicles of various sizes, etc.) or in a real membrane (see Garnier-Lhomme et al. in this volume). First, we present applications of NMR for studying lipids dissolved in organic solution. The study of lipids in membranes requires the use of solid-state NMR, which we present in a second part.

7.2 Materials

7.2.1 Analysis of Lipids Using Multinuclear Solution NMR

7.2.1.1 Samples, Preparation Tools, and Measuring Cells

1. $CDCl_3$ (99.9 % atom D, 0.1% TMS) (Aldrich).
2. Lipids: liver phosphatidylcholine (PtdCho), liver phosphatidylethanolamine (PtdEth), liver phosphatidylinositol (PtdIns), 1,2-dipalmitoyl-*sn*-glycero-3-phosphocholine (DPPtdCho), 1,2-dioleoyl-*sn*-glycero-3-phosphoglycerol (DOPG), cholesterol > 98% pure, brain sphingomyelin (SM), ceramide (Avanti Polar Lipids) See structures in Fig. 7.1.

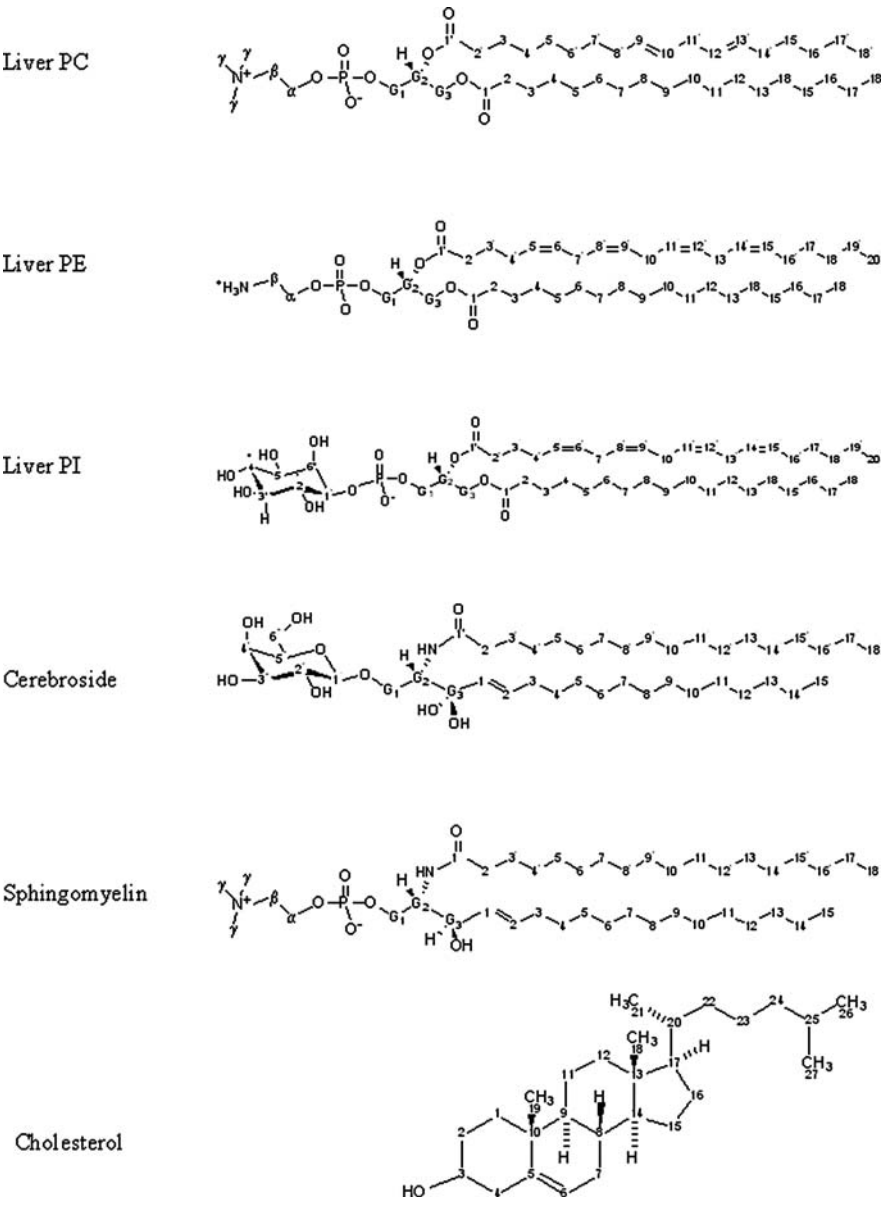

Fig. 7.1 Molecular structures of selected lipids with numbering for Tables 7.1–7.4

3. 2-ml micro-centrifuge tubes (VWR, France).
4. MS2 Minishaker (VWR).
5. 5-mm-diameter NMR glass tube (Cortec, France).

7.2.1.2 NMR Instrumentation for ^{1}H NMR

1. NMR Spectrometer: Bruker Avance 400 operating at 400.13 MHz (Bruker, Wissembourg, France).
2. NMR liquid-state probe: QNP $^{1}H/^{13}C$-^{31}P-^{19}F 5-mm liquid probe equipped with Z gradient and ^{2}H lock. Probe is tuned to 400.13 MHz.
3. PC station with Topspin software v1.3 (Bruker).

7.2.1.3 NMR Instrumentation for ^{13}C NMR

1. NMR spectrometer: Bruker Avance 400 operating at 100.61 MHz (Bruker).
2. NMR liquid-state probe: QNP $^{1}H/^{13}C$-^{31}P-^{19}F 5-mm liquid probe equipped with Z gradient and ^{2}H lock. Probe is tuned to 100.61 MHz for channel ^{13}C and to 400.13 MHz for channel ^{1}H.
3. PC station with Topspin software v1.3 (Bruker).

7.2.1.4 NMR Instrumentation for Two-Dimensional NMR (^{31}P-^{1}H)

1. NMR spectrometer: Bruker Avance 400 operating at 161.97 MHz (Bruker).
2. NMR liquid-state probe: QNP $^{1}H/^{13}C$-^{31}P-^{19}F 5-mm liquid probe equipped with Z gradient and ^{2}H lock. Probe is tuned to 161.97 MHz for channel ^{31}P and to 400.13 MHz for channel ^{1}H.
3. PC station with Topspin software v1.3 (Bruker) (*see* Note 1).

7.2.1.5 Data Analysis

1. PC computer loaded with Topspin 2.0 software (Bruker) and Origin software V7.5 (OriginLab Corp., Northhampton, MA).
2. NMR Friend V1.2 plug-in software to import and treat NMR spectra on Origin software developed by Sébastien Buchoux, UMR5144 CNRS-University Bordeaux 1, France.

7.2.2 Analysis of Membranous Lipids Using Solid-State NMR

7.2.2.1 Samples, Preparation Tools, and Measuring Cells

1. 90% ultra pure water (miliQ-system) + 10% deuterated water ($^{2}H_2O$), v:v (Eurisotop, Saint-Aubin, France).
2. Deuterium-depleted water, $^{1}H_2O$ (Isotec-Sigma-Aldrich, France).
3. Lipids: 1,2-dipalmitoyl-$^{2}H_{62}$-*sn*-glycero-3-phosphocholine (16:0/16:0 DPPtdCho-$^{2}H_{62}$), liver phosphatidylethanolamine (PtdEth), egg PtdEth, liver phosphatidylcholine (PtdCho), brain sphingomyelin (SM), and cholesterol Avanti Polar Lipids, USA.
4. Table-top centrifuge Eppendorf (VWR).

5. 2-ml micro-centrifuge tubes (VWR).
6. MS2 Minishaker (VWR).
7. Water bath, 50°C.
8. Liquid nitrogen, 50 ml in 500-ml Dewar.
9. Zirconia (ZrO_2) 4-mm-diameter magic angle spinning (MAS) rotor of HR-MAS type (50 µl) and of CP-MAS type (100 µl) (Cortec).

7.2.2.2 NMR Instrumentation for 31P

1. NMR spectrometer equipped for solid state: Bruker Avance 300 operating at 121.5 MHz (Bruker).
2. NMR probe: $^{1}H/\{^{13}C\text{-}^{17}O\}$, 4-mm CP-MAS probe tuned at 121.5 MHz (channel 31P) and 300.13 MHz (channel 1 H); equipped with temperature regulation (thermocouple and heater).
3. PC station with TopSpin software v1.3 (Bruker).
4. Bruker BCU (air-cooling) and VT (variable-temperature) units to control temperature on sample using dry airflow.

7.2.2.3 NMR Instrumentation for ^{2}H

1. NMR spectrometer equipped for solid state: Bruker Avance 500 operating at 76.77 MHz (Bruker).
2. NMR probe: low gamma $^{1}H/\{^{13}C\text{-}^{17}O\}$ 4-mm CP-MAS probe tuned at 76.77 MHz; equipped with temperature regulation (thermocouple and heater).
3. PC station with TopSpin software v1.3 (Bruker).
4. Bruker BCU (air-cooling) and VT (variable-temperature) units to control temperature on sample using dry airflow.

7.2.2.4 NMR Instrumentation for HR-MAS ^{1}H-NMR

1. NMR spectrometer equipped for solid state: Bruker Avance 500 operating at 500.16 MHz (Bruker).
2. NMR probe: $^{1}H/^{13}C$, 4 mm HR-MAS probe tuned at 500.16 MHz, equipped with temperature regulation (thermocouple and heater).
3. PC station with TopSpin software v1.2 (Bruker).
4. Bruker BCU (air-cooling) and VT (variable-temperature) units to control temperature on sample using dry airflow.
5. Bruker pneumatic MAS unit to control sample rotation at the magic angle.

7.2.2.5 Data Analysis

1. PC computer loaded with Topspin 2.0 software (Bruker) and Origin software V7.5 (OriginLab Corp.).

2. NMR Friend V1.2 plug-in software to import and treat NMR spectra on Origin software developed by Sébastien Buchoux, UMR5144 CNRS-University Bordeaux 1 (*see* Note 2).

7.3 Methods

7.3.1 Analysis of Lipids Using Multinuclear Solution NMR

The simplest liquid-state NMR experiment (*see* Subheading 7.3.1.1) leads to one-dimensional (1D) high-resolution spectrum, that is, very sharp lines of variable intensity dispersed along a frequency axis. In order to obtain such a spectrum, the lipid must be entirely dissolved in solution. Aggregates will lead to broader lines, from which accurate information can no longer be extracted. Three types of information can be obtained from a high-resolution 1D-NMR spectrum: (1) The position of a NMR line, the chemical shift expressed in ppm, shows the local electric environment of the nucleus (atom) in the molecule. In principle, this allows identification of the molecular species using standard tables of chemical shifts. (2) Some lines exhibit fine structure; they are split into multiplets (doublets, triplets, etc.), providing information on the number of nearest neighboring nuclei. This is also used for molecular structure identification. (3) The intensity of a given line is proportional to the number of nuclei giving rise to the signal. This means that NMR is a quantitative method and can be used for determining either molecular structure or the proportion of different species in mixtures. In the following, two examples of 1D liquid-state NMR of liquids are given (Figs. 7.2 and 7.3).

For more complex molecular structures or for lipid mixtures, 1D-NMR is limited because spectra are crowded with hundreds or thousands of lines. Two-dimensional (2D-NMR) or three-dimensional NMR is then used. Of the many experiments possible to decipher the structure of molecules in solution that are usually used in structural biology with proteins or nucleic acids, only one 2D-NMR experiment will be presented that allows the structural assignment of phospholipids in a mixture (Fig. 7.4).

7.3.1.1 Structural Determination of Phosphatidylinositol (PtdIns), Sphyngomyelin (SM), and Cholesterol (CH) Using ^{1}H-NMR in Solution

1. The lipids are dissolved in C $^{2}HCl_3$ up to a concentration of 10 mM. Clean and dry 5-mm sample tubes are filled with 500 µl of the solution.
2. The sample tube is placed in the magnetic field, the measuring probe is properly tuned to 400.13 MHz, and the space and time homogeneity is adjusted by a deuterium "lock" system using the deuterated solvent as a reference.

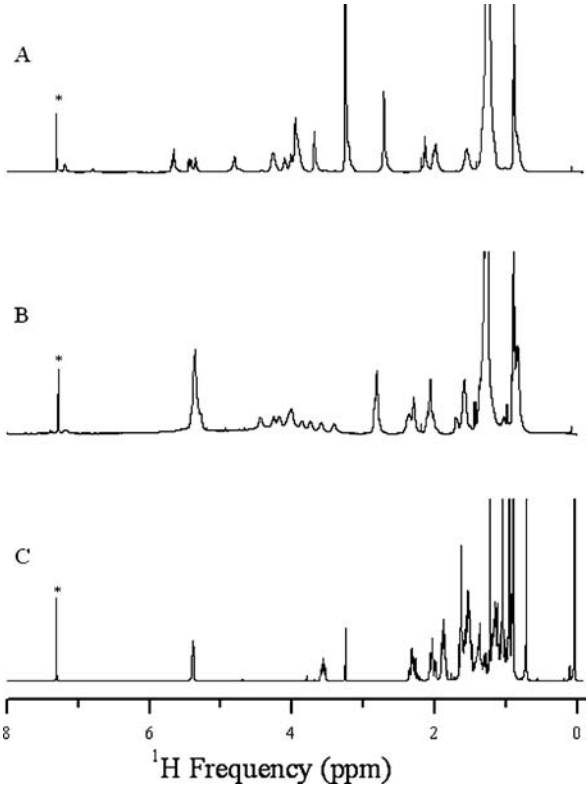

Fig. 7.2 (a) Solution ^{1}H-NMR spectra of liver PtdCho, (b) liver PtdIns, and (c) cholesterol dissolved in deuterated choloroform $C^{2}HCl_3$ containing traces of TMS as reference (0 ppm). Asterisk denotes solvent peak

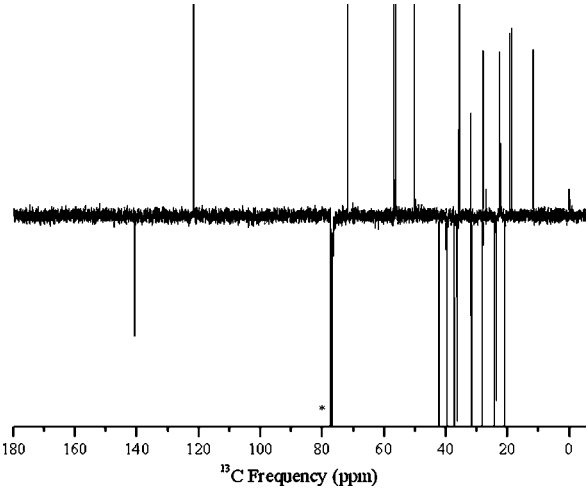

Fig. 7.3 Solution ^{13}C-NMR spectrum of cholesterol dissolved in deuterated choloroform $C^{2}HCl_3$ containing traces of TMS as reference (0 ppm). Acquisition is designed such that CH_3 and CH groups appear as single positive lines and CH_2 and quaternary carbons as single negative lines. Asterisk denotes solvent peak

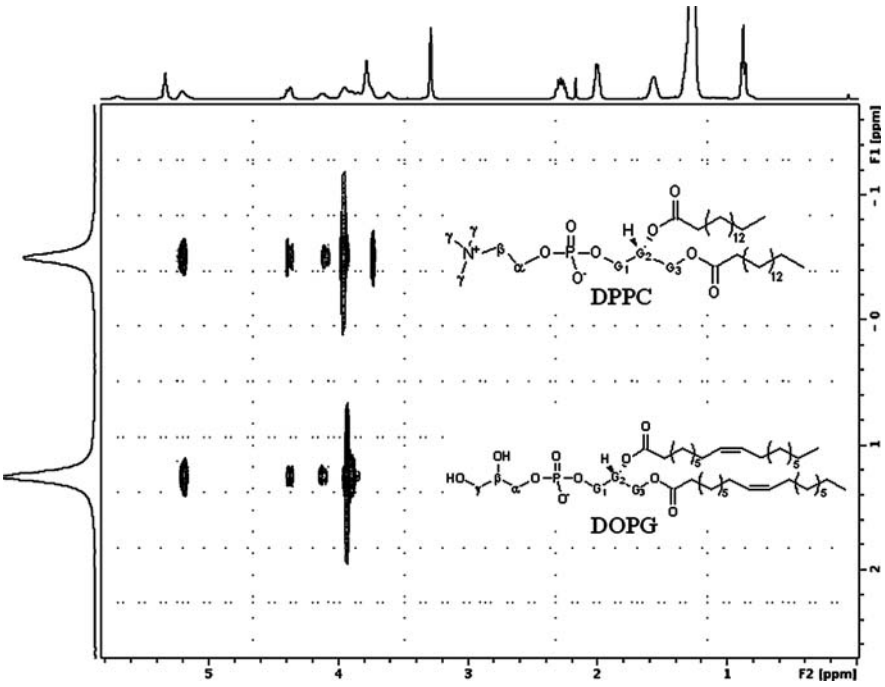

Fig. 7.4 Solution {^{31}P-^{1}H} NMR two-dimensional correlation map of DPPtdCho and POPG dissolved in deuterated choloroform C^2HCl_3. ^{1}H chemical shifts are on the horizontal bottom axis with a ^{1}H 1D-spectrum on the top axis. ^{31}P chemical shifts are on the vertical right axis with a ^{31}P 1D-spectrum on the left axis. A trace in the 2D map indicates that there are through-bond correlations (closeness) between phosphorus and protons

3. ^{1}H NMR spectroscopy is performed at 400.13 MHz, a so-called 90° single-pulse sequence is used, with a pulse duration (P1) of 13 μs (*see* Note 3), a time domain (TD) set to 32 K points, a spectral width (SW) of 20 ppm, and a relaxation delay (D1) of 2 s (*see* Note 4). The number of scans is set to 16 (*see* Note 5). These conditions determine a total acquisition time of 70 s for the time-dependent signal (FID).
4. Processing parameters: Noise filtering with an exponential window of the FID, characterized by the Lorentzian line-broadening factor [lb = 0.3 Hz (*see* Note 6)], is used. This noise filtering generally improves the signal-to-noise ratio, but at the cost of resolution. The Fourier transformation is applied to get the spectrum, and its phase is adjusted to correct for unavoidable time delays in acquisition (Fig. 7.2). Referencing (the rightmost signal of TMS is set to 0 ppm), peak picking (measure of chemical shifts in ppm), and peak integration (measure line areas) are part of the relevant processing parameters.
5. The strategy for structure elucidation is to determine the functional groups and then link the groups to the entire molecule (*see* Note 7). Table 7.1 reports the structural assignment of ^{1}H chemical shifts for selected lipids.

Table 7.1 ^{1}H chemical shifts of lipids in $C^{2}HCl_3$ [Ambient temperature, reference TMS (0 ppm)]

	N	Cerebroside	Liver PtdIns	Sphingomyelin	Liver PtdEth	Liver PtdCho	M	Cholesterol
Head group	1"/α	4.25	4.26	3.72	3.97	4,25		
	2"/β	3.86	4.05	3.92	3.20	3.65		
	3"/γ	3.73	3.86	3.34	8.29	3.23		
	4"	3.53	3.41					
	5"	3.44	3.75					
	6"	3.93	3.60					
Backbone	G1	4.22/4.34	4.46/4.18	3.92	4.17/4.42	4.14/4.39		
	G2	5.39	5.30	5.21	5.23	5.21		
	G3	7.01	4.02	4.14	4.10	3.92		
Fatty acyl chains	1	5.8		5.36	nd		1	nd
	1'				nd		2	nd
	2	5.66	2.30/2.37	5.36	2.26/2.31	2.25/2.32	3	3.51
	2'	2.24	2.30/2.37	2.27/2.29	2.26/2.31	2.25/2.32	4	2.28
	3	2.06	1.70/1.58	2.00	1.59	1.58	5	
	3'	1.85	1.70/1.58	1.57	1.59	1.58	6	5.35
	4	1.27	1.29	1.25	1.27	1.25	7	nd
	4'	1.27	2.08	1.25	2.05	1.25	8	nd
	5	1.27	1.29	1.25	1.27	1.25	9	nd
	5'	1.27	5.38	1.25	5.37	1.25	10	
	6	1.27	1.29	1.25	1.27	1.25	11	nd
	6'	1.27	5.38	1.25	5.37	1.25	12	nd
	7	1.27	1.29	1.25	1.27	1.25	13	
	7'	1.27	2.81	1.25	2.82	1.25	14	nd
	8	1.27	1.29	1.25	1.27	1.25	15	nd
	8'	1.27	5.38	1.25	5.37	2.05	16	nd
	9	1.27	1.29	1.25	1.27	1.25	17	nd
	9'	1.27	5.38	1.25	5.37	5.36	18	0.68
	10	1.27	1.29	1.25	1.27	1.25	19	1.12
	10'	1.27	2.81	1.25	2.82	5.36	20	nd
	11	1.27	1.29	1.25	1.27	1.25	21	0.91
	11'	1.27	5.38	1.25	5.37	2.81	22	nd
	12	1.27	1.29	1.25	1.27	1.25	23	nd
	12'	1.27	5.38	1.25	5.37	5.36	24	nd
	13	1.07	1.29	1.25	1.27	1.25	25	nd
	13'	1.27	2.81	1.25	2.82	5.36	26	0.86
	14	0.88	1.29	1.25	1.27	1.25	27	0.87
	14'	1.27	5.38	1.25	5.37	2.05		
	15		1.29	0.88	1.27	1.25		
	15'	1.27	5.38	1.25	5.37	1.25		
	16		1.29		1.27	1.25		
	16'	1.27	1.29	1.25	2.05	1.25		
	17		1.29		1.27	1.25		
	17'	1.27	1.29	1.25	1.25	1.25		

Table 7.1 (continued)

N	Cerebroside	Liver PtdIns	Sphingomyelin	Liver PtdEth	Liver PtdCho	M Cholesterol
18		0.87		0.89	0.88	
18'	1.07	2.08	0.88	1.27	0.88	
19						
19'	0.88	1.29		1.27		
20'		0.87		0.89		

nd = not determined. Numbers separated by "/" (e.g., 4.46/4.18) indicate two lines of chemical shifts.

7.3.1.2 Structural Determination of Cholesterol (CH) Using ^{13}C-NMR (Proton J-mod Experiment) in Solution

1. The lipids are dissolved in C $^{2}HCl_3$ up to a concentration of 10 mM. Clean and dry 5-mm sample tubes are filled with 500 µl of the solution.
2. The sample tube is placed in the magnetic field, the measuring probe is properly tuned to 100.61 MHz and 400.13 MHz, and the space and time homogeneity is adjusted by a deuterium "lock" system using the deuterated solvent as a reference.
3. ^{13}C NMR spectroscopy was performed at 100.61 MHz, a APT pulse sequence [4] was used, with a pulse length of 13 µs (*see* Note 3), a time domain (TD) set to 32 K points, a spectral width (SW) of 25 kHz, a relaxation delay (D1) of 3 s (*see* Note 4), and an evolution delay (D20) of 7 ms (D20 = $1/J_{CH}$ with J_{CH} = 145 Hz). The number of scans was set to 3 K (*see* Note 5). These conditions determine a total acquisition time of 3 h.
4. Processing parameters: Noise filtering with an exponential window of the FID, characterized by the Lorentzian line-broadening factor [lb = 2 Hz (*see* Note 6)], is used. A Fourier transformation is applied to get the spectrum, and its phase is adjusted to correct for unavoidable time delays in acquisition. Referencing (the rightmost signal of TMS is set to 0 ppm) and peak picking (measure of chemical shifts in ppm) are part of the relevant processing parameters.
5. The NMR sequence is set such that signals of CH and CH_3 groups appear positive and signals of CH_2 and quaternary carbons (the solvent C $^{2}HCl_3$ as well) appear negative (*see* Fig. 7.2). This allows the straightforward assignment of functional groups. Table 7.2 reports the structural assignment of ^{13}C chemical shifts for cholesterol, cerebroside, sphingomyelin, liver PtdEth, and liver PtdCho.

7.3.1.3 Structural Assignment of Phospholipids in a Solution Mixture Using a {^{31}P-^{1}H} 2D-NMR Experiment

1. The lipids are dissolved in C $^{2}HCl_3$ up to a concentration of 10 mM. Clean and dry 5-mm sample tubes are filled with 500 µl of the solution.

Table 7.2 ^{13}C chemical shifts of lipids in C^2HCl_3 [Ambient temperature, reference TMS (0 ppm)]

	N	Cerebroside	Sphingomyelin	Liver PtdEth	Liver PtdCho	M	Cholesterol
Head group	1"/α	104.57	63.37	63.09	63.56		
	2"/β	69.82	66.32	40.80	66.17		
	3"/γ	72.12	54.37		54.18		
	4"	74.28					
	5"	76.02					
	6"	62.30					
Backbone	G1	69.12	66.32	63.80	62.89		
	G2	53.90	63.01	70.74	70.55		
	G3	72.60	70.51	62.78	59.39		
Fatty acyl chains	1	134.31	129.7/130.02	174.66	173.80	1	37.18
	1'	175.00	173.2/173.58	174.66	173.80	2	31.60
	2	130.27	129.7/130.02	34.59	34.14	3	71.73
	2'	37.08	34.32	34.59	34.14	4	42.23
	3	33.11	27.23	23.19	24.88	5	140.68
	3'	27.97	24.91	23.19	24.88	6	121.74
	4	30.50	29.34–31.92	29.82–40.94	22.66–31.91	7	31.82
	4'	30.50	29.34–31.92	29.74	22.66–31.91	8	nd
	5	30.50	29.34–31.92	29.82–40.94	22.66–31.91	9	50.05
	5'	30.50	29.34–31.92	127.52–132.51	22.66–31.91	10	36.42
	6	30.50	29.34–31.92	29.82–40.94	22.66–31.91	11	21.01
	6'	30.50	29.34–31.92	127.52–132.51	22.66–31.91	12	39.71
	7	30.50	29.34–31.92	29.82–40.94	22.66–31.91	13	nd
	7'	30.50	29.34–31.92	26.11	22.66–31.91	14	56.69
	8	30.50	29.34–31.92	29.82–40.94	22.66–31.91	15	24.23
	8'	30.50	29.34–31.92	127.52–132.51	27.27	16	28.16
	9	30.50	29.34–31.92	29.82–40.94	22.66–31.91	17	56.07
	9'	30.50	29.34–31.92	127.52–132.51	127.83/129.89	18	11.79
	10	30.50	29.34–31.92	29.82–40.94	22.66–31.91	19	19.33
	10'	30.50	29.34–31.92	26.11	127.83/129.89	20	35.70
	11	30.50	29.34–31.92	29.82–40.94	22.66–31.91	21	18.65
	11'	30.50	29.34–31.92	127.52–132.51	25.56	22	36.12
	12	30.50	29.34–31.92	29.82–40.94	22.66–31.91	23	23.75
	12'	30.50	29.34–31.92	127.52–132.51	127.83/129.89	24	39.45
	13	23.25	29.34–31.92	29.82–40.94	22.66–31.91	25	27.94
	13'	30.50	29.34–31.92	26.11	127.83/129.89	26	22.50
	14	14.42	26.29	29.82–40.94	22.66–31.91	27	22.75
	14'	30.50	29.34–31.92	127.52–132.51	27.27		
	15		14.10	29.82–40.94	22.66–31.91		
	15'	30.50	29.34–31.92	127.52–132.51	22.66–31.91		
	16			29.82–40.94	22.66–31.91		
	16'	30.50	29.34–31.92	29.74	22.66–31.91		
	17			23.07	22.66–31.91		
	17'	30.50	26.29	29.82–40.94	22.66–31.91		

Table 7.2 (continued)

N	Cerebroside	Sphingomyelin	Liver PtdEth	Liver PtdCho	M Cholesterol
18		14.10	14.62	14.09	
18'	23.25		29.82–40.94	14.09	
19					
19'	14.42		23.07		
20					
20'			14.62		

nd = not determined. Range numbers (e.g., 127.52–132.51) indicate that more than two lines in the range cannot be assigned with confidence. Numbers separated by "/" (e.g., 127.83/129.89) indicate two lines of chemical shifts, which cannot be assigned with confidence.

2. The sample tube is placed in the magnetic field, the measuring probe is properly tuned to 161.94 MHz and 400.13 MHz, and the space and time homogeneity is adjusted by a deuterium "lock" system using the deuterated solvent as a reference.
3. $\{^{31}P\text{-}^{1}H\}$ two-dimensional NMR spectroscopy was performed at 161.94 MHz and 400.13 MHz. Parameters for the inverse HMQC-TOCSY sequence [5, 6] are ^{1}H and ^{31}P 90° pulses, respectively, 13 μs and 5 μs (*see* Note 3), recycle delay (D1) 2s (*see* Note 4), a spectral width (SW2) in the F2 dimension of 12 ppm (1,024 points), an SW1 in the F1 dimension of 20 ppm (256 increments), acquisition mode in Echo-antiEcho on F1 and quadrature on F2, DIPSI mixing time of 101 ms (22 cycles), $J_{PH} = 7$ Hz , ^{31}P-decoupling during acquisition, and the number of scans was set to 80 (*see* Note 5). These conditions determine a total acquisition time of 13 h.
4. Data sets were processed with QSINE windows functions in both directions with SSB = 2 (*see* Note 8). Once the double Fourier transform has been performed, the phase is adjusted in the F2 dimension only. The F1 dimension is in Magnitude mode. A 2D map is plotted such as peaks are projected onto the plane (Fig. 7.5).
5. Phosphorus chemical shifts were referenced relative to 85% of H_3PO_4 (0 ppm), and ^{1}H chemical shifts to TMS (0 ppm) (Fig. 7.5).
6. The so-called correlation peaks in Fig. 7.5 are found at the intersection of vertical and horizontal lines linking protons and phosphorus that are close through bonds (in the molecular structure). They allow assignment of structures in a mixed sample. ^{31}P-NMR chemical shifts of common lipids are given in Table 7.3.

7.3.2 Analysis of Membranous Lipids Using Solid-State NMR

The membrane that defines the cell entity or the cell organelles is by its very nature a medium that is halfway between a liquid and a solid. Called "soft

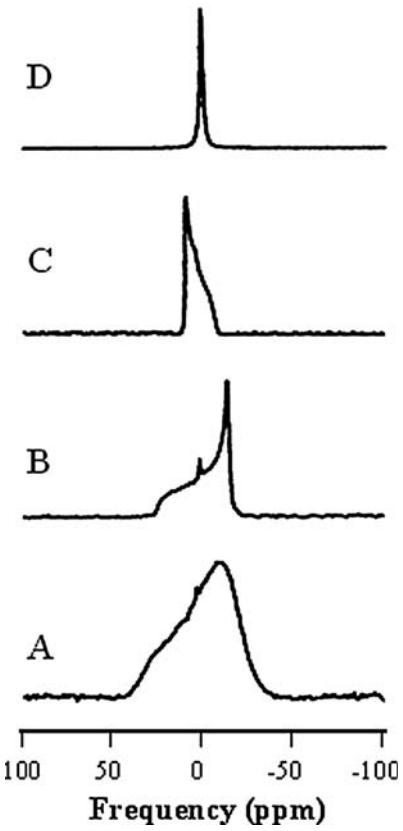

Fig. 7.5 Solid-state wide-line ^{31}P-NMR solid-state spectra of Egg PtdEth dispersed in water (liposomes). Protons are broadband decoupled from phosphorus. (a) Lamellar gel phase, T = −10°C; (b) lamellar fluid phase, T = 20°C; (c) hexagonal phase, T = 50°C; (d) isotropic phase (small vesicles, micelles, etc.), T = 90°C

matter," this state is, by definition, a liquid crystalline medium whose anisotropic properties are essential for membrane function and cells. Molecules embedded, such as lipids (or membrane proteins), may undergo many dynamic processes such as lateral diffusion in the bilayer plane, transverse diffusion from one membrane leaflet to the other, and conformational changes in the interior

Table 7.3 ^{31}P chemical shifts of lipids in C^2HCl_3 [Ambient temperature, reference 85% H_3PO_4 (0 ppm)]

	DPPtdCho	Lyso PtdCho	SM	CL	PtdIns	PtdSer	PtdEth
PO4	−0.51	0.10	0.30	0.51	0.0, −0.2	0.25	0.43

Source: Adapted from Pearce et al. [23].
DPPtdCho = dipalmitoylphosphatidylcholine; Lyso PtdCho = lysophosphatidylcholine; SM = sphingomyelin; CL = cardiolipin; PtdIns = phosphatidylinositol; PtdSer = phosphatidylserine; PtdEth = phosphatidylethanolamine.

Table 7.4 ^{1}H chemical shifts of liposomal lipids in H_2O/D_2O (90/10) [Ambient temperature, reference TSP (0 ppm)]

	N	Sphingomyelin	Liver PtdEth	Liver PtdCho
Head group	α	nd	3.97	3.99
	β	nd	3.22	3.66
	γ	3.66	7.87	3.21
Backbone	G1	nd	nd	nd
	G2	5.31	5.29	5.31
	G3	4.00	4.03	4.27
Fatty acyl chains	1	5.71		
	1'			
	2	5.71	2.40	2.28
	2'	2.22/2.31	nd	2.28
	3	2.02	1.57	1.57
	3'	1.60	nd	1.57
	4	1.29	1.24	1.25
	4'	1.29	2.00	1.25
	5	1.29	1.24	1.25
	5'	1.29	nd	1.25
	6	1.29	1.24	1.25
	6'	1.29	nd	1.25
	7	1.29	1.24	1.25
	7'	1.29	2.75	1.25
	8	1.29	1.24	1.25
	8'	1.29	nd	2.02
	9	1.29	1.24	1.25
	9'	1.29	nd	nd
	10	1.29	1.24	1.25
	10'	1.29	2.75	nd
	11	1.29	1.24	1.25
	11'	1.29	nd	2.77
	12	1.29	1.24	1.25
	12'	1.29	nd	nd
	13	1.29	1.24	1.25
	13'	1.29	2.75	nd
	14	1.29	1.24	1.25
	14'	1.29	nd	2,02
	15	0.88	1.24	1.25
	15'	1.29	nd	1.25
	16		1.24	1.25
	16'	1.29	2.00	1.25
	17		1.24	1.25
	17'	1.29	1.24	1.25
	18		0.85	0.86
	18'	0.88	1.24	0.86
	19			
	19'		1.24	
	20'		0.85	

nd = not determined. Numbers separated by "/" (e.g., 2.22/2.31) indicate two lines of chemical shifts.

membrane. They may also group as patches in the membrane plane that are named "rafts" to picture the rigidity of these membrane domains that swim in a "sea" of more fluid lipids and proteins. Understanding the structure and dynamics of membrane components will not reveal the function of lipids (or proteins) but will provide insight toward deciphering complex biological processes such as cell recognition, fusion, trafficking, apoptosis, energetic, signal transduction, etc.

Two general types of spectra can be obtained using solid-state NMR: "wide line" and "high resolution." Wide-line NMR can be sensitive to membrane symmetry (Fig. 7.5) and molecular motions (Fig. 7.6). It is a useful tool to determine the nature of membrane phases (lamellar, hexagonal, isotropic, etc.) [7, 8] and track membrane dynamics (membrane fluidity, fusion, gel, liquid-ordered, and fluid states). The well-known regulating effect of cholesterol on membrane phases (increasing the fluidity of ordered phases and decreasing that of fluid phases) can easily be monitored by using lipids that are deuterated [9–11]. Wide-line NMR can also probe average orientations of molecules embedded in membranes (membrane topology) [9, 10, 12] when used with X-ray structural information. The latter will not be presented here. The 3D structure of molecules in membranes is also obtained by making use of magic angle sample spinning, a technique that leads to pseudo "high-resolution" spectra as in the liquid state, where the sample is still in the membrane "liquid crystalline" state (Fig. 7.7). Another facet of NMR is relaxation studies, which this chapter does not discuss. Briefly, this aspect brings together the measurement of the speed of molecular motion and activation energies, allowing us to picture membrane dynamics from the atomic level, where intramolecular motion dominates, to the cell level, where membrane hydrodynamic modes of motion play an important role [13–15].

7.3.2.1 Determination of Lipid Phase (Lamellar, Hexagonal, Isotropic) Using Wide-Line ^{31}P-NMR

1. Appropriate amounts of phospholipids are weighed and a suitable volume of water is added to obtain a lipid hydration (water mass/total mass) 80% (w/w). Lipid concentration is of the order of 200 mM.
2. The hydrated sample is then vigorously shaken in a vortex mixer, frozen in liquid nitrogen, and heated to 50°C for 10 min in a water bath. This cycle of liposome (multilamellar vesicles) formation is repeated three to five times until a milky dispersion is obtained at room temperature.
3. The resulting dispersion is transferred into a 4-mm NMR ZrO_2 rotor (100 µl) that is placed in the magnetic field. The measuring probe is properly tuned to 121.5 MHz (^{31}P channel) and 300.13 MHz (^{1}H channel) and the space homogeneity is adjusted to the optimum level.

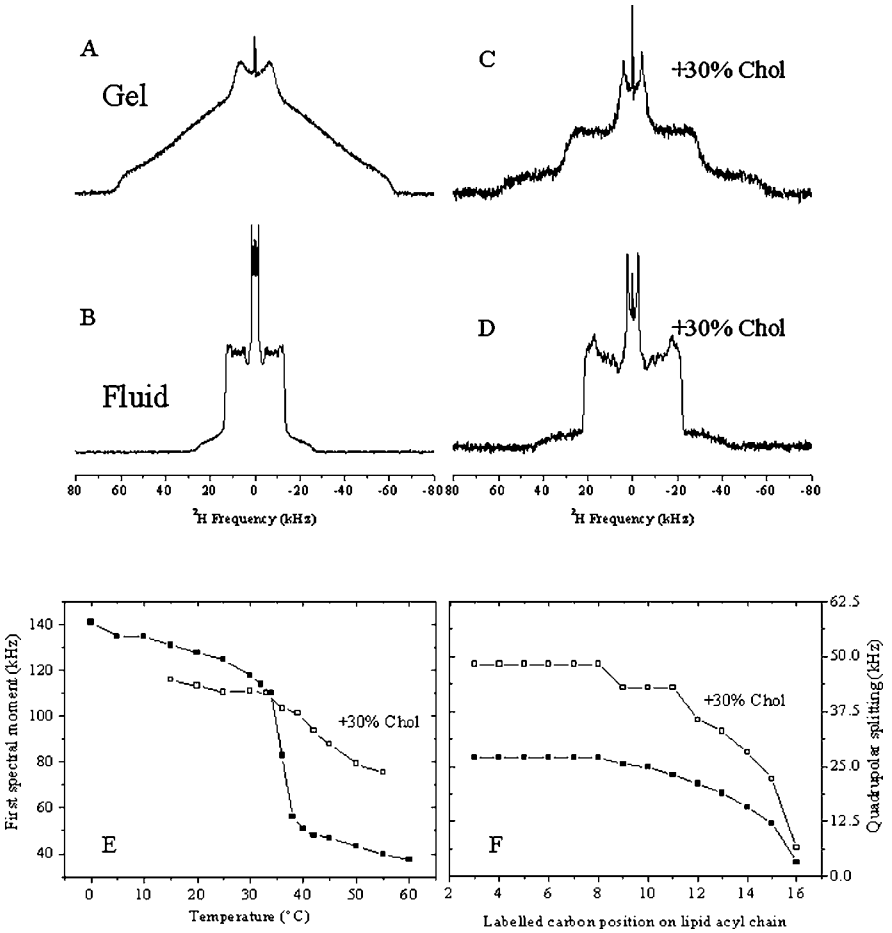

Fig. 7.6 Solid-state wide-line ^{2}H-NMR spectra of DPPtdCho-$^2H_{62}$with and without cholesterol dispersed in water (liposomes). (a) DPPtdCho, T = 10°C; (b) DPPtdCho, T = 40°C; (c) DPPtdCho/cholesterol (2/1 molar), T = 10°C, (d) DPPtdCho/cholesterol (2/1 molar), T = 40°C. (e) First spectral moment as a function of temperature for DPPtdCho (filled symbol) and DPPtdCho/cholesterol (empty symbol) spectra. (f) Quadrupolar splittings for DPPtdCho acyl chains at 40°C in the presence (empty symbols) and absence (filled symbols) of cholesterol

4. Using the variable-temperature setup (VT and BCU units), samples are allowed to equilibrate 15–30 minutes at a given temperature before the time-dependent NMR signal (FID) is acquired; the temperature is regulated to ±1°C (*see* Note 9).
5. ^{31}P-NMR spectroscopy is performed at 121.5 MHz. FID are acquired using a phase-cycled Hahn echo-pulse sequence with gated broadband proton decoupling [16]. Typical acquisition parameters were as follows: $\pi/2$ pulse

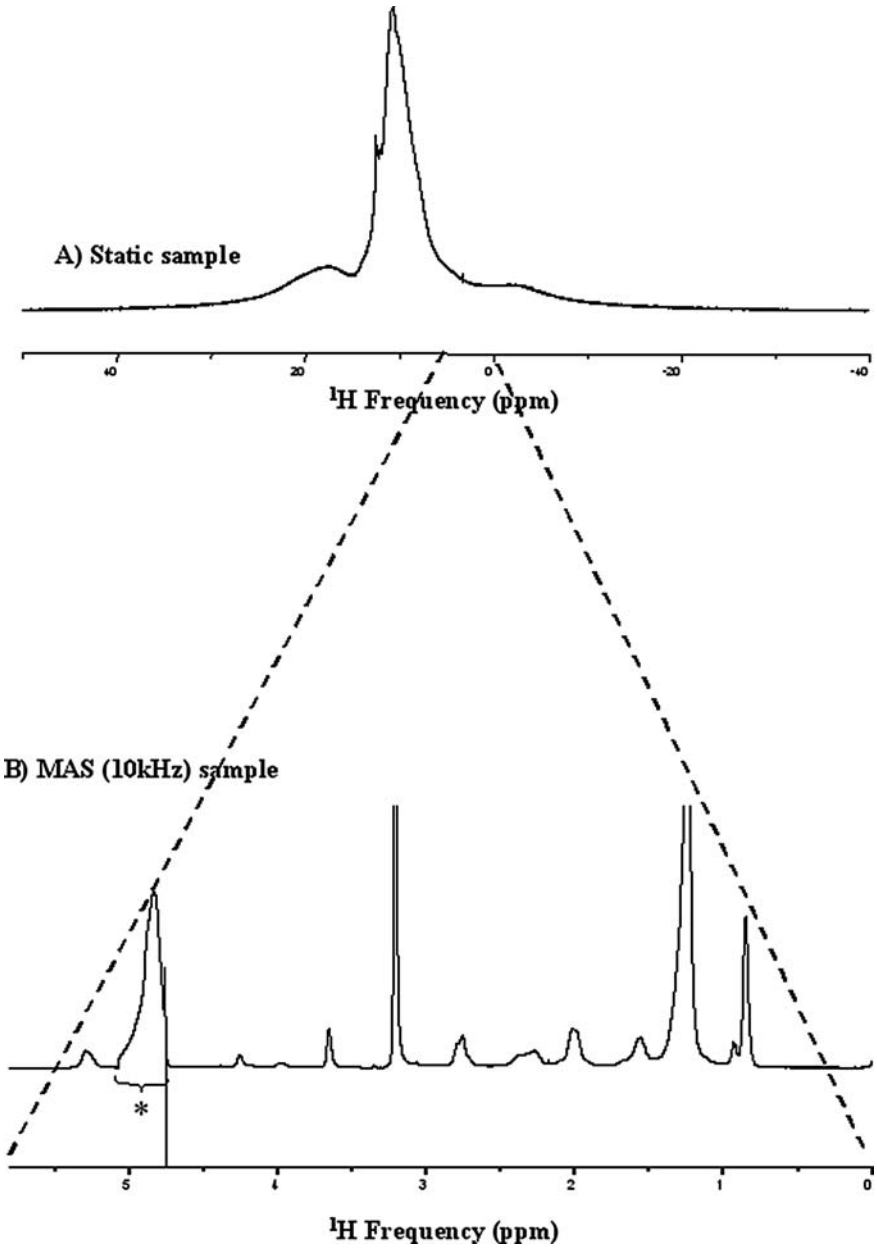

Fig. 7.7 Solid-state "high-resolution" magic angle spinning ^{1}H-NMR spectrum of liver PtdCho dispersed in water containing 10% D_2O. Water suppression (asterisk) was used during signal acquisition. (a) Spectrum without spinning; (b) with MAS rate = 10 kHz. Note the change in *x*-scale from (a) 90 ppm to (b) 6 ppm

width (P1) of 14.5 μs (*see* Note 10), spectral window (SW) of 32 kHz, interpulse delay (D6) of 50 μs, and repetition delay (D1) of 5 s. Typically, 512 scans are recorded in 42 minutes.

6. Processing parameters: Noise filtering with an exponential window of the FID, characterized by the Lorentzian line-broadening factor (lb = 10–50 Hz), is used. A Fourier transformation is applied to get the spectrum, and its phase is adjusted to correct for unavoidable time delays in acquisition. Reference is made to 85% H_3PO_4 (0 ppm). The width of the spectrum is measured and used to calculate the chemical shift anisotropy (CSA).
7. The spectrum at −10°C (Fig. 7.5a) is broad and characteristic of a gel phase where the shielding tensor of the phosphate begins showing nonaxial symmetry due to the very restricted dynamics of the phase.
8. The spectrum obtained at 20°C (Fig. 7.5b) is much narrower along the frequency axis and shows a shape characteristic of a lamellar fluid phase with axial symmetry (only one intense peak on the right and a shoulder on the left).
9. The spectrum obtained at 50°C (Fig. 7.5c) has a width reduced by a factor ca. 2 with respect to that at 20°C and has a reverse symmetry (intense peak on the left and shoulder on the right) characteristic of a hexagonal phase.
10. A phase with isotropic symmetry (Fig. 7.5d) (cubic, micelles, etc.) occurs at 90°C: A single, very intense sharp line appears and is centered at ca. 0 ppm.

7.3.2.2 Determination of Lipid Dynamics in Lamellar Bilayers (Gel, Fluid, Liquid-Ordered) Using Wide-Line ^{2}H-NMR

1. Appropriate amounts of phospholipids are weighed (*see* Note 11).
2. A suitable volume of deuterium-depleted water, ^1H_2O, was added to obtain a lipid hydration of 80% (v/w). Hydration is defined as the mass of water over the total mass of the system (phospholipids and water).
3. The hydrated sample is then vigorously shaken in a vortex mixer, frozen in liquid nitrogen, and heated to 50°C for 10 min in a water bath. This cycle of liposome (multilamellar vesicles) formation is repeated three to five times until a milky dispersion is obtained at room temperature.
4. The resulting dispersion is transferred into a 4-mm NMR ZrO_2 rotor (100 μl) that is placed in the magnetic field (*see* Note 12). The measuring probe is properly tuned to 76.77 MHz (^{2}H channel) and the space homogeneity is adjusted to the optimum level.
5. Using the variable-temperature setup (VT and BCU units), samples are allowed to equilibrate 15–30 minutes at a given temperature before the time-dependent NMR signal (FID) is acquired; the temperature is regulated to ±1°C (*see* Note 9).
6. ^{2}H NMR spectroscopy was performed at 76.77 MHz. NMR spectra were acquired using a solid quadrupolar echo-pulse sequence [17]. Typical

acquisition parameters were as follows: spectral window of 500 kHz, $\pi/2$ pulse width 3 μs (*see* Note 13), interpulse delay of 30 μs. A recycle delay of 1 s was used. Typically, 512–1,024 scans were accumulated in 8–15 minutes.

7. Processing parameters: Noise filtering with an exponential window of the FID, characterized by the Lorentzian line-broadening factor (lb = 50–300 Hz), is used. A Fourier transformation is applied to get the spectrum, and its phase is adjusted to correct for unavoidable time delays in acquisition. The peak-to-peak separation, called the "quadrupolar splitting," that can be obtained, in principle, for nonequivalent C-^{2}H bonds can be measured on some spectra. Spectral moments can also be used to estimate width and shape changes in spectra [13, 18].
8. The spectrum at 10°C for DPPtdCho-$^2H_{62}$ liposomes (Fig. 7.6a) is characteristic of a gel phase where the quadrupolar interaction occurring for each C-^{2}H bond (there are 62 deuterium-labeled positions on the acyl chains of DPPtdCho-$^2H_{62}$) reveals nonaxial symmetry due to the very restricted chain dynamics and to the symmetry of the phase. No peak-to-peak measurement can be measured on such spectrum, except for the central broad doublet assigned to the chain-end deuterated methyl groups. The first moment is calculated using a routine built in the Origin software.
9. The spectrum obtained at 40°C for DPPtdCho-$^2H_{62}$ liposomes (Fig. 7.6b) is much narrower along the frequency axis and shows a shape characteristic of a lamellar fluid phase with axial symmetry. The overall spectrum is nonetheless complex because it represents the superposition of all spectra coming from all C-^{2}H bonds. Several peak-to-peak separations, quadrupolar splittings, can be measured and plotted as a function of the labeled carbon position along the acyl chain (Fig. 7.6f). Spectral deconvolution [19, 20] can be applied here for more resolution.
10. The spectrum at 10°C for DPPtdCho-$^2H_{62}$/cholesterol (2/1) liposomes (Fig. 7.6c) is characteristic of a liquid-ordered phase where the quadrupolar interaction occurring for each C-^{2}H bond reveals axial symmetry due to the axial diffusion of lipids in the membrane.
11. The spectrum at 40°C for DPPtdCho-$^2H_{62}$/cholesterol (2/1) liposomes (Fig. 7.6d) is characteristic of a liquid-ordered phase with greater dynamics than at 10°C (spectrum of smaller width). Several peak-to-peak separations, quadrupolar splittings, can be measured and plotted as a function of the labeled carbon position along the acyl chain (Fig. 7.6f).
12. Spectra were recorded as a function of temperature, and the first moment was calculated and plotted against temperature (Fig. 7.6e). Elevated values are found for gel-phase temperatures and depict an ordered rigid state, whereas smaller values are found above the gel-to-fluid phase transition temperature (ca. 37°C) for pure DPPtdCho-$^2H_{62}$ liposomes and depict a disordered lamellar fluid phase. If cholesterol has been added, the transition is nearly smoothed out, demonstrating the

regulating effect of cholesterol: It increases the fluidity of ordered phases and decreases that of fluid phases.

13. Peak-to-peak separation, so-called quadrupolar splittings, measured for individual C-^{2}H bonds report on local space and time angular fluctuations. When plotted against labeled acyl chain position, they report on local dynamics (order/disorder) (Fig. 7.6f). The greater the quadrupolar splitting, the higher the order (fewer bond fluctuations). C-^{2}H bonds close to the glycerol backbone (positions 2–8) are much more ordered than those near the bilayer center (positions 12–16).

7.3.2.3 Determination of Lipid Molecular Structure in a Membrane Environment Using ^{1}H HR-MAS

1. Appropriate amounts of phospholipids were weighed. In case of lipid mixtures, lipids are dissolved in organic solvent ($CHCl_3$/MeOH), the solvent is evaporated, water is added, and the sample is shaken in a vortex mixer and lyophilized to remove solvent traces.
2. A suitable volume of ultra pure water mixed with deuterated water (90:10, v:v) containing traces of TSP (trimethylsilylpropionic acid) as a reference (0 ppm) was added to obtain a lipid hydration of 80% (v/w). Hydration is defined as the mass of water over the total mass of the system (phospholipids and water).
3. The hydrated sample is then vigorously shaken in a vortex mixer, frozen in liquid nitrogen, and heated to 50°C for 10 min in a water bath. This cycle of liposome (multilamellar vesicles) formation is repeated three to five times until a milky dispersion is obtained at room temperature.
4. The resulting dispersion is transferred into a 4-mm NMR ZrO2 rotor for "high-resolution MAS NMR" (50 µl) that is placed in the magnetic field.
5. Speed for magic angle spinning is set to 7–10 kHz using the pneumatic unit device. Using the variable-temperature setup (VT and BCU units), samples are allowed to equilibrate 15–30 min at 30°C before the time-dependent NMR signal (FID) is acquired; the temperature is regulated to ±1°C. The measuring probe is properly tuned to 500.16 MHz, and the space and time homogeneity is adjusted by a deuterium "lock" system using the deuterated solvent as a reference.
6. ^{1}H-NMR spectroscopy was performed at 500.16 MHz. NMR spectra were acquired using a single-pulse sequence with water suppression [21]. Typical acquisition parameters are pulse duration (P1) of 5.5 µs, a time domain (TD) set to 32 K points, a spectral width (SW) of 20 ppm, and a relaxation delay (D1) of 3 s. The number of scans is set to 16. These conditions determine a total acquisition time of 90 s for the time-dependent signal (FID).
7. Processing parameters: Noise filtering with an exponential window of the FID, characterized by the Lorentzian line-broadening factor (lb = 0.3 Hz), is used. This noise filtering generally improves the signal-to-noise ratio, but at the cost of resolution. A Fourier transformation is applied to get the

spectrum and its phase is adjusted to correct for unavoidable time delays in acquisition (Fig. 7.7). Referencing (residual water signal is assigned to 4.7 ppm), peak picking (measure of chemical shifts in ppm), and peak integration (measure of line areas) are part of the relevant processing parameters.

8. The spectrum obtained in the absence of rotation (Fig. 7.7a) is characteristic of an unresolved proton spectrum of a membrane phase. No peak-to-peak measurement can be measured on such a spectrum.
9. The spectrum obtained for a MAS speed of 10 kHz (Fig. 7.7b) shows a resolution that is akin to that obtained in liquids, the sample still being under the form of liposomes. Referencing, peak picking, and peak integration can now be applied.
10. The strategy for structure elucidation is the same as for lipids in solution (*see* Subheading 7.3.1.1). 2D-NMR experiments (COSY, TOCSY) are often needed for complete assignment. Table 7.3 reports the structural assignment of ^{1}H chemical shifts for selected lipids in liposomal form.

Notes

1. Data may also be treated on the computer that drives the spectrometer. Most spectrometer-linked computers are now PCs.
2. Spectral moment calculations or spectral de-Pake-ing may not be available on computers driving spectrometers. They can nonetheless be implemented on PCs by obtaining the source code from the authors [13, 20].
3. P1 is determined with a routine provided on all spectrometers (POPT on Bruker software). It must be determined individually for samples with different solvents (because of the different dielectric constants that may modify the P1 value).
4. Relaxation delays are also determined using a routine provided on spectrometers, which allows calculation of spin lattice relaxation time, T_1. D1 is usually set to $5*T_1$ for optimum relaxation delay.
5. The number of scans is chosen such that the signal-to-noise ratio is greater than approximately 50.
6. Line broadening is set in order to filter spectral noise without marked modification of peak line width.
7. Many groups can be identified by their ^{1}H chemical shifts using chemical shift tables [22] and coupling constants (multiplet separation). Two-dimensional NMR experiments (COSY, TOCSY) are sometimes needed for complete assignment.
8. More sophisticated window filtering can be used since they are available with most spectrometer software.
9. Experiments may sometimes be run overnight implementing a temperature variation from low to high temperatures and back to low to detect possible sample hysteresis.
10. Same as Note 3 indicates, but the presence of salt may alter the P1 duration.
11. With lipid mixtures (DPPC/cholesterol), lipids are dissolved in organic solvent ($CHCl_3$/MeOH), the solvent is evaporated, water is added, and the sample is shaken in a vortex mixer and lyophilized to remove solvent traces. All these experiments can be run with DPPtdCho-$^{2}H_{31}$ (less expensive) instead of DPPtdCho-$^{2}H_{62}$. The number of scans must then be increased by a factor of 2.
12. In order to facilitate the transfer into the rotor, it may be wise to vary (increase or decrease) the temperature to be in a fluid state. The sample may then be easily poured into the rotor.

13. The pulse must be very short to acquire very wide spectra (hundreds of kHz). Using longer pulse widths will lead to intensity loss in the outer verges of the spectrum and hence errors in spectral moment calculation.

References

1. Simons K, Ehehalt R. Cholesterol, lipid rafts, and disease. J Clin Invest 2002;110: 597–603.
2. Simons K, Ikonen E. How cells handle cholesterol. Science 2000;290:1721–6.
3. Byrne RD, Barona TM, Garnier M, Koster G, Katan M, Poccia DL, Larijani B. Nuclear envelope assembly is promoted by phosphoinositide-specific PLC with selective recruitment of phosphatidylinositol enriched membranes. Biochem J 2004;387:393–400.
4. Braun S, Kalinowski H-O, Berger S. 150 and More Basic NMR Experiments. Weinheim, Germany: Wiley-VCH; 1998:596.
5. Henke J, Willker W, Engelmann J, Liebfritz D. Combined extraction techniques of tumor cells and lipid/phospholipid assignment by two-dimensional NMR spectroscopy. Anticancer Res 1966;16:1417–27.
6. Palmer AG, Cavanagh J, Wright PE, Rance M. Sensitivity improvement in proton-detected two-dimensional heteronuclear correlation NMR spectroscopy. J Magn Reson 1991;93:151–70.
7. Marinov R, Dufourc EJ. Cholesterol stabilizes the hexagonal type II phase of 1-palmitoyl-2-oleoyl *sn* glycero-3-phosphoethanolamine. A solid state ^{2}H and ^{31}P NMR study. J Chim Physiq 1995;92:1727–31.
8. Marinov R, Dufourc EJ. Thermotropism and hydration properties of POPE and POPE-cholesterol systems as revealed by solid state ^{2}H and ^{31}P-NMR. Eur Biophy J 1996;24:423–31.
9. Aussenac F, Tavares M, Dufourc EJ. Cholesterol dynamics in membranes of raft composition: A molecular point of view from ^{2}H and ^{31}P solid state NMR. Biochemistry 2003;42:1383–90.
10. Dufourc EJ, Parish EJ, Chitrakorn S, Smith ICP. Structural and dynamical details of cholesterol-lipid interaction as revealed by deuterium NMR. Biochemistry 1984;23: 6063–71.
11. Pott T, Maillet JC, Dufourc EJ. Effects of pH and cholesterol on DMPA membranes: A solid state ^{2}H- and ^{31}P-NMR study. Biophys J 1995;69:1897–908.
12. Marsan MP, Muller I, Ramos C, Rodriguez F, Dufourc EJ, Czaplicki J, Milon A. Cholesterol orientation and dynamics in dimyristoylphosphatidylcholine bilayers: A solid state deuterium NMR analysis. Biophys J 1999;76:351–9.
13. Dufourc EJ. Solid state NMR in biomembranes. In Larijani B, Rosser CA, Woscholski R, eds. Chemical Biology. London: John Wiley & Sons, Ltd.; 2006:113–31.
14. Dufourc EJ, Mayer C, Stohrer J, Althoff G, Kothe G. Dynamics of phosphate head groups in biomembranes. Comprehensive analysis using phosphorus-31 nuclear magnetic resonance lineshape and relaxation time measurements. Biophys J 1992;61:42–7.
15. Dufourc EJ, Smith ICP. A detailed analysis of the motions of cholesterol in biological membranes by ^{2}H-NMR relaxation. Chem Phys Lipids 1986;41:123–35.
16. Rance M, Byrd RA. Obtaining high-fidelity spin-1/2 powder spectra in anisotropic media: Phase-cycled Hahn echo spectroscopy. J Magn Reson 1983;52:221–40.
17. Davis JH. Deuterium magnetic resonance study of the gel and liquid crystalline phases of dipalmitoylphosphatidylcholine. Biophys J 1979;27:339–58.
18. Davis JH, Jeffrey KR, Bloom M, Valic MI, Higgs TP. Quadrupolar echo deuteron magnetic resonance spectroscopy in ordered hydrocarbon chains. Chem Phys Lett 1976; 42:390–4.

19. Bloom M, Davis JH, Mackay AL. Direct determination of the oriented sample NMR spectrum for systems with local axial symmetry. Chem Phys Lett 1981;80:198–201.
20. Sternin E, Bloom M, Mackay, AL. De-Pake-ing of NMR spectra. J Magn Reson 1983;55:274–82.
21. Piotto M, Saudek V, Sklenar V. Gradient-tailored excitation for single-quantum NMR spectroscopy of aqueous solutions. J Biomol NMR 1992;2:661–666.
22. Pretsch E, Bühlmann P, Affolter C. Structure Determination of Organic Compounds. Berlin: Springer-Verlag; 2000:421.
23. Pearce JM, Shifman MA, Pappas AA, Komoroski RA. Analysis of phospholipids in human amniotic fluids by 31P-NMR. Magn Reson Med 1991;21:107–16.

Chapter 8
Spatial Localization of PtdInsP_2 in Phase-Separated Giant Unilamellar Vesicles with a Fluorescent PLC-delta 1 PH Domain

Xavier Mulet, Erika Rosivatz, Ka Kei Ho, Béatrice L.L.E. Gauthé, Oscar Ces, Richard H. Templer and Rudiger Woscholski

Abstract This chapter describes a method for the preparation of giant unilamellar vesicles containing phosphatidylinositol 4,5-bisphosphate that are larger than 20 μm in size. The phospholipids composition of the vesicular membrane is such that fluid lamellar and liquid-ordered or gel phases are formed and separate within the confines of one vesicle. It outlines the preparation of a protein fluorescent label, pleckstrin homology domain from phospholipase C-delta 1, that binds specifically to phosphatidylinositol 4,5-bisphosphate. Using fluorescence microscopy, the presence and spatial position of this phosphorylated phosphatidylinositol lipid on the lipid membrane have been located with the pleckstrin homology domain. We show that phosphatidylinositol 4,5-bisphosphate and the phospholipase C-delta 1 pleckstrin homology domain are located to the fluid phase of the vesicle membrane. This approach can therefore show how membrane physical properties can affect enzyme binding to phosphatidylinositol 4,5-bisphosphate and thus further the understanding of important membrane processes such as endocytosis.

Keywords Giant unilamellar vesicles · phosphatidylinositol 4,5-bisphosphate · phospholipase C-delta 1 · PH domain

Abbreviations BSA: bovine serum albumin; DOPtdCho: dioleylphosphatdylcholine; DOPtdEth: dioleyl-phosphatdylethanolamine; GUV: giant unilamellar vesicle; NBD: [(7-nitro-2-1,3-benzoxadiazol-4-yl)amino]dodecanoyl; PH: pleckstrin homology; PtdInsP_2: phosphatidylinositol 4,5-bisphosphate; PLC: phospholipase C.

X. Mulet
Chemical Biology Centre, Imperial College, London, Exhibition Road, London SW7 2AZ, UK
e-mail: xavier.mulet@imperial.ac.uk

B. Larijani et al. (eds.), *Lipid Signaling Protocols*, DOI: 10.1007/978-1-60327-115-8_8, 135

8.1 Introduction

Phospholipid membranes and their properties, such as curvature and hydrophobic mismatch, have recently come under much scrutiny and have been the focus of several reviews [1–4]. These lipid bilayers show complex phase transition behavior [5], which can be observed in cell membranes during processes such as vesicle fission [6]. When giant unilamellar vesicles (GUVs) are formed from multiple lipid components, they can laterally separate into coexisting liquid phases, or domains, with distinct compositions [7]. Imaging of this compartmentalization is possible through the use of fluorescence imaging. Two fluorescent dyes preferentially locating within different lipid phases allow one to visualize the different domains. Here we outline a protocol that localizes a particular lipid species within a specific domain of the GUV with the use of a lipid-specific protein probe.

In particular, we are interested in the segregation and therefore spatial localization of phosphatidylinositol 4,5-bisphosphate (PtdInsP_2) and a specific recognition domain for it: the phospholipase C(PLC)-delta 1 pleckstrin homology (PH) domain. In our study, two types of GUVs are formed: from a ternary lipid mixture of dioleoylphosphatidylcholine (DOPtdCho), dioleoylphosphatidylethanolamine (DOPtdEth) and PtdInsP_2, as well as from a quaternary mixture of the lipids sphingomyelin (SM), cholesterol, DOPtdCho, and PtdInsP_2. We show binding without segregation to the ternary lipid system (Fig. 8.1 and Color Plate 1); in phase-separated GUVs, sphingomyelin and cholesterol enrich in a liquid phase with short-range order in the fatty acid chains [liquid-ordered phase (L_o)], while DOPtdCho forms a separate liquid disordered (L_d) phase. At physiologically relevant temperatures, these phases coexist and separate. The use of a PtdInsP_2 specific fluorescent probe adds a further dimension to the results that are acquired using such a biomimetic system as it allows spatial localization of PtdInsP_2. With the PLC-delta 1 PH domain probe, we can locate the presence of the PtdInsP_2 exclusively to the liquid-disordered phase. The vesicles with associated proteins are shown in Figs. 8.2 and 8.3 (Color Plates 2 and 3). This system can be adapted to other phosphorylated phosphatidylinositol molecules, such as phosphatidylinositol 4-phosphate and related binding domains found in cells.

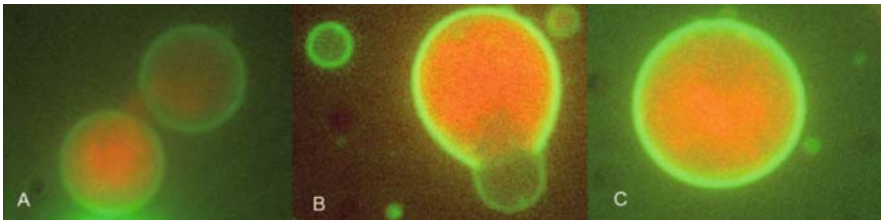

Fig. 8.1 85:10:5 mol% DOPtdCho/DOPtdEth/PtdInsP_2 vesicles, membrane labeled with DOPtdEth-NBD and PLC-delta 1 PH domain. No lipid segregation is observed here, but binding of the protein to PtdInsP_2 is distinctly observed. To view this figure in color, see color insert

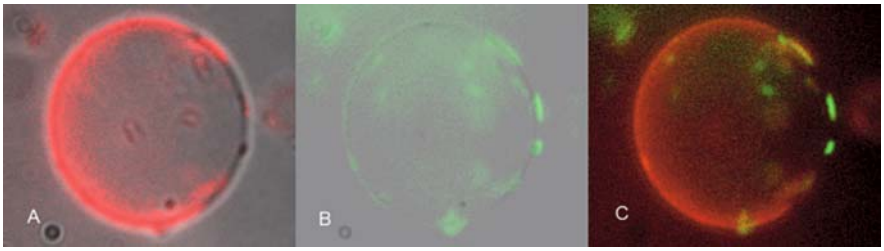

Fig. 8.2 (a) 45/40/5/10 mol% DOPtdCho/SM/Chol/PtdInsP_2 vesicles, liquid-disordered membrane labeled with DOPtdEth-NBD with brightfield image. (b) PLC-delta 1 PH domain and with brightfield image shown here, clear lipid domain separation is shown. (c) Highlights presence of protein domain and thus PtdInsP_2 in the liquid-disordered phase. To view this figure in color, see color insert

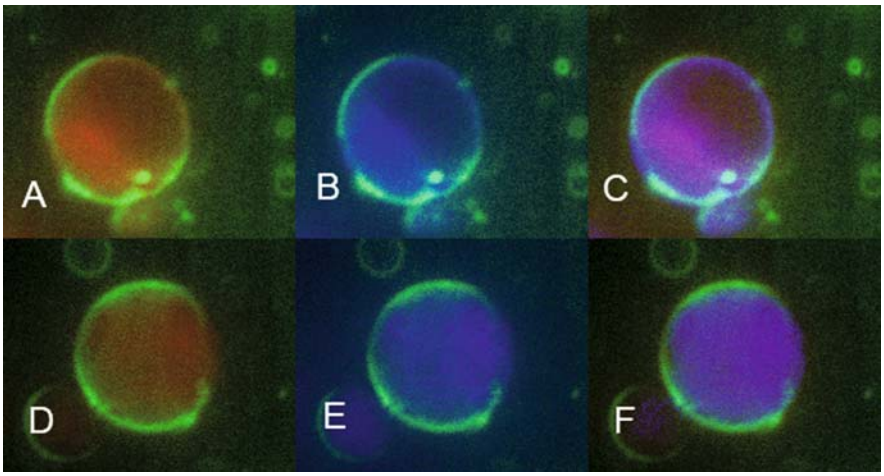

Fig. 8.3 (a) and (d) 55/15/5/25 DOPtdCho/SM/Chol/PtdInsP_2 vesicles, liquid-disordered membrane labeled with DOPtdEth-NBD with PLC-delta 1 PH domain. (b) and (e) Vesicle membranes labeled with perylene and PtdInsP_2 labeled with PLC-delta 1 PH domain. (c) and (f) Highlights the presence of protein domains and thus PtdInsP_2 in the liquid-disordered phase. To view this figure in color, see color insert

8.2 Materials

8.2.1 Lipids, Preparations of Slides for Microscope Chamber and Buffers

1. Dioleylphosphatydilcholine (DOPtdCho) and dioleylphosphatidylethanolamine (DOPtdEth) Sphingomyelin (SM) were both supplied as lyophilized powders from Avanti Lipids (Alabaster, AL, USA). PtdInsP_2 was obtained

from Lipid Products (Surrey, UK) dissolved in chloroform. These phospholipids and cholesterol (Sigma, Dorset, UK) were used without further purification (*see* Subheading 8.3.1).
2. The fluorescent lipid 1,2-dioleoyl-*sn*-glycero-3-phosphoethanolamine-N-(7-nitro-2-1,3-benzoxadiazol-4-yl) (Avanti Lipids) was used to label the liquid-disordered phase. It was used in ratios ranging from 1:500 to 1:1,000 fluorophore:lipid molecules (*see* Subheading 8.3.1). Perylene was used as a membrane probe also in 1:500 to 1:1,000 ratios (*see* Subheading 8.3.1).
3. The chloroform and methanol used for lipid solution preparation are both HiPerSolv for HPLC quality (BDH, UK) (*see* Subheading 8.3.1).
4. The microscope cover slips (22 mm × 26 mm, VWR, Leicestershire, UK) were cut with a diamond cutter to the desired size for mounting onto a sample cell. Compressed air is used to remove the majority of the dust particulates (*see* Subheading 8.3.4).
5. Fatty acid-free bovine serum albumin (BSA) 1% w/v in 200 mM glucose, 20 mM Tris-HCl, pH 7.4, is used to coat glass slides of the sample cell (*see* Subheading 8.3.4) prior to the addition of vesicles to prevent interactions between the glass surface and lipid membranes (*see* Note 1).
6. 200 mM sucrose and 20 mM Tris-HCl, pH 7.4, at 25°C are used for vesicle preparation (*see* Subheading 8.3.2). It is filtered with a 0.2-μm syringe filter (Sartorius, Epsom, UK) prior to use.
7. The imaging solution of 200 mM glucose and 20 mM Tris-HCl, pH 7.4, at 25°C is used for vesicle imaging (*see* Subheading 8.3.4). It is filtered with a 0.2-μm syringe filter (Sartorius) prior to use.

8.2.2 Protein Expression and Purification Buffers

Note: See Subheading 8.3.3 for protocol.

1. Ampicillin inoculation stock solution ×1,000: 100 mg/ml in 50% glycerol and stored at −20°C.
2. Isopropyl β-D-1-thiogalactopyranoside (IPTG) ×1,000 stock, 100 mM, made up in 50% glycerol and stored at −20°C for 3 months (BDH, UK) was used to induce protein expression.
3. 10 × Lysis buffer: 500 mM Tris-base, 20 mM ethylene-diaminetetraacetic acid (EDTA), 100 mM benzamidine, 10 mM dithiothreitol (DTT), 10% Triton X-100, and 100 μg/ml soybean trypsin inhibitor. To be stored at 4°C. Add 1 mM phenylmethylsulphonylfluoride (PMSF) before use.
4. PMSF ×1,000 stock: 100 mM, made up in 50% ethanol and stored at −20°C for 3 months.
5. The glutathione S-transferase-fusion (GST) proteins were affinity-purified using glutathione sepharose 4B (GE Healthcare, Amersham, UK).

6. Elution buffer: 20 mM reduced glutathione, 500 mM NaCl (pH 8.0), 0.02% β-mercaptoethanol (10 μl/50 ml) made up in 50% glycerol and stored at −20°C. Check pH before each use (pH 7), as the buffer will not work effectively under alkaline conditions.

8.2.3 Protein Dialysis

The dialysis membrane used for fluorescently labeled protein purification was Spectra/Pore (12-14,000 MWCO) for overnight dialysis against 2 × 2 L of 10 mM potassium phosphate, 0.15 mM NaCl, pH 7.2, with 0.2 mM sodium azide buffer.

8.3 Methods

8.3.1 Lipid Solution Preparation

Lipids are dissolved in a 3:1 chloroform:methanol mixture. They are kept in an amber glass vial with Teflon-lined cap to prevent lipid degradation. The vial is also filled with an inert gas (nitrogen or argon) to prevent lipid oxidation. Vesicle compositions can be varied by mixing various lipids to obtain the desired mixture composition (lipid concentration 10 mg/mL). The stock lipid solution may be kept at −20°C for a week. Argon gas can be added to the lipid/chloroform vial to prevent oxidation.

A typical lipid composition is 85:10:5 mol% DOPtdCho:DOPtdEth:PtdInsP_2. This composition allows efficient binding of the probe to the fluorescent protein, and lipid probes are normally used in a 1,000:1 lipid:fluorophore ratio. The formation of phase-separated vesicles is performed by choosing a lipid composition that will lead to phase coexistence. Two suggested compositions are 45/40/5/10, 55/15/5/25 mol% of SM/DOPtdCho/PtdInsP_2/cholesterol. If grown above the liquid ordered to disordered phase transition (60°C for these compositions), the lipids will mix effectively, thus creating a homogeneous lipid composition. Segregation of lipid components can be achieved by decreasing the temperature below that of the sphingomyelin gel to fluid phase transition [8].

8.3.2 Vesicle Formation by Swelling

1. The Teflon discs (1 mm thick, and with diameter suitable for a 100-ml beaker) were roughened on one side using fine glass paper to ensure an evenly rough surface with large area.

2. The Teflon discs may be reused but must be thoroughly cleaned and roughened with glass paper prior to fresh lipid layer deposition.
3. Prior to coating, the Teflon discs were immersed in a chloroform:methanol (3:1) mixture to ensure complete removal of any previous lipidic species.
4. The Teflon discs and gas-tight Hamilton syringes, used for lipid deposition, are rinsed with a 3:1 $CHCl_3$:CH_3OH v/v mixture and must be left to completely air-dry prior to lipid deposition.
5. A Hamilton glass syringe (*see* Note 2) was used to evenly coat 20 to 30 µl of lipid (10 mg/ml) chloroform mixture. If a fluorescent lipid probe is required (typically 1:1,000), then samples should be kept in the dark by enveloping the container in aluminum foil.
6. The syringe needle was used to spread (*see* Note 3) the lipid solution as thinly as possible onto the entire roughened side of the Teflon discs in order to ensure a thin layer deposition.
7. Once spread, the disc was placed rapidly under vacuum for at least 4 h to remove all traces of solvent.
8. Prehydration (*see* Note 4) of lipids was carried out with argon or nitrogen bubbled through 37°C distilled water for 10 min with the Teflon disc placed at the bottom of the 100-ml beaker.
9. Sucrose (*see* Note 5) solution was equilibrated at 37°C prior to addition in beaker (solution may be kept for 1 week), for nonphase-separated vesicles and above 60°C for phase-separated vesicles.
10. 10 ml of 200 mM sucrose was added per 100-ml beaker (filtered with 0.2-µm syringe filter) to ensure complete immersion of the disc in the solution.
11. The beaker was sealed with parafilm and incubated at 37°C overnight, for nonphase-separated vesicles, and above 60°C for vesicles capable of phase separation.
12. Three hours before they were needed, the vesicles were removed from the incubator and left to equilibrate at room temperature.
13. If correctly followed, the protocol yielded an opaque vesicular cloud suspension above the Teflon surface, which was easily gathered using a Pasteur pipette.
14. Once harvested, the vesicle suspension was diluted fivefold in equiosmotic glucose buffer to obtain solutions with different refractive indices in and out of the vesicular lumen (*see* Subheading 8.3.4 for further details).

8.3.3 Protein Sample Preparation

A PtdInsP_2-specific phospholipase (PLC)-delta 1 PH 2x domain (54.7 kDa), described by Yagisawa et al. [9], was used to label the PtdInsP_2-containing vesicles. The PH domain construct of the PLC-delta 1 was cloned into the pGEX-4T2 expression vector (Pharmacia). A DH5α strain of *Escherichia coli* was heat-shock-transformed with the expression and the protein was expressed

as follows. Several mg of glutathione S-transferase(GST)-fusion protein were regularly obtained using the described method for expression and purification.

Though samples did contain a cleaved GST component, this did not affect the results, as no membrane binding was observed upon prior incubation of the PH domain with inositol 1,4,5-trisphosphate, since this occupies the lipid's binding site. Incubation of a lipid phosphatase that hydrolyzes phosphate from the lipid head group (data not shown) inhibited any protein binding to the vesicles (data not shown), showing the specificity of the protein domain to PtdInsP_2.

The protein expression and purification are as follows:

1. Inoculate eight 10-ml LB-bouillon (with relevant selection antibiotic, ampicillin in this case) with transformed bacteria and grow overnight, shaking (225–250 rpm) at 37°C.
2. Dilute two 10-ml culture into 1,000-ml LB medium + antibiotic, thus yielding 4 L. Grow overnight as before.
3. After first 24 h growth, add antibiotic again. Grow overnight as before.
4. Induce cells with 0.1 mM (final concentration, F.C.) IPTG and grow overnight, shaking (225–250 rpm) at 16°C.
5. Harvest bacteria by centrifugation (7,700 rcf, 10 min, 4°C). Discard supernatant and resuspend bacteria in 25 ml of distilled water; this typically generates 50 ml of bacterial suspension.
6. Add lysozyme (10 mg/ml) and incubate at 4°C for 2 h.
7. Transfer cells to −20°C overnight (or longer).
8. Thaw cells upside down on ice, occasionally shaking vigorously to shear DNA. Add 10× lysis buffer (to 1× F.C.) immediately on removal from −20°C.
9. Add 50 µl 1000× PMSF (protease inhibitor) stock and fresh soybean trypsin inhibitor. Samples should become viscous as lysis occurs.
10. Lyse cells with ultra-Thorax once thawed. Samples should become highly viscous. Keep on ice until all samples are treated sufficiently. Lysis will continue over time as lysozyme destroys bacterial cell walls and osmotic stress in samples causes hydrolysis. Add 50 µl of 1000× PMSF.
11. Transfer samples to manual homogenizer, on ice, to complete lysis.
12. Start with smaller piston (loose) and homogenize with repeated strokes. Sample viscosity reduces as homogenization proceeds.
13. Change to large (tight) piston and give several strokes to ensure complete cell lysis (*see* Note 6).
14. Continue until whole sample has been treated and is again fluid.
15. Add 50 µl of PMSF stock (*see* Note 7).
16. Ultra-centrifuge samples using SS-34 rotor (23,500 rcf, 15–25 min, 4°C).
17. Gently shake GST beads to resuspend, and pour approximately 0.5 ml into 50-ml Falcon, add excess distilled water, and pulse-spin (600 rcf, room temperature). Remove 49 ml of supernatant (loose pellet) and repeat wash.

18. Pour homogenate supernatant onto beads (do not disturb homogenate pellet), shake, and add 0.5 M (FC) NaCl (salt addition reduces both viscosity and nonspecific binding) and 50 µl of 1000× PMSF.
19. Spin sample (550 rcf, 1 min, RT).
20. Decant supernatant, reload, add 0.5 M (FC) NaCl, and repeat spin (*see* Note 8).
21. Continue until all sample has been loaded to beads. If aggregates form, 0.5 M (F.C.) NaCl will greatly reduce nonspecific binding.
22. Wash beads with ddaq and 0.5 M (FC) NaCl; shake vigorously to disrupt aggregates and spin (550 rpm, 1 min, RT). Samples can be left after this wash if necessary. Remove supernatant (loose pellet).
23. Repeat washes with ddaq (salt no longer needs to be added) until there is no foam indicating the presence of Triton. Distilled must be ultra-pure (18.2 MΩ, molecular grade) and all detergent traces must be removed because they will interfere with downstream experiments (three to four washes are usually required).
24. Transfer beads to a 2-ml microcentrifuge tube and pulse-spin.
25. Pipette off ddaq and replace with 1 ml of elution buffer.
26. Elute protein overnight at −20°C. Pipette eluted protein off beads and store at −20°C. The beads can be reused.
27. Protein recovery was checked by SDS PAGE and Western blotting (α-GST for GST-fusion proteins, 10-µl sample) or SDS PAGE Coomassie (data not shown).

This PH domain protein was subsequently labeled with an Alexa fluor 546 protein labeling kit (Invitrogen, Paisley, UK) and dialyzed with 12-kDa dialysis membrane (*see* Subheading 8.2.1), to minimize the observed background signal.

8.3.4 Microscopy and Preparation of Micromanipulation Cell

Microscopy is performed on a Nikon Eclipse TE2000-E inverted microscope (Nikon UK Ltd., Surrey, UK), controlled with IPLab (BD Biosciences Bioimaging, Rockville, MD) software. X 20 Hoffman Modulation (Hoffman Modulation Optics, Greenvale, NY) optics are essential for the successful brightfield imaging of vesicles. Fluorescent imaging is performed with a x20 plan fluorite lens. The data are recorded with an air-cooled CCD camera (Orca ER, Hamamatsu, Japan).

The vesicle samples are contained within an in-house designed temperature-controlled sample cell. The chamber that holds the vesicles must be prepared prior to vesicle addition to prevent the vesicles from adhering to the glass surfaces of the slides. The chamber itself consists of an assembly of stainless steel plates with an integrated water flow temperature control system. The sample cell is prepared as follows:

1. The glass slides were mounted, using vacuum grease, onto the sample chamber and the temperature of the chamber set.
2. A BSA solution drop was added between the two glass slides so that it covered a small area (1 cm^2).
3. One hour of incubation at room temperature ensured coating of the glass surfaces with BSA.
4. The sucrose vesicle suspension was diluted at least five times in equiosmotic glucose solution to increase the contrast during the imaging process.
5. The BSA solution was removed and replaced with the vesicle suspension.
6. The vesicles required 20 minutes to settle to the bottom of the chamber.
7. GUVs are distinguishable from multilamellar vesicles due to undulations of the membrane.
8. The vesicle was be incubated with the desired enzyme; in the case of Figs. 8.1, 8.2, and 8.3, with 0.1 nmol of labeled PH domain. It may be necessary to alter the buffer conditions to prevent protein aggregation (*see* Note 9).
9. Following incubation of approximately an hour, binding of the protein to the lipid is clearly observable, as shown in Fig. 8.1. It becomes possible to localize the presence of the PtdInsP_2 by using the PH domain and, for phase-separated vesicles, to locate the presence of PtdInsP_2 in the different membrane domains (Figs. 8.2 and 8.3).
10. Phase separation can be analyzed by comparing the localization of the PH domain to that of the perylene and NDB fluorophore lipid probe. The presence of the PH domain in the liquid-disordered region indicates that the PH domain binds specifically to PtdInsP_2 present in the liquid-disordered phase.

Notes

1. BSA must be fatty acid-free to prevent interference with the lipid membrane and prevent contamination. The presence of fatty acids would lead to weaker vesicles.
2. Different Hamilton syringes should be used for different lipid types to prevent cross contamination. The syringes should be thoroughly rinsed before and after every use.
3. Spreading the solution with one even stroke appears to produce a greater proportion of unilamellar vesicles, as it forms an even film.
4. This is a crucial step and omission of this step drastically lowers yield of vesicles.
5. Sucrose solution is used to fill the lumen of the vesicles due to its greater density than glucose. This causes the vesicles to sink to the bottom of the observation chamber when placed in a glucose solution. Locating the vesicles is thus possible.
6. Check viscosity and repeat homogenization with a large piston if samples have become too viscous (high viscosity prevents efficient centrifugation).
7. From this point, samples cannot be allowed to stand between steps.
8. Performing several repeat loadings is better than splitting the beads and loading all of the sample at the same time.
9. BSA may be necessary to prevent aggregation of the protein sample caused by rapid dilution of the protein stock. The presence of approximately 1 mg/ml of fatty acid-free BSA should prevent the formation of protein aggregates (shown in Fig. 8.4 and Color Plate 4).

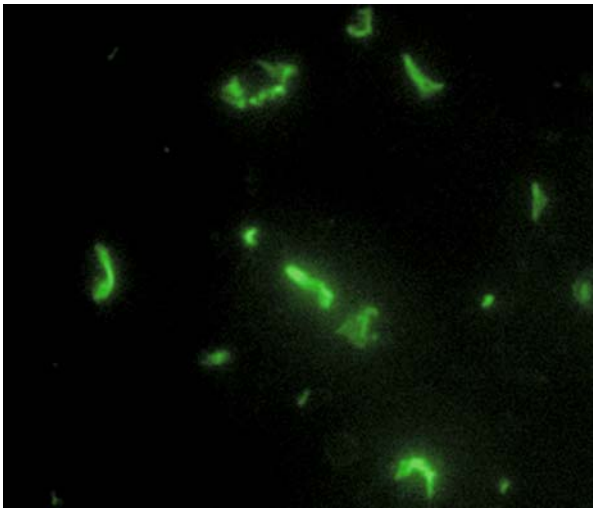

Fig. 8.4 PH domain fibrils formed without BSA in imaging solution. To view this figure in color, see color insert

References

1. Ces O, Mulet X. Physical coupling between lipids and proteins: A paradigm for cellular control. Signal Transduc 2006;6:112–32.
2. Zimmerberg J, Kozlov MM. How proteins produce cellular membrane curvature. Nat Rev Mol Cell Biol 2005;7:9–19.
3. McMahon HT, Gallop JL. Membrane curvature and mechanisms of dynamic cell membrane remodelling. Nature 2005;438:590–6.
4. van den Brink-van der Laan E, Killian JA, de Kruijff B. Nonbilayer lipids affect peripheral and integral membrane proteins via changes in the lateral pressure profile. Biochim Biophys Acta 2004;1666:275–88.
5. Seddon JM. Structure of the inverted hexagonal (HII) phase, and non-lamellar phase transitions of lipids. Biochim Biophys Acta 1990;1031:1–69.
6. Dobereiner HG, Kas J, Noppl D, Sprenger I, Sackmann E. Budding and fission of vesicles. Biophys J 1993;65:1396–403.
7. Baumgart T, Hess ST, Webb WW. Imaging coexisting fluid domains in biomembrane models coupling curvature and line tension. Nature 2003;425:821–4.
8. de Almeida RF, Fedorov A, Prieto M. Sphingomyelin/phosphatidylcholine/cholesterol phase diagram: Boundaries and composition of lipid rafts. Biophys J 2003;85:2406–16.
9. Yagisawa H, Hirata M, Kanematsu T, Watanabe Y, Ozaki S, Sakuma K, Tanaka H, Yabuta N, Kamata H, Hirata H, et al. Expression and characterization of an inositol 1,4,5-trisphosphate binding domain of phosphatidylinositol-specific phospholipase C-delta 1. J Biol Chem 1994;269:20179–88.

Chapter 9
Studying Cell-to-Cell Interactions: An Easy Method of Tethering Ligands on Artificial Membranes

Sebastian J. Fleire and Facundo D. Batista

Abstract Extensive studies have been performed in order to understand the interaction of receptors with soluble ligands. However, we know very little of the parameters that regulate the interaction of receptors with membrane-bound ligands. Artificial lipid bilayers can be used to mimic cell-to-cell interactions, but a major challenge remains how to tether molecules to these membranes. We describe a simple and reliable method to tether ligands on glass-supported artificial bilayers containing biotinylated lipids. In this system, the model antigen hen egg lysozyme (HEL) is tethered through a fluorescently labeled streptavidin-monobiotinylated anti-HEL antibody bridge. This allows us to study the interaction of HEL-specific B cells with the tethered antigen by a variety of microscopy techniques. We recently used this system to study the activation of B cells by membrane antigens.

Keywords Artificial lipid bilayers · membrane ligands · cell-to-cell interactions

9.1 Introduction

Artificial lipid membranes have been extensively used as simplified models of the plasma membrane for the last 40 years, particularly in electrophysiology studies [1, 2]. The introduction of glass-supported planar lipid bilayers expanded the artificial membrane technology by allowing the study of cell–membrane interactions by fluorescence microscopy [3]. Since then, artificial

F.D. Batista
Lymphocyte Interaction Laboratory, London Research Institute, Cancer Research UK, 44 Lincoln's Inn Fields, London, WC2A 3PX, UK
e-mail: facundo.batista@cancer.org.uk

B. Larijani et al. (eds.), *Lipid Signaling Protocols*, DOI: 10.1007/978-1-60327-115-8_9,

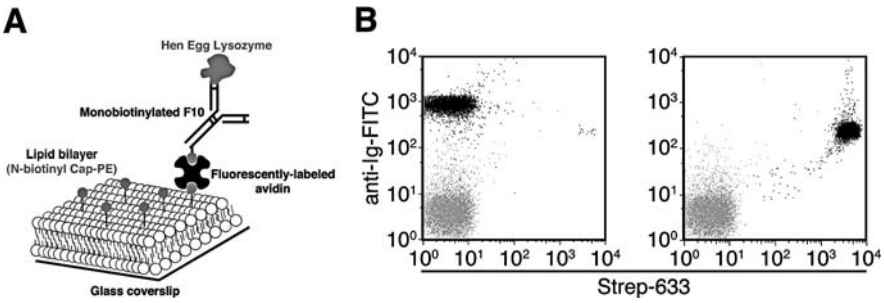

Fig. 9.1 Method used to tether antigens on artificial lipid bilayers. (a) Lipid bilayers containing biotinylated lipids (N-biotinyl Cap-PE) are generated on the surface of glass coverslips. The HEL antigen is then tethered through a monobiotinylated F10 antibody–avidin bridge. "As the…" avidin is fluorescently labeled, the antigen bound "through the F10 can be visualized." (b) Streptavidin-coated beads are used to estimate the degree of biotinylation of the F10 antibody. The beads are coated with the biotinylated F10 and then labeled with an anti-mouse Ig-FITC and streptavidin-Alexa Fluor 633. The degree of biotinylation can be distinguished by the levels of streptavidin-Alexa Fluor 633 staining, as shown by the FACS profiles of beads coated with a monobiotinylated (left panel) or a polybiotinylated F10 antibody (right panel). Uncoated control beads are shown in grey

lipid bilayers have become an invaluable model system in immunology to study the interaction of cells with membrane ligands [4–7]. We have recently adapted this system to quantitatively study the early stages of B cell activation by membrane antigens [8, 9]. For this, we took advantage of transgenic MD4 B cells that express a B cell receptor (BCR) specific for the model antigen, hen egg lysozyme (HEL). We developed a simple method for tethering HEL on artificial lipid bilayers containing biotinylated lipids through an avidin-monobiotinylated anti-HEL antibody bridge (Fig. 9.1). The interaction between the tethered antigen and the B cells can then be monitored by a variety of microscopy techniques. This simple and reliable method to tether ligands on artificial bilayers can easily be extended to study other receptor–ligand interactions.

9.2 Materials

9.2.1 Preparation of Liposomes and Glass-Supported Artificial Lipid Bilayers

1. Lipid stocks of the following phospholipids dissolved in chloroform are obtained from Avanti Polar Lipids: 1,2-dioleoyl-sn-glycero-3-phosphocholine (DOPC), 1,2-dioleoyl-*sn*-glycero-3-phosphoethanolamine-NBD (PE-NBD), and 1,2-dioleoyl-*sn*-glycero-3-phosphoethanolamine-N-(Cap Biotinyl) (N-biotinyl Cap-PE). Phospholipid solutions are kept at −20°C, sealed, and overlaid with argon (to minimize oxidation).

2. Glass vials (3 ml) with silicon twist cap (Chromacom).
3. Slide-A-Lyzer dialysis cassettes, MWCO = 3.5 kDa (Pierce).
4. Dialysis buffer: 25 mM Tris-HCl, 150 mM NaCl, pH 8. The buffer is degassed by vacuum or by bubbling with N_2 for 20 min before filtering (0.22-μm membrane, Millipore).
5. Liposome buffer: 25 mM Tris-HCl, 150 mM NaCl, 2% octylglucoside (Roche), pH 8. The required volume (usually 10 ml) is prepared by adding octylglucoside to the dialysis buffer.
6. Sulphochromic solution (Fisher) and acetone (Analar) are used to clean glass coverslips.
7. Millex-GP syringe filter units, 0.22 μm (Millipore).
8. FCS2 closed chamber system with the corresponding temperature controller (Bioptechs, Inc.).
9. Blocking buffer: phosphate buffered saline (PBS), 2% fetal calf serum.
10. Chamber buffer: PBS, 0.5% fetal calf serum, 2 mM Mg^{2+}, 0.5 mM Ca^{2+}, 1 g/l D-glucose, pH 7.4.
11. Avidin-Alexa Fluor 488 (Molecular Probes).
12. HEL (Sigma).
13. Quantum Simply Cellular anti-mouse IgG calibrated beads (Bangs Laboratories, Inc.).

9.2.2 Monobiotinylation of the F10 Monoclonal Antibody

1. EZ-Link sulfo-NHS-LC-LC-biotin reagent (Pierce). Stock solution in DMSO at 200 mg/ml.
2. Slide-A-Lyzer dialysis cassettes, MWCO = 10.0 kDa (Pierce).
3. Streptavidin-coated beads, 5 μm diameter (Bangs Laboratories, Inc.).
4. Streptavidin-Alexa Fluor 633 (Molecular Probes).
5. Rabbit polyclonal anti-mouse Ig-FITC antibody (PharMingen).

9.2.3 B Cell Isolation and Culture

All the solutions and reagents are purchased from Gibco (Bethesda, MD), except where indicated, and kept at 4°C.

1. RPMI Glutamax-I medium supplemented with 10% fetal calf serum, 10 mM HEPES, 10 IU/ml of penicillin and streptomycin antibiotics, and 50 μM 2-mercaptoethanol (Sigma).
2. Cell strainers, 70 μm (Falcon).
3. Lympholyte (Cedarlane, Ontario, Canda).
4. Erytrocyte lysis buffer: 0.75% Tris-HCl, 0.2% NH_4Cl (Analar), pH 7.2.
5. Dynabeads mouse pan-T magnetic beads (Dynal Biotech ASA, Oslo, Norway).

9.2.4 Scanning Electron Microscopy

1. Fixative: 4% paraformaldehyde (Sigma) solution in PBS (freshly prepared).
2. OsO_4 (Sigma).
3. Hexamethyldisilazane (HMDS, Sigma).

9.2.5 F-actin Staining

1. Fixative: see previous paragraph.
2. Permeabilizing buffer: PBS, 0.1% Triton X-100 (Sigma).
3. Blocking/staining solution: PBS, 2% bovine serum albumin (Sigma), 0.05% Tween-20, 0.1% NaN_3.
4. Phalloidin-Alexa Fluor 543 stock solution in DMSO (Molecular Probes).

9.3 Methods

9.3.1 Preparation of Liposomes

Liposomes are prepared by detergent dialysis [9].

1. The chloroform in the lipid solutions is evaporated under an N_2 stream in a glass vial. Solvent traces are removed by high vacuum for two hours (we usually use a lyophylizer). The thin film of dry lipids is then resuspended in a liposomes buffer to obtain a 2 mM solution (10 × stock), and sonicated until clear (usually five cycles of 10 s each at medium power).
2. The resuspended labeled lipids (NBD-PE or N-biotinyl Cap-PE) are mixed with unlabeled DOPC in a 1:50 molar ratio and then diluted 1:10 with liposome buffer.
3. The solutions are then filtered (syringe filter 0.22 μm, Millipore) and dialyzed against dialysis buffer for 36 h, with buffer exchange every 12 h.
4. After dialysis, the liposomes solutions are filtered again (0.22 μm), aliquoted in twist-cap tubes (1.5 ml), and overlaid with argon. Solutions kept at 4°C and protected from the light are stable for long periods of time (2–4 years).

9.3.2 Monobiotinylation of the F10 Monoclonal Antibody

The monobiotinylated F10 anti-HEL monoclonal antibody is prepared by incubating the antibody with limiting concentrations of the sulfo-NHS-biotin reagent (Pierce).

1. Dissolve (or dialyze) the purified monoclonal antibody at 1 mg/ml in an amine-free buffer (pH > 7) and aliquot in 1 ml fractions.

2. Add varying concentrations of the sulfo-NHS-biotin reagent. Usually, final concentrations of 0.1–0.01 μg/ml should yield monobiotinylated species of antibody.
3. Leave to react for 30 min at room temperature, and then dialyze against PBS with several changes of buffer to remove the excess reagent.
4. The degree of biotinylation of the antibody is evaluated by FACS with streptavidin-coated beads as described below.
5. Prepare 100 μl of a dilution 1:50 (in PBS with 2% fetal calf serum) of each aliquot of the biotinylated antibody and mix each sample with 1 μl of beads in an Eppendorf tube. Incubate for 20 min at room temperature with agitation (to prevent the beads from settling in the bottom of the tube) and wash.
6. Incubate the beads with 100 μl of streptavidin-Alexa Fluor 633 (1:400 dilution) and an anti-mouse Ig-FITC antibody for 20 min at room temperature with agitation and wash.
7. Analyze by FACS. The monobiotinylated antibody can be distinguished from polybiotinylated antibody by the levels of streptavidin-Alexa Fluor 633 staining (Fig. 9.1b).

9.3.3 Preparation of Glass-Supported Artificial Lipid Bilayers

Artificial membranes are prepared by liposome spreading on clean glass coverslips [4].

1. Glass coverslips (25 mm, Bioptechs) are treated overnight in sulphochromic solution and then rinsed with distilled water and acetone. The excess acetone is removed by aspiration with a glass Pasteur pipette.
2. Liposomes containing NBD-PE or N-biotinyl Cap-PE are mixed at appropriate ratios with DOPC liposomes to get the required molecular densities.
3. Liposome drops (usually 0.8 μl) are deposited on the glass coverslips, and then the FCS2 chambers are assembled following the manufacturer's instructions (Bioptechs, Inc.). After 20 min of incubation, the chambers are flushed and incubated for at least 1 h in blocking buffer (*see* Note 1).
4. To tether the antigen, the chambers are successively incubated with 1 ml of avidin-Alexa Fluor 488 (concentration $\approx$ 1 μg/ml), 1 ml of monobiotinylated F10 antibody (concentration $\approx$ 50 μg/ml), and 1 ml of the HEL antigen (concentration $\approx$ 200 ng/ml). All the incubations are performed at room temperature for 10–15 min each in chamber buffer. To eliminate the excess of reagents, the chambers are washed between incubations with at least 5 ml of buffer.
5. Antigen molecules can freely diffuse on these bilayers as assessed by fluorescence recovery after photobleaching (FRAP) (Fig. 9.2a). Furthermore, the diffusion rate is comparable to the diffusion of single labeled lipid molecules (NBD-PE) on bilayers (Fig. 9.2b).

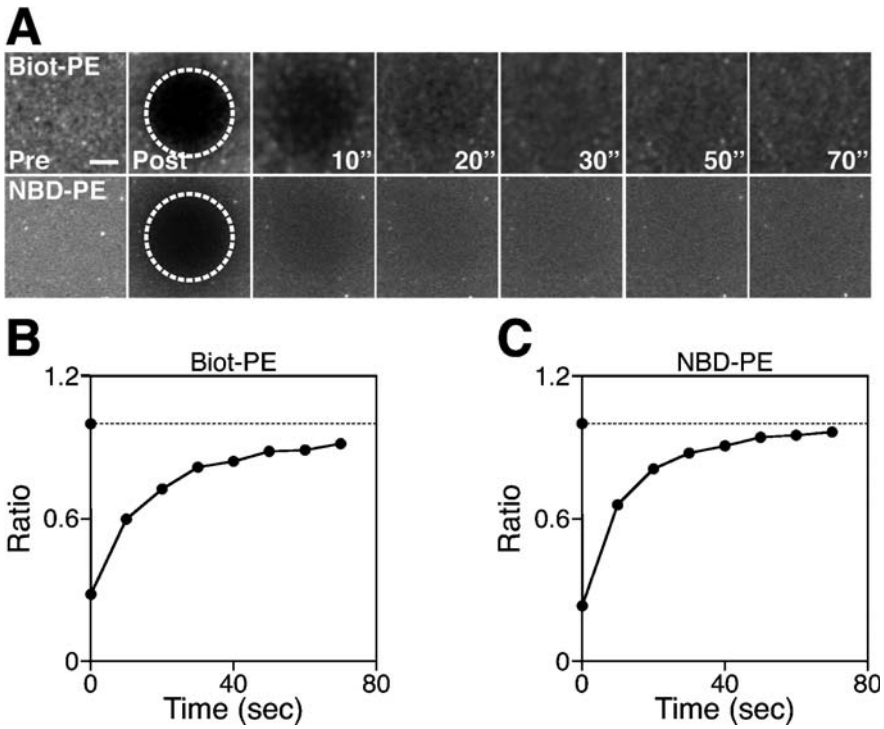

Fig. 9.2 Diffusion of antigen on lipid bilayers. (a) FRAP experiments of lipid bilayers containing biotin-PE lipids (top panels) or NBD-PE lipids (bottom panels). A spot on the lipid bilayer (white dotted circle) was bleached with 25 laser pulses, and the fluorescence recovery was followed for 2 min. Scale bar: 2 μm. Fluorescence recovery (expressed as ratio = mean intensity at time *n* after bleaching/mean intensity at *t* = prebleaching) of lipid bilayers containing (b) biotin-PE and (c) NBD-PE lipids is represented as a function of time

9.3.4 Determination of Molecular Densities

Molecular densities are determined with a fluorometric assay using calibrated beads. Calibrated beads of discrete antibody binding capacities (ABC = numbers of molecules of mouse IgG per bead) are available from Bangs Laboratories. These beads have also a defined diameter (5 μm) and therefore a defined density of antibody.

1. Coat the calibrated beads with the F10 antibody (non-biotinylated) used to tether the antigens according to manufacturer's protocol. Stain the beads with an anti-mouse kappa chain antibody fluorescently labeled with phycoeritrine (PE). FACS analysis shows five populations with defined levels of fluorescence (Fig. 9.3a). These populations are also evident when visualized by confocal microscopy Fig. 9.3b).

2. Acquire images of the beads by confocal microscopy and measure the mean fluorescence of each population (*see* Note 2). Build a calibration curve with the ABC of each population and their mean fluorescence values (Fig. 9.3c, d).
3. Prepare artificial bilayers with different dilutions of N-biotinyl Cap-PE (*see* Subheading 9.3.3). Load them with avidin-Alexa Fluor 488 and the monobiotinylated F10. Incubate the bilayers with the anti-mouse kappa chain antibody fluorescently labeled with phycoeritrine (PE) for 15 min. Wash the chamber and measure the mean fluorescence of the bilayer at the different dilutions.
4. Compare the fluorescence values of the bilayer with the calibration curve obtained with the beads and determine the density of antigen (*see* Note 3).

9.3.5 Purification of Splenic Naïve B Cells

B cells are purified from the spleens of transgenic MD4 mice with a negative selection protocol.

1. Disrupt the spleen on a cell strainer with a syringe plunger (2.5 ml) and wash with PBS (three times, 3 ml each). Purify the total splenocytes with a lympholyte gradient.
2. Lyse the red blood cells with erythrocyte lysis buffer (1 ml for 5 min) and wash with RPMI 10% medium.
3. Incubate with the magnetic beads for 1 h at 4°C to deplete the T cells.
4. The cells are then incubated for 1–2 h at 37°C to allow macrophages to adhere to the plate.

9.3.6 Interaction of B Cells with Artificial Lipid Bilayers

The interaction of B cells with the HEL-loaded artificial bilayers can be analyzed by different microscopy techniques (*see* Note 4).

1. The cells are injected in a chamber buffer into the FCS2 closed chamber (usually $1–5 \times 10^6$ cells), and real-time kinetics of interaction are followed by confocal microscopy (Fig. 9.4a).
2. B cells accumulate the freely diffusing antigen on these bilayers (Fig. 9.4a). Contacts with the bilayer are visualized by interference reflection microscopy (IRM, grayscale) (Fig. 9.4a).
3. Quantitative analysis can be also performed on the antigen recognition process, and antigen accumulation can be expressed as the total number of molecules (Fig. 9.4b).
4. Morphological changes can be analyzed by scanning electron microscopy (SEM). B cells are fixed at different times of contact with the bilayer with 1 ml of prewarmed 4% paraformaldehyde (Sigma) for 10 min at 37°C (*see* Note 5).

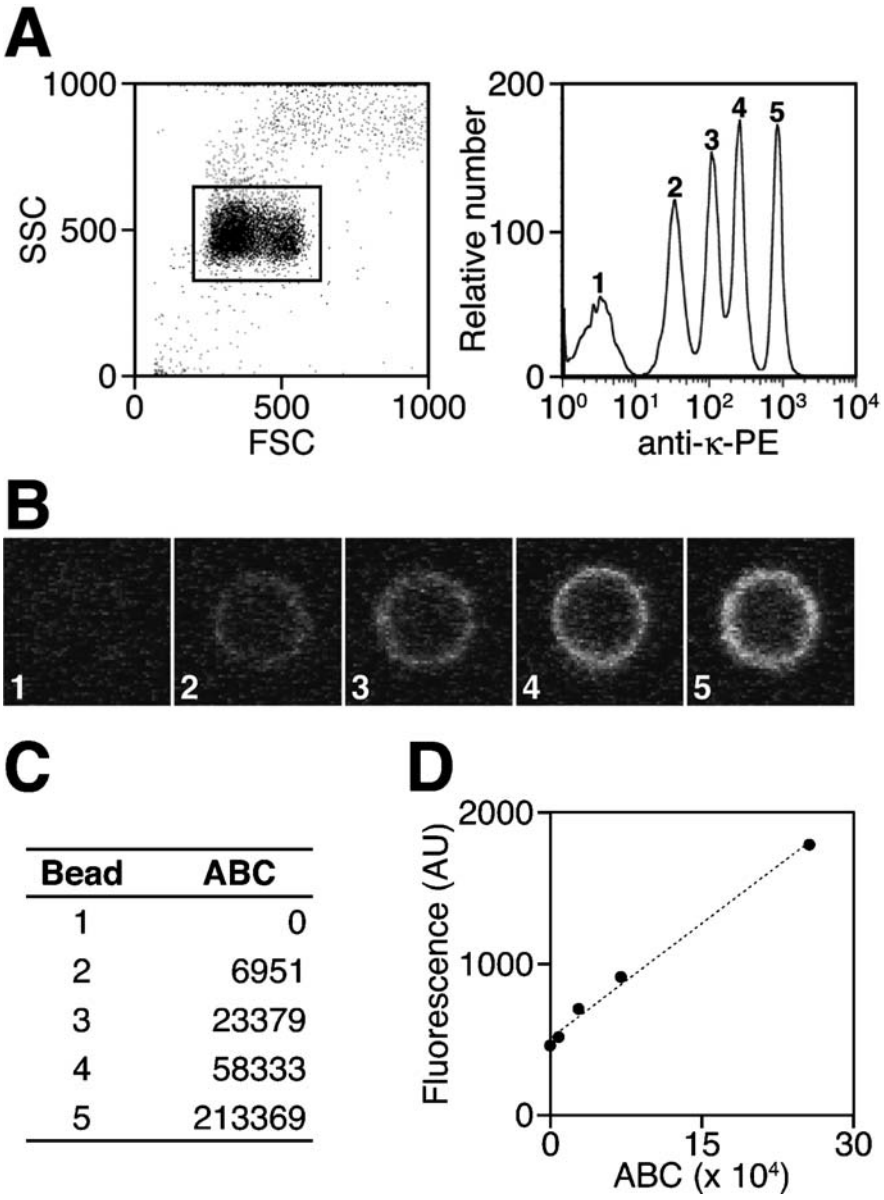

Bead	ABC
1	0
2	6951
3	23379
4	58333
5	213369

Fig. 9.3 Estimation of the antigen density on lipid bilayers. (a) FACS analysis of the calibrated beads coated with F10 antibody and an anti-kappa-PE antibody shows five populations with different levels of antibody. (b) These populations are also evident when the beads are analyzed by confocal microscopy. (c) Antibody-binding capacities (ABC) of the different calibrated beads are used to estimate the density of antigen. (d) Calibration curve derived from the intensity of the fluorescence measured by confocal microscopy of the different populations of calibrated beads and their respective ABCs

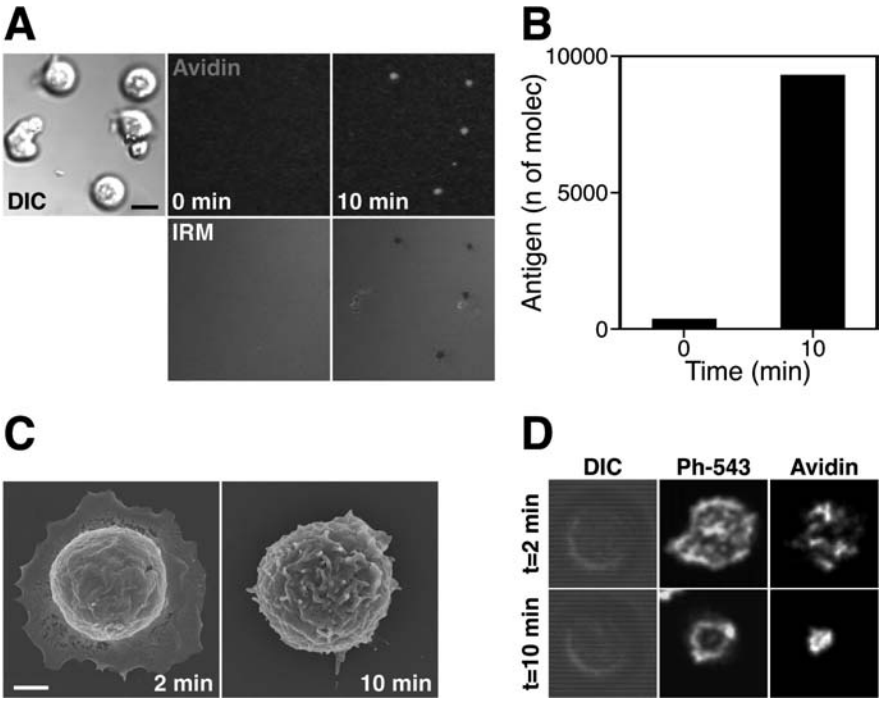

Fig. 9.4 Interaction of B cells with antigen-loaded lipid bilayers. (a) The interaction of MD4 naïve B cells planar lipid bilayers containing HEL antigen at a density of 150 molecules/μm^2 is followed by confocal microscopy. The antigen is aggregated in a central cluster after 10 minutes. The bottom panels show the contacts with the bilayers as assessed by IRM (grayscale). Scale bar: 2 μm. (b) The quantification of the number of molecules accumulated as a function of the time of contact with the bilayer. (c) B cells in contact with antigen-loaded bilayers are fixed at different time points with 4% paraformaldehyde. Cell morphology is then analyzed by SEM. Scale bar: 1 μm. (d) Fixed B cells can be also labeled with phalloidin-Alexa Fluor 543 (Ph-543) and analyzed by confocal microscopy to visualize actin reorganization

Then they are washed with phosphate buffer (PBS), treated for 1 h with 1% OsO_4, and washed again with PBS. After dehydration in absolute ethanol, the cells are treated for 2 min with hexamethyldisilazane (HMDS, Sigma), air-dried, and coated with platinum. Fig. 9.4c shows SEM analysis of B cells interacting with an antigen-loaded membrane fixed at the indicated time points.

5. B cells fixed on artificial bilayers can be also analyzed by immunolabeling (*see* Note 6). After fixation, the cells are washed with PBS (1–2 ml) and treated with permeabilizing buffer (1 ml) for 5 min. The cells are then blocked for at least 1 h with blocking/staining solution and stained with phalloidin-Alexa Fluor 543 (1:1,000 dilution in blocking/staining solution, 1 ml) for 15 min at room temperature. After washing with 2 ml of blocking/staining solution, the cells can be visualized under the confocal microscope. An example of the procedure is shown in Fig. 9.4d.

Notes

1. Liposomes drops are circled with a marker on the top glass slide of the FCS2 chamber system, so that they can easily be found after flushing with buffer. The flushing should be done carefully to avoid any air bubbles, which disrupt the lipid bilayers by contact.
2. The mean fluorescence of the different beads is measured at the midplane by confocal microscopy (usually, a pinhole resulting in an optical slice of 1 μm is used). Any image handling software is appropriate for this task.
3. The density of the antibody of the beads is estimated from the ABC and their surface area (diameter 5 μm). The calibration curve is derived then from the density of the antibody and the mean fluorescence of each bead.
4. The same system can be applied to study other cell-to-cell interactions, as any monobiotinylated ligand can be tethered with the biotinylated lipids/fluorescently labeled avidin approach.
5. After this step, the coverslips are dismounted from the FCS2 chambers to facilitate the processing. Only the cells in contact with the bilayer will be visible by SEM, as they are the only ones that remain attached to the coverslip.
6. The entire procedure is performed inside the chambers, as this facilitates the incubations.

References

1. Hladky SB, Haydon DA. Discreteness of conductance change in bimolecular lipid membranes in the presence of certain antibiotics. Nature 1970;225:451–3.
2. Mueller P, Rudin DO, Tien HT, Wescott WC. Reconstitution of cell membrane structure *in vitro* and its transformation into an excitable system. Nature 1962;194:979–80.
3. Hafeman DG, von Tscharner V, McConnell HM. Specific antibody-dependent interactions between macrophages and lipid haptens in planar lipid monolayers. Proc Natl Acad Sci USA 1981;78:4552–6.
4. Brian AA, McConnell HM. Allogeneic stimulation of cytotoxic T cells by supported planar membranes. Proc Natl Acad Sci USA 1984;81:6159–63.
5. Dustin ML, Ferguson LM, Chan PY, Springer TA, Golan DE. Visualization of CD2 interaction with LFA-3 and determination of the two-dimensional dissociation constant for adhesion receptors in a contact area. J Cell Biol 1996;132:465–74.
6. Grakoui A, Bromley SK, Sumen C, Davis MM, Shaw AS, Allen PM, Dustin ML. The immunological synapse: A molecular machine controlling T cell activation. Science 1999;285:221–7.
7. Groves JT, Dustin ML. Supported planar bilayers in studies on immune cell adhesion and communication. J Immunol Methods 2003;278:19–32.
8. Carrasco YR, Batista FD. B-cell activation by membrane-bound antigens is facilitated by the interaction of VLA-4 with VCAM-1. EMBO J 2006;25:889–99.
9. Carrasco YR, Fleire SJ, Cameron T, Dustin ML, Batista FD. LFA-1/ICAM-1 interaction lowers the threshold of B cell activation by facilitating B cell adhesion and synapse formation. Immunity 2004;20:589–99.

Chapter 10
Ceramide-Induced Transbilayer (Flip-Flop) Lipid Movement in Membranes

F.-Xabier Contreras, Ana-Victoria Villar, Alicia Alonso and Félix M. Goñi

Abstract Lipids in biological membranes are asymmetrically distributed across the bilayer. The choline-containing lipids, phosphatidylcholine (PtdCho) and sphingomyelin (SM), are more abundant in the external leaflet. In contrast, the amino-containing glycerophospholipids, phosphatidylserine (PtdSer) and phosphatidylethanolamine (PtdEth), are located preferentially on the cytoplasmic leaflet. The maintenance of transbilayer lipid asymmetry is essential for normal membrane function, and disruption of this asymmetry is associated with cell activation or pathological condition. The physiological role of ceramide formation in response to cell stimulation remains controversial. Ceramide formation serves many different functions at various locations in the cell. Despite the limited capacity for spontaneous intracellular diffusion or membrane flip-flop of lipids in membranes, we have found that ceramide production, via sphingomyelinase action or addition of external ceramide, induces the transbilayer lipid motion of the lipids within the cellular membrane. This chapter outlines various commonly used assays for measuring lipid flip-flop induced by ceramide in cell and model membranes.

Keywords Cell membrane · ceramide · sphingomyelinase · flip-flop · transmembrane lipid movement · apoptosis · plasma membrane

10.1 Introduction

The mammalian plasma membrane (PM) outer leaflet contains mainly phosphatidylcholine (PtdCho), sphingomyelin (SM), and glycolipids. The inner leaflet is rich in phosphatidylethanolamine (PtdEth) and contains practically all of the phosphatidylserine (PtdSer). This lipid asymmetry is possible because of the slow spontaneous transmembrane diffusion of phospholipids [1] and because several membrane proteins are involved in maintaining this lipid asymmetry [2, 3].

F.M. Goñi
CSIC and University of the Basque Country, Bilbao, Spain
e-mail: felix.goni@ehu.es

B. Larijani et al. (eds.), *Lipid Signaling Protocols*, DOI: 10.1007/978-1-60327-115-8_10,

Among the proteins that catalyze the movement of lipids across the membrane, two ATP-dependent classes have been described. The best-characterized activity is aminophospholipid translocase or "flippase." This protein transports PtdSer from the outer monolayer to the inner face of the plasma membrane. The second ATP-dependent activity, catalyzed by "floppases," transports lipids in the opposite direction [4, 5, 6]. Finally, three ATP-independent and relatively nonspecific scramblase activities have been reported [7]. These Ca^{2+}-dependent proteins occur in RE, plasma membrane, and mitochondria and may play an important role in plasma membrane reorganization in response to cell stimulation, e.g., during platelet activation or apoptosis. The dissipation of transbilayer lipid asymmetry results in the exposure of PtdSer on the surface of the cell, which activates recognition of the cell by macrophages [8, 9].

The sphingolipid ceramide is generated during cellular stress and apoptosis, either by the *de novo* synthesis or via the action of a neutral or acid sphingomyelinase [10, 11, 12, 13]. Recent studies have related the enhanced production of ceramide to TNF-induced apoptosis of some long-term culture cell lines [14, 15]. Evidence to support this notion includes the observed activation of stimulated sphingomyelinase activity and the fact that treatment of cells with exogenous ceramide results in effects similar to those observed after the addition of TNF or other SMase-activating stimuli. The identification of targets that can mediate ceramide action has supported its prominent role in signal transduction. Ceramide is known to activate the serine threonine phosphatases PP1 and PP2 [16], protein kinase (CAPK) [17], and dephosphorylated PKCα with consequent inactivation [18]. In the lipid bilayer, the generation of ceramide increases the volume of hydrocarbon chains within the lipid bilayer, thereby enhancing its propensity to form hexagonal II phase [19]. Besides the generation of a hydrophobic interaction site for proteins, ceramide changes the membrane fluidity and permeability [20, 21] and facilitates membrane fusion [22, 23], the budding process [24], the formation of ceramide-rich domains [25, 26], and lipid flip-flop [27, 28, 29].

Three specific methods appropriate for the measurement of lipid flip-flop induced by ceramide are discussed below. The chemical method protocol (Method 1) allows the detection of lipid flip-flop measuring the enzyme activity of SMase and neuraminidase, leading to the production of ceramide and sialic acid, respectively. This method has three major steps: (a) preparation of vesicles containing entrapped neuraminidase; (b) insertion of GM3 ganglioside (substrate of neuraminidase) in the outer monolayer of the vesicles; (c) measurement of GM3 and SM hydrolysis. Methods 2 and 3 are fluorimetric assays that use phospholipids labeled with a fluorophore to measure lipid movement across the bilayer. Method 2 is based on fluorescence resonance energy transfer (FRET) between NBD-PE and a rhodamine (Rho) bound to an irrelevant IgG. This method consists of three major steps: (a) production of ghost membranes labeled in both monolayers with NBD-PE; (b) reduction of the NBD-PE present in the outer monolayer, leading to ghost membranes labeled only in the inner leaflet; (c) measurement of the

energy transfer between NBD-PE flopped toward the outer monolayer and Rho-IgG present in the external media. Method 3 is based on the excimer-forming capacity of the fluorescent probe pyrene, incorporated into phosphatidylcholine analogs. The main step of this method is the asymmetric incorporation of pyPC in the outer monolayer of vesicles [29, 30]. This method is described in Müller et al. [30], where additional information may be found.

10.2 Material

10.2.1 Lipids

1. Egg sphingomyelin (SM), egg (PtdEth), cholesterol (Ch) (Avanti Polar Lipids, Alabaster, AL), monosialoganglioside (GM3) (Larodan AB, Sweden), egg ceramide, and N-(7-nitrobenzene-2-oxa-1,3-diazol-4-yl) phosphatidylethanolamine (NBD-PE) (Molecular Probes, Eugene, OR) were dissolved in chloroform/methanol (2/1) and stored at −20 °C.
2. 1-lauryl-2-(1'-pyrenebutyroyl)-sn-glycero-3-phosphocholine (pyPC) was synthesized as described in Müller et al. [30], dissolved in chloroform/methanol (2/1), and stored in aliquots at −20 °C.

10.2.2 Enzymes

1. Sphingomyelinase (EC 3.1.4.12) from *Bacillus cereus* (Sigma–Aldrich, St. Louis, MO) was used at 1.6 U/ml on vesicles and at 0.6 U/ml for erythrocyte assays (*see* Note 1).
2. Neuraminidase was added to the hydration buffer at 0.16 U/ml. The nonentrapped neuraminidase was removed by gel filtration through Sephadex G-75 (Amersham Biosciences, Uppsala, Sweden).

10.2.3 Materials for Method 1

1. Hydration buffer: 10 mM HEPES, 200 mM NaCl, 10 mM $CaCl_2$, 2 mM $MgCl_2$, pH 6.5, supplemented with neuraminidase (0.16 U/ml) (*see* Note 2).
2. Triton X-100 (0.1 w/v) prepared in HEPES buffer and stored at 4 °C.
3. Sephadex G-75 (Amersham Biosciences) prepared in water in presence of diazide and stored at 4 °C.
4. Lipid extraction mixture used to measure sphingomyelinase and neuraminidase activity was chloroform/methanol/hydrochloric acid (200/100/1, v/v/v) (*see* Note 3).

10.2.4 Materials for Method 2

1. Tetramethylrhodamine goat antimouse (Rho-IgG) (Molecular Probes) stored at 4 °C.
2. Human blood cells provided by the blood bank.
3. Wash buffer: 0.9% NaCl. Store at room temperature.
4. Lysis buffer: 1.2 mM acetic acid, 4 mM $MgSO_4$, pH 3.2. Store at 4 °C (*see* Note 4).
5. Reseal buffer: HEPES buffer supplemented with 3 μM NBD-PE. Store at 4 °C (*see* Note 5).
6. 0.6 mM sodium dithionite (Fluka Biochemika, AG, Switzerland) in HEPES buffer (*see* Note 6).

10.3 Methods

10.3.1 Measurement of Flip-Flop Movement Using the Chemical Method (Method 1)

10.3.1.1 Preparation of Liposomes

Large unilamellar vesicles (LUV) were prepared as described by Mayer et al. [31].

1. Co-dissolve the lipids at the desired ratio in chloroform/methanol (2:1). SM should be 33–50 mol%.
2. Remove organic solvent by evaporation under a nitrogen stream followed by storage under vacuum in the dark for 2 h.
3. Resuspend the dry lipid film in HEPES buffer supplemented with neuraminidase (0.16 U/ml).
4. Pass the suspension 10 times through polycarbonate filters of 0.1-μm pore diameter using an extruder (under N_2 pressure).
5. Remove nonentrapped neuraminidase by gel filtration through Sephadex G-75.

10.3.1.2 Incorporation of Glycolipids to the Outer Monolayer

1. Dry GM3 ganglioside (10 mol% of the total lipids).
2. Resuspend the lipid in methanol. The organic solvent will be 5% of the vesicle suspension volume.
3. Add the methanolic glycolipid solution to vesicles, and after vortex mixing, incubate the mixture for 15 min at room temperature (*see* Note 7).

10.3.1.3 Measurement of Flip-Flop Motion

1. Add sphingomyelinase (1.6 U/ml) to the LUV suspension prepared as above.
2. At fixed times after the SMase addition, remove aliquots (50 μl) from the reaction mixture and mix with the extraction mixture (250 μl). This step will produce two clear phases: an upper, aqueous phase and a lower, organic phase.

3. After 60 minutes' reaction time, add Triton X-100 (0.5% v/v) to cause membrane disruption and release of neuraminidase. Ninety minutes after the SMase addition, remove a final aliquot that will mark the reaction endpoint.
4. Measure sphingomyelinase activity by assaying the phosphorous content in the aqueous phase of the extraction mixture as described by Bottcher et al. [32].
5. Measure the sialic acid formed by neuraminidase hydrolysis of GM3 in the aqueous phase using the resorcinol-sialic acid assay described by Wybenga et al. [33].
6. Plot the percentage of GM3 and ceramide hydrolysis vs. time (Fig. 10.1a, b).

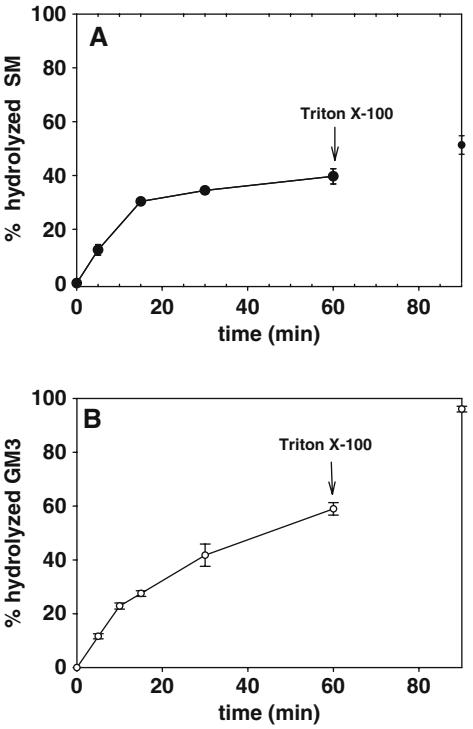

Fig. 10.1 Sphingomyelinase induces transbilayer translocation of GM3 in model membranes. (a) SM hydrolysis by SMase. (b) GM3 hydrolysis by entrapped neuraminidase. (Reprinted from Contreras et al. [28], with permission.)

10.3.2 Measurement of Flip-Flop Movement by FRET (Method 2)

10.3.2.1 Ghost Membrane Preparation

Human erythrocyte membranes were obtained using a modified Steck and Kant method [34].

1. Wash (centrifuge in a bench centrifuge for 10 min at 3,000 rpm at 4 °C in 0.9% NaCl) the membranes obtained from 20 ml of erythrocyte concentrate three times.
2. Resuspend the pellet with cold 1.2 mM acetic acid, 4 mM $MgSO_4$, pH 3.2 buffer, leave for 30 min at 4 °C, and finally centrifuge for 10 min at 3,000 rpm.

3. Resuspend the pellet with HEPES buffer supplemented with 3 μM NBD-PE, and then sterilize membrane and allow to reseal, incubating at 37 °C for 1 h.
4. Centrifuge for 10 min at 14,500 × *g* and resuspend in the same buffer. Repeat this step three times.
5. Layer the resulting membrane suspension over 43% (w/v) sucrose in 25 mM Tris-HCl, pH 7.4. Centrifuge for 60 min at 27.500 × *g*. Finally, harvest the resealed ghosts floating on top of the sucrose gradient.
6. Wash the ghost membranes by centrifugation three times for 10 min at 14,500 × *g* at room temperature in HEPES buffer.
7. At this step, the ghost membranes are fluorescently labeled in both leaflets. To reduce and quench the fluorescence of the outer leaflet label, use 0.6 mM sodium dithionite. Reduction can be followed in a spectrofluorometer.
8. Remove excess dithionite by centrifugation for 10 min at 14,500 × *g* at room temperature.
9. Finally, resuspend in HEPES buffer ghost membranes labeled only in the inner leaflet.

10.3.2.2 Fluorescence Energy Transfer in Ghost Membranes

1. Add SMase (0.16 U/ml) to ghost membranes (90 μM in lipid) in 1 ml.
2. At regular times, remove aliquots from the reaction mixture (100 μl) and mix with Rho-IgG (20 μg/ml) in HEPES buffer.
3. Measure the fluorescence intensity of NBD-PE and Rho-IgG in a spectrofluorometer (*see* Note 8).
4. Plot the data of NBD-PE and Rho-IgG fluorescence vs. time (Fig. 10.2).

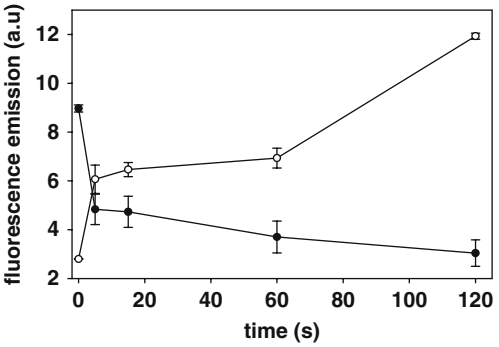

Fig. 10.2 Transbilayer movement of NBD-PE induced by SMase in model membranes. (•) NBD-PE fluorescence intensity. (○) Rho-IgG fluorescence intensity. (Reprinted from Contreras et al. [28], with permission.)

10.3.3 Measurement of Flip-Flop Movement Using the Pyrene Method (Method 3)

10.3.3.1 Liposome Preparation

Liposomes are prepared as described above (*see* Subheading 10.3.1.1) except that the buffer is not supplemented with neuraminidase.

10.3.3.2 Asymmetric Incorporation of pyPC

To label vesicles with pyPC only in the outer monolayer:

1. Under a nitrogen stream, dry an appropriate amount of pyPC prepared in chloroform/methanol.
2. Leave in a vacuum chamber for 1 h.
3. Resuspend the dry lipid in a small volume of ethanol.
4. Add an aliquot (5 mol% total lipid concentration) to the liposome preparation.
5. After vortex-mixing, leave the system to equilibrate for 15 min.

10.3.3.3 Ceramide Preparation

1. Dry ceramide in organic solvent under nitrogen.
2. Remove final traces of solvent, leaving the dry lipid in a vacuum chamber for 1 h in the dark.
3. Resuspend dry lipids in a small volume of ethanol.

10.3.3.4 Construction of the Calibration Curve

1. Prepare liposomes by mixing different concentrations of probe with the main lipids in organic solvent before vesicle preparation.
2. Measure the fluorescence intensity of the excimer (I_E) ($\lambda_{ex} = 344$ nm; $\lambda_{em} = 465$ nm) and monomer (I_M) ($\lambda_{ex} = 344$ nm; $\lambda_{em} = 395$ nm) for each LUV preparation containing different concentration of pyPC.
3. Plot the I_E and I_M data vs. pyPC concentration in the bilayer (Fig. 10.3).
4. The I_E/I_M ratio of pyPC measured in vesicles corresponds to the excimer and monomer intensities of analogs in both leaflets, outer (I_E^0, I_M^0) and inner (I_E^i, I_M^i):

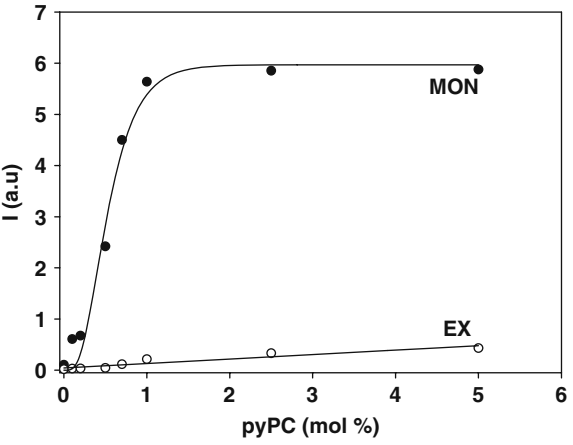

Fig. 10.3 Intensities of pyrene monomers (•) measured at 395 nm and excimers (○) measured at 465 nm as a function of pyPC concentration. PyPC was symmetrically incorporated into the bilayers. (Reprinted from Contreras et al. [29], with permission.)

$$\frac{\mathbf{I_E}}{\mathbf{I_M}} = \frac{\mathbf{I_E^0} + \mathbf{I_E^i}}{\mathbf{I_M^0} + \mathbf{I_M^i}}$$

To relate the observed I_E/I_M to the degree of pyPC distribution q between the leaflets,

$$\mathbf{q} = \frac{\mathbf{C_i}}{\mathbf{C_i} + \mathbf{C_0}}$$

where C_i and C_o are the probe concentrations in the inner and outer monolayers, respectively. The data from Fig. 3 can be used to construct the calibration curve (Fig. 4). This curve is the origin of the q-values obtained in all the experiments. For more details on the construction of the calibration curve, see Müller et al. [30].

10.3.3.5 Measurement of pyPC Flip-Flop

1. To vesicles labeled with pyPC, add the desired amount of ceramide (10 mol% of the final lipid concentration) or SMase (1.6 U/ml).
2. At regular times, measure the fluorescence intensities of excimers at 465 nm (I_E) and monomers at 395 nm (I_M) (*see* Note 9) using a spectrofluorometer (excitation wavelength is 344 nm).
3. Measure the I_E/I_M ratio, which allows us to calculate the extent of the flip-flop [30]. When flip-flop occurs, there is a reduction in the excimer-monomer ratio, due to the dilution of the probe in both monolayers.
4. Estimate the extent of flip-flop using the calibration curve for the appropriate pyrene concentration.
5. Plot the flip-flop extent vs. time (Fig. 5).

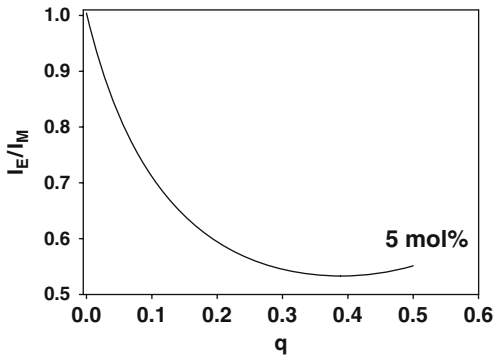

Fig. 10.4 I_E/I_M ratios for different transbilayer distributions q in model membranes containing 5 mol% of pyPC. I_E and I_M are the sum of the corresponding values in the inner (i) and the outer (o) leaflets, respectively. ($I_E^0 + I_E^i$) and ($I_M^i + I_M^0$) were obtained from the experimental data in Fig. 10.3. (Reprinted from Contreras et al. [29], with permission.)

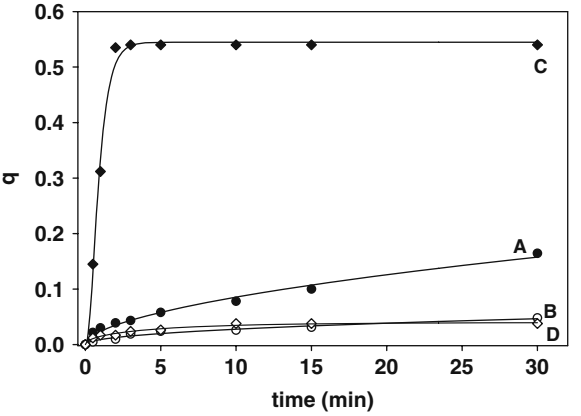

Fig. 10.5 Transbilayer movement (flip-flop) of pyPC induced by ceramide in model membranes. The following components were added at time 0 to vesicles labeled in the outer leaflet with pyPC: (curve A) egg ceramide; (curve B) ethanol; (curve C) sphingomyelinase; and (curve D) none. (Reprinted from Contreras et al. [29], with permission.)

Notes

1. To avoid nonspecific hydrolysis of contaminant phospholipase C during SMase activity, perform the experiments in the presence of 2 mM *o*-phenanthroline.
2. To obtain reproducible assays, add the neuraminidase to the hydration buffer just at the time of vesicle preparation. Do not prepare a hydration buffer stock with neuraminidase, because the protein will lose its activity with time.
3. It is important to prepare the extraction mixture the same day of the experiment. The extraction mixture could also be prepared without hydrochloric acid, but the aqueous and organic phases will be separated less neatly.
4. Keep the lysis buffer cold, because erythrocyte lysis seems to increase with cold buffer.
5. Add the desired amount of NBD-PE into the buffer just before the resealing step.
6. Sodium dithionite has to be prepared freshly before adding it to labeled vesicles to obtain good reduction.
7. Alternatively, glycolipids can be added in ethanolic solution.
8. Fluorescence energy transfer between NBD and Rho is monitored in a continuously stirred cuvette. Excitation and emission wavelengths were 465 and 535 nm for NBD-PE and 530 nm and 575 nm for Rho-PE, respectively. To prevent contamination from scattered light, it is advisable to use a cutoff filter (515 nm).
9. To simplify interpretation of the data, the I_E/I_M value obtained after pyPC incorporation to the outer leaflet of vesicles was set to 1. This method can also be used with ghost or other cell membranes.

References

1. Kornberg RD, McConnell HM. Lateral diffusion of phospholipids in a vesicle membrane. Proc Natl Acad Sci USA 1971;68:2564–8.
2. Connor J, Schroit AJ. Determination of lipid asymmetry in human red cells by resonance energy transfer. Biochemistry 1987;26:5099–105.
3. Zachowski A, Herrmann A, Paraf A, Devaux PF. Phospholipid outside-inside translocation in lymphocyte plasma membranes is a protein-mediated phenomenon. Biochim Biophys Acta 1987;897:197–200.

4. Van Helvoort A, Smith AJ, Sprong H, Fritzsche I, Schinkel AH, Borst P, van Meer G. MDR1 P-glycoprotein is a lipid translocase of broad specificity, while MDR3 P-glycoprotein specifically translocates phosphatidylcholine. Cell 1996;87:507–17.
5. Rust S, Rosier M, Funke H, Real J, Amoura Z, Piette JC, Deleuze JF, Brewer HB, Duverger N, Denefle P, Assmann G. Tangier disease is caused by mutations in the gene encoding ATP-binding cassette transporter 1. Nat Genet 1999;22:352–5.
6. Brooks-Wilson A, Marcil M, Clee SM, Zhang LH, Roomp K, van Dam M, Yu L, Brewer C, Collins JA, Molhuizen HO, Loubser O, Ouelette BF, Fichter K, Ashbourne-Excoffon KJ, Sensen CW, Scherer S, Mott S, Denis M, Martindale D, Frohlich J, Morgan K, Koop B, Pimstone S, Kastelein JJ, Genest J, Jr., Hayden MR. Mutations in ABC1 in Tangier disease and familial high-density lipoprotein deficiency. Nat Genet 1999;22:336–45.
7. Sims PJ, Wiedmer T. Unraveling the mysteries of phospholipid scrambling. Thromb Haemost 2001;86:266–75.
8. Fadok VA, Bratton DL, Frasch SC, Warner ML, Henson PM. The role of phosphatidylserine in recognition of apoptotic cells by phagocytes. Cell Death Differ 1998; 5:551–62.
9. Connor J, Pak CC, Schroit AJ. Exposure of phosphatidylserine in the outer leaflet of human red blood cells. Relationship to cell density, cell age, and clearance by mononuclear cells. J Biol Chem 1994;269:2399–404.
10. Hannun YA, Luberto C. Ceramide in the eukaryotic stress response. Trends Cell Biol 2000;10:73–80.
11. Levade T, Jaffrezou JP. Signalling sphingomyelinases: Which, where, how and why? Biochim Biophys Acta 1999;438:1–17.
12. Perry DK. Ceramide and apoptosis. Biochem Soc Trans 2000;27:399–404.
13. Goñi FM, Alonso A. Sphingomyelinases: Enzymology and membrane activity. FEBS Lett 2002;531:38–46.
14. Spiegel S, Foster D, Kolesnick R. Signal transduction through lipid second messengers. Curr Opin Cell Biol 1996;8:159–67.
15. Kolesnick RN, Kronke M. Regulation of ceramide production and apoptosis. Ann Rev Physiol 1998;60:643–5.
16. Dobrowsky RT, Hannun YA. Ceramide stimulates a cytosolic protein phosphatase. J Biol Chem 1992;267:5048–51.
17. Zhang Y, Yao B, Delikat S, Bayoumy S, Lin XH, Basu S, McGinley M, Chan-Hui PY, Lichenstein H, Kolesnick R. Kinase suppressor of ras is ceramide-activated protein kinase. Cell 1997;89:63–72.
18. Lee JY, Hannun YA, Obeid LM. Ceramide inactivates cellular protein kinase C alpha. J Biol Chem 1996;271:13169–74.
19. Veiga MP, Arrondo JL, Goni FM, Alonso A. Ceramides in phospholipid membranes: Effects on bilayer stability and transition to nonlamellar phases. Biophys J 1999;76:342–50.
20. Montes LR, Ruiz-Argüello MB, Goñi FM, Alonso A. Membrane restructuring via ceramide results in enhanced solute efflux. J Biol Chem 2002;277:11788–94.
21. Siskind LJ, Colombini M. The lipids C_2- and C_{16}-ceramide form large stable channels. Implications for apoptosis. J Biol Chem 2000;275:38640–4.
22. Basañez G, Ruiz-Argüello MB, Alonso A, Goñi FM, Karlsson G, Edwards K. Morphological changes induced by phospholipase C and by sphingomyelinase on large unilamellar vesicles: A cryo-transmission electron microscopy study of liposome fusion. Biophys J 1997;72:2630–7.
23. Ruiz-Argüello MB, Basañez G, Goñi FM, Alonso A. Different effects of enzyme-generated ceramides and diacylglycerols in phospholipid membrane fusion and leakage. J Biol Chem 1996;271:26616–21.
24. Holopainen JM, Angelova MI, Kinnunen PKJ. Vectorial budding of vesicles by asymmetrical enzymatic formation of ceramides in giant liposomes. Biophys J 2000;78:830–8.

25. Bollinger CR, Teichgraber V, Gulbins E. Ceramide-enriched membrane domains. Biochim Biophys Acta 2005;1746:284–94.
26. Gulbins E, Li PL. Physiological and pathophysiological aspect of ceramide. Am J Physiol Regul Integr Comp Physiol 2006;290:R11–R26.
27. Lopez-Montero I, Rodríguez N, Cribier S, Pohl A, Velez M, Devaux PF. Rapid transbilayer movement of ceramides in phospholipid vesicles and in human erythrocytes. J Biol Chem 2005;280:25811–9.
28. Contreras FX, Villar AV, Alonso A, Kolesnick RN, Goñi FM. Sphingomyelinase activity causes transbilayer lipid translocation in model and cell membranes. J Biol Chem 2003;278:37169–74.
29. Contreras FX, Basanez G, Alonso A, Herrmann A, Goñi FM. Asymmetric addition of ceramides but not dihydroceramides promotes transbilayer (flip-flop) lipid motion in membranes. Biophys J 2005;88:348–59.
30. Müller P, Schiller S, Wieprecht T, Dathe M, Herrmann A. Continuous measurement of rapid transbilayer movement of a pyrene-labeled phospholipid analogue. Chem Phys Lipids 2000;106:89–99.
31. Mayer LD, Hope MH, Cullis PR. Vesicles of variable sizes produced by a rapid extrusion procedure. Biochim Biophys Acta 1986;858:161–8.
32. Bottcher GJF, Van Gent CM, Pries C. A rapid and sensitive submicro phosphorus determination. Anal Chim Acta 1961;24:203–4.
33. Wybenga LE, Epand RF, Nir S, Chu JWK, Sharom FJ, Flanagan TD, Epand RM. Glycophorin as a receptor for Sendai virus. Biochemistry 1996;35:9513–9.
34. Steck TL, Kant JA. Preparation of impermeable ghosts and inside-out vesicles from human erythrocyte membranes. Methods Enzymol 1974;31:172–80.

Chapter 11
Effects of Sterols on the Development and Aging of *Caenorhabditis elegans*

Eun-Young Lee, Pan-Young Jeong, Sun-Young Kim, Yhong-Hee Shim, David J. Chitwood and Young-Ki Paik

Abstract Although *Caenorhabditis elegans* lacks several components of the *de novo* sterol biosynthetic pathway, it requires sterols as essential nutrients. Supplemental cholesterol undergoes extensive enzymatic modification in *C. elegans* to form certain sterols of unknown function. Since sterol metabolism in *C. elegans* differs from that in other species, such as mammals and yeast, it is important to examine how sterols regulate worm physiology. To examine the functions of sterols in *C. elegans*, a sterol-feeding experiment was carried out and several critical parameters, such as brood size, growth rate, and life span, were measured. In addition, the change in lipid distribution in *C. elegans* can be both qualitatively and quantitatively determined by various methods, including staining and chromatographic techniques. Taken together, the effects of sterols on *C. elegans* are very prominent and can be easily assessed using the techniques described here.

Keywords *C. elegans* · sterol · gas-liquid chromatography · reproduction · signaling · aging

Abbreviations AY-9944: *trans*-1,4-bis(2-chlorobenzylaminomethyl) cyclohexane dihydrochloride; 25-Azacoprotsane-HCl: 25-aza-5β-cholestane hydrochloride; BM15.766: 4-(2-[1-(4-chlorocinnamyl)piperazin-4-yl]ethyl)-benzoic acid; Hoechst No. 33342: (2'-[4-Ethoxyphenyl]-5-[4-methyl-1-piperazinyl]-2,5'-bi-1 H-benzimidazole); NGM: nematode growth medium; sitosterol: 5-cholesten-24-ethyl-3β-ol; stigmastanol: 24α-ethyl-5α-cholestan-3β-ol; U18666A: 3β-(2-diethylaminoethoxy)-androstenone HCl; 7DHC: 7-dehydrocholesterol; GLC: gas-liquid chromatography; TLC: thin-layer chromatography.

Y.-K. Paik
Yonsei Proteome Research Center, Biomedical Proteome Research Center, Department of Biochemistry, Yonsei University, 134 Shinchon-dong, Sudamoon-Ku, Seoul, 120-749, Korea
e-mail: paikyk@yonsei.ac.kr

B. Larijani et al. (eds.), *Lipid Signaling Protocols*, DOI: 10.1007/978-1-60327-115-8_11,

11.1 Introduction

The purpose of this chapter is to describe the process by which the effects of sterols on *C. elegans* are analyzed in the laboratory with respect to development, reproduction, growth, and aging. Sterols are important constituents of eukaryotic cell plasma membranes; a change in sterol composition greatly affects membrane permeability and lipid bilayer fluidity [1, 2]. Data accumulated in recent years demonstrate that sterols (e.g., cholesterol) are also actively involved in broad physiological reactions, including organ development, dauer formation, chemosensation, and germ cell proliferation [3]. Fungi, plants, and mammals have complex sterol biosynthetic pathways, which enzymatically catalyze more than 30 reactions [2]. However, *C. elegans* is incapable of *de novo* sterol biosynthesis due to a deficiency in the enzymes of sterol biosynthesis; it does, however, take up exogenous sterols for normal growth and development [4]. For example, our earlier physiological studies on the role of cholesterol during development showed that germ-line development and aging of *C. elegans* have been severely affected by sterols [5–7]. Once taken up by *C. elegans*, sterols can undergo extensive enzymatic modification to form permissive sterols (e.g., 7-DHC, cholesterol) by certain sterol-modifying enzymes (e.g., 7-cholesterol desaturase, sterol 24-dealkylase) [4]. *C. elegans* appears to contain homologues of enzymes preceding farnesyl pyrophosphate biosynthesis, a major branching point for the biosynthesis of other major isoprenoids [4]. In contrast to mammals, where cholesterol is the major sterol, *C. elegans* contains 7-dehydrocholesterol (7-DHC) as its major sterol [6]. The cholesterol-signaling pathway has been the subject of many developmental studies since *C. elegans* is known to have a much simpler organ system for the investigation of this pathway. This chapter is intended to provide necessary information on the systematic analysis of the effects of sterols on worm physiology, particularly as they relate to sterol-related signaling pathways in *C. elegans*.

11.2 Materials

11.2.1 Nematode Strains and Growth Medium to Study the Effects of Sterols

1. Prepare *E. coli* (OP50) in liquid culture.
2. Strain N2 is used as a wild-type strain for most analyses. It is provided by the *Caenorhabditis* Genetics Center (http://biosci.umn.edu/CGC/Strains/strains.htm). A nematode growth medium (NGM) plate is prepared as follows. Stock solutions of 1 M $CaCl_2$, 1 M $MgSO_4$, and 1 M KH_2PO_4 should be autoclaved prior to use. Prepare medium containing the following reagents: 3 g of NaCl, 2.5 g of bacto-peptone, 17 g of agar, and distilled water to a final volume of 1 L. Autoclave for 20 min and cool to 55°C by stirring. While the medium is still warm, add the following reagents: 1 ml

of sterol (5 mg/ml in ethanol), 1 ml of 1 M $CaCl_2$, 1 ml of 1 M $MgSO_4$, and 25 ml of 1 M KH_2PO_4 (pH 6.0). The agar solution can be poured into Petri dishes until half-full. The liquid culture of *E. coli* OP50 (50 µl) is seeded onto NGM plates and grown overnight at room temperature.

3. M9 buffer: 3 g of KH_2PO_4, 6 g of $Na_2HPO_4 \cdot 2\,H_2O$, 5 g of NaCl, and distilled water to a final volume of 1 L. Adjust the buffer to pH 7.0 and autoclave. After autoclaving, add 1 ml of 1 M $MgSO_4$.
4. S basal buffer: 5.85 g of NaCl, 1 g of K_2HPO_4, 6 g of KH_2PO_4, 1 ml of cholesterol (5 mg/ml in ethanol), and distilled water to a final volume of 1 L. Sterilize by autoclaving.
5. 1 M potassium citrate (pH 6.0): 20 g of citric acid monohydrate, 293.5 g of tri-potassium citrate monohydrate, and distilled water to a final volume of 1 L. Sterilize by autoclaving.
6. Trace metals solution: 1.86 g of disodium EDTA, 0.69 g of $FeSO_4 \cdot 7\,H_2O$, 0.2 g of $MnCl_2 \cdot 4\,H_2O$, 0.29 g of $ZnSO_4 \cdot 7\,H_2O$, 0.025 g of $CuSO_4 \cdot 5\,H_2O$, and distilled water to a final volume of 1 L. Sterilize by autoclaving and store in the dark.
7. 1 M $CaCl_2$: 111 g of $CaCl_2$ in 1 L of distilled water. Sterilize by autoclaving.
8. S medium: 1 L of S basal buffer, 10 ml of 1 M potassium citrate (pH 6), 10 ml of trace metals solution, 3 ml of 1 M $CaCl_2$, and 3 ml of 1 M $MgSO_4$. Add components using sterile technique and do not autoclave.
9. Sterol stock solution: The sterols (Steraloids, Sigma) used for this experiment are sitosterol, cholesterol, and 7-DHC. The sterol stock solution for sterol feeding is prepared at a concentration of 10 mg/ml in ethanol and should not be autoclaved.
10. Sterol biosynthesis inhibitor stock solution: AY-9944, azacoprostane (10 mg/ml in ethanol, should not be autoclaved).

11.2.2 Preparation of Reagents for Sterol Analysis by GLC and TLC

1. Gas-liquid chromatography (GLC): Hewlett Packard 5890 II gas chromatograph, flame ionization detection (FID), capillary column (SAC-5)-5% diphenyl, 95% dimethylsiloxane, 30 m × 0.25 mm, inner diameter of 0.25 mm, oven temperature of 280°C, detector temperature of 300°C, carrier gas N_2, flow rate of 2.44 ml/min.
2. 25% methanolic KOH: Dissolve 25 g KOH in methanol and bring to a final volume of 100 ml.
3. 5α-cholestane (Sigma, C8003).
4. TLC plate: silica gel 60_{F254} plate (Merck).
5. Solvents: All sterol extraction procedures should be performed in glass using commercially available HPLC-grade solvents. The extracted sterols should be kept under nitrogen gas in a dark glass bottle.

6. TLC apparatus: Rectangular glass tanks are used. It is advisable to line the inside of the tanks with Whatman filter paper to saturate the surrounding atmosphere. Development solutions are poured into the tank at least 1 h prior to use.
7. Standard sterols: Stock solutions of pure samples of standard sterols are prepared by dissolving the sterols in chloroform (10 mg/ml) and storing at −20°C until use.
8. Detection of lipids on the TLC plate: Prepare a solution of 10% $CuSO_4$/8% H_3PO_4 just prior to staining.

11.2.3 Hoechst 33342, Filipin, and Sudan Black B Staining

1. GCP slide: Soak glass slide in 0.1% polylysine solution and dry at room temperature overnight. (If stored at 4°C, the GCP slide is usable for more than 1–2 weeks).
2. STEG buffer: 40 mM NaCl, 10 mM Tris·HCl (pH 7.4), 1 mM EDTA (pH 8.0), and 20% glycerin.
3. 0.1% polylysine (Sigma, P8920).
4. Hoechst 33342 (Sigma, B6621).
5. Filipin (Sigma).
6. Sudan Black B solution: A saturated solution of Sudan Black B (Sigma, S2380) in 70% ethanol is filtered through a 0.45-μm syringe filter prior to use.

11.2.4 Microscopy and Photography

1. Microscope: Axiovert 135 (Zeiss).
2. Manipulator: Microforge MF-830 (Narishige).
3. Micro-coverglass: 48 mm × 60 mm No. 1 (THOMAS Red Label).
4. T-max 400 film (Kodak).
5. Dektol developer (Kodak) and HYPAM fixer (ILFORD).
6. Image capture: AxioCam (Zeiss).

11.3 Methods

Sterol metabolism in *C. elegans* is quite different from that in other species, such as mammals and yeast, due to its inability to synthesize sterols *de novo*. To examine sterol functions in *C. elegans*, a sterol-feeding experiment was carried out in which certain critical parameters, such as brood size, growth rate, and life span, could be determined. In addition, a change in lipid distribution in

C. elegans can be qualitatively detected by Sudan black staining for fat accumulation and filipin labeling for cholesterol localization. With nuclear staining techniques, the effects of sterols on germ-line development and egg laying can also be observed. The degree of the egg-laying defective phenotype becomes severe when sterol modification is perturbed by treatment with either azacoprostane HCl or AY9944. Taken together, the effects of sterols on *C. elegans* development are very prominent and easily assessed using the techniques described here.

11.3.1 Measurements of Growth Rate and Body Size of C. elegans Fed Dietary Sterols

1. Wild-type N2 is grown at either 20°C or 25°C on 87-mm NGM agar plates containing *E. coli* (OP50).
2. For the sterol-feeding experiment, worms are grown under different concentrations of cholesterol (e.g., 0, 5, 50, or 100 μg/ml).
3. Ten L4 hermaphrodites or worms at mixed stages are collected by washing the plates with M9 buffer.
4. The growth rate of worms on each agar plate is determined by the observation of characteristic stage-specific morphologies under the microscope.
5. Individual worms at specific stages are placed on an agar pad and body lengths are measured (*see* Fig. 11.1).

11.3.2 Measurement of Brood Size, Embryonic Lethality, and Percent Development

To investigate whether sterols regulate worm development, one can examine the effects of sterol biosynthesis inhibitors on worm growth and reproduction using the following protocol.

1. L4-stage N2 worms are individually cloned onto agar plates in the presence or absence of sterol biosynthesis inhibitor at either 20°C or 25°C.
2. The worms are transferred to new plates at 24-hr intervals.
3. An embryo is scored as dead if it did not hatch after 24 h.
4. The brood size is defined as the sum of both nonhatched and hatched embryos (*see* Note 1).
5. Embryonic lethality can be calculated as the number of nonhatched embryos divided by the sum of nonhatched and hatched embryos.
6. The percent development is calculated as the number of hatched embryos that reach adulthood. Usually, an average value is obtained from three independent experiments where at least five cloned hermaphrodites were used (*see* Table 11.1) [5].

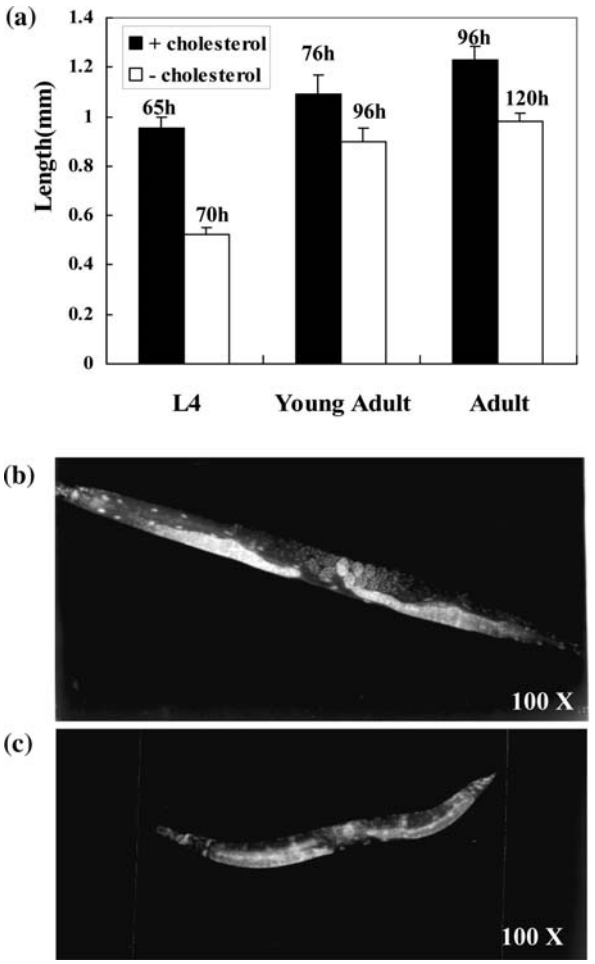

Fig. 11.1 Comparison of sizes of worms grown with or without cholesterol. (a) Size of worms measured at different stages with (closed bar) and without (open bar) cholesterol at 20°C. The time after egg laying to L4, young adult, or adult stage, is indicated on the top of the bar. The average values of 10 worms are presented. (b) Adult worm after growth for 96 h with cholesterol. (c) Adult worm after growth for 120 h without cholesterol. ((a) is reproduced from Shim et al. [5] with permission. (b) and (c) are unpublished data provided by Shim Y-H)

Table 11.1 Effect of cholesterol starvation on *C. elegans* development

Strain	Average Brood Size		Embryonic Lethality (%)	Development (%)
	Cholesterol 5 μg/ml			
	+	–		
P0	362 ± 28.0 (100%)	—	0.8 ± 0.2	96.7 ± 1.8
F1	—	315 ± 17.6 (87%)	2.9 ± 0.5	88.3 ± 0.9
F2	—	243 ± 36.3 (67%)	1.6 ± 2.1	89.6 ± 3.7
F3	—	222 ± 7.3 (61%)	2.8 ± 1.1	91.2 ± 3.8

Values are expressed as the mean ± standard deviation ($n = 5$) and the percentage of the control group grown in the presence of cholesterol. (Reproduced from Shim et al. [5] with permission).

11.3.3 Measurement of Life Span of C. elegans Fed Different Sterol Concentrations

Aging is associated with the accumulation of molecular and cellular damage that correlates with a decline in normal physiological function. To determine how sterols in the diet affect the age of *C. elegans*, the mean life span was determined. We have tested the hypothesis that life span can be affected in part by changes in sterol composition. The following protocol is applied to measure the mean life span of *C. elegans* fed different concentrations of cholesterol.

1. Synchronous populations are obtained by hatching eggs from a gravid adult in M9 buffer.
2. The hatched L1 larvae are placed on NGM agar plates that contain different concentrations of sterols, at both 20°C and 25°C (*see* Note 2). Lifespan assays are typically carried out at either 20°C or 25°C. A mean adult life span at 20°C is approximately 23–24 days. At 25°C, the average is approximately 14 days. Since 25°C yields a shorter life span, be sure that any mutant you may use is viable and behaves normally at 25°C.
3. Worms are observed daily and are scored as dead if they do not move in response to prodding with a toothpick. The mean life span is determined from the percentage of worms alive on a given day (*see* Table 11.2).

Table 11.2 Changes in the physiological characteristics of *C. elegans* in response to sterols

Strain	NGM (±) Cholesterol 5 μg/mL	* Mean Life Span (± S.D., days) $n = 20$	†Brood Size (mean ± S.D.) $n = 20$	Adult Number (mean ± S.D.) $n = 20$	‡ Percent Development (egg → adult)
N2	+	21 ± 5.1	252 ± 22	229 ± 14	90.8 ± 5.5
	–	16 ± 1.2	119 ± 10	76 ± 6	63.9 ± 5.0

*To measure both survival and mean life span (MLS) of F1 progeny in either cholesterol-supplemented medium (CSM) or sterol-depletion medium (SDM), worms were counted every day and dead ones were eliminated.

†Brood sizes of F3 progeny on either CSM or SDM plates are defined as the total number of nonhatched and hatched eggs of each hermaphrodite and expressed as the mean ± standard deviation ($n = 20$).

‡Percent development is defined as the number of adults divided by the total number of eggs. Each mean ± S.D. value was derived from three separate determinations.

Source: Reproduced from Lee et al. [6] with permission.

11.3.4 Treatment of Worms with Sterol Biosynthesis Inhibitors

1. Five hundred microliters of AY9944 (Sigma; 2 mM) were spread onto NGM plates (87 mm) containing cholesterol (5 μg/ml). To make serial plates that contain different concentrations of inhibitor, the stock solution of AY-9944 is sequentially diluted with distilled water and added onto the plate as described above.

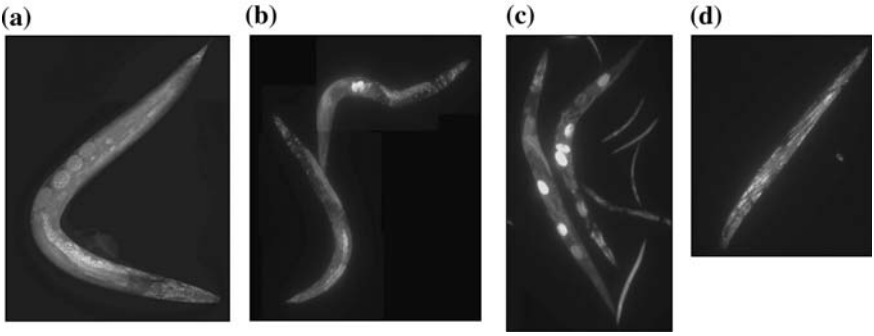

Fig. 11.2 Effects of AY-9944 on egg laying of *C. elegans*. Bag-of-worm and egg-laying defective phenotypes became severe as concentrations of AY-9944 were increased. The sizes of the adults also decreased. (a) N2 worms. (b) Worms grown on an NGM plate containing 5 μg/ml of sitosterol and 30 μM AY-9944. (c) 60 μM AY9944. (d) 120 μM AY-9944

2. Worms are placed onto plates with agar chunks containing mixed-staged N2 worms and grown at 20°C for 5–7 days.
3. Morphological changes (e.g., egg-laying defects) are observed with nuclear staining techniques under microscopy (*see* Fig. 11.2).

11.3.5 Preparation of C. elegans Membrane Fractions

This experiment was performed to obtain membrane fractions for various purposes before or after perturbation by altering sterol concentrations in the agar or liquid medium. Such membrane fractions can be used to assay enzymes related to sterol metabolism (e.g., 7-DHCR).

1. Prepare liquid culture as follows: Add 250 ml of S medium to a sterilized 1–2 L flask.
2. Inoculate the S medium with a concentrated *E. coli* OP50 pellet made from 2–3 L of an overnight culture.
3. Wash each of four large NGM plates of *C. elegans* with 5 ml of S medium and add to the 250-ml flask.
4. Place the flask on a shaker at 20°C and shake vigorously so that the culture is well oxygenated.
5. Cultures should be monitored by checking a drop of the culture under the microscope. If the food supply is depleted (the solution is no longer visibly cloudy), add more concentrated *E. coli* (OP50) suspended in S medium. When there are many adult animals in each drop, the culture is ready to be harvested. This usually occurs on the 4th or 5th day.
6. Place the flask on ice for 15 min to allow the worms to settle.
7. Aspirate most of the liquid from the flask.

8. Transfer the remaining liquid to a 50-ml sterile, conical centrifuge tube and centrifuge at 4,000 × *g* for 5 min to pellet the worms. Aspirate the remaining liquid.
9. The final pellets are resuspended in distilled water, loaded onto a sucrose gradient (final 35%), and centrifuged at 1,500 × *g* for 5 min at 4°C.
10. Preparation of membrane fractions: Prepare buffer A containing 0.1 M potassium phosphate buffer (pH 7.4), 1 mM reduced glutathione, and 0.5 mM EDTA plus a protease inhibitor cocktail tablet (Boehringer Mannheim).
11. Harvest worms from liquid culture and wash repeatedly in S medium to remove bacteria.
12. Collect washed worms by centrifugation at 1,500 × *g* for 10 min.
13. Resuspend the pellets into two volumes of buffer A and then disrupt the pellets with a Teflon homogenizer.
14. Centrifuge the homogenates at 1,500 × *g* for 10 min at 4°C to remove cuticles and large pieces of debris.
15. Centrifuge the supernatant (whole homogenate: WH) at 105,000 × *g* for 1 h.
16. Resuspend the pellets (microsomes) containing the membrane fractions in buffer A.

11.3.6 Analysis of Sterols in C. elegans by GLC

The aim of this experiment was to consider how one could measure the endogenous sterol content that is present in *C. elegans*. Although 7-DHC is the main sterol in *C. elegans* that is detected by GLC, its levels can be altered when the worms receive different drugs during growth. To examine the quantitative change in sterol content after sterol biosynthesis inhibitor treatment (i.e., wild-type N2 grown in the presence of azacoprostane or AY-9944), total lipids are extracted from the nematodes, saponified, and quantified with GLC using an internal standard according to the following protocol.

1. Worms are treated with sterol biosynthesis inhibitors (e.g., AY-9944).
2. Prepare microsomes from the total homogenates of worms that were treated with sterol biosynthesis inhibitors as described in Subheading 11.3.5
3. Add an equal volume of 25% methanolic KOH to the membrane fractions (from Subheading 11.3.6) and heat at 80°C for 15 min (saponification). As an internal standard, certain amounts of 5α-cholestane can be added.
4. Extract nonsaponifiable sterols with two volumes of petroleum ether and dry under N_2 gas. Dissolve in chloroform.
5. Quantify the sterols by GLC. Measure the peak sterol area relative to that of an internal standard (5α-cholestane). The relative retention time (compared with a cholesterol standard) are 1.070 for 7-dehydrocholesterol (7-DHC) under conditions described above (*see* Note 3) [5, 6].

11.3.7 Analysis of Fatty Acids and Other Lipids in C. elegans by TLC

1. Add an equal volume of chloroform:methanol (2:1) to the total worm homogenate (from Subheading 11.3.5) and sonicate (bath-type sonicator) for 15 min at room temperature.
2. Centrifuge the mixture at 4,000 × *g* for 5 min.
3. Filter the organic fraction with Whatman paper (No. 2) and dry under N_2 gas.
4. Redissolve the lipid samples in 50 μl of chloroform and apply the sample as a small streak that measures 1.5 cm from the bottom edge of precoated TLC plates (Silica gel 60, 20 cm × 20 cm).
5. Develop the TLC plate in the presence of a solvent mixture of hexane: diethyl ether (1:1) in a presaturated chamber until the solvent front reaches approximately 1.5 cm from the top of the plate; quickly mark the solvent front's position.
6. Alternatively, separate sterols on a one-dimensional TLC plate using two solvent systems: hexane/diethyl ether/acetic acid (80:20:1) and hexane/chloroform/acetone/acetic acid (10:35:10:1), respectively [8].
7. Immerse the developed TLC plate quickly into a freshly made 10% $CuSO_4$/8% H_3PO_4 aqueous solution and heat at 180°C on a hot plate.
8. Sterols and lipids will become blue-brown in color (*see* Note 4).
9. The quantities of sterols and lipids are determined by densitometry and compared with 10–20 μg of a standard compound on the same plate (Sigma).
10. If necessary, lipids can be eluted from the TLC plate by cutting out the stained area with a sharp blade or spatula and performing a solvent extraction. The extracted lipids can be further analyzed by counting (for radioactive lipids) in a liquid scintillation counter or quantified by GLC using an internal standard.

11.3.8 Sudan Black B Staining

This method is very useful for the qualitative analysis of fatty acids present in the body of *C. elegans* (i.e., intestine and hyperdermis). When worms are stressed during early life (i.e., L1 or early L2), they go into the dauer phase, an alternative to L3, in order to overcome the given environmental stress [9]. To prepare for this phase, they accumulate fats inside the body that can be detected qualitatively by Sudan Black B staining. In addition, this technique can be used to detect changes in fat deposits in response to a dauer-inducing pheromone (e.g., daumone) [10], nutritional signal, or genetic mutation. Several lipids, including phospholipids, neutral fats, and sterols, are stained intensely by Sudan Black B. For convenience, the following protocol is prepared for the

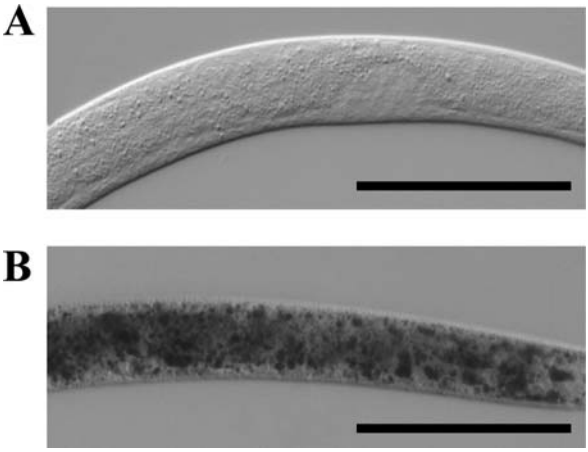

Fig. 11.3 Nomarski photographs showing abundant fat storage visualized with Sudan Black B staining. (a) Normal L3 stage grown in favorable conditions. (b) Dauer larval stage grown on plates containing 384 mM daumone and 160 mg dead *E. coli* as a food source. Scale bar: 50 mm

general observation of fat deposits under dauer or dauer-like phases that are induced by pure daumone [10].

1. Wash worms through a 5-μm nylon mesh with M9 or PBS buffer to remove bacteria.
2. Incubate worms in 5–6 ml of the same buffer for another 30 min to remove bacteria in the gut, if desirable.
3. Transfer worms to a tube and add 10% paraformaldehyde (PF) stock to a final concentration of 1% (w/v), mix well, and freeze in dry ice/ethanol. Frozen samples may be processed immediately or stored indefinitely at −80°C (*see* Note 5).
4. Repeat the freeze-thaw the worm in 1% PF for three times.
5. After the final thaw, incubate samples on ice with an occasional agitation for 10 min.
6. Wash the fixed worms in cold distilled water at least three times.
7. Dehydrate worms through 25%, 50%, and 70% ethanol sequentially. Keep worms in each gradient for 2 min.
8. Add 2–5 volumes of Sudan Black B solution to the worms and incubate for 30–60 min.
9. Wash worms with 15–25% ethanol for 5–10 min and photograph (*see* Note 6) (see Fig. 11.3, Jeong P–Y et al., unpublished data).

11.3.9 Filipin Staining

The sterol-rich plasma membrane domains can be stained *in vivo* with filipin.

1. Place 20 drops of water or M9 buffer (~1–2 μl) on a GCP slide, and put several worms onto each water drop.

2. Evaporate water drops quickly near the flame of an alcohol lamp (*see* Note 7).
3. Drop approximately 15–20 µl of filipin (10 µg/ml in STEG buffer) onto a coverslip (40 mm × 24 mm) and overlay the coverslip onto the worms; flatten but do not squish the sample.
4. Remove extra filipin solution.
5. Observe using microscope equipped with epifluorescence optics and CCD camera.

11.3.10 Nuclear Staining of Worms by Hoechst 33342

The morphology of intact worms can be visualized by nuclear staining with Hoechst 33342 (Sigma). This method is used for detecting the cell viability of *C. elegans*.

1. Place 20 drops of water or M9 buffer (~1–2 µl) on a GCP slide, and put several worms onto each water drop.
2. Evaporate the water drops quickly near the flame of an alcohol lamp (*see* Note 7).
3. Drop approximately 15–20 µl of Hoechst 33342 (10 µg/ml in STEG buffer) onto a coverslip (40 mm × 24 mm) and overlay the coverslip onto the worms; flatten but do not squish the sample.
4. Remove extra Hoechst solution.
5. Observe using microscope equipped with epifluorescence optics and CCD camera.

Acknowledgments This study was supported by a grant from the Korean Health 21 R&D project, Ministry of Health & Welfare, Republic of Korea (A030003 to YKP), by the Technology Development Program of the Ministry of Agriculture and Forestry, Republic of Korea (606001-53-1-SB010 to YKP), and by a grant from the Basic Research Program that is supported by KOSEF (RO1-2005-000-11021-0 to YHS).

Notes

1. Embryonic lethality is defined as the number of nonhatched embryos divided by the sum of nonhatched and hatched embryos. The percent development is defined as the number of hatched embryos that reach adulthood [5].
2. When life span is determined, 5-fluoro-2'-deoxyuridine (FDUR, Sigma, F0503) is also used. Forty micromolar FDUR added to the NGM plates inhibits progeny growth, and worms do not lay eggs [8]. Dissolve FUDR in distilled water and sterilize through a filter. Add FUDR to the medium at the same time as Ca, Mg, etc. after autoclaving.
3. To observe a well-resolved sterol peak by GLC, one of the critical parameters is oven temperature. Because sterols of *C. elegans* are present in trace amounts, which make it difficult to obtain a pure sterol fraction, selecting an oven temperature between 260–300°C is very important.

4. Lipids are separated in the order of cholesterol, lanosterol, free fatty acids, triglyceride, cholesterol ester, and squalene from the bottom of the plate.
5. A 10% paraformaldehyde (PF) stock should be made fresh at least once a week by dissolving 1 g of PF in 10 ml of hot water (preheated in a microwave oven). Add 1–2 drops of 2 N NaOH and incubate at 55–60°C for 15 min.
6. The final step (washing with 15–25% ethanol) is needed for reducing the background.
7. If worms are overdried, nuclei do not stain. Flaming the worms for 5–10 s is sufficient. Overlay the coverslip steadily to avoid forming a bubble. Seal the edge of the coverslip with transparent nail polish.

References

1. Nes WR, MeKean ML. Biochemistry of Steroids and Other Isopentenoids. New York: University Park Press; 1977.
2. Faust JR, Trzaskos JM, Gaylor JL. Cholesterol biosynthesis. In Yeagle, PL, ed. Biology of Cholesterol. Boca Raton, FL: CRC Press; 1988.
3. Kurzchalia TV, Ward S. Why do worms need cholesterol? Nat Cell Biol 2003;5:684–8.
4. Chitwood DJ. Biochemistry and function of nematode steroids. Crit Rev Biochem Mol Biol 1999;34:273–84.
5. Shim YH, Chun JH, Lee EH, Paik YK. Role of cholesterol in germ-line development of *Caenorhabditis elegans*. Mol Reprod Dev 2002;61:358–66.
6. Lee EY, Shim YH, Chitwood DJ, Hwang SB, Lee JH, Paik YK. Cholesterol-producing transgenic *Caenorhabditis elegans* lives longer due to newly acquired enhanced stress resistance. Biochem Biophys Res Commun 2005;328:929–36.
7. Choi BK, Chitwood DJ, Paik YK. Proteomic changes during disturbance of cholesterol metabolism by azacoprostane treatment in *Caenorhabditis elegans*. Mol Cell Proteomics 2003;10:1086–95.
8. Beanan MJ, Strome S. Characterization of a germ-line proliferation mutation in *C. elegans*. Development 1992;116:755–66.
9. Riddle D, Albert P. Riddle D, Blumenthal T, Meyer B, Priess J., eds. *C. elegans* II, Genetic and environmental regulation of dauer larva development. pp 739–768. Cold Spring Harbor, NY: Cold Spring Harbor Laboratory Press; 1997.
10. Jeong PY, Jeong MK, Yim YH, Kim HK, Park MS, Hong MS, Lee MT, Kim YH, Kim K, Paik YK. Chemical structure and biological activity of the *Caenorhabditis elegans* dauer-inducing pheromone. Nature 2005;433:541–5.
11. Baugh LR, Hill AA, Brown EL, Hunter CP. Quantitative analysis of mRNA amplification by *in vitro* transcription. Nucleic Acids Res 2001;29:E29.

Chapter 12
Proteomic Analysis of the Sterol-Mediated Signaling Pathway in *Caenorhabditis elegans*

Byung-Kwon Choi, Yun-Kyung Shin, Eun-Young Lee, Pan-Young Jeong, Yhong-Hee Shim, David J. Chitwood and Young-Ki Paik

Abstract Since *Caenorhabditis elegans* is incapable of *de novo* cholesterol biosynthesis, it must utilize other nonpermissive sterols that are present in the environment by converting them into cholesterol for cellular function. The inhibition of sterol conversion to cholesterol in *C. elegans* by various sterol biosynthesis inhibitors (SBIs) is known to cause serious defects in the development of these worms. To determine the biochemical consequences of these physiological abnormalities, one can perform a proteomic analysis of worms of a certain stage that are grown in the presence of SBIs in order for the differential expression of proteins involved in the sterol-mediated signaling pathway to be identified. For example, reductions in the expression of lipoprotein family members, such as vitellogenin-2 and vitellogenin-6, are prominent in azacoprostane-treated worms. This phenomenon is also seen in worms treated with AY-9944, which blocks the conversion of 7-dehydrocholesterol, a major sterol present in *C. elegans*, to cholesterol.

Keywords *C. elegans* · proteome · sterol biosynthesis inhibitor · 2-DE · 25-azacoprostane-HCl · AY-9944 · 7-dehydrocholesterol · MALDI-TOF · sitosterol

12.1 Introduction

C. elegans is an excellent animal model organism in which to study the *in vivo* sterol effects on signal transduction that are relevant to human disease [1,2,3]. Since *C. elegans* lacks the enzymes required for *de novo* sterol biosynthesis, it must utilize other sterols for cellular function [4]. In addition to genetics and

Y.-K. Paik
Yonsei Proteome Research Center, Biomedical Proteome Research Center, Department of Biochemistry, Yonsei University, 143 Shinchon-dong, Sudamoon-Ku, Seoul, 120-749, Korea
e-mail: paikyk@yonsei.ac.kr

B. Larijani et al. (eds.), *Lipid Signaling Protocols*, DOI: 10.1007/978-1-60327-115-8_12,

reverse-genetics tools, a proteomic study of *C. elegans* now enables the identification of sterol-mediated signaling and reproductive pathways [5]. To analyze sterol-mediated signaling pathways in *C. elegans*, expression proteomics can be performed under conditions whereby specific perturbations of sterol metabolism are caused by the addition of sterol biosynthesis inhibitors (SBIs) or modifying agents to the growth media [2]. The resulting proteome map may produce a protein list that contains different protein populations that are present in qualitative abundance and the identification of a set of proteins under conditions of sterol metabolism disturbance [4]. For example, a 2D map of differentially expressed proteins that were obtained from the proteomic analysis of *C. elegans* grown in the presence of azacoprostane, an inhibitor of sterol 24-reductase (which catalyzes the conversion of desmosterol to cholesterol) [6, 7, 8], presents useful information about those proteins that were either upregulated or downregulated by perturbations of sterol metabolism. Similarly, when the exogenous sterol supply is restricted, many physiological abnormalities, including growth inhibition, egg-laying defects, and endomitotic (*emo*) phenocopy, are easily observed [1, 2, 9]. To analyze the protein expression changes in those worms that are grown in the presence of various SBIs in the media, different proteomics techniques, such as gel-based [e.g., two-dimensional electrophoresis (2-DE) and nongel-based, two-dimensional liquid chromatography (2D-LC)] coupled to mass spectrometry (MS) can be applied [5, 10]. This chapter demonstrates that SBI treatment causes a substantial change in the levels of many sterol-related proteins, which can be analyzed by 2-DE as described here.

12.2 Materials

12.2.1 Nematode Culture

1. Prepare *E. coli* (OP50) in liquid culture as a food source.
2. The wild-type strain *C. elegans* (N2) [11] was provided by the *Caenorhabditis* Genetics Center (http://biosci.umn.edu/CGC/Strains/strains.htm).
3. Nematode growth medium (NGM) for liquid: Combine 1 L of media containing 3 g/L of NaCl, 2.5 g/L of bacto-peptone, 17 g/L of agar, 1 ml of sterol (5 mg/ml in ethanol), 1 ml of of 1 M $CaCl_2$, 1 ml of 1 M $MgSO_4$, and 25 ml of 1 M KH_2PO_4 (pH 6).
4. M9 buffer: 3 g of KH_2PO_4, 6 g of $Na_2HPO_4 \cdot 2\,H_2O$, 5 g of NaCl, and distilled water to a final volume of 1 L. Adjust the buffer to pH 7 and autoclave. After autoclaving, add 1 ml of 1 M $MgSO_4$.
5. S basal buffer: 5.85 g of NaCl, 1 g of K_2HPO_4, 6 g of KH_2PO_4, 1 ml of cholesterol (5 mg/ml in ethanol), and distilled water to a final volume of 1 L. Sterilize by autoclaving.

6. 1 M potassium citrate (pH 6) solution: 20 g of citric acid monohydrate, 293.5 g of tri-potassium citrate monohydrate, and distilled water to a final volume of 1 L. Sterilize by autoclaving.
7. Trace metals solution: 1.86 g of disodium EDTA, 0.69 g of $FeSO_4 \cdot 7\,H_2O$, 0.2 g of $MnCl_2 \cdot 4\,H_2O$, 0.29 g of $ZnSO_4 \cdot 7\,H_2O$, 0.025 g of $CuSO_4 \cdot 5\,H_2O$, and distilled water to a final volume of 1 L. Sterilize by autoclaving and store in the dark.
8. 1 M $CaCl_2$: 111 g $CaCl_2$ in 1 L of distilled water. Sterilize by autoclaving.
9. S medium: 1 L of S basal buffer, 10 ml of 1 M potassium citrate (pH 6), 10 ml of trace metals solution, 3 ml of 1 M $CaCl_2$, and 3 ml of 1 M $MgSO_4$. Add components using sterile technique and do not autoclave.
10. Sterol stock solution: the sterols (Steraloids, Sigma) used for this experiment are sitosterol, cholesterol, and 7-DHC. The sterol stock solution for sterol feeding is prepared at a concentration of 10 mg/ml in ethanol and should not be autoclaved.
11. Sterol biosynthesis inhibitors stock solution: The compound 25- azacoprostane HCl (25-aza-5β-cholestane hydrochloride) and triparanol are prepared as 5 mg/ml and 25 mg/ml stock solutions in ethanol, respectively.

12.2.2 Growth Medium to Study the Effects of Sterols

1. Tenfold cholesterol overfeeding stock solution: 25 mg/ml of cholesterol in ethanol. Store at 4°C.
2. Cholesterol overfeeding: (a) Stock solutions of 1 M $CaCl_2$, 1 M $MgSO_4$, and 1 M KH_2PO_4 should be autoclaved prior to use. (b) Prepare medium containing the following reagents: 3 g of NaCl, 2.5 g of bacto-peptone, 17 g of agar, and distilled water to a final volume of 1 L. Autoclave for 20 min and cool to 55°C with stirring. (c) While the medium is still warm, add the following reagents: 2 ml of sterol (25 mg/ml in ethanol), 1 ml of 1 M $CaCl_2$, 1 ml of 1 M $MgSO_4$, and 25 ml of 1 M KH_2PO_4 (pH 6). The agar solution can be poured directly into Petri dishes until half-full.
3. The liquid culture of *E. coli* OP50 (50 μl) is seeded onto NGM plates and grown overnight at room temperature.

12.2.3 Sample Preparation for Two-Dimensional Electrophoresis (2-DE)

1. Buffer A: 50 mM Tris·HCl, 5 mM EDTA, 7 M urea, 2 M thiourea, 4% CHAPS {3-[(3-cholamidoprophyl)dimethylammonio]-1-propansulfonate}, and protease inhibitor cocktail.

2. Protease inhibitor (Complete Protease Inhibitor Cocktail, Roche, Cat. no. 11 697 498 001, 20 tablets): One tablet contains protease inhibitors (antipain, bestatin, chymostatin, leupeptin, pepstatin, aprotinin, phosphoramidon, EDTA) sufficient for a 50-ml cell extract. Prepare 25X stock solutions in the 2-ml water. Stock solution is stable at least 12 weeks at −15°C to −20°C.
3. The protein concentration of the soluble fraction was determined by the Bradford method [12] using bovine serum albumin as a standard. Aliquots were stored at −70°C until use.

12.2.4 Two-Dimensional Electrophoresis

1. Buffer B: 7 M urea, 2 M thiourea, 2% (v/v) IPG buffer (nonlinear pH gradient 3–10), 2 % CHAPS, 15 mM DTT, and a trace of bromophenol blue.
2. Immobiline Dry Strip, nonlinear pH 3–10 (18 cm, GE Healthcare).
3. Equilibrating solution: 375 mM Tris-HCl (pH 8.8), 6 M urea, 2% SDS, and 5 mM tributyl phosphine (TBP) (*see* Note 1).
4. Embedding solution: 0.5% agarose, 24.8 mM Tris-HCl (pH 8.3), 192 mM glycine, 0.1% SDS, and a trace of bromophenol blue.
5. Multiphor or IPGphor (GE Healthcare).
6. GS-710 image scanner (Bio-Rad).
7. Image Master Platinum 5.0 (GE Healthcare).

12.2.5 In-Gel Trypsin Digestion

1. Sequencing grade-modified trypsin (Promega, V5111, 100 μG, 18,100 U/mg).
2. 50 mM ammonium bicarbonate.

12.2.6 Desalting of Peptides and MALDI Plating

1. Gel Loader tips (20-μl capacity, Cat. no. 0030 048.083, Eppendorf).
2. Poros 10 R2 resin (1-1118-02, 0.8 g, PerSeptive Biosystems) (*see* Note 2).
3. Oligo R3 resins (1-1339-03, 6.3 g, PerSeptive Biosystems).
4. Acetonitrile (ACN) (HPLC grade).
5. 2% formic acid in 70% ACN.
6. 0.1% Trifluoroacetic acid in 70% ACN.
7. 1-ml syringe.
8. Matrix: α-cyano-4-hydroxy cinnamic acid (CHCA) (Sigma) (*see* Note 3).

12.2.7 Matrix-Assisted Laser Desorption/Ionization–Time-of-Flight–Mass Spectrometry Analysis (MALDI-TOF-MS)

1. Voyager DE Pro Mass spectrometry (Applied Biosystems).
2. 4800 MALDI-TOF/TOF (Applied Biosystems).
3. Opti-TOF^{TM} 384 well Insert (123 mm × 81 mm, 1016491, Applied Biosystems).

12.2.8 Competitive Reverse Transcription-Polymerase Chain Reaction

1. Genomic DNA of *C. elegans* in mixed stages: Genomic DNA was extracted from wild-type *C. elegans* using a genomic DNA isolation kit (Nucleogene).
2. TRI reagent (Molecular Research Center).
3. Moloney murine leukemia virus reverse transcriptase (Invitrogen).
4. DNase I (Takara).
5. Random hexamer (Promega).
6. GeneAmp 2400 PCR thermal cycler (Perkin Elmer Life Science).

12.3 Methods

12.3.1 Nematode Culture

To grow *C. elegans* in liquid media (S media), worms are grown on an NGM agar plate containing 5 μg/ml of β-sitosterol (Steraloids Inc.) and supplied OP50 *E. coli* strain as a food source.

1. Collected worms from the NGM plate were inoculated into flasks containing S medium with 5 μg/ml of β-sitosterol (Steraloids Inc.).
2. 25-azacoprostane hydrochloride (5 μg/ml) and triparanol (25 μg/ml) were added [13, 14].
3. Worms were grown for 8 days at 20°C.
4. The suspension was transferred into a 2 ml microcentrifuge tube.
5. An equal volume of 70% sucrose was added and incubated for 10 min on ice (see Note 4).
6. Centrifuge for 10 min at 12,000 x *g* at 4°C.
7. Worms were washed with M9 buffer and stored at −70°C until use.

12.3.2 Nematode Growth on Overfed Cholesterol Plate

1. Strain N2 used as a wild-type strain is provided by the *Caenorhabditis* Genetics Center.

2. Worms are grown at 20°C on NGM agar plates containing 5 μg/ml, or 50 μg/ml of cholesterol.
3. Worms are washed with 70% sucrose solution and M9 buffer to eliminate any contaminant proteins.
4. Grown worms are suspended with an appropriate volume of sample buffer. Or, if it is not used right away, it can be suspended with distilled water and stored at −70°C until use (*see* Note 5).

12.3.3 Two-Dimensional Electrophoresis

12.3.3.1 Sample Preparation for Two-Dimensional Electrophoresis (2-DE)

1. Worms were washed with M9 buffer and stored at −70°C until use.
2. Worms were washed with distilled water and suspended in an appropriate volume of sample buffer A.
3. Suspensions were sonicated for approximated for 30 s, three times on ice at 60% duty cycle, 6 power output, and centrifuged at 36,000 x *g* for 40 min at 4°C.
4. The supernatant were transferred in to a new tube.
5. The protein concentration in the soluble fraction was determined by the Bradford method [12] using bovine serum albumin as a standard.
6. Aliquots were stored at −70°C until use.

12.3.3.2 Sample Preparation for 2-DE from Cholesterol-Overfed Worms

1. Worms were washed with M9 buffer and spun down three times at 3,000 × *g* for 3 min and suspended with an appropriate volume of sample buffer A.
2. Suspensions were sonicated for approximately 30 s on ice.
3. The soluble fractions were precipitated by TCA (Trichloroacetic acid) and spun at 36,000 × *g* for 40 min at 4°C
4. The resulting pellet was washed with 99% cold acetone and dried at room temperature for 10 min.The dried pellet was resuspended in 500 μl of sample buffer A without dye.
5. The protein concentration of the soluble fraction was determined by the Bradford method [12] using bovine serum albumin as a standard. Aliquots were stored at −70°C until use.

12.3.3.3 2-DE

1. Suspend protein sample (100 μg for analytical gels and 1 mg for preparative gels) in sample buffer B to obtain a final volume of 350 μl.
2. Apply aliquots of *C. elegans* proteins in sample buffer onto an immobilized pH gradient strip (IPG) (Immobiline Dry Strip, nonlinear gradient pH 3–10, 18 cm; GE Healthcare) (*see* Note 6) that had been rehydrated with sample protein solution at 20°C for 14 h.

3. Perform isoelectric focusing at 20°C under a current limit of 50 μA/strip as follows: 100 V for 2 h, 300 V for 2 h, 1,000 V for 1 h, 2,000 V for 1 h, and then continuous at 3,500 V until reaching optimal voltage hour (Vh). Perform focusing for a total of 67,000 Vh for preparative samples (*see* Note 7) [2].
4. IPG strips are equilibrated for 20 min by gently shaking in buffer containing 375 mM Tris·HCl (pH 8.8), 6 M urea, 2% SDS, 5 mM TBP, 2.5% acrylamide solution, and 20% glycerol. In the second dimension of electrophoresis, vertical SDS-gradient slab gels (9–16%; dimensions 180 × 200 × 1.5 mm) are used (*see* Note 8).
5. The equilibrated IPG strips are cut to size, and then these slab gels are overlaid with embedding solution.
6. Electrophoresis is conducted at a constant 15 mA per gel. After protein fixation in 40% methanol and 5% phosphoric acid for at least 1 h, the gels are stained with Coomassie Brilliant Blue (CBB) G-250 overnight.
7. After destaining, gel images are obtained using a GS-710 image scanner (Bio-Rad). The gel images are processed with Image Master Platinum (GE Healthcare).
8. Comparative 2-DE gels with cholesterol and cholesterol overfeeding of *C. elegans* are shown in Fig. 12.1.

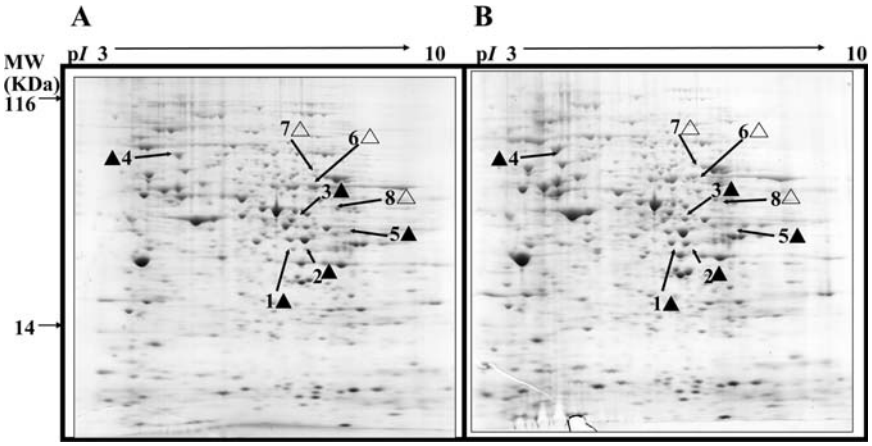

Fig. 12.1 Comparative 2-DE gel with cholesterol and cholesterol overfeeding of *C. elegans*. (a) 2-DE gel image of 5 μg/mL cholesterol-treated worms. Proteins that were extracted from wild-type worms were separated on a nonlinear pH 3–10 IPG strip followed by electrophoresis on a 9–16% SDS-polyacrylamide gel. The gel was stained with Coomassie Brilliant Blue. Each labeled numeral indicates a protein for which the expression level was 1.5-fold upregulated (▲ > 1.5-fold: lipid metabolism-related proteins) or downregulated (Δ < 1.5-fold: carbohydrate- and energy metabolism-related proteins). (b) 2-DE gel image of 50 μg/ml cholesterol-treated worms. Shown in the gels are 1. alcohol dehydrogenase (K12G11.3), 2. alcohol dehydrogenase (K12G11.3), 3. ATP synthase alpha and beta subunits (Y49A3A.1), 4. ATP synthase alpha and beta subunits (Y49A3A.1), 5. acyl-Coenzyme A dehydrogenase short branched chain (K06A5.6), 6. ALDH6A3, ALdehyde deHydrogenase (alh-8), 7. glutamate dehydrogenase (ZK829.4), 8. phosphoglycerate kinase (T03F1.3)

12.3.4 2D Gel Image Analysis

1. Import the gel image (recommended 16-bit, TIFF file format) and convert to the ImageMaster file (*.mel).
2. Detect protein spots and determine the volume and percent volume of each spot. Percent volume is the normalized value that remains relatively independent of variations between gels, particularly those caused by varying experimental conditions, and are often irrelevant.
3. Select the differentially expressed protein spots.
4. Search the Swiss-Prot and NCBInr databases using the Matrix Science (http://www.matrixscience.com) search engine.
5. A typical 2D map of proteins expressed in *C. elegans* grown in the presence of two different SBIs (25-azacoprostane HCl and triparanol) is shown in Fig. 12.2 (hypothetical proteins) and Fig. 12.3 (vitellogenin-2 and -6).

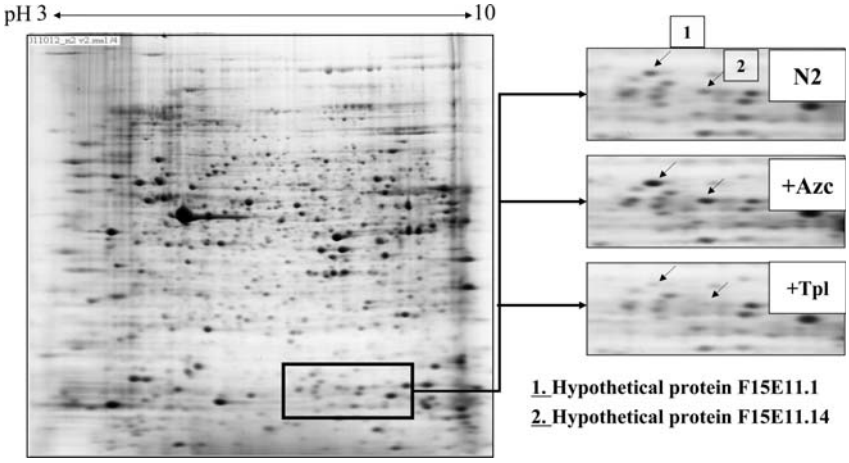

Fig. 12.2 2D gel pattern of *C. elegans* at mixed stages that are grown in the presence of three different sterol biosynthesis inhibitors. Proteins extracted from wild-type N2 *C. elegans* that were treated with or without azacoprostane and triparanol were separated on the nonlinear pH 3–10 IPG strip, followed by a 9–16% SDS-polyacrylamide gel electrophoresis. In the boxed area, two hypothetical proteins show their altered expression after treatment with azacoprostane and triparanol. Right side: 2D gel image of drug-treated worms; N2: wild-type worm; Azc: 25-azacoprostane HCl; Tpl: triparanol

12.3.5 Destaining and In-Gel Trypsin Digestion

1. Pick (or excise) the protein spot with an end-cut yellow tip and transfer the picked gel piece into a 1.5-ml Eppendorf tube.
2. Wash the gel piece with distilled water.

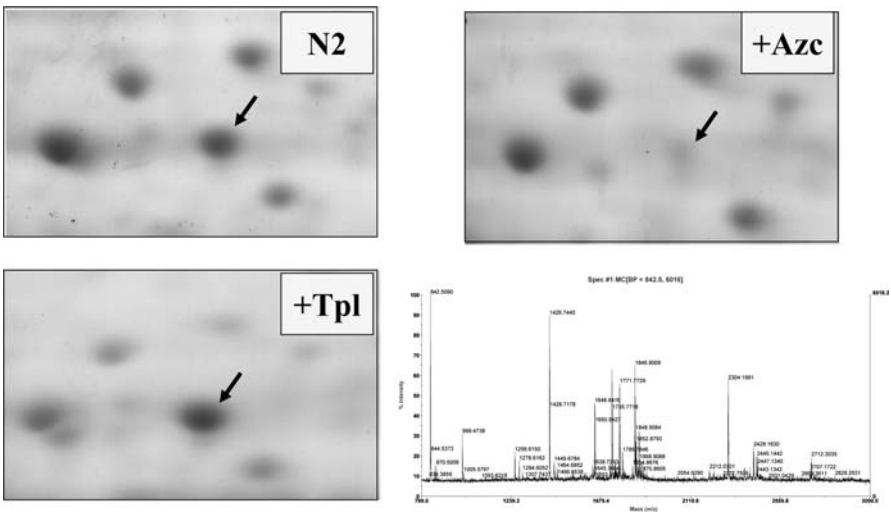

Fig. 12.3 Altered expression of the vitellogenin-6 precursor following treatment with azacoprostane and triparanol. The arrow indicates the vitellogenin-6 precursor protein on a 2D gel, and the mass spectrum shown above was obtained from the Voyager DE Pro MALDI-TOF MS. To identify the protein, the spot on the gel was excised with the end-cut pipette tip, destained, dehydrated, and digested with trypsin followed by MALDI-TOF MS (right side of the bottom panel). The digested peptide was mixed with matrix, applied to the plate, and analyzed under 20-kV accelerating voltage, 75% grid voltage, 0% guide-wire voltage, 120-ns delay, and low mass gate of 800. Aza: 25-azacoprostane HCL; Tpl: triparanol

3. Add 50 µl of 50 mM NH_4HCO_3 (pH 7.8):ACN (6:4) and shake for 10 min.
4. Repeat step 3 until the Coomassie Brilliant Blue G250 dye disappears (2–5 times).
5. Decant the supernatant and dry the gel in a SpeedVac for 10 min.
6. Add 5 µl of trypsin (12.5 µg/µl in 50 mM NH_4HCO_3) and leave the gel on ice for 45 min (*see* Note 9).
7. Add 10 µl of 50 mM NH_4HCO_3.
8. Incubate the gel at 37°C for 12–24 h.

12.3.6 Desalting of Peptides and MALDI Plating

1. Resin packing: Twist the column body (GELoader tip, Eppendorf) near the end of the tip and push the resin solution [Poros R2:Oligo R3 (1:1) in 70% ACN] with a 1-ml syringe. The packed resin length is 2–3 mm long [15, 16].
2. Equilibration of the column: Add 20 µl of a 2% formic acid solution and push the solution through the column with the 1-ml syringe.

3. Peptide binding: Add the peptide solution (approximately 10–12 μl) and push the solution through the column with the syringe.
4. Washing: Add 20 μl of a 2% formic acid solution and push the solution through the column with the syringe.
5. MALDI spotting: Add 1 μl of the matrix solution (CHCA, 10 mg/ml in 70% ACN and 2% formic acid) and directly spot the eluted peptides and matrix mixture onto the MALDI plate.
6. Reuse the column: Add 20 μl of 100% ACN and push the ACN through the column with the syringe and repeat the equilibration step (step 2).

12.3.7 MALDI-MS and Peptide Mass Fingerprinting

12.3.7.1 MALDI-TOF/TOF

1. Analyze the peptide mass fingerprinting (PMF) with a 4800 MALDI-TOF/TOF mass spectrometer (Applied Biosystems) equipped with a 355-nm Nd:YAG laser. The pressure in the TOF analyzer is approximately 7.6e-07 Torr.
2. Obtain the mass spectra in the reflection/delayed extraction mode with an accelerating voltage of 20 kV and sum the data from 500 laser pulses.
3. Calibrate the spectrum with the tryptic autodigested peaks (m/z 842.5090 and 2211.1064) and obtain the mono-isotopic peptide masses with Data Explorer 3.5 (PerSeptive Biosystems).
4. Search the Swiss-Prot and NCBInr databases using the Matrix Science (http://www.matrixscience.com) search engine.

12.3.7.2 MALDI-TOF

1. Analyze the trypsin-digested peptides (desalted from Subheading 12.3.5) using the Voyager DE Pro MALDI-TOF (Applied Biosystems).
2. The peptide mixture that was eluted from the custom-made Poros R2 column is placed on the plate with CHCA in 70% acetonitrile [15, 17].
3. TOF measurements use the following parameters: 20 kV accelerating voltage, 75% grid voltage, 0% guide-wire voltage, 120-ns delay, and low mass gate of 500. Internal calibration is also performed using autodigestion peaks of porcine trypsin [$(M + H)^+$, 842.5090 and 2211.1064].
4. The peptide mass profiles produced by MALDI-MS are analyzed using search programs, such as UCSF's MS-Fit 4.0.6 (http://prospector.ucsf.edu/), Matrix Science Ltd.'s MASCOT (http://www.matrixscience.com/cgi/search_form.pl?FORMVER=2&SEARCH=PMF), and Rockefeller University's ProFound (Version 4.10.5) (http://129.85.19.192/profound_bin/WebProFound.exe), with the NCBI database. A mass tolerance of 20 ppm is used for masses that are measured in reflector mode.

12.3.8 Competitive Reverse Transcription-Polymerase Chain Reaction

For quantitative analysis of the mRNA of the identified proteins by 2-DE, quantitative reverse transcription (RT)-polymerase chain reaction (PCR) was carried out using target template RNA plus mimic RNAs (which share the same primer annealing sites but differ in length) as previously reported [18]. In the current study, *C. elegans* genomic DNAs for both VIT-2 and the VIT-6 precursor fragment that contain introns of 52 and 91 base pairs, respectively, are used as mimics. Mimic mRNAs are added to the reaction at the RT stage in order to control for cDNA synthesis efficiency as well as for PCR. Each mimic DNA is prepared from the genomic DNA of *C. elegans* by PCR and is used for preparing cRNA by *in vitro* transcription. After the cRNAs are mixed with total RNA from each condition (with or without azacoprostane), first-strand cDNA is synthesized using the M-MLV reverse transcriptase. Then, PCR amplification with the same primer sets is performed. After PCR, the resulting PCR amplification products are visualized by ethidium bromide in a 3% agarose gel and quantified using an ImageMaster program (GE Healthcare) (Fig. 12.4).

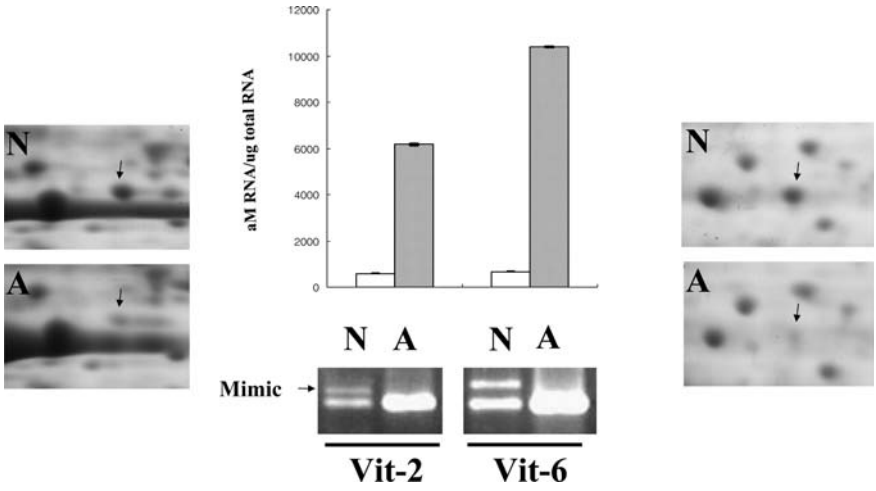

Fig. 12.4 Protein and mRNA expression of VIT-2 and VIT-6 genes following treatment of *C. elegans* with azacoprostane. VIT-2 and VIT-6 protein levels are visible on the gels on the left and right sides of the figures. Shown at the center are the mean mRNA levels that were calculated as described in Heading 2, "Methods." VIT-2 and VIT-6 mRNA levels were 591 ± 9.77 and 674 ± 27.7 amol mRNA/μg total RNA ($n = 3$) under normal (N) conditions, respectively, but were 6,171 ± 23.79 and 10,375 ± 26.25 ($n = 3$), respectively, after azacoprostane (A) treatment. The data are expressed as aM (10^{-18} M) mRNA/μg total RNA. (Reproduced from Choi et al. [2] with permission.)

12.3.8.1 Genomic DNA and Mimic Construction

1. Genomic DNA fragments that are used as mimics in quantitative RT-PCR are initially amplified from genomic DNA of *C. elegans* that is extracted from wild-type worms using a Genomic DNA Isolation Kit (Nucleogen) according to the manufacturer's instructions.
2. The PCR mixture contains the genomic DNA template and TAKARA ExTaq DNA polymerase (Takara, Japan) in the presence of a 1.5 mM Mg^{2+} buffer (pH 7.9), 100 μM dNTPs, and 0.4 μM each primer: VIT-2 (forward, 5'-GAGAAGGA-CACCGAGCTCATCC-3'; reverse, 5'-TCTCGACTTCTTGGATTTGCTC-3'), and VIT-6 precursor (forward, 5'-CTCTCTTGGGAGCGGCACTCG-3'; reverse, 5'-CTCTTGGTGCTCACGGTTCATGC-3').
3. PCR is carried out in the GeneAmp 2400 PCR thermal cycler (Perkin Elmer) using 30 cycles of 94°C for 30 s, 52°C for 45 s, and 72°C for 1 min.
4. The resulting PCR fragments are ligated into the pGEM-T Easy Vector (Promega).
5. The nucleotide sequence of each plasmid is confirmed by DNA sequencing analysis using the Big Dye Terminator sequencing method (Perkin Elmer).

12.3.8.2 cDNA Synthesis

1. Tributyl phosphine (TBP) can be used as the reducing agent of protein disulfide bond instead of DTT. However, its concentration must be empirically optimized.
2. The RNAs are treated with DNase I (Takara) and extracted with phenol/chloroform. The absence of genomic DNA is confirmed by PCR with a sample of total RNA using the primers described above.
3. The first-strand cDNA is synthesized using 1 μg of total RNA, M-MuLV reverse transcriptase (Gibco BRL), 1 mM dNTPs, 0.5 μg of random hexamers (Promega), and 20 U of RNAsin (Promega) in a 20-μl volume. The mixture is incubated at 37°C for 1 h, and the reactions were terminated by heating at 95°C for 5 min.
4. PCR is carried out as described above using 1 μl of cDNA. The nucleotide sequences of amplified fragments are confirmed by DNA sequencing analyses as described above.

12.3.8.3 cRNA Preparation

1. One microgram of the template plasmid, containing the genomic DNA mimics, is transcribed using the Riboprobe *in vitro* transcription system (Stratagene) according to the manufacturer's instructions.
2. DNA templates are removed by DNase I treatment at 37°C for 30 min. The cRNA is subsequently purified by phenol/chloroform extraction and stored at −80°C.

12.3.8.4 mRNA Expression

1. cDNA synthesis is achieved using 2 μg of total RNA from either the azacoprostane-treated or the untreated control worms, using the cRNAs of the VIT-2 and VIT-6 precursors as internal standards in the reaction. Initially, 2.04 fM VIT-2 and 2.5 fM VIT-6 precursor mimic cRNA and 0.2 μg of random hexamers (Promega) are incubated at 70°C for 5 min. This step is followed by the addition of 40 U of M-MuLV reverse transcriptase and its buffer (Gibco BRL) and 30 U of ribonuclease inhibitor (GE Healthcare).
2. Incubation is conducted at 25°C for 15 min, 37°C for 1 h, and 95°C for 5 min. At the end of the incubation, reaction products are diluted to 50 μl. PCR is performed in a 50-μl volume containing 10 μl of the diluted cDNA synthesis reaction, TAKARA ExTaq DNA polymerase, and its buffer [1.5 mM Mg^{2+} (pH 7.9)], 1 mM dNTPs, and 1 μM each primer set. The thermal cycling program is run for 23 cycles at 94°C for 30 s, 54°C for 45 s, and 72°C for 45 s (*see* Note 10). The resulting PCR amplification products are visualized by ethidium bromide in a 3% agarose gel and quantified using an ImageMaster program (GE Healthcare) (*see* Note 11) (Fig. 12.4).

Acknowledgments This study was supported by a grant from the Korean Health 21 R&D project, Ministry of Health & Welfare, Republic of Korea (A030003 to YKP), by the Technology Development Program of the Ministry of Agriculture and Forestry, Republic of Korea (606001-53-1-SB010 to YKP), and by a grant from the Basic Research Program that is supported by KOSEF (RO1-2005-000-11021-0 to YHS). We thank Dr. David Chitwood for his generous gift of 25-azacoprostane HCl for this work.

Notes

1. Tributyl phosphine (TBP) can be used for both the reduction and alkylation of disulfide bonds instead of DTT and iodoacetamide. However, its concentration must be empirically optimized.
2. Poros R2 [7] is used for desalting and concentrating the digested peptide mixture. For this procedure, 100–300 nl of Poros R2 (20–30-μm bead size; PerSeptive Biosystems) is packed in a constricted Gel Loader tip (Eppendorf) as previously described [6, 8]. Ten microliters of the peptide mixture from the digestion supernatant were diluted to 40 μl in 2% formic acid, loaded onto the Poros R2 column, and washed with 20 μl of 2% formic acid. For MALDI-TOF MS analysis, the peptides were eluted with 2 μl of matrix solution (10 mg/ml of CHCA in 70% ACN) directly onto the MALDI target in a very small droplet.
3. α-cyano-4-hydroxycinnamic acid (CHCA) is purified before use. First, CHCA is dissolved in warm ethanol until it is saturated, then two or three volumes of cold water are added, and the mixture is incubated for 24 h at −20°C The precipitate is filtered using Whatman filter paper, dried completely, and stored at −80°C until use.
4. It is very important to use ice-cold 70% sucrose; otherwise, *C. elegans* will not easily float on top of the solution.
5. It is very important to remove excessive distilled water before storing at −70°C.

6. IPG buffer nonlinear pH 3–10 must be optimized for the condition of the sample protein.
7. Because the pH gradient is fixed in the gel, the focused proteins are more stable at their isoelectric points. IPG strips can be stored at −80°C until 2D SDS-PAGE analysis.
8. In principle, proteins are denatured in a single step during the reduction and alkylation procedure. Tributylphosphine breaks protein disulfide bonds. Acrylamide reacts with the sulfhydryl groups on cysteine residues and thus prevents disulfide bonds from reforming.
9. If excessive amounts of trypsin are not removed, most of the peptide peaks will be buried in the baseline when the samples are analyzed by MALDI-TOF mass spectrometry because the intensity of the autodigested trypsin peak is relatively higher than the actual peptide peaks.
10. Competitive PCR at higher cycle numbers ($\geq$ cycle 30) can cause heteroduplex formation, which is composed of a single-stranded, internal standard cDNA and a single-stranded sample cDNA and is visible on the gel as a faint third band that migrates more slowly than the sample cDNA, and can interfere with precise quantification. The cycle number must be optimized.
11. The amount of unknown template RNA was calculated from the ratio of template:mimic band intensities as the amount of mRNA in amol/μg of total RNA.

References

1. Shim YH, Chun JH, Lee EY, Paik YK. Role of cholesterol in germ-line development of *Caenorhabditis elegans*. Mol Reprod Dev 2002;61:358–66.
2. Choi B-K, Chitwood DJ, Paik YK. Proteomic Changes during disturbance of cholesterol metabolism by azacoprostane treatment in *Caenorhabditis elegans*. Mol Cell Proteomics 2003;2:1086–95.
3. Kurzchalia TV, Ward S. Why do worms need cholesterol? Nat Cell Biol 2003;5:684–8.
4. Hieb WF, Rothstein M. Sterol requirement for reproduction of a free-living nematode. Science 1968;160:778–80.
5. Paik YK, Jeong SK, Lee EY, Jeong PY, Shim YH. *Caenorhabditis elegans*: An invaluable model organism for the proteomics studies of the cholesterol-mediated signalling pathway. Expert Rev Proteomics 2006;3:1–15.
6. Bottjer KP, Weinstein PP, Thompson MJ. Effects of an azasteroid on growth, development and reproduction of the free-living nematode *Caenorhabditis briggsae* and *Panagrellus redivivus*. Comp Biochem Physiol B 1985;82:99–106.
7. Chitwood DJ, Lusby WR. Metabolism of plant sterols by nematodes. Lipids 1991;26:619–27.
8. Bae SH, Paik YK. Cholesterol biosynthesis from lanosterol: Development of a novel assay method and characterization of rat liver microsomal lanosterol Δ^{24}-reductase. Biochem J 1997;326:609–16.
9. Merris M, Wadsworth WG, Khamrai U, Bittman R, Chitwood DJ, Lenard J. Sterol effects and sites of sterol accumulation in *Caenorhabditis elegans*: Developmental requirement for 4alpha-methyl sterols. J Lipid Res 2003;44:172–81.
10. Biomarker discovery from the plasma proteome using multidimensional fractionation proteomics. Curr Opin Chem Biol 2006;10:42–9.
11. Brenner S. The genetics of *Caenorhabditis elegans*. Genetics 1974;77:71–94.
12. Bradford MM. A rapid and sensitive method for the quantitation of microgram quantities of protein utilizing the principle of protein-dye binding. Anal Biochem 1976;72:248–54.
13. Svoboda JA, Thompson MJ, Robbins WE. Azasteroids: Potent inhibitors of insect molting and metamorphosis. Lipids 1972;7:553–6.
14. Chitwood DJ, Lusby WR, Lozano R, Thompson MJ, Svoboda JA. Sterol metabolism in the nematode *Caenorhabditis elegans*. Lipids 1984;19:500–6.

15. Choi B-K, Cho Y-M, Bae S-H, Zoubaulis CC, Paik Y-K. Single-step perfusion chromatography with a throughput potential for enhanced peptide detection by matrix-assisted laser desorption/ionization-mass spectrometry. Proteomics 2003;3:1955–61.
16. Gobom J, Nordhoff E, Mirgorodskaya E, Ekman R, Roepstorff P. Sample purification and preparation technique based on nano-scale reversed-phase columns for the sensitive analysis of complex peptide mixtures by matrix-assisted laser desorption/ionization mass spectrometry. J Mass Spectrom 1999;34:105–16.
17. Larsen MR, Sørensen GL, Fey SJ, Larsen PM, Roepstorff P. Phospho-proteomics: Evaluation of the use of enzymatic de-phosphorylation and differential mass spectrometric peptide mass mapping for site specific phosphorylation assignment in proteins separated by gel electrophoresis. Proteomics 2001;1:223–38.
18. Zimmermann K, Mannhalter JW. Technical aspects of quantitative competitive PCR. BioTechniques 1996;21:268–72, 274–79.

Chapter 13
Studying the Subcellular Localization and DNA-Binding Activity of FoxO Transcription Factors, Downstream Effectors of PI3K/Akt

Abdelkader Essafi, Ana R. Gomes, Karen M. Pomeranz, Aleksandra K. Zwolinska, Rana Varshochi, Ursula B. McGovern and Eric W.-F. Lam

Abstract This chapter describes methods for studying downstream events of the PI3 K/Akt signaling cascade, focusing on the FoxO transcription factors. These approaches also represent alternative means for gauging the phosphoinositide-3 kinase/Akt activity. We describe protocols for the fractionation of cytoplasmic and nuclear protein extracts and for studying transcription factor DNA-binding activity *in vitro* and *in vivo*.

Keywords FoxO · PI3 kinase · Akt · transcription factor

13.1 Introduction

The phosphoinositide-3 kinase (PI3 K)-PKB/Akt signal transduction pathway regulates vital cellular functions and responses, such as proliferation, differentiation, DNA repair, defense against oxidative stress damage, and apoptosis, in response to hormones, growth factors, and other environmental cues [1–3]. Hyperactivation of this pathway contributes to tumor formation, tumor metastasis, and resistance to standard cancer therapy [1, 4–6]. Transcription factors integrate cellular signals with the transcription machinery to regulate gene expression. The mammalian FoxO (forkhead box O subclass) family of transcription factors, FoxO1, FoxO3a, FoxO4, and FoxO6, are critical downstream effectors of the protein kinases Akt(PKB) and SGK (serum and glucocorticoid inducible kinase), which relay PI3 K signals to target genes [7,8]. These FoxO proteins function as transcriptional factors that interact with the core consensus

E.W.-F. Lam
Cancer Research UK Laboratories, Department of Oncology, MRC Cyclotron Building, Imperial College London, Hammersmith Hospital, Du Cane Road, London, W12 ONN, UK
e-mail: eric.lam@imperial.ac.uk

B. Larijani et al. (eds.), *Lipid Signaling Protocols*, DOI: 10.1007/978-1-60327-115-8_13,

genomic DNA sequence GTAAA(C/T)A to modulate target gene expression in the nucleus [7]. In the presence of growth or survival factors, activated PKB/Akt phosphorylates FoxO proteins at the three conserved residues in the nucleus and creates docking sites for the 14-3-3 proteins [9, 10]. Phosphorylated FoxOs bind to the 14-3-3 proteins and relocalize to the cytoplasm, strongly suggesting that the 14-3-3 proteins play an important role in the export of FoxO transcription factors [9–11]. PKB/Akt phosphorylation also reduces the DNA-binding ability of FoxO and enhances its degradation [8]. In the absence of mitogenic/survival signals, FoxO proteins are dephosphorylated at the Akt phosphorylation sites, bind to responsive elements, and activate target genes that are important for cell cycle arrest and apoptosis [3,12]. In this chapter, we describe an indirect functional approach to investigate PI3 K/Akt activity by studying FoxO protein expression and shuttling between nuclear and cytoplasmic compartments. We also investigate the binding of the FoxO transcription factors to promoter responsive elements in response to PI3 K signaling *in vitro* by oligonucleotide pulldown as well as *in vivo* using chromatin immunoprecipitation.

13.2 Materials

13.2.1 Cell Culture, Chemicals, Buffers, and Equipment

1. Cell lines: human breast carcinoma cell line MCF-7 and human B-lymphoid CML cell line BV173 (originally from ATCC).
2. Dulbecco's Modified Eagle's Medium (DMEM) (Sigma, Dorset, UK) supplemented with 10% fetal bovine serum (FBS) (Invitrogen, Paisley, UK) for MCF-7 cells and RPMI-1640 (Sigma, Dorset, UK) with 10% FBS for BV173 cells.
3. Phosphate buffered saline (PBS): 13.7 M NaCl, 2.7 mM KCl, 10 mM Na_2HPO_4, 1.8 mM KH_2PO_4 (adjust to pH 7.4 with HCl). Store at room temperature after autoclaving.
4. Solution of 0.25% (w/v) trypsin and 1 mM ethylenediamine tetraacetic acid (EDTA) in PBS (Sigma, Dorset, UK).
5. Stock 10 mM PI3-kinase inhibitor LY294002 (Cat. no. 440204; Calbiochem, Nottingham, UK) solution in DMSO (Calbiochem). Store in aliquots at −20°C.
6. Solutions need to be prepared freshly by dilution in PBS to a working concentration of 1 mM.
7. Stock 100 μM Paclitaxel (Sigma, Poole, UK) solution in ethanol is stored in aliquots at −20°C. Working solutions need to be prepared freshly by dilution in PBS to a working concentration of 1 μM.

8. SDS-PAGE (sodium dodecyl sulfate-polyacrylamide gel electrophoresis) equipment.
9. 0.5 M PMSF (phenylmethylsulfonyl fluoride) stock in ethanol stored at −20°C.
10. Anti-Phospho-FKHRL1/FoxO3a (Thr32) (Cat. no. 07-695) and total anti-FKHRL1 antibodies (Cat. no. 06-951) (Upstate, Dundee, UK).

13.2.2 Buffer Preparation

To avoid protein degradation during the process, the following buffers and all the described steps should be performed on ice.

13.2.2.1 Buffers to Be Used in Nuclear and Cytosolic Protein Extraction

1. Pre-buffer: 20 mM HEPES, 20 mM KCl, 0.2 mM EDTA, 0.2 mM EGTA, 1.6 mM KOH, Protease Inhibitor Tablets (Roche Complete^{TM}protease cocktail): 1 tablet/10 ml buffer (*see* Note 2).
2. Buffer A (cytosolic buffer): 10 mM HEPES, 10 mM KCl, 0.1 mM EDTA, 0.1 mM EGTA, 2 mM DTT, Protease Inhibitor Tablets (Roche Complete^{TM} protease cocktail): 1 tablet/10 ml buffer.
3. Buffer B (nuclear buffer): 10 mM HEPES, 10 mM KCl, 0.1 mM EDTA, 0.1 mM EGTA, 2 mM dithiothreitol (DTT), 400 mM NaCl, 1% NP-40, Protease Inhibitor Tablets (Roche Complete^{TM} protease cocktail): 1 tablet/10 ml buffer.

13.2.2.2 Buffers to Be Used in Biotinylated Oligonucleotide Pulldown Assay

1. Sample buffer 1 (for 1D analysis): 0.1 M Tris-HCL, pH 6.8, 0.2 M DTT, 4% (w/v) SDS, 20% (v/v) glycerol, 0.1% (w/v) bromophenol blue.
2. Sample buffer 2 (for 2D analysis): 7 M urea, 2 M thiourea, 0.4% CHAPS.

13.2.2.3 Buffers to Be Used in Chromatin Immunoprecipitation (ChIP)

1. TE (Tris-EDTA) buffer: 100 mM Tris-HCl (pH 8.0), 10 mM EDTA (pH 8.0).
2. Sonication buffer: 1% (w/v) SDS, 10 mM EDTA, 50 mM Tris-HCl (pH 8.1), 1 mM phenylmethyl sulfonyl fluoride, 1 × Roche Complete^{TM}protease inhibitor cocktail.
3. TSE I buffer (low-salt immune complex wash buffer): 0.1% (w/v) SDS, 1% (v/v) Triton X-100, 2 mM EDTA, 20 mM Tris-HCl, pH 8.1, 150 mM NaCl.
4. TSE II buffer (high-salt immune complex wash buffer): 0.1% (w/v) SDS, 1% (v/v) Triton X-100, 2 mM EDTA, 20 mM Tris-HCl, pH 8.1, 500 mM NaCl.
5. TSE III buffer: 25 mM NaCl, 1% (v/v) NP40, 1% (w/v) deoxycholate, 1 mM EDTA, 10 mM Tris-HCl, pH 8.1.

6. DNA extraction solution: 0.1 M $NaHCO_3$, 1% (w/v) SDS.
7. Salmon sperm DNA: 10 μg/μl stock plus BSA.

13.3 Methods

13.3.1 Nuclear and Cytosolic Protein Fractionation

13.3.1.1 Cell Preparation

1. Adherent cells are collected from 70% confluent flask by scraping/trypsinization and centrifugation.
2. The cells are washed once with ice-cold PBS and then pelleted by centrifugation for 5 min at 300 × *g*. Cells are then resuspended in 1 ml of ice-cold PBS and transferred to an Eppendorf tube. Another centrifugation is performed at 300 × *g* for 3–5 min in order to pellet the cells.

13.3.1.2 Cytosolic Protein Extraction

1. After thawing the prepared buffers on ice, 50–150 μl of buffer A are added to the cell pellet, which is then vortexed and incubated for 5–20 min on ice.
2. In order to lyse the cells, NP40 is added to a final concentration of 1% (v/v) and mixed for 10 s.
3. Centrifuge at 13,000 × *g* for 5 min at 4°C to separate the supernatant containing the cytosolic protein extract from the pellet consisting of the nuclear extract.
4. This protein fraction (cytosolic extract) can be snap-frozen and stored at −70°C.

13.3.1.3 Nuclear Protein Extraction

1. The resulting pellet is washed in 1,000 μl of buffer A, followed by spinning at 13,000 × *g* for 5 min, and the supernatant is then discarded.
2. The pellet containing the nuclear material is resuspended in 30–50 μl of buffer B, vortexed for 10 s, and incubated with rotation in the cold room, for 15 min.
3. After incubation, the samples are centrifuged at 13,000 × *g* for 5 min at 4°. The supernatant containing the nuclear protein extract is collected, while the pellet is discarded.
4. As described for the cytosolic protein extract, this protein fraction can be snap-frozen and stored at −70°C.
5. For nuclear/cytosolic protein fractionation analysis, 20–100 μg of nuclear/cytosolic protein are analyzed by SDS-PAGE and proteins investigated by Western blot analysis (Fig. 13.1).

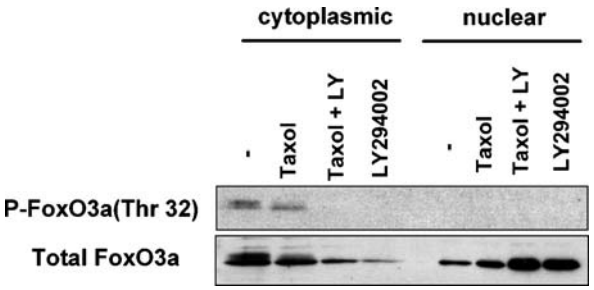

Fig. 13.1 Nuclear and cytoplasmic fractionation experiments were performed to analyze the relative amounts of FoxO3a in the nucleus and cytoplasm, following treatment of MCF-7 cells with 10 nM taxol or 25 μM LY294002 alone or in combination. Paclitaxel (taxol) has been shown to mediate the nuclear translocation of FoxO3a through inhibiting Akt activity. Western blot analysis results showed that the majority of FoxO3a in the control cycling MCF-7 cells was located in the cytoplasm and that following treatment with taxol LY294002, or their combination, FoxO3a was predominantly located in the nucleus. Consistent with this, the results also showed that the Akt-phosphorylated forms of FoxO3a, which are found only in the cytosolic fraction, were downregulated with taxol treatment and abolished by LY294002. These results together suggested that inhibition of the PI3 K/Akt activity by LY294002 or taxol results in a decrease of FoxO3a expression in the cytoplasm and an increase in FoxO3a in the nucleus, most likely the consequence of a translocation of FoxO3a into the nucleus

13.3.2 Transcription Factor-DNA Affinity Precipitation (Oligonucleotide Pulldown Assay)

This approach can be used for studying and identifying protein complexes binding to a particular response element on transcriptional promoters, silencers, and enhancers. This method has an advantage over mobility-shift (band-shift) and antibody super-shift analysis, as it can be used for studying large protein complexes, which will not enter the 4–5% PAGE gel often employed for mobility-shift and super-shift with antibodies. This protocol can also be scaled up in a column for enriching protein complexes.

13.3.2.1 Annealing Primers

1. Biotinylated and non-biotinylated primers (Invitrogen, UK) are diluted in TE to a final stock concentration of 1 mM.
2. A 0.2 mM solution of double-stranded oligonucleotides is reconstituted in 500 mM NaCl, 20 mM Tris-HCl (pH 7.5), 5 mM EDTA (pH 8).
3. Primers are heated to 100°C for 5 min and left to cool gradually to room temperature to facilitate annealing (*see* Note 3).

13.3.2.2 Biotinylated Oligonucleotide Pulldown Assay

1. Biotinylated double-strained oligonuceotides are coupled to strepavidin-agarose beads (Sigma UK) in a 100-μl PBS solution containing 10% (v/v)

fetal calf serum (FCS), 20 µl of a 50% (v/v) slurry of strepavidin-agarose beads (Sigma), and 1 µl of 0.2 mM annealed biotinylated oligonucleotide.
2. Beads are left to incubate with the oligonuceotides while rotating on a rotary wheel for 2 h at room temperature.
3. Following incubation, the oligonucleotide-coupled beads are spun down at 13,000 × *g* in a bench-top microfuge for 2 min and the supernatant discarded.
4. Twenty to 100 µg of nuclear lysate (prepared as described in Subheading 13.3.1.3; *see* also Note 4 for preparation of the nuclear lysate) are then added to the biotinylated oligo-coupled beads along with 1 µg of sheared salmon sperm DNA (Sigma, UK) and competitor non-biotinylated double-stranded oligonucleotides containing a wild-type or mutant consensus site for prospective binding proteins (*see* Note 4).
5. Samples are left mixing on a rotary wheel at 4°C for 1 h and subsequently incubated for 10 min at 30°C in a water bath. The beads are then washed 5–6 times in PBS containing protease inhibitors (Roche Complete^{TM} cocktail).
6. The proteins are eluted from the beads by the addition of 2 × gel sample buffer (sample buffer 1) for one-dimensional analysis by SDS-PAGE. For analysis by 2D-electrophoresis, however, proteins are eluted from the beads using sample buffer for analysis by 2D-electrophoresis (sample buffer 2). Separated proteins are then transferred onto PVDF or nitrocellulose membranes and analyzed by Western blotting using specific antibodies (Fig. 13.2).

13.3.3 Chromatin Immunoprecipitation (ChIP)

Chromatin immunoprecipitation allows the investigation of the *in vivo* occupancy of a particular gene promoter region by transcription factors [8, 12–14]. This procedure is characterized by a multistep procedure as follows:

1. DNA-binding proteins are cross-linked to DNA with formaldehyde *in vivo*.
2. The chromatin is isolated, followed by sonication to shear DNA along with bound proteins into small fragments.
3. Antibodies specific to the prospective DNA-binding protein(s) are added to isolate the complex by precipitation. The precipitated proteins are denaturated to free bound DNA fragments.
4. DNA fragments that are isolated after immunoprecipitation are amplified by PCR using specific primers spanning the target binding site.

13.3.3.1 Stimulation of Cells

Stimulate cells (approximately 1×10^7 cells) on a 10-cm dish as appropriate. An extra dish can be used for estimation of the cell number required.

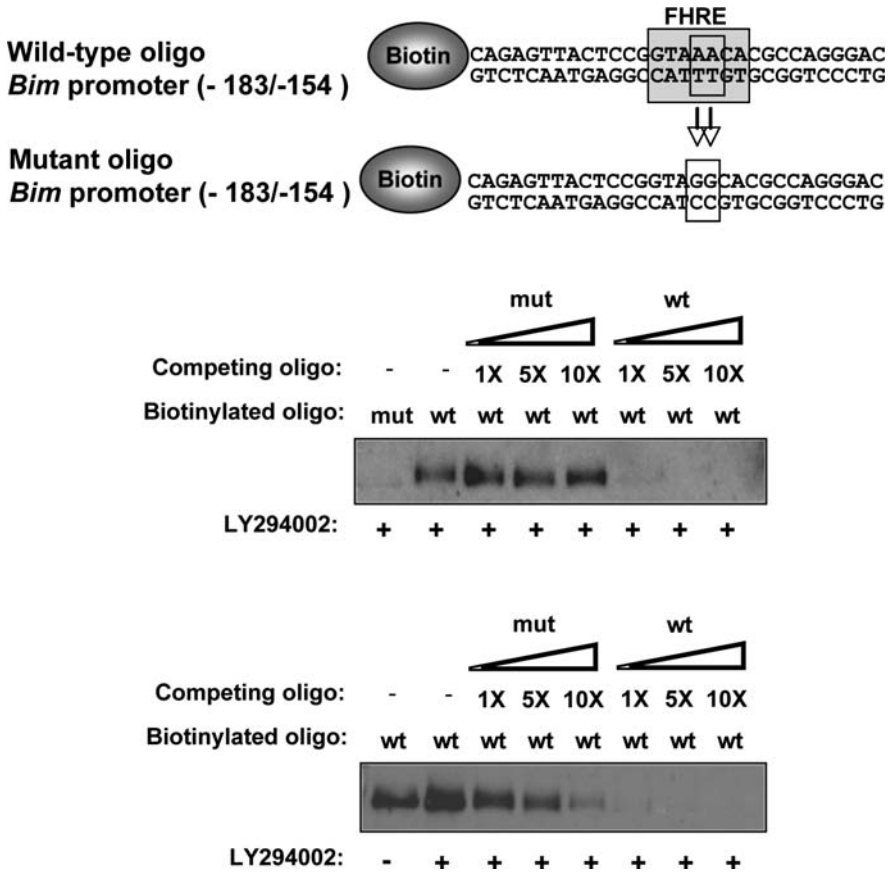

Fig. 13.2 Pulldown experiment was performed to study the binding of FoxO3a to the FHRE of the human *Bim* promoter. Nuclear extracts were prepared from MCF-7 cells using the high-salt buffer as described. After diluting with 2 volumes of the low-salt lysis buffer, 50 μg of the cell extracts were incubated at 30°C for 10 min with either 0.5 nmol of the 5'-biotinylated double-stranded wild-type (5'-CAGAGTTACTCCGGTAAACACGCCAGGGAC-3') or mutant (5'- CAGAGTTACTCCGGTA*GG*CACGCCAGGGAC-3') oligonucleotides previously coupled to streptavidin agarose beads. The wild-type oligonucleotide corresponded to the region of –139 to –145 of the human *Bim* promoter. After incubation, the biotinylated oligonucleotide-coupled streptavidin beads were washed at least six times with the low-salt buffer containing 150 mM NaCl and denatured in SDS-sample buffer before running on an SDS-acrylamide gel. The separated proteins were then Western blotted for FoxO3a using specific antibodies. For competition experiments, the extracts were incubated with the wild-type oligonucleotide-coupled beads in the presence of 1x, 5x, or 10x molar excess of either the wild-type or mutant non-biotinylated oligonucleotide. The result showed that FoxO3a bound to the wild-type FHRE oligonucleotide but not a similar mutant oligonucleotide with the FHRE mutated. The result also showed that LY294002 treatment increased the binding of FoxO3a to the FHRE. This interaction depends on the FHRE, as the FoxO3a binding could be compared against using increasing amounts of an oligonucleotide containing the FoxO site, but not a similar oligonucleotide with the FHRE mutated

13.3.3.2 Chromatin Cross-Linking

1. Add formaldehyde directly to culture medium to a final concentration of 1% (w/v) and incubate for 10 min at 37°C, followed by the addition of glycine to 0.136 M and incubation for a further 10 min.
2. Suspension cells: Cells are collected by centrifugation and washed with PBS. The cells are then suspended in 10 ml of PBS, 1% (w/v) of formaldehyde is added, and the mix is incubated at 37°C for 10 min. To reverse the cross-linking, 0.136 M of glycine is added and incubated for an extra 10 min. The cells are then washed and pelleted by centrifugation.
3. Aspirate medium and wash with cold PBS. Scrape the cells into a conical tube and centrifuge the cells for 4 min at 300 × *g* at 4°C.

13.3.3.3 Sonication

1. Resuspend the cell pellet in the appropriate volume (approximately 300 µl) of sonication buffer and incubate for 10 min on ice. Sonicate the cell lysate in four 10-s pulses at maximum power. The number of sonications can be experimentally established for each cell line.
2. Centrifuge samples for 10 min at 13,000 × *g* at 4°C to remove the debris and then dilute the supernatant five times with sonication buffer (to total volume of 1.5 ml), of which 1/10 is retained as input control.

13.3.3.4 Immunoprecipitation

1. DNA shearing is controlled by running a fraction of the sonicated chromatin on a 2% (w/v) agarose gel to ensure that the fragmented DNA is of size 200 to 500 bp.
2. To prevent nonspecific binding, the chromatin solution is precleared through incubation with 2 µg of sonicated single-stranded herring sperm DNA (Sigma) and 45 µl of 50% (v/v) slurry of protein G-Sepharose (Pharmacia) beads for 30 min at room temperature.
3. The beads are then removed by brief centrifugation, and the supernatant fraction is collected. This fraction is divided between the prospective antibody and the nonspecific IgG antibody.
4. Add the immunoprecipitating antibody (in appropriate amount) to the retrieved supernantant and incubate for 2 h at room temperature (or overnight at 4°C), with rotation and in the presence of 2 µg of sonicated single-stranded herring sperm DNA (Sigma) and 45 µl of a 50% (vol/vol) slurry of protein G-Sepharose (Pharmacia) beads.
5. For a negative control, use a nonspecific antibody for immunoprecipitation. Pellet the beads by gentle centrifugation (700 to 1,000 × *g* at 4°C, ~1 min).
6. Carefully remove the supernatant that contains the unbound, nonspecific DNA.

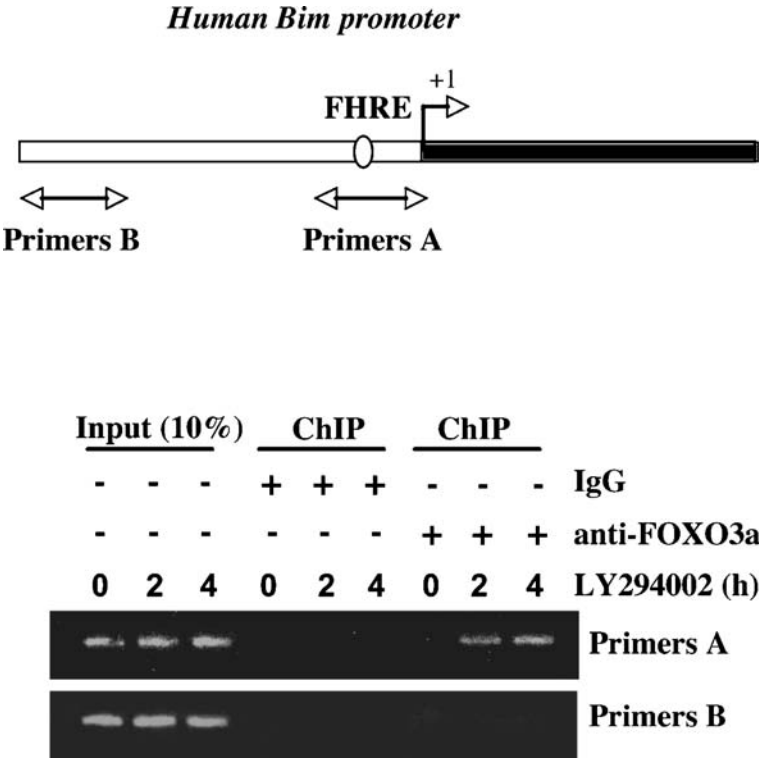

Fig. 13.3 Chromatin immunoprecipitation (ChIP) was used to study the binding of FoxO3a to its target gene *Bim* following LY294002 treatment. BV173 cells were treated with 25 μM LY294002 for 0, 2, and 4 h. Protein-DNA complexes were formaldehyde cross-linked, and chromatin was immunoprecipitated with either a FoxO3a-specific or an isotype-IgG control antibody. PCR primer pairs were designed to selectively detect the Forkhead Response Element (FHRE) in the human *Bim* gene promoter (A primers). PCRs were then performed on the purified DNA purified using the Qiagen PCR Purification Kit according to the manufacturer's protocol. PCRs were then performed on the purified DNA, prepared according to the Qiagen *Taq* PCR Handbook, in the presence of 2.5 mM $MgCl_2$, at 55°C, for 28 cycles, using the following primers: primer A forward (−421/−401)(5'-TCGCGAGGAC-CAACCCAGTC-3'), primer A reverse (+12/−8)(5'- CCGCTCCTACGCCCAATCAC-3'), primer B forward (+885/+908)(5'-GTACGCTTGAGAAAGCGAACGCAG-3'), primer B reverse (+681/+658)(5'-AGCTGAGGACCTGCTCGTAGTATC-3'). Analysis of the PCR products was performed on a standard 2% (w/v) agarose gel, by electrophoresis in Tris-acetate EDTA buffer. LY294002 treatment caused an increase in FoxO3a binding to the promoter region containing the FHRE. To ensure proper DNA shearing, we used primers detecting unrelated regions of the *Bim* promoter (B primers, about 500 bp upstream of the FHRE). PCR analysis with control primers B showed no specific chromatin precipitation with either the anti-FoxO3a or the control antibodies. These experiments therefore demonstrate that PI3 K activity has an important role in regulating binding of active FoxO3a complexes to the FHRE of the *Bim* promoter. The ChIP analysis results revealed association of FoxO3a with the *Bim* promoter upon LY294002 treatment, while no binding was detected in the untreated condition

7. Wash the precipitate for 3–5 min on a rotating platform with each of the following buffers, in the order given: PBS, sonication buffer, TSE I (low-salt buffer), TSE II (high-salt buffer), TSE III, and PBS. Note that the washing conditions may differ slightly depending upon the antibody's affinity for the antigen.

13.3.3.5 DNA Extraction and PCR

1. After the sequential washings, extract the immunoprecipitated chromatin (or the input control) by adding 300 µl of freshly prepared extraction solution and incubate at 65°C for 6 h (or overnight) to reverse the protein/histone-DNA cross-links.
2. Purify the sample using a QIAGEN PCR Purification Kit according to the manufacturer's protocol. The samples can be stored at −20°C if necessary.
3. Purified DNA is amplified by PCR according to the QIAGEN Taq PCR handbook, in the presence of 2.5 mM MgCl at about 55°C for 28 cycles, using specially designed primer sets (Fig. 13.3).

Notes

1. After preparing the described buffers A and B, they can be frozen (kept) at −20°C in 5-ml and 3-ml aliquots, respectively.
2. Roche Complete^{TM} protease cocktail tablets of *Complete Protease Inhibitors Cocktail Tablets* are used in the preparation of all buffers. According to the manufacturer, each tablet contains a combination of the following protease inhibitors: Aprotinin, Bestatin, Calpain Inhibitor I, Calpain Inhibitor II, Chymostatin, E-64, Leupeptin, α2-Macroglobulin, Pefabloc SC, Pepstatin, PMSF, TLCK-HCL, Trypsin Inhibitor (chicken), and Trypsin (soybean).
3. Heated primers are left to cool gradually in the heating block to room temperature to facilitate annealing.
4. The nuclear lysates have to be diluted with at least 2x volume of low-salt buffer to less than 150 mM NaCl before being used for oligonucleotide pulldown.

References

1. Fresno Vara JA, Casado E, de Castro J, Cejas P, Belda-Iniesta C, Gonzalez-Baron M. PI3 K/Akt signalling pathway and cancer. Cancer Treat Rev 2004;30:193–204.
2. Fruman DA, Meyers RE, Cantley LC. Phosphoinositide kinases. Ann Rev Biochem 1998;67:481–507.
3. Song G, Ouyang G, Bao S. The activation of Akt/PKB signaling pathway and cell survival. J Cell Mol Med 2005;9:59–71.
4. Campbell RA, Bhat-Nakshatri P, Patel NM, Constantinidou D, Ali S, Nakshatri H. Phosphatidylinositol 3-kinase/AKT-mediated activation of estrogen receptor alpha: A new model for anti-estrogen resistance. J Biol Chem 2001;276:9817–24.
5. Nicholson KM, Anderson NG. The protein kinase B/Akt signalling pathway in human malignancy. Cell Signal 2002;14:381–95.

6. Osaki M, Oshimura M, Ito H. PI3 K-Akt pathway: Its functions and alterations in human cancer. Apoptosis 2004;9:667–76.
7. Greer EL, Brunet A. FOXO transcription factors at the interface between longevity and tumor suppression. Oncogene 2005;24:7410–25.
8. Sunters A, Madureira PA, Pomeranz KM, Aubert M, Brosens JJ, Cook SJ, Burgering BM, Coombes RC, Lam EW. Paclitaxel-induced nuclear translocation of FOXO3a in breast cancer cells is mediated by c-Jun NH2-terminal kinase and Akt. Cancer Res 2006;66:212–20.
9. Obsilova V, Vecer J, Herman P, Pabianova A, Sulc M, Teisinger J, Boura E, Obsil T. 14-3-3 Protein interacts with nuclear localization sequence of forkhead transcription factor FoxO4. Biochemistry 2005;44:11608–17.
10. Vogt PK, Jiang H, Aoki M. Triple layer control: Phosphorylation, acetylation and ubiquitination of FOXO proteins. Cell Cycle 2005;4:908–13.
11. Hermeking H, Benzinger A. 14-3-3 proteins in cell cycle regulation. Semin Cancer Biol 2006;16:183–92.
12. Sunters A, Fernandez de Mattos S, Stahl M, Brosens JJ, Zoumpoulidou G, Saunders CA, Coffer PJ, Medema RH, Coombes RC, Lam EW. FoxO3a transcriptional regulation of Bim controls apoptosis in paclitaxel-treated breast cancer cell lines. J Biol Chem 2003;278:49795–805.
13. Essafi A, Fernandez de Mattos S, Hassen YA, Soeiro I, Mufti GJ, Thomas NS, Medema RH, Lam EW. Direct transcriptional regulation of Bim by FoxO3a mediates STI571-induced apoptosis in Bcr-Abl-expressing cells. Oncogene 2005;24:2317–29.
14. O'Neill LP, Turner BM. Immunoprecipitation of native chromatin: NChIP. Methods 2003;31:76–82.

Chapter 14
Measurement of PTEN Activity *in vivo* by Imaging Phosphorylated Akt

Erika Rosivatz and Rudiger Woscholski

Abstract This chapter describes an indirect approach to measure PTEN's lipid phosphatase activity *in vivo*. PTEN counteracts phosphatidylinositol 3-kinase action in dephosphorylating 3-phosphorylated phosphoinositides. Therefore, PtdIns(3,4,5)P_3-dependent activation and phosphorylation of the survival kinase Akt can be used as readout for cellular PTEN activity. Here we have outlined a detailed procedure employing a phosphoserine-specific anti-Akt antibody to examine the content of phosphorylated Akt by immunofluorescence and its dependence on PTEN activity.

Keywords PTEN lipid phosphatase activity · immunofluorescence · phospho-specific antibody · pS473 Akt detection · Akt localization

Abbreviation BSA: bovine serum albumin; PtdIns(3,4,5)P_3: phosphatidylinositol 3,4,5-trisphosphate; PtdIns(3,4)P_2: phosphatidylinositol 3,4-bisphosphate; PTEN: phosphatase and tensin homologue

14.1 Introduction

Tensin homologue deleted on chromosome 10 (PTEN) is a major tumor suppressor protein that dephosphorylates membrane phosphatidylinositol lipids such as PtdIns(3)*P*, PtdIns(3,4)P_2, and PtdIns(3,4,5)P_3, thus counteracting the action of PI3-kinases and its downstream targets [1, 2]. In dephosphorylating intracellular PtdIns(3,4,5)P_3, PTEN prevents the activation of the survival signaling kinase Akt, which can be monitored by detecting phosphorylation at two sites (T308 and S473) with commercially available antibodies [3]. This modification of Akt is a specific readout for PTEN lipid phosphatase activity, because Akt

E. Rosivatz
Division of Cell and Molecular Biology, Imperial College London, Exhibition Road, London, SW7 2AZ, UK
e-mail: e.rosivatz@imperial.ac.uk

B. Larijani et al. (eds.), *Lipid Signaling Protocols*, DOI: 10.1007/978-1-60327-115-8_14,

translocation to the plasma membrane and its phosphorylation have been shown to be strictly dependent on PtdIns(3,4,5)P_3 levels [4, 5].

The chapter describes how to specifically detect a phosphorylated site within the carboxy terminus (S473) of Akt in fixed cells with a commercially available monoclonal antibody. We outline the procedure for labeling the antibody with a fluorophore and its application on fixed cells for fluorescence microscopy. Our results show that it detects the phosphorylated form of Akt only, as the signal is abolished in starved cells and upon PI3 kinase inhibition, whereas it is enhanced upon PTEN inhibition. Furthermore, peptide competition studies underline its specificity and total Akt signals (phosphorylated and nonphosphorylated forms of Akt) merge with the phospho signals. The results obtained are consistent with Western blotting and additionally provide spatial information. The method described represents a useful tool in order to assess PTEN activity *in vivo*.

14.2 Materials

14.2.1 Cell Culture and Preparation of Coverslips

1. Cell lines: NIH 3T3 mouse fibroblasts.
2. Dulbecco's Modified Eagle's Medium (DMEM) (Sigma, Dorset, UK) supplemented with 10% fetal bovine serum (FBS, Invitrogen).
3. Microscope coverslips (Ø 13 mm) were heated in 1 M HCl for 4 h at 55°C, rinsed in water three times, rinsed once in 100% ethanol p.a., separately dried on filter paper, and baked in a glass jar covered with foil (*see* Note 1).
4. Phosphate buffered saline (PBS) (10X stock): 1.37 M NaCl, 27 mM KCl, 100 mM Na_2HPO_4, 18 mM KH_2PO_4 (adjust to pH 7.4 with HCl if necessary). Prepare working solution by dilution of one part with nine parts water and autoclave before storage at room temperature.
5. Solution of trypsin (0.25%) and ethylenediamine tetraacetic acid (EDTA) (1 mM).
6. Insulin (bovine; Sigma, Dorset, UK) is dissolved at 1 mg/ml in 0.02 M HCl, filter-sterilized, and stored in single-use aliquots at −20°C. Working solutions are prepared by dilution in PBS to a concentration of 100 μg/ml.
7. PI3-kinase inhibitor LY 294002 solution in DMSO (10 mM) (Calbiochem, Nottingham, UK). Working solutions need to be prepared freshly by dilution in water to a concentration of 1 mM.
8. PTEN inhibitor RV001: Dipotassium bisperoxo(picolinato)oxovanadate (V) (Calbiochem, Nottingham, UK) stock solution is prepared in water at a concentration of 2 mM. Working solutions are prepared by dilution in water to a final concentration of 20 μM, which can be stored in aliquots at −20°C.

14.2.2 Immunofluorescence for Phosphorylated (S473) and Total Akt

1. Phosphate buffered saline (PBS): Prepare as described in Subheading 14.2.1.
2. Fixative: paraformaldehyde (Sigma, Dorset, UK). Prepare a 4% (w/v) solution in PBS fresh for each experiment (*see* Note 2).
3. Quench solution: 50 mM NH4Cl in PBS.
4. Permeabilization solution: 0.1% (v/v) Triton X-100 in PBS.
5. Blocking buffer: 3% (w/v) fatty acid-free BSA (Sigma, Dorset, UK) in PBS (*see* Note 3).
6. Zenon Mouse IgG Labeling Kit (Molecular Probes) Alexa Fluor 488 Mouse IgG2b (Molecular Probes, Eugene, OR) (*see* Note 4).
7. Mouse monoclonal anti-Phospho-Akt (Ser473) antibody from the IgG2b isotype (Cat. no. 587F11, Cell Signaling, Danvers, MA) (*see* Note 5).
8. Optional: phospho-peptide (1 mg/ml) corresponding to the S473 phosphorylated carboxy terminal region of Akt.
9. Zenon Rabbit IgG Labeling Kit Alexa Fluor 594 (Molecular Probes, Eugene, OR) (*see* Note 4).
10. Rabbit anti-Akt antibody (Cat. no. 9272, Cell Signaling, Danvers, MA).
11. Nuclear stain: 300 nM DAPI (4,6-diamidino-2-phenylindole) in water.
12. Mounting medium: Antifade (Molecular Probes, Eugene, OR).

14.2.3 Microscopy and Software

1. Nikon TE 2000 fluorescence microscope equipped with a 100x Fluor oil lens and band-pass filters for DAPI, FITC, and TRITC with excitation wavelengths of 340–380, 465–495, and 540–580 nm, respectively, and with emission wavelengths of 435–485, 515–555, and 572–605 nm, respectively.
2. Digital acquisition: CCD camera (Hamamatsu, Hertfordshire, UK).
3. Software: ImageJ (National Institutes of Health, Bethesda, MD) (*see* Note 6).

14.3 Methods

The antibody to the active, phosphorylated form of Akt is sufficiently sensitive to allow detection on the plasma membrane after growth factor stimulation. Treatment with 1 μg/ml of insulin for 2 minutes provides a positive control for the activation of Akt in many cell types [6–10]. However, after prolonged treatment with insulin, Akt translocates to the nucleus and may not be detectable on the membrane [11]. Therefore, it is important to terminate the samples rapidly after stimulation to obtain reproducible results.

One sample that has been preincubated with a PI3-kinase inhibitor (either LY 294002 or Wortmannin) before insulin stimulation should be included as a negative control in order to determine the background (autofluorescence) of cells.

In order to modulate PTEN activity and test its influence in the cell system of interest, we chose to use a small-molecule PTEN inhibitor [12]. When using Akt phosphorylation as a readout for PTEN activity, basal stimulation of PI3-kinase is required, because its product, PtdIns(3,4,5)P_3, is one of PTEN's substrates, on which Akt phosphorylation strictly depends [13]. Therefore, after the cells have been preincubated with the PTEN inhibitor, we stimulated with very low amounts of insulin, which would not activate Akt on their own, but result in a strong signal under these conditions.

14.3.1 Preparation of Samples for Assaying PTEN Activity

1. The PTEN-expressing NIH 3T3 fibroblasts are passaged when approaching confluence with trypsin/EDTA to provide new maintenance cultures on 100-mm tissue dishes. Experimental cultures are seeded in a 24-well dish containing sterile coverslips. One 13-mm coverslip/well is required for each experimental data point, and each data point should be carried out in duplicates or triplicates. A 1:20 split of the cells will provide subconfluent cultures that can be starved in DMEM without serum after 24 h for up to 12 h (*see* Note 7) so that by the time the cells are stopped, individual cells are clearly visible in the immunofluorescence.
2. All the materials required for the treatment and termination protocol are made ready: insulin at an appropriate stock concentration for 1:1,000 or 1:10,000 dilution, respectively, into the cultures, PTEN inhibitor ready for addition to the cells at a final concentration of 500 nM, LY 294002 stock solution diluted into water for a final concentration of 100 μM in the culture, PBS, and 4% paraformaldehyde.
3. The cultures are treated with PI3 kinase and PTEN modulators according to the protocol and then stimulated for 2 minutes. For full stimulation, 1 μg/ml of insulin is required. For PTEN inhibitor-treated cells, a basal stimulation of PI3 kinase is achieved with 0.1 μg/ml of insulin. A negative control without PTEN inhibitor and 0.1 μg/ml of insulin must be included. After the treatment, the medium is removed by aspiration and the coverslips are gently rinsed twice with ice-cold PBS (~500 μl/well).
4. Any residual liquid is removed by aspiration and 4% PFA solution is added immediately onto the coverslips. Cells are fixed for 10 minutes at room temperature (*see* Note 8).
5. The paraformaldehyde is discarded and the samples are washed three times for 2 minutes each with PBS.
6. Residual formaldehyde is quenched by incubation in NH4Cl for 10 minutes at room temperature, followed by a further two washes with PBS.

7. The cells are permeabilized by incubation in 0.1% Triton X-100/PBS for 5 minutes at room temperature and then rinsed twice with PBS.
8. The samples are blocked with fatty acid-free BSA solution for 30 minutes at room temperature.
9. Meanwhile, 1 µg of anti-Phospho-Akt antibody is labeled by diluting it into 15 µl of PBS and combining it with Alexa fluorescent Fab fragment (component A). The solution is incubated at room temperature for 5 minutes and then blocked with 5 µl of blocking solution provided with the kit (component B) for 5 minutes or until usage (*see* Notes 4 and 9).
10. Optional: In order to test the specificity of the phospho-specific antibody, a peptide competition sample can be included. Peptide competition: Mouse monoclonal anti-Phospho-Akt (Ser473) antibody is incubated with phospho-peptide (1 mg/ml) corresponding to the S473 phosphorylated carboxy terminal region of Akt or with blocking solution, respectively. After 30 minutes of incubation, the antibody can be labeled as described in step 9 (*see* Note 5).
11. The BSA solution is removed from the coverslips and replaced with the labeled anti-Phospho-Akt antibody diluted 1:200 in 3% BSA for 1 h at room temperature (*see* Note 10) under aluminium foil. Optionally, two samples are incubated with the peptide blocked and mock BSA blocked antibody, respectively.
12. The room lights should be dimmed for all subsequent steps.
13. Optional step: The antibody recognizing total Akt can be labeled meanwhile with a fluorophore that emits at a different wavelength scope than the one used for phospho Akt (e.g., Alexa 594) as described in step 9 of this section and used for a second staining (as described in step 11) after the coverslips have been washed three times with PBS.
14. The coverslips are washed three times with PBS and DAPI is added for 10 minutes at room temperature to stain for the nuclei.
15. The coverslips are removed from the wells by lifting each one with a syringe needle and grabbing the edge with tweezers. Then they are separately dipped into PBS 10 times, followed by a short dip into distilled water.
16. The coverslips are carefully inverted into a drop of mounting medium on a microscope slide. Nail varnish is used to seal the sample (*see* Note 11). When the varnish is dry, the slides can be viewed or stored in the dark at −20°C.

14.3.2 Assaying PTEN Activity by Fluorescence Microscopy of Phosphorylated Akt

1. Using a 100x Fluor oil lens, the slides are viewed under a fluorescence microscope with a band-pass excitation filter of 340–380-nm wavelength to

(a)

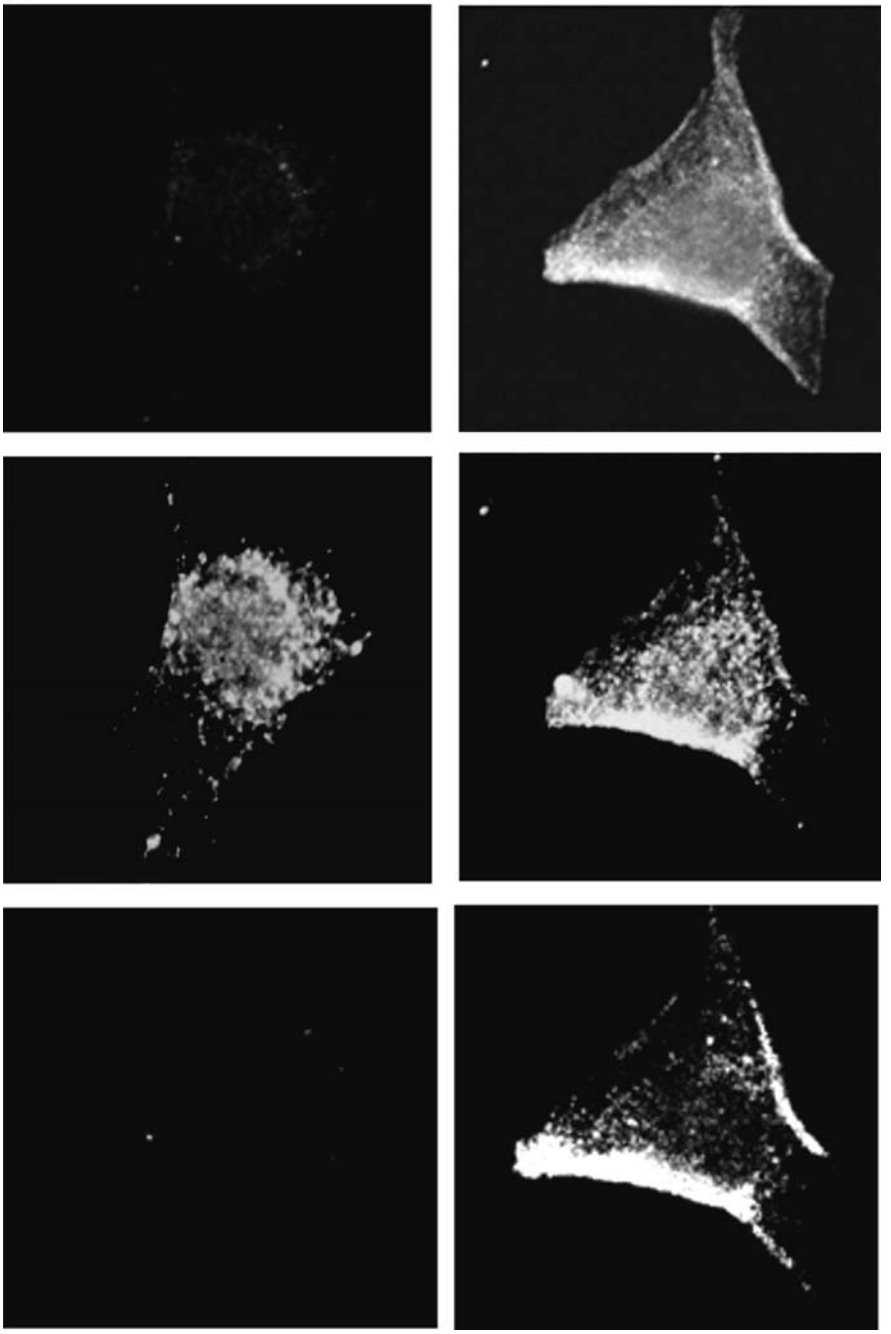

(continued)

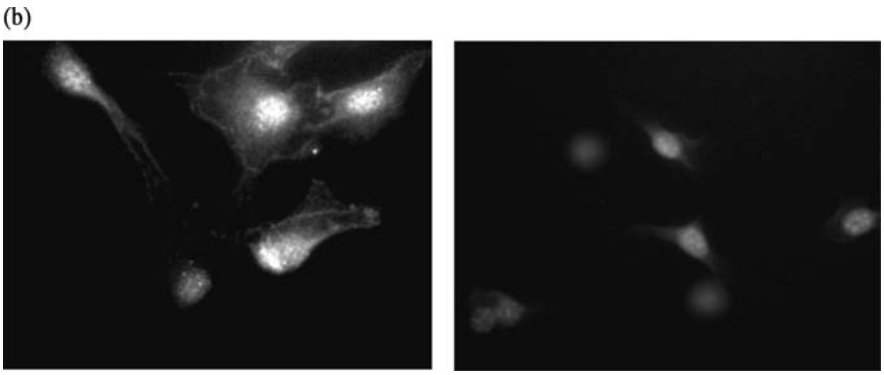

Fig. 14.1 Demonstrating Phospho-Akt (587F11) antibody specificity. (a) Double immunofluorescent staining with the phospho Akt antibody labeled with Alexa Fluor 488 and an Alexa Fluor 594 labeled total Akt antibody. Starved NIH3T3 fibroblasts were treated with low amounts of insulin (0.1 μg/ml) (left column), or Akt activating amounts of insulin (1 μg/ml) (right column). Fluorescence was imaged in FITC channel for phospho (S473) Akt (top row) and TRITC channel for total Akt (middle row). Images were merged and analyzed for colocalization as indicated in positive pixels common to both FITC and TRITC channels (bottom row). Nonstimulated cells are negative for the phosphorylated form of Akt, whereas total Akt is mainly detected in the cytoplasm. In contrast, stimulated cells display high amounts of phosphorylated Akt on the membrane, which is also detected with the antibody for total Akt and therefore colocalizes nicely. Dependence on growth factor stimulation and colocalization with total Akt demonstrate the specificity of the phospho-specific antibody used in this study. (b) Peptide competition study: NIH 3T3 cells were stimulated with 1 μg/ml of insulin for 2 minutes and fixed with 4% PFA. Immunostaining for phosphorylated Akt and nuclear counterstaining with DAPI show that peptide blocking of the antibody with a phosphopeptide corresponding to the carboxy terminal region of Akt abolishes immunoreaction of the phospho Akt antibody (right), whereas control incubation with BSA does not block immunoreaction and phospho-Akt staining can be seen on the plasma membrane (left)

induce DAPI fluorescence (blue emission) and 465–495 nm for Alexa 488 fluorescence (green emission) representing phospho Akt. Optional: Total Akt fluorescence is viewed with a band-pass filter of 572–605 nm (red emission).

2. Images are digitally acquired with a CCD camera for each fluorophore separately and processed with ImageJ Software (National Institutes of Health, Bethesda, MD). The RGB Stack Merge Plugin can be used to overlay different channels and phase contrast images. And the Colocalization Finder Plugin is useful to quantify colocalized pixels. Examples of the signals for phosphorylated Akt and total Akt are shown in Fig. 14.1a (*see* Note 12).
3. All pictures are acquired using the same exposure time and are processed equally in order to obtain comparable data sets. Examples for indirect PTEN activity reflected in Akt phosphorylation are shown in Fig. 14.2.

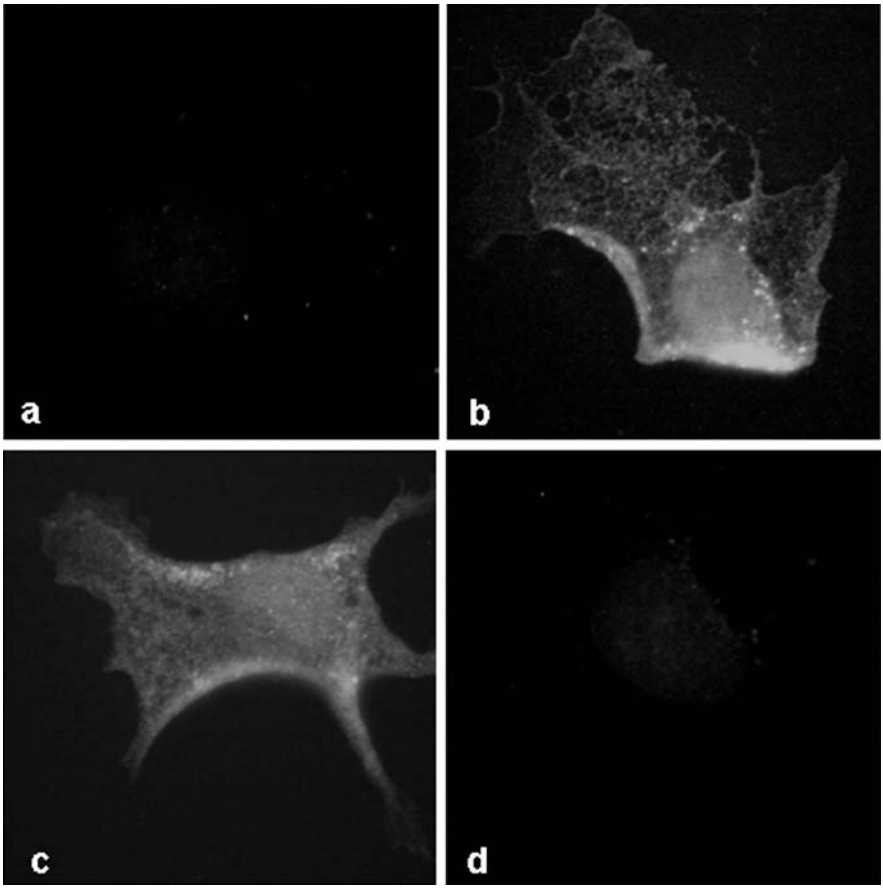

Fig. 14.2 Using S473 phosphorylated Akt as a readout for PTEN activity in NIH 3T3 fibroblasts. NIH3T3 were treated with (a) a vehicle or (c) with 500 nM RV001 PTEN inhibitor. After 15 minutes, low amounts of insulin (0.1 μg/ml) were added to both samples for 2 minutes. After fixation, cells were stained with the phospho-specific Akt antibody (587F11) labeled with Alexa Fluor 488. Fluorescence imaged in FITC channel shows that PTEN inhibition triggers (a) Akt phosphorylation on the membrane, comparable to (b) Akt activity in fully insulin-stimulated cells (1 μg/ml). This indicates that in dephosphorylating PtdIns(3,4,5)P_3, PTEN contributes substantially to controlling Akt activity in NIH 3T3 cells. (d) Inhibition of PI3-kinase with 100 μM LY 294002 before insulin stimulation (1 μg/ml) abolishes Akt phosphorylation completely

Acknowledgments We thank Peter Parker (Cancer Research UK) for providing the phosphopeptide. This work was supported by MRC and BBSRC.

Notes

1. All solutions should be prepared in water that has a resistivity of 18.2 MΩ/cm^{-1}. This standard is referred to as "water" in the text.
2. Paraformaldehyde takes a long time to dissolve. Heating and alkaline conditions accelerate the process. We recommend the following procedure: 1.2 g of paraformaldehyde is

suspended in 1.5 ml of water. Heat carefully in a 80°C water bath under a fume hood and add 0.5 M NaOH until completely dissolved. The solution is topped up with PBS to 30 ml and the pH adjusted to 7.4 by adding 1 M HCl (use indicator strips, as paraformaldehyde can destroy the pH electrode).

3. It is essential to use fatty acid-free BSA. We found that it increases the signal-to-noise ratio substantially.
4. We have also tried detection with commonly used fluorophore tagged antimouse secondary antibodies, but they were found not to be sensitive enough for detection of phospho Akt or gave a high background and unspecific binding. However, total Akt can be detected with a Cy5 conjugated mouse antirabbit antibody (Jackson Immunoresearch, West Grove, PA).
5. We have found this monoclonal phospho Akt antibody to be excellent for immunofluorescence. We also tested polyclonal antibodies against phospho Akt, but these displayed substantial unspecific (nuclear) binding. We tested the specificity of the mouse monoclonal antibody by phospho peptide competition (Fig. 14.1b). The immunofluorescence results were confirmed by Western blotting (data published elsewhere [12]).
6. We highly recommend ImageJ, which is a public-domain Java image processing program. The source code is freely available and no license is required. It is available for Windows, Mac OS, Mac OS X, and Linux. Supported by downloadable plug-ins, it can display, edit, analyze, process, save, and print 8-bit, 16-bit, and 32-bit images. It can read many image formats, including TIFF, GIF, JPEG, BMP, DICOM, FITS, and "raw." We tested more than 10 different programs for scientific image processing and found ImageJ the most versatile and reliable software for microscopic image processing and quantification.
7. The protocol can be adapted for use on other cell lines. However, we strongly recommend establishing the amounts of insulin (or any other growth factor) that are required for full stimulation of Akt by, for example, Western blotting. A dose-response curve is also required in order to determine the amounts of insulin for basal PI3-kinase activity that would not activate Akt. Only upon inhibition of PTEN should the Akt response be triggered (given that PTEN is functional in the respective cell line). Apply all solutions gently in order not to wash away the cells and to ensure even antibody binding throughout the coverslip.
8. Once labeled, the antibody should be used within 30 minutes. However, the amount of antibody for labeling can be reduced.
9. For economy, only 100 µl of diluted antibody per sample needs to be used. Alternatively, even less antibody solution is required when the coverslips are put upside down on a drop (20 µl) of antibody solution on parafilm.
10. Air bubbles should not get trapped in the mounting medium. Slow application of the top layer minimizes their appearance, and carefully tapping the coverslip might let them disappear.
11. The negative control and the positive control should be viewed first in order to establish the optimal exposure time, so that the negative control emits minimal light and the positive control is not overexposed and shows low background.

References

1. Maehama T, Dixon JE. The tumor suppressor, PTEN/MMAC1, dephosphorylates the lipid second messenger, phosphatidylinositol 3,4,5-trisphosphate. J Biol Chem 1998;273:13375–8.
2. Leslie NR, Downes CP. PTEN: The down side of PI 3-kinase signalling. Cell Signal 2002;14:285–95.
3. Stephens L, Anderson K, Stokoe D, Erdjument-Bromage H, Painter GF, Holmes AB, Gaffney PR, Reese CB, McCormick F, Tempst P, Coadwell J, Hawkins PT. Protein kinase B kinases that mediate phosphatidylinositol 3,4,5-trisphosphate-dependent activation of protein kinase B. Science 1998;279:710–4.

4. Ramaswamy S, Nakamura N, Vazquez F, Batt DB, Perera S, Roberts TM, Sellers WR. Regulation of G1 progression by the PTEN tumor suppressor protein is linked to inhibition of the phosphatidylinositol 3-kinase/Akt pathway. PNAS 1999;96:2110–5.
5. Andjelkovic M, Alessi DR, Meier R, Fernandez A, Lamb NJ, Frech M, Cron P, Cohen P, Lucocq JM, Hemmings BA. Role of translocation in the activation and function of protein kinase B. J Biol Chem 1997;272:31515–24.
6. Borgatti P, Martelli AM, Bellacosa A, Casto R, Massari L, Capitani S, Neri LM. Translocation of Akt/PKB to the nucleus of osteoblast-like MC3T3-E1 cells exposed to proliferative growth factors. FEBS Lett 2000;477:27–32.
7. Ono H, Katagiri H, Funaki M, Anai M, Inukai K, Fukushima Y, Sakoda H, Ogihara T, Onishi Y, Fujishiro M, Kikuchi M, Oka Y, Asano T. Regulation of phosphoinositide metabolism, Akt phosphorylation, and glucose transport by PTEN (phosphatase and tensin homolog deleted on chromosome 10) in 3T3-L1 adipocytes. Mol Endocrinol 2001;15:1411–22.
8. Hill MM, Andjelkovic M, Brazil DP, Ferrari D, Fabbro D, Hemmings BA. Insulin-stimulated protein kinase B phosphorylation on Ser-473 is independent of its activity and occurs through a staurosporine-insensitive kinase. J Biol Chem 2001;276:25643–6.
9. Motley ED, Eguchi K, Gardner C, Hicks AL, Reynolds CM, Frank CD, Mifune M, Ohba M, Eguchi S. Insulin-induced Akt activation is inhibited by angiotensin II in the vasculature through protein kinase C-alpha. Hypertension 2003;41:775–80.
10. Qi HL, Zhang Y, Ma J, Guo P, Zhang XY, Chen HL. Insulin/protein kinase B signalling pathway upregulates metastasis-related phenotypes and molecules in H7721 human hepatocarcinoma cell line. Eur J Biochem 2003;270:3795–805.
11. Meier R, Alessi DR, Cron P, Andjelkovic M, Hemmings BA. Mitogenic activation, phosphorylation, and nuclear translocation of protein kinase Bbeta. J Biol Chem 1997;272:30491–7.
12. Schmid AC, Byrne RD, Vilar R, Woscholski R. Bisperoxovanadium compounds are potent PTEN inhibitors. FEBS Lett 2004;566:35–8.
13. Frech M, Andjelkovic M, Ingley E, Reddy KK, Falck JR, Hemmings BA. High affinity binding of inositol phosphates and phosphoinositides to the pleckstrin homology domain of RAC/protein kinase B and their influence on kinase activity. J Biol Chem 1997;272:8474–81.

Chapter 15
Analysis of Phosphatidylinositol 3,4,5 Trisphosphate 5-Phosphatase Activity by *in vitro* and *in vivo* Assays

Lisa M. Ooms, Jennifer M. Dyson, Anne M. Kong and Christina A. Mitchell

Abstract Phosphatidylinositol 3,4,5 trisphosphate [PtdIns(3,4,5)P_3] is a potent membrane-bound signaling molecule transiently synthesized by phosphoinositide 3-kinase (PI3-kinase) in response to extracellular agonists. PtdIns(3,4,5)P_3 signals need to be strictly controlled. PtdIns(3,4,5)P_3 recruits and binds effectors that function in oncogenic signaling pathways. PtdIns(3,4,5)P_3 activates cell proliferation, growth, and migration as well as regulating insulin signaling. The inositol polyphosphate 5-phosphatase family of enzymes dephosphorylate and thereby modulate PtdIns(3,4,5)P_3 levels, attenuating PI3-kinase-dependent signaling. PtdIns(3,4,5)P_3 5-phosphatase enzyme activity can be assessed *in vitro* by analysis of the hydrolysis of radiolabeled or fluorescently labeled PtdIns(3,4,5)P_3 and *in vivo* by visualization of the recruitment and turnover of the PtdIns(3,4,5)P_3-specific biosensor GFP-PH/ARNO or other PtdIns(3,4,5)P_3 binding proteins at the plasma membrane.

Keywords Phosphatidylinositol 3,4,5 trisphosphate · inositol polyphosphate 5-phosphatase · thin layer chromatography · confocal immunofluorescence · plasma membrane · growth factor stimulation · phosphoinositide biosensor

Abbreviations 5-phosphatase: Inositol polyphosphate 5-phosphatase; DMSO: Dimethyl sulfoxide; PI3-kinase: Phosphoinositide 3-kinase; PH: Pleckstrin homology; PtdIns(4,5)P_2: Phosphatidylinositol 4,5 bisphosphate; PtdIns(3,4,5)P_3: Phosphatidylinositol 3,4,5 trisphosphate; PtdSer: Phosphatidylserine; TLC: Thin layer chromatography.

15.1 Introduction

Phosphoinositide 3-kinase (PI3-kinase) phosphorylates phosphatidylinositol 4,5 bisphosphate [PtdIns(4,5)P_2] at the plasma membrane following agonist stimulation to transiently generate the lipid signaling molecule

C.A. Mitchell
Department of Biochemistry and Molecular Biology, Monash University, Wellington Road, Clayton 3800, Victoria, Australia
e-mail: christina.mitchell@med.monash.edu.au

B. Larijani et al. (eds.), *Lipid Signaling Protocols*, DOI: 10.1007/978-1-60327-115-8_15,

phosphatidylinositol 3,4,5 trisphosphate [PtdIns(3,4,5)P_3] [1]. PtdIns(3,4,5)P_3 regulates many cellular processes, including cell proliferation, inhibition of apoptosis, insulin signaling, actin dynamics, and cell migration [2]. PtdIns(3,4,5)P_3 recruits proteins that contain modular domains such as pleckstrin homology (PH) domains found in the serine threonine kinase Akt and its activating kinase PDK1. PtdIns(3,4,5)P_3 localizes PH domain-containing proteins at the plasma membrane and thereby regulates their allosteric activation [1]. In addition to Akt, the PH domains of ARNO, Btk, and GRP1 also specifically bind to PtdIns(3,4,5)P_3 [3–7].

The signals generated by PtdIns(3,4,5)P_3 are regulated by PTEN and/or the inositol polyphosphate 5-phosphatases (5-phosphatases) [8]. The 5-phosphatases specifically remove the 5-position phosphate from the inositol ring of the membrane-bound phosphoinositides PtdIns(4,5)P_2, PtdIns(3,4,5)P_3, and PtdIns(3,5)P_2, forming PtdIns(4)P, PtdIns(3,4)P_2, and PtdIns(3)P, respectively. Additionally, some 5-phosphatases can also hydrolyze the soluble inositol phosphates Ins(1,4,5)P_3 and Ins(1,3,4,5)P_4 at the 5-position phosphate, forming Ins(1,4)P_2 and Ins(1,3,4)P_3, respectively. Currently, 10 mammalian and four yeast family members have been identified that all contain a conserved 300 amino acid 5-phosphatase domain [9]. Each 5-phosphatase displays varying substrate preferences [10], but most are capable of hydrolyzing both the phosphoinositides and inositol phosphates. To date, nine of the 10 mammalian 5-phosphatases exhibit PtdIns(3,4,5)P_3 5-phosphatase activity *in vitro*. PtdIns(3,4,5)P_3 5-phosphatases include Synaptojanin-1 and -2, SHIP-1 and -2, PIPP, 72-kDa 5-phosphatase, OCRL, SKIP, and the type II 5-phosphatase, which regulate numerous cellular processes including synaptic vesicle recycling, immune cell function, insulin signaling, neurite elongation, and endosomal trafficking [8, 11–13].

The gold standard for demonstrating PtdIns(3,4,5)P_3 5-phosphatase activity is via analysis of total cellular PtdIns(3,4,5)P_3 levels in intact cells. Cells are labeled with [^{3}H]-inositol followed by short-term growth factor stimulation, extraction of lipids, deacylation, and HPLC analysis of lipid reaction products in comparison to known standards [14]. However, this may be technically challenging depending on the cell type and cannot be undertaken for transiently transfected cells with less than 50% transfection efficiency or a mixed cell population. Also, such analysis cannot determine localized PtdIns(3,4,5)P_3 turnover on specific membrane microdomains such as membrane ruffles, or in specific subcellular compartments of highly specialized cells such as the neurite growth cone.

Alternative techniques that have recently been developed include analysis of the plasma membrane recruitment of PtdIns(3,4,5)P_3-specific biosensors in transiently transfected cells. The advantage of this technique is that single-cell analysis of PtdIns(3,4,5)P_3 turnover can be determined. In addition, many of the 5-phosphatases are large proteins, which may be challenging to express as purified recombinant proteins. Furthermore, the 5-phosphatases often form multiprotein complexes with receptors and/or other signaling proteins, which may affect their enzyme activity. To enable analysis of PtdIns(3,4,5)P_3 5-phosphatase activity of specific 5-phosphatases in transfected cells or to

quantify PtdIns(3,4,5)P_3 5-phosphatase activity in multiprotein complexes, an immunoprecipitation-based assay has been developed. We describe the use of radiolabeled ^{32}P-PtdIns(3,4,5)P_3; however, a commercially available PtdIns(3,4,5)P_3 substrate together with malachite green may be equally effective.

15.2 Materials

15.2.1 In vitro PtdIns(3,4,5)P_3 5-Phosphatase Assays

15.2.1.1 Transfection of COS-1 Cells

1. Dulbecco's Modified Eagle's Medium (DMEM, Gibco/BRL, Bethesda, MD) supplemented with 10% fetal bovine serum (JRH Biosciences, Lenexa, KS), 100 U/ml of penicillin/0.1% streptomycin (Sigma, St Louis, MO), and 2 mM L-glutamine (JRH Biosciences).
2. Trypsin (JRH Bioscicences): 0.12% Trypsin, 0.02% EDTA, 0.04% glucose.
3. 25x dextran/chloroquine: 400 µg/ml of DEAE dextran (Sigma), 100 µM chloroquine (Sigma). Sterilize by filtration through a 0.2-µm filter. Store at −20°C indefinitely. A working aliquot can be stored at 4°C for two weeks.
4. Phosphate buffered saline (PBS): Prepare a 10x stock with 1.37 M NaCl, 27 mM KCl, 100 mM Na_2HPO_4, 18 mM KH_2PO_4 (adjust to pH 7.4). Store at room temperature and dilute one volume with nine volumes of water to prepare a working solution. Sterilize by autoclaving.
5. 10% DMSO in PBS: Mix one volume of DMSO (Sigma) with nine volumes of sterile PBS.
6. Lysis buffer: 20 mM Tris-HCl, pH 7.4, 150 mM NaCl, 1% Triton X-100 (v/v), store at 4°C, and use ice-cold. One Complete Mini Protease Inhibitor Cocktail tablet (Roche Diagnostics, Mannheim, Germany) should be dissolved in 10 ml of the lysis buffer just prior to use for harvesting the cells following transfection (this solution cannot be stored).
7. Cell scrapers (Falcon, Bedford, MA).

15.2.1.2 Immunoprecipitation of Recombinant Proteins

1. Tris-saline: Prepare a 10x stock with 200 mM Tris-HCl, pH 7.4, 1.5 M NaCl, and store at room temperature. Dilute one volume with nine volumes of water to prepare a working solution.
2. Protein A Sepharose CL-4B (Amersham Biosciences, Uppsala, Sweden).

15.2.1.3 Labeling of PtdIns(3,4,5)P_3 Substrate

1. PtdIns(4,5)P_2 (Sigma) is resuspended at 2 mg/ml in a mixture of chloroform:-methanol:10 mM HCl (20:9:1). Lipid stocks should be stored in 100-µl

aliquots in dark glass vials at −20°C. The lids should be sealed with Parafilm or an equivalent to prevent evaporation of the solvent.
2. L-α Phosphatidyl-L-serine (PtdSer) stock (Sigma) is resuspended at 5 mg/ml in a mixture of chloroform:methanol:10 mM HCl (20:9:1) and stored as above for PtdIns(4,5)P_2.
3. Nitrogen cylinder with regulator.
4. Lipid resuspension buffer: 20 mM HEPES, pH 7.5, 1 mM $MgCl_2$, 1 mM EGTA.
5. PtdSer carrier lipid: Place 5 μg of PtdSer per reaction into a microcentrifuge tube and dry under a stream of nitrogen. Resuspend the lipid in 10 μl of lipid resuspension buffer and sonicate for 5 min in a water-bath sonicator. PtdSer carrier lipid should be prepared fresh on the day required but can be stored for several hours at room temperature.
6. Recombinant PI3-kinase: obtained from Dr Meredith Layton, Ludwig Institute, Australia [15]. Store at −20°C.
7. 20x kinase buffer: 400 mM HEPES, pH 7.8, 100 mM $MgCl_2$, 20 mM EGTA.
8. Unlabeled 2.5 mM ATP (Sigma). Store at −20°C.
9. Adenosine 5'-[γ-^{32}P]triphosphate ~3,000 Ci/mmol, 10 mCi/ml. Store at −20°C (Perkin Elmer Life Sciences, Boston, MA; we use frozen, not the 4°C stabilized label).
10. 1 M HCl. Measure 45.8 ml of water into a 50-ml tube and add 4.2 ml of concentrated HCl. Be careful when handling concentrated HCl; only use it in a fume hood.
11. Chloroform-saturated 2 M KCl: Dissolve 3.73 g of KCl in 25 ml of water and add 5 ml of chloroform. Mix the solution by shaking vigorously and then allow the phases to separate. Only use the top aqueous layer for lipid extractions. The solution can be stored at room temperature for months as long as the chloroform layer is replaced as it evaporates.
12. Chloroform:methanol (1:1, v/v): Mix equal volumes of chloroform and methanol. This solution should be freshly prepared before use, ensuring that the solution does not turn cloudy.

15.2.1.4 PtdIns(3,4,5)P_3 5-Phosphatase Assays

1. TLC plates: Partisil K6 Silica Gel 60 Å (250-μm layer) channeled concentration zone TLC plates (Whatman, Maidstone, UK). TLC plates need to be oxalate-treated prior to use by incubating plates horizontally in oxalate solution [1% potassium oxalate (w/v), 50% ethanol (v/v), 2 mM EDTA] for 30 s. Drain off the excess liquid and then dry the plates vertically on an absorbent paper towel overnight at room temperature (*see* Note 2). Oxalate-treated TLC plates can be stored at room temperature for months before use.
2. Hairdryer.
3. TLC tank: Cover the two widest sides of the tank with pieces of gel blotting paper (Schleicher and Scheull Bioscience, Dassel, Germany). Add freshly

prepared tank solvent (130 ml of propan-1-ol, 8 ml of glacial acetic acid, 680 µl of orthophosphoric acid, and 61.32 ml of water; ensure that the solution is clear) to the TLC tank, seal the lid in place with vacuum grease, and allow the tank to equilibrate at room temperature overnight (*see* Note 3).
4. Super Rx medical X-ray film (Fuji, Tokyo, Japan).

15.2.1.5 SDS-Polyacrylamide Gel Electrophoresis (SDS-PAGE)

1. Running gel buffer: 0.75 M Tris-HCl, pH 8.8. Store at room temperature.
2. Stacking gel buffer: 0.25 M Tris-HCl, pH 6.8. Store at room temperature.
3. 10% SDS (Amresco, Solon, OH). Dissolve 100 g of SDS in 1 L of water. Store at room temperature. SDS powder is a respiratory irritant and should only be handled in the fume hood.
4. 30% acrylamide/bis solution (because unpolymerized solution is neurotoxic, exposure should be avoided; Bio-Rad Laboratories, Hercules, CA).
5. Ammonium persulfate (APS): 14 mg/ml of APS (Bio-Rad Laboratories) in water.
6. N,N,N',N'-tetramethylethylene-diamine (TEMED, Sigma).
7. Running buffer: 25 mM Tris-HCl, 190 mM glycine, 0.1% (w/v) SDS; store at room temperature.
8. Prestained molecular weight markers: Page Ruler (Fermentas, Burlington, Ontario, Canada).
9. 2x Laemmli buffer: 40 mM Tris-HCl, pH 6.8, 4% SDS (w/v), 20% glycerol (v/v), 0.002% bromophenol blue (w/v), 10% 2-mercaptoethanol (v/v).
10. Transfer buffer: 25 mM Tris-HCl, 190 mM glycine, 20% (v/v) methanol; store at room temperature.
11. PVDF membrane (Pall Life Sciences, Pensacola, FL).
12. Gel blotting paper (Schleicher and Scheull Bioscience).
13. Blocking buffer: 5% skim milk (w/v) in Tris-saline, prepared fresh.
14. Primary antibody: appropriate antibody to detect the protein of interest diluted in 10 ml of Tris-saline.
15. Secondary antibody: appropriate HRP-conjugated secondary antibody diluted in 10 ml of Tris-saline.
16. Western Lightning enhanced chemiluminescence solution (Perkin Elmer Life Sciences, Boston, MA) and Super Rx medical X-ray film (Fuji).

15.2.2 In vivo PtdIns(3,4,5)P_3 5-Phosphatase Assays

15.2.2.1 Transfection of COS-1 Cells with GFP-PH/ARNO

1. GFP-PH/ARNO plasmid was obtained from Dr. Tamas Balla (National Institutes of Health, Bethesda, MD).
2. 13-mm coverslips (Menzel, Braunschweig, Germany). Coverslips should be placed into a glass jar and sterilized by autoclaving.

3. Epidermal growth factor (EGF; BD Biosciences, Bedford, MA) or other appropriate growth factor. Store at −20°C in single-use aliquots to avoid freeze-thawing. Prepare stimulation media by adding EGF to serum-free DMEM to a final concentration of 100 ng/ml.

15.2.2.2 Immunofluorescence

1. 3% paraformaldehyde (BDH, Victoria, Australia). Paraformaldehyde is toxic and should be prepared in a fume hood. Heat approximately 300 ml of water to 80°C in a glass beaker, stirring continuously on a heated stirrer. Add 15 g of paraformaldehyde, stirring continuously for 30 min at 80°C. At this stage, most of the paraformaldehyde will have gone into solution; however, the solution will still appear cloudy. Add 50 ml of 10x PBS, stirring continuously at 80°C (for a final concentration of 1x PBS). After the addition of the 10x PBS, the solution should appear clear. Adjust the pH to 7.4 using HCl and then add water to a final volume of 500 ml. Freeze in aliquots at −20°C. Paraformaldehyde can be stored indefinitely at −20°C, but avoid freeze-thawing.
2. 0.1% Triton X-100 (Sigma) in PBS: Mix 50 µl of Triton X-100 with 50 ml of PBS and vortex. Store at room temperature.
3. Staining dish. To prepare the dish, two pieces of gel blotting paper are placed in the bottom of an agar plate and dampened with water. The blotting paper is then covered with a piece of Parafilm (or equivalent) and the coverslips placed on top of the Parafilm, cell side facing up. This setup can be reused, but the gel blotting paper needs to be dampened before each use.
4. 1% BSA fatty acid free (Bovogen, Victoria, Australia) in PBS: Mix 0.5 g of BSA with 50 ml of PBS; vortex. Store in aliquots at −20°C.
5. Primary antibody to detect protein of interest diluted in 1% BSA.
6. Secondary antibody conjugated to AlexaFluor®594 (or equivalent) diluted in 1% BSA. Protect the solution from the light.
7. Glass slides (Menzel).
8. Slow Fade solution (Molecular Probes, Eugene, OR).

15.3 Methods

15.3.1 In vitro PtdIns(3,4,5)P_3 5-Phosphatase Assays

The method outlined below describes *in vitro* PtdIns(3,4,5)P_3 5-phosphatase assays performed using radiolabeled PtdIns(3,4,5)P_3 and immunoprecipitated proteins from intact cells. These assays can also be performed with purified recombinant 5-phosphatases as well as immunoprecipitated endogenous 5-phosphatases or multiprotein complexes that may contain 5-phosphatases immunoprecipitated from mammalian cells.

15.3.1.1 Transfection of COS-1 Cells

COS-1 cells may be transiently transfected with a construct encoding the 5-phosphatase of interest, or a protein that complexes with a 5-phosphatase, prior to immunoprecipitation of the recombinant protein from cell lysates. While the method describes the transfection of one 5-phosphatase construct, it can easily be adapted to assess the effects of other proteins such as 5-phosphatase-binding partners on PtdIns(3,4,5)P_3 5-phosphatase activity by transiently co-transfecting the cells with multiple constructs. The 5-phosphatase construct can also be transfected into different cell types, although the transfection method may need to be optimized. The cells can also be treated with specific growth factors or inhibitors as required.

1. COS-1 cells are maintained in DMEM supplemented with 10% fetal bovine serum in 100-mm tissue culture dishes.
2. For transfection, 100-mm tissue culture dishes of COS-1 cells at ~80% confluence are split 1:2 and incubated for 4 h at 37°C in a humidified 5% CO_2 incubator to allow the cells to adhere. One 100-mm tissue culture dish is required for the transfection of each construct.
3. Replace the media with 5 ml of DMEM without fetal bovine serum.
4. Add 200 µl of 25x dextran/chloroquine and 5 µg of a DNA construct encoding either the 5-phosphatase of interest or the empty vector alone as a negative control. The amount of DNA added to the transfection may need to be increased depending on the activity of the promoter.
5. Mix gently and incubate at 37°C for 2 h in a humidified 5% CO_2 incubator (*see* Note 4).
6. Discard the media/dextran/chloroquine/DNA mix.
7. Add 5 ml of 10% DMSO in PBS and incubate for 2 min at room temperature. The time of this incubation is critical.
8. Aspirate the DMSO/PBS mix.
9. Add 8 ml of DMEM containing serum and incubate the cells at 37°C overnight in a humidified 5% CO_2 incubator.
10. Split the cells 1:2 to generate two 100-mm tissue culture dishes for each construct and incubate at 37°C in a humidified 5% CO_2 incubator overnight.
11. Wash the cells twice with ice-cold Tris-saline.
12. Add 1 ml of ice-cold lysis buffer to each dish (with protease inhibitors) and scrape the cells from the dish with a cell scraper.
13. Incubate at 4°C for 1 h, with gentle agitation.
14. Centrifuge 13,000 × *g* for 10 min.
15. Transfer the Triton-soluble supernatant to a fresh tube for immunoprecipitation of the recombinant protein of interest. This protocol will generate 2x 1 ml of Triton-soluble supernatant for each construct.

15.3.1.2 Immunoprecipitation of Recombinant Proteins

The transiently expressed recombinant 5-phosphatase or binding partner or receptor is immunoprecipitated from cell lysates using specific antibodies. It is

also possible to immunoprecipitate endogenous 5-phosphatase proteins from cells or multiprotein complexes that contain a 5-phosphatase.

1. For each construct, transfer 100-µl aliquots of protein A Sepharose [50% slurry (v/v)] to two microcentrifuge tubes. Transfer an additional 100 µl of protein A Sepharose to a separate tube as a blank control reaction for the PtdIns(3,4,5)P_3 5-phosphatase assay.
2. Centrifuge the protein A Sepharose for 15 s at 13,000 × *g* and then discard the supernatant.
3. Wash the protein A Sepharose pellets three times with 1 ml of ice-cold lysis buffer (without protease inhibitors) and discard the final wash.
4. Set the blank tube aside at 4°C for use in the PtdIns(3,4,5)P_3 5-phosphatase assays described in Subheading 15.3.1.4.
5. Add 1 ml of the Triton-soluble supernatant prepared as described in Subheading 15.3.1.1.
6. Incubate at 4°C overnight with gentle agitation (a rotating wheel is ideal; *see* Note 5).
7. Centrifuge the immunoprecipitations at 1,000 × *g* for 10 s and remove the supernatant.
8. Wash the pellets three times with 1 ml of ice-cold lysis buffer (without inhibitors).
9. Wash the pellets three times with 1 ml of ice-cold 1x kinase buffer and discard the final wash.
10. Use one immunoprecipitation for PtdIns(3,4,5)P_3 5-phosphatase assays as described in Subheading 15.3.1.4. Add 50 µl of 2x Laemmli buffer to the other immunoprecipitation and analyze by Western blotting (Subheading 15.3.1.5) to confirm the expression/immunoprecipitation of the recombinant protein of interest.

15.3.1.3 Labeling of PtdIns(3,4,5)P_3 Substrate

The radiolabeled PtdIns(3,4,5)P_3 substrate is generated by incubating unlabeled PtdIns(4,5)P_2 with recombinant PI3-kinase and [γ^{32}P]ATP to produce PtdIns([^{32}P]3,4,5)P_3. The protocol outlined below describes the use of recombinant PI3-kinase from a noncommercial source. However, active recombinant PI3-kinase is also available from a number of commercial sources such as Upstate (Lake Placid, NY), Biomol (Plymouth Meeting, PA), and Jena Bioscience (Jena, Germany).

1. Add 6.7 µl of PtdIns(4,5)P_2 stock and 2.4 µl of PtdSer stock to a microcentrifuge tube.
2. Dry the lipids under a stream of nitrogen gas using a glass Pasteur pipette attached via plastic tubing to the regulator on the nitrogen cylinder (*see* Note 6).
3. Resuspend the lipids in 200 µl of lipid resuspension buffer (*see* Note 7).
4. Sonicate for 5 min in a water-bath sonicator.

5. Mix 18 µl of water, 2 µl of 2.5 mM ATP, 1 µg of recombinant PI3-kinase (in 5 µl), 5 µl of 20x kinase buffer, 50 µl of PtdIns(4,5)P_2/PtdSer mix, and 20 µl [γ^{32}P]ATP (3,000 Ci/mmol) (ensure that appropriate shielding is used when working with [γ^{32}P]ATP; *see* Note 8).
6. Incubate the reaction at room temperature overnight.
7. Stop the reaction by adding 100 µl of 1 M HCl.
8. Add 10 µl pf PtdSer carrier lipid, 200 µl of chloroform:methanol (1:1), and 500 µl of chloroform-saturated 2 M KCl to the substrate reaction.
9. Vortex briefly, and then centrifuge at 10,000 × *g* for 5 min to separate the organic and aqueous phases.
10. Transfer the bottom organic layer to a clean microcentrifuge tube using a Gilson pipette (or equivalent). It is very important not to transfer any of the top layer during this step. Depress the plunger of the pipette almost to the first stop, and then insert the pipette tip into the bottom organic layer. Fully depress the plunger to the first stop to expel a small amount of air and any of the top aqueous layer within the pipette tip. Carefully draw up almost all of the bottom organic layer and withdraw the pipette.
11. Dry the PtdIns([^{32}P]3,4,5)P_3 under a stream of nitrogen as above. Care must be taken during this step to prevent spillage of the radioactive substrate (*see* Note 8).
12. Resuspend the lipid in 500 µl of lipid resuspension buffer.
13. Sonicate for 5 min in a water-bath sonicator.

15.3.1.4 PtdIns(3,4,5)P_3 5-Phosphatase Assays

To measure PtdIns(3,4,5)P_3 5-phosphatase activity *in vitro*, the radiolabeled PtdIns([^{32}P]3,4,5)P_3 substrate generated in Subheading 15.2.1.3 is incubated with the recombinant immunoprecipitated 5-phosphatase (Subheadings 15.3.1.1 and 15.3.1.2) and then the lipid reaction products are extracted and separated by thin layer chromatography.

1. Add 5 µl of 20x kinase buffer and 50 µl of PtdIns([^{32}P]3,4,5)P_3 to the immunoprecipitate pellets prepared in Subheading 15.3.1.2.
2. Incubate for 30 min at 37°C. This time can be shortened to 10 min if submaximal hydrolysis of PtdIns(3,4,5)P_3 is required to compare subtle differences in 5-phosphatase activity.
3. Stop the reactions by adding 100 µl of 1 M HCl (*see* Note 9).
4. Add 10 µl of PtdSer carrier lipid, 200 µl of chloroform:methanol (1:1), and 500 µl of chloroform-saturated 2 M KCl to each reaction.
5. Vortex briefly and then centrifuge at 10,000 × *g* for 5 min to separate the organic and aqueous phases.
6. Transfer the bottom organic layer to a clean microcentrifuge tube, ensuring that none of the top layer is transferred (see Subheading 15.3.1.3, step 10).
7. Pipette the whole organic layer from a reaction onto the loading zone of a lane on an oxalate-treated TLC plate. Heat the plate with a hairdryer on the lowest warm setting during loading to facilitate solvent evaporation (*see* Note 10).

8. Place the plate into the prepared TLC tank with the samples at the bottom and incubate at room temperature until the solvent front almost reaches the top of the TLC plate (approximately 4–5 h).
9. Remove the plate from the TLC tank and place on an absorbent paper towel behind suitable shielding to dry.
10. Cover the plate with plastic wrap and place into an X-ray film cassette with an intensifying screen. Tape the edges of the plate to the cassette to prevent the plate from moving during exposure.
11. Expose the plate to X-ray film at room temperature (start with a 2-h exposure, but an overnight or longer exposure may be required if the signal is low).
12. Determine the percentage of PtdIns(3,4,5)P_3 hydrolysis by comparing the intensity of the PtdIns(3,4)P_2 spot to the PtdIns(3,4,5)P_3 spot for each sample by densitometry. An example of the results obtained is shown in Fig. 15.1a.

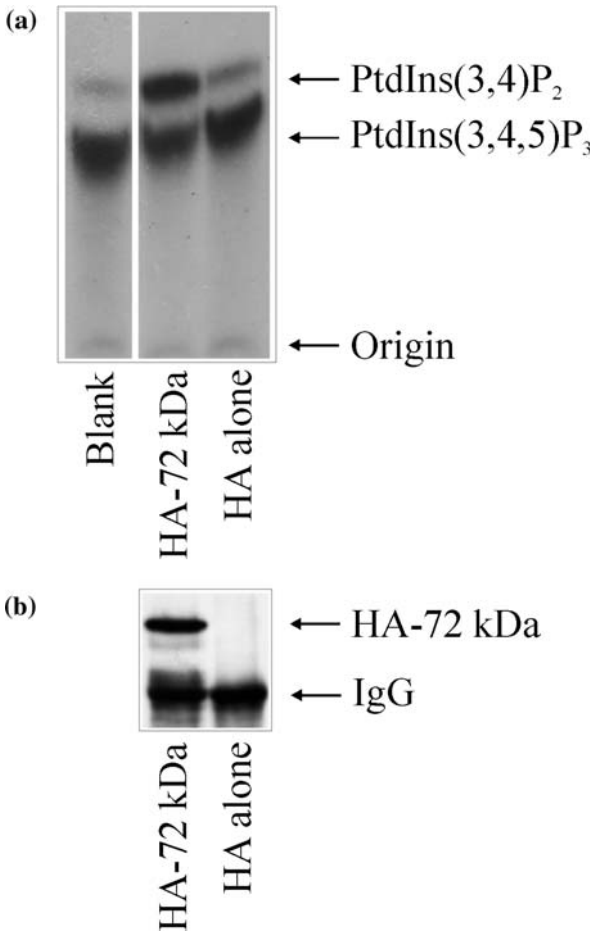

Fig. 15.1 *In vitro* PtdIns(3,4,5)P_3 5-phosphatase assays. (a) COS-1 cells were transiently transfected with plasmids encoding HA empty vector alone (HA alone) or HA-72-kDa 5-phosphatase (HA-72-kDa). Forty-eight hours after transfection, cells were harvested and the 1% Triton X-100-soluble fractions were immunoprecipitated with HA antibodies. HA alone and HA-72-kDa immunoprecipitates were subjected to PtdIns([^{32}P]3,4,5)P_3 5-phosphatase assays and the lipid products were resolved by TLC. The origin and migration of PtdIns(3,4,5)P_3 and PtdIns(3,4)P_2 are shown on the right. (b) COS-1 cells were transiently transfected and immunoprecipitated as in (a). HA alone and HA-72-kDa immunoprecipitates were subjected to SDS-PAGE and immunoblotted with HA antibodies. The migration of HA-72-kDa 5-phosphatase (HA-72 kDa) and IgG is indicated on the right

15.3.1.5 Western Blotting of Immunoprecipitated Recombinant Proteins

Following PtdIns(3,4,5)P_3 5-phosphatase assays with radiolabeled substrate, duplicate immunoprecipitates prepared in Subheading 15.3.1.2 are Western blotted with appropriate antibodies to confirm the expression and immunoprecipitation of the recombinant 5-phosphatase.

1. The following instructions are for a Bio-Rad mini-gel electrophoresis and transfer system but can be adapted to suit other systems. The glass plates should be wiped clean with methanol prior to use.
2. Prepare a 0.75-mm-thick 10% gel by mixing 2.5 ml of running gel buffer, 1.6 ml of 30% acrylamide/bis solution, 50 µl of 10% SDS, 0.57 ml of water, 250 µl of 14 mg/ml APS, and 10 µl of TEMED. Pour into the prepared casting apparatus, leaving space (~2 cm) for the stacking gel, and overlay with distilled water. Allow the gel to polymerize (~15 min).
3. Pour off the water from the running gel.
4. Prepare the stacking gel by mixing 2.5 ml of the stacking gel buffer, 0.65 ml of 30% acrylamide/bis solution, 50 µl of 10% SDS, 1.55 ml of water, 250 µl of 14 mg/ml APS, and 10 µl of TEMED. Fill up the casting apparatus with the stacking gel mix and then insert the comb. Allow the gel to polymerize (~15–30 min).
5. Remove the comb and rinse the wells with running buffer using a disposable plastic transfer pipette. Insert thin strips of gel blotting paper into the wells to remove the buffer from the wells. Assemble the gel unit into the tank.
6. Boil the samples at 100°C for 10 min and then centrifuge briefly to pellet the protein A Sepharose. Load 30 µl of a sample (avoiding the protein A Sepharose) into a well. Load prestained molecular weight markers into one well and then fill all of the wells with running buffer.
7. Fill the tank with running buffer, connect the gel unit to the power supply, and run at 200 V until the blue dye front has just run off the gel.
8. Disconnect the electrophoresis unit from the power supply, disassemble, and discard the stacking gel.
9. Cut a sheet of PVDF membrane just larger than the gel. Mark one corner of the membrane with a soft pencil to allow identification and orientation of the membrane in subsequent steps. Briefly wet the membrane in methanol and then rinse in water followed by transfer buffer.
10. Lay the transfer cassette open on the bench. Wet a sponge in transfer buffer and place on the transfer cassette followed by a piece of gel blotting paper. Wet another piece of gel blotting paper, transfer the gel to the blotting paper, and place into the transfer cassette. Carefully overlay the PVDF membrane onto the gel, remove any air bubbles, and then cover with another two pieces of gel blotting paper and a sponge soaked in transfer buffer.
11. Place the transfer cassette into the transfer tank, ensuring that the gel is facing the cathode, and then place an ice block and magnetic stirrer into the tank.

12. Fill the tank with transfer buffer, connect to the power supply, and switch on the magnetic stirrer. Transfer at 250 mA for 1 h.
13. Disassemble the transfer apparatus and confirm that the prestained molecular weight markers have transferred to the membrane. Discard the gel and blotting paper.
14. Incubate the membrane in 50 ml of blocking buffer for 1 h at room temperature with gentle agitation.
15. Briefly rinse the membrane three times with Tris-saline and then place it into a heat-sealable plastic bag. Add the primary antibody to the bag and remove the air bubbles. Heat-seal the top of the bag and incubate at 4°C overnight with gentle agitation (*see* Note 12).
16. Remove the primary antibody (*see* Note 13) and then wash the membrane three times with Tris-saline for 5 min each wash (*see* Note 14).
17. Place the membrane into a heat-sealable bag and add the secondary antibody. Again remove the air bubbles and heat-seal the bag. Incubate at room temperature for 1 h with gentle agitation.
18. Wash the membrane as in step 16.
19. Mix 2.5 ml of each of the ECL reagents in a plastic container. Incubate the membrane in the ECL mix for 1 min, making sure that the membrane is evenly coated.
20. Remove the blot from the ECL reagent and gently blot with paper towel to remove excess liquid. Cover the membrane with plastic wrap, place into an X-ray cassette, and secure with tape. Expose the membrane to film for a suitable time (start with a 2-min exposure and adjust the time accordingly). An example of the results is shown in Fig. 15.1b.

15.3.2 In vivo PtdIns(3,4,5)P_3 5-Phosphatase Assays

The protocol described below outlines the measurement of plasma membrane PtdIns(3,4,5)P_3 levels in COS-1 cells. However, this method can be easily adapted to any cell line that can be transfected with the GFP-PH/ARNO construct. In addition, other PtdIns(3,4,5)P_3-specific GFP-PH fusion proteins can be used including GFP-PH/Btk. This method can also be utilized to analyze the turnover of PtdIns(3,4,5)P_3 in specialized cellular compartments such as neurite growth cones. To analyze the generation of PtdIns(3,4)P_2, the product of PtdIns(3,4,5)P_3 hydrolysis by 5-phosphatases, the same protocol can be repeated using the PH domain of TAPP1, which binds only PtdIns(3,4)P_2 [16].

15.3.2.1 Transfection of COS-1 Cells with GFP-PH/ARNO

COS-1 cells are co-transfected with the GFP-PH/ARNO biosensor and a construct encoding the 5-phosphatase of interest or a protein that may regulate 5-phosphatase activity. While this method describes PtdIns(3,4,5)P_3 analysis in

cells overexpressing a 5-phosphatase, knockdown of the protein of interest by RNAi methods can also be used.

1. Transfect a 100-mm dish of COS-1 cells using the dextran/chloroquine method described in Subheading 15.3.1.1. Follow steps 1–9 and add 5 μg of GFP-PH/ARNO DNA in step 4 in addition to 5 μg of a construct encoding the 5-phosphatase of interest or empty vector alone as a control. Incubate the cells at 37°C overnight.
2. Trypsinize the cells with 2 ml of trypsin and then add 6 ml of DMEM containing serum. Sterilize a pair of forceps with 70% ethanol and transfer four coverslips per transfection to separate wells of a 24-well dish. Add 400 μl of media containing serum and 100 μl of cells (*see* Note 15). Incubate at 37°C for ~6 h.
3. Replace the media with 500 μl of DMEM without serum and incubate overnight (16 h) at 37°C.
4. Thaw the paraformaldehyde fix and prepare the stimulation media containing 100 ng/ml of EGF (*see* Note 16). Label the wells of the 24-well dish 0, 1, 5, and 10 min for each transfection.
5. Remove the media from the 10-min wells and add 500 μl of stimulation media. Incubate at 37°C for 5 min, remove the media from the 5-min wells, and add 500 μl of stimulation media. Incubate at 37°C for 4 min and then repeat for the 1-min wells. Incubate the dish for a further 1 min at 37°C.
6. Immediately aspirate the culture media from all of the wells and add ~500 μl of paraformaldehyde fix (*see* Note 17). Incubate for 20 min at room temperature.
7. Remove the paraformaldehyde and add ~500 μl of 0.1% Triton X-100 in PBS. Incubate for 2 min at room temperature.
8. Remove the 0.1% Triton X-100 in PBS and wash the coverslips three times with PBS (*see* Note 18).

15.3.2.2 Immunofluorescence

Following transient transfection, the cells are stimulated with a growth factor to promote plasma membrane PtdIns(3,4,5)P_3 production and are then fixed, permeabilized, and stained with specific antibodies to detect the recombinant 5-phosphatase.

1. Transfer the coverslips from the tissue culture dish to a staining/Petri dish (*see* Note 19).
2. Block the coverslips with 40 μl of 1% BSA in PBS for 20 min at room temperature.
3. Incubate the coverslips with 40 μl of primary antibody (diluted in 1% BSA in PBS) for 1 h at room temperature.
4. Wash the coverslips three times with PBS (*see* Note 20).

5. Incubate the coverslips with 40 µl of AlexaFluor® 594-conjugated secondary antibody (or equivalent, diluted in 1% BSA in PBS) for 45 min at room temperature protected from the light.
6. Wash the coverslips three times with PBS.
7. Mount the coverslips on glass slides using 1.5 µl of antifade mounting solution per coverslip and seal the edges with nail polish (*see* Note 21).

15.3.2.3 Microscopy and Analysis

Images of fixed cells are acquired by confocal laser scanning microscopy. Single optical sections are taken through the middle of the cell such that the plasma membrane and the cytosol are visibly distinct (*see* Note 22). An example of this is shown in Fig. 15.2. Use ImageJ analysis software to quantify the recruitment of the GFP-PH/ARNO biosensor to the plasma membrane [17] (*see* Note 23). This is achieved by measuring and expressing the pixel fluorescence intensity at the plasma membrane as a ratio of the cytosolic fluorescence intensity, which is used to standardize for differential expression between individual cells. For each cell to be analyzed, the average pixel fluorescence intensity of three separate representative areas of defined size at the plasma membrane (e.g., 50 pixels) and three areas of defined size in the cytosol (e.g., 100 pixels) are determined (see Note 24). The ratio of plasma membrane to cytosolic pixel fluorescence intensity is then calculated [13]. At least 10 cells per time point should be analyzed from three separate experiments.

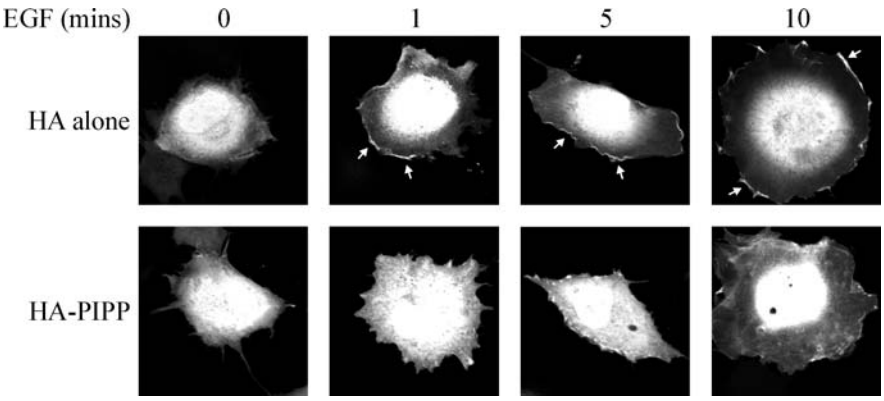

Fig. 15.2 *In vivo* PtdIns(3,4,5)P_3 5-phosphatase assays. COS-1 cells were transiently co-transfected with plasmids encoding GFP-PH/ARNO and either HA empty vector (HA alone) or HA-PIPP 5-phosphatase (HA-PIPP). Cells were serum-starved and, where indicated, stimulated with 100 ng/ml of EGF for 1, 5, or 10 min and stained with HA antibodies to identify co-transfected cells (not shown). Arrows indicate plasma membrane localization of GFP-PH/ARNO. Images were captured using confocal microscopy

Acknowledgments The authors would like to thank Dr. Tamas Balla for the GFP-PH/ARNO construct, Dr. Meredith Layton for the recombinant PI3-kinase, and Drs. Absorn Sriratana and Richard Huysmans for technical assistance.

Notes

1. All solutions should be prepared in water with a resistivity of 18.2 MΩ-cm. All buffers and reagents used should be at room temperature unless otherwise stated.
2. While standard silica 60 TLC plates can be used, channeled concentration zone plates lanes allow quicker sample application and result in sharper bands with better resolution. Following oxalate treatment, TLC plates must be dried vertically and placed into the TLC tank in the same orientation in which they were dried. Concentration zone plates should be dried with the zone at the bottom. If concentration zone plates are not used, the bottom of the plate should be marked by ruling a line 1 cm from the bottom with a soft pencil, which serves as the origin on which the samples are loaded. If channeled plates are not used, the samples should be loaded 1 cm apart on the TLC plate.
3. The walls of the TLC tank need to be lined with gel blotting paper to saturate the chamber atmosphere with solvent vapor. Gel blotting paper can be stuck to the sides of the tank with tape, although most tapes are not able to withstand the solvents used in the tank. Alternatively, the paper can be placed against the sides of the tank and held in place with the TLC plate. Do not allow the gel blotting paper to come in contact with the silica of the TLC plate. The TLC tank should be poured at least the day before use to allow it to equilibrate properly. The tank can be used for two weeks providing the lid is tightly sealed with vacuum grease to prevent evaporation of the solvent.
4. Extending the dextran/chlroquine/DNA incubation to 3 h may improve the transfection efficiency. However, it is important to monitor the cells during this time as the longer incubation can promote cell death.
5. If protein degradation is an issue, the immunoprecipitations can be incubated for 2 h instead of overnight. Also, the samples can be precleared with protein A Sepharose prior to immunoprecipitation to decrease nonspecific binding if necessary.
6. Be careful when drying lipids under nitrogen (especially when labeled with ^{32}P) to prevent the lipids from being blown out of the tube by the gas stream. Perform this procedure in a fume hood to minimize exposure to aerosols. Also, be careful not to overdry the lipids, as they will become impossible to resuspend—the lipids should be dried until the liquid just disappears.
7. When resuspending lipids, scrape the sides of the microcentrifuge tube with a pipette tip to remove any bound lipid.
8. Suitable shielding and personal protection must be used when working with ^{32}P. Dispose of waste according to local guidelines. Ensure that the microcentrifuge tubes used have tight-fitting lids that do not leak when vortexed.
9. If necessary, the 5-phosphatase assays can be stopped with 100 µl of 1 M HCl and then stored at 4°C overnight (with appropriate shielding). The extraction and separation can then be continued the next day.
10. Use a hairdryer to warm the plate, but do not put it too close to the plate as too much airflow over the plate can make loading the samples very difficult and blow them across the plate.
11. The timeline for the *in vitro* PtdIns(3,4,5)P_3 5-phosphatase assays is as follows. Day 1: Transfect COS-1 cells. Day 2: Split transfected cells 1:2. Day 3: Prepare cell lysates, immunoprecipitate protein of interest, perform PtdIns(3,4,5)P_3 labeling reaction, prepare TLC tank, oxalate-treat plates. Day 4: Extract PtdIns(3,4,5)P_3 substrate, perform PtdIns(3,4,5)P_3 5-phosphatase assays.
12. Depending on the antibody, this incubation can be performed at room temperature for 1 h.

13. Primary antibodies can be reused several times. Following incubation with the membrane, transfer the antibody to a 10-ml tube and add sodium azide to a final concentration of 0.1% (this is only necessary following the first use). Sodium azide is toxic and should be handled in a fume hood. Store the diluted antibody at 4°C. Additional antibody can be added after three uses to boost the signal strength.
14. The washes can be extended to 10 minutes each if necessary to remove background signals. Tween 20 can also be added to a final concentration of 0.1% to decrease the background.
15. The cells must not be more than ~50% confluent when harvested; otherwise, contact inhibition will prevent the cells from being properly stimulated by the growth factor treatment. The cell density may need to be adjusted to ensure that the cells do not become overconfluent.
16. Various concentrations of EGF can be used to stimulate the cells. In addition, other methods of cell stimulation can be used.
17. 4% formaldehyde is also a suitable fixative as an alternative to paraformaldehyde. To make 4% formaldehyde, mix 5 ml of a 40% formaldehyde solution (BDH), 5 ml of 10x PBS, and 40 ml of water.
18. Washing steps to remove growth media, fixative, and permeabilizing solution do not require an incubation period. Simply apply the PBS and aspirate.
19. The volume of antibody required for immunostaining can be reduced by using a staining/Petri dish. To prepare the dish, two pieces of gel blotting paper are placed in the bottom of an agar plate and dampened with water. The blotting paper is then covered with a piece of Parafilm (or equivalent) and the coverslips placed on top of the Parafilm, cell side facing up. This setup can be reused, but the gel blotting paper needs to be dampened before each use.
20. Washing steps to remove unbound antibody require a 30-second incubation period of the coverslips with the PBS. To further minimize nonspecific staining with either primary or secondary antibodies, the incubation period during the PBS washes can be extended to anywhere from 5–30 minutes per wash.
21. Prior to mounting the coverslip on the glass slide, gently dab the edge of the coverslip onto a Kimwipe to remove excess PBS. Avoid trapping air bubbles under the coverslips: Slowly apply the coverslip to the mounting media by gently guiding it onto the media using fine forceps or a needle.
22. The selection of appropriate cells to an image is critical. A wide variation in the level of expression of the fusion proteins will be apparent. Avoid imaging cells with high levels of protein expression, which can cause aberrant cell behavior and reduced responsiveness to hormonal or GF stimulation [7]. It is also preferable to choose separated cells to minimize the influence of cell-cell contact on cellular responses to hormonal or GF stimulation. Laser attenuation should be set at levels such that the signal is not saturating.
23. The ImageJ program can be downloaded from rsb.info.nih.gov/ij/.
24. The level of pixel fluorescence intensity should be fairly uniform throughout the cytosol. Higher cytosolic fluorescence observed near the center of the cell compared to the periphery may indicate that the cell has not completely spread due to high expression levels of the GFP-fusion protein and interference with normal cell adhesion processes.

References

1. Cantley LC. The phosphoinositide 3-kinase pathway. Science 2002;296:1655–7.
2. Czech MP. PIP2 and PIP3: Complex roles at the cell surface. Cell 2000;100:603–6.
3. Salim K, Bottomley MJ, Querfurth E, Zvelebil MJ, Gout I, Scaife R, Margolis RL, Gigg R, Smith CI, Driscoll PC, Waterfield MD, Panayotou G. Distinct specificity in the

recognition of phosphoinositides by the pleckstrin homology domains of dynamin and Bruton's tyrosine kinase. EMBO J 1996;15:6241–50.
4. Venkateswarlu K, Oatey PB, Tavare JM, Cullen PJ. Insulin-dependent translocation of ARNO to the plasma membrane of adipocytes requires phosphatidylinositol 3-kinase. Curr Biol 1998;8:463–6.
5. Venkateswarlu K, Gunn-Moore F, Oatey PB, Tavare JM, Cullen PJ. Nerve growth factor- and epidermal growth factor-stimulated translocation of the ADP-ribosylation factor-exchange factor GRP1 to the plasma membrane of PC12 cells requires activation of phosphatidylinositol 3-kinase and the GRP1 pleckstrin homology domain. Biochem J 1998;335(Pt 1):139–46.
6. Varnai P, Rother KI, Balla T. Phosphatidylinositol 3-kinase-dependent membrane association of the Bruton's tyrosine kinase pleckstrin homology domain visualized in single living cells. J Biol Chem 1999;274:10983–9.
7. Varnai P, Bondeva T, Tamas P, Toth B, Buday L, Hunyady L, Balla T. Selective cellular effects of overexpressed pleckstrin-homology domains that recognize PtdIns(3,4,5)P_3 suggest their interaction with protein binding partners. J Cell Sci 2005;118:4879–88.
8. Mitchell CA, Gurung R, Kong AM, Dyson JM, Tan A, Ooms LM. Inositol polyphosphate 5-phosphatases: Lipid phosphatases with flair. IUBMB Life 2002;53:25–36.
9. Whisstock JC, Wiradjaja F, Waters JE, Gurung R. The structure and function of catalytic domains within inositol polyphosphate 5-phosphatases. IUBMB Life 2002;53:15–23.
10. Schmid AC, Wise HM, Mitchell CA, Nussbaum R, Woscholski R. Type II phosphoinositide 5-phosphatases have unique sensitivities towards fatty acid composition and head group phosphorylation. FEBS Lett 2004;576:9–13.
11. Dyson JM, Kong AM, Wiradjaja F, Astle MV, Gurung R, Mitchell CA. The SH2 domain containing inositol polyphosphate 5-phosphatase-2: SHIP2. Int J Biochem Cell Biol 2005;37:2260–5.
12. Lowe M. Structure and function of the Lowe syndrome protein OCRL1. Traffic 2005;6:711–9.
13. Ooms LM, Fedele CG, Astle MV, Ivetac I, Cheung V, Pearson RB, Layton MJ, Forrai A, Nandurkar HH, Mitchell CA. The inositol polyphosphate 5-phosphatase, PIPP, is a novel regulator of phosphoinositide 3-kinase-dependent neurite elongation. Mol Biol Cell 2006;17:607–22.
14. Hama H, Torabinejad J, Prestwich GD, DeWald DB. Measurement and immunofluorescence of cellular phosphoinositides. Methods Mol Biol 2004;284:243–58.
15. Layton MJ, Harpur AG, Panayotou G, Bastiaens PI, Waterfield MD. Binding of a diphosphotyrosine-containing peptide that mimics activated platelet-derived growth factor receptor beta induces oligomerization of phosphatidylinositol 3-kinase. J Biol Chem 1998;273:33379–85.
16. Kimber WA, Trinkle-Mulcahy L, Cheung PC, Deak M, Marsden LJ, Kieloch A, Watt S, Javier RT, Gray A, Downes CP, Lucocq JM, Alessi DR. Evidence that the tandem-pleckstrin-homology-domain-containing protein TAPP1 interacts with Ptd(3,4)P_2 and the multi-PDZ-domain-containing protein MUPP1 *in vivo*. Biochem J 2002;361:525–36.
17. Abramoff M, Magelhaes P, Ram S. Image processing with ImageJ. Biophoton Int 2004;11:36–42.

Chapter 16
Measuring Phospholipase D Activity in Insulin-Secreting Pancreatic β-Cells and Insulin-Responsive Muscle Cells and Adipocytes

Rosanna Cazzolli, Ping Huang, Shuzhi Teng and William E. Hughes

Abstract Phospholipase D (PLD) is an enzyme producing phosphatidic acid and choline through hydrolysis of phosphatidylcholine. The enzyme has been identified as a member of a variety of signal transduction cascades and as a key regulator of numerous intracellular vesicle trafficking processes. A role for PLD in regulating glucose homeostasis is emerging as the enzyme has recently been identified in events regulating exocytosis of insulin from pancreatic β-cells and also in insulin-stimulated glucose uptake through controlling GLUT4 vesicle exocytosis in muscle and adipose tissue. We present methodologies for assessing cellular PLD activity in secretagogue-stimulated insulin-secreting pancreatic β-cells and also insulin-stimulated adipocyte and muscle cells, two of the principal insulin-responsive cell types controlling blood glucose levels.

Keywords Phospholipase D · insulin · GLUT4 · adipocyte 3T3-L1 · myotube · L6 · MIN6 · pancreatic β-cell

16.1 Introduction

Phospholipase D (PLD) was first described as a lecithinase in the 1940 s [1] and is now recognized as a phosphodiesterase that catalyzes the hydrolysis of the most abundant cellular membrane phospholipid, phosphatidylcholine (lecithin). In mammalian cells, phosphatidylcholine hydrolysis by PLD produces soluble choline and phosphatidic acid. In the 1980 s, this activity, which in unstimulated cells is generally quite low, was seen to be increased by a number of agonists including a variety of growth factors, cytokines, and hormones [2]. PLD has consequently often been thought of as a signaling enzyme; indeed, its activity is associated with a number of signaling cascades (reviewed by Jenkins and Frohman [3]). In addition, PLD activity has also been associated with a

W. E. Hughes
Phospholipid Biology Group, Department of Medicine, Garvan Institute of Medical Research, University of New South Wales, St. Vincent's Hospital, Sydney, New South Wales, Australia

B. Larijani et al. (eds.), *Lipid Signaling Protocols*, DOI: 10.1007/978-1-60327-115-8_16,

number of intracellular vesicular trafficking processes (also reviewed by Jenkins and Frohman), including those associated with the Golgi [4], endocytosis [5], and exocytosis from neurons [6] and endocrine cells [7, 8]. Phospholipase D activity has also been associated with increases in the uptake of glucose triggered by the hormone insulin [9, 10]. However, in many of these vesicle trafficking processes, the direct role for the activity of the enzyme is only partially understood.

A primary function of the hormone insulin in mammalian organisms is to control glucose homeostasis. This is achieved through appropriately regulated exocytosis of insulin from pancreatic β-cells, which, in turn, regulates major metabolic processes, including the promotion of glucose uptake into adipocytes and myotubes and the inhibition of gluconeogenesis in the liver. Insulin exocytosis and its metabolic effects are mediated by a complex series of signaling cascades, defects in which can cause diabetes. In the case of insulin secretion from pancreatic β-cells, signaling cascades are triggered by a variety of stimuli, such as glucose, hormones, or neurotransmitters. Subsequent metabolic and receptor-mediated signaling cascades generally result in an increase in cytosolic calcium, which then triggers insulin vesicle/granule exocytosis [11–13]. In the case of muscle and adipose cells, signaling is initiated when insulin binds to its receptor(s). Activated receptor(s) phosphorylate and recruit downstream effector proteins, in two principal signaling cascades involving phosphatidylinositol 3-kinase (PI3 K) and protein kinase B (PKB/Akt) or a Ras-mitogen-activated protein kinase (MAPK) pathway [14]. Glucose uptake into muscle and adipose tissues is regulated by insulin via the PI3 K-PKB-dependent arm of the insulin signaling pathway, resulting in the exocytosis of vesicles containing the glucose transporter, GLUT4, from intracellular compartments to the plasma membrane. Fusion of these vesicles with the plasma membrane allows glucose to enter the cell via facilitated transport through GLUT4 [15].

Phospholipase D activity has been associated with both stimulated insulin exocytosis from pancreatic β-cells [7] and insulin-dependent fusion of GLUT4-containing vesicles with the plasma membrane in adipocytes [10] and muscle cells (Cazzolli and Hughes, unpublished data).

Studies into the role of cellular PLD activity are normally relatively straightforward, with good and specific assays having been in use for a number of years [16]. However, studies particularly with respect to the enzyme's role in insulin-signaling cascades and insulin-regulated vesicular trafficking are complicated by the requirements for maintaining and differentiating insulin-sensitive cell lines. Specifically, measuring cellular PLD activity, without attenuating insulin's effect on its signaling cascade, is a major concern if meaningful insight into the role of this enzyme is to be achieved. Here we present detailed protocols for culturing and differentiating insulin-secreting and insulin-responsive cell lines, with particular emphasis on ensuring that the responsiveness of the cells is maintained. We provide protocols to radioactively label cellular phospholipids within appropriately differentiated cells and to produce a metabolically stable

and unique labeled phospholipid PLD product. We also detail phospholipid extraction protocols and a chromatographic separation technique to allow quantitation of the PLD product, providing an indication of relative cellular PLD activity.

16.2 Materials

16.2.1 Cell Culture for MIN6 Pancreatic β-Cells, L6 Myoblasts, and 3T3-L1 Fibroblasts

1. MIN6 murine pancreatic β-cells (*see* Note 1) are grown in high-glucose (25 mM) Dulbecco's Modified Eagle Medium (DMEM; Gibco/BRL) supplemented with 10% fetal calf serum (FCS; Trace, Melbourne, Australia), 15 mM HEPES, 50 IU/ml of penicillin, and 50 μg/ml of streptomycin (Gibco/BRL). Similarly supplemented low-glucose (5 mM) DMEM (Gibco/BRL) is also used.
2. L6 rat skeletal myoblasts (*see* Note 1) are grown in minimal essential media-α (αMEM; Gibco/BRL, Gaithersburg, MD) supplemented with 10% fetal calf serum (FCS; Trace, Melbourne, Australia) and 1% antibiotic/antimycotic (Gibco/BRL; equivalent to 100 U/ml of penicillin G sodium, 100 μg/ml of streptomycin sulfate, and 0.25 μg/ml pf amphotericin B).
3. 3T3-L1 fibroblasts (*see* Note 1) are grown in DMEM (Gibco/BRL) supplemented with 10% fetal bovine serum (FBS; HyClone, Logan, UT), 2 mM glutamine (Gibco/BRL), 100 IU/ml of penicillin, and 100 μg/ml of streptomycin (Gibco/BRL).
4. Modified Krebs-Ringer bicarbonate buffer (KRB; *see* Note 2): 136 mM NaCl, 4.7 mM KCl, 5 mM $NaHCO_3$, 1.2 mM $MgSO_4$ (7 H_2O), 1.2 mM KH_2PO_4, 1 mM $CaCl_2$, 10 mM HEPES (pH 7.4), glucose 2.8 or 25 mM, 0.5% albumin (bovine serum; BSA, Sigma, A7030).
5. Insulin (Sigma; St Louis, MO) or, alternatively, the human insulin analog Actrapid^{TM} from Novo Nordisk (Copenhagen, Denmark) was used. For 3T3-L1 fibroblast differentiation, prepare a 2-mg/ml insulin stock (Sigma) in 3 mM HCl and store at 4°C. To use, dilute 1:500 in complete media.
6. Dexamethasone (Sigma): Prepare a stock solution at 0.39 mg/ml in 100% ethanol, store at −20°C. Dilute 1:4,000 in media for differentiation.
7. 3-Isobutyl-1-methylxanthine (IBMX, Sigma): Prepare fresh each time. Make a stock of 57.5 mg/ml in dimethyl sulfoxide (DMSO) and dilute 1:500 in complete media for differentiation.
8. Trypsin (JRH Biosciences): equivalent to 0.012% trypsin in Dulbecco's PBS with 0.02% EDTA and 0.04% glucose.
9. 10 mM phosphate buffered saline: 137 mM NaCl, 2.7 mM KCl, 4.3 mM $Na_2HPO_4.7\,H_2O$, 1.4 mM KH_2PO_4.

16.2.2 In vivo *Phospholipase D Assay*

1. Palmitic acid [9,10-^{3}H(N)] (American Radiolabeled Chemicals, St Louis, MO, or Perkin Elmer, Boston, MA); myristic acid [9,10-^{3}H(N)] is from Perkin Elmer.
2. Phorbol 12-myristate 13-acetate (PMA, Sigma) is dissolved at 0.1 mM in DMSO and stored in aliquots at −80°C.
3. A 10 μM working solution of insulin for PLD assay is made fresh by diluting neat insulin (Actrapid^{TM}) 1:60 into water. This working solution can then be diluted 1:100 directly into culture medium to give a final concentration of insulin of 100 nM.

16.2.3 Phospholipid Extraction, Separation, and Quantification

1. Chloroform and methanol, analytical grade (Sigma).
2. 0.88% KCl (Sigma) in water.
3. Thin layer chromatography plates: LK5D Silica Gel 150 A (Whatman, UK).
4. 1,2-Dipalmitoyl-*sn*-Glycero-3-Phosphobutanol (PtdBut) is from Avanti Polar Lipids (Alabaster, AL).
5. 1% oxalic acid (Sigma); 2 mM EDTA (Sigma) w/v in methanol:water 2:3 (*see* Note 3).
6. Butan-1-ol; ethyl acetate; 2,2,4-trimethyl pentane; acetic acid (glacial); all analytical grade; and iodine (Sigma).
7. EN^{3}Hance (Perkin Elmer).
8. Teflon cell scrapers (Fisher).
9. Scintillation fluid, Ultima Gold XR (Perkin Elmer).

16.3 Methods

16.3.1 Cell Culture and Differentiation

16.3.1.1 Culture of MIN6 Pancreatic β-Cells

MIN6 pancreatic β-cells are maintained at 37°C and 5% CO_2 in supplemented DMEM (as described above). Stock flasks are usually split every 3 to 4 days, when the cells are approximately 60–70% confluent. MIN6 cells are well differentiated and do not grow well when split too hard, growing best when allowed to readhere in small clumps of two to three cells rather than as single cells. MIN6 cells secrete insulin in response to glucose as a secretory stimulus but lose this capacity after approximately passage 42. Consequently, cells are routinely tested for secretory competence (by insulin RIA, protocols not detailed here) and are generally only used between passages 25–42. For

experimentation cells, $\sim 5 \times 10^6$ cells/well of a 6-well plate are incubated overnight in high-glucose DMEM (as described above) before incubation for 24–48 h in low-glucose DMEM (as described above).

16.3.1.2 Culture and Differentiation of L6 Myoblasts

L6 myoblasts are maintained at 37°C and 5% CO_2 in supplemented αMEM (as described above). Stock 10-cm dishes (Falcon) are usually split every 3 to 4 days, when the cells are approximately 60–70% confluent. L6 myotubes will align and spontaneously start to differentiate if they reach full confluency. Hence, to avoid selecting for myoblasts with a nonfusing phenotype, it is imperative that stock dishes of L6 myoblasts are not allowed to exceed 60–70% confluency. Furthermore, stocks should not be kept beyond 12 to 15 passages, as their ability to differentiate and their response to insulin will be diminished. For splitting, dishes are washed twice in 5 ml of warm PBS and then rinsed in 1 ml of warm trypsin, most of which is then removed. The dish is incubated for approximately 3 minutes at 37°C, and then 5 ml of warm supplemented α-MEM (10% FCS plus antimicrobials) is added to harvest the cells. Usually, the cells are split 1:6–1:10 into new 10-cm stock dishes.

In order to differentiate the myoblasts into myotubes for experiments, the cells are seeded in supplemented αMEM, with one 10-cm dish at approximately 80–90% confluence usually being sufficient to seed two 12-well plates (2×10^4 cells/well) or one 6-well plate (6×10^4 cells/well). At confluence, usually 3 to 4 days after seeding, the media is changed to αMEM supplemented with only 2% FCS and antimicrobials, to initiate differentiation. This media is changed daily for the first 3 to 4 days of the differentiation process and every 2 days thereafter. The cells are used after approximately 5 to 7 days of differentiation.

16.3.1.3 Culture and Differentiation of 3T3-L1 Fibroblasts

Murine 3T3-L1 fibroblasts are cultured in DMEM (as above) at 37°C in 8% CO_2 (*see* Note 4). These cells can be passaged at least 10 times (and probably longer) provided the fibroblasts are maintained rigorously. Differentiation is based on established protocols [17]. Plates/flasks are usually split every 4 days and seeded at a lower cell density to prevent cells from becoming confluent. Normally, a 15-cm plate or T150 flask can be seeded with $6–10 \times 10^4$ cells. For differentiation, 3T3-L1 fibroblasts are seeded at 18×10^4 cells/well and 10×10^4 cells/well for 6-well and 12-well dishes, respectively, and fed with fresh media every 4 days. Differentiation is induced according to established protocols. Briefly, 3T3-L1 fibroblasts are allowed to grow at least 2 days past confluence (8 days after plating). Differentiation is induced (on day 0) with complete medium containing 0.25 μM dexamethasone, 4 μg/ml of insulin, and 500 μM 3-isobutyl-1-methylxanthine. After 4 days in differentiation media, the cells are

fed with complete medium containing 4 μg/ml of insulin (*see* Note 5). After 4 more days, the cells are refed every 2 days with complete medium. Differentiation is monitored by noting the accumulation of lipid droplets, which typically appear by day 4 of differentiation. Cells are considered fully differentiated between days 8 and 12.

16.3.2 In vivo *Phospholipase D Activity Assay*

Cellular PLD activity can be measured most readily using an *in vivo* transphosphatidylation reaction [16]. Measuring PLD activity through depletion of phosphatidylcholine substrate is not possible, as phosphatidylcholine makes up a significant proportion of total cellular phospholipid and the component metabolized by PLD is generally very small. In addition, there are, of course, numerous PLD-independent routes by which phosphatidylcholine can be metabolized. Similarly, phosphatidic acid, the product of PLD hydrolysis, can be rapidly synthesized and metabolized in an agonist-stimulated, PLD-independent manner and is also therefore unsuitable for use as a measurement of cellular PLD activity. PLD activity has been monitored using a single-cell microscope-based Forester Resonant Energy Transfer assay. However, this is unsuitable for routine activity screens and requires specialist equipment [18]. PLD retains the unique ability to transphosphatidylate primary alcohols such as ethanol or butan-1-ol and will, in the presence of primary alcohol, produce phosphatidlyalcohol in preference to phosphatidic acid. Accumulation of phosphatidylalcohol, which is generally metabolically stable, can be used as an indication of relative PLD activity when control (basal) and treated conditions are compared. However, we and others have found that alcohol substrate (such as butan-1-ol) decreases insulin receptor activation [10, 19, 20]. Therefore, insulin is added first for 5 minutes to preactivate insulin receptor before the addition of butan-1-ol to increase the sensitivity of the assay. PMA, a potent activator of cellular PLD, is used as a positive control.

16.3.2.1 MIN6 Phospholipase D Activity Assay

1. MIN6 pancreatic β-cells in 6-well plates are incubated in the presence of 4 μCi/ml [^{3}H] palmitic acid or myristic acid in supplemented low-glucose DMEM for a minimum of 7 h.
2. Media is aspirated and the cells briefly washed into modified KRB before being incubated in fresh modified KRB for 30 min.
3. For stimulated PLD activity, cells are then incubated with or without an appropriate stimulus, such as secretagogues including glucose (11.1 -> 25 mM), carbamoylcholine (cholinergic receptor agonist 100 μM), or hormones, in modified KRB containing 0.3% butan-1-ol for 30 min to 1 h. For

PMA-stimulated PLD activity, cells are incubated with 100 nM PMA and 0.3% butan-1-ol for 30 min.
4. At the end of incubation, aspirate the medium and add 0.5 ml of ice-cold methanol to each well of the 6-well plate.
5. Cells are scraped and collected into microcentrifuge tubes on ice.

16.3.2.2 L6 Myotube Phospholipase D Activity Assay

1. L6 myotubes in 6-well plates are incubated in the presence of 4 μCi/ml [^{3}H] palmitic acid or myristic acid in serum-free α-MEM for a minimum of 7 h.
2. For insulin-stimulated PLD activity, myotubes are incubated with 1, 50, or 100 nM insulin for 5 min prior to the addition of 0.3% butan-1-ol for 30 min. For PMA-stimulated PLD activity, myotubes are incubated with 100 nM PMA and 0.3% butan-1-ol for 30 min.
3. At the end of incubation, aspirate the medium and add 0.5 ml of ice-cold methanol to each well of the 6-well plate.
4. Myotubes are scraped and collected into microcentrifuge tubes on ice.

16.3.2.3 3T3-L1 Adipocyte Phospholipase D Activity Assay

1. 3T3-L1 adipocytes in 6-well or 12-well plates are serum-starved overnight (0.5% BSA in DMEM) in the presence of 4 μCi/ml [^{3}H] palmitic acid.
2. For insulin-stimulated PLD activity, adipocytes are incubated with 100 nM insulin for 5 min prior to the addition of 0.3% 1-butanol for 30 min. For PMA-stimulated PLD activity, cells are incubated with DMEM containing 100 nM PMA and 0.3% butan-1-ol for 30 min.
3. At the end of incubation, aspirate the medium and add 0.5 ml of ice-cold methanol to each well of the 6-well plate. It is important to note that special care must be taken not to damage the cell monolayer, because the monolayer is fragile at this time and can be damaged by suction or the careless addition of media.
4. Adipocytes are scraped and collected into microcentrifuge tubes on ice.

16.3.3 Phospholipid Extraction, Separation, and Quantification

1. To the methanol cell extracts, add 0.5 ml of chloroform, for a final chloroform:methanol ratio of 1:1. Mix well by vortex and incubate for 15 min at room temperature.
2. Add 0.45 ml of water or 0.88% KCl solution to each tube and mix well by vortex.
3. Centrifuge for 5 min at ~800 × *g* to promote phase separation.

4. Carefully remove the upper aqueous phase and take 20 µl of the lower organic phase for scintillation counting to determine total labeled phospholipids (*see* Note 6). The remainder of the organic phase is dried by vacuum centrifugation or under a nitrogen stream. At this point the samples can either be spotted onto pre-equilibrated TLC plates (as described below) or stored at −20°C for future processing.
5. LK5DF silica gel TLC plates are activated by soaking in 1% oxalic acid/2 mM EDTA in methanol:water (2:3), described in step 5 of Subheading 16.2.3, for 2 min before baking in an oven for at least 15 min at 110°C (*see* Note 7).
6. Resuspend the dried samples in 25 µl of chloroform/methanol (19:1;v/v). If desired, 50 µg of authentic PtdBut can be included in the chloroform/methanol resuspending solution as an internal standard, where iodine is to be used to visualize phospholipids.
7. Sample are spotted onto activated TLC plates at least 2 cm from the bottom of the plate (*see* Note 8).
8. When dry, the plate is developed in a TLC tank and pre-equilibrated (*see* Note 9) with the organic phase of ethylacetate:trimethylpentane:acetic acid:water (110:50:20:100; v/v/v/v). These solvents should be mixed in a separating funnel in a fume hood and allowed to stand until the upper organic and lower inorganic phases are separated. The upper phase is used to fill a TLC tank to a depth of no more than 2 cm.
9. Chromatographic separation in this solvent system takes approximately 1.5 h, by which time the solvent front is usually 2–3 cm from the top of the plate. The plate is removed from the TLC tank and briefly air-dried in the fume hood.

10a. The plate can be placed in a iodine atmosphere tank to stain for about 15–30 min. Use a soft pencil to mark the position of PtdBut, the retention factor (Rf) of which should be 0.3–0.4. Dry the plate in the hood until all the yellowish staining is gone.

10b. Alternatively, radiolabeled phospholipids can be visualized through a combination of autoradiography and fluorography. For this method, the TLC plates can be sprayed three times with a fluorescent intermediate autoradiography enhancer (EN^{3}Hance; *see* Note 10). The plates should be sprayed while still in the fume hood and allowed to dry for 10 min between each spray. The plates are exposed on film for about 5 days at –80°C. Once the film has been developed, the TLC plate can be oriented on the film over a lightbox to identify the position of PtdBut, the retention factor (Rf) of which should be 0.3–0.4. An example is shown in Fig. 16.1.

11. PtdBut spots are scraped from the plate into approximately 0.5 ml of methanol and scintillation fluid and used for counting in a scintillation counter.
12. An assessment of PLD activity is calculated as [^{3}H]-PtdBut and can be related to percentage of total phospholipids as required.

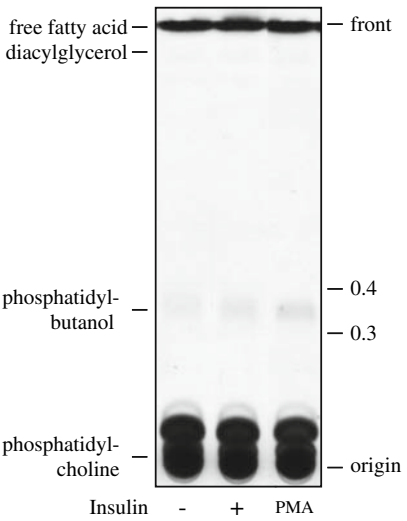

Fig. 16.1 An example of radiolabeled L6 myotube phospholipids separated by TLC. L6 cells were cultured as described and labeled with [^{3}H] myristic acid for 7 h before 10 minutes of treatment with or without 100 nM insulin or 10 nM PMA (as indicated) prior to the addition of 0.3% (v/v) butan-1-ol. Phospholipids were extracted and separated before visualization as described

Notes

1. MIN6 murine pancreatic β-cells are from Miyazaki et al. [21]; L6 rat skeletal myoblasts and 3T3-L1 murine fibroblasts are from ATCC.
2. Modified Krebs-Ringer bicarbonate buffer (KRB) is made up fresh from a 2x stock of 272 mM NaCl, 9.4 mM KCl, 10 mM $NaHCO_3$, 2.4 mM $MgSO_4$ (7 H_2O), 2.4 mM KH_2PO_4 with distilled water. To this are added $CaCl_2$ and HEPES to a final concentration of 1 mM and 10 mM, respectively, and glucose to a final concentration of either 2.8 or 25 mM. The solution is bubbled with ~5% CO_2 for 15 minutes and pH 7.4 confirmed. Albumin (bovine serum, BSA) is added to a final concentration of 5% (w/v) and the resultant solution is used within 1 h.
3. Add 400 μl of 500 mM EDTA to 60 ml of water and dissolve 1 g of oxalic acid in this solution. Once all the oxalic acid has dissolved, add 40 ml of methanol. Final concentrations are 1% oxalic acid:2 mM EDTA in methanol:water (2:3).
4. We have found that 3T3-L1 fibroblasts differentiate substantially better in an 8% CO_2 environment rather than 5% CO_2.
5. It is important to note that special care must be taken not to damage the cell monolayer, because the monolayer is extremely fragile at this time and can be damaged by suction or the careless addition of media.
6. Cell debris and protein form a white precipitate at the interface, which should also be carefully removed.
7. We use activated TLC plates. Once cooled, however, plates remain usable for several days/weeks.
8. Spots should be kept as small as possible to give the best resolution. To help achieve this, samples can be spotted in small increments (placed to be above the solvent level in the tank).
9. To help saturate the atmosphere of the tank, it should be lined with blotting paper prewetted with the organic solvent solution. Place the lid on the tank and allow it to saturate for at least 30 minutes before placing TLC plates inside.
10. As described in the manufacturer's instructions, it is important to avoid oversaturating the TLC plate when spraying with EN^{3}Hance.

References

1. Hanahan DJ, Chaikoff IL. The phosphorous-containing lipides of the carrot. J Biol Chem 1947;168:233–40.
2. Exton JH. Phospholipase D-structure, regulation and function. Rev Physiol Biochem Pharmacol 2002;144:1–94.
3. Jenkins GM, Frohman, MA. Phospholipase D: A lipid centric review. Cell Mol Life Sci 2005;62:2305–16.
4. Chen YG, Siddhanta A, Austin CD, Hammond SM, Sung TC, Frohman MA, Morris AJ, Shields D. Phospholipase D stimulates release of nascent secretory vesicles from the trans-Golgi network. J Cell Biol 1997;138:495–504.
5. Shen Y, Xu L, Foster DA. Role for phospholipase D in receptor-mediated endocytosis. Mol Cell Biol 2001;21:595–602.
6. Humeau Y, Vitale N, Chasserot-Golaz S, Dupont JL, Du G, Frohman MA, Bader MF, Poulain B. A role for phospholipase D1 in neurotransmitter release. Proc Natl Acad Sci USA 2001;98:15300–5.
7. Hughes WE, Elgundi Z, Huang P, Frohman MA, Biden TJ. Phospholipase D1 regulates secretagogue-stimulated insulin release in pancreatic beta-cells. J Biol Chem 2004;279:27534–41.
8. Vitale N, Caumont AS, Chasserot-Golaz S, Du G, Wu S, Sciorra VA, Morris AJ, Frohman MA, Bader MF. Phospholipase D1: A key factor for the exocytotic machinery in neuroendocrine cells. EMBO J 2001;20:2424–34.
9. Emoto M, Klarlund JK, Waters SB, Hu V, Buxton JM, Chawla A, Czech MP. A role for phospholipase D in GLUT4 glucose transporter translocation. J Biol Chem 2001;275:7144–51.
10. Huang P, Altshuller YM, Hou JC, Pessin JE, Frohman MA. Insulin-stimulated plasma membrane fusion of Glut4 glucose transporter-containing vesicles is regulated by phospholipase D1. Mol Biol Cell 2005;16:2614–23.
11. Straub SG, Sharp GW. Glucose-stimulated signaling pathways in biphasic insulin secretion. Diabetes Metab Res Rev 2002;18:451–63.
12. Gilon P, Henquin JC. Mechanisms and physiological significance of the cholinergic control of pancreatic beta-cell function. Endocr Rev 2001;22:565–604.
13. Bratanova-Tochkova TK, Cheng H, Daniel S, Gunawardana S, Liu YJ, Mulvaney-Musa J, Schermerhorn T, Straub SG, Yajima H, Sharp GW. Triggering and augmentation mechanisms, granule pools and biphasic insulin secretion. Diabetes 2002; 51 (Suppl 1):S83–S90.
14. Taniguchi CM, Emanuelli B, Kahn CR. Critical nodes in signalling pathways: Insights into insulin action. Nat Rev Mol Cell Biol 2006;7:85–96.
15. Bryant NJ, Govers R, James DE. Regulated transport of the glucose transporter GLUT4. Nat Rev Mol Cell Biol 2002;3:267–77.
16. Morris AJ, Frohman MA, Engebrecht J. Measurement of phospholipase D activity. Anal Biochem 1997;252:1–9.
17. Bogan JS, McKee AE, Lodish HF. Insulin-responsive compartments containing GLUT4 in 3T3-L1 and CHO cells: Regulation by amino acid concentrations. Mol Cell Biol 2001;21:4785–806.
18. Hughes WE, Larijani B, Parker PJ. Detecting protein-phospholipid interactions. Epidermal growth factor-induced activation of phospholipase D1b *in situ*. J Biol Chem 2002;277:22974–9.
19. Seiler AE, Henderson A, Rubin R. Ethanol inhibits insulin receptor tyrosine kinase. Alcohol Clin Exp Res 2000;24:1869–72.
20. Xu J, Yeon JE, Chang H, Tison G, Chen GJ, Wands J, de la Monte S. (2003) Ethanol impairs insulin-stimulated neuronal survival in the developing brain: Role of PTEN phosphatase. J Biol Chem 278:26929–37.

21. Miyazaki J, Araki K, Yamato E, Ikegami H, Asano T, Shibasaki Y, Oka Y, Yamamura K. Establishment of a pancreatic beta cell line that retains glucose-inducible insulin secretion: Special reference to expression of glucose transporter isoforms. Endocrinology 1990;127:126–32.

Chapter 17
Protein Kinase C as an Effector of Lipid-Derived Second Messengers

Marie-Hélène Paclet, Jan K. Davidson-Moncada, Guillermo López-Lluch, Dongmin Shao and Lodewijk V. Dekker

Abstract Members of the protein kinase C family are major effectors of lipid second messengers. We describe three protocols to assess protein kinase C activity in polymorphonuclear leukocytes (neutrophils). These methods are useful to study the activation and function of protein kinase C in these immune cells. Since neutrophils provide a ready source of human primary tissue, these methods are also useful for pharmacological studies on the protein kinase C system and for evaluation of protein kinase C activators and inhibitors in the context of human primary cells. Furthermore, since protein kinase C activity is determined by a number of lipid-generating signaling systems, the methods described here can also be employed to study the pharmacology of these "upstream" signaling systems.

Keywords Protein kinase C · PKC · neutrophils · lipid rafts · translocation

Abbreviations PKC: Protein kinase C; MβCD: Methyl-β-cyclodextrin; PBS: Phosphate buffered saline; TLCK: N-α-p-tosyl-L-lysine chloromethyl ketone; DFP: Di-isopropyl fluorophosphate.

17.1 Introduction

Protein kinase C (PKC) is a major component of the intracellular systems that translate extracellular cues into cellular responses [1–3]. The basic intracellular signal transduction pathway is dependent on the ability of particular cell surface receptors to stimulate the activity of phospholipase C, which in turn acts upon phosphatidylinositol-4,5-bisphosphate to yield the second messengers diacylglycerol and Ca^{2+} [via inositol-(1,4,5) trisphosphate], which both act as allosteric activators of PKC. Once activated, PKC is thought to

L.V. Dekker
School of Pharmacy, Centre for Biomolecular Sciences, University Park, University of Nottingham, Nottingham, NG7 2RD, UK
e-mail: lodewijk.dekker@nottingham.ac.uk

B. Larijani et al. (eds.), *Lipid Signaling Protocols*, DOI: 10.1007/978-1-60327-115-8_17,

contribute to the cellular response by phosphorylation and modulation of effector proteins. It has recently become clear that inputs from other lipid-generating systems impinge on this basic control pathway. In particular, phosphatidylinositol-3,4,5-trisphosphate (PtdInsP_3) activates phosphoinositide-dependent kinase-1, which phosphorylates numerous kinases including PKC, a modification that is essential to its activity [4]. Since PtdInsP_3 itself can be seen as a second messenger, it thus appears that PKC activity is determined by the intracellular availability of a number of such messengers. The function of PKC is checked on this basis, not just acutely after receptor activation, when a burst of second messenger is generated, but also in time—by the continued presence of low amounts of second messenger inside the cell—and in space—by restricting the availability of second messenger inside the cell. Further control of PKC activity is dictated by its interaction with (subsets of) intracellular binding proteins, resulting in the compartmentalization of the kinase and its activity. This mechanism is now seen as a major means of control of intracellular PKC action.

PKC constitutes a family of kinases. The ability of these kinases to respond to (lipid) second messengers depends on the presence of certain conserved domains in their primary structure. Thus, diacylglycerol binds to the so-called C1 domain, which is also the binding site for phorbol esters, pharmacological activators of PKC [5]. The presence of C1 domains in other gene families explains why PKC is not the sole target of diacylglycerol/phorbol ester. The C2 domain of the classical isotypes (PKC-α, -β, and -γ) has long been identified as a major target for Ca^{2+}, and the presence of a Ca^{2+}-binding C2 domain in many other proteins conveys Ca^{2+} dependence upon many of these proteins [6]. In a recent innovation, the C2 domain of the PKC-ε isotype has been shown to be a target for phosphatidic acid, providing further complexity of this established signal transduction chain [7]. Domains such as the C2 domain of PKC-δ and the PB1 domain (in atypical PKCs) have been identified as protein interaction domains [8–12], with multiple other sites in the kinase also serving this function.

PKC isotypes are expressed throughout the body, although a degree of tissue specificity is attributed to some isotypes. Most, if not all, cell types express multiple PKC isotypes. The ubiquitous presence of PKC isotypes almost certainly reflects their importance for overall cell function. PKC function has been established using numerous approaches, ranging from genetic deletion to RNA interference and from cell biology to pharmacology. Such studies have revealed the importance of PKC isotypes for receptor signaling, cellular homeostasis, and cell survival/apoptosis as well as the regulation of more specialized cell functions in numerous tissues. Based upon these studies, PKC is considered a target in many indications, including inflammatory, cardiovascular, and neurological conditions. At the same time, PKC itself is a "readout" for those second messenger systems that lie "upstream." Overall, the study of the PKC system is a worthwhile endeavor in a basic biological as well as a more applied context.

Protocols for the general study of PKC are available from a recent volume in this series [13]. In this chapter, we present a number of techniques we employed when studying PKC isotype function in primary polymorphonuclear leukocytes (neutrophils). These cells are major participants in the innate immune response to infection. Therefore, the study of PKC isotypes in these cells is relevant in the general area of infection, inflammation, and associated diseases. However, since these cells provide a ready source of primary human tissue, which is generally difficult to obtain, they can be used for easy pharmacological evaluation of PKC inhibitors and activators on human isotypes in a native context. Furthermore, through the study of PKC itself, the system can be used for evaluation of its upstream activating systems, including the phospholipase C and possibly the phosphoinositide kinase systems. In interpreting the technology, it should be noted that neutrophils only contain a limited subset of PKC isotypes and that they lack PKC-γ, PKC-ε, and possibly PKC-θ [14]. This makes the assay systems described here useful filters for pharmacological evaluation of isotype-specific blockers. For instance, the NADPH oxidase response (Subheading 17.3.1) should not be affected by PKC-ε-, PKC-γ-, and possibly PKC-θ-specific blockers if these are truly specific for these isotypes.

One of the main functional responses of PKC in neutrophils is activation of the NADPH oxidase. We describe an NADPH oxidase measurement relying on oxygen consumption [15], which in our hands has been useful to assess both direct activation of PKC (using phorbol esters) and receptor activation of PKC (in the example, the Fcγ receptor) and for the evaluation of PKC antagonists on these different stimuli [16]. It should be noted that the response is also highly sensitive to wortmannin, indicating that the assay may be used to evaluate PI-3 kinase isotype function and pharmacology in these cells.

As mentioned, PKC itself is regulated by various signaling intermediates. The study of PKC in neutrophils is useful for evaluation of these upstream systems. We developed a simple redistribution assay using the disappearance of PKC from the cytosol fraction as readout [17]. The response most likely reflects activation of PKC, although the assay does not provide a mechanistic insight into PKC function since the target compartment is not defined (this may be plasma membrane, intracellular membranes, or cytoskeleton). Nevertheless, the assay has the advantage of being highly reliable and quantifiable; even when using these primary cells that are not synchronized in any way and may represent a heterogeneous population, we observed very little sample variation. Redistribution of PKC could be induced by phorbol esters as well as native receptors; in our example, it is the fMLP receptor. As such, this assay can be used to study the pharmacology of this receptor and its immediate signaling components. In a more involved analysis, we describe a fractionation protocol to isolate lipid rafts from neutrophils [18]. This membrane compartment is a subcellular target area for PKC isotypes, and PKC redistribution to this area may also be used as a measure of its activation.

17.2 Materials

17.2.1 Isolation of Neutrophils from Fresh Blood or Buffy Coats and NADPH Oxidase Assay

1. Blood sourced in the form of a "buffy coat," as supplied by the national blood bank, or taken from healthy volunteers was used to provide neutrophil isolates (*see* Note 1).
2. Phosphate buffered saline (PBS): Prepare 10x stock of 1.37 M NaCl, 27 mM KCl, 100 mM Na_2HPO_4, 18 mM KH_2PO_4 (adjust to pH 7.4 with HCl if necessary) and autoclave before storage at room temperature. PBS can also be purchased as powder or pills (e.g., Sigma).
3. Saline (0.9% w/v NaCl). Prepared as 10x solution.
4. 2x saline prepared from the above.
5. 2% (w/v) Dextran (ICN Biochemicals, Costa Mesa, CA) in 0.9% (w/v) NaCl solution, filtered on 0.22-μm filters and stored at 4°C.
6. Ficoll-Hypaque (Lymphoprep^{TM}) (Nycomed Pharma AS, Oslo, Norway).
7. Heparin (Sigma).
8. Conical centrifugation tubes (e.g., 50-ml Falcon).
9. RPMI 1640 (Gibco/Invitrogen).
10. Hemocytometer (Neubauer improved, Marienfeld, Germany).
11. Oxygen electrode (e.g., Rank Brothers, Cambridge, UK, www.rankbrothers.co.uk).
12. Chart recorder or computer connected to electrode.
13. Sodium dithionite (Sigma).

17.2.2 PKC Cytosol Depletion Assay

1. Sonication buffer: 10 mM Pipes (pH 7.0), 100 mM KCl, 3 mM NaCl, 35 mM $MgCl_2$, 20 μM leupeptin, 1.5 μM pepstatin, 10 μM TLCK (N-α-p-tosyl-L-lysine chloromethyl ketone), 10 μM di-isopropylfluorophosphate (DFP), 10 mM glycerophosphate, 25 mM NaF.
2. Sucrose cushion: 15% (w/w) sucrose in 10 mM Pipes (pH 7.0), 100 mM KCl, 3 mM NaCl, 35 mM $MgCl_2$, 20 μM leupeptin, 1.5 μM pepstatin, 10 μM TLCK, 10 μM DFP, 10 mM glycerophopsphate, 25 mM NaF.
3. SDS-PAGE gel (10% running gel). Gels can be purchased commercially (e.g., Invitrogen). Alternatively, for a 10-ml 10% running gel, combine 2.5 ml of 40% acrylamide/bisacrylamide, 0.15 ml of 20% SDS, 3.75 ml of 1 M Tris-Cl, pH 8.8, 3.6 ml of distilled water. Mix, add 10 μl of TEMED and 50 μl of 20% fresh ammonium peroxodisulfate, and pour in gel sandwich, leaving space for a stacking gel. Overlay the gel with saturated 1-butanol. Allow the gel to polymerize, wash away the butanol with distilled water, and insert an appropriate comb. Make a stacking gel consisting of 1.67 ml of 40% acrylamide/bisacrylamide, 50 μl of 20% SDS, 1.25 ml of 1 M Tris-Cl, pH 6.8, and 7 ml of

distilled water, mix, add 10 µl of TEMED and 50 µl of 20% fresh ammonium peroxodisulfate, mix, and pour into gel sandwich. Allow to set for 1 h.
4. Laemmli buffer consisting of 62.5 mM Tris-Cl, pH 6.8, 2% SDS, 10% glycerol, 1 mM β-mercaptoethanol, 0.1 mg/ml of bromophenol blue [19]. Prepare as a 4x stock solution.
5. Gel running buffer appropriate to the gel system used [25 mM Tris, 192 mM glycine, 0.1% (w/v) SDS, pH 8.8].
6. Towbin buffer [25 mM Tris, 129 mM glycine, 0.01% (w/v) SDS, 20% (v/v) methanol, pH 8.3) [20].
7. 3MM filter paper (Whatman) and Nitrocellulose (GE Healthcare, Amersham, UK).
8. PBS containing 0.05% (v/v) Tween 20. It can be purchased as pills.
9. PBS containing 0.05% (v/v) Tween 20 and either 2% (w/v) or 1% (w/v) fat-free milk powder.
10. Rabbit polyclonal immunoglobulins directed against PKC-βI (C-16), PKC-βII (C-18), PKC-δ (C-20), and PKC-ζ (C-20) (Santa Cruz Biotechnology, Santa Cruz, CA).
11. Secondary antibody, goat antirabbit (GE Healthcare, Amersham, UK).
12. ECL® detection kit (GE Healthcare, Amersham, UK).

17.2.3 PKC Recruitment to Lipid Rafts

1. HNE buffer: 20 mM HEPES, pH 7.0, 150 mM NaCl, 5 mM EDTA, 1% (v/v) Triton X-100.
2. Sucrose gradient: Prepare 80% (w/v) sucrose in HNE buffer and store at −20°C. From this, prepare solutions of 30% and 5% sucrose by diluting in HNE buffer.
3. Methyl-β-cyclodextrin (MβCD, Sigma).
4. RPMI-1640 (Gibco/Invitrogen).
5. 10x PBS.
6. Protease inhibitors (Sigma): Leupeptin: 1000x stock of 10 mg/ml in ethanol; DFP 1000x stock of 1 M in propanol-2; Pepstatin A: 1000x stock of 10 mg/ml in water; TLCK 1000x stock of 10 mg/ml in water; Aprotinin: 1000x stock of 10 mg/ml in water; PMSF: phenylmethylsulphonyl fluoride 1000x stock of 0.2 M in ethanol. Store protease inhibitors in aliquots at −20°C.
7. Materials for SDS-PAGE and Western blotting as described in Subheading 17.2.2.

17.3 Methods

17.3.1 Isolation of Neutrophils from Fresh Blood or Buffy Coats and NADPH Oxidase Assay

1. a. From buffy coat: Dilute buffy coats with 30% volume of normal saline. Add heparin to 5 U/ml. Mix gently by inversion, but do not shake (*see* Note 2).
   b. From fresh blood: Add 5 units of heparin/ml blood.

2. Add equal volume of 2% dextran for a final concentration of 1% (*see* Note 3). Mix by inversion (4–5 times). Do not shake (*see* Note 2).
3. Leave to sediment at room temperature for 1 h (a clear upper layer can be seen).
4. Recover the upper layer containing leukocytes in 50-ml Falcon tubes (40 ml per tube).
5. Underlay the cells with a 10-ml cushion of Ficoll-Hypaque using wide Pasteur pipettes to obtain a 20% final volume Ficoll-Hypaque cushion.
6. Centrifuge at 800 × *g* for 10 min at room temperature.
7. Aspirate supernatant and interphase.
8. Resuspend the pellet in water for 10–20 s (this will lyse any erythrocytes).
9. Immediately add an equal volume of 2x saline.
10. Centrifuge at 300 × *g* for 5 min at room temperature.
11. Leukocyte pellet will be around 95% pure neutrophils, which can be checked by flow cytometry.
12. Resuspend cells in RPMI 1640 (*see* Note 2).
13. Count cells using a hemocytometer.
14. Set up the oxygen electrode following the manufacturer's instructions (www.rankbrothers.co.uk).
15. The maximum response can be calibrated using dithionite. Dithionite is a reducing agent that will "consume" all oxygen. The concentration of dissolved molecular oxygen in water at 37°C is 230 nmol/ml [15].
16. Perform the incubations on a time schedule.
17. Resuspend neutrophils in RMPI 1640 (Gibco/Invitrogen), at 5×10^7 cells/ml (*see* Note 2).
18. Preincubate 1 ml of the neutrophil suspension for 15 min with the desired concentration of inhibitor.
19. Place 1 ml of neutrophil suspension (5×10^7 cells) inside the electrode chamber and close the chamber.
20. Equilibrate for 2 min.
21. Add stimulus (e.g., PMA) at a concentration of 0.1 μg/ml.
22. Follow response for 5 min or as long as desired.
23. NADPH oxidase activity can be quantified by determining the maximum rate of oxygen consumption (mol O_2 consumed/min/10^7 PMNs) (Fig. 17.1).

17.3.2 PKC Cytosol Depletion Assay

1. Resuspend neutrophils (*see* Subheading 17.3.1) at 1×10^8 cells/ml in RPMI 1640 medium (*see* Note 2).
2. Divide into 100-μl fractions (1×10^7 cells) in 1.5-ml Eppendorf tubes and stimulate as required. In the example, cells were stimulated with 10 μM fMLP for 5 min at 37°C or with 400 nM PMA for 5 min at 37°C.
3. Stop the reaction by adding 8 volumes (800 μl) of ice-cold PBS. Place the tube on ice.

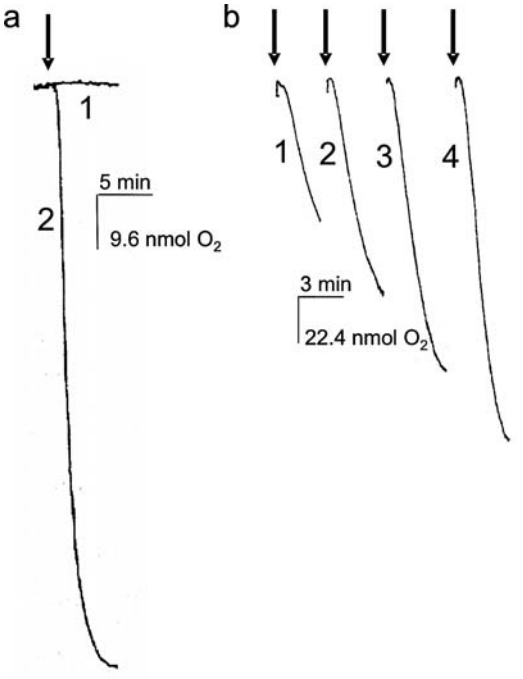

Fig. 17.1 Neutrophil oxygen consumption assays. (a) 5×10^7 neutrophils were preincubated for 5 minutes at 37°C in a Clark cell and then treated with (trace 2) (50 nmol O_2/min/5×10^7neutrophils) or without (trace 1) (0.9 nmol O_2/min/5×10^7neutrophils) PMA (0.1 μg/ml) and the oxygen consumption was determined. (b) Neutrophils were incubated with increasing concentrations of IgG-opsonized *S.aureus* (the ratio of particles:cells was 1.5, 3, 6, and 9, increasing oxygen consumption to 39, 47, 64, and 89 nmol O_2/min/5×10^7neutrophils, respectively). Arrows indicate the point of stimulation after preincubation at 37°C and stabilization of the trace. Inset: PMA and IgG-opsonized *S.aureus*-induced oxygen consumption rates in the presence of PKC inhibitors

	IC_{50} NADPH oxidase	
Compound	**PMA**	**Opsonized *S.aureus***
Bisindolylmaleimide I	2.1 ± 0.27 μM	2.4 ± 0.41 μM
Ro-31-8220	580 ± 22 nM	3.6 ± 2.6 μM
Go 6976	602 ± 92 nM	380 ± 24 nM

4. Centrifuge the cells at 14,000 × *g* for 1 min at 4°C.
5. Resuspend the cell pellet in 400 μl of ice-cold sonication buffer. Sonicate cells three times for 5 s on ice (*see* Note 4).
6. Centrifuge at 1,000 × *g* for 15 min to remove nuclei and unbroken cells.
7. Collect the (postnuclear) supernatant containing both membrane and cytosolic proteins and layer on a 15% (w/w) sucrose cushion.
8. Centrifuge at 150,000 × *g* for 75 min at 4°C (TLS 55 rotor; Beckman Instruments, Fullerton, CA). Collect the top fraction representing the cytosol.
9. Analyze an aliquot by SDS-PAGE. Add 4x Laemmli buffer to the sample and load the gel. Run for 1 h at 30 mA (depending on the gel system used).
10. Transfer proteins onto a nitrocellulose membrane at 100 mA for 1 h (*see* Note 5).

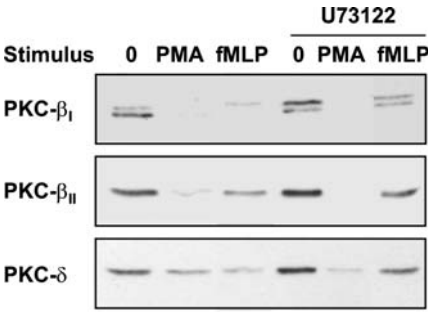

Fig. 17.2 Pharmacological analysis of PKC activation. Western blot analysis of cytosolic fractions isolated from neutrophils stimulated by either PMA (400 nM) or fMLP (10 μM) for 5 minutes at 37°C. Where indicated, neutrophils were preincubated in presence of 5 μM U73122 (phospholipase C inhibitor) for 30 minutes at 37°C. Cytosolic fractions were collected after centrifugation at 150,000 × *g* for 75 minutes at 4°C on a sucrose cushion as described in Subheading 17.3.2. Cytosolic proteins (20 μg or 10 μg in the case of PKC-δ) were loaded on SDS-PAGE followed by immunoblotting with specific polyclonal antibodies (*see* Subheading 17.3.2). The immune complexes were detected by ECL. The depletion of PKC-βI, PKC-βII, and PKC-δ from cytosol is correlated with PKC activation. Reduced depletion is observed after pretreatment with the phospholipase C blocker in fMLP-treated cells but not in PMA-treated cells

11. Incubate the nitrocellulose membrane in PBS/0.05% Tween 20/2% milk powder for 1 h at room temperature.
12. Incubate the membrane overnight at 4°C with polyclonal antibodies directed against PKC- βI (dilution 1:1000 in PBS/0.05% Tween 20/1% milk powder), PKC-βII (dilution 1:1000 in PBS/0.05% Tween 20/1% milk powder), PKC-δ (dilution 1:2000 in PBS/0.05% Tween 20/1% milk powder), or PKC-ζ (dilution 1:500 in PBS/0.05% Tween 20/1% milk powder) (*see* Note 6).
13. Wash the membranes extensively with PBS/0.05% Tween 20.
14. Incubate the membranes in goat antirabbit immunoglobulin secondary antibody conjugated with peroxidase (dilution 1:5,000 in PBS/0.05% Tween 20/1% milk powder).
15. Wash the membranes extensively with PBS/0.05% Tween 20.
16. Incubate the membrane with ECL® detection reagents and expose to film for different lengths of time (exposure time depends on the strength of the signal, typically around 20 s). Process the film.
17. The decrease in cytosolic PKC amount after neutrophil stimulation represents a measure of its activation (see Note 7) (Fig. 17.2) [17].

17.3.3 PKC Recruitment to Lipid Rafts

1. Chill all the solutions on ice.
2. Prewarm neutrophils (*see* Subheading 17.3.1) at 37°C for 5 min, then stimulate cells with desired stimulus (*see* Note 2).

3. Stop reactions by adding 50 volumes of cold PBS.
4. Centrifuge at 900 × *g* for 5 min at 4°C and keep cell pellet on ice.
5. For cholesterol depletion, incubate neutrophils (1×10^7cells/ml) in 2 ml of RPMI-1640 with 10 mM MβCD (or control without MβCD) for 30 min.
6. Centrifuge at 900 × *g* for 5 min, and then keep cells on ice.
7. Add 1 μl of DFP stock solution onto the cells and incubate on ice for 5–10 min.
8. Add 1 ml of HNE buffer containing protease inhibitors listed above (except DFP) and incubate on ice for 30 min.
9. Homogenize the cells with 20 up-and-down strokes in a Dounce homogenizer (*see* Note 4).
10. Add 1 ml of 80% sucrose stock in HNE buffer to the cell lysate to give a final concentration of 40% sucrose; mix well.
11. Add 1.0 ml of the mixture to a prechilled Beckman thin-wall 2.4-ml ultracentrifuge tube. Then carefully lay 1.0 ml of 30% sucrose and 0.4 ml of 5% sucrose in HNE buffer on top of the cell lysate.
12. Centrifuge at 250,000 × *g* for 2.5 h in a bench-top ultracentrifuge in a TLS-55 rotor.
13. After spinning, fractionate the gradient from top to bottom in 10 fractions (240 μl each fraction).
14. Neutrophil rafts generally fractionate in fraction 2. As marker for rafts, the presence of flotillin can be determined by Western blotting as described in Subheading 17.3.2.
15. The presence of PKC isotypes in rafts can be assessed by SDS-PAGE and Western blotting as described in Subheading 17.3.2.
16. An example of this analysis is shown in Shao et al. [18].

Notes

1. Because neutrophils are human primary cells, due care must be exercised in handling the cells. Local ethical approval for the use of these cells may be required, and specific safety precautions may need to be put in place for their handling. For advice, readers are referred to their local ethical and safety committees.
2. To avoid unintentional stimulation, cells should be handled carefully, with minimal physical manipulation. Cells should not be shaken or vortexed. Transfer of cells is best done using wide-barrelled pipettes. Generally, neutrophils from fresh blood respond more reproducibly to receptor stimulation than neutrophils isolated from buffy coat. In our experience, cell longevity, and therefore reproducibility of measurements, is more consistent in RPMI 1640 medium than in PBS.
3. Dextran may also be added from a 10% stock to achieve a 1% final concentration. However, sedimentation tends to be affected by cell density, and so dilution of the buffy coat may need to be adjusted.
4. Neutrophils contain numerous proteolytic enzyme systems that mainly reside inside intracellular vesicles. Upon extraction, these enzymes may be liberated and affect the proteins in the extract. Even when extracting in denaturing conditions (e.g., SDS extraction), significant proteolysis can still occur. Extractions during which intracellular vesicles

are not broken tend to give the least breakdown of PKC [e.g., pulse sonication in sonication buffer (Subheading 17.3.2)]. In some cases, the addition of a small amount of diisopropyl fluorophosphate stock solution to the cells prior to fractionation aids in the recovery of intact proteins.

5. The following protocol works for a Hoeffer semidry system. Wear gloves throughout the procedure. Cut 3 MM filter paper and nitrocellulose to the size of the gel. Soak three 3MM filters in Towbin buffer and place on the semidry electrode. Wet the nitrocellulose and place on the filters, avoiding air bubbles. Place the gel on the nitrocellulose, again avoiding air bubbles. It is useful to wet the gloves in Towbin buffer prior to gel handling; this prevents the gloves from sticking to the gel. Soak three 3 MM filters in Towbin buffer and place on the gel. Remove any air bubbles by rolling a rod over the filter. Close the semidry unit and transfer at 100 mA for 1 h. After transfer, mark the orientation of the gel using pencil. Colored markers can serve as orientation markers and should be used when feasible.
6. We used a heat sealer to seal the filter in a small plastic pocket and used a 4-ml buffer for the incubation. Filters can be sealed back to back if they need to be incubated with the same antibody. The filter can be rotated on a wheel in the cold room or in a cold cabinet.
7. Redistribution of classical and novel PKCs is taken as measure of activation, based on the fact that PKC-activating phorbol esters and diacylglycerols induce recruitment to the plasma membrane. Atypical PKC isotypes do not respond to these factors. Nevertheless, they may show changes in localization on receptor stimulation, which may still reflect activation. We observed that cytosolic PKC-ζ is reduced in response to fMLP but not to phorbol ester [17].

References

1. Parker PJ, Dekker LV. Protein Kinase C. Austin, TX: Molecular Biology Intelligence Unit, Landes; 1997.
2. Dekker LV. Protein Kinase C. Austin, TX: Molecular Biology Intelligence Unit, Landes; 2004.
3. Parker PJ, Murray-Rust J. PKC at a glance. J Cell Sci 2004;117:131–2.
4. Le Good JA, Ziegler WH, Parekh DB, Alessi DR, Cohen P, Parker PJ. Protein kinase C isotypes controlled by phosphoinositide 3-kinase through the protein kinase PDK1. Science 1998;281:2042–5.
5. Pearson M, Hurley JH. Structure, function and membrane interactions of C1 domains. In Dekker LV, ed. Protein Kinase C. Austin, TX: Landes; 2004:8–15.
6. Nalefski EA. Structural and functional specialization of C2 domains in protein kinase C. In Dekker, LV, ed. Protein Kinase C. Austin, TX: Landes; 2004:16–35.
7. Jose Lopez-Andreo M, Gomez-Fernandez JC, Corbalan-Garcia S. The simultaneous production of phosphatidic acid and diacylglycerol is essential for the translocation of protein kinase Cepsilon to the plasma membrane in RBL-2 H3 cells. Mol Biol Cell 2003;14:4885–95.
8. Dekker LV, Parker PJ. Regulated binding of the protein kinase C substrate GAP-43 to the VO/C2 region of protein kinase C-delta. J Biol Chem 1997;272:12747–53.
9. Lopez-Lluch G, Bird MM, Canas B, Godovac-Zimmerman J, Ridley A, Segal AW, Dekker LV. Protein kinase C-delta C2-like domain is a binding site for actin and enables actin redistribution in neutrophils. Biochem J 2001;357:39–47.
10. Sanchez P, De Carcer G, Sandoval IV, Moscat J, Diaz-Meco MT. Localization of atypical protein kinase C isoforms into lysosome-targeted endosomes through interaction with p62. Mol Cell Biol 1998;18:3069–80.
11. Wilson MI, Gill DJ, Perisic O, Quinn MT, Williams RL. PB1 domain-mediated heterodimerization in NADPH oxidase and signaling complexes of atypical protein kinase C with Par6 and p62. Mol Cell 2003;12:39–50.

12. Benes CH, Wu N, Elia AE, Dharia T, Cantley LC, Soltoff SP. The C2 domain of PKCdelta is a phosphotyrosine binding domain. Cell 2005;121:271–80.
13. Newton AC. Protein Kinase C Protocols. Totawa, NJ: Humana Press; 2003.
14. Dekker LV. Protein kinase C isotype function in neutrophils. In Dekker LV, ed. Protein Kinase C. Austin, TX: Landes; 2004:165–90.
15. Segal AW, Coade SB. Kinetics of oxygen consumption by phagocytosing human neutrophils. Biochem Biophys Res Commun 1978;84:611–7.
16. Davidson-Moncada JK, Lopez-Lluch G, Segal AW, Dekker LV. Involvement of protein kinase D in Fc gamma-receptor activation of the NADPH oxidase in neutrophils. Biochem J 2002;363:95–103.
17. Paclet MH, Davis C, Kotsonis P, Godovac-Zimmermann J, Segal AW, Dekker LV. N-formyl peptide receptor subtypes in human neutrophils activate L-plastin phosphorylation through different signal transduction intermediates. Biochem J 2004;377:469–77.
18. Shao DM, Segal AW, Dekker LV. Lipid rafts determine efficiency of NADPH oxidase activation in neutrophils. FEBS Lett 2003;550:101–6.
19. Laemmli UK. Cleavage of structural proteins during the assembly of the head of bacteriophage T4. Nature 1970;227:680–5.
20. Towbin H, Staehelin T, Gordon J. Electrophoretic transfer of proteins from polyacrylamide gels to nitrocellulose sheets: Procedure and some applications. Proc Natl Acad Sci USA 1979;76:4350–4.

Chapter 18
Detection of Myotubularin Phosphatases Activity on Phosphoinositides *in vitro* and *ex vivo*

Holger Maria Rohde, Hélène Tronchère, Bernard Payrastre and Jocelyn Laporte

Abstract Phosphoinositides (PPIn) are important regulators of cellular processes like intracellular protein transport, cellular proliferation, apoptosis, and cytoskeletal organization. The amount and localization of these membrane-bound second messengers are regulated through a set of specific phospholipases, lipid kinases, and phosphatases. The elucidation of PPIn-phosphatases and their cellular function has gained much attention because phosphatase dysregulation is often associated with human genetic diseases. Our laboratory has identified the 3'-PPIn-phosphatase myotubularin 1 (MTM1) mutated in X-linked myotubular myopathy (XLMTM). In addition, a whole family of myotubularin-related proteins (MTMR1–MTMR13) has been discovered. Some of them display phosphatase activity, whereas for other family members no enzymatic activity could be detected. Nevertheless, these "dead phosphatases" myotubularins are conserved throughout evolution and probably exert regulatory function by heteromeric interaction with active phosphatase members. It was shown that MTM1 and related phosphatases act on PtdIns3*P* and PtdIns(3,5)P_2; both PPIn species are important regulators of endocytic pathways. We describe two methods to determine phosphatase activity and substrate specificity of myotubularins. One is an immunoprecipitation-phosphatase assay, testing the activity of myotubularin immunoprecipitated from overexpressing cells on artificial PPIn. The other method analyzes phosphatase activity indirectly *ex vivo* in transiently transfected mammalian cells. The presence and subcellular localization of the myotubularin substrate PtdIns3*P* were determined using a specific binding domain (2xFYVE) produced recombinantly as a biosensor.

Keywords Myotubularin · phosphatidylinositol · phosphatase · biosensor · phosphatase assay · phosphoinositides · FYVE domain · endosome

J. Laporte
Institut de Génétique et de Biologie Moléculaire et Cellulaire (IGBMC), Department of Neurobiology and Genetics, Illkirch, France; INSERM U596, Illkirch, France; CNRS, UMR7104, Illkirch, France; Université Louis Pasteur, Strasbourg, France; Collège de France, chaire de Génétique Humaine, Illkirch, France
e-mail: mtm@igbmc.u-strasbg.fr

B. Larijani et al. (eds.), *Lipid Signaling Protocols*, DOI: 10.1007/978-1-60327-115-8_18,

Abbreviations PPIn: phosphoinositides; PS: phosphatidylserine; MTM: Myotubularins; XLMTM: X-linked myotubular myopathy; CMT: Charcot-Marie-Tooth; TLC: Thin-layer chromatography; IP: immuno-precipitation; PBS: phosphate buffer saline; GFP: green fluorescent protein; PFA: paraformaldehyde.

18.1 Introduction

In eukaryotic cells, phosphatidylinositol can be phosphorylated on its inositol ring into seven distinct phosphoinositides (PPIn), which have been implicated in a variety of cellular processes, including actin rearrangement, cell survival and mitogenesis, and membrane and protein trafficking. These phosphoinositides act as precursors of second messengers or directly influence signaling pathways depending on the localization and availability of specialized PPIn binding proteins (for review, see [1] and [2]).

The myotubularin (MTM1) gene is mutated in X-linked myotubular myopathy (XLMTM, OMIM 310400), a congenital disorder resulting in severe and generalized muscle weakness in affected newborn males [3]. MTM1 was shown to dephosphorylate PtdIns3*P* and PtdIns(3,5)P_2 into PtdIns and PtdIns5*P*, respectively [4–7]. Sequence analysis revealed the presence of a conserved phosphatase domain encompassing a protein tyrosine phosphatase (PTP) motif with catalytically active cysteine and arginine residues (CX_5R) [8]. This PTP phosphatase protein superfamily also includes most of the PPIn phosphatases.

Further research led to the discovery of a whole family of proteins that were named myotubularin-related proteins (MTMR), consisting of 14 members in humans. Within this family, both catalytically active and inactive myotubularins exist. For the "dead phosphatases," the canonical PTP domain is also conserved, but they lack enzymatic activity due to mutations of the catalytically active cysteine and arginine residues [9, 10]. Besides MTM1, two further members from this family (MTMR2, an active phosphatase, and MTMR13, a dead phosphatase) are also known to be implicated in other human diseases, such as demyelinating neuropathies (Charcot-Marie-Tooth disease, CMT4B [11, 12]). The difference in pathology of these diseases compared to XLMTM suggests a tissue-specific function for the different myotubularin family proteins and indicates that dead phosphatases cooperate with active homologues [13, 14].

We propose two methods to identify and characterize the enzymatic activity of myotubularin and related 3'PPIn-phosphatases and their respective disease causing mutants from cells that transiently overexpress these proteins. For the first part, lipid phosphatase activity is assayed *in vitro* on artificial phosphatidylinositol species using immunoprecipitated myotubularin. Here, tagged myotubularin versions are transiently overexpressed in mammalian cells and purified using a standard immune precipitation protocol. Using this IP-phosphatase assay method, we are able to quickly investigate different disease mutants.

In a second step to verify and compare the enzymatic activity in a cellular context, we utilize a biotinylated biosensor probe specific for PtdIns3*P* (GST-2xFYVE [15]) to determine the presence and localization of the myotubularin substrates within the cells. So far we have used this method only qualitatively to verify the *in vitro* data; we have recently followed this strategy to characterize a novel human PPIn phosphatase, hJUMPY [16].

18.2 Materials

18.2.1 Cell Culture and Transfection

1. For Cos-1 cells: Dulbecco's Modified Eagle Medium (DMEM, Invitrogen), supplemented with 5% fetal calf serum (FCS, PanBiotech), 1% glucose, and 40 μg/ml of gentamicin.
2. For HEK293 cells: DMEM (Gibco) supplemented with 5% FCS and 1% penicillin/streptomycin.
3. Solution of trypsine (0.05%) in phosphate buffered saline (PBS).
4. Effectene transfection reagent (Qiagen, Düsseldorf, Germany).
5. Myotubularin and myotubularin-related protein coding sequences cloned into eukaryotic expression vectors, or any putative PPIn phosphatase to be tested.

18.2.2 Cell Lysis and Myotubularin Immunoprecipitation

1. Cell lysis/immunoprecipitation buffer: 20 mM Tris-HCl, pH 7.4, 150 mM NaCl, 4 mM EDTA, 0.1% TritonX-100.
2. Laemmli buffer for SDS-PAGE 4x concentrated: 8% SDS, 40% glycerol, 240 mM Tris-HCl, pH 6.8, 400 mM dithiothreitol (DTT), 0.004% bromophenol blue.
3. Protein A Sepharose 4 fast flow, protein G Sepharose 4 fast flow (Amersham, UK) prepared as a 50% slurry in lysis buffer.
4. Disposable cell scraper.
5. SDS-PAGE gel system.

18.2.3 Lipid Phosphatase Assay in vitro

1. Fluorescent lipids: di-C16-NBD6 or di-C6-NBD6 PtdIns3*P*, PtdIns4*P*, PtdIns5*P*, PtdIns(3,4)P_2, PtdIns(3,5)P_2, PtdIns(3,4,5)P_3, stored in a chloroform/methanol solution (v/v) at –20°C under a nitrogen atmosphere at a concentration of 0.5 μg/μl (Echelon Biosciences, Salt Lake City, UT).

2. Other lipids stocks including various phosphoinositides, phosphatidylinositol, and phosphatidylserine PS (Sigma, St Louis, MO, Avanti Polar lipids, Alabaster, AL, or Echelon Biosciences, Salt Lake City, UT) are stored in chloroform/methanol (v/v) at –20°C under a nitrogen atmosphere.
3. [γ-^{32} P]ATP (3,000 Ci/mmol, 370 MBq/ml), stored at 4°C; immunopurified PI 3-Kinase [17].
4. Phosphatase assay buffer with fluorescent lipids: 50 mM ammonium acetate, pH 6.8, 2 mM DTT.
5. Phosphatase assay buffer with radioactive lipids: 20 mM 2-(N-Morpholino) ethanesulfonic acid (MES) (pH 6.5) containing 2.5 mM EDTA and 8 mM KCl.
6. Chloroform (VWR), methanol, acetone, acetic acid, 2-propanol, chloridric acid (Sigma-Aldrich).
7. Iodine vapor for visualization of PPIn standards.
8. Thin layer chromatography (TLC) plates, 20-cm × 20-cm silica gel 60 (0.2 mm thickness; Merck).
9. TLC plates premigration buffer: H_2O (90 ml), potassium oxalate (1.5 g), EDTA (100 mM, 3 ml), and methanol (60 ml).
10. Equipment: UV gel illumination/camera system, PhosphorImager system, nitrogen evaporator, sonicator, microfuge, dry-bath shaking incubator, glass TLC tank.

18.2.4 Production of the Biotinylated PtdIns3P Biosensor

1. GST-2xFYVE expression vector (2xFYVE domain courtesy of H. Stenmark, Norway [15], subcloned into pGEX4T3; Amersham), transformed into BL21 bacteria (Stratagene).
2. Bacteria growth medium 2xYT (16 g of bacto tryptone, 10 g of bacto yeast extract, 5 g of NaCl at 1,000 ml, pH 7.0), supplemented with 2% glucose, 100 μg/ml of ampicillin.
3. Lysis buffer: PBS containing 1% Triton X-100, 1% Tween 20, protease inhibitor (leupeptin, pepstatin A, aprotinin, antipain, chymostatin, each at 2.5 μg/ml of final concentration).
4. Glutathione-Agarose beads (Amersham Pharmacia).
5. Glutathione elution buffer: 100 mM Tris-HCl, pH 8.0, 120 mM NaCl, 20 mM glutathione reduced.
6. Isopropyl-β-D-Thiogalactopyranoside, IPTG (Sigma); 100 mM stock is prepared by dissolving powder into H_2O and sterile-filtering; store aliquots at −20°C; use at a final concentration of 0.5 mM.
7. BiotinTag Micro Biotinylation Kit (Sigma Cat. no. B-TAG) containing the BAC-sulfo-NHS biotinylation reagent (biotinamido hexanoic acid 3-sulfo-N-hydroxysuccinide ester), micro-spin columns prepacked with

Sephadex G-50 resin, 100 mM sodium phosphate buffer, pH 7.2, and 10 mM PBS, pH 7.4 (1.9 mM KH_2PO_4, 8.1 mM, 138 mM NaCl).
8. Centricon concentrator, 30-kDa cutoff (Millipore).
9. Dimethylsulfoxide (DMSO), pure grade (Sigma).

*18.2.5 Confocal Imaging of GFP-Myotubularin and Detection of PtdIns3*P Biosensor

1. Microscope slides SuperFrost Plus (25 mm × 75 mm × 1 mm, Menzel-Gläser, Germany), glass coverslips, and 6-well cell culture plates (Greiner).
2. Phosphate buffered saline (PBS).
3. Paraformaldehyde (4% w/v solution in PBS), prepared by carefully warming the solution on a stirring hot plate (fume hood). Best used fresh, but aliquots can be frozen for storage.
4. Streptavidin-Alexa 594 (Molecular Probes) for fluorescent detection of biotin-GST-2xFYVE biosensor.
5. 4′,6-Diamidino-2-phenylindole dihydrochloride (DAPI, Serva); 1 μg/ml in H_2O; keep aliquots in the dark.
6. Antifading mounting medium: 80% glycerol, 5% propyl gallate in PBS.

18.3 Methods

To investigate the enzymatic activity of different myotubularin proteins and mutants, we established a phosphatase assay examining the enzymatic function of myotubularin and used immunoprecipitated proteins from transiently overexpressing mammalian cells. First, this established method bypasses the time-consuming process of generating recombinant proteins *in vitro*, especially when testing different mutants. Second, it allows the post-translational modifications of proteins expressed in a mammalian system to occur.

We also take the advantage of transient transfection of myotubularin expression constructs into mammalian cells to verify *ex vivo* the results obtained from the IP-phosphatase assay. Here, cells expressing fluorescently tagged myotubularin versions are analyzed visually for their content of the myotubularin substrate PtdIns3*P*. This PPIn species is faithfully detected by a specific biosensor, GST-2xFYVE, which itself is labeled fluorescently using a biotin-streptavidin binding system. This also permits us to analyze the subcellular localization of the remaining PtdIns3*P* substrate. Moreover, both approaches enable the activation of signaling pathways and cell processes before enzymatic activity measurement.

18.3.1 Cell Culture and Transfection of Myotubularin Variants

Standard cell culture is performed using well-established mammalian cell lines (Cos-1; HEK293) and conducted under standard conditions (37°C, 5% CO_2, humidified atmosphere); cells were maintained by continuous passages and counted using a hematocytometer.

1. Cos-1 cells: For confocal analysis of GFP-tagged myotubularin variants and their influence on the intracellular level of PtdIns3*P*, respective mammalian expression constructs are transfected. Before transfection, 6-well plates are prepared with glass coverslips fitting into the wells under sterile conditions; then Cos-1 cells are seeded at a density of 300,000 cells per well.
2. For HEK293 cells, trypsinized cells are seeded in 6-well plates at a density of 300,000 cells/well 24 h before transfection.
3. After 12–24 h, cells have reached a confluency of 50–70% and are ready for transfection. For liposomal transfection, the transfection reagent Effectene (Qiagen) is utilized. In each well, 0.4 μg of DNA is mixed with 3.2 μl of Enhancer and 75 μl of EC buffer; incubate for 5 min. Then, 6 μl of Effectene reagent is added and vortexed for 10 s. After 10 min of incubation at room temperature, the complex is added on the cells for transfection.
4. Twenty-four hours after transfection, cells are washed once in cold PBS and either fixed with 4% PFA for microscope analysis (Cos-1 cells; *see* Subheading 18.3.5) or lysed in lysis buffer to proceed with immunoprecipitation (HEK293 cells; *see* Subheading 18.3.2).

18.3.2 Cell Lysis and Immune Precipitation

1. Wash adherent cells once with cold PBS and add 500 μl of lysis buffer per well. Incubate on ice for 5 min, scrape cells, and transfer to microfuge tube, then mix by rotation for 20 min at 4°C.
2. Spin at top speed in microfuge for 10 min, take supernatant, transfer to a new microfuge tube, and do a preclearing with 20 μl of a 50% slurry protein A Sepharose, rotating for 30 min at 4°C.
3. Spin at top speed in microfuge for 10 min. Take 450 μl of supernatant and process for myotubularin immunoprecipitation using tag-specific or protein-specific antibodies and 30 μl of a 50% slurry protein A Sepharose. Rotate for 3 h at 4°C.
4. Wash the beads four times with lysis buffer and twice with the fluorescent or radioactive lipids phosphatase assay buffer. Centrifugations were done at 1,500 × *g* for 2 min. After the last wash, divide the supernatant into three aliquots.

5. One third is used to check the success of immune precipitation. Resuspend beads in Laemmli buffer, boil for 8 min, and run samples on a 10% SDS-PAGE gel. Transfer onto nitrocellulose membrane and reveal myotubularin proteins using a tag-specific antibody followed by horse radish peroxidase (HRP)-linked anti-mouse secondary antibody and enhanced chemiluminescence system (ECL, Pierce).

18.3.3 Phosphatase Assay on Immunoprecipitated Myotubularins

18.3.3.1 Assay Using Fluorescent Substrates

Fluorescent phosphoinositides can be used as substrates to investigate the activity and specificity of either recombinant or immunoprecipitated PPIn phosphatases. Such assays have been used to determine the specificity of PTEN, SHIP, and myotubularin phosphatases [18]. This method is useful for a rapid characterization of a phosphatase activity and for the identification of its substrate specificity.

1. Prepare the silica gel plates by running in the oxalate premigration buffer to the top. Place in a fume hood until dried and in a drying oven at 70°C for 20 min prior to use.
2. Dry 1 μg of fluorescent substrate under a nitrogen stream in a glass tube and resuspended in 30 μl of 50 mM ammonium acetate (pH 6) plus 2 mM DTT by vortexing.
3. Add immunoprecipitated myotubularins (10 μl of bead volume) and incubate the mixture for 30 min at 30°C with shaking.
4. For the di-C6-NBD6, stop the reaction by centrifugation (10,000 × *g*, for 2 min) to pellet the beads. Remove the supernatant and add to glass tube with 100 μl of acetone. Dry the supernatant under a nitrogen stream at 37°C; resuspend in 30 μl of methanol/2-propanol/acetic acid (5/5/2; v/v) and spot onto a pre-oxalated TLC plate. Run in the solvent system: chloroform/methanol/acetone/acetic acid/water (70/50/20/20/20, v/v) to 2 cm from the top of the plate (approximately 2 h; *see* Note 1).
5. For the di-C16-NBD6, stop the reaction by adding 60 μl of water, 100 μl of 2.4 N HCl, and 400 μl of chloroform/methanol (v/v). Shake vigorously and centrifuge at 3,000 × *g* for 5 min. Transfer the organic phase to a glass tube and dry under a nitrogen stream at 37°C. Resuspend in 30 μl of methanol/2-propanol/acetic acid (5/5/2; v/v) and spot onto a pre-oxalated TLC plate. Run in the solvent system: chloroform/acetone/methanol/acetic acid/water (80/30/26/24/14, v/v).
6. Fluorescent lipids are visualized by UV light (*see* Note 2; sample results are shown in Fig. 18.1).

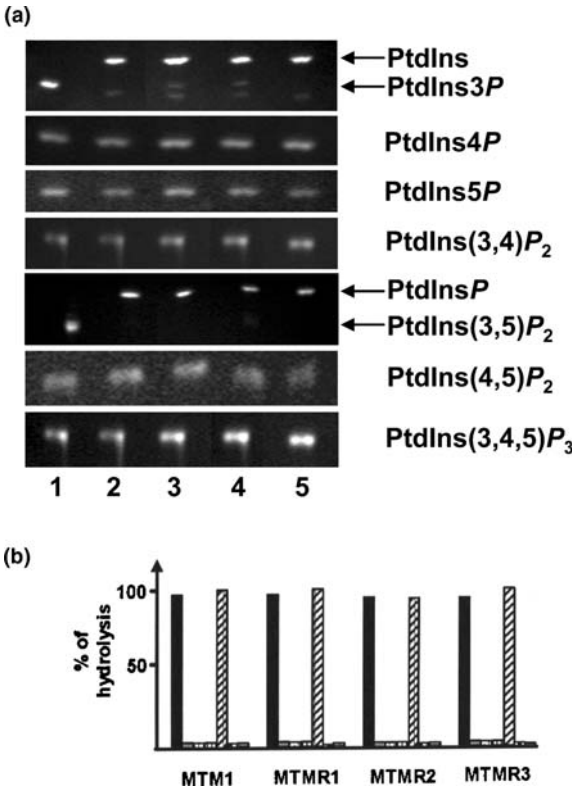

Fig. 18.1 Substrate specificity of MTM1 and MTMRs *in vitro*. (a) Empty vector (lane 1), MTM1 (lane 2), MTMR1 (lane 3), MTMR2 (lane 4), and MTMR3 (lane 5) were transiently expressed in HEK 293 cells and immunoprecipitated using protein-specific or tag-specific antibodies. The immunoprecipitates were tested for *in vitro* phosphatase activity using fluorescent C6-NBD-PPIn according to the described method. Lipid products were separated on TLC, and the fluorescence was measured on a UV table. Tested substrates are indicated on the right. All myotubularins specifically dephosphorylate PtdIns3*P* and PtdIns(3,5)P_2. (b) Percentage of hydrolysis of the different fluorescent lipid substrates are reported for each myotubularin, standardized to the vector control in the following alignment from left to right: PtdIns3*P*, PtdIns4*P*, PtdIns5*P*, PtdIns(3,4)P_2, PtdIns(3,5)P_2, PtdIns(4,5)P_2, and PtdIns(3,4,5)P_3. (Pictures taken from Fig. 3 of Tronchère et al. [7], with permission from ASBMB Journals.)

18.3.3.2 Assay Using Radioactive Substrates

1. Prepare the radioactive substrates [^{32}P]PtdIns3*P* or [^{32}P]PtdIns(3,5)P_2 using C16-phosphatidylinositol/phosphatidylserine (1/2, w/w) vesicles or di-C16-PtdIns5*P*/PS vesicles, respectively, [γ-^{32}P]ATP and immunopurified Class IA PI 3-kinase by incubation for 15 min at 37°C under shaking [7].
2. Separate the [^{32}P]PtdIns3*P* and [^{32}P]PtdIns(3,5)P_2 formed by TLC in the solvent system: chloroform/acetone/methanol/acetic acid/water

(80/30/26/24/14, v/v) on a pre-oxalated plate. After visualization of the radioactive spots by PhosphorImager, scrap them off the TLC plate and resuspend the silica in 500 µl of HCl (2 N). Add 1 ml of chloroform/methanol (v/v) and vortex thoroughly for 2 min at room temperature. After centrifugation (7,000 × *g* for 5 min), collect the organic phase.

3. For one assay, add about 30,000 dpm of TLC-purified [^{32}P]PtdIns3*P* or [^{32}P]PtdIns(3,5)P_2 together with 50 µg of PS in chloroform/methanol (v/v) and 5 µg of di-C16-PtdIns3*P* or di-C16-PtdIns(3,5)P_2. Dry the mixture under a nitrogen stream, and resuspend in 40 µl of 20 mM MES (pH 6.5) containing 2.5 mM EDTA and 80 mM KCl. Sonicate three times for 1 min at 4°C (20 kHz).
4. Incubate the reaction mixture containing 20 µl of immunoprecipitated myotubularin or other phosphatases to test and 40 µl lipid vesicles for 15 min at 37°C with shaking.
5. Stop the reaction by adding 400 µl of chloroform/methanol (v/v) and 140 µl of 2.4 N HCl. Vortex the sample thoroughly for 2 min at room temperature. After centrifugation (10,000 × *g* for 5 min), collect and dry the organic phase under a nitrogen stream.
6. Resuspend the dried lipid samples in a minimal volume (60 µl) of chloroform/methanol (v/v) and spot onto a pre-oxalated TLC plate.
7. Separate [^{32}P]PtdIns3*P* or [^{32}P]PtdIns(3,5)P_2 on a pre-oxalated plate by TLC using chloroform/acetone/methanol/acetic acid/water (80/30/26/24/14, v/v) as a solvent system.
8. Visualize the radioactive spots by a PhosphorImager. di-C16-PtdIns, di-C16-PtdIns3*P*, di-C16-PtdIns5*P*, and di-C16-PtdIns(3,5)P_2 standards are resolved on the same TLC and visualized using iodine vapors.
9. Quantify the amount of hydrolyzed [^{32}P]PtdIns3*P* or [^{32}P]PtdIns(3,5)P_2 by scrapping of the corresponding spots and count samples in a beta-counter by scintillation to calculate the specific activity of the phosphatase (*see* Note 3).

18.3.4 Production and Biotinylation of PtdIns3P Biosensor

1. The production of GST-tagged 2xFYVE recombinant protein was accomplished in bacteria, using a modified pGEX protocol from Amersham for induction and expression. No problems with the solubility of the protein have been encountered, and the amount of protein was always sufficient. To control the production process, small aliquots can be taken at different steps to analyze the success of the purification protocol.
2. Starting from a glycerol stock or an agarose media plate, prepare a starter culture in 10 ml of 2xYT bacterial growth medium in a bigger culture vessel (at least five times bigger) and culture it overnight (37°C, shaking at 220 rpm).

3. The following morning, establish a growing culture by diluting the starter culture 1:10 into a 2 L culture shaker vessel and cultivate it with shaking at 37°C. For monitoring the growth of the bacteria, the OD_{600} of the culture was measured.
4. After 2–3 h of growth, when the OD_{600} has reached 0.7–0.9, production of the protein is induced by adding 0.5 mM f.c. IPTG to the growing bacteria culture.
5. After 2 h of induction, the bacteria are harvested by centrifugation. At this point, the OD_{600} normally reached values of about 1.5. To remove residual medium, the bacteria pellet is washed once with 20 ml of ice-cold PBS.
6. Resuspend the bacteria in 20 ml of lysis buffer without added detergents and lyse the cells by sonication. Resuspended cells are placed on ice and sonicated in intervals for a total time of 2 min (10 s/10 s, 37%). Then, detergents (1% Triton X-100, 1% Tween 20) are added and the bacterial lysate is incubated, shaking for 20 min at 4°C.
7. To purify the GST domain-containing recombinant protein, the bacterial lysate is cleared by centrifugation. To the supernatant, add 0.5 ml of glutathione agarose beads and let the protein bind overnight at 4°C.
8. To remove unbound material, the glutathione beads have to be centrifuged and washed three times. Here, 10 ml of ice-cold lysis buffer (including detergents) is added to the beads, left shaking for 10 min at 4°C, and the beads sedimented with soft centrifugation (10 min, 1,500 × *g*). At each step, the supernatant is discarded, but control samples may be taken.
9. To reduce residual detergent, repeat this washing step once with PBS without detergents.
10. To elute the desired protein from the beads, incubate beads twice with 500 µl of elution buffer. In both cases, incubate shaking for 20 min at room temperature, then spin down beads at 1,500 × *g* to collect the supernatant, which contains the eluted protein. Both eluates are pooled, and the protein content is measured using the Bradford method. For prolonged storage, the protein can be frozen at −80°C with 20% glycerol.
11. For labeling the GST-2xFYVE protein with biotin, the Biotin Tag Kit (Sigma) is utilized. Normally described for labeling of IgG, this protocol is specially suited for small-scale labeling of proteins under mild reaction conditions and uses an activated biotin (BAC-Sulfo-NHS) as the labeling reagent. This reagent is prepared by dissolving one vial of labeling reagent (5 mg of BAC-Sulfo-NHS) with 30 µl of DMSO, followed by adding 970 µl of PBS and vortexing.
12. The eluted protein was dialyzed overnight into 100 mM sodium phosphate buffer (*see* Note 4). After that, the protein concentration was adjusted at around 5 mg/ml, as verified by the Bradford method.

13. To start the biotinylation reaction, add 20 µl of the labeling reaction to 100 µl of the GST-2xFYVE protein solution (= 500 µg protein). Incubate the tube for 30 min at room temperature; gently flick the tube from time to time.
14. For equilibration, resuspend the Sephadex G-50 resin in the microcolumns (supplied by manufacturer) by vortexing, then add 200 µl of PBS, and place into an Eppendorf tube. After spinning in a microcentrifuge (700 × *g* for 1 min), remove the flowthrough and repeat this equilibration step twice with 300 µl of PBS.
15. To separate and recover the biotinylated protein from unbound biotin and the reaction mixture, apply the biotinylation mixture carefully onto the top of the column and spin in a microcentrifuge (700 × *g* for 2 min).
16. Elute column three times with 200 µl of PBS (microcentrifuge), collect and pool eluates, and determine the protein concentration using the Bradford method.
17. Additional washing steps are performed with 3x 200 µl of PBS using a centricon concentrator (Millipore, cutoff 30 kDa). To increase the protein concentration, concentrate pooled eluates down to 200 µl (one third of the original eluates' volume; *see* Notes 5 and 6).

18.3.5 Confocal Detection of PtdIns3P Levels in Transfected Cells

1. Before proceeding with the labeling protocol, it is advisable to check transfected cells for expression of the GFP-tagged myotubularin version via live cell microscopy. For myotubularin, a transfection time of 24 h was sufficient to obtain clear results of enzymatic activity, but this may be titrated for other phosphatases.
2. If the transfection results are fine, remove the medium and wash wells with PBS. After that, cells are fixed with 4% paraformaldehyde, overnight at 4°C (*see* Note 7). As paraformaldehyde evaporates and is slightly noxious, seal the cell culture vessel with Saran wrap.
3. After fixing, wash slides with PBS for 5 min. Block unspecific binding sites with 5% bovine serum albumin (BSA, w/v) for 30 min in PBS. Wash again with PBS (*see* Note 8).
4. Incubate the GST-2xFYVE biosensor protein at a final concentration of 5 µg/ml for 60 min and then wash three times with PBS.
5. To detect the bound biotinylated biosensor protein, incubate with streptavin-Alexa 594 for 30 min and then perform three washings with PBS.
6. For an eventual nuclear counterstain, incubate with DAPI (5 min, 1 µg/ml) followed by three washings with PBS.
7. Mount the glass plates onto a microscope slide using an antifading solution (examples of the results obtained are shown in Fig. 18.2).

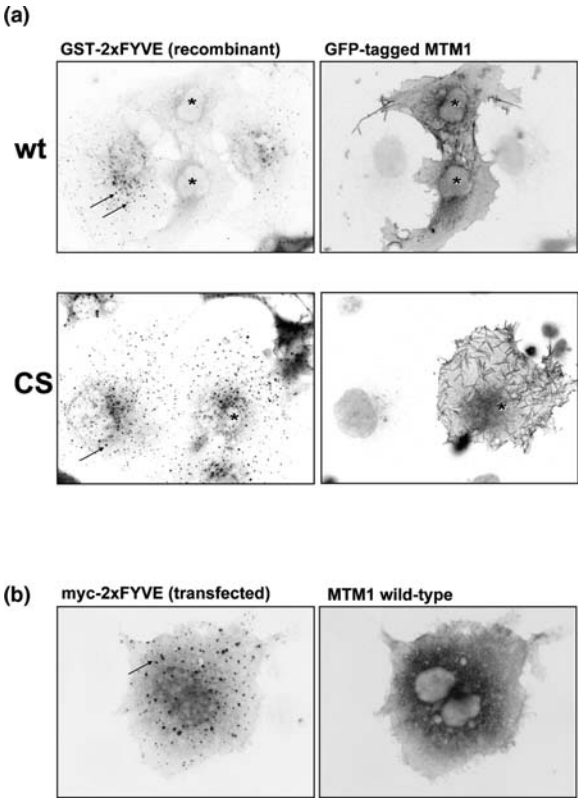

Fig. 18.2 Myotubularin dephosphorylates endosomal PtdIns3*P ex vivo*. (a) Cos-1 cells were grown on glass slides and transiently transfected with GFP-tagged myotubularin constructs [pictures on the right: wild-type and phosphatase dead C375S (CS) mutant, respectively]. After fixation, PtdIns3*P* was detected using the biotinylated GST-2xFYVE biosensor protein, as seen in the corresponding pictures on the left. For untransfected cells and cells expressing the phosphatase dead mutant, a clear punctuated staining of endosomes becomes visible, whereas cells expressing wild-type myotubularin are devoid of PtdIns3*P* staining. (b) Cells were co-transfected with a myc-tagged 2xFYVE expression construct and myotubularin wild type. Although myotubularin phosphatase is nicely expressed, the overexpressed 2xFYVE biosensor still detects endosomal PtdIns3*P* in the cell. This indicates that for double-transfection protocols, the 2xFYVE biosensor is not applicable, as it probably has a higher affinity for PtdIns3*P* and blocks access of myotubularin phosphatases to their substrate. [Part (b) adapted from Fig. 7 of Laporte et al. [20], with permission from The Company of Biologists.) Transfected cells are highlighted with stars and examples of PtdIns3*P*-positive endosomes with arrows

Acknowledgments We thank Jean-Louis Mandel for support and Harald Stenmark for the 2xFYVE tandem domain. This work was supported by the Institut National de la Santé et de la Recherche Médicale, the Centre National de la Recherche Scientifique, the Collège de France, and the Association Française contre les Myopathies. H.M.R. is recipient of a Deutsche Forschungsgemeinschaft fellowship no. RO3070/1-1.

Notes

1. Migration solvents should be prepared and filled into the TLC tank 1 to 2 days before the migration to get perfect saturation of the tank. Second, it is important to keep the solvent tank and perform the migration experiment in a room with a constant temperature around 19°C.
2. For the fluorescent lipid-based IP-phosphatase assay, it is important to check fluorescent lipids from the reaction quite soon on small TLC plates (8 cm × 3 cm), as they are not stable and get degraded or hydrolyzed [even if kept in chloroform/methanol (1/1) at 4°C].
3. For quantification of the specific activity of a PPIn phosphatase, the radioactive assay is more appropriate. The phosphatase activity of myotubularins can be measured using di-C16-NBD6 or di-C6-NBD6 phosphoinositides [7, 19].
4. For the biotinylation reaction, it is important to rebuffer the eluted recombinant proteins from the glutathione elution buffer into the biotinylation reaction buffer, as amine-containing buffer may inhibit the biotinylation reaction.
5. After finishing the biotinylation, it is important to wash and to concentrate the obtained eluates from the Sephadex column with PBS with a centricon concentrator. Although the eluates' concentration is sufficient for diluting the biosensor to the working concentration, no positive results have been obtained using the eluates directly. Most likely, residual biotins are quenching this sensitive detection method.
6. Although the biotinylation reaction itself should not be problematic, it is advisable to control its success by resolving the biotinylated GST-2xFYVE on a SDS-PAGE, followed by detection with streptavidin-horseradish peroxidase and enhanced chemiluminescence system.
7. For the fixation procedure, it is important to keep the cells in the fixation solution (4% PFA in PBS) with gentle shaking overnight. This has proven to be important for permeabilization, as no detergents or other permeabilization step will be added.
8. For proper detection of the lipid signaling molecule PtdIns3*P* using the 2xFYVE probe, it is important to avoid detergents like Triton X-100 during all incubation and washing steps. It is very likely that such detergents, even at very low concentrations, will wash out the lipids within the sample and avoid proper detection.

References

1. De Matteis MA, Godi A. PI-loting membrane traffic. Nat Cell Biol 2004;6:487–92.
2. Simonsen A, Wurmser AE, Emr SD, Stenmark H. The role of phosphoinositides in membrane transport. Curr Opin Cell Biol 2001;13:485–92.
3. Laporte J, Hu LJ, Kretz C, Mandel JL, Kioschis P, Coy JF, Klauck SM, Poustka A, Dahl N. A gene mutated in X-linked myotubular myopathy defines a new putative tyrosine phosphatase family conserved in yeast. Nat Genet 1996;13:175–82.
4. Berger P, Bonneick S, Willi S, Wymann M, Suter U. Loss of phosphatase activity in myotubularin-related protein 2 is associated with Charcot-Marie-Tooth disease type 4B1. Human Mol Genet 2002;11:1569–79.
5. Blondeau F, Laporte J, Bodin S, Superti-Furga G, Payrastre B, Mandel JL. Myotubularin, a phosphatase deficient in myotubular myopathy, acts on phosphatidylinositol 3-kinase and phosphatidylinositol 3-phosphate pathway. Human Mol Genet 2000;9:2223–9.
6. Taylor GS, Maehama T, Dixon JE. Inaugural article: Myotubularin, a protein tyrosine phosphatase mutated in myotubular myopathy, dephosphorylates the lipid second messenger, phosphatidylinositol 3-phosphate. Proc Natl Acad Sci USA 2000;97:8910–5.
7. Tronchère H, Laporte J, Pendaries C, Chaussade C, Liaubet L, Pirola L, Mandel J-L, Payrastre B. Production of PtdIns(5)*P* by the phosphoinositide 3-phosphatase myotubularin in mammalian cells. J Biol Chem 2004;279:7308–12.

8. Fauman E, Saper MA. Structure and function of the protein tyrosine phosphatases. Trends Biochem Sci 1996;21:413–7.
9. Clague MJ, Lorenzo O. The myotubularin family of lipid phosphatases. Traffic 2005;6:1063–9.
10. Laporte J, Bedez F, Bolino A, Mandel J-L. Cooperation and specificity of catalytically active and inactive myotubularin phosphoinositides phosphatases. Human Mol Genet 2003;12:285–92.
11. Azzedine H, Bolino A, Taieb T, Birouk N, Di Duca M, Bouhouche A, Benamou S, Mrabet A, Hammadouche T, Chkili T, Gouider R, Ravazzolo R, Brice A, Laporte J, LeGuern E. Mutations in MTMR13, a new pseudophosphatase homologue of MTMR2 and Sbf1, in two families with an autosomal recessive demyelinating form of Charcot--Marie-Tooth disease associated with early-onset glaucoma. Am J Human Genet 2003;72:1141–53.
12. Bolino A, Muglia M, Conforti FL, LeGuern E, Salih MA, Georgiou DM, Christodoulou K, Hausmanowa-Petrusewicz I, Mandich P, Schenone A, Gambardella A, Bono F, Quattrone A, Devoto M, Monaco AP. Charcot-Marie-Tooth type 4B is caused by mutations in the gene encoding myotubularin-related protein-2. Nat Genet 2000;25:17–9.
13. Berger P, Berger I, Schaffitzel C, Tersar K, Volkmer B, Suter U. Multi-level regulation of myotubularin-related protein-2 phosphatase activity by myotubularin-related protein-13/set-binding factor-2. Human Mol Genet 2006;15:569–79.
14. Robinson FL, Dixon JE. The phosphoinositide-3-phosphatase MTMR2 associates with MTMR13, a membrane-associated pseudophosphatase also mutated in type 4B Charcot-Marie-Tooth disease. J Biol Chem 2005;280:31699–707.
15. Gillooly DJ, Morrow IC, Lindsay M, Gould R, Bryant NJ, Gaullier JM, Parton RG, Stenmark H. Localization of phosphatidylinositol 3-phosphate in yeast and mammalian cells. EMBO J 2000;19:4577–88.
16. Tosch V, Rohde HM, Tronchère H, Zanoteli E, Monroy N, Kretz C, Dondaine N, Payrastre B, Mandel JL, Laporte J. A novel PtdIns3*P* and PtdIns(3,5)P_2 phosphatase with an inactivating variant in centronuclear myopathy. Human Mol Genet 2006;15:3098–106.
17. Payrastre B. Phosphoinositides: Lipid kinases and phosphatases. Methods Mol Biol 2004;273:201–12.
18. Taylor GS, Dixon JE. An assay for phosphoinositide phosphatases utilizing fluorescent substrates. Anal Biochem 2001;295:122–6.
19. Laporte J, Liaubet L, Blondeau F, Tronchère H, Mandel JL, Payrastre B. Functional redundancy in the myotubularin family. Biochem Biophys Res Commun 2002;291:305–12.
20. Laporte J, Blondeau F, Gansmuller A, Lutz Y, Vonesch JL, Mandel JL. The PtdIns3*P* phosphatase myotubularin is a cytoplasmic protein that also localizes to Rac1-inducible plasma membrane ruffles. J Cell Sci 2002;115:3105–17.

Chapter 19
Quantification of Multiple Phosphatidylinositol 4-Kinase Isozyme Activities in Cell Extracts

Mark G. Waugh, Shane Minogue and J. Justin Hsuan

Abstract A wide spectrum of intracellular signaling events mediated by up to seven different phosphorylated forms of phosphatidylinositol (PtdIns) occurs in all eukaryotic cells. The activities of multiple, nondegenerate PI kinases and phosphatases control these signaling events. The PI 4-kinase isozymes account for the major PI kinase activity in many different cell types, and the activity of each isozyme is differentially regulated. The ability to measure and distinguish the activity of individual enzymes is therefore important and forms the subject of the methods in this chapter. We describe the use and application of a versatile radiometric assay to measuring PI 4-kinase activity in a variety of biochemical contexts, from purified enzymes to membrane preparations and permeabilized cells. Until a suitable nonradioactive reagent becomes available, this assay is destined to remain the most widely used method.

Keywords Phosphatidylinositol · phosphatidylinositol kinase · phosphoinositide · phospholipid · enzyme assay · kinase · phosphorylation · thin layer chromatography · cell signaling

Abbreviations Gro-PIns: Glycerophosphoinositol; GFP: Green fluorescent protein; HPLC: hHgh-performance liquid chromatography; PtdIns: Phosphatidylinositol; PI 4-kinase: Phosphatidylinositol 4-kinase; PtdIns4*P*: Phosphatidylinositol 4-phosphate; PtdIns(4,5)P_2: Phosphatidylinositol 4,5-bisphosphate; PtdOH: Phosphatidic acid; PLC: Phospholipase C; PI4KIII: Type III PI kinases; PI4KII: Type II PI kinases; TX-100: Triton X-100; PBS: Phosphate buffered saline; TLC: Thin Layer Chromatography.

M.G. Waugh
Centre for Molecular Cell Biology, Department of Medicine, Royal Free and University College Medical School, Hampstead, London NW3 2PF, UK
e-mail: m.waugh@medsch.ucl.ac.uk

B. Larijani et al. (eds.), *Lipid Signaling Protocols*, DOI: 10.1007/978-1-60327-115-8_19,

19.1 Introduction

Phosphatidylinositol 4-kinases (PI 4-kinases) are a family of lipid kinases that catalyze the formation of phosphatidylinositol 4-phosphate (PtdIns4*P*) via the phosphorylation of phosphatidylinositol (PtdIns) on the 4'-position of the inositol residue [1]. Mammalian PtdIns 4-kinases fall into two main structural groups: (1) the type III PI kinases (PI4KIII) that were cloned based on their homology to yeast (*Saccharomyces cerevisiae*) PI 4-kinases and to the PI 3-kinase family (type I PI kinases), and (2) the type II PI kinases (PI4KII) that were purified and cloned more recently [2, 3]. The two mammalian PI4KIII enzymes, the 230-kDa α-isoform and the 92-kDa β-isoform [4, 5], have yeast orthologs termed Stt4 and Pik1, respectively [6, 7], while the two mammalian PI4KII enzymes, the 55-kDa α- and β-isoforms, have a single yeast ortholog called Lsb6 [8, 9]. It is important to note that PI 4-kinases are both structurally and enzymatically distinct from PI 5-phosphate 4-kinases (also known as type II PIPKs or PIPKINs), which catalyze the synthesis of PI 4,5-bisphosphate [PtdIns(4,5)P_2] and have no activity against PtdIns [10].

It is becoming increasingly clear that different isozymes are co-expressed by a variety of cell types and have nonredundant biological functions. It is therefore often necessary to perform isoform-specific assays. The two mammalian PI4 K types are commonly distinguished biochemically because, like PI 3-kinases, PI4KIII isozymes are sensitive to inhibition by the compounds wortmannin and LY294002, while PI4KII isozymes are sensitive to inhibition by the monoclonal antibody 4C5G and micromolar concentrations of adenosine [1]. These enzymatic differences are consistent with the low sequence similarity between the PI4KII and PI4KIII/PI 3-kinase families.

In mammalian cell lines, PI4KIIα is the most abundant and easily detected PI kinase activity. It is also constitutively membrane-associated, at least partially via posttranslational palmitoylation [2]. In contrast to PI4KIIα, the lipid kinase activities of the yeast Lsb6 [8] and mammalian PI4KIIβ [11] enzymes do not appear to contribute significantly to total cellular PtdIns4*P* levels, and their activities may be difficult to assay without some form of purification, such as immunoprecipitation. Apart from the possibility of the activity of any individual isozyme being too low to detect, the protocols described here can be employed to quantify the lipid kinase activity of any PI 4-kinase enzyme. The core requirements to detect activity are neutral pH (commonly pH 7.4), Mg^{2+} ions to form the Mg.[γ-^{32}P]ATP complex required as the phosphate donor in many kinase reactions, and EGTA to chelate free Ca^{2+} ions that can inhibit PI4KII activity. The substrates required for the assay are the phospholipid PtdIns (either added in the form of mixed micelles or vesicles, or already present in membrane preparations) and ATP that is spiked with radioactive [γ^{32}P]-ATP in order to allow detection of the [^{32}P]PtdIns4*P* product (*see* Note 1). The nonionic detergent Triton X-100 (TX-100) is often added to the assay when exogenous PtdIns substrate is included, because TX-100 greatly enhances PI4 K

and inhibits PI 3-kinase activities [12]. The presentation of PtdIns in membranes, vesicles, and micelles is usually sufficient to compare different activities where the linearity of the assay is established. However, in order to estimate intrinsic enzymatic properties, such as K_m and V_{max} values, approximations are required to quantify PtdIns concentrations (reviewed in Carman et al. [13]).

Finally, for simplicity, the core method we describe here covers the assay we routinely use for lysates prepared from cultured mammalian cell lines. A similar methodology can be extended to the analysis of other cell types, immunoprecipitates, and membrane and tissue preparations (*see* Notes 2 and 3).

19.2 Materials

19.2.1 Cell Lysis

1. Phosphate buffered saline (PBS) with Ca^{2+} and Mg^{2+} (Gibco). Note that it worth checking that the pH of new batches is 7.4.
2. Lysis buffer: PBS (or 50 mM Tris-HCl, pH 7.4, 150 mM NaCl) containing 1% TX-100, 1 mM EDTA, 1 mM EGTA, 0.1% 2-mercaptoethanol, stored at 4°C. Just before use, add COMPLETE™ protease inhibitors (Roche Diagnostics), or 1 mM phenylmethylsulphonyl fluoride (from a 200-mM stock in ethanol, stored at −20°C), 1 mM benzamidine, 1 μM aprotinin, and 1 μM leupeptin. (Note that RIPA buffer at 4°C does not appear to destroy PI 4-kinase activity and can be employed for more aggressive solubilization.)

19.2.2 PI 4-Kinase Assay

1. Assay buffer (2x): 20 mM Tris-HCl, pH 7.4, 20 mM $MgCl_2$, 1 mM EGTA, and 0.8% TX-100 (*see* Notes 4–7). Store at 4°C.
2. PtdIns [10x, small, unilamellar vesicles (SUVs)]: Resuspend lyophilized lipid (Avanti Polar Lipids) in its vial with 1–2 ml of chloroform and transfer to a suitable tube, e.g., 2-ml microfuge tube. The chloroform is then evaporated off in a fume hood under a very gentle stream of nitrogen gas. Resuspend the dried lipid in water (90% of final stock volume, based on a usual final stock concentration of 500 μM), place on ice, and sonicate with a fine-probe sonicator to form vesicles (conditions depend on the sonicator being used, but overheating must be avoided and the final susupension should appear cloudy). The stock is then aliquoted and stored at −20°C (under nitrogen for long-term storage). The purity of commercially available PtdIns can sometimes be an issue of concern. Phosphoinositides from Avanti Polar Lipids tend to be of good quality. Several other forms of lipid substrate are commonly used; indeed, secondary lipids and physical presentation can have a large effect on enzyme activity. As this area is complicated, the reader is referred to the literature for more information (e.g., [13–15]).

3. ATP containing radiolabeled [γ^{32}P]-ATP (0.05–0.3 MBq per assay tube): Stocks of unlabeled (carrier) ATP, where required, should be either freshly prepared or used from frozen stocks to minimize autohydrolysis. We generally store 100x aliquots at –20°C and use final concentrations of 10–100 μM. Accurate quantification of ATP concentration can be performed spectrophotometrically using an extinction coefficient at 259 nm of 15.4×10^3 $M^{-1}cm^{-1}$ (pH 7.0). Specific activity is determined directly by counting small, diluted aliquots alongside assay samples.
4. Quench: 1 M HCl.
5. Phase extraction reagents: 3:3:1 chloroform:methanol:1 M HCl (unless otherwise specified, all solvent ratios are given by volume and should be added gradually and in the order they are written, with mixing) and 1:1 methanol:1 M HCl, both for use with the acidic TLC resolving buffer (*see* Notes 8 and 9).

19.2.3 Thin Layer Chromatography (TLC) and Quantification

1. TLC plates: We prefer to use silica plates with lane divisions (Merck Silica 60, glass plates without fluorescence indicator).
2. Oxalate buffer for activating TLC plates: 1% w/v potassium oxalate, 20% v/v methanol, and 1 mM EDTA.
3. Phosphoinositide standards: Unlabeled PtdIns, PtdIns*P*, PtdInsP_2, and PtdInsP_3 are available from several suppliers, including Avanti Polar Lipids, and [^{3}H]PtdIns and [^{3}H]PtdInsP_2 are available from Perkin Elmer.
4. TLC acidic resolving buffer: 65:35 propan-1-ol:2 M acetic acid and 1% 5 M H_3PO_4. Note that the acidic and basic (see step 5) buffers can be reused for several consecutive runs in the TLC tank. The TLC running buffer is highly volatile, however, and care needs to be exercised when opening the tank's lid due to the release of organic vapors.
5. TLC basic resolving buffer: 45:35:11:3 chloroform:methanol:28% ammonia:water [16].
6. Scintillation cocktail(s): We routinely use Ready Safe (Beckman-Coulter) because of its disposal properties and compatibility with a wide range of samples. Note, however, that large-volume samples containing a high salt concentration, such as ion-exchange high-performance liquid chromatography (HPLC) fractions, will require a more specialized cocktail, such as Ultima-Flo AP (Perkin Elmer) for ammonium phosphate gradients.

19.3 Methods

19.3.1 Cell Lysis

See Note 5 for information on affinity precipitation and Chapter 26 for the preparation of cell homogenates.

1. Cells are placed on ice and washed twice in ice-cold PBS, pH 7.4, to remove the culture medium.
2. Ice-cold lysis buffer is added. After 5 min on ice, lysates are transferred to microfuge tubes, employing cell scrapers if necessary to improve recovery of lysates, and cleared by centrifugation for 10 min at 20,000 $\times$ *g* at 4°C. Supernatants are transferred to fresh tubes on ice.

19.3.2 PI 4-Kinase Assay

1. Samples to be assayed are aliquoted into 1.5-ml microfuge tubes (uncoated) and an equal volume of 2x assay buffer containing PtdIns and ATP at the desired concentrations is added. Tubes are sealed and incubated at 20°C (note that the yeast Lsb6p PI 4-kinase activity is thermally labile [8]) for 20–30 min. We normally assay 50 µl of sample; thus, the volumes referred to hereafter are based on this initial starting volume. However, the assay can be scaled up or down by proportional adjustment of reagents.
2. Reactions are terminated through the addition of 20 µl of 1 M HCl, which also serves to protonate the head groups of acidic phospholipids lipids, thereby neutralizing their charge and making them more amenable to organic extraction. Acid addition also denatures proteins, aiding their precipitation at the aqueous–organic interface in the subsequent extraction steps.
3. Lipids are extracted by adding 200 µl of 3:3:1 chloroform:methanol:1 M HCl. Samples may be vortexed and pulse-centrifuged using a bench-top centrifuge to improve phase partitioning.
4. The lipid-containing chloroform forms the lower phase, 50% of which is pipetted off to fresh tubes. This organic phase contains the protonated [^{32}P]PtdIns4*P* reaction product, while the radiolabeled ATP remains in the aqueous upper phase.
5. 200 µl of 1:1 methanol:1 M HCl is added to further clean up the organic phase. Tubes are then vortexed and recentrifuged as before, and a 30-µl volume is removed from the bottom phase to clean tubes. Although not completely free of other labeled compounds, this fraction should now be sufficiently pure to identify [^{32}P]PtdIns4*P* following TLC. If necessary, the volume of the organic fraction can be reduced under a continuous stream of liquid nitrogen in a fume hood. Care is needed to normalize volumes of sample required for comparison.

19.3.3 TLC and Quantification

1. Silica 60 TLC plates (Whatman) are briefly submerged in oxalate buffer, dried in an oven at 110°C for 20 min, and then cooled. Impregnating the silica

with EDTA and oxalate sequesters any free metal ions that could chelate anionic phospholipids such as PtdIns4*P*. It is also important to use dry plates: If the plates are not to be used immediately, they should be redried before use.

2. The organic phase containing [^{32}P]PtdIns4*P* is spotted in small aliquots (0.5–1 µl) onto the origin of each strip on cooled TLC plates, well above the level of the mobile phase. Repeated spotting with drying is possible to increase loadings, but heating should be avoided.
3. The plates are then placed in the TLC tank pre-equilibrated with acidic resolving buffer (~1–2 cm depth) and allowed to develop over at least 3–4 h until the solvent front has reached at least 75% of the plate's height.

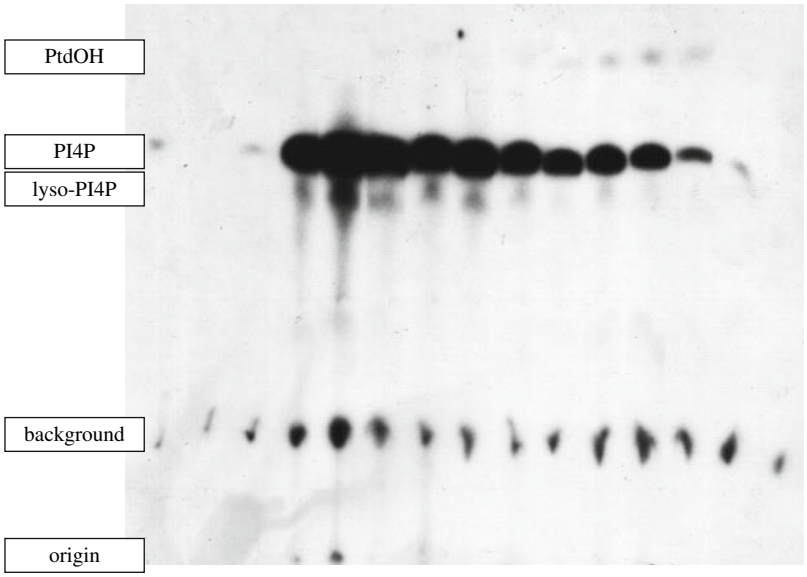

Fig. 19.1 Phosphorimage of a TLC separation of PI 4-Kinase assay products. Other bands that are often seen, especially when endogenous membrane PtdIns is used as a substrate, include the highly mobile phosphatidic acid (PtdOH) and, to a lesser extent, PtdIns(4,5)P_2. If care is not taken to minimize oxidation of the samples prior to TLC, there is also a possibility of forming lyso-PtdIns4*P*, which, because of its reduced hydrophobicity, is less mobile in the organic phase. There is often a smear of radioactive substance in the loading area of the plate, which could be unresolved [^{32}P]ATP- or [^{32}P]-labeled proteins that are hydrophobic and end up partitioning into the organic phase during the assay extraction procedures (background). PI4P standards include commercially available [^{3}H]PtdIns and [^{3}H]PtdIns(4,5)P_2, which can be imaged by an appropriate phosphorimaging screen or by fluorography. Alternatively, unlabeled PtdIns and PtdIns4*P* (10–100 nmol) can be loaded with labeled samples and visualized by a variety of reagents using the appropriate safety measures, including incubation in iodine vapor or lightly spraying with 5–10% phosphomolybdic acid in ethanol (Sigma) followed by heating at 120°C for 10 minutes, or with 0.1% 1-anilo-8-naphthalene sulfonate or 1 mM 6-*p*-toludino-2-naphthalene sulfonate, which permit visualization of phosphoinositides as fluorescent spots under ultraviolet light (reviewed in [29]). Another alternative standard, which has a limited lifetime and has to be run in parallel lanes, is [^{32}P]PtdIns4*P* generated using recombinant PI 4-kinase and extracted from silica plates

Plates can be allowed to develop overnight if desired. [Note that plates can be developed and samples spotted using different solvent mixtures. For example, PtdIns3*P* separation from PtdIns4*P* can be improved using the borate system described by Walsh and coworkers [27] (*see* Note 10). Furthermore, we have occasionally employed a basic solvent mixture to improve the separation of PtdIns*P* from other polyphosphoinositides (*see* Note 8).]

4. The TLC plate is then removed from the tank and allowed to dry in a fume hood for 30 min. Spots containing radiolabeled lipid are visualized either by autoradiography using X-ray film or by phosphorimaging (Fig. 19.1). Phosphorimaging is advantageous in that spot visualization can be directly coupled with quantification of the incorporated radiolabel. If autoradiography is used, the plate has to be aligned with the developed autoradiograph in order to identify spots of interest. In such instances, spotting a very small amount of radiolabel in a couple of visible points greatly facilitates the accurate alignment of the TLC plate and corresponding autoradiograph. Strips are then lightly sprayed with water (to reduce dispersal of silica) and the radiolabeled areas of interest scrapped off with a clean blade to scintillation vials. The level of [^{32}P]PtdIns4*P* can be accurately quantified using a scintillation counter after adding scintillation cocktail or via Cerenkov counting.

Acknowledgments We gratefully acknowledge the generous support of the Wellcome Trust and the Wolfson Foundation.

Notes

1. Using [^{3}H]PtdIns as a substrate combined with a method to quantify the formation of [^{3}H]PtdIns4*P* allows nonradioactive ATP to be employed. One problem with this technique is that the proportion of PtdIns converted to PtdIns4*P* is usually quite low, often less than 1%. Hence, the radiolabeled lipid products at the end of the reaction will contain a vast excess of [^{3}H]PtdIns relative to [^{3}H]PtdIns4*P*. This necessitates a very effective TLC separation to definitively separate and identify the different phosphoinositides.
2. The PI 4-kinase assay can also be used to look for PI 4-kinase activities present via direct or indirect association in affinity precipitates or immunoprecipitates. Such precipitations can be carried out by a variety of protocols. However, following the last washes to remove nonspecifically bound proteins, the beads are exchanged twice into PI 4-kinase assay buffer and then the assay is carried out as detailed before. If intact membrane fractions, for example caveolae, are to be immunoprecipitated, PI 4-kinase activity can subsequently be assayed using endogenous membrane-associated substrate in the absence of detergent.

   As high background binding of PI 4-kinase activity is common, it is vital to determine the level of specifically and nonspecifically bound activity. Probably due to their acylation, the type II PI 4-kinases in particular readily attach to Sepharose beads and can be difficult to remove by standard detergent-washing techniques. To overcome this problem, it is essential to ensure that relevant controls are assayed in parallel and also to preblock the beads in 0.1% (w/v) fatty acid-free BSA to reduce nonspecific protein binding. Results from experiments missing such controls are unreliable. In our experience, the magnetic Dynabeads can sometimes give reduced nonspecific binding of PI 4-kinases compared with Sepharose-based media.

3. Another variation of the method is to assay PI 4-kinase activity in cells permeabilized using streptolysin O [17, 18]. While the full details of this method are beyond the scope of this review, it is important to note that in such experiments it is often important to maintain steady-state levels of at least PtdIns and PtdIns4*P* prior to assay by providing physiological concentrations of ATP and Ca^{2+}. Other important components include soluble proteins such as PtdIns transfer proteins [19].
4. In some instances, it is useful to measure [^{32}P]PtdIns4*P* production by membrane-associated PI 4-kinases using endogenous PtdIns as substrate. In these instances, neither exogenous PtdIns nor TX-100 is added. This is because TX-100 will dissolve many biological membranes, resulting in the solubilization and dilution of both PI 4-kinase and the PtdIns substrate away from the membrane into the assay buffer.
5. It is possible to distinguish between PI4KII and PI4KIII activity by assessing the sensitivity of [^{32}P]PtdIns4*P* generation to various inhibitors. PI4KIII activity is sensitive to wortmannin (IC_{50} 50 nM) and LY-294002 (IC_{50} 100 μM). It is important to include an appropriate vehicle control in such inhibitor experiments, as compounds such as wortmannin are often dissolved in DMSO, which, we have noted, can in itself be stimulatory to PI 4-kinase activity. PI4KII activity can be inhibited by micromolar adenosine (IC_{50} 20–50 μM) and the monoclonal antibody 4C5G [20]. PI4 K activities are all sensitive to inhibition by phenylarsene oxide [1]., One study indicated differential levels of sensitivity: IIIα > IIIβ > IIβ > IIα [21].

   The only reliable way to distinguish among isoforms is first to immunoprecipitate with noninhibitory antibodies and then to assay for activity as detailed in Note 2. For example, it is possible to immunoprecipitate PI4KIIα from solubilized membrane fractions that also contain PI4KIIβ in order to determine the relative contribution of each isoform to PI 4-kinase activity. In the absence of suitable subtype-specific antisera, an alternative approach is to immunoprecipitate recombinant green fluorescent protein (GFP)-tagged PI 4-kinase isozymes expressed in cultured cell lines. This technique works particularly well because of the availability of commercial antibodies that efficiently immunoprecipitate GFP.

   For affinity precipitation, it is vital to preclear lysates wherever possible. As an example for immunoprecipitations, add an aliquot of the protein A or protein G matrix being used [e.g., protein A Sepharose (GE Healthcare) or antibody-coupled Dynabeads (Invitrogen)] and incubate for 30 min at 4°C with mixing. Centrifuge briefly to clear, and then remove supernatants to fresh tubes. Add the anti-PI 4-kinase antibody precoupled to the matrix being used, wash in lysis buffer, and then incubate for 1 h at 4°C with mixing. A control sample should include a separate antibody instead of the anti-PI 4-kinase antibody (*see* Note 2).
6. Assaying bacterially expressed recombinant PI 4-kinases can be problematic due to their low specific activity. Bacterially expressed recombinant PI4KII isozymes are inactive unless a detergent such as TX-100 is added. This is probably due to low solubility and the absence of posttranslational palmitoylation, which is thought to promote membrane localization and activity of at least the PI4KIIα isozyme. In contrast, PI4KIIα expressed in mammalian cells and purified by immunoprecipitation is active against exogenously added PtdIns substrate in the absence of TX-100. Nonetheless, the basal activity of the enzyme is greatly enhanced by detergent addition. This is an important consideration when using the PI 4-kinase assay to screen for exogenous regulators of this enzyme class, as the positive effect of regulators on activity can be masked by the large stimulatory effect of TX-100 in the assay.
7. When assaying PI 4-kinase activities from cell lysates, it may be useful to minimize PtdIns4*P* degradation by phosphatases such as Sac1 [22]. While there are no generic inhibitors of PtdIns phosphatases, the activity of Sac1 phosphatases is suppressed by TX-100. Additional inhibitors include Cu^{2+}, Zn^{2+}, and Mg^{2+} ions [23] and N-ethylmaleimide [24]. However, in our experience, phosphatase activity is not a commonly encountered problem when assaying PI 4-kinase activity. Phospholipase C (PLC) activity can also

potentially lead to PtdIns4*P* degradation, and a commercially available PLC inhibitor such as U73122 (BioSource) may be included if PLC activity is a concern. While this is normally not a problem, it can become important in co-immunoprecipitation experiments where PLC is a component of an immuno-complex, such as, for example, in immunoprecipitates of activated tyrosine kinase growth factor receptors [17, 25].

8. The solvent system detailed here is widely used as it also permits the separation of PtdIns, PtdIns*P*, PtdInsP_2, and PtdInsP_3. However, it has a disadvantage in that it takes at least 3 h to develop the plate. Separation by a basic TLC system is much more rapid but affords much less resolution of phosphoinositide isoforms. The basic running buffer consists of 45:35:11:3 chloroform:methanol:ammonia (28%):water [16]. In this system, sufficient separation occurs to visualize PtdIns4*P* using plate development times typically less than an hour.
9. While extraction with chloroform:methanol works very well, some workers prefer to remove the top rather than the bottom phase from the assay mix in order to reduce contamination by the aqueous phase. One such method based on that reported by Wetzker et al. [26] entails incubating samples with 25 mM Tris-HCl, pH 7.5, 10 mM $MgCl_2$, 70 μM ATP, 1.5% TX-100 containing 200 μM PtdIns and 5 μCi of [$\tilde{\gamma}$ ^{32}P]ATP for 20 minutes at 37°C. Reactions are stopped by the addition of 1 ml of 13:7 hexane/isopropanol and 0.2 ml of 8:0.25 2 M KCl/conc. HCl. Tubes are sealed, vortexed, and allowed to settle, aided by a brief low-speed spin before 0.5 ml of the organic (upper) phase is transferred to fresh tubes containing 0.5 ml of 0.1 M HCl. After vortexing again, a 0.2-ml aliquot of the final organic phase is removed to fresh tubes for analysis by TLC.
10. Due to the prevalence of PI 4-kinase activity in many cell types, a common mistake is to misidentify PI 4-kinase activity as PI 3-kinase activity. This is usually due to the fact that both molecules are identical in charge and size and hence do not display significantly different mobilities on TLC. One approach to distinguish between PI 3-kinases and PI 4-kinases is to carry out the assay in the presence of exogenous PtdIns and TX-100, as the detergent selectively stimulates PI 4-kinase activity. Alternatively, carrying out the assays in the presence of PI 3-kinase inhibition with low concentrations of wortmannin and/or LY-294002 will discriminate between PI 3-kinases and PI 4-kinases (i.e., 2 μM wortmannin and 10 μM LY-294002) and will have little effect on type III PI 4-kinase activity but should inhibit PI 3-kinase activity.

    Another approach is to use the method of Walsh et al. [27] to resolve PtdIns3*P* and PtdIns4*P* by TLC. This method uses radiolabeled PtdIns3*P* and PtdIns4*P* standards run in parallel with the reaction products. TLC plates are first soaked in 4.5% CDTA and then dried at 110°C for at least 10 min. The plates are then developed in a solution composed of 17 ml of methanol, 60 ml of chloroform, and 45 ml of pyridine, which is made using continuous stirring. Then 12 g of boric acid are added, followed by 7.5 ml of ddH_2O, and finally 2.6 g of 2,6-di-tert-butyl-4-methylphenol and 75 μl of technical-grade ethoxyquin. In this solvent system, PtdIns3*P* has a slightly higher mobility than PtdIns4*P*.

    A more rigorous approach is to carry out the reaction as before but instead of separating the reaction products by TLC, HPLC using a strong anion-exchange resin can be employed. This form of chromatography affords a much better resolution of phosphoinositide isomers than TLC but requires several more steps in preparing the reaction products for analysis. The procedure is the same as far as drying under nitrogen the assay reaction products extracted in the chloroform phase. However, in order to allow separation by HPLC, the reaction products first need to be deacylated to form the corresponding glycerophosphoinositol (Gro-*P*Ins) phosphates. It is important to consult the original deacylation procedure described in detail by Clarke and Dawson [28]. Briefly, deacylation is carried out by treatment with methylamine (100:80:20 methylamine:methanol:butanol) at 50°C for 1 h, which results in the conversion of PtdIns4*P* to Gro-*P*Ins4*P*. The reaction mixture is then resuspended in propanol and dried under nitrogen. The dried lipids are then redissolved in water and finally extracted with 20:4:1 butanol/petrol ether/ethyl formate. The deacylated, water-soluble products are then

separated on an HPLC column, commonly using ^{3}H-labeled glycero-phosphoinositol phosphate standards to identify peaks corresponding to the various ^{32}P-labeled products and procedures based on the methods originally described by Stephens et al. [16]. Strong anion-exchange columns are developed with an $(NH_4)_2HPO_4$ gradient, and the eluate analyzed by scintillation counting either inline or via fraction collection.

References

1. Balla A, Balla T. Phosphatidylinositol 4-kinases: Old enzymes with emerging new functions. Trends Cell Biol 2006;16:351–361.
2. Barylko B, Gerber SH, Binns DD, Grichine N, Khvotchev M, Sudhof TC, Albanesi JP. A novel family of phosphatidylinositol 4-kinases conserved from yeast to humans. J Biol Chem 2001;276:7705–8.
3. Minogue S, Anderson JS, Waugh MG, dos Santos M, Corless S, Cramer R, Hsuan JJ. Cloning of a human type II phosphatidylinositol 4-kinase reveals a novel lipid kinase family. J Biol Chem 2001;276:16635–40.
4. Nakagawa T, Goto K, Kondo H. Cloning, expression, and localization of 230-kDa phosphatidylinositol 4-kinase. J Biol Chem 1996;271:12088–94.
5. Nakagawa T, Goto K, Kondo H. Cloning and characterization of a 92 kDa soluble phosphatidylinositol 4-kinase. Biochem J 1996;320:643–9.
6. Flanagan CA, Schnieders EA, Emerick AW, Kunisawa R, Admon A, Thorner J. Phosphatidylinositol 4-kinase: Gene structure and requirement for yeast cell viability. Science 1993;262:1444–8.
7. Yoshida S, Ohya Y, Goebl M, Nakano A, Anraku Y. A novel gene, STT4, encodes a phosphatidylinositol 4-kinase in the PKC1 protein kinase pathway of *Saccharomyces cerevisiae*. J Biol Chem 1994;269:1166–72.
8. Han GS, Audhya A, Markley DJ, Emr SD, Carman GM. The *Saccharomyces cerevisiae* LSB6 gene encodes phosphatidylinositol 4-kinase activity. J Biol Chem 2002;277:47709–18.
9. Shelton SN, Barylko B, Binns DD, Horazdovsky BF, Albanesi JP, Goodman JM. *Saccharomyces cerevisiae* contains a type II phosphoinositide 4-kinase. Biochem J 2003;371:533–40.
10. Oude Weernink PA, Schmidt M, Jakobs KH. Regulation and cellular roles of phosphoinositide 5-kinases. Eur J Pharmacol 2004;500:87–99.
11. Waugh MG, Minogue S, Blumenkrantz D, Anderson JS, Hsuan JJ. Identification and characterization of differentially active pools of type II alpha phosphatidylinositol 4-kinase activity in unstimulated A431 cells. Biochem J 2003;376:497–503.
12. Whitman M, Kaplan D, Roberts T, Cantley L. Evidence for two distinct phosphatidylinositol kinases in fibroblasts. Implications for cellular regulation. Biochem J 1987;247:165–74.
13. Carman GM, Deems RA, Dennis EA. Lipid signalling enzymes and surface dilution kinetics. J Biol Chem 1995;270:18711–4.
14. Hubner S, Couvillon AD, Kas JA, Bankaitis VA, Vegners R, Carpenter CL, Janmey PA. Enhancement of phosphoinositide 3-kinase (PI 3-kinase) activity by membrane curvature and inositol-phospholipid-binding peptides. Eur J Biochem 1998;258:846–53.
15. Torchilin VP, Weissig V. Liposomes: A Practical Approach. Oxford: Oxford University Press; 2003.
16. Stephens L, Hawkins PT, Downes CP. Metabolic and structural evidence for the existence of a third species of polyphosphoinositide in cells: D-phosphatidyl-myo-inositol 3-phosphate. Biochem J 1989;259:267–76.
17. Kauffmann-Zeh A, Thomas GM, Ball A, Prosser S, Cunningham E, Cockcroft S, Hsuan JJ. Requirement for phosphatidylinositol transfer protein in epidermal growth factor signalling. Science 1995;268:1188–90.

18. Fensome A, Cunningham E, Prosser S, Tan SK, Swigart P, Thomas G, Hsuan J, Cockcroft S. ARF and PITP restore GTP gamma S-stimulated protein secretion from cytosol-depleted HL60 cells by promoting PIP2 synthesis. Curr Biol 1996;6:730–8.
19. Hsuan J, Cockcroft S. The PITP family of phosphatidylinositol transfer proteins. Genome Biol 2001;2.
20. Endemann GC, Graziani A, Cantley LC. A monoclonal antibody distinguishes two types of phosphatidylinositol 4-kinase. Biochem J 1991;273:63–6.
21. Balla A, Tuymetova G, Barshishat M, Geiszt M, Balla T. Characterization of type II phosphatidylinositol 4-kinase isoforms reveals association of the enzymes with endosomal vesicular compartments. J Biol Chem 2002;277:20041–50.
22. Hughes WE, Cooke FT, Parker PJ. Sac phosphatase domain proteins. Biochem J 2000;350:337–52.
23. Guo S, Stolz LE, Lemrow SM, York JD. SAC1-like domains of yeast SAC1, INP52, and INP53 and of human synaptojanin encode polyphosphoinositide phosphatases. J Biol Chem 1999;274:12990–5.
24. Maehama T, Taylor GS, Slama JT, Dixon JE. A sensitive assay for phosphoinositide phosphatases. Anal Biochem 2000;279:248–50.
25. Kauffmann-Zeh A, Klinger R, Endemann G, Waterfield MD, Wetzker R, Hsuan JJ. Regulation of human type II phosphatidylinositol kinase activity by epidermal growth factor-dependent phosphorylation and receptor association. J Biol Chem 1994;269:31243–51.
26. Wetzker R, Klinger R, Hsuan J, Fry MJ, Kauffmann-Zeh A, Muller E, Frunder H, Waterfield M. Purification and characterization of phosphatidylinositol 4-kinase from human erythrocyte membranes. Eur J Biochem 1991;200:179–85.
27. Walsh JP, Caldwell KK, Majerus PW. Formation of phosphatidylinositol 3-phosphate by isomerization from phosphatidylinositol 4-phosphate. Proc Natl Acad Sci USA 1991;88:9184–7.
28. Clarke NG, Dawson RM. Alkaline O leads to N-transacylation. A new method for the quantitative deacylation of phospholipids. Biochem J 1981;195:301–6.
29. Henderson RJ, Tocher DR. Thin-layer chromatography. In Hamilton RJ, Hamilton S, eds. Lipid Analysis: A Practical Approach. Oxford: IRL Press at Oxford University Press; 1992:65–111.

Chapter 20
Phospholipid-Interacting Proteins by Solution-State NMR Spectroscopy

Keiichiro Kami, Sundaresan Rajesh and Michael Overduin

Abstract Signaling lipids are found in specific subcellular membranes, where they recruit and regulate cytosolic proteins and contribute to bilayer structure and dynamics. These interactions are vital for signaling and membrane trafficking pathways and contribute to the organization, growth, and differentiation of the cell. However, the analysis of the physical and chemical mechanisms of membrane interaction and lipid recognition is technically challenging, motivating the development of new NMR methods to study lipid and bilayer binding by peripheral membrane proteins in solution. We describe methods that have been optimized for the FYVE and phox (PX) domains of the EEA1 and Vam7p proteins, respectively, both of which specifically recognize phosphatidylinositol 3-phosphate (PtdIns3*P*) within endocytic membranes. Solution-state NMR methods were used to characterize the phosphoinositide and membrane interaction sites and affinities and can be used to illustrate protein:micelle structures and phospholipid specificities. The methods are generally applicable and can be used to discover and characterize the phospholipid interactions of other membrane-interacting protein domains.

Keywords PX domain · FYVE domain · peripheral membrane protein · phosphoinositide binding · phospholipid interactions · NMR · protein structure

Abbreviations DHPC: dihexanoyl- or diheptanoyl-phosphatidylcholine; DPC: dodecylphosphocholine; GST: glutathione S-transferase; HSQC: heteronuclear single quantum coherence; PC: phosphatidylcholine; PI: phosphatidyl inositol; TCEP: tris (2-carboxyethyl) phosphine.

M. Overduin
CR-UK Institute for Cancer Studies, School of Medicine, University of Birmingham, Birmingham B15 2TT, UK
e-mail: m.overduin@bham.ac.uk

B. Larijani et al. (eds.), *Lipid Signaling Protocols*, DOI: 10.1007/978-1-60327-115-8_20,

20.1 Introduction

Phospholipids are important for cellular signaling and receptor trafficking and are responsible for the recruitment, assembly, and regulation of many protein complexes. Roughly one third of all proteins are transmembrane. Another large but undercharacterized fraction of the proteome consists of peripheral membrane proteins that bind to or insert partially into the bilayer. These proteins can be constitutively localized to the membrane or can be recruited by signaling events such as the phosphorylation of a lipid head group. The paradigm of the group is the zinc-stabilized FYVE domain, which binds specifically to PtdIns3*P* in a pH-dependent manner [1]. The functionally analogous PX domain is found in proteins including phospholipases, protein kinases, PI-kinases, SNAREs, and sorting nexins but exhibits more diverse binding specificities [2]. Other examples of phospholipid binding modules, including BAR, C1, C2, CALM, ENTH, FERM, Gla, PDZ, PH, PTB, SH2, START, and Tubby domains, have been found [3–16]; collectively, these are responsible for recruiting hundreds of proteins to membrane surfaces.

The protein domains that interact with membrane surfaces remain poorly understood due to practical hurdles including difficult expression and purification, poor solubility, and weak lipid interactions. Moreover, there are many distinct phospholipids and glycolipids that can be specifically recognized or that influence the structures and dynamics of the bilayer and interacting proteins. The lipid recognition mechanisms can involve multiple steps of membrane docking and insertion, as well as changes in protein structure and activity. Characterizing and exploiting these interactions requires high-resolution structural and dynamic information in a context that mimics the chemical and physical properties of the membrane, such as can be provided by NMR methods.

20.2 Materials

20.2.1 Transformation of E. coli *to Express Target Proteins*

1. Expression vector such as pGEX (GE Healthcare) or pET (Novagen) with inserts encoding the structural domains plus glutathione S-transferase fusions (pGEX) or His_6 tags (pET) for convenient affinity purification.
2. To design inserts, the boundaries of conserved structural domains in membrane-interacting proteins can be predicted using programs such as FoldIndex [17] and RONN [18], and conserved sequences identified using programs such as PSI-Blast [19], and ClustalW [20].
3. Competent cells: *E. coli* BL21(DE3) for expression and DH5α for DNA manipulation (*see* Note 1).

20.2.2 Expression and Isotope Labeling of Protein

1. Rich media (LB) for production of unlabeled protein: Dissolve tryptone (10 g/L), yeast extract (5 g/L), and NaCl (10 g/L), and autoclave to sterilize just prior to use.
2. Minimal M9 medium base: 1 L of deionized H_2O with 33.5 mM Na_2HPO_4, 44.1 mM KH_2PO_4, and 17.1 mM NaCl, autoclaved prior to use.
3. Minimal M9 medium for production of ^{15}N-isotope labeled protein: Add the following filter-sterilized solutions to the M9 base: 10 ml of 20% (w/v) glucose, 4 ml of 25 % (w/v) [^{15}N]-NH_4Cl (Cambridge Isotope Laboratories, Inc.), 2 ml of 1 M $MgSO_4$, 1 ml of 100 mM $CaCl_2$, and 1 ml of metal mixture containing 4 mM $ZnSO_4$, 1 mM $MnSO_4$, 4.7 mM H_3BO_3, and 0.7 mM $CuSO_4$.
4. Isopropyl-β-D-thiogalactoside (IPTG): a 1 M filter-sterilized stock with distilled water, and stored as frozen 1-ml aliquots.

20.2.3 Protein Purification

20.2.3.1 Lysis of Cells

1. Lysozyme stored as a powder at 4°C until use at room temperature.
2. 20% (v/v) Triton X-100 in 20 mM phosphate buffer (pH 7.4) dissolved and stored at room temperature.
3. Complete™ protease inhibitor tablets (Boehringer Mannheim). For His-tagged protein purification, use Complete EDTA-free tablets.

4a. Phosphate buffered saline (PBS) prepared with 10 mM Na_2HPO_4, 1.8 mM KH_2PO_4, 140 mM NaCl, and 2.7 mM KCl, and adjusted to pH 7.4 with conc. HCl.

4b. 50 mM Tris-HCl, pH 7.5, 250 mM NaCl, and 0.5 mM TCEP.

20.2.3.2 Affinity Purification, Elution, and Buffer Exchange

1. Disk filter: A low-protein binding filter should be used to filter the supernatant, such as Millex®-HV (Millipore) or Acrodisc® (Pall Corporation).

For purification of GST-tagged proteins:

2. Affinity resin slurry: Equilibrate resin such as Glutathione Sepharose 4B (GE Healthcare) in running buffer as a 50% slurry. Store at 4°C.
3. Wash buffer 1: 50 mM phosphate (pH 7.0), 150 mM KCl, and 0.5% Triton X-100.
4. Wash buffer 2: 50 mM phosphate (pH 7.0) and 150 mM KCl.
5. Elution buffer: Prepare fresh with 10–20 mM reduced glutathione in 200 mM Tris, pH 8.0, and 250 mM NaCl.
6. Concentrator: e.g., Amicon® Ultra-15 centrifugal filter devices (Millipore).

For His_6-tagged proteins:

7. Column: HisTrap column (1 ml) (GE Healthcare).
8. Equilibration buffer: 50 mM Tris-HCl, pH 7.5, 250 mM NaCl, 25 mM Imidazole, and 0.5 mM TCEP.
9. Wash buffer: same as above.
10. Elution buffer: 50 mM Tris-HCl, pH 7.5, 250 mM NaCl, 500 mM Imidazole, and 0.5 mM TCEP.
11. Concentrator: Vivaspin concentrator centrifugal filter devices (Vivascience).

20.2.3.3 Protease Digestion and Removing the Cleaved Protein

1. Dissolve lyophilized thrombin (Sigma-Aldrich) at 1 NIH unit per μl in PBS (10 mM Na_2HPO_4, 1.8 mM KH_2PO_4, 140 mM NaCl, and 2.7 mM KCl; adjust to pH 7.4). Store in small aliquots at −80°C.
2. Benzamidine Sepharose 4 Fast Flow (GE Healthcare) is washed with pure water and equilibrated with wash buffer 2. Store at 4°C.

20.2.3.4 Refolding by Dialysis

1. Dissolve guanidine hydrochloride at 6 M in pure water, and filter the solution.
2. Dialysis buffer: 50 mM phosphate (pH 7.0) and 150 mM KCl.
3. Dialysis membrane: Wash SnakeSkin® Pleated Dialysis Tubing (Pierce) with pure water before use.

20.2.3.5 Chromatographic Purification

1. Disk filter: Millex®-HV (Millipore) or Acrodisc® (Pall Corporation).
2. Column: HiTrap SP, RESOURCE S, etc. (GE Healthcare) for ion-exchange chromatography; Superdex 75/200 (GE Healthcare) for size exclusion.
3. For ion exchange, buffer A: 20 mM phosphate (pH 7.4); buffer B: 1 M NaCl and 20 mM phosphate (pH 7.4). Mix appropriate volumes of buffers A and B to prepare desired salt concentration. (For size exclusion, *see* Subheading 20.2.4.)

20.2.4 Estimation of Protein Size and Oligomeric State

1. Use a size exclusion column with appropriate molecular weight exclusion limit to discriminate monomers from multimers, e.g., Superdex200 10/300 GL (GE Healthcare).
2. To avoid nonspecific interactions of proteins with gel matrix, the running buffer should include up to 150 mM salt, e.g., 50 mM phosphate (pH 7.0) and 150 mM NaCl.
3. Standard protein samples are commercially available, e.g., Gel Filtration Calibration Kit (GE Healthcare).

20.2.5 Preparation of Protein Samples for 1D NMR

Prepare 600 µl of an NMR sample containing 0.05 to 1 mM unlabeled protein in a buffer such as (1) 250 mM potassium phosphate (pH 7.0), (2) 50 mM potassium phosphate, 100 mM KCl (pH 7.0), or (3) 25 mM perdeuterated Tris (Cambridge Isotope Laboratories), 200 mM KCl (pH 7.0), in addition to 1 mM DTT, 1 mM $NaNO_3$, and 10% ^2H_2O. Optimal NMR solution conditions for protein solubility can be screened by microdrop analysis [21].

20.2.6 Lipid Binding

1. Prepare 600 µl of an NMR sample containing 0.05 to 1 mM ^{15}N-labeled protein in a 25 mM Tris, 200 mM KCl (pH 7.0) buffer containing 1 mM DTT, 1 mM $NaNO_3$, and 10% ^2H_2O.
2. Short acyl chain phospholipids such as dioctanoyl (diC8) PtdIns3*P* and detergents such as dodecylphosphocholine are available from companies such as Anatrace, Avanti Polar Lipids, Matreya, Echelon Biosciences, and Sigma-Aldrich. They are prepared as stock solutions in the NMR buffer, and the pH is adjusted with HCl and NaOH solutions if necessary.

20.2.7 Micelle Interaction by NMR

1. For 1D NMR studies, a stock solution of perdeuterated detergent such as dodecylphosphocholine (d_{38}-DPC) or dihexanoyl-PC (Cambridge Isotope Laboratories) is prepared in the NMR buffer. After dissolving, measure the correct solution volume, calculate the correct detergent concentration, and adjust the pH.
2. For 2D ^{15}N-HSQC NMR studies, micelles composed of detergent such as diheptanoyl-PC (DHPC; Avanti Polar Lipids) are prepared by dissolving detergent in the NMR buffer as described above.

20.2.8 Micelle Insertion Using Spin Doxyls and NMR

Stock solutions of 5- or 16-doxyl-stearic acid (DSA; Sigma Aldrich) are prepared in methanol, and working solutions for titrations are aliquoted immediately. The methanol is then evaporated under vacuum before being added to an NMR sample containing ^{15}N-labeled protein ($\geq$200 µM) and detergent micelles, preferably at an excess concentration that saturates the bound state of the protein. A water-bath sonicator used at this stage helps in better dispersion of the DSA into the micelles.

20.3 Methods

20.3.1 Transformation of E. coli *to Express Target Proteins*

1. As freshly transformed bacteria express more protein, add 1 ng of plasmid to 10 µl of the BL21 competent cells; mix and place on ice for 30 min.
2. Incubate the tube containing the cells at 42°C for 45 s and then leave on ice for a few minutes.
3. Add 200 µl of prewarmed rich growth media to the transformed cells and incubate for 1 h at 37°C.
4. Plate 100 µl of the cell mixture onto an LB plate containing ampicillin and incubate the plate at 37°C overnight.
5. Prepare a glycerol stock by inoculating an isolated single colony into 2 ml of LB media, incubate at 37°C for 6 h, mix 500 µl of the culture with 500 µl of 60% glycerol, and store at −80°C.

20.3.2 Expression and Isotope Labeling of Protein

1. Prepare first culture in LB media by inoculating 10 µl of a fresh colony or glycerol stock of the transformed *E. coli* BL21 strain into 2 ml of LB medium and incubate with agitation at 37°C for 6 h.
2. Prepare a second culture by inoculating 500 µl of the LB culture into 100 ml of M9 medium, and incubate overnight in a 2 L baffled flask at 25°C.
3. Prepare a third culture by inoculating the 100-ml M9 culture into 1 L of M9 media. Agitate the cells in a 5 L baffled flask to an OD_{600} of between 0.6 and 0.7 (about 3 h) at 37°C before changing to 20°C and shaking for a further hour. Subsequently induce the culture for protein expression by adding 1 ml of 1 M IPTG, and incubate overnight to induce protein expression.
4. Harvest the cells by centrifugation at 10,000 × *g* for 15 min at 4°C, resuspend the cell pellet in 20 ml of PBS, and store at −80°C unless used immediately.

20.3.3 Protein Purification

1. Lysis of cells: Thaw the cells in an appropriate buffer in a water bath, adding lysozyme powder and then 20% (v/v) Triton X-100 to a final concentration of 1%, mixing gently to avoid bubbles. Rotate for 20 min at 4°C. Sonicate the solution for 30-s bursts on ice until the solution become less viscous and clears. Alternatively, a high-pressure cell disrupter such as a FRENCH® press (Thermo Electron) can be used to lyse cell membranes and walls, resulting in a complete and uniform cell lysis.
2. Affinity purification: Centrifuge the lysate at 75,000 × *g* for 45 min at 4°C. Filter the supernatant with Millex®-HV (Millipore), add buffer-equilibrated

glutathione (e.g., Sepharose 4B, GE Healthcare) slurry to the filtrate, and mix for 30 min at 4°C. Pour the mixture into an empty column, and wash the resin with 2 bed volumes of wash buffer 1 and then with 5 bed volumes of wash buffer 2 (*see* Note 2 for His_6-tagged proteins).

3. Elution of fusion proteins: Add elution buffer to each column, and collect the eluate containing the protein in 15-ml tubes placed under each column (*see* Note 3 for His_6-tagged proteins).
4. Buffer exchange: Exchange the elution buffer for the protease digestion buffer using a concentrator, aiming for a final filtrate volume of about 10 ml (*see* Note 4 for His_6-tagged proteins).
5. Protease digestion: Add an appropriate amount of protease to digest the protein sample overnight without causing spurious degradation based on initial trial digestions, and mix gently at room temperature or, if necessary, at a lower temperature. If proteolytic degradation occurs, use an expression vector that encodes a cleavage site for a higher-specificity PreScission protease or TEV protease.
6. Removing the cleaved protein: Set two different columns in tandem; one is packed with the same bed volume of the glutathione Sepharose resin as used in the purification of the GST-fusion protein, the other with Benzamidine Sepharose resin. Put a 50-ml tube under the lower column to collect the flow-through. Gently pour the digested sample solution into the upper column. To wash out the remaining target protein in the columns, add ~5 ml of wash buffer 2 into the upper column. The GST-cleaved protein should be found in the flow-through fraction. Total volume is ca. 15 ml (*see* Note 5 for His_6-tagged proteins).
7. Refolding by dialysis: Some proteins, such as the Vam7p PX domain, give better NMR spectra after refolding, presumably due to the removal of heterogeneity. Such proteins can be mixed with an equal volume of 6 M guanidine-HCl; the mixture is placed in a dialysis membrane tube, which is then closed. The tube is placed into 1 L of the dialysis buffer, gently stirred at room temperature for several hours, and then dialyzed into fresh buffer again overnight. Note that refolding of other proteins may require other methods [22].
8. Final purification: Ion-exchange chromatography (manually using a syringe) or size exclusion [23] in an FPLC system such as an Akta Purifier (GE Healthcare) or similar system is usually required to prepare the protein with at least 95% purity for quantitative NMR experiments, although a lower purity is sufficient for preliminary 1D NMR studies, such as assessing the structural integrity.

Purification example: Filter the protein sample solution with 0.45-μm disk filter and syringe, and load the sample solution into a pre-equilibrated cation-exchange column such as HiTrap SP (GE Healthcare). Wash the column with dialysis buffer that is equivalent to two times the column bed volume. Elute the bound proteins by increasing the concentration of NaCl stepwise (e.g., 300, 500, 700, 800, and 1,000 mM) (Fig. 20.1).

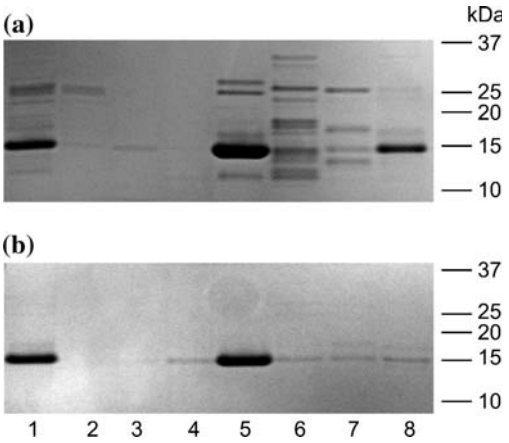

Fig. 20.1 SDS-PAGE analysis of the Vam7 PX domain purification by cation-exchange chromatography with HiTrap SP column (a) before and (b) after refolding. Lane 1, input sample after the GST-tag cleaved; lane 2, flow-through; lane 3, the first eluted fraction at 300 mM NaCl; lane 4, the second one at 300 mM NaCl; lane 5, 500 mM; lane 6, 700 mM; lane 7, 800 mM; lane 8, 1,000 mM. The fraction eluted at 500 mM NaCl (lane 5) contains the correctly folded Vam7 PX domain

20.3.4 Estimation of Protein Size and Oligomeric State (see *Note 6*)

1. Equilibrate a size exclusion column such as Superdex 200 or Superdex 75 10/300 GL (GE Healthcare) with an appropriate running buffer on a chromatography system.
2. Load globular protein standards of known molecular weight such as ribonuclease A, chymotrypsinogen A, ovalbumin, albumin, aldolase, catalase, ferritin, etc., which have been filtered through 0.45-μm filters, into the column and measure their elution volumes (V_e) at the recommended flow rate. Sample volumes should be under 2% of the total column volume (V_t) to achieve maximum resolution.
3. Calculate the K_{av} values for the standards and prepare a calibration curve of K_{av} against the logarithm of their molecular weights based on the following equation:

$$K_{av} = (V_e - V_0)/(V_t - V_0),$$

   where V_e is the elution volume of each protein, V_0 is the column void volume (equal to the elution volume of Blue Dextran), and V_t is the total bed volume of the column.
4. Measure the elution volume of the target protein and estimate its apparent molecular weight with the calibration curve determined in step 3.

20.3.5 Preparation of Lipid Binding Domain Samples

20.3.5.1 Determination of Protein Concentration by UV Absorption

1. Estimate the protein concentration by preparing a dilution series of the protein sample with an appropriate buffer (e.g., 50 mM phosphate, pH 7.0, 150 mM KCl) for measurement of the absorbance at 280 nm (A_{280}), spinning the protein sample beforehand at a high speed to remove any particulate matter.
2. Compare the absorbance to a reference buffer solution in a UV spectrometer; ideally, a quartz cuvette should be used for the measurements, although some disposable UV-compatible plastic cuvettes are also available. Ensure that cuvettes are clean, rinsed with ethanol, and free of bubbles.
3. Absorbance readings should typically be in the range between 0.1–1.0. Certain chemicals such as dithiothreitol (DTT) and Triton X-100 should be removed beforehand as they interfere with the measurement.
4. Calculate the protein concentration using a Web tool such as ProtParam using the A_{280} value, the extinction coefficient of the protein, and the dilution factor of the sample [24].

20.3.5.2 Solution Conditions

It is advisable to test several parameters (e.g., buffer salts, ionic strength, pH, temperature, and additives) before deciding on a final solution condition for a protein domain. For example, in the case of the Vam7-PX domain, it was found that high ionic strength—and, in particular, high phosphate concentration—was important for long-term protein solubility. On the other hand, it was also found that the ^{1}H and ^{15}N resonances of the PX domain were significantly different between Tris and phosphate buffers. This suggests that some solution components interact with the protein and that the phosphate buffer interferes with the binding of PX domain to PtdIns3*P* [25].

Generally, a protein will precipitate near its isoelectric point (pI) due to low solubility as a result of cancellation of net charge on the protein. Consequently, the pH of the solution should be set at least 1 unit away from the theoretical pI of the protein. The theoretical pI values can be calculated via Web-based tools [24], with a pH between 6 and 7 often being most suitable.

Although nonspecific protein aggregation may be avoided by adjusting the above parameters, some additives may also be helpful to stabilize the protein. The choice of additives for a given protein depends on the properties of each protein. For example, reducing reagents, e.g., DTT or TCEP, are effective at preventing aggregation by disulfide bonding via free cysteines. Nondetergent sulphobetaines (NDSB; available from Anatrace or Sigma-Aldrich) may also be useful to aid in solubilizing some proteins [26]. The simultaneous addition of the charged L-amino acids Arg and Glu at 50 mM to the buffer reduced aggregation during protein concentration and increased the lifetime and stability of some NMR samples [27].

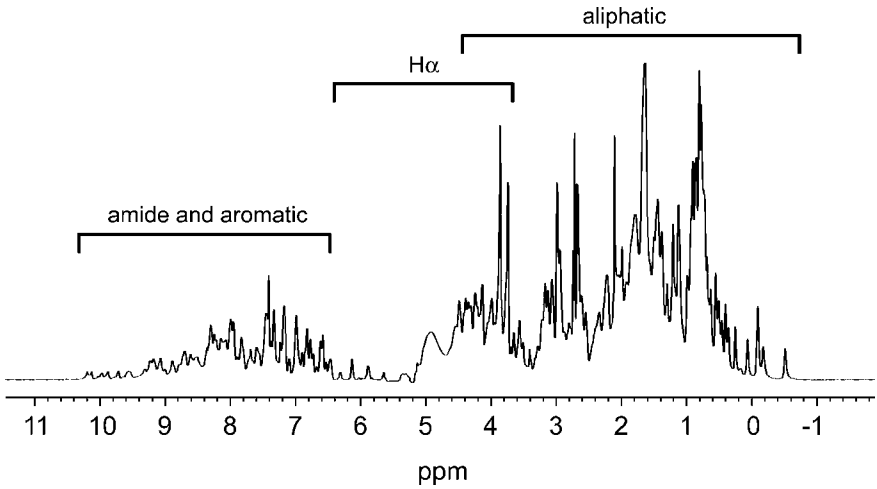

Fig. 20.2 One-dimensional ^{1}H NMR spectrum of the Vam7 PX domain (0.5 mM). Approximate regions of amide, aromatic, Hα, and aliphatic protons are indicated on the spectrum. See the text for more details

20.3.5.3 1D NMR of Protein

One-dimensional proton NMR spectra provide rapid information on whether a protein possesses a stable three-dimensional structure and whether the sample conditions are suitable for detailed NMR analysis. Measure a 1D ^{1}H NMR spectrum with a spectral width of at least −3 to 12 ppm. Dispersed peaks upfield of 0 ppm indicate that the methyl groups in amino acid side chain are buried in the hydrophobic core of a folded protein. Peaks in the region between 5.5 and 6.25 ppm indicate Hα signals of residues in a β strand conformation. Amide signal dispersion downfield of 8.5 ppm also supports the existence of a secondary structure in the protein (Fig. 20.2). A preliminary 1D proton NMR spectrum is typically first obtained from an unlabeled protein (500 μM–1 mM) on a 500- or 600-MHz NMR spectrometer, although only one third this amount of protein is needed if cryogenic probes are available due to their higher sensitivity, particularly with low-salt samples.

20.3.6 Lipid Binding

20.3.6.1 Lipid Titrations and 2D HSQC NMR

Lipid binding affinity and specificity can be characterized by comparing two-dimensional [^{1}H, ^{15}N]-HSQC spectra of ^{15}N-labeled proteins into which a soluble form of a PI such as a dibutanoyl (diC_4) or diC_8 form or another short-chain phospholipid is added stepwise (Fig. 20.3a and Color Plate 5). Chemical shift

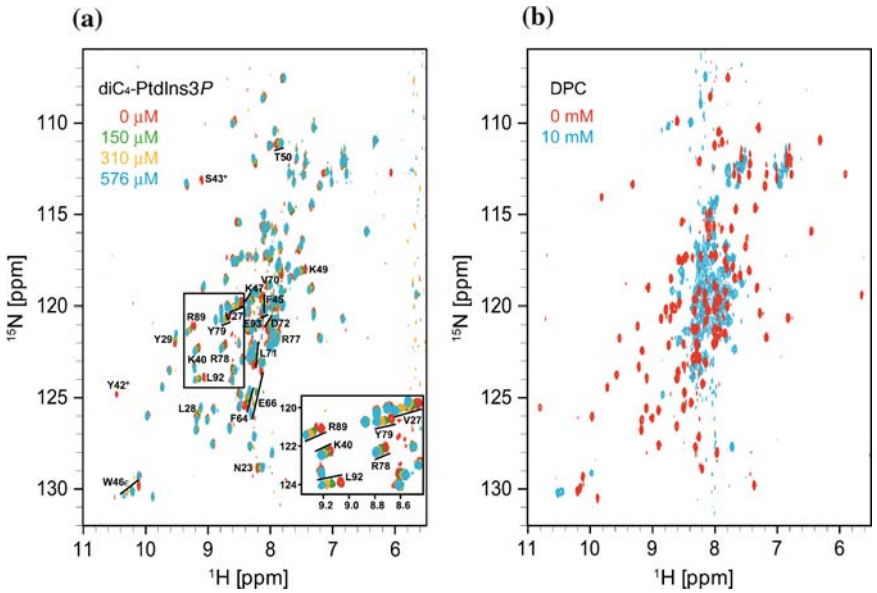

Fig. 20.3 NMR spectra were recorded at 25°C on Varian INOVA 800-MHz spectrometer. The ^{1}H-^{15}N heteronuclear single-quantum coherence (HSQC) spectra of 75 μM uniformly ^{15}N-labeled Vam7 PX domain were collected while (a) diC_4-PtdIns3*P* or (b) DPC was titrated in the buffer condition of (a) 50 mM Tris (pH 7.0) including 200 mM KCl, 1 mM TCEP, and 1 mM NaN_3 or in (b) 50 mM phosphate (pH 7.0) including 100 mM KCl, 1 mM TCEP, and 1 mM NaN_3. Residues with an asterisk (Y42 and S43) in (a) disappeared when diC_4-PtdIns3*P* was added. To view this figure in color, see color insert

changes of the amide cross peaks are observed during direct interactions and are normalized as described in the next section.

20.3.6.2 Normalized Chemical Shift Perturbations

The normalized change in the ^{1}H and ^{15}N chemical shift of each amide group is calculated using Equation (1):

$$N\Delta\delta = 10 \times [(\delta_H)^2 + (\delta_N \times (\gamma_N/\gamma_H))^2]^{1/2}, \quad (1)$$

where $N\Delta\delta$ is the normalized chemical shift change, δ_H is the observed ^{1}H chemical shift change, δ_N is the observed ^{15}N chemical shift change, and γ_N and γ_H are the gyromagnetic ratios of ^{15}N and ^{1}H, respectively [28] (Fig. 20.4).

20.3.6.3 Affinity Estimation

The dissociation constant can be determined by titrating diC_4-PtdIns3*P* into a ^{15}N-labeled protein NMR sample and monitoring the chemical shift changes by

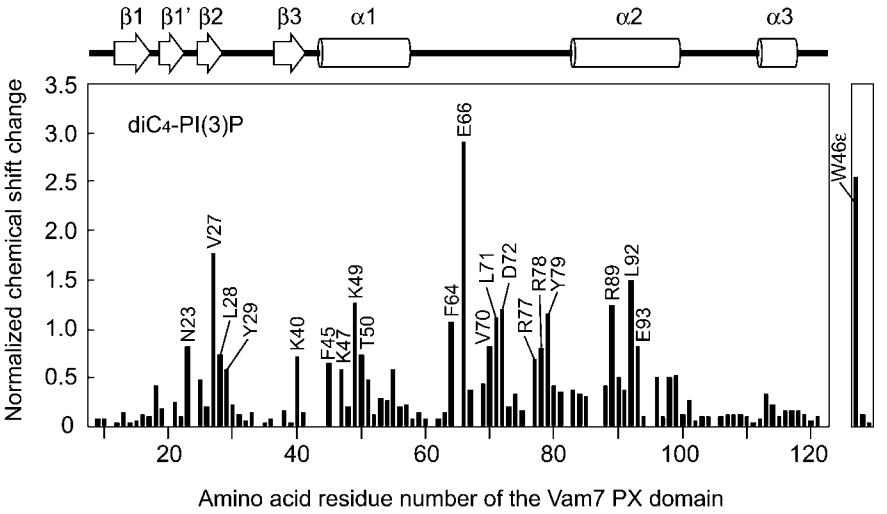

Fig. 20.4 The panel shows the normalized chemical shift changes induced after adding 567 μM diC$_4$-PtdIns3*P*. The normalized chemical shift change was calculated based on Equation (1). The secondary structure is shown above the panel

^{1}H, ^{15}N HSQC experiments. If the binding is in a fast exchange regime on the NMR timescale, the dissociation constant (K_d) is estimated based on Equation (2) by a nonlinear least-squares analysis percent-maximum chemical shift change.

$$N\Delta\delta = N\Delta\delta_{max} \times [(L + P_T + K_d) - ((L + P_T + K_d)^2 - (4 \times L \times P_T))^{1/2}]/[2 \times PT], \quad (2)$$

where $N\Delta\delta$ is the chemical shift change at each step, $N\Delta\delta_{max}$ is the change in chemical shift at saturation, L is the ligand concentration, and P_T is the total protein concentration (*see* Note 7).

20.3.6.4 Assigning Resonances and Mapping Lipid Binding Sites

The backbone resonances of a protein are sequentially assigned using several triple-resonance spectra [e.g., HNCA, HNCACB, CBCA(CO)NH, etc.] obtained from ^{15}N, ^{13}C-labeled protein that has been prepared using minimal media [29]. Large proteins (e.g., over 20 kDa) may also require deuteration to obtain high-quality spectra. Once the backbone signals are assigned, the chemical shift difference of each signal can be mapped according to residue number and onto the structure of the protein, allowing rational mutagenesis of binding-site residues to perturb subcellular localization and biological activity.

20.3.7 Micelle Interaction by NMR

To investigate the structural features of membrane binding modules for membrane interactions, a membrane-mimicking micelle system composed of detergent molecules such as DPC or DHPC is often employed in NMR experiments. DPC has a phosphocholine head group similar to that of the most abundant natural membrane phospholipid, PC. Moreover, it contains a single 12-carbon alkyl chain and forms small (~19-kDa) neutral micelles [30] suitable for NMR studies. Some other detergents that can also be used for NMR studies include DHPC, CYCLOFOS-4, β-D-octylglucoside, and CHAPS. The mode of micelle insertion may be extrapolated to bilayer interactions and tested by measuring the effects of mutations of the residues involved on vesicle association.

20.3.7.1 Micelle Titrations by 1D and HSQC NMR

1. Micelle interactions are monitored by titrating unlabeled or perdeuterated detergent micelle solution into a sample containing between 60 and 200 μM ^{15}N-labeled or unlabeled protein, respectively. Detergent concentrations are increased stepwise from near the critical micelle concentration, typically through the 1–10-mM range.
2. Monitor micelle binding by comparing ^{1}H,^{15}N HSQC spectra of ^{15}N-labeled sample at each step of the titration (*see* Note 8). Continue the titration until either saturation of the micelle interaction is approached (as evidenced by the lack of significant additional chemical shift changes) or protein denaturation occurs (as evidenced by the disappearance of resolved NMR resonances).

20.3.7.2 Affinity Estimation and Mapping Membrane-Interacting Residues

1. The changes in ^{1}H and ^{15}N chemical shift are normalized as described in affinity estimation using Equation (2).
2. Obtain the approximate micellar concentration by dividing the value of a detergent molecular concentration by the average aggregation number. These values are available in the literature [31] but may be influenced by additives such as salt and protein. The average aggregation number for each detergent micelle can be estimated by pulsed field gradient NMR methods [32].
3. Affinity estimation of micelle interaction and mapping the interacting residues are performed in the same manner as described in Subheading 20.3.6.

20.3.8 Estimation of Depth and Angles of Membrane Insertion with Spin Doxyls

An NMR sample containing the protein bound to phospholipid ligand and micelle is prepared, and the spin label such as DSA is added stepwise,

starting at concentrations below that of the micelle and protein sample. The concentration of the spin label is increased until the NMR spectra reveal significant line broadening in a subset of $^{1}H,^{15}N$ peaks, typically near the equimolar ratio of spin label to micelle [33]. The line broadening is measured as a decrease in the intensities (or volumes) of the backbone amide resonances. Significant levels of intensity reduction should be greater than the average plus one standard deviation. As a control, a second sample is prepared identically except for the lack of the specific phospholipid ligand, revealing whether nonspecific micelle insertion also occurs. The chemical shifts of the protein resonances in the HSQC spectrum should not be perturbed, as this would indicate a chemical interaction with the spin label. The broadened peaks correspond to amide groups that are located near the average position of the spin doxyl within the micelle. For example, the 5-DSA broadens the peaks of residues positioned at the level of the phospholipid head groups or below, while the 16-DSA broadens those of the most deeply buried residues.

Notes

1. In instances where codon bias of human sequences prove problematic to express sufficient amounts of protein in *E. coli*, bacterial strains optimized for codon bias such as BL21 (RIL) from Strategene or BL21(codon plus) need to be used.
2. For His-tagged proteins, dilute the lysate threefold with equilibration buffer and load onto the HisTrap column according to manufacturer's instruction (GE Healthcare). After application, wash the protein-loaded column with a further 5 column volumes of the same buffer to remove unbound samples.
3. His-tagged proteins are best eluted with an Imidazole gradient of 25 mM to 500 mM Imidazole in equilibration buffer over a 20-column volume.
4. Imidazole-containing protein fractions are concentrated and buffer-exchanged using a Vivaspin centrifugal concentrator of the appropriate molecular weight cutoff.
5. In case of a His-tagged protein, the cleaved tag is removed by passing the protease-digested protein sample through a HisTrap column to remove the cleaved tag. The flow-through from the column contains both protease and His-tag cleaved protein, which is subsequently applied onto Benzamidine Sepharose to remove the protease, e.g., thrombin. Any residual protease activity in the final flow-through may be removed by a size exclusion chromatography using a Superdex 200 10/300 GL column.
6. In addition to gel filtration [34], other methods including analytical ultracentrifugation [35], dynamic light scattering [36], and pulsed field gradient NMR [32] can be used to estimate the molecular weight of a protein.
7. To estimate the affinity correctly, the ligand should be added until chemical shifts no longer change, and the total volume of the ligand added in the protein NMR sample should be less than 10% (i.e., 60 µl) of the original protein sample.
8. Some detergents have denaturing effects. For example, the Vam7-PX domain is denatured by several detergents at concentrations below 10 mM (Fig. 20.3b and Color Plate 5). On the other hand, the FYVE domain is more stable in the presence of detergents, being held together by two zinc coordination sites.

References

1. Lee SA, Eyeson R, Cheever ML, Geng JM, Verkhusha VV, Burd C, Overduin M, Kutateladze TG. Targeting of the FYVE domain to endosomal membranes is regulated by a histidine switch. Proc Natl Acad Sci USA 2005;102:13052–7.
2. Cheever ML, Sato TK, de Beer T, Kutateladze TG, Emr SD, Overduin M. Phox domain interaction with PtdIns(3)*P* targets the Vam7 t-SNARE to vacuole membranes. Nat Cell Biol 2001;3:613–8.
3. Ford MG, Pearse BM, Higgins MK, Vallis Y, Owen DJ, Gibson A, Hopkins CR, Evans PR, McMahon HT. Simultaneous binding of PtdIns(4,5)P_2 and clathrin by AP180 in the nucleation of clathrin lattices on membranes. Science 2001;291:1051–5.
4. Overduin M, Cheever ML, Kutateladze TG. Signalling with phosphoinositides: Better than binary. Mol Interv 2001;1:150–9.
5. Lee E, Marcucci M, Daniell L, Pypaert M, Weisz OA, Ochoa GC, Farsad K, Wenk MR, De Camilli P. Amphiphysin 2 (Bin1) and T-tubule biogenesis in muscle. Science 2002;297:1193–6.
6. Johnson JE, Giorgione J, Newton AC. The C1 and C2 domains of protein kinase C are independent membrane targeting modules, with specificity for phosphatidylserine conferred by the C1 domain. Biochemistry 2000;39:11360–9.
7. Mikoshiba K, Fukuda M, Ibata K, Kabayama H, Mizutani A. Role of synaptotagmin, a Ca^{2+} and inositol polyphosphate binding protein, in neurotransmitter release and neurite outgrowth. Chem Phys Lipids 1999;98:59–67.
8. Stolt PC, Jeon H, Song HK, Herz J, Eck MJ, Blacklow SC. Origins of peptide selectivity and phosphoinositide binding revealed by structures of disabled-1 PTB domain complexes. Structure 2003;11:569–79.
9. Iyer LM, Koonin EV, Aravind L. Adaptations of the helix-grip fold for ligand binding and catalysis in the START domain superfamily. Proteins 2001;43:134–44.
10. Zwaal RF, Comfurius P, Bevers EM. Lipid-protein interactions in blood coagulation. Biochim Biophys Acta 1998;1376:433–53.
11. Tokonzaba E, Capelluto DG, Kutateladze TG, Overduin M. Phosphoinositide, phosphopeptide and pyridone interactions of the Abl SH2 domain. Chem Biol Drug Des 2006;67:230–7.
12. Boggon TJ, Shan WS, Santagata S, Myers SC, Shapiro L. Implication of tubby proteins as transcription factors by structure-based functional analysis. Science 1999;286:2119–25.
13. Harlan JE, Hajduk PJ, Yoon HS, Fesik SW. Pleckstrin homology domains bind to phosphatidylinositol-4,5-bisphosphate. Nature 1994;371:168–70.
14. Peter BJ, Kent HM, Mills IG, Vallis Y, Butler PJ, Evans PR, McMahon HT. BAR domains as sensors of membrane curvature: The amphiphysin BAR structure. Science 2004;303:495–9.
15. Niggli V, Andreoli C, Roy C, Mangeat P. Identification of a phosphatidylinositol-4,5-bisphosphate-binding domain in the N-terminal region of ezrin. FEBS Lett 1995;376:172–6.
16. Zimmermann P, Meerschaert K, Reekmans G, Leenaerts I, Small JV, Vandekerckhove J, David G, Gettemans J. PIP(2)-PDZ domain binding controls the association of syntenin with the plasma membrane. Mol Cell 2002;9:1215–25.
17. Prilusky J, Felder CE, Zeev-Ben-Mordehai T, Rydberg EH, Man O, Beckmann JS, Silman I, Sussman JL. FoldIndex: A simple tool to predict whether a given protein sequence is intrinsically unfolded. Bioinformatics 2005;21:3435–38.
18. Yang ZR, Thomson R, McNeil P, Esnouf RM. RONN: The bio-basis function neural network technique applied to the detection of natively disordered regions in proteins. Bioinformatics 2005;21:3369–76.
19. Altschul SF, Madden TL, Schaffer AA, Zhang J, Zhang Z, Miller W, Lipman DJ. Gapped BLAST and PSI-BLAST: A new generation of protein database search programs. Nucleic Acids Res 1997;25:3389–402.

20. Thompson JD, Higgins DG, Gibson TJ. CLUSTAL W: Improving the sensitivity of progressive multiple sequence alignment through sequence weighting, position-specific gap penalties and weight matrix choice. Nucleic Acids Res 1994;22:4673–80.
21. Lepre CA, Moore JM. Microdrop screening: A rapid method to optimize solvent conditions for NMR spectroscopy of proteins. J Biomol NMR 1998;12:493–9.
22. Armstrong N, de Lencastre A, Gouaux E. A new protein folding screen: Application to the ligand binding domains of a glutamate and kainate receptor and to lysozyme and carbonic anhydrase. Protein Sci 1999;8:1475–83.
23. Sheehan D, O'Sullivan S. Fast protein liquid chromatography. Methods Mol Biol 2004;244:253–8.
24. Gasteiger E, Gattiker A, Hoogland C, Ivanyi I, Appel RD, Bairoch A. ExPASy: The proteomics server for in-depth protein knowledge and analysis. Nucleic Acids Res 2003;31:3784–8.
25. Cheever ML, Kutateladze TG, Overduin M. Increased mobility in the membrane targeting PX domain induced by phosphatidylinositol 3-phosphate. Protein Sci 2006;15:1873–82.
26. Vuillard L, Braun-Breton C, Rabilloud T. Non-detergent sulphobetaines: A new class of mild solubilization agents for protein purification. Biochem J 1995;305(Pt 1):337–43.
27. Golovanov AP, Hautbergue GM, Wilson SA, Lian LY. A simple method for improving protein solubility and long-term stability. J Am Chem Soc 2004;126:8933–9.
28. Amezcua CA, Harper SM, Rutter J, Gardner KH. Structure and interactions of PAS kinase N-terminal PAS domain: Model for intramolecular kinase regulation. Structure 2002;10:1349–61.
29. Kay LE. Pulsed field gradient multi-dimensional NMR methods for the study of protein structure and dynamics in solution. Prog Biophys Mol Biol 1995;63:277–99.
30. Vinogradova O, Sonnichsen F, Sanders CR. On choosing a detergent for solution NMR studies of membrane proteins. J Biomol NMR 1998;11:381–6.
31. le Maire M, Champeil P, Moller JV. Interaction of membrane proteins and lipids with solubilizing detergents. Biochim Biophys Acta 2000;1508:86–111.
32. Altieri AS, Hinton DP, Byrd RA. Association of biomolecular systems via pulsed field gradient NMR self-diffusion measurements. J Am Chem Soc 1995;117:7566–7.
33. Kutateladze TG, Capelluto DG, Ferguson CG, Cheever ML, Kutateladze AG, Prestwich GD, Overduin M. Multivalent mechanism of membrane insertion by the FYVE domain. J Biol Chem 2004;279:3050–7.
34. Goetz H, Kuschel M, Wulff T, Sauber C, Miller C, Fisher S, Woodward C. Comparison of selected analytical techniques for protein sizing, quantitation and molecular weight determination. J Biochem Biophys Methods 2004;60:281–93.
35. Lebowitz J, Lewis MS, Schuck P. Modern analytical ultracentrifugation in protein science: A tutorial review. Protein Sci 2002;11:2067–79.
36. Wilson WW. Light scattering as a diagnostic for protein crystal growth—A practical approach. J Struct Biol 2003;142:56–65.

Chapter 21
Revealing Signaling in Single Cells by Single- and Two-Photon Fluorescence Lifetime Imaging Microscopy

Damien Alcor*, Véronique Calleja* and Banafshé Larijani

Abstract Lipids are actively involved in many cellular processes. Their roles pivot toward determining membrane structure, compartment targeting, and membrane fusion but also regulation of cell signaling via their interactions with proteins and the production of second messengers. As they play a key role in cell signaling, the study of protein–protein interaction and protein conformation change in relationship with their interaction with lipids is of major importance. Until recently, the ability to detect *in situ* and in real time the dynamics of various biological events and signals without perturbing the cellular environment has been a real challenge. However, the emergence of fluorescence imaging of cells and tissues has allowed the dynamic aspects of the cell to be investigated in a more physiological context than the disassembled model systems employed in traditional biochemical analysis. This chapter highlights some of the many biological applications and uses of frequency- and time-domain fluorescence lifetime imaging microscopy (FLIM) applied to the detection of Förster resonance energy transfer (FRET). The first part describes a FRET system, the second part discusses its study by FLIM, and the third part describes the application of these methods to a panel of biological questions such as (1) spatio-temporal interaction of protein kinase B (PKB) with 3-phosphoinositide dependent protein kinase-1 (PDK1), (2) PKB conformation change, (3) dynamics of PKB activation, (4) interaction of phosphatidylinositol transfer protein (PITP) and phospholipase D (PLD) with lipids.

Keywords Fluorescence lifetime imaging microscopy (FLIM) · FRET · protein conformation · protein–lipid interactions · PKB/Akt · PDK1 · PITP · PLD

B. Larijani
Cell Biophysics Laboratory, Lincoln's Inn Fields Laboratories, Cancer Research UK, 44 Lincoln's Inn Fields, London WC2A 3PX, UK
e-mail: banafshe.larijani@cancer.org.uk

*These authors equally contributed to the work.

B. Larijani et al. (eds.), *Lipid Signaling Protocols*, DOI: 10.1007/978-1-60327-115-8_21,

Abbreviations PKB: protein kinase B; PDK1: 3-phosphoinositide-dependent protein kinase 1; PLD: Phospholipase D; PITP: Phosphatidylinositol Transfer Protein; PDGF: Platelet Derived Growth Factor; BSA: Bovine Serum Albumin; HRP: Horse Radish Peroxydase; mRFP: monomeric Red Fluorescent Protein (Accession no: AF506027); EGFP: Enhanced Green Fluorescent Protein; YFP: Yellow Fluorescent Protein; Cy3: Cyan 3 dye; SDS-PAGE: sodium dodecyl sulfate-polyacrylamide gel electrophoresis; DCS: Donor Calf Serum; PH domain: Plextrin Homology domain; PCR: Polymerase Chain Reaction; MOWIOL: Mowiol 4-88; DABCO: 1,4-diazabicyclo-[2.2.2]-octane; FRET: Förster Resonance Energy Transfer; FLIM: Fluorescence Lifetime Imaging Microscopy; FD-FLIM: Frequency Domain-FLIM; TD-FLIM: Time Domain-FLIM, Tau (or have been used to refer to the lifetimes in the figures or in the text); TCSPC: Time Correlated Single Photon Counting.

21.1 Introduction

One of the difficulties in understanding molecular signaling in biological systems is caused by the temporal and spatial regulation of protein activity. The localization and compartmentalization of these processes are strongly dependent on lipids, and the relationship between lipids and protein activity is part of a growing field of interest. The local lipid composition and its changes are known to be important for membrane structure and function as well as for the regulation of protein activity and trafficking. Due to the spatial and dynamic aspect of these processes, invasive methods only provide partial information that does not account for the heterogeneity within a single cell. However, this heterogeneity is of major importance in cell signaling since it is an essential component of the acute regulation of cellular processes.

The use of fluorescence has played a critical role in the progress of cell biology. Indeed, it is a relatively noninvasive technique that allows us to address, both spatially and temporally, the molecular mechanisms in single cells. The development of confocal microscopy and two-photon excitation has led to the possibility of resolving the localization of protein or organelles with micrometer precision. The use of FRET in biology has provided a breakthrough in fluorescence imaging and in the understanding of biological mechanisms. By detecting resonance energy transfer between a donor and an acceptor fluorophore, it has been possible to detect intermolecular interactions, like protein–protein or protein–lipid interactions, but also protein conformational changes. The transfer of energy occurs only if the fluorophores are less than 10 nm apart. FRET enables the detection of events that are two orders of magnitude smaller than light microscopy resolution. Since the distance range within which FRET occurs has about the dimensions of a protein, intermolecular FRET reflects specific interactions as opposed to co-localization of molecules. A steady-state image can be acquired therefore, and transient/unstable interactions can be detected that might not have been

observed by classical methods like co-immunoprecipitation. Different techniques have been developed to detect FRET [1, 2]. Among them, the detection of FRET by measurement of the lifetime of the donor fluorophore has been exploited. Upon FRET, the lifetime of the donor is reduced as energy is nonradiatively transferred, via a dipole-dipole coupling, to the acceptor [3]. Fluorescence lifetime imaging microscopy (FLIM) provides a pixel-by-pixel lifetime map of the cell. In-house FLIM platforms have been developed to detect FRET by measuring lifetime in the frequency domain (FD) and in the time domain (TD). The FD-FLIM uses a one-photon epi-fluorescence excitation mode that provides rapidity. The instrument has also been developed to be an automated high-throughput prototype. The TD-FLIM, using a two-photon excitation, provides a high spatial resolution ($\sim$0.4 μm in x and y) with 3D information ($\sim$1 μm in z). The TCSPC (time-correlated single-photon counting) detection mode gives a very robust and accurate measurement of the lifetime, allowing the detection of small variations.

21.2 Materials

21.2.1 Time-Domain FLIM

1. All the images were acquired on a modified TE 2000-E inverted microscope (Nikon Ltd., Tokyo, Japan).
2. The lifetime measurements were obtained using an SPC 830 time-correlated single-photon counting (TCSPC) electronic card (Becker and Hickl, Berlin, Germany) in the reverse stop-start mode.
3. A mode-locked tunable Ti:sapphire laser Mira 900 (Coherent, UK) pumped by a solid-state diode laser Verdi (Coherent, London, UK) was used for the excitation.
4. The laser beam was analyzed using a Wave Scan laser spectrometer and Mini autocorrelator system (APE, Berlin, Germany).
5. The excitation power was adjusted with neutral density filters (New Focus, San Jose, CA, USA) set before the scanning system.
6. The scanning system was developed by the Advanced Technology Development group (Gray Cancer Institute, London, UK).
7. The laser beam was focused with a 40x oil immersion objective lens 1.3 NA, Plan-Fluor (Nikon, Kingston upon Thames, UK).
8. The fluorescence was detected through the same objective in a descanned configuration and detected with a fast photomultiplier (Hamamatsu, Welwyn Garden City, UK) after a combination of dichroic beam splitter 565 LP (Chroma Technology Corp., Rockingham, USA) and band-pass filter 510/10 (Chroma Technology Corp., Rockingham, USA).
9. Epi-fluorescence intensity images of both GFP and RFP were obtained by using the mercury lamp source of the TE 2000-E microscope.

10. Fluorescence was detected with a cooled CCD camera (Hamamatsu ORCA-ER, Welwyn Garden City, UK).
11. The cubes set in the TE 2000-E microscope turret were FITC (Nikon, Kingston upon Thames, UK) for GFP and G-2A (Nikon, Kingston upon Thames, UK) for RFP.
12. TCSPC images were acquired with MPTR software developed by the Advanced Technology Development Group (Gray Cancer Institute, UK).
13. TCSPC images were converted into lifetime maps with TRI2 software developed by the Advanced Technology Development Group (Gray Cancer Institute, London, UK).
14. Quantitative analysis of the lifetime maps were done on Origin software V7.5 (OriginLab Corp., Northampton, MA).

21.2.2 Frequency-Domain FLIM

1. A detailed description of the frequency-domain FLIM apparatus can be found elsewhere [4, 5].
2. Zeiss Plan-APOCHROMAT 100x/1.4 NA phase 3 oil objective (Carl Zeiss Ltd., Welwyn Garden City, Hertfordshire, UK).
3. Argon/Krypton laser (Coherent UK Ltd., Cambridgeshire Business Park Ely, Cambridgeshire, UK).
4. Dichroic beam splitter: Q 505 LP (Chroma Technology Corp., Rockingham, VT).
5. Narrow-band emission filter 514/10 (Delta Lys & Optik, Lyngby, Denmark).
6. Mercury arc lamp Zeiss Attoarc 2 (Carl Zeiss Ltd., Welwyn Garden City, Hertfordshire, UK).
7. High Q Cy3 filter set: exciter, HQ 535/50; dichroic, Q 565 LP; emitter, HQ 610/75 LP (Chroma Technology Corp., Rockingham, VT).
8. IPLab Spectrum software, version 3.1.2 c (Scanalytics, Inc., Fairfax, VA).

21.2.3 Protein–Protein Interaction: PKB/PDK1 Interaction

21.2.3.1 Construct Design

1. pCMV5-HA-PKB was provided by Brian A. Hemmings, as described elsewhere [6].
2. pCMV5-EGFP-PDK1 was provided by Jongsun Park, as described elsewhere [7].
3. pRSET B-mRFP was provided by Dr Roger Tsien (University of California).

4. Oligonucleotides (Sigma-Genosys, Sigma-Aldrich, Gillingham, Dorset, UK).
5. mRFP sens: agagaattcgccgccaccatggcctcctccgaggacgtcatcaaggagttcatgcgc.
6. mRFP anti: atcgaattctgcaccggtggagtggcggccctcggcgcgctcgtactgttcc.
7. EcoRI less-sens: gccacgctgtcctccgcaattcgagct ctagaggatcccgg.
8. EcoRI less-antisens: ccgggatcctctagagctcgaattgcggaggacagcgtggc.
9. Molecular biology enzymes (New England BioLabs UK Ltd.).

21.2.3.2 Expression/Activity

1. Human purified platelet-derived growth factor (PDGF) (Cat. no. 120-HD, R&D Systems, Minneapolis, MN).
2. Lysis buffer: 20 mM Tris-HCl (pH 7.4), 150 mM NaCl, 100 mM NaF, 10 mM $Na_4P_2O_7$, 10 mM EDTA.
3. Complete protease inhibitor cocktail tablet (Hoffmann-La Roche, Basel, Switzerland).
4. Bradford assay (Cat. no. 500-0006) using Bio-Rad protein assay (Bio-Rad Laboratories GmbH, Muenchen, Germany).
5. Sample buffer: 125 mM Tris-HCl (pH 6.8), 6% SDS, 20% glycerol, 0.02% bromophenol blue.
6. 2-mercaptoethanol (Cat no. M-6250, Sigma-Aldrich, Gillingham, Dorset, UK).
7. 4–12% polyacrilamide precast gels (Invitrogen, Paisley, UK).
8. Polyvinylidene difluoride membranes (PVDF) (Cat. no. IPVH 00010, Millipore UK, Watford, Hertfordshire, UK).
9. TBS-T: 10 mM Tris-HCl (pH 7.4), 150 mM NaCl, 0.05%, Tween 20.
10. Bovine serum albumin (BSA) 30% solution (A 3424) ultra high avidity (Sigma-Aldrich, Gillingham, Dorset, UK).
11. Phospho-Akt (Thr-308) was a rabbit polyclonal antibody (Cat. no. 9275, Cell Signaling, New England BioLabs UK).
12. Phospho-Akt (Ser-473) (Cat. no. 9271) was a rabbit polyclonal antibody (Cell Signaling, New England BioLabs UK).
13. Mouse monoclonal anti HA antibody (in house, CR-UK antibody production).
14. Mouse monoclonal anti GFP antibody (in house, CR-UK antibody production).
15. Secondary goat antirabbit HRP antibodies (Amersham Biosciences UK, Buckinghamshire, UK).
16. Secondary sheep antimouse HRP-antibodies (Amersham Biosciences UK, Buckinghamshire, UK).
17. Marvel milk powder (food store or VWR International, Merck House, Poole, UK).
18. ECL (Amersham Biosciences UK, Buckinghamshire, UK).

21.2.3.3 Cell Culture and Transfections

1. NIH3T3 cells (Cat no. CRL-1658, ATCC, LGC Promochem, Teddington, Middlesex, UK).
2. Dulbecco's Modified Eagle Medium (DMEM) (in house, medium production; same composition as commercial one).
3. Donor bovine serum (Cat. no. 16030074, Invitrogen, Paisley, UK).
4. 35-mm glass-bottomed microwell dishes (Cat. no. P35G-1.5-14-C, MatTek Corp., Ashland, MA).
5. Lipofect AMINE and PLUS reagent (Cat. no. 18324-012 and no. 11514-015, Invitrogen, Paisley, UK).
6. OPTIMEM with Glutamax (Cat. no. 51985, Invitrogen, Paisley, UK).
7. Poly-L-lysine 0.01% solution (Cat. no. P4707, Sigma-Aldrich, Gillingham, Dorset, UK).
8. Bovine serum albumin (BSA) fatty acid-free, endotoxin-free (Cat. no. A8806-5 G, Sigma-Aldrich, Gillingham, Dorset, UK).

21.2.3.4 Antibody Labeling

1. Anti-HA mouse monoclonal antibody (in house, CR-UK antibody production).
2. N,N-Bis (2-hydroxyethyl) glycine (also known as bicine) (Cat. no. B 8660, Sigma-Aldrich, Gillingham, Dorset, UK).
3. Dimethylformamide (DMF) (Cat. no. D 4551, Sigma-Aldrich, Gillingham, Dorset, UK).
4. Cyan-3 monoreactive dye (Cat. no. PA23001, Amersham Biosciences UK, Buckinghamshire, UK).
5. Gel permeation chromatography Econo-Pac 10 DG columns (Cat. no. 732-2010, Bio-Rad Laboratories, Hertfordshire, UK).
6. Millex-GV 0.22-μm syringe filter (Cat. no. SLVGV 004SL, Millipore, Bedford, MA).

21.2.3.5 Fixation and Mounting

1. Human purified platelet-derived growth factor (PDGF) (Cat. no. 120-HD, R&D Systems, Minneapolis, MN).
2. Paraformaldehyde (PFA) (Cat. no. P-6148, Sigma-Aldrich, Gillingham, Dorset, UK).
3. Triton X-100 (Cat. no. T-9284, Sigma-Aldrich, Gillingham, Dorset, UK).
4. Sodium borohydride ($NaBH_4$) (Sigma-Aldrich, Gillingham, Dorset, UK).
5. Mowiol 4-88 (Cat. no. 475904, Calbiochem, Merck KGaA, Darmstadt, Germany).
6. Millex-HV 0.45-μm syringe filter (Cat. no. SLHV033RS, Millipore, Bedford, MA).
7. DABCO (Cat. no. D-2522, Sigma-Aldrich, Gillingham, Dorset, UK).

21.2.4 Change in Conformation: PKB Conformation

21.2.4.1 Construct Design

1. GFP-PKB (MOUSE PKBα) was provided by Sandra Watton and described as pEGFP-HA-Akt construct [8].
2. The GFP-PKB-RFP construct was created by adding PCR-amplified mRFP (containing an EcoRI site in the N-terminal and an XbaI site in the C-terminal) instead of YFP in the vector pCDNA3-EGFP-PKB-YFP [9] using the oligos mRFP-Ct sens and mRFP-Ct antisens.

21.2.4.2 Expression/Activity

1. Human purified platelet-derived growth factor (PDGF) (Cat. no. 120-HD, R&D Systems, Minneapolis, MN).
2. Lysis buffer: 20 mM Tris-HCl (pH 7.4), 150 mM NaCl, 100 mM NaF, 10 mM $Na_4P_2O_7$, 10 mM EDTA.
3. Complete protease inhibitor cocktail tablet (Hoffmann-La Roche, Basel, Switzerland).
4. Bradford assay using Bio-Rad protein assay (Cat. no. 500-0006, Bio-Rad Laboratories GmbH, Muenchen, Germany).
5. Sample buffer: 125 mM Tris-HCl (pH 6.8), 6% SDS, 20% glycerol, 0.02% bromophenol blue.
6. 2-mercaptoethanol (Cat. no. M-6250, Sigma-Aldrich, Gillingham, Dorset, UK).
7. 4–12% polyacrilamide precast gels (Invitrogen, Paisley, UK).
8. Polyvinylidene difluoride membranes (PVDF) (Cat. no. IPVH 00010, Millipore UK, Watford, Hertfordshire, UK).
9. TBS-T: 10 mM Tris-HCl (pH 7.4), 150 mM NaCl, 0.05%, Tween 20.
10. Bovine serum albumin (BSA) 30% solution (A 3424) ultra high avidity (Sigma-Aldrich, Gillingham, Dorset, UK).
11. Phospho-Akt (Thr-308) is a rabbit polyclonal antibody (Cat. no. 9275, Cell Signaling, New England BioLabs UK).
12. Anti-Akt is a rabbit polyclonal antibody (Cat. no. 9272, Cell Signaling, New England BioLabs UK).
13. Secondary goat antirabbit HRP-antibodies (Amersham Biosciences UK, Buckinghamshire, UK).
14. Marvel milk powder (food store or VWR International, Merck House, Poole, UK).
15. ECL (Amersham Biosciences UK, Buckinghamshire, UK).

21.2.4.3 Cell Culture and Transfections

1. NIH3T3 cells (Cat. no. CRL-1658, ATCC, LGC Promochem, Teddington, Middlesex, UK).

2. Dulbecco's Modified Eagle Medium (DMEM) (in house, medium production; same composition as commercial one).
3. Donor bovine serum (Cat. no. 16030074, Invitrogen, Paisley, UK).
4. 35-mm glass-bottomed microwell dishes (Cat. no. P35G-1.5-14-C, MatTek Corp. Ashland, MA).
5. Lipofect AMINE and PLUS reagent (Cat. no. 18324-012 and no. 11514-015, Invitrogen, Paisley, UK).
6. OPTIMEM with Glutamax (Cat. no. 51985, Invitrogen, Paisley, UK).

21.2.4.4 Fixation and Mounting

1. Human purified platelet-derived growth factor (PDGF) (Cat. no. 120-HD, R&D Systems, Minneapolis, MN).
2. Paraformaldehyde (PFA) (Cat. no. P-6148, Sigma-Aldrich, Gillingham, Dorset, UK).
3. DABCO (Cat. no. D-2522, Sigma-Aldrich, Gillingham, Dorset, UK).

21.2.5 Protein–Lipid Interaction: PLD and PITP

21.2.5.1 Construct Design

1. The design of the fusion between GFP and PITPβ (GFP-PITP) has been described elsewhere [10].
2. The design of the fusion between GFP and PLDb (GFP-PLD) has been described elsewhere [11].

21.2.5.2 Cell Culture and Transfections

1. COS-7 cells were obtained from Prof. Shamshad Cockcroft's laboratory, University College London (UCL).
2. Dulbecco's Modified Eagle's Medium (DMEM) in PITP experiments (Sigma-Aldrich, Gillingham, Dorset, UK).
3. Fetal bovine serum in PITP experiments (GIBCO, Invitrogen, Paisley, UK).
4. Herring sperm carrier DNA (Promega UK, Southam, UK).
5. Poly-L-lysine 0.01% solution (Cat. no. P4707, Sigma-Aldrich, Gillingham, Dorset, UK).
6. 35-mm glass-bottomed microwell dishes (Cat. no. P35G-1.5-14-C, MatTek Corporation, Ashland, MA).
7. HeLa Ohio cells (in house, CR-UK cell production).
8. Dulbecco's Modified Eagle's Medium (DMEM) (in house, CR-UK media production; can be found commercially).
9. Fetal bovine serum in PLD experiments (Sera Laboratories International, Horsted Keynes, UK).

10. FuGENE 6 transfection reagent (Roche Diagnostics-Roche Applied Science, Indianapolis, IN).

21.2.5.3 Preparation of Fluorescently Labeled Cells by Liposomes

1. BODIPY 542/574 C_6 phosphatidylinositol (-PI) (Molecular Probes, Invitrogen, Paisley, UK).
2. Polyamine carriers Shuttle PIP carrier-1 (Molecular Probes, Invitrogen, Paisley, UK).
3. BODIPY 530/550 C5 human phosphatidylcholine (-PC) (Molecular Probes, Invitrogen, Paisley, UK).

21.2.5.4 Stimulation, Fixation, and Mounting

1. Epithelial growth factor (EGF) (Cat. no. E-1257, Sigma-Aldrich, Gillingham, Dorset, UK).
2. Paraformaldehyde (PFA) (Cat. no. P-6148, Sigma-Aldrich, Gillingham, Dorset, UK).
3. Immunofluore mounting medium (ICN Biomedicals Inc., Costa Mesa, CA).
4. Mowiol (Cat. no. 475904, Calbiochem, Merck KGaA, Darmstadt, Germany).
5. DABCO (Cat. no. D-2522, Sigma-Aldrich, Gillingham, Dorset, UK).

21.2.5.5 Analysis and Statistics

GraphPad InStat software (version 3.0 for Mac-2001, Apple Computer).

21.2.6 Reporter of Phosphorylation State/Activity: PKB Phosphorylation

21.2.6.1 Construct Design

The fusion of GFP in the N-terminal of PKBα has been described elsewhere [8]. That construct was formerly referred to as pEGFP-HA-Akt.

21.2.6.2 Cell Culture and Transfections

1. NIH3T3 cells (Cat. no. CRL-1658, ATCC, LGC Promochem, Teddington, Middlesex, UK).
2. Dulbecco's Modified Eagle Medium (DMEM) (in house, medium production; same composition as commercial one).
3. Donor bovine serum (Cat. no. 16030074, Invitrogen, Paisley, UK).
4. Lipofect AMINE and PLUS reagent (Cat. no. 18324-012 and no. 11514-015, Invitrogen, Paisley, UK).
5. OPTIMEM with Glutamax (Cat. no. 51985, Invitrogen, Paisley, UK).

6. Poly-L-lysine 0.01% solution (Cat. no. P4707, Sigma-Aldrich, Gillingham, Dorset, UK).
7. Bovine serum albumin (BSA) fatty acid-free, endotoxin-free (Cat. no. A8806-5 G, Sigma-Aldrich, Gillingham, Dorset, UK).

21.2.6.3 Stimulation, Antibody Treatment, and Mounting

1. Human purified platelet-derived growth factor (PDGF) (Cat. no. 120-HD, R&D Systems, Minneapolis, MN).
2. Paraformaldehyde (PFA) (Cat. no. P-6148, Sigma-Aldrich, Gillingham, Dorset, UK).
3. Triton X-100 (Cat. no. T-9284, Sigma-Aldrich, Gillingham, Dorset, UK).
4. Sodium borohydride ($NaBH_4$) (Sigma-Aldrich, Gillingham, Dorset, UK).
5. Phospho-PKB Ser-473 was a rabbit polyclonal antibody raised against the C-terminal phosphopeptide HFPQF*p*SYSASS of Akt1 from Julian Downward's laboratory (CR-UK, London).
6. Cyan-3 monoreactive dye (Cat. no. PA23001, Amersham Biosciences UK, Buckinghamshire, UK).
7. Millex-GV 0.22-μm syringe filter (Cat. no. SLVGV 004SL, Millipore, Bedford, MA).
8. Mowiol (Cat. no. 475904, Calbiochem, Merck KGaA, Darmstadt, Germany).
9. DABCO (Cat. no. D-2522, Sigma-Aldrich, Gillingham, Dorset, UK).

21.3 Methods

21.3.1 Assembly of the System of Interest

21.3.1.1 Choice of the FRET Pair

1. Unlike intensity-based methods, detection of FRET by fluorescence lifetime reduces the constraints regarding spectral mixing of the fluorescence emission of the donor and the acceptor [12, 13]. Only the fluorescence from the donor is detected; no contamination of the acceptor fluorescence needs to be considered.
2. In FRET, one critical parameter is the efficiency of the transfer of energy currently known as the FRET efficiency. This parameter gives the expected variation of the lifetime upon RET and is defined as $\eta_{FRET} = 1 - \tau_{DA}/\tau_D$. To observe a significant change, the system has to be optimized so that the FRET efficiency variation is maximal. The following parameters must be considered: (a) the donor brightness (defined as the product of the absorption cross section at one or two photons and the quantum yield of fluorescence) to obtain a high-fluorescence signal. This will have direct implications on the acquisition time. The quantum yield of the donor's fluorescence directly affects the efficiency of the energy transfer; (b) the overlap between

the emission spectra of the donor and the absorption spectra of the acceptor (take into account the absorption extinction coefficient of the acceptor in the overlap integral); (c) the photostability of both the donor and the acceptor; (d) oligomer formation should be avoided. This increases the size of the fluorescent protein relative to the tagged protein (steric hindrance) and they generally lead to complex intensity decays that cannot be analyzed by a mono-exponential fit.

3. When possible, estimate the distance between the two fluorescent proteins by molecular modeling with double-tagged proteins (for conformational change) or complexes (for intermolecular interactions). Ensure that the intermolecular or intramolecular distance is about the Förster radius associated to the fluorescent pair used. When studying intermolecular interactions, FRET detection is favored due to an equilibrium between a non-FRETing state and a FRETing state. Nevertheless, when studying conformational change, the two fluorescent proteins are kept close to each other and the distance between them varies by a finite quantity. Thus, it is preferable that the variation of distance takes place between $0.5R_0$ and $1.5R_0$, where the FRET efficiency is the most sensitive.

21.3.1.2 Linker

For the following reasons, the fluorescent proteins that are fused to the protein of interest need to be linked by inert linkers (such as 6 glycines):

1. Biocompatibility: Neutrality of the sequence in term of secondary structure and biomolecular recognition.
2. Flexibility: Reduces the dependence of the fluorescent protein movement relative to the protein to which it is fused. The tumbling of the fluorescent protein, resulting from the flexibility of the linker, minimizes the effect of the anisotropy factor in terms of resonance energy transfer.
3. No quenching: Charged or aromatic amino acids might lead to the quenching of the fluorescence.

21.3.1.3 Labeling Strategy

1. Immuno-labeling will allow the detection of endogenous and overexpressed proteins. This method permits the detection of the activation status of the protein. However, unspecific binding of the antibody and their size (MW: 150,000) can be a problem in some types of experiments.
2. Fluorescent proteins are genetically encoded with the sequence coding of the protein of interest. They are much smaller (MW: 25,000) compared to antibodies. After transfection, the genetically encoded protein can be transient or stable. Two fluorescent proteins can be fused at specific positions within the protein, allowing the double tag of a single protein with both the donor and the acceptor to monitor the conformation change.

21.3.1.4 Cell Lines

1. When possible, use cells that can be easily maintained in culture.
2. Cells also have to be easily transfectable; otherwise, microinjection needs to be performed.
3. To be imaged, it is preferable to use cells that can be attached on the surface of a glass coverslip (with or without poly-L-lysine).

21.3.1.5 Mounting

1. The samples can be mounted either on coverslips or on MatTek dishes. The first one allows the samples to be kept for months at −20°C. This is a "dry storage." Unlike coverslips, working with MatTek dishes permits live experiments to be performed. It is a "wet storage," and care must be taken not to allow the sample to dry.
2. Treatment of cells in MatTek dishes is milder compared to the coverslips. During the mounting and fixation steps, cells on MatTek dishes need less manipulation; mounting with Mowiol, in particular, is not required. The lifetime measured in both conditions might be slightly different due to the mounting medium.

21.3.2 Time-Domain FLIM

21.3.2.1 Prior to Acquisition

1. The room temperature is maintained at 18–19°C, while the cooling system for the lasers (Verdi and Mira 900) is set at 17°C. The room temperature must be kept close to the temperature set on the cooling system to avoid water condensation on cooled parts of the lasers.
2. The laser cavity is left to stabilize for 30 min after having started to pulse. If the room temperature is stable, the laser should pulse stably just a few minutes after having been switched on and only some small readjustments of the cavity might be necessary.
3. For reproducible data, the laser parameters need to be recorded. For two-photon excitation of GFP (*see* Note 1), the laser is tuned to 890 nm and pumped at 6 W. The Ti:sapphire laser generates 125-fs pulses with a repetition rate of 76.26 MHz (*see* Note 2) and an average power output of 450 mW.
4. The instrument response function (IRF) is acquired by using a strong scattering surface (aluminum foil). The IRF is constant if the instrument setup is not modified.
5. The excitation power is measured unfocused at the sample position or, more conveniently, after the neutral density filters (*see* Note 3).
6. Alignment of the excitation needs to be done directly per experimental condition by maximizing the intensity of an arbitrary cell (coverslip or MatTek). The incidence of the excitation beam is adjusted with two mirrors

situated before the scanner. If no major readjustment of the laser cavity was done and if the room temperature is stable, then the alignment with the sample is stable.

21.3.2.2 Acquisition

1. To have an adequate magnification and collection factor, a 40x oil objective with a high N.A. (1.3) is used. Only a small drop of oil is necessary to establish the optical interface between the objective and the sample.
2. Swap to the mercury lamp and finely readjust the focus by observing the fluorescence.
3. Find a cell through the eyepiece. The focus needs to be readjusted by swapping between the eyepiece and the camera.
4. It is useful to record the position of the cell on the coverslip, as it will simplify its relocation. Thus, a single cell can be used as a reference to verify the stability of the lifetime measurement from one day to the next.
5. The intensity image of the donor and acceptor is acquired with a mercury lamp (*see* Note 4). Take note of the acquisition parameters (exposure, frame average, gain, binning). They have to be adjusted to have the best image possible but without any photobleaching (*see* Note 5).
6. Swap to the two-photon excitation and adjust the vertical position of the objective to select a plane of the cell. It can be done either by maximization of the signal or by focusing on an arbitrary plane of the cell (*see* Note 6).
7. Zoom tightly on the cell or the region of interest.
8. Make a pre-acquisition of a few scans to control the pulse pile-up and signal level, and decide on the total number of scans.
9. After acquisition, control the photobleaching of the donor by comparing it to the pre-acquisition. In absence of photobleaching, the final photon count should be proportional to the number of scans.
10. Swap back to the mercury lamp to check if the acceptor has not photobleached.

The acquisition settings need to be adjusted to avoid photobleaching (*see* Note 7) and to detect enough photons so that the signal-to-noise ratio is high enough for the data analysis (Fig. 21.1 and Color Plate 6) (*see* Note 8).

1. The power of the laser beam, measured unfocused on the sample plane, is set to 9 mW with a combination of neutral optical density filters.
2. Usually, the acquisition time is fixed at 300 s for less bright cells; it may be reduced to 30 s for brighter ones (*see* Note 9).
3. For a resolution of 256 × 256 pixels, a dwelling time of 17 μs per pixel (1.5 s/frame) is used (*see* Note 10).
4. The photobleaching is evaluated by comparing the photon count to time. These settings keep the photobleached fraction of GFP inferior to 2% during the acquisitions.

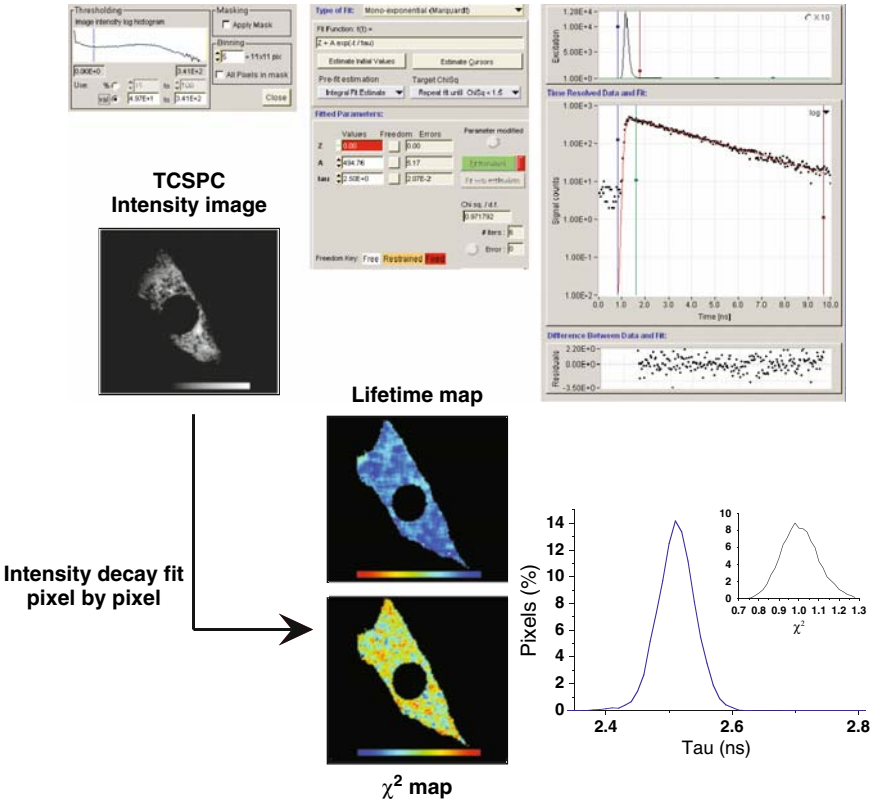

Fig. 21.1 Converting TCSPC intensity image in a fluorescence lifetime map. The TCSPC intensity image is thresholded to remove the background (blue vertical line on the intensity histogram) and the binning set to an adequate value (*see* Note 11). The intensity image is fitted pixel by pixel using a fitting model (*see* Note 15). A mono-exponential Marquardt fit is commonly used, but a range of different models is available (bi-/tri-exponential Marquardt as well as a stretched mono-exponential). The fitted parameters as well as the calculated reduced χ^2 are shown for the selected pixel. The instrument response function is convolved with the fit function to determine the closeness to the fit. The fit result (red line), at the given pixel, is represented on the raw data (black dots) and the residual calculated for the fitted part of the intensity decay (starting at the green vertical line). All the pixels are fitted to provide the lifetime map as well as the χ^2 map (represented in pseudo-color scale). The histogram representing the percentage of pixels at each lifetime can be plotted for quantitative analysis. The χ^2 histogram is usually centered on 1 with a standard deviation of 0.1. To view this figure in color, see color insert

5. Depending on the fluorescence intensity of the cells, the photon count at the maximum of the intensity decay varies from 100 counts to 1,000 counts after a spatial binning of 11 × 11 pixels (*see* Note 11).
6. The count rate frequency is kept below 10^6 photon/s, to avoid pulse pile-up (*see* Note 12).

21.3.2.3 Vertical Stacks

1. Using two-photon excitation, the images of the cell can be acquired at different positions along the excitation axis. This is done by moving the position of the objective along the excitation axis. The two-photon excitation has the advantage that it does not require the use of a pinhole and it reduces the risk of photobleaching outside the focal plane. It is possible to acquire sections from the bottom to the top of the cell with a resolution of about 1 µm that is limited by the size of the excitation volume.
2. The vertical stack can be used to identify and locate compartments within either the cytoplasm or the nucleus but also to analyze the localization of the protein of interest at the plasma membrane (Fig. 21.2 and Color Plate 7). Apart from the middle section of the cell, the signal of fluorescence usually decreases as the excitation volume reaches the edges of the cell. It is thus necessary to adjust the acquisition conditions so the signal obtained at the extremities of the cell is high enough for the accurate analysis of the lifetime.

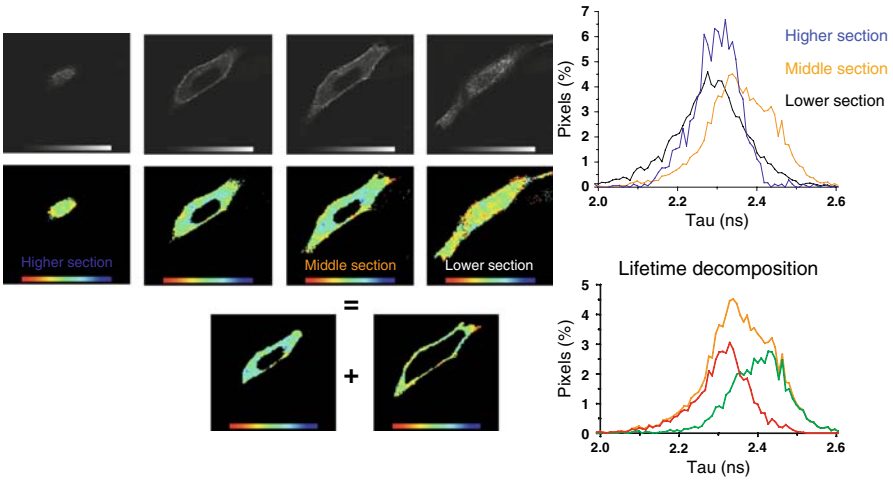

Fig. 21.2 Acquiring a Z stack. Sections from the bottom to the top membrane of NIH3T3 cell were co-transfected with GFP-PDK1 and RFP-PKB. Sections were acquired every 1 µm. A sample of the acquired sections is shown. The stimulation with PDGF induced the translocation of GFP-PDK1 to the plasma membrane, characterized by the bright edges of the cell. The lifetime map of each section was calculated. The histograms show the lifetime distribution of the higher (blue line), middle (orange line), and lower (black line) sections. The spatial decomposition of the middle section of the plasma membrane (red line) and cytoplasmic components (green line) show that the average fluorescence lifetime at the plasma membrane is identical at the edge of the cell as well as the top and bottom membranes. To view this figure in color, see color insert

21.3.2.4 Fitting the Intensity TCSPC Images

The analysis of the TCSPC intensity images was acquired with the MPTR software and analyzed with TRI2 to extract the lifetime information from the TCSPC measurements (Fig. 21.1). The intensity images were converted in lifetime maps by fitting pixel by pixel the fluorescence intensity decay. The maps are represented in pseudo-color. The variation of the lifetime within the cells is monitored by plotting the histograms representing the normalized number of pixels of the cells at a given lifetime. Lifetime and intensity distribution histograms are analyzed using Origin.

1. Threshold low-intensity background.
2. Mask surrounding of the cell (*see* Note 13).
3. Select the binning according to the signal-to-noise level and resolution used during the acquisition.
4. Choose a suitable model for the intensity decay fit (*see* Notes 14 and 15).
5. The residuals as well as the χ^2 distribution need to be verified to make sure the fit is accurate [3]. A χ^2 of 0.1 is commonly obtained for cells transfected with the donor only.

21.3.2.5 Signal and Accuracy

1. A low photon count results in the broadening of the lifetime distribution of a single cell. Thus, a decrease in the photon count induces a higher error in the τ measurement. Nevertheless, the average value of the lifetime is not affected, so the signal may be decreased as long as the distribution width stays smaller than lifetime changes expected due to FRET. If the width of the distribution becomes wider than the amplitude of the lifetime variation upon FRET, it might appear as a random error rather than a specific change. In addition, the required photon count depends on the complexity of the model fitted to the data (*see* Note 15).
2. The determination of a lower-intensity threshold is important for the following reasons: (a) The intensity within a single cell can be very heterogeneous and some regions have low intensity. It is necessary to know if the lifetime measurement of those pixels is reliable or not; (b) if the fluorophore is highly prone to photobleaching, the excitation power and the acquisition time need to be reduced. But one needs to make sure not to go below the minimum photon count; (c) a low expression level of the construct causes difficulties in having high photon counts; (d) overexpression of certain constructs can lead to a nonphysiological response of the cells to stimuli. Thus, it might be necessary to select only the cells with low expression levels.
3. In principle, it is possible to increase the photon count by increasing the spatial binning (*see* Note 11) or by having longer acquisitions. Nevertheless, longer acquisitions necessitate ensuring the long-term stability of the sample (photo-damage of the sample, photobleaching of the

fluorophores, etc.) as well as that of the instrument (mechanical drift, temperature stability, etc.).

21.3.2.6 Fluorescence Lifetime Maps: Spatial Decomposition

1. Two-photon excitation TCSPC lifetime imaging permits access to the local information within the cell. To quantify and analyze this information accurately, it is necessary to take into account the inherent heterogeneity of the cells.
2. Due to the heterogeneous distribution of molecules such as proteins and lipids, some regions might be strongly depleted and thus might be associated with low-intensity pixels. Under these conditions, the lifetime analysis of low-intensity pixels will be inaccurate and lead to a large dispersion of the values. When analyzing the distribution histogram, the spatial information is lost and those inaccurate pixels can dramatically affect the analysis. Therefore, it is necessary to analyze the local lifetime as opposed to the lifetime of the whole cell. So, the high-intensity pixels can be fitted and analyzed with the histogram accurately, while the low-intensity ones can be analyzed separately and the fitting parameters adjusted adequately.
3. The molecular interactions take place in specific subcellular compartments of the cell. The smaller the compartment, the lower the contribution of the pixels to the lifetime distribution histogram. Thus, the local variation will remain unnoticed. Local variations need to be spatially isolated in order to be exposed. This is performed on the lifetime intensity maps, prior to analysis.
4. In some cases, the lifetime distribution clearly shows two different populations. This occurs when the donor exhibits two well-defined lifetimes. The population of pixels for each lifetime has to be significant compared to one another. However, in most cases, there is an overlap of subpopulations. This may be due to lifetimes that are not different enough or because of a continuous distribution between the two extreme populations. However, if the lifetime variation is localized spatially, two subpopulations can be defined and spatially separated on the cell lifetime map [Fig. 21.4 a, b and Color Plate 9]. Hence, we can determine the mean τ value of the cell and of the different pixel populations as well as their relative percentage.

21.3.2.7 Fluorescence Lifetime Distribution: Histogram Normalization

The proportion of pixels with a given lifetime can be determined from the distribution histogram. It is also useful to compare how this proportion varies from cell to cell in different experimental conditions. Since the shape and size of the cells can vary considerably, it is necessary to normalize the histograms by the total number of pixels in the cell so that they can be directly comparable.

21.3.2.8 Normalized Lifetime Variation

1. Comparing absolute lifetimes between different experiments can be difficult because of the variability that arises from the instrument setup, temperature changes, mounting medium, and cell passage. To reduce the impact on the analysis of such variability, it is preferable to express the results in terms of normalized lifetime variations, which are calculated as $(\tau_{ref} - \tau_i)/\tau_{ref}$, where τ_{ref} is the reference lifetime and τ_i the lifetime considered. These two values can be defined differently depending on how the analysis is carried out.
2. When detected by FLIM, FRET results in a variation of the donor lifetime. One way of studying this variation consists of comparing the fluorescence lifetime in cells that have only the donor to cells that have both donor and acceptor. In this case, τ_{ref} is defined as the average lifetime of the donor alone and τ_i as the lifetime at a given pixel (for local changes) or as the average lifetime (for global changes) in the presence of both donor and acceptor. τ_{ref} is determined for each measurement.
3. If the average lifetime of the cells with both the donor and the acceptor varies considerably relative to τ_{ref} and if the variation due to FRET is small, then it would be preferable to analyze the relative local variation within a single cell as a diagnostic of the heterogeneity of the FRET response. In this case, τ_{ref} can be defined as the highest lifetime in the cell and τ_i as the lowest.

21.3.2.9 Pseudo-Color Lifetime Window

When comparing cell lifetime maps in pseudo-color, it is necessary to have the same scale for each of them to identify color and lifetime. Nevertheless, if the variation from cell to cell is high compared to the intracellular variation, a common scale will hide those local intracellular changes. To emphasize these changes, a narrow pseudo-color scale needs to be used.

21.3.2.10 Reducing Variability

Variability is observed when detecting FRET *in cells*. It can be attributed to the instrument itself [14] but also to cell-to-cell variability (resulting from their different response to stimuli) and to the local environment within a single cell. Nevertheless, other factors that can be controlled may also introduce variability.

1. When studying interaction between two species (for example, GFP-PDK1 and RFP-PKB; *see* Subheading 21.3.4), the proportion of interacting and noninteracting species depends on their affinity constant. The variation of the lifetime depends directly on the ratio [PDK1:PKB]/[PDK1] = K_f.[PKB], where [PDK1:PKB] is the concentration in complex and [PDK1] and [PKB] are, respectively, the concentrations of noncomplexed GFP-PDK1 and RFP-PKB. The variation of the average lifetime is directly dependent on the product K_f.[PKB]. Thus, a low concentration of PKB relative to $1/K_f$ may lead to a loss of interaction. Most of the time,

K_f is not known, and so it is important to screen different concentration ranges to find the right range of concentration and be able to detect the interaction by FRET.

2. Another important factor is the ratio of the donor and acceptor concentrations. Indeed, when the total concentration of the donor is high compared to the total concentration of the acceptor, only a small fraction of the total donor will transfer its energy to the acceptor. In these conditions, only a very small variation of the average fluorescence lifetime can be expected and FRET might not be detected. So, it is necessary to work with an excess of acceptor compared to the donor (to an extent that does not induce nonspecific FRET). Nevertheless, in cells, the concentrations of both donor and acceptor are not easily determined. The relative intensities of both fluorophores cannot be compared directly due to the different absorption and emission properties of the fluorophores as well as the different collection factors associated with their fluorescence detection. At low FRET efficiency, or small percentage of interacting species, it is possible to relate FRET detection to the steady-state intensity ratio $I_{\text{Acceptor}}/I_{\text{Donor}}$ obtained by exciting the sample in epi-fluorescence successively using the FITC and G-2A cubes (for GFP, RFP fluorophore pair). Thus, for a given system, it is possible to experimentally determine a FRET detection threshold $(I_{\text{Acceptor}}/I_{\text{Donor}})_{\text{min}}$.
3. Cell response varies depending on the number of cell passages. It is generally possible to observe the cellular response such as protein translocation to the plasma membrane. Nevertheless, this readout is not available if translocation is prevented. To ensure that the cells are responding, control experiments always need to be done in parallel.

21.3.3 Frequency-Domain FLIM

21.3.3.1 Principles of Phase Measurements

1. Phase methods provide an average lifetime where sinusoidally modulated light is used to excite the sample. The lag in the emitted fluorescence signal compared to the excitation signal permits measurement of a phase shift (φ) and a relative modulation depth (m).
2. Using a Fourier transformation, two independent parameters, tau phase (τ_p) and tau modulation (τ_m), can be derived from (φ) and (m) measurements. The average lifetime is defined as $[\tau_p + \tau_m]/2$.
3. The FRET efficiency can be mapped in a single cell by determining the lifetime of the donor fluorophore at each pixel of the image. The FRET efficiency is calculated as $\eta = 1 - < \tau_{da} > / < \tau_d >$, where $< \tau_{da} >$ is the lifetime of the donor at a given pixel in the presence of the acceptor, and $< \tau_d >$ is the average lifetime of the donor in the absence of the acceptor [5, 15–17].

21.3.3.2 Instrumentation and Acquisition

1. A detailed description of the frequency FLIM instrument setup can be found elsewhere [5].
2. For cellular acquisitions, a sequence of 16 images is taken at successive modulation angles of 45° plus an image of the background.
3. In most cases, the acquisition's exposure time is chosen depending on the fluorescence intensity of the cell and can vary from 50 to 1,000 ms. The acquired and saved image sequences are analyzed.
4. All images are taken with a Zeiss Plan-APOCHROMAT 100x/1.4 numerical aperture, phase 3 oil objective, and images are recorded at a modulation frequency of 80.218 MHz.
5. In our experiments, the donor GFP is excited by the 488-nm line of an Argon/Krypton laser, and emission is detected through a dichroic beam splitter Q 505 LP and narrow-band emitter filter BP 514/10.
6. Acceptor images are acquired with a 100 W Mercury arc lamp (Zeiss Attoarc 2) as a source of sample illumination combined with a high Q Cy3 filter set (exciter: HQ 535/50, dichroic: Q 565 LP, emitter: HQ 610/75 LP; Chroma Technology).
7. FLIM images are detected by an image intensifier–charge-coupled detector. The acceptor images can be acquired with the same camera used for the FLIM images or with an OCRA camera to gain resolution (*see* Note 16).

21.3.3.3 Data Analysis

1. The analysis of the image sequence (see previous subheading) is carried out using the IP Lab software.
2. Prior to image analysis, the background is thresholded. This is done by our automated analysis software.
3. The two independent parameters τ_p and τ_m are calculated via Fourier transformations.
4. An average of the lifetime phase and modulation is calculated for each pixel ($[\tau_p + \tau_m]/2$). Care has to be taken for τ_p and τ_m to have close values. Otherwise, these independent parameters cannot be averaged.
5. For visualization purposes, the average lifetime map is pseudo-colored with high lifetimes in blue and short lifetimes in red. It is important to note that the pseudo-color scale may differ for each set of experiments. Therefore, regardless of the color, it is essential to consider in each experiment the values of the lifetimes.
6. The data analysis was formerly performed manually, with the determination of the correct thresholding and the average lifetime map done by the operator. In collaboration with Pierre Leboucher at College de France, an automatic analysis of the data is now implemented. In addition to an increased speed in the data treatment, a nonbiased analysis resulting from the automatic thresholding has dramatically improved the reproducibility of the results.

21.3.4 Protein–Protein Interaction: PKB|PDK1 Interaction

To date, the molecular mechanism by which PDK1 interacts with PKB has not been elucidated. To assess in single cells the binding mechanism of PKB to its activation partner PDK1, the resonance energy transfer was exploited. A fusion protein was generated by genetically encoding human PDK1 with GFP (donor) in the N-terminal of PDK1. For PKB, either HA-tagged PKB recognized by a Cy3-labeled anti-HA antibody (Fig. 21.3 and Color Plate 8) was used as an acceptor or the genetically encoded fusion of mRFP in the N-terminal of PKB was produced (Fig. 21.4). NIH3T3 cells were transfected with GFP-PDK1

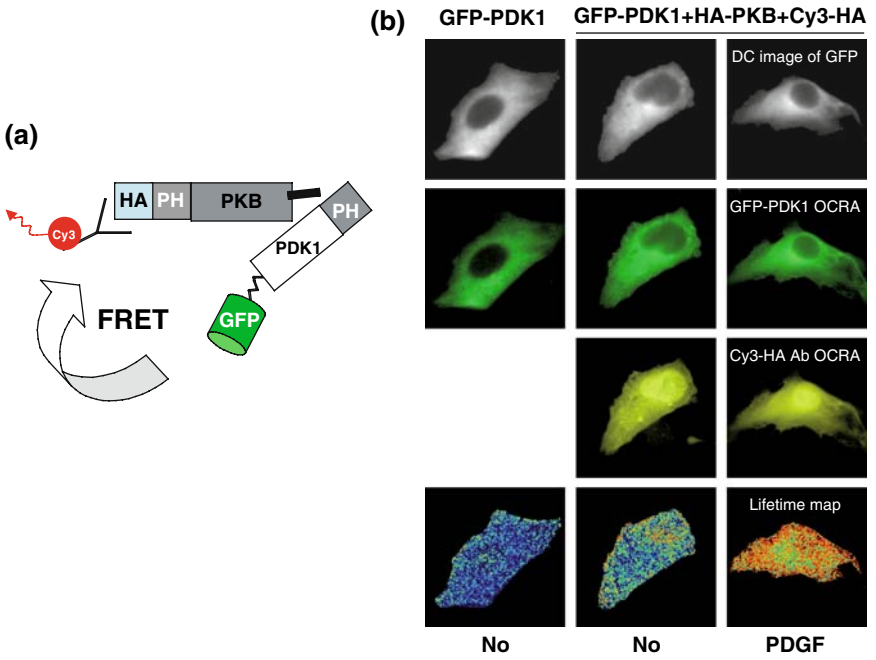

Fig. 21.3 GFP-PDK1/RFP-PKB interaction determined by frequency-domain FLIM. (a) The experimental configuration is represented where cells are transfected with HA-PKB and recognized by a Cy3 labeled anti-HA antibody. The latter is used as an acceptor to monitor FRET when HA-PKB interacts with GFP-PDK1. (b) Frequency FLIM images of NIH3T3 cells transfected either with GFP-PDK1 alone (donor) or with HA-PKB. Where indicated, the cells were incubated with an anti-HA antibody labeled with Cy3 (acceptor) and treated for 5 min with 30 ng/ml of PDGF. The top panels represent the intensity images of the donor GFP-PDK1 (DC image) after thresholding and mathematical treatment. The central panels show the use of an OCRA camera in addition to frequency FLIM images to provide a better-resolution image of the FRET partners (donor in green and acceptor in yellow). The bottom panels represent the lifetime maps of the cells in a pseudo-color scale from 1.6 ns (red) to 2.1 ns (blue). The data show that upon PDGF treatment, PDK1 interacts with PKB at the edge of the cell with an efficiency of about 15% (1.7 ns) but also in the cytoplasm with an efficiency of about 7% (1.85 ns). To view this figure in color, see color insert

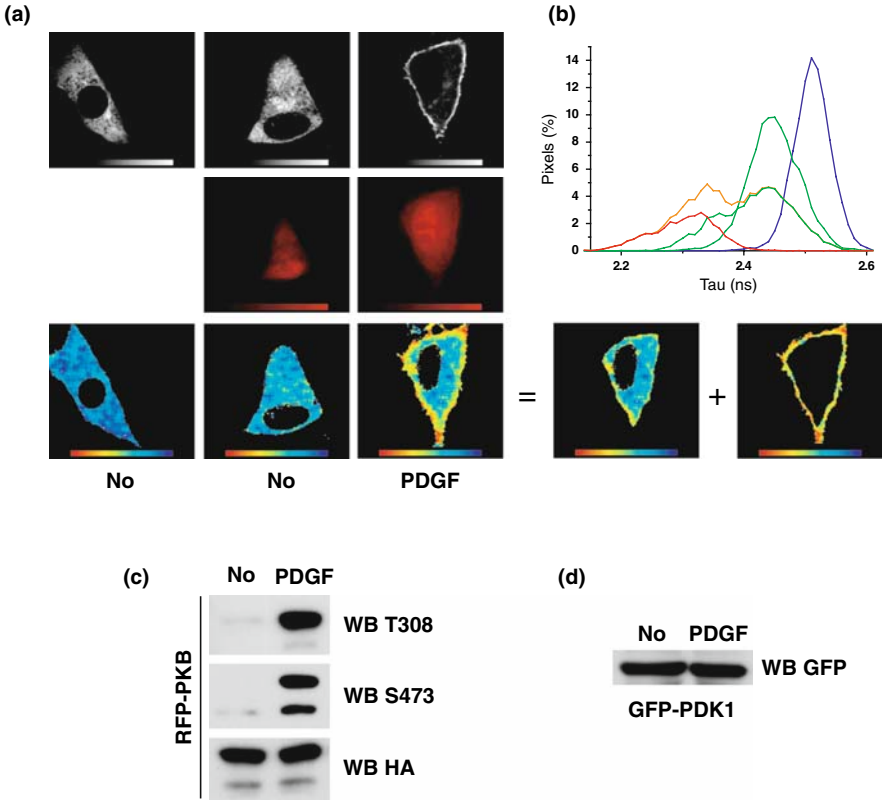

Fig. 21.4 GFP-PDK1/RFP-PKB interaction determined by time-domain FLIM. (a) Two-photon FLIM images of NIH3T3 cells transfected either with GFP-PDK1 alone or with RFP-PKB are shown. The top panels present intensity images of GFP-PDK1 after two-photon excitation. The central panels represent intensity images of RFP-PKB obtained with a mercury lamp. The bottom panels represent the calculated lifetime maps of the donor GFP-PDK1. The lifetimes are in pseudo-color scale from 2.0 ns (red) to 2.7 ns (blue). Where indicated, the cells were stimulated for 5 min with 30 ng/ml of PDGF. The lifetime map of the stimulated condition is decomposed into its cytoplasmic and plasma-membrane contribution. The average FRET efficiency is 4% in the cytoplasm and 8.4% at the plasma membrane. These results show that PKB interacts with PDK1 at the plasma membrane upon PDGF but also in the cytoplasm in stimulated as well as basal conditions. (b) The graph represents the lifetime distributions of GFP-PDK1 alone (blue) and GFP-PDK1 with RFP-PKB prior to (green) or upon (orange) PDGF stimulation. The light green and red distributions represent, respectively, the contribution of the cytoplasm and plasma membrane to the stimulated cell (orange distribution). (c) The expression of RFP-PKB in NIH3T3 treated with PDGF as indicated was determined by Western blot with an anti-HA antibody. The phosphorylation of Thr 308 and Ser 473 was detected by phosphospecific antibodies. (d) The expression of GFP-PDK1 in NIH3T3 treated or not with PDGF for 5 min was verified using an anti-GFP antibody. To view this figure in color, see color insert

and HA-PKB or RFP-PKB and their behavior was followed upon stimulation with PDGF. FRET was monitored by FD-FLIM as well as TD-FLIM. The resonance energy transfer was detected by the decrease in the donor lifetime in the presence of the acceptor.

21.3.4.1 Construct Design

1. pCMV5-HA-PKB construct encoding hemaglutinin (HA) epitope-tagged human PKB α (HA-PKB) has been described elsewhere [6].
2. The GFP-tagged full-length human PDK1 (GFP-PDK1) was generated by inserting the GFP fragment between EcoR I and Bgl II in pCMV5-Myc-PDK1 to give pCMV5-EGFP-PDK1, as previously described [7].
3. PCR-amplified monomeric RFP was subcloned in the N-terminal of HA-PKB in the vector pCMV5-HA-PKB using an EcoRI site (*see* Note 17). mRFP was PCR-amplified from pRSET B-RFP using the oligonucleotides mRFP-sens and mRFP-antisens.

21.3.4.2 Expression/Activity

In order to verify that the fluorescent tags have not modified the protein function, the expression and activity of the fusion proteins need to be determined.

1. Transfected NIH3T3 cells from a 6-well plate were stimulated for 5 min with 30 ng/ml of PDGF.
2. Cells were put on ice, washed once with PBS, and solubilized for 15 min in lysis buffer supplemented with COMPLETE protease inhibitor cocktail tablet.
3. The cells were scraped and spun for 5 min at 14,000 rpm in a cold bench centrifuge.
4. The protein content of the supernatant in each condition was determined by Bradford assay as recommended by the manufacturer.
5. To terminate the reaction, 4X SDS sample buffer supplemented with 10% β-mercaptoethanol was added and the samples boiled for 5 min.
6. The proteins were separated on a 4–12% polyacrylamide gel by SDS-PAGE and transferred on PVDF membrane.
7. The membranes were incubated in blocking buffer TBS-0.2% Tween 20 (TBS-T) supplemented with 3% BSA for a minimum of 1 h prior to incubation with the different antibodies. Phospho-Akt (Thr-308) antibody or phospho-Akt (Ser-473) was used at 1:1,000 for 2–3 h in the same buffer. Anti-HA and Anti-GFP antibody were used at 1:2,000 and 1:5,000, respectively, for 1 h in the same buffer. The membranes were washed four times for 15 min in TBS-T 1% milk prior to incubation with the secondary HRP antibodies. HRP antibodies were used at 1:5,000 in TBS-T 5% milk for 1 h (*see* Note 18). Western blots were revealed by incubation with ECL.

21.3.4.3 Cell Culture and Transfection

1. NIH3T3 cells were maintained in DMEM 10% donor bovine serum before trypsinization and plating.
2. Cells were seeded at 30,000 on poly-L-lysine-coated coverslips in 24-well plates. For MatTek dishes (*see* Note 19) and 6-well plates, cells were seeded at 150,000.
3. Transfections were done with 0.4 μg (24-well plate) or 2 μg (MatTek or 6-well plate) of GFP-PDK1. For the co-transfections on coverslips, 0.4 μg of GFP-PDK1 and 0.1 μg of HA-PKB were used. For the MatTek dishes, 2 μg of each of the constructs (GFP-PDK1 and RFP-PKB) were employed.
4. For transfections, Lipofect AMINE/PLUS reagent in OPTIMEM medium was used as recommended by the manufacturer.
5. After 3 h in the transfection mix, the medium was replaced with DMEM 10% donor bovine serum.
6. Cells were starved in DMEM 0.2% BSA for 18 h before stimulation. If not starved, experiments were performed 24 h after transfection (*see* Note 20).

21.3.4.4 Antibody Labeling

1. Concentrated HA monoclonal antibody (at least 1 mg/ml) (*see* Note 21) in PBS (*see* Note 22) was used for the labeling.
2. 50 μl of freshly prepared bicine were added to a minimum of 300 μl of the concentrated antibody in a 2-ml capped glass vial containing a small stirrer bar.
3. 20 μl of DMF-reconstituted monoreactive Cy3 dye were added to the preparation drop by drop. The preparation was then incubated at room temperature in the dark for 1 h with constant stirring (*see* Note 23).
4. After 1 h, the labeled antibody was separated from the excess unconjugated Cy3 dye by gel permeation chromatography (using a P10 column) (*see* Note 24).
5. The column was first washed and equilibrated with 3 × 5 ml of PBS before the loading. Labeled antibody and unconjugated Cy3 were eluted with PBS. The labeled antibody was collected in first position and stored at 4°C.
6. A dye/protein ratio between 1 and 2 was measured by spectroscopy UV/Vis (*see* Note 25).

21.3.4.5 Fixation and Mounting

1. Preparation of the Mowiol: Mix 6 ml of water with 2.4 g of Mowiol and 6 ml of glycerol in a 50-ml Falcon tube with a stirrer bar. Mix gently by reversing the tube several times (do not expect the mix to homogenize yet). Add 12 ml of 200 mM Tris-HCl, pH 8.5. Incubate the Falcon tube overnight at 50°C in a beaker containing water on a hot plate with stirring. Filter through a 0.45-μm syringe filter and store at 4°C. Before use, add 2.5% (w/v) of DABCO.

2. NIH3T3 cells in MatTek dishes (Fig. 21.4) were treated for 5 min with 30 ng/ml of PDGF and washed twice with PBS before being fixed with a solution of 4% paraformaldehyde in PBS for 12 min.
3. The dishes were washed twice with PBS; then 2 ml of PBS containing 2.5% DABCO as an antifade (*see* Note 26) were added to the dishes.
4. For the conditions on coverslips (Fig. 21.3), the cells were treated for 5 min with 30 ng/ml of PDGF, washed twice with PBS, and fixed with a solution of 4% paraformaldehyde in PBS for 12 min.
5. The cells were washed with PBS and permeabilized with 0.2% Triton-X100 in PBS for 5 min before being incubated with 1 mg/ml of sodium borohydride ($NaBH_4$) in PBS for another 5 min (*see* Note 27).
6. Following a wash with PBS and 10 minutes' incubation in blocking buffer PBS supplemented with 1% BSA, the cells were incubated for 1 h with 0.22-μm-filtered (*see* Note 28) anti-HA antibody labeled with Cy3 in the same buffer.
7. The coverslips were washed twice with PBS and once with water before being mounted on slides with the mounting medium Mowiol (*see* Note 29) containing 2.5% (w/v) DABCO as an antifade.
8. Dishes and coverslips were stored at 4°C.

21.3.5 Change in Conformation: PKB Conformation

To monitor the change in conformation of PKB conformation, a reporter was constructed. Full-length PKB with genetically encoded, and enhanced GFP in the N-terminal and monomeric RFP on the C-terminal (GFP-PKB-RFP) were designed. Variations in PKB conformation were monitored by changes in the donor lifetime by two-photon FLIM (Fig. 21.5 and Color Plate 10). These changes were due to variations in distance and/or orientations of the two chromophores fused to PKB.

21.3.5.1 Construct Design

1. GFP-PKB (mouse PKB α), provided by Sandra Watton, has been previously described as pEGFP-HA-Akt construct [8].
2. The GFP-PKB-RFP construct was created by exchanging PCR-amplified mRFP (containing an EcoRI site in the N-terminal and an XbaI site in the C-terminal) instead of YFP in the previously described vector pCDNA3-EGFP-PKB-YFP [9]. The oligos mRFP-Ct sens and mRFP-Ct antisens were used for the PCR amplification (*see* Note 30).

21.3.5.2 Expression/Activity

1. Transfected NIH3T3 cells from a 6-well plate were stimulated for 5 min with 30 ng/ml of PDGF.

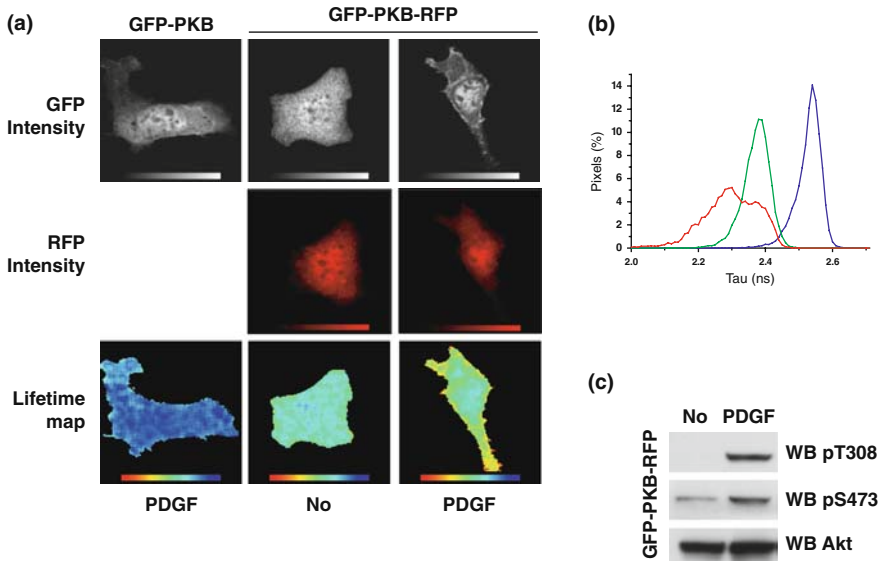

Fig. 21.5 Change in conformation of GFP-PKB-RFP monitored by time-domain FLIM. (a) Two-photon FLIM images of NIH3T3 cells transfected with either GFP-PKB or GFP-PKB-RFP are shown. Where indicated, the cells were treated with 30 ng/ml of PDGF for 5 min. Upon PDGF treatment, the construct translocates to the plasma membrane (intensity images in top panels). The lifetimes are represented in a pseudo-color scale from 2.20 ns (red) to 2.65 ns (blue). The average FRET efficiency is 4.3% for GFP-PKB-RFP in the cytoplasm and 8.6% at the plasma membrane. (b) The graph represents the lifetime distributions of GFP-PKB alone (blue), GFP-PKB-RFP prior to (green) or upon (red) PDGF stimulation. (c) The expression and phosphorylation state of GFP-PKB-RFP prior to and upon PDGF stimulation is revealed by using an anti-pan PKB antibody (WB Akt) and the Thr 308 phosphorylation by using an anti-phosphospecific antibody. To view this figure in color, see color insert

2. Cells were put on ice, washed once with PBS, and solubilized for 15 min in lysis buffer supplemented with COMPLETE protease inhibitor cocktail tablet.
3. The cells were scraped and centrifuged at 14,000 rpm for 5 min.
4. The protein content of the supernatant in each condition was determined by Bradford assay as recommended by the manufacturer.
5. To terminate the reaction, 4X SDS sample buffer supplemented with 10% β-mercaptoethanol was added and the samples boiled for 5 min.
6. The same amount of protein per well was separated on a 4–12% polyacrylamide gel by SDS-PAGE. The gels were transferred on PVDF membrane.
7. Membranes were incubated in blocking buffer TBS-T supplemented with 3% BSA for a minimum of 1 h prior to incubation with the different antibodies. Phospho-Akt (Thr-308) and Pan Akt antibodies were used at 1:1,000 at 4°C overnight in the same buffer. The primary antibodies were washed four times for 15 min in TBS-T 1% milk and incubated with the secondary HRP-antibodies for 1 h. HRP antibodies were used at 1:5,000 in TBS-T 5% milk. Western blots were revealed by incubation with ECL.

21.3.5.3 Cell Culture and Transfections

1. NIH3T3 cells were maintained in DMEM 10% donor bovine serum before trypsinization and plating.
2. The cells were seeded at 150,000 in a MatTek dish or in a well of a 6-well plate.
3. The transfection was done with 2 μg of DNA using Lipofect AMINE/PLUS reagent in OPTIMEM medium as recommended by the manufacturer.
4. After 3 h in the transfection mix, the medium was replaced with DMEM 10% donor bovine serum.
5. The experiments were performed 48 h after transfection.

21.3.5.4 Fixation and Mounting

1. NIH3T3 cells seeded in MatTek dishes were treated for 5 min with 30 ng/ml of PDGF and washed twice with PBS prior to fixation with a solution of 4% paraformaldehyde in PBS for 12 min.
2. The dishes were washed twice with PBS, and 2 ml of PBS containing 2.5% DABCO were added to the dishes.
3. Dishes were stored at 4°C.

21.3.6 Protein–Lipid Interaction: PLD and PITP

Phosphatidylinositol transfer proteins (PITP) have a role in signal transduction and traffic and have the ability to transfer phosphatidylinositol (PI/PtdIns) and phosphatidylcholine (PC/PtdCho) between membranes. Using GFP-PITP as a donor and fluorescent (BODIPY)-PI as an acceptor, we describe the dynamic interaction of PITP with PtdIns at the plasma membrane when stimulated with EGF using FD-FLIM [Fig. 21.6a and Color Plate 11].

A second example of protein–lipid interaction is illustrated by the study of the phospholipase D (PLD) activation [Fig. 21.6b and Color Plate 11]. PLD catalyzes the hydrolysis of phosphatidylcholine to phosphatidic acid (PA or PtdOH) and is involved, among other functions, in the regulation of membrane traffic. Here, GFP-PLD interaction with membrane BODIPY-PC in intact cells is monitored by FD-FLIM.

21.3.6.1 Construct Design

1. The design of the fusion between GFP and PITPβ (GFP-PITP) has been described elsewhere [10].
2. The design of the fusion between GFP and PLDb (GFP-PLD) has been described elsewhere [11].

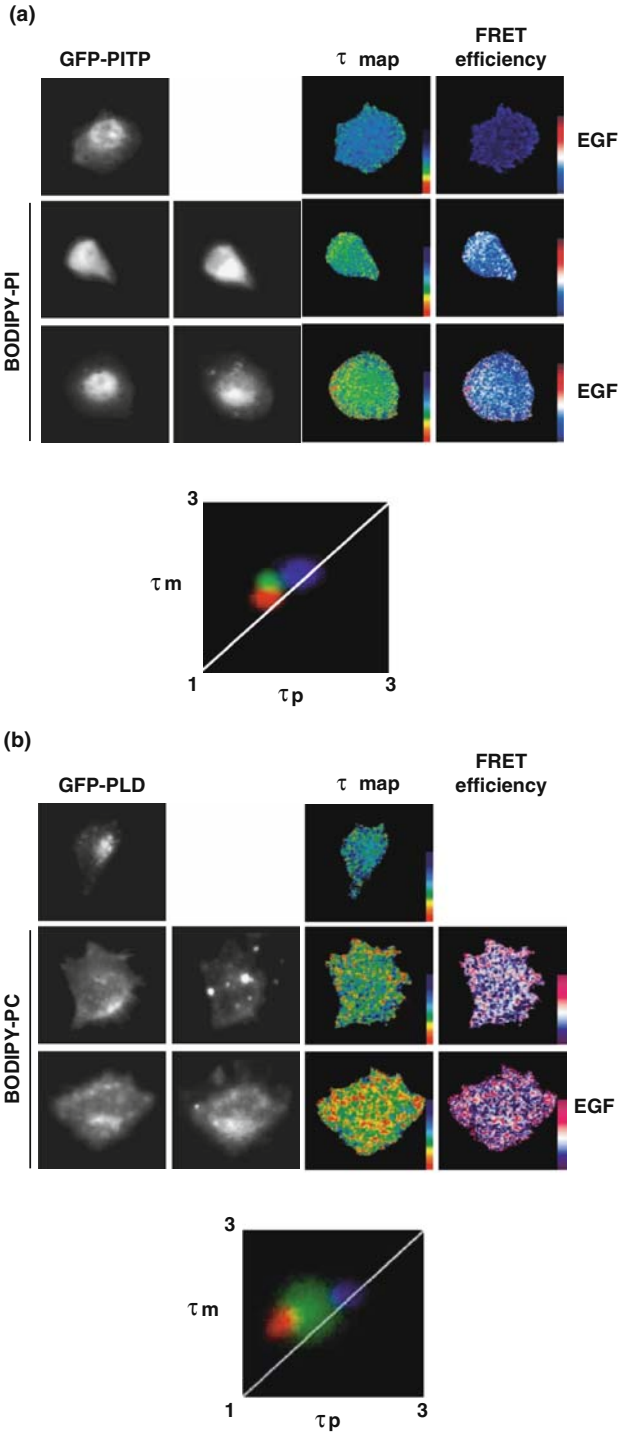

(See Fig. 21.6 Legend on next page)

21.3.6.2 Cell Culture and Transfections

1. COS-7 cells were grown in DMEM supplemented with 10% heat-inactivated fetal bovine serum. These cells were used for PITP experiments (Fig. 21.6a).
2. For electroporation (two pulses of 500 V and 125 μF), the cells were mixed with 0.7 μg of GFP-PITP and 35 μg of Herring sperm carrier DNA.
3. The cells were plated onto poly-L-lysine-coated coverslips or glass-bottomed dishes for microscopy and were used 24 h after transfection.
4. Prior to treatment with EGF, DMEM medium was exchanged for serum-free medium for a minimum of 1 h.
5. For PLD experiments (Fig. 21.6b), HeLa Ohio cells were grown in DMEM supplemented with 10% fetal bovine serum.
6. HeLa cells were transiently transfected with GFP-PLD constructs using FuGENE 6, as previously described [11], according to the manufacturer's protocol (Roche).

21.3.6.3 Preparation of Fluorescently Labeled Cells by Liposomes

1. For PITP experiments, liposomes containing 40 μM BODIPY-PI, labeled on the acyl chain (BODIPY 542/574 C_6 PI), were conjugated with polyamine carriers Shuttle PIP carrier-1 as described elsewhere ([18] and Molecular Probes' information sheet).
2. For PLD experiments, liposomes containing 20 μM PC (dipalmitoyl, Sigma) and 20 μM fluorescent phospholipid labeled on the acyl chain BODIPY 530/

Fig. 21.6 GFP-PITP/BODIPY-PtdIns and GFP-PLD/BODIPY-PtdCho interactions monitored by frequency-domain FLIM. (a) COS-7 cells were transfected with GFP-PITP, incubated with BODIPY-PtdIns for 15 min, and stimulated for 15 min with 35 ng/ml of EGF as indicated before being fixed. The average lifetime of GFP-PITP in cells that are incubated only with BODIPY-PtdIns decreases at the Golgi and the plasma membrane. Upon EGF stimulation, a further reduction in the lifetime of GFP-PITP is observed. The FRET efficiency maps indicate that the FRET efficiency can increase locally up to 40%. GFP lifetime is from 1.5 ns (red) to 2.1 ns (dark blue), and the efficiency scale is 0% (dark blue) to 40% (dark red). The cumulative lifetimes of GFP-PITP from three experiments (seven cells per experiment) are plotted on two-dimensional histograms, showing the phase (τ^p) and modulation (τ^m) for all pixels. GFP-PITP alone is shown in blue, while GFP-PITP together with BODIPY-PtdIns in unstimulated cells is in green and in EGF-stimulated cells is in red. A concomitant decrease in both τ^p and τ^m, and the resultant diagonal shift, indicates a reduction in the GFP lifetime due to FRET. (b) HeLa cells expressing GFP-PLD were incubated with liposomes containing BODIPY-PtdCho and then treated with 100 ng/ml of EGF for 30 min as indicated. The lifetime of GFP is from 1.6 ns (red) to 2.1 ns (blue). The FRET efficiency is also shown in a pseudo-color scale from purple (0%) to magenta (30%). The data indicate that GFP-PLD interacts with BODIPY-PtdCho; this interaction is increased by EGF treatment. The cumulative lifetimes from six experiments are plotted on a two-dimensional histogram showing lifetime phase (τ^p) and modulation (τ^m) for all pixels. The lifetimes are shown for GFP-PLD alone (blue), in the presence of BODIPY-PtdCho in nonstimulated cells (green) or EGF–treated cells (red). The diagonal shift indicates that FRET occurs between BODIPY-PtdCho and GFP-PLD and is increased in the presence of EGF. To view this figure in color, see color insert

550 C5 PC were prepared on resuspension in PBS by probe sonication (MSE Microsonicator) for three 10-s cycles at 20 W.
3. Cos-7 or Hela cells prepared on poly-L-lysine-coated glass coverslips were incubated at 37°C for 15 min with BODIPY lipids, and excess lipid was removed by washing with PBS before mounting.

21.3.6.4 Stimulation, Fixation, and Mounting

1. Labeled Cos-7 cells (PITP experiment) were stimulated with 35 ng/ml of EGF at 37°C for 15 min.
2. Cos-7 cells were washed, fixed with a solution of 4% paraformaldehyde in PBS, and mounted with 1:1 immunofluore mounting medium.
3. Hela cells were stimulated for 30 min with 100 ng/ml of EGF (PLD experiment). After PBS wash, the coverslips were mounted using Mowiol containing 2.5% DABCO.

21.3.6.5 Analysis and Statistics

1. For PITP experiments, images were thresholded in such a manner that the signal-to-noise ratio was systematically 2:1, and therefore the plasma membrane was not eliminated.
2. To determine the localized lifetime, the *x*- and *y*-coordinates of the regions of interest (plasma membrane and Golgi) on the intensity image were determined, and the same coordinates were used to determine the localized lifetimes.
3. GraphPad InStat software (version 3.0 for Mac 2001) was used for the statistical analysis. An unpaired *t*-test with Welch correction was used to determine the significance of the change in localized lifetimes at the plasma membrane with and without EGF stimulation (seven or more cells were analyzed per experiment; $n = 3$). The p values were determined at a 95% confidence interval.
4. The average GFP lifetime without acceptor was calculated from 10 cells per experiment, and the average GFP lifetime in the presence of acceptor was deduced from seven cells per experiment. Each experiment was repeated three times. The cumulative lifetimes of GFP-PITP alone and those with acceptor fluorophore are plotted on two-dimensional histograms. The average population variation, a concomitant decrease in τ_p and τ_m, indicates a reduction in GFP lifetime due to FRET.
5. For PLD experiments, the average GFP lifetime without acceptor was calculated from eight cells, and the average GFP lifetime with acceptor was deduced from six cells. Each experiment was repeated three times.
6. The cumulative lifetimes of GFP-PLD alone and that measured with acceptor fluorophore were plotted on two-dimensional histograms. The population variation, a concomitant decrease in τ_d and τ_m, indicates a reduction in GFP lifetime due to FRET.

21.3.7 Reporter of Phosphorylation State/Activity: PKB Phosphorylation

The activation state of PKB is strongly correlated with its phosphorylation on two sites, the threonine 308 in the kinase domain and the serine 473 on the C-terminal regulatory region. We have developed a method where we can monitor *in situ* PKB activation upon PDGF stimulation by measuring the Ser 473 phosphorylation status on a PKB. GFP-PKB was used as the donor and a Cy3-labeled anti-Ser473 antibody as the acceptor for FRET. The genetically encoded fusion protein GFP-PKB was expressed in NIH3T3 cells and the Cy3-labeled anti-Ser473 antibody incubated on permeabilized cells after fixation. Upon PKB activation, phosphorylated Ser 473 is recognized by the Cy3-labelled anti-Ser473 antibody and a decrease in the lifetime of GFP-PKB indicates FRET can be measured (Fig. 21.7 and Color Plate 12).

21.3.7.1 Construct Design

The fusion of GFP in the N-terminal of mouse PKB α has been described elsewhere [8]. That construct was formerly referred to as pEGFP-HA-Akt.

21.3.7.2 Cell Culture and Transfections

1. NIH3T3 cells were maintained in DMEM 10% donor bovine serum before trypsinization and plating.
2. The cells were seeded at 30,000 on poly-L-lysine-coated glass coverslips in 24-well plates.
3. The transfections were done with 0.4 μg of GFP-PKB DNA construct using Lipofect AMINE/PLUS reagent in OPTIMEM medium as recommended by the manufacturer. The cells were left for 3 h in the transfection mix, and then the medium was removed and replaced by DMEM containing 10% donor bovine serum.
4. The experiments were performed after overnight starvation in DMEM containing 0.2% BSA.

21.3.7.3 Stimulation, Antibody Treatment, and Mounting

1. The cells were treated for 5 min with 30 ng/ml of PDGF and then washed twice in PBS before being fixed with a solution of 4% paraformaldehyde in PBS for 12 min.
2. The cells were washed in PBS and permeabilized with 0.2% Triton-X100 in PBS for 5 min before incubation with 1 mg/ml of sodium borohydride ($NaBH_4$) in PBS for 5 min.
3. Following a wash with PBS and 10 minutes' incubation in the blocking buffer PBS supplemented with 1% BSA, the cells were incubated for 1 h

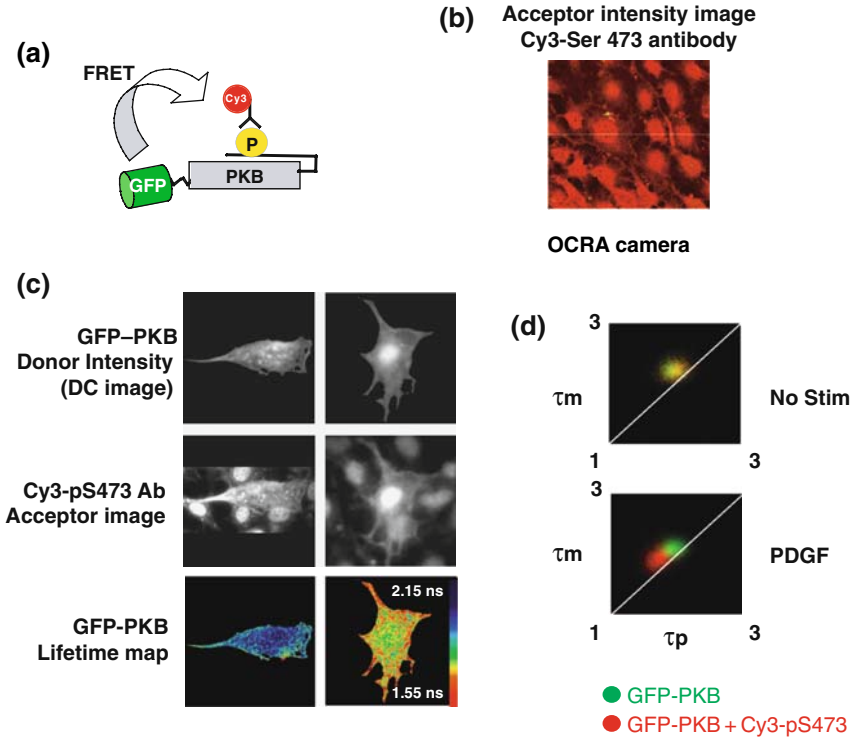

Fig. 21.7 Monitoring *in situ* GFP-PKB phosphorylation. (a) The experimental configuration is shown, where GFP-PKB is used as the donor and an anti-Ser473 antibody labeled with Cy3 is used as an acceptor to monitor FRET when PKB serine 473 is phosphorylated and recognized by the antibody. (b) The acceptor intensity image shows the homogenous distribution of incubated Cy3-labeled Ser473 antibody in NIH3T3 cells, taken with an OCRA camera. (c) Frequency FLIM images of NIH3T3 cells expressing GFP-PKB. The cells were treated with 30 ng/ml of PDGF for 5 min as indicated prior to fixation and incubation with an anti-Ser473 antibody labeled with Cy3. The top panels represent intensity (DC) images of GFP-PKB. The central panels represent intensity images of the Cy3-labeled anti-Ser473 antibody, and the bottom panels represent the calculated lifetime maps of the donor GFP-PKB. The lifetimes in pseudo-color scale are from 1.55 ns (red) to 2.15 ns (blue). This example shows that upon PDGF stimulation, FRET occurs at the edge of the cell, strongly suggesting that PKB phosphorylation upon stimulation occurs at the plasma membrane. (d) The cumulative lifetimes of GFP-PKB from three experiments are plotted on two-dimensional histograms, showing the phase (τ_p) and modulation (τ_m) for all pixels. GFP-PKB alone is shown in green and GFP-PKB together with Cy3-labeled anti-Ser473 antibody is in red. The top histogram shows the complete overlapping of the green and red dots, indicating that unspecific FRET is not occurring due to the presence of the Cy3-labeled antibody. However, upon PDGF stimulation (the bottom histogram), the concomitant decrease in both τ_p and τ_m and the resultant diagonal shift of the red dot indicates a reduction in the GFP lifetime due to Cy3-labeled Ser473 antibody recognition of PKB phosphorylation, allowing FRET to occur. To view this figure in color, see color insert

with 0.22-μm filtered anti-Ser473 antibody labeled with Cy3 in the same buffer.
4. The coverslips were washed twice with PBS and once with water before being mounted on slides with Mowiol containing 2.5% (w/v) DABCO as an antifade.

Acknowledgments The authors would like to thank Prof. Borivoj Vojnovic and the Advanced Technology Development Group (Drs. Paul Barber and Rosalind Locke) at Gray Cancer Institute for setting up the two-photon FLIM and Pierre Leboucher at College de France Paris for the automation of the frequency-domain FLIM analysis. This work was supported by EU Grant QLK3-CT-2000-01038 and Basic Technology Grant EPSRC-GA3191.

Notes

1. Apart from the blue fluorescent proteins (BFP, Sapphire), fluorescent proteins display a maximum two-photon absorption cross section above 900 nm. It is possible to tune the Mira 900 to a wavelength higher than 900 nm, but it is necessary to purge the cavity with dry N_2 and keep it under continuous flux.
2. The lifetime of the donor must be about $1/(4f)$, where f is the frequency of the pulsed excitation. Pulsed lasers have a frequency of 80 MHz, which reduces the lifetime measurement to a maximum of about 3 ns. Nevertheless, it can be extended to almost any lifetime range by reducing the pulse frequency with a pulse picker.
3. The two measurements can be quite different depending on the optical path in between the two positions. It is more convenient to measure the power after the neutral density filters since it does not necessitate the removal of the sample from the microscope stage. It can be critical if the power has to be adjusted and measured during experiments. In any case, both values should vary proportionally.
4. Emission "cross talk" ("bleed through") is a common problem in FRET experiments because of the constraints imposed by the overlap of the donor emission and acceptor absorption spectra. In these conditions, it is common for the emission spectra of the donor and the acceptor to partially overlap, resulting in a possible contamination of the acceptor channel with fluorescence of the donor. Using narrow band-pass filters for the collection of the fluorescence of both the donor and the acceptor reduces the collection factor, but, more importantly, it minimizes the risk of cross talk. No cross talk was detected when using the GFP/RFP pair. However, when using eYFP as a donor in place of GFP with the same set of cubes as for GFP/RFP, bleed through was detected in the RFP channel, due to the red-shifted fluorescence of YFP compared to GFP. It is not a problem for the detection of FRET by fluorescence lifetime [using a (535 ± 15)-nm band-pass filter] since only YFP fluorescence is detected.
5. Attention must be paid to the photobleaching during localization and observation of the cells with the mercury lamp. Even if FRET is detected by the variation of lifetime of the donor, it is important to pay attention to the photostability of both the donor and the acceptor since damage to the acceptor will affect directly the FRET efficiency as well as the proportion of the FRETing population.
6. Usually, the image is acquired at the cell's mid-section, which is actually defined as the plane where the nuclear size is maximal.
7. In TD-FLIM, only the donor fluorescence has to be collected. Nevertheless, great care must be given for both donor and acceptor photobleaching. This can affect the lifetime of the donor either directly [19] or indirectly by affecting the proportion of "FRETing and non-FRETing" species. The photobleaching must be calibrated and minimized for every

fluorophore since they all exhibit a different photostability. In two-photon excitation, absorption spectra are usually broader than in one-photon excitation and might overlap. Consequently, a two-photon excitation of the donor can also be accompanied by the acceptor excitation. It is important that the excitation of the acceptor does not lead to its own photobleaching. Another side effect of the acceptor absorption is its possible fluorescence emission. This fluorescence would make the analysis more complicated if FRET is measured by the intensity ratio $I_{\text{donor}}/I_{\text{acceptor}}$ since I_{acceptor} should only result from FRET-sensitized emission. It is not a problem in the case of the detection of FRET by measuring the lifetime of the donor, since the fluorescence of the donor, collected through a narrow band-pass filter, should not be contaminated by the fluorescence of the acceptor.

8. It is preferable to decide the number of scans for cells with a heterogeneous intensity distribution and low-intensity pixels in some regions, so that the low-intensity pixels will present a high final count to be fitted correctly for the data analysis.
9. For a dwelling time of 17 μs and a rate of 10^6 photon/s, almost 1 minute is necessary to acquire an image with 1,000 counts at the maximum of the intensity decay after a binning of 11 × 11 pixels. For low-intensity cells, considering that the power of the excitation is limited by the photobleaching, the photon-count rate falls rapidly below 10^6 photon/s, and acquisitions take longer. Thus, to keep the acquisition time not longer than a few minutes, it is necessary to compromise on the photon count and consequently on the signal-to-noise ratio. A photon count of about 100 at the maximum of the intensity decay is enough to be able to fit a mono-exponential. When varying the photon count, the lifetime distribution keeps the same average value, but its width increases. This may be a problem if the lifetime variations are smaller than the distribution width.
10. The resolution has to be adjusted with regards to the magnification factor. Keeping a high resolution with a high magnification does not improve the image quality and dramatically increases the risk of photobleaching.
11. Spatial binning consists of putting together the collected photons of adjacent pixels into a single bin. It is an easy way to increase the photon count per representative pixel without increasing either the acquisition time or the excitation power. Nevertheless, it leads to a decrease in the spatial resolution and might mask local lifetime variations by averaging pixels that present different lifetimes. Binning has to be performed carefully when studying changes at the plasma membrane, in vesicles, or in any subcellular compartment. The increase in the binning tends to flatten the lifetime variations.
12. In case of count rates higher than 10^6 photon/s, the excitation power has to be reduced.
13. Masking the cells surrounding the cell of interest is important for the use of histograms since other cells will directly contribute to it.
14. The intensity decay is fitted in the linear part (y-axis in $\log_{10}$ scale) of the intensity decay. The instrument response function has a full-width-half-maximum of about 200 ps, which should not affect the lifetime calculation, which is commonly higher than 2 ns in the presence or absence of FRET [20].
15. The complexity and characteristic time of a fluorophore intensity decay are sensitive to both its environment and its intrinsic photophysical properties. Thus, cell heterogeneity, the complexity of the protein interactions, as well as the photophysics of the donor fluorophore do not expect mono-exponential decays [21]. The decays are rather expected to be complex and be modeled by a lifetime distribution or by the sum of mono-exponential decays. When detecting intermolecular interactions by FRET, photons from both interacting and noninteracting species are collected. Similarly, when detecting conformational changes, the fusion protein leads to variations of FRET efficiency due to a change of distance and/or the relative orientation of the two fluorescent proteins. Again, when measuring the fluorescence intensity decay, photons associated with the different conformations are collected. Thus, in both

cases, the intensity decays must follow a multi-exponential law. Already a bi-exponential fit (based on a two-state modeling of the system, in which each state exhibits a mono-exponential intensity decay) necessitates a minimum photon count of 1,000 at the maximum of the intensity decay to have an adequate signal-to-noise ratio. Considering the limitations such as photobleaching and low concentration of fusion protein in cells, the number of photons necessary to proceed accurately with a multi-exponential analysis would be prohibitive. In addition, to identify the contribution of two lifetimes to the decay accurately, it is preferable that they differ by about a factor of two [3], which is generally not the case with fluorescent proteins. Taking this in consideration, data might better be analyzed using a mono-exponential fit and FRET quantified by measuring the relative variation of the lifetime obtained from the mono-exponential fit.

16. To provide a high spatial resolution, the detection system for lifetime measurement is not optimized. To provide a better quality for the cell's intensity image, the OCRA camera is used.
17. An extra EcoRI site (in the vector) C-terminal of PKB was eliminated by direct site mutagenesis prior to the subcloning of RFP using the primers EcoRI less-sens and EcoRI less-antisens.
18. It is important to note here that the wash and the incubation of the secondary antibody are done in milk and not BSA. This is due to the fact that the prepared BSA used here contains azide. Having azide in the wash or the secondary antibody incubation prior to ECL will prevent the revealed.
19. For imaging, MatTek dishes with a coverslip thickness of 0.16–0.19 mm are recommended to match microscope objective characteristics. A thinner or thicker thickness can greatly reduce fluorescence.
20. To reduce the basal activity of the protein of interest prior to stimulation, starvation of the cells is usually used. However, NIH3T3 cells have been proven to be very sensitive to starvation, with an increased percentage of dead or unhealthy cells. For this reason, depending on the experiment, the cells may have been starved or not. Note that PKB's potency of activation was not affected by the absence of starvation.
21. For appropriate labeling, the quantity of the antibody needs to be above 200 μg. The antibody concentration is also a very important factor that will depend on each specific antibody.
22. Buffers containing primary amino groups such as Tris and glycine will inhibit the conjugation reaction.
23. Care should be taken to prevent foaming of the antibody solution by stirring too strongly. The 2-ml capped glass vial can be covered with aluminum foil to keep the solution in the dark.
24. A Bio-GelTM P-10 column with a minimum of 1-cm diameter and 12-cm length packed volume is required.
25. For reproducibility reasons, it is important to determine the protein-to-dye ratio, i.e., the number of dyes per molecule of antibody. First, the protein concentration will be determined by measuring the absorbance of the collected antibody at 280 nm in a spectrophotometer. Then, the Cy3 concentration is determined by measuring the absorbance at 552 nm. The molar extinction coefficients will be 150,000 $M^{-1}cm^{-1}$ at 552 nm for the Cy3 dye and 170,000 $M^{-1}cm^{-1}$ at 280 nm for the antibody. The extinction coefficient will vary for different proteins. The calculation is corrected for the absorbance of the dye at 280 nm (approximately 8% of the absorbance at 552 nm). [Cy3 dye] = Abs at 552 nm/150,000.

$$[\text{Antibody}] = [(\text{Abs at } 280\text{nm} - (0.08 \times \text{Abs at } 552\,\text{nm})]/170{,}000.$$

$$\text{Dye/protein ratio} = [\text{dye}]/[\text{antibody}] = [(1.13 \cdot (\text{A552})]/[\text{A280} -; (0.08 \times (\text{A552})].$$

26. Due to its antioxidant properties, DABCO minimizes the photobleaching, improving the lifetime of dyes. It is used as an antifade reagent in fluorescence experiments.
27. Sodium borohydride ($NaBH_4$) is an effective and very selective special reducing agent. It quenches any remaining PFA and also removes most of the cellular autofluorescence. It reacts across double bonds, thereby reducing the pi-bond interactions that result in autofluorescence. It is used to quench, for instance, unreacted glutaraldehyde, which is very fluorescent if not reduced. Use at 0.1%.
28. Filtering the labeled antibody on a 0.22-μm filter is essential to clean the antibody before incubating the coverslips and must be done on a very small filter to avoid loss of material.
29. Mowiol mount is a PVA-based mount. It hardens overnight after slide preparation, one advantage of its used is that cells under the coverslip do not dry, and it does not require the coverslips to be sealed with nail polish.
30. An additional Xba I site in GFP-PKB-YFP was initially removed by direct site mutagenesis before subcloning mRFP.

References

1. Jares-Erijman EA, Jovin TM. FRET imaging. Nat Biotechnol. 2003;21(11):1387–95.
2. Jares-Erijman EA, Jovin TM. Imaging molecular interactions in living cells by FRET microscopy. Curr Opin Chem Biol. 2006;10(5):409–16.
3. Lakowicz J. Principles of fluorescence spectroscopy. 2nd ed. New York: Kluwer Academic Plenum Publishers; 1999. pp. 380–83.
4. Gadella TW, Jovin TM, Clegg RM. Fluorescence lifetime imaging microscopy (FLIM): spatial resolution of microstructures on the nanosecond time scale. Biophys Chem. 1993;48(2):221–39.
5. Squire A, Bastiaens P.I. Three dimensional image restoration in fluorescence lifetime imaging microscopy. J Microsc. 1999;193(Pt 1):36–49.
6. Alessi DR, Andjelkovic M, Caudwell B, Cron P, Morrice N, Cohen P, Hemmings BA. Mechanism of activation of protein kinase B by insulin and IGF-1. Embo J. 1996;15(23):6541–51.
7. Park J, Hill MM, Hess D, Brazil DP, Hofsteenge J, Hemmings BA. Identification of tyrosine phosphorylation sites on 3-phosphoinositide-dependent protein kinase-1 and their role in regulating kinase activity. J Biol Chem. 2001;276(40):37459–71.
8. Watton SJ, Downward J. Akt/PKB localisation and 3' phosphoinositide generation at sites of epithelial cell-matrix and cell-cell interaction. Curr Biol. 1999;9(8):433–6.
9. Calleja V, Ameer-Beg SM, Vojnovic B, Woscholski R, Downward J, Larijani B. Monitoring conformational changes of proteins in cells by fluorescence lifetime imaging microscopy. Biochem J. 2003;372(Pt 1):33–40.
10. Swigart P, Insall R, Wilkins A, Cockcroft S. Purification and cloning of phosphatidylinositol transfer proteins from Dictyostelium discoideum: homologues of both mammalian PITPs and Saccharomyces cerevisiae sec14p are found in the same cell. Biochem J. 2000;347(Pt 3):837–43.
11. Hughes WE, Parker PJ. Endosomal localization of phospholipase D 1a and 1b is defined by the C-termini of the proteins, and is independent of activity. Biochem J. 2001;356(Pt 3):727–36.
12. Wallrabe H, Periasamy A. Imaging protein molecules using FRET and FLIM microscopy. Curr Opin Biotechnol. 2005;16(1):19–27.
13. Thaler C, Koushik SV, Blank PS, Vogel SS. Quantitative multiphoton spectral imaging and its use for measuring resonance energy transfer. Biophys J. 2005;89(4):2736–49.
14. Hanley QS, Subramaniam V, Arndt-Jovin DJ, Jovin TM. Fluorescence lifetime imaging: multi-point calibration, minimum resolvable differences, and artifact suppression. Cytometry. 2001;43(4):248–60.

15. Wu P, Brand L. Resonance energy transfer: methods and applications. Anal Biochem. 1994;218(1):1–13.
16. Wouters FS, Verveer PJ, Bastiaens PI. Imaging biochemistry inside cells. Trends Cell Biol. 2001;11(5):203–11.
17. Clegg RM, Murchie AI, Lilley DM. The solution structure of the four-way DNA junction at low-salt conditions: a fluorescence resonance energy transfer analysis. Biophys J. 1994;66(1):99–109.
18. Ozaki S, DeWald DB, Shope JC, Chen J, Prestwich GD. Intracellular delivery of phosphoinositides and inositol phosphates using polyamine carriers. Proc Natl Acad Sci U S A. 2000;97(21):11286–91.
19. Tramier M, Zahid M, Mevel JC, Masse MJ, Coppey-Moisan M. Sensitivity of CFP/YFP and GFP/mCherry pairs to donor photobleaching on FRET determination by fluorescence lifetime imaging microscopy in living cells. Microsc Res Tech. 2006;69(11):933–9.
20. Treanor B, Lanigan PM, Suhling K, Schreiber T, Munro I, Neil MA, Phillips D, Davis DM, French PM. Imaging fluorescence lifetime heterogeneity applied to GFP-tagged MHC protein at an immunological synapse. J Microsc. 2005;217(Pt 1):36–43.
21. Lee KC, Siegel J, Webb SE, Leveque-Fort S, Cole MJ, Jones R, Dowling K, Lever MJ, French PM. Application of the stretched exponential function to fluorescence lifetime imaging. Biophys J. 2001;81(3):1265–74.

Chapter 22
Phosphoinositide (PI) 3-Kinase Assays

Michael J. Fry

Abstract The regulation of phosphoinositide (PI) 3-kinase activities has been linked to many normal and disease-related processes, including cell survival, cell growth and proliferation, cell differentiation, cell motility, and intracellular vesicle trafficking. However, as the family of enzymes has now grown to include eight true members, in three functional classes, plus several related protein kinases that are also inhibited by the widely used PI 3-kinase selective inhibitors, wortmannin and LY294002, extended methodologies are required to identify which type of kinase is involved in a particular cellular process, or protein complex, under study. A robust *in vitro* PI 3-kinase assay, suitable for use with immunoprecipitates, or purified proteins, is described here together with a series of modifications of substrate and assay conditions that will aid researchers in the identification of the particular class and isoform of PI 3-kinase that is involved in a signaling process under investigation.

Keywords Phosphatidylinositol · phosphoinositide 3-kinase · Vps34 · Wortmannin · LY294002 · immunoprecipitation · *in vitro* PI 3-kinase assay · thin layer chromatography

Abbreviations CDTA: trans-1,2-diaminocyclohexane-N,N,N',N'-tetra-acetic acid; DMSO: dimethylsulphoxide; EDTA: diaminoethanetetra-acetic acid; PBS: phosphate buffered saline; PI: phosphoinositide; PMSF: phenylmethylsulfonyl fluoride; PtdCho: phosphatidylcholine; PtdEth: phosphatidylethanolamine; PtdIns: phosphatidylinositol; PtdSer: phosphatidylserine; TLC: thin layer chromatography.

M.J. Fry
School of Biological Sciences, Division of Biomolecular Science, AMS Building, University of Reading, Whiteknights, Reading, Berkshire, RG6 6AJ, UK
e-mail: m.j.fry@reading.ac.uk

B. Larijani et al. (eds.), *Lipid Signaling Protocols*, DOI: 10.1007/978-1-60327-115-8_22,

22.1 Introduction

Over 20 years have passed since a minor lipid kinase activity was discovered associated with retroviral oncogene products and growth factor receptors [1–4]. This activity later turned out to have a novel specificity for the 3' position OH group of the inositol ring [5]. This receptor-/oncogene-linked kinase activity is now known to be attributable to a class Ia subclass of phosphoinositide (PI) 3-kinase. PI 3-kinase activity has been shown to be involved in diverse normal and disease cellular processes including cell growth, oncogenic transformation, cell survival, insulin-stimulated glucose uptake, and protein trafficking [6–9]. Selective inhibitors of PI 3-kinase activity have proved a popular tool in implicating PI 3-kinases in many different biological responses. The most widely used are two cell-permeable inhibitors: wortmannin, a steroid-like toxin isolated from soil bacteria [10] (*see* Note 1), and LY294002, a bioflavonoid derived from quercetin [11] (*see* Note 2).

However, in the last 10 years, the PI 3-kinase family has grown to include eight mammalian enzymes, encoded by distinct genes, that catalyze the phosphorylation of the 3'-OH group of phosphatidylinositol (PtdIns) and a range of other phosphoinositides including PtdIns(4)*P*, PtdIns(5)*P*, and PtdIns(4,5)P_2 [9]. These enzymes have been organized into three classes (I–III) based on different enzyme domain structures and on their *in vitro* substrate specificities [12]. An additional class IV enzyme subgroup includes the proteins mTOR, ATM, ATR, and DNA-PK and possesses sequence homology to the catalytic region of the true PI 3-kinases, but which possess only a protein kinase, and not a lipid kinase activity [13,14]. The class I subfamily of PI 3-kinases consists of four catalytic subunits: three class Ia subunits (p110α, p110β, and p110δ) that are mainly, but not exclusively, protein-tyrosine kinase-regulated via the p85 family of regulatory adaptor proteins that possess phosphotyrosine-binding SH2 domains, and a single class Ib isoform, p110γ, which is mainly G protein-coupled receptor (GPCR)-regulated and binds to p101/p84 regulatory subunits [8,9]. The main *in vivo* product of both class Ia and Ib isoforms is phosphatidylinositol(3,4,5)-trisphosphate [PtdIns(3,4,5)P_3], but these enzymes will readily utilize PtdIns and PtdIns(4)*P* as substrates *in vitro* [6–9]. The class I PI 3-kinases control a range of cellular functions including cell proliferation, cell differentiation, cell survival, and cell migration depending on the cell type [6–9], and there is evidence that the different isoforms have both redundant and non-redundant functions. There are three mammalian class II PI 3-kinase isoforms, PI3 K-C2α, PI3 K-C2β/Hs-C2-PI3 K, and PI3 K-C2γ [9,15]. *In vitro* their preferred substrates are PtdIns and PtdIns(4)*P*, but not PtdIns(4,5)P_2, resulting in the production of PtdIns(3)*P* and PtdIns(3,4)P_2 [9,15]. Recent evidence suggests that their *in vivo* product may be PtdIns(3)*P* [16]. There are currently no known regulatory subunits for class II PI 3-kinases [15]. There is a single class III isoform in mammals, which is the homologue of the sole yeast PI 3-kinase, Vps34 [17]. Class III PI 3-kinases are all PtdIns-specific PI 3-kinases that make PtdIns(3)*P*

mainly on intracellular vesicles, where it plays a role in the regulation of intracellular trafficking [6–9, 17]. The Vps34 protein has an adaptor called Vps15 in yeast that is a myristylated protein serine/threonine kinase [17]; a homologue, p150, is present in mammalian cells [8, 9].

Wortmannin inhibits all three classes of PI 3-kinase enzymes, some PtdIns 4-kinase isoforms, and all members of the class IV PIK-related kinases over the nM- to low-μM-concentration range [18]. LY294002 also inhibits all the PI 3-kinase family members, including the class IV protein kinases in the μM-concentration range [18]. Variation is observed, however, for individual isoforms from species to species as to the concentrations required for inhibition. For example, yeast Vps34p and a bovine PtdIns-specific PI 3-kinase are reported to be relatively insensitive to wortmannin [15]. The use of wortmannin is further complicated since the class II PI 3-kinase, PI3 K-C2α, requires high nM to μM concentrations for inhibition [19].

Given the current broad interest in the involvement of PI 3-kinases in diverse cellular functions and the increasing interest from drug companies in targeting these enzymes in various therapies [20,21], there is a clear need for simple and appropriate assays that rapidly allow the type of PI 3-kinase present in a sample to be determined. This is especially relevant as there is not a well-characterized panel of antibodies available that allows clear determination of which isoforms of PI 3-kinase are present in a lysate, or immunoprecipitate, by Western blotting. The widely used *in vitro* PI 3-kinase assay, using PtdIns as a substrate, fails to adequately address this, as all the known PI 3-kinases, and other enzymes such as the abundant PI 4-kinases, can phosphorylate this lipid to produce a PtdIns(X)*P* species that cannot easily be distinguished from PtdIns(3)*P* on the commonly used TLC systems. The method that follows describes a basic, robust *in vitro* PI 3-kinase assay, modified from published assays for this activity [4, 5, 22,23], that is suitable for use on either a purified enzyme or on an immunoprecipitate containing a PI 3-kinase activity. A series of inhibitor controls and modifications to this standard protocol are described that will provide the researcher with more insight as to the class of enzyme under study in a particular sample.

22.2 Materials

22.2.1 Cell Culture, Cell Lysis, and Immunoprecipitation

1. Dulbecco's Modified Eagle's Medium (DMEM) (Invitrogen) supplemented with 10% (v/v) fetal bovine serum (FBS) (Invitrogen) and 100 U/ml of penicillin and 100 μg/ml of streptomycin (Invitrogen).
2. Phosphate buffered saline (without Ca^{2+} and Mg^{2+}) (Invitrogen).
3. 0.25% (w/v) Trypsin/1 mM EDTA (Invitrogen).
4. Wortmannin (Sigma) was dissolved in dimethyl sulphoxide (DMSO) at 10 mM, stored in single-use aliquots at −20°C, and then diluted further in DMSO and/or cell culture media immediately prior to use (*see* Note 1).

5. LY294002 (Calbiochem or Tocris) was dissolved in DMSO at 50 mM, stored in single-use aliquots at −20°C, and then diluted further in DMSO and/or cell culture media immediately prior to use (*see* Note 2).
6. Lysis buffer (*see* Note 3): 10 mM Tris-HCl, pH 7.4 (at 4°C), 1% (v/v) Triton X100, 5 mM EDTA, 50 mM NaCl, 50 mM NaF (*see* Note 4). Make fresh on day of use. Add sodium orthovanadate (200–500 μM final) (*see* Note 5), 1× Complete™ EDTA-free protease inhibitor cocktail (Boehringer Mannheim) and PMSF (2 mM final) immediately before use.
7. Cell scrapers (Fisher Scientific).
8. Eppendorf brand 1.5-ml microcentrifuge tubes (*see* Note 6).
9. The following antibodies have all been tested and found to work in immunoprecipitation/PI 3-kinase assays: anti-PI 3-kinase, p85 N-SH3, clone AB6, monoclonal antibody (05-212), and anti-PI 3-kinase p85 rabbit antiserum (06-195) (Upstate). Anti-p110α monoclonal antibody (P94520) from Transduction Laboratories. Rabbit polyclonal anti-p110α antibody (sc-7174), rabbit polyclonal anti-p110β antibody (sc-602), rabbit polyclonal anti-p110δ antibody (sc-7176), and rabbit polyclonal anti-p110γ antibody (sc-7177) were from Santa Cruz. Mouse monoclonal anti-phosphotyrosine antibody, clone 4 G10 (05-321) from Upstate. Many antibodies have been successfully used to immunoprecipitate PI 3-kinase activity in association with receptors and adaptors.
10. Protein A- or G-Sepharose (Amersham).

22.2.2 PI 3-Kinase Assay

1. Phosphatidylserine (PtdSer), PtdIns, and PtdIns(4,5)P_2 were purchased from Avanti Polar Lipids. PtdIns(4)*P* and bovine brain phosphoinositides were purchased from Sigma.
2. 2× PI 3-kinase assay buffer (50 mM HEPES, pH 7.4, 100 mM NaCl, 1 mM dithiothreitol).
3. ATP-mix: 16.6 mM $MgCl_2$, 333.3 μM ATP, 1 mCi/15 μl [γ-^{32}P] ATP (specific activity > 5,000 Ci/mmol) (Amersham).
4. 1 M HCl.
5. Chloroform:methanol (1:1, by volume) (*see* Note 7).
6. Methanol:1 M HCl (1:1, by volume).

22.2.3 Lipid Analysis by Thin Layer Chromatography (TLC)

1. 1% (w/v) oxalic acid, 1 mM EDTA in water:methanol (6:4, by volume).
2. TLC developing solution: chloroform:methanol:4 M NH_4OH (9:7:2, by volume).
3. 20-cm × 20-cm plastic-backed Silica gel 60 TLC plates (without fluorescent indicator) (Merck) (*see* Note 8).
4. Rectangular (27 × 26.5 × 7 cm) TLC developing tank with lid (Aldrich).
5. 3 MM chromatography paper (Whatman).
6. Chloroform:methanol (4:1, by volume).

22.3 Methods

The activity of a PI 3-kinase can be measured *in vitro* by monitoring the incorporation of ^{32}P into a phosphoinositide substrate. The most commonly used substrate is PtdIns, either alone or as a mixed vesicle with a second non-phosphorylatable carrier lipid such as phosphatidylserine (PtdSer), phosphatidylcholine (PtdCho), or phosphatidylethanolamine (PtdEth). This type of assay can be performed on purified enzyme but is most commonly carried out in conjunction with immunoprecipitation of the PI 3-kinase by one of several strategies: (1) direct immunoprecipitation of a PI 3-kinase using an antibody directed against either the catalytic subunit or an associated regulatory subunit; (2) immunoprecipitation of the PI 3-kinase activity using an antibody directed against a protein with which the PI 3-kinase associates, e.g., to an activated receptor or associated adaptor protein; (3) immunoprecipitation of PI 3-kinase activity using anti-phosphotyrosine antibodies. Assay type 1, using antibodies to the catalytic or regulatory subunit of the PI 3-kinase, potentially allows kinetic measurements to be made on the kinase, by comparing activity before and after stimulation by treatment of cells with a growth factor. In practice, only small changes (up to twofold) in activity are usually seen by this approach. This is likely to be in part due to the fact that stimulation of cells by growth factors tends to activate only a fraction of the available receptors and downstream signaling molecules such as PI 3-kinase. The possible positive and negative effects of antibody binding to the PI 3-kinase also have to be considered here on a case-by-case basis, and immunoprecipitated activities need to be related back to the amount of PI 3-kinase protein immunoprecipitated under each condition by Western blotting with isoform-specific antisera where available. The assays described in types 2 and 3 tend to result in much larger observed changes in the measured PI 3-kinase activity associated with the immunoprecipitate, as they largely reflect recruitment of the PI 3-kinase into the complex rather than changes in intrinsic activity. In the case of PDGF stimulation of NIH 3T3 fibroblasts, followed by immunoprecipitation with anti-phosphotyrosine antibodies, 50- to 100-fold more associated PI 3-kinase activity has been reported following stimulation.

The protocol presented below is a standard PtdIns-based kinase assay that has been tested in all the above assay formats and generally gives good results in the first experiment. In its basic format, however, it does fail to distinguish between a range of PI 3-kinase and other PtdIns kinases, and so it is followed by a brief discussion as to how the standard assay can be readily modified to provide greater information to the researcher as to which type of PI kinase is being studied.

22.3.1 Cell Culture, Cell Lysis, and Immunoprecipitation

1. HeLa cells were grown as a monolayer and were passaged before they reached confluence using trypsin/EDTA to release them from the culture

dish. Maintenance cultures were passaged in 10-cm tissue culture dishes, and experiments were routinely carried out on 6-cm dishes. Irrespective of the cell line under study, in our experience one 6-cm dish for each experimental point is a good starting point (*see* Note 9). To induce a quiescent state, and to reduce the basal PI 3-kinase activity to a minimum, cells were starved overnight in low-serum [0.5% (v/v) FBS] media (*see* Note 10).

2. Prepare a suitable amount of the working lysis buffer solution by adding the inhibitors [100–500 μM sodium orthovanadate, 1× Complete^{TM} EDTA-free protease inhibitor cocktail (Boehringer Mannheim), and 2 mM PMSF (*see* Note 11)] immediately prior to use.
3. Stimulate the cells with an appropriate agonist for an appropriate length of time or number of times (*see* Note 12). Nonstimulated control cells are lysed and analyzed in the same manner as the agonist-stimulated cells. Wash the cells twice with ice-cold PBS (on dish if cells form an adherent monolayer, or by centrifugation if a suspension cell line), carefully removing the media at each step by aspiration.
4. Lyse cells with a minimum volume of ice-cold lysis buffer (use 1 ml for a 10-cm dish of HeLa cells: ~2 million cells and 250–300 μl for a 6-cm dish) (*see* Note 13). From this point on, all procedures should be carried out at 4°C.
5. Scrape cells from dish into a prechilled 1.5-ml Eppendorf microcentrifuge tube. Vortex the tube and then leave on ice for 20 min for lysis to occur. Vortex briefly again and then spin the lysate at full speed (~10,000–14,000 × *g*) in a refrigerated microcentrifuge for 20 min at 4°C to remove the detergent's insoluble material. The supernatant was then transferred to a fresh, chilled Eppendorf tube. The protein concentration of the different cell lysates was measured in a spectrophotometer at 595 nm using Coomassie protein assay reagent (Pierce).
6. After adjusting the concentrations of each sample, add an appropriate amount of the resultant supernatant to prechilled tubes containing an appropriate amount of primary antiserum. Incubate 1–2 h on the wheel at 4°C. Longer incubations often result in higher backgrounds and can lead to loss of kinase activity. If necessary, add a secondary antibody after 1 h.
7. While the lysate is incubating with the primary antibody, the protein A-Sepharose (or protein G-Sepharose depending on the species and isotype of antibody being used) is prepared by swelling the resin for 1 h at 4°C in ~10 dry pellet volumes of lysis buffer. The resin is then gently washed with several pellet volumes of lysis buffer before use to remove any loosely bound protein A/G. Add protein A-Sepharose (30–40 μl of a 50% solution in lysis buffer is usually plenty and gives a visible pellet). Use a Gilson pipette with a tip cut to give a wider-diameter aperture when transferring the resin between tubes. Continue incubation at 4°C for a further 45 min.
8. Pellet the immune complex by a brief spin in the microcentrifuge (~30 s at 10,000 × *g*). Collect and store the supernatant if required for SDS-PAGE and Western blotting. Wash the immune pellet with 1 ml of lysis buffer.

Repeat this wash step at least twice. Additional wash steps can be included here to increase the stringency, e.g., a 0.5 M LiCl, or 1 M NaCl, in 10 mM Tris-HCl (pH 7.4) wash, again depending on the antibody (*see* Note 14). Finally, wash the immune pellet once with 1 ml of 1× kinase buffer (*see* Note 15).

22.3.2 PI 3-Kinase Assay

22.3.2.1 Preparation of TLC Tank

1. A glass chromatography tank, just big enough to hold the TLC plate, should be cleaned and then lined with 3 MM filter paper on three sides.
2. The mobile-phase solvent mixture is added to a depth around 1–2 cm (*see* Note 16).
3. The tank is covered with its lid and then gently shaken to wet the filter paper.
4. The tank should then be left for at least 1 h to saturate the air with mobile-phase vapor (*see* Note 17).

22.3.2.2 Preparation of Lipid Vesicles

1. Lipids were dissolved as a 10-mg/ml stock solution in chloroform and stored at −20°C. For the standard assay, vesicles of PtdIns only will work fine. Vesicles were made up freshly on the day of use as a 1 mg/ml working solution by drying the appropriate amount of the lipid stock solution under a stream of inert gas (e.g., nitrogen) on ice (*see* Note 18).
2. While the immunoprecipitate is incubating with the protein A-Sepharose, the dried lipids were resuspended in 5 mM HEPES (pH 7.4) by vortexing and vesicles were formed by ultrasonic treatment of the suspension for 5–10 min in an ice-cold ultrasonic water bath. The lipid suspension, which initially appears cloudy, should turn clear (*see* Note 19).

22.3.2.3 PI 3-Kinase Assay Using PtdIns as Substrate

1. The immune complex pellet from the immunoprecipitation was washed twice with 1 ml of 2× kinase buffer (50 mM HEPES, pH 7.4, 100 mM NaCl, 1 mM dithiothreitol) and then resuspended in 25 µl of 2× kinase buffer (*see* Note 20).
2. 10 µl lipid vesicles (final concentration: 200 µg/ml in a 50 µl reaction) were mixed with the immune complex pellet and preincubated for 20 min at 4°C.
3. The enzymatic reaction was started by adding 15 µl of the ATP mix [final concentration in a 50 µl reaction: 5 mM $MgCl_2$, 100 µM ATP (sodium salt)

(*see* Note 21), 1 μCi [γ-^{32}P] ATP (specific activity > 5,000 Ci/mmol) (Amersham) (*see* Note 22)].
4. The reaction was incubated for 5–10 min at 30°C and terminated by the addition of 100 μl of 1 M HCl (*see* Note 23).
5. The lipids were extracted by the addition of 200 μl of chloroform:methanol (1:1, by volume) and mixed for 5 s per sample using a vortex, and then the two phases were separated by centrifugation for 2 min at room temperature in a microfuge.
6. The upper, aqueous phase was discarded (take care to remove all this layer as it contains the highly radioactive, unused [^{32}P]ATP).
7. The remaining lower, organic phase was then washed with 80 μl of methanol:1 M HCl (1:1, by volume).
8. After centrifugation, the upper phase was again discarded and the lower organic phase was transferred to a fresh tube.
9. The lipids were evaporated to dryness under vacuum in a Speed Vac (*see* Note 24).
10. Samples were either loaded immediately onto TLC plates and analyzed or stored overnight at –20°C under nitrogen (or other inert gas).

22.3.3 Lipid Analysis by TLC

1. Lipid products were routinely separated by TLC (*see* Note 25). Silica plates (silica gel 60, Merck) were impregnated by immersing them in 1 mM EDTA, 1% (w/v) oxalic acid, water:methanol (3:2, by volume) (*see* Note 26). The plates were allowed to dry for at least 1 h at room temperature and were activated for 15–30 min at 110°C in an oven before use (*see* Note 27).
2. The dried lipid reaction products were dissolved in 30 μl of chloroform: methanol (4:1, by volume) and spotted onto the pretreated silica plate (*see* Note 28). Lipid standards were also loaded at this time.
3. For assays using PtdIns as substrate, TLC plates were routinely developed in chloroform:methanol:4 M NH_4OH (9:7:2, by volume) (*see* Note 29).
4. When the solvent front has reached a suitable point (usually 1–2 cm from the top of the plate), the TLC plate is removed from the tank, the position of its front is marked with a pencil (*see* Note 30), and then it is placed in a fume hood to air-dry. Drying time can be increased by using a hair dryer at a low temperature setting (again in a fume hood).
5. Once the TLC plate is dry, the reaction products were visualized by exposing the TLC plates to autoradiography film overnight at room temperature; alternatively, the TLC plates were exposed to a phosphor screen for 2–6 h and the reaction products were quantified using a PhosphorImager (Molecular Dynamics) (*see* Note 31) (Fig. 22.1).
6. Standard lipids (*see* Note 32) were visualized by exposure to iodine vapor (*see* Note 33).

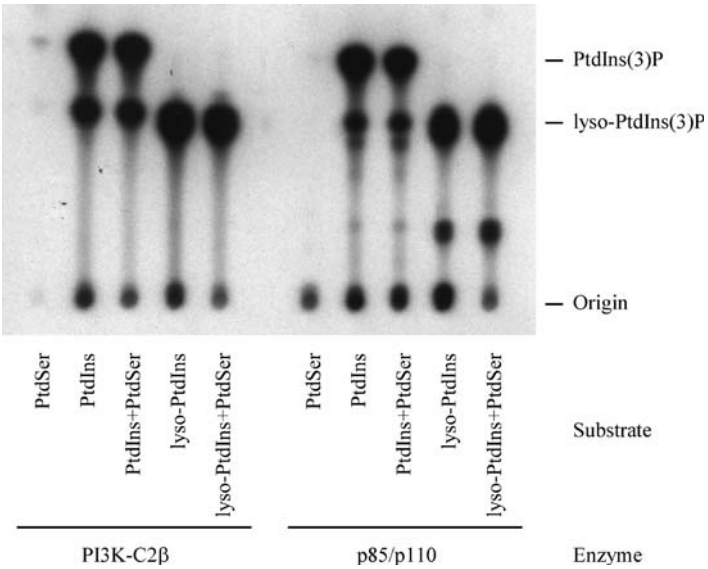

Fig. 22.1 PI 3-kinase assays performed with PtdIns and lyso-PtdIns as substrates resolved by TLC in a developing solution of chloroform:methanol:4 M NH_4OH. Control untransfected, and HA-tagged PI3 K-C2β transfected, HeLa cells were lysed and immunoprecipitations were carried out using anti-HA (clone 12CA5, Boehringer Mannheim) and anti-p85 antibodies (Upstate), respectively. The immune complexes were collected on protein A-Sepharose beads, washed, and then assayed for PI 3-kinase activity. Assays were performed in the presence of 5 mM $MgCl_2$ using PtdIns, lyso-PtdIns as substrates in the absence or presence of PtdSer (1:1 molar ratio) as a carrier. The phosphorylated lipids were resolved by TLC on silica gel plates in a developing solution of chloroform:methanol:4 M NH_4OH (9:7:2, by volume), and the labeled lipid spots were revealed by autoradiography. The radioactive material at the origin is likely to be residual ATP carried over during the extraction. Note the presence of a lipid species co-migrating with [^{32}P] lyso-PtdIns(3)*P* in the PtdIns assays. The identity of the additional radioactive spot in the p85/p110 assays using lyso-PtdIns as substrate remains unclear. It can be seen that in these assays the presence or absence of PtdSer carrier has little effect on the assay

22.3.4 Modifications of the Standard Assay to Distinguish Among the Different Classes of PI 3-Kinase That May Be Present

As noted earlier, while the preceding method is rapid and robust, it is not selective for any particular PI 3-kinase class or isoform, as they are all able to utilize PtdIns as a substrate. The following sections suggest simple inhibitor controls and modifications to the substrate and cations used in the assay that allow greater insight into the likely class of PI 3-kinase accounting for the activity under investigation.

22.3.4.1 Use of Inhibitors

While wortmannin and LY294002 are selective only for the PI 3-kinase family, and not for the individual isoforms, they can be used in control assays to confirm that the activity present is likely to be a PI 3-kinase. These inhibitors can be added to the cells for 30 minutes prior to cell lysis or can be added to the immune pellet at step 2 of Subheading 22.3.2.3, prior to the addition of lipids. Otherwise, the assay and TLC are carried out as described above. In parallel, a control assay can also be performed in the presence of 200 μM adenosine, which should significantly inhibit any contaminating type II PI 4-kinase activity without significantly affecting any PI 3-kinase activity present. Adenosine should be added at step 2 of Subheading 22.3.2.3, prior to the addition of lipids. Alternate TLC systems are available that can resolve PtdIns(3)*P* from PtdIns(4)*P* (*see* Note 34).

As already mentioned, a number of pharmaceutical companies are working on isoform-selective PI 3-kinase inhibitors [18,20,21]. It is likely that some of these will soon start making it into chemical catalogs and will complement the assays above and provide more insight into the isoform of PI 3-kinase present in an immunoprecipitate.

22.3.4.2 Use of Different Lipid Substrates in Assay

PtdIns tends to be the lipid of choice in PI 3-kinase assays for several reasons: (1) Historically, the first assays were carried out with this lipid when the kinase under study was assumed to be a PtdIns-specific kinase. (2) PtdIns is cheap compared with the more highly phosphorylated, lower-abundance PtdIns(4)*P* and PtdIns(4,5,)P_2. (3) The more highly phosphorylated lipids (PtdInsP_3 in particular; *see* Note 35) are more difficult to extract and handle and to resolve by simple TLC techniques. The use of PtdIns(4)*P* and PtdIns(4,5)P_2 as substrates can, however, shed light on the class of PI 3-kinase present. An activity that can utilize PtdIns(4,5)P_2 is strong evidence for the activity being from either class Ia or Ib, as neither the class II or class III PI 3-kinases can use this lipid effectively as a substrate (*see* Note 36). An activity that can utilize both PtdIns and PtdIns(4)*P*, but not PtdIns(4,5)P_2, is likely to belong to the class II family of PI 3-kinase. An activity that can only utilize PtdIns as a substrate is likely to be a class III enzyme (although care has to be taken here to exclude contaminating PI 4-kinase activities).

When utilizing more highly phosphorylated phosphoinositides as substrates, alternate TLC systems that provide better resolution, of PtdIns(3,4,5)P_3 in particular, are recommended (*see* Note 37) (Fig. 22.2).

22.3.4.3 Use of Different Cations in Assay

The use of 5–10 mM Mn^{2+} and Ca^{2+} ions, for Mg^{2+}, in the PtdIns substrate-based PI 3-kinase assay can also help to resolve the class of isoform present.

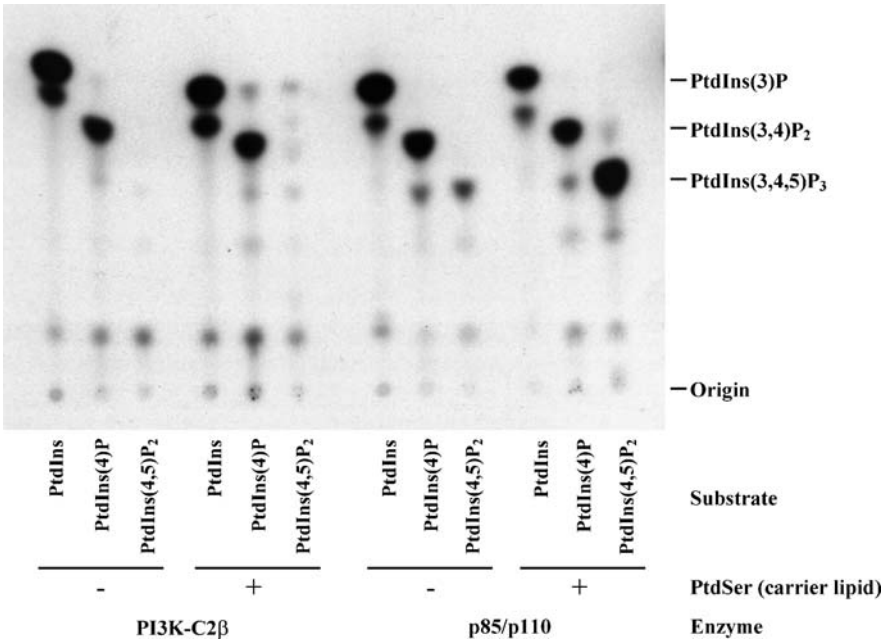

Fig. 22.2 Separation of PtdIns(3)*P*, PtdIns(3,4)P_2, and PtdIns(3,4,5)P_3 by TLC in *n*-propanol: acetic acid:water. Control untransfected, and HA-tagged PI3 K-C2β transfected, HeLa cells were lysed, and immunoprecipitations were carried out using anti-HA (clone 12CA5, Boehringer Mannheim) and anti-p85 antibodies (Upstate), respectively. The immune complexes were collected on protein A-Sepharose beads, washed, and then assayed for PI 3-kinase activity. Assays were performed in the presence of 5 mM $MgCl_2$ using PtdIns, PtdIns(4)*P*, or PtdIns(4,5)P_2 as substrates in the absence (−) or presence (+) of PtdSer (1:1 molar ratio) as a carrier. The phosphorylated lipids were resolved by TLC on silica gel plates in a developing solution of *n*-propanol:glacial acetic acid:water (64:2:33, by volume) and the radioactive spots were revealed by autoradiography. Note the greatly enhanced ability of the p85/p110 class Ia PI 3-kinase preparation to utilize PtdIns(4,5)P_2 as a substrate when presented together with PtdSer

Class I enzymes exhibit maximal activity when 5–10 mM Mg^{2+}/ATP is used, having only around 25% activity with 5–10 mM Mn^{2+}/ATP and <10% activity in the presence of Ca^{2+}/ATP. Class II PI 3-kinases show maximal activity in the presence of Ca^{2+}/ATP, with 60–70% activity with Mn^{2+}/ATP and 25–35% activity with Mg^{2+}/ATP [24, 25]. If PtdIns(4)*P* is used as a substrate, class II PI 3-kinases show a marked reduction in their activity toward this lipid in the presence of Ca^{2+}/ATP (the cation used has no effect on the inability of this class of PI 3-kinase to utilize PtdIns(4,5)P_2 as a substrate [24]). Class III PtdIns 3-kinases show maximal activity in the presence of Mn^{2+}/ATP, 60–70% activity with Mg^{2+}/ATP, and around 50% maximal activity with Ca^{2+}/ATP. To make use of these cations, calcium chloride or manganese chloride is substituted in place of magnesium chloride in the ATP mix solution at step 3 of Subheading 22.3.2.3.

Acknowledgments The author would like to thank both former colleagues and members of his laboratory for discussions over many years that have led to the formulation of these assays. Thanks also to Mike Lau for assistance in preparing the figures.

Notes

1. Wortmannin is a cell-permeable, irreversible inhibitor of PI 3-kinases. At concentrations between 1 and 100 nM, wortmannin is fairly selective for the PI 3-kinase superfamily, although it shows little selectivity for the individual isoforms. However, one problem with this inhibitor is that wortmannin is unstable in aqueous buffered solutions. This is particularly relevant when it is used in any cell-based assays. It has been reported that 90% of its inhibitory activity toward PI 3-kinase is lost after 3 h at 37°C in 20 mM Tris-HCl (pH 7.4) [26]. At 4°C the stability is much better. Its covalent mode of interaction through a lysine side chain when inhibiting PI 3-kinase suggests that wortmannin may also interact with other proteins, especially at pH > 8.0. Although wortmannin has been shown to interact with the PI 3-kinase via its ATP binding site, a number of reports suggest that it acts as a noncompetitive inhibitor with respect to ATP.
2. LY294002 is a cell-permeable, ATP-competitive, reversible inhibitor of PI 3-kinases. In the low-μM range, it shows good specificity for the PI 3-kinases over other kinase families, although, like wortmannin, it shows little selectivity for individual isoforms within the PI 3-kinase family. LY294002 is much more stable in aqueous solutions than wortmannin and, when used in cell-based assays, its effects can be observed for days without the need for readdition. However, as this inhibitor is reversible, extensive washings of immunoprecipitated PI 3-kinase preparations that have been inhibited *in vivo* can result in removal of the inhibitor and restoration of the kinase activity.
3. The lysis buffer composition varies depending upon the aim of the experiment, but this is a standard lysis buffer for looking at protein–protein interactions and for immunoprecipitating both protein and lipid kinases for *in vitro* assay. It is fairly gentle and works with most kinases.
4. All solutions are prepared with water that has a resistivity of 18.3 mΩ-cm and were filter-sterilized before use.
5. Vanadate must be in the correct valancy state for it to act as an effective inhibitor of protein-tyrosine phosphatases and phosphoinositide phosphatases. A 10 mM stock solution that is stable for long-term storage at −20°C and short-term storage at 4°C can be prepared as follows: (a) Weigh out the sodium orthovanadate and dissolve in approximately 70% of the final volume of water. (b) Bring the solution to a boil and then cool to room temperature. (c) Adjust the solution to pH 10. (d) Repeat steps a and c as necessary until the pH remains stable (at pH 10) and the solution remains clear (rather than turning yellow). (e) Adjust the solution to the final required volume. Filter-sterilize the solution and store in 50-ml and 10-ml aliquots at –20°C. The vanadate is now predominantly in the valency state, which most effectively inhibits phosphatase activities. Suggested working concentrations are 100–500 μM in lysis buffers. A 10-ml working aliquot may be stored at 4°C for several weeks. Yellowing of the solution on storage at 4°C, or the presence of a yellow precipitate, suggests that the solution is going bad. Discard and then thaw a fresh aliquot.
6. The use of Eppendorf brand microcentrifuge tubes is recommended for PI 3-kinase assays. Traditionally, lipid work is carried out in glass tubes, but this is not convenient for the assays described here. We have found that some brands of microcentrifuge tubes have coatings that are sensitive to organic solvents. This problem often only becomes apparent after loading the TLC plate, when a discolored residue can be observed at the point of sample loading at the origin. This tends to result in the aberrant migration of the

sample on the TLC plate. This problem has not been encountered when using Eppendorf brand microcentrifuge tubes.

7. Analar or better grade should be used for all TLC solvents.
8. Glass- or aluminum-backed TLC plates are also suitable for this assay. The glass-backed plates have the advantage of being more rigid and less prone to curling up upon heat activation and of "sagging" during chromatography.
9. Although many PI 3-kinase activities seem to be ubiquitous, the absolute amount of a given isoform present can vary dramatically between cells types. For example, the class II PI 3-kinase isoform, PI3 K-C2β, has been reported to be ubiquitously expressed, but we have found that it is not present in all cells and that, where it is present, the amount can vary 100-fold among cell types [24].
10. The length and exact conditions of serum deprivation required to bring cells to a state of quiescence will depend on the type of cell line under study and the particular stimulus to be employed. The method described has been used with NIH 3T3, 3T3-L1, COS-7, and HeLa cells and can be easily adapted for use with other cell types.
11. PMSF is highly unstable in aqueous solutions, with a lifetime of less than 30 minutes, and therefore should be added immediately before use.
12. For agonists acting through protein-tyrosine kinase receptors, stimulation times of between 5 and 15 minutes should capture activated or recruited PI 3-kinase.
13. It is important to keep everything cold from cell lysis through to the final assay, as some kinases are very fragile. In general, working on the bench in an ice bucket is fine. If in doubt, carry out all steps up to the kinase assay in a cold room.
14. Extensive washing of the immunoprecipitate at this stage is essential for two reasons. First, PI 3-kinases are inhibited by non-ionic detergents; thus, if not removed prior to assay, the detergents used for cell lysis will compromise the assay. Second, PI 4-kinases are strongly activated by non-ionic detergents. A type II PI 4-kinase activity predominates in whole cell extracts even in the absence of detergents and has been reported to associate nonspecifically with immunoprecipitates. Thus, if contaminating PI 4-kinase activity is not removed, it can mask an underlying PI 3-kinase activity or lead a researcher to believe that a PI 3-kinase activity is present where, in fact, it does not exist. On the widely used TLC systems, PtdIns(3)*P* does not resolve from PtdIns(4)*P*. This type II PI 4-kinase activity is inhibited by adenosine (K_i = 20 μM), whereas PI 3-kinases are resistant to adenosine, so this inhibitor should be used as a control to resolve contamination issues.
15. In many cases where a suitable Western blotting antibody is available for either the precipitated PI 3-kinase isoform or the associated protein, it is useful to split the immune pellet before the last wash step and take a fraction of the sample for SDS-PAGE and Western blotting. Removing one third to one half is usually sufficient for Western blotting, leaving one half to two thirds of the immunoprecipitate for the kinase assay.
16. It is important to ensure that the depth of solvent in the chromatography tank (1–2 cm) will be below the level of the origin line used for sample loading on the TLC plate. Extra care should be taken on this point when using plastic- or aluminum-backed TLC plates, as they can "sag" a little when placed in the tank.
17. It is important that the tank is allowed to saturate with mobile-phase vapor prior to chromatography. If the chamber is not saturated, the rising solvent will evaporate from the surface of the TLC plate, especially at the edges. This will result in "smiling" of the samples. This can be a greater problem where mixtures of solvents are used as the mobile phase, as in the case in the lipid separations described here, and in extreme cases this can lead to multiple solvent fronts developing. Solvents in tanks, especially when they are mixtures, should be replaced frequently, as their composition will likely change over time when one component is more volatile than the others. Monitoring the R*f* values (*see* Note 30) for various lipids over time will help keep track of how rapidly the solvent goes off.

18. While lipid vesicles composed solely of PtdIns tend to work fine in the assay described, this presents the lipid in a way far removed from the *in vivo* situation. Many labs have utilized various lipid mixtures with the phosphoinositide embedded in vesicles of carrier lipids such as PtdSer, PtdEth, and PtdCho. Where these have been used with PtdIns as a substrate, the two lipids are often combined in the final vesicles in a 1:1 molar ratio. PtdIns(4)*P* and PtdIns(4,5)P_2 in particular tend to work better as substrates when mixed with carrier lipids and have been used at molar ratios of substrate to carrier ranging from 1:4 to 1:10, with final concentrations of PtdIns(4,5)P_2 ranging from 50 μM to 250 μM (Fig. 22.2). There is no clear standard for which mixtures work best. An alternative to the use of carrier lipid is cholate [23] (*see* Note 36).
19. Care should be taken when preparing lipid stock solutions. When gauging the output of your sonicator, it is best to treat the lipid in short, 30-second bursts until the optimum time for vesicle production is identified. Oversonication will result in oxidized lipids. Probe-type sonicators are also suitable for preparing lipid vesicles, but extreme care should be taken, as it is very easy to oversonicate with these devices. Sonicate the lipids on ice with short (5-second) bursts until the solution clears, keeping a close watch on the temperature of the lipids.
20. Five to 10 μl of whole cell lysate can be used as a suitable positive control for the PI kinase assay. The whole cell lysate contains highly active PI 4-kinase due to the presence of the non-ionic detergent in the lysis buffer (and little or no PtdIns 3-kinase activity due to the inhibitory effects of this detergent on PI 3-kinases). In the standard assay, the ^{32}P-labeled PtdIns(4)*P* produced allows the likely position of any PtdIns(X)*P*s on the TLC plate to be pinpointed after sample separation. When running other TLC systems that can resolve PtdIns(3)*P* from PtdIns(4)*P*, then it will allow a clear distinction to be made as to whether the activity under investigation is a PI 3-kinase or not. Recombinant purified PI 3-kinases (Alexis Biochemicals—bovine p110α/p85 and human p110γ) can also be purchased if control PI 3-kinase activity [or a [^{32}P]-labeled PtdIns(3)*P*] standard is required.
21. If you are aiming to carry out kinetic analysis on your PI 3-kinase, then you will need to have an accurate stock of ATP. The following method describes how to produce such a solution. 100 mM ATP stock (10 ml): Dissolve 0.66 g of ATP in 3–4 ml of water. Extra weight allows for hydrated ATP species (MW ATP anhydrous = 515.2). Adjust the pH to 7.5 with NaOH. OD_{259} ATP = 15.4 = 1 mM, 1,540 = 100 mM. Dilute 10 μl 1:10^4. Read OD_{259}. Using $C_1V_1 = C_2V_2$ (C = molar concentration, V = volume in ml), calculate the additional amount of water to dilute solution to 100 mM. Dispense in 1-ml aliquots in sterile 1.5-ml Eppendorf tubes and store at −20°C.
22. Depending on the amount and activity of the PI 3-kinase under investigation, you may want to use anywhere between 0.5 and 20 μCi of [^{32}P]ATP per assay point.
23. Phosphoinositides should be exposed to acidic and basic solvents for as short a time as possible, as they are prone to hydrolysis. If this precaution is taken, then the concentrations of such solvents used herein will not cause significant degradation of these lipids.
24. If a rotating Speed Vac is not available, then an alternative is to dry the lipids down under a nitrogen gas stream.
25. While TLC provides a simple way to analyze phosphorylated lipids, it is difficult to unequivocally determine the identity of a species by this approach. In particular, on most TLC systems, PtdIns(3)*P*, PtdIns(4)*P*, and PtdIns(5)*P* run at the same position. Currently, the most widely used methodology for defining the identity of a given phosphorylated inositol lipid is by use of HPLC (*see* Chapter 3). In the future, mass spectrometry may provide an alternative, but currently, lipid analysis by this approach is restricted to a few laboratories.
26. TLC plates should be wetted in a single flowing movement. If a plate does not wet evenly, or regions of the plate fail to wet, then it should be discarded. TLC plates often contain calcium sulfate as a binder. Inositol phospholipids bind strongly to calcium; if this is not prevented by oxalate treatment, the migration of the lipids will be retarded.

27. After dipping the plates in the oxalic acid solution, the plates are allowed to air-dry for 15 minutes. They are then transferred to an oven preset to 110°C and baked for 30 minutes to activate the silica gel. For the best reproducibility, it is important that the baking time and temperature used are consistent between experiments and that the plates are loaded immediately. Silica gel will rapidly deactivate in a moist atmosphere. If plates are not to be used immediately, they should be stored in a dessiccator.
28. It is important to take appropriate care when loading your samples to achieve the best possible results. The width of a clear 12-in. ruler (~3–3.5 cm) provides a suitable loading guide for placing the origin above the base of the TLC plate. Solvent depth should be around 1–2 cm. Alternatively, a TLC spotting guide designed for this purpose can be used. Samples can be applied to the plate as either discrete spots or linear bands along the origin. Space samples evenly across the origin, leaving ~1 cm between samples. Loading can be achieved using either a Hamilton syringe or a Gilson pipette (P2, P10, or P20). The sample should be applied a few μl (1–5) at a time, allowing the sample time to dry between repeat applications. This can be aided using a hairdryer at low temperature (take care not to evaporate off any unloaded sample). It is important not to scrape, or scratch, the adsorbent layer of the TLC plate when loading the sample, as this will cause the mobile phase to elute unevenly, resulting in spot distortion. Loading too much sample will cause tailing of the sample after chromatography. Not allowing the sample to dry between applications will cause spreading of the sample, and rings of sample may be apparent after separation.
29. This buffer system is suitable for resolving PtdIns(X)*P* from PtdIns and PtdIns(4,5)P_2, but is not good for separating PtdIns(3)*P* from PtdIns(4)*P* (*see* Notes 34 and 36).
30. R*f* values can be derived for lipid standards and for unknowns. The R*f* value for a given sample component is given by

$$\frac{\text{distance migrated by sample component}}{\text{distance migrated by solvent front}}.$$

These R*f* values are affected by a number of variables, including the saturation of the chamber with solvent vapor, quality and quantity of the mobile phase, plate activity, and chromatographic technique and conditions. These values are thus not absolutes but are worth monitoring as they will give a good indication as to the reproducibility of your methodology and when problems may occur.
31. The identity of the radioactive spots as lipids can be confirmed by scraping them from the first plate and then deacylating the lipids. Lipids were deacylated by the method of Clarke and Dawson [27]. A 0.75-ml aliquot of monomethylamine [33% (v/v) in industrial methylated spirits]:methanol:*n*-butanol (50:15:5 by volume) was added to either silica scrapings from TLC or dried lipids, and the mixture was incubated at 53°C for 50 minutes. Reactions were stopped on ice and the samples dried *in vacuo* prior to the addition of 1 ml of water and 1.2 ml of *n*-butanol:light petroleum:ethyl formate (20:40:1, by volume). After phase separation, the lower phase was washed with a further 1.2 ml of the butanol mixture prior to the addition of 100 μl of 50 mM mannitol (Sigma) and then was freeze-dried *in vacuo*. These deacylated products can be analyzed either by HPLC (*see* Chapter 3) or by a second TLC of the deacylated material on DEAE-cellulose plates (Whatman) in 250 mM KH_2PO_4 (pH 3.0, adjusted with phosphoric acid). Make sure that the chamber atmosphere is saturated prior to run. 3 MM paper on three sides is best. Run the plate until solvent front is approximately 2 cm from top (for a 20-cm plate), which takes approximately 2 h. Deacylated PtdInsP_3 runs approximately 2 cm from origin. ATP migrates further.
32. It is a good idea to run lipid standards on all TLC plates to aid in identifying spots, as depending on the source and care taken with lipids, there may be a number of species

present on the TLC plate. Commonly observed breakdown products are lyso-phospholipid forms of the lipids in use (which can be used as substrates by PI 3-kinases) [24]. These usually run slower than the intact inositol phospholipids and thus may be confused with more highly phosphorylated species. The majority of the substrate will usually not be converted, so this will provide one standard across the plate. The amounts of this present can be useful for judging the reproducibility of lipid extraction. The use of a standard for the product of the kinase reaction is also recommended. If the assay is with PtdIns as substrate, then PtdIns(4)*P* is usually a suitable standard, as this co-migrates with PtdIns(3)*P* in most commonly used TLC systems for phospholipids. As a cheaper alternative to highly purified individual phosphoinositide species, a mixed phosphoinositide fraction containing PtdIns, PtdIns(4)*P*, and PtdIns(4,5)P_2 can be used.

33. Iodine provides a simple, nondestructive method for identifying the migration position of the lipid substrate and of any lipid standards. A chromatography tank is set up with a few crystals of iodine in the bottom. Warming the tank will cause the iodine to vaporize. When the TLC plate is placed in the tank, the iodine reveals the lipids as yellow/brown spots of varying intensity and color. Upon removing the plate from the tank, the outline of the spots should be marked with a soft pencil, as the color will be rapidly lost within about 30 minutes. It is recommended that the plate is placed in a fume hood to allow the iodine to be removed.
34. **TLC method for separation of PtdIns(3)*P* from PtdIns(4)*P* [28].** (a) 35 ml of methanol, 32 ml of chloroform, and 24 ml of pyridine were mixed in a bottle. (All steps were carried out in a fume hood to avoid exposure to the harmful pyridine fumes.) Then 6.3 g of boric acid were added and the bottle was shaken occasionally until this completely dissolved (this can take some time). Next, 4 ml of water and 1.6 ml of concentrated formic acid were added and the solution was transferred into the developing tank. (b) 0.9 g of CDTA was dissolved in 30 ml of 0.33 M NaOH. Once the CDTA was dissolved, 60 ml of ethanol were added. Silica plates were dipped face down in the CDTA solution. Excess liquid was allowed to drain, and then the plates were air-dried in a fume hood. Immediately prior to use, the plates were activated for 30 minutes at 110°C. Once the plates were cool, lipids were spotted as described earlier. (c) Development of the TLC plates was performed in a saturated tank lined with 3 MM paper. Development was stopped when the solvent front was 2 cm from the top of the plate. Plates were left for 2–3 h to air-dry in the fume hood prior to autoradiography or PhosphorImaging. Iodine detection of the separated lipids is not possible mainly due to the pyridine on the plate. In this TLC system, PtdIns(4)*P* migrates with an R*f* of 0.46 and PtdIns(3)*P* migrates slightly faster, with an R*f* of 0.51 [28]. Although the two lipids do separate, it is advisable to routinely use PtdIns(4)*P* and PtdIns(3)*P* standards when using this TLC system.
35. It has been suggested that the class II enzyme PI3 K-C2α has a weak activity toward PtdIns(4,5)P_2 when presented in mixed vesicles with PtdSer [19]. The identity of this spot was not confirmed by HPLC and so remains uncertain. In our hands, the class II PI 3-kinase, PI3 K-C2β, shows no significant activity toward PtdIns(4,5)P_2 [24].
36. **Modifications to PI 3-kinase assay when using PtdIns(4,5)P_2 as a substrate.** There are few published methods for the quantitative analysis of PtdInsP_3. Our basic assay is as described in Domin et al. [19]. Prepare PtdIns(4,5)P_2 at 2 mg/ml by sonication in 50 mM HEPES (pH 8.0), 2.5% (w/v) cholate (sodium salt). The cholate seems to improve presentation of the substrate [23, 24]. Use 10 µl of this PtdInsP_2 preparation in a 50-µl assay instead of the PtdIns. Lipid extractions are carried out as described except that it is a good idea to back-extract the first discarded aqueous layer with 200 µl of fresh $CHCl_3$:MeOH (1:1, by volume). The resultant $CHCl_3$ phase from this extraction is then pooled with the first $CHCl_3$ phase. This is done because PtdInsP_3 is highly polar and tends to be lost into the aqueous phase. It is very difficult to get good quantitative extractions of PtdInsP_3. Note, however, that you need to take care with these extractions, as ATP migrates on the TLC plate in most systems very close to the

PtdInsP_3. Some batches of [^{32}P]ATP may also contain impurities, which will resolve near the origin on the TLC systems described. If unexpected radioactive spots are observed near the origin, then a control extraction of just the [^{32}P]ATP mix in the kinase buffer can be performed to identify any radioactive species that may originate in the ATP solution. The identity of the radioactive spots as lipids can be confirmed by scraping them from the first plate, deacylating the lipids (*see* Note 30), and then performing HPLC (*see* Chapter 3) or a second TLC of the deacylated material on DEAE-cellulose plates (Whatman) (*see* Note 30).

37. **TLC system when using PtdIns(X)*P* or PtdIns(4,5)P_2 as substrate for separation of PtdIns*P*, PtdInsP_2, and PtdInsP_3.** Developing solution: *n*-propanol:glacial acetic acid:-water (64:2:33 by volume). Silica gel 60 plates (Merck) were dipped in 1% (w/v) oxalic acid, 1 mM EDTA in water:methanol (3:2, by volume) and allowed to air-dry. Immediately prior to use, the plates were heat-activated in an oven at 110°C for 30 minutes. TLC plates were spotted and run as described for a standard TLC system. Running time is 4–5 h. Note that this buffer system is not good for separating PtdIns(3)*P* from PtdIns(4)*P*.

References

1. Sugimoto Y, Whitman M, Cantley LC, Erikson RL. Evidence that the Rous sarcoma virus transforming gene product phosphorylates phosphatidylinositol and diacylglycerol. Proc Natl Acad Sci USA 1984;81:2117–21.
2. Macara IG, Marinetti GV, Balduzzi PC. Transforming protein of avian sarcoma virus UR2 is associated with phosphatidylinositol kinase activity: Possible role in tumorigenesis. Proc Natl Acad Sci USA 1984;81:2728–32.
3. Whitman M, Kaplan DR, Schaffhausen B, Cantley L, Roberts TM. Association of phosphatidylinositol kinase activity with polyoma middle-T competent for transformation. Nature 1985;315:239–342.
4. Fry MJ, Gebhardt A, Parker PJ, Foulkes JG. PI turnover and transformation of cells by Abelson murine leukaemia virus. EMBO J 1985;4:3173–8.
5. Whitman M, Downes CP, Keeler M, Keller T, Cantley L. Type I phosphatidylinositol kinase makes a novel inositol phospholipid, phosphatidylinositol-3-phosphate. Nature 1988;332:644–6.
6. Fry MJ. Structure, regulation and functional of phosphoinositide 3-kinases. Biochim Biophys Acta 1994;1226:237–68.
7. Rameh LE, Cantley LC. The role of phosphoinositide 3-kinase lipid products in cell function. J Biol Chem 1999;274:8347–50.
8. Katso R, Okkenhaug K, Ahmadi K, White S, Timms J, Waterfield MD. Cellular functions of phosphoinositide 3-kinases: Implications for development, homeostasis, and cancer. Ann Rev Cell Dev Biol 2001;17:615–75.
9. Foster FM, Traer CJ, Abraham SM, Fry MJ. The phosphoinositide (PI) 3-kinase family. J Cell Sci 2003;116:3037–40.
10. Arcaro A, Wymann MP. Wortmannin is a potent phosphatidylinositol 3-kinase inhibitor: The role of phosphatidylinositol3,4,5-trisphosphate in neutrophil responses. Biochem J 1993;296:297–301.
11. Vlahos CJ, Matter WF, Hui KY, Brown RF. A specific inhibitor of phosphatidylinositol 3-kinase, 2-(4-morpholinyl)-8-phenyl-4 H-1-benzopyran-4-1 (LY294002). J Biol Chem 1994;269:5241–8.
12. Domin J, Waterfield MD. Using structure to define the function of phosphoinositide 3-kinase family members. FEBS Lett 1997;410:91–5.

13. Kastan MB, Lim DS. The many substrates and functions of ATM. Nat Rev Mol Cell Biol 2000;1:179–86.
14. Dann SG, Thomas G. The amino acid sensitive TOR pathway from yeast to mammals. FEBS Lett 2006;580:2821–9.
15. Traer CJ, Foster FM, Abraham SM, Fry MJ. Are class II phosphoinositide 3-kinases potential targets for anticancer therapies? Bull Cancer 2006;93:E53–8.
16. Maffucci T, Cooke FT, Foster FM, Traer CJ, Fry MJ, Falasca M. Class II phosphoinositide 3-kinase defines a novel signaling pathway in cell migration. J Cell Biol 2005;169:789–99.
17. Stack JH, Emr SD. Vps34p required for yeast vacuolar protein sorting is a multiple specificity kinase that exhibits both protein kinase and phosphatidylinositol-specific PI 3-kinase activities. J Biol Chem 1994;269:31552–62.
18. Knight ZA, Gonzalez B, Feldman ME, Zunder ER, Goldenberg DD, Williams O, Loewith R, Stokoe D, Balla A, Toth B, Balla T, Weiss WA, Williams RL, Shokat KM. A pharmacological map of the PI3-kinase family defines a role for p110α in insulin signalling. Cell 2006;125:733–47.
19. Domin J, Pages F, Volinia S, Rittenhouse SE, Zvelebil MJ, Stein RC, Waterfield MD. Cloning of a human phosphoinositide 3-kinase with a C2 domain that displays reduced sensitivity to the inhibitor wortmannin. Biochem J 1997;326:139–47.
20. Ward S, Sotsios Y, Dowden J, Bruce I, Finan P. Therapeutic potential of phosphoinositide 3-kinase inhibitors. Chem Biol 2003;10:207–13.
21. Workman P. Inhibiting the phosphoinositide 3-kinase pathway for cancer treatment. Biochem Soc Trans 2004;32:393–6.
22. Whitman M, Kaplan D, Roberts T, Cantley L. Evidence for two distinct phosphatidylinositol kinases in fibroblasts. Implications for cellular regulation. Biochem J 1987;247:165–74.
23. Woscholski R, Kodaki T, Palmer RH, Waterfield MD, Parker PJ. Modulation of the substrate specificity of the mammalian phosphatidylinositol 3-kinase by cholesterol sulfate and sulfatide. Biochemistry 1995;34:11489–93.
24. Lau MR. Characterisation of the class II phosphoinositide 3-kinase, PI3 K-C2β. Ph.D. thesis, University of London; 2000.
25. Arcaro A, Volinia S, Zvelebil MJ, Stein R, Watton SJ, Layton MJ, Gout I, Ahmadi K, Downward J, Waterfield MD. Human phosphoinositide 3-kinase C2β, the role of calcium and the C2 domain in enzyme activity. J Biol Chem 1998;273:33082–90.
26. Woscholski R, Kodaki T, McKinnom M, Waterfield MD, Parker PJ. A comparison of demethoxyviridin and wortmannin as inhibitors of phosphatidylinositol 3-kinase. FEBS Lett 1994;342:109–14.
27. Clarke NG, Dawson RMC. Alkaline *O* -> *N*-transacylation. A new method for the quantitative deacylation of phospholipids. Biochem J 1981;195:301–6.
28. Walsh JP, Caldwell KK, Majerus PW. Formation of phosphatidylinositol 3-phosphate by isomerisation from phosphatidylinositol 4-phosphate. Proc Natl Acad Sci 1991; 88:9164–87.

Chapter 23
Measurement of Phosphatidylinositol and Phosphatidylcholine Binding and Transfer Activity of the Lipid Transport Protein PITP

Shamshad Cockcroft

Abstract Mammalian cells have evolved proteins that can extract single lipids from membranes and sequester them in their hydrophobic cavity. These proteins, collectively known as lipid transport proteins, play essential roles in many aspects of lipid metabolism, lipid signaling, and membrane traffic. Phosphatidylinositol transfer proteins (α and β) are lipid transport proteins that specifically bind phosphatidylinositol or phosphatidylcholine in their hydrophobic cavity and facilitate their transfer from one membrane compartment to another. In addition, PITPβ can facilitate sphingomyelin transfer. This chapter describes methods to monitor the transfer and binding activity of PITPs using a variety of assays, including an assay that uses microsomes as a donor and liposomes as an acceptor of PtdIns. For phosphatidylcholine and sphingomyelin transfer, liposomes are used as a donor compartment and mitochondria as an acceptor compartment. A separate method describes the use of permeabilized cells as a source of donor lipids and liposomes as an acceptor membrane. In addition to lipid transfer, methods to identify the lipids that occupy the hydrophobic cavity of PITPs are discussed.

KeyWords Phosphatidylinositol · phosphatidylcholine · phospholipid transfer proteins · phosphatidylinositol transfer proteins · liposomes · microsomes · lipid binding

Abbreviations PtdIns: Phosphatidylinositol; PtdCho: Phosphatidylcholine; SM: Sphingomyelin; PITP: Phosphatidylinositol transfer proteins; LTP: Lipid transfer proteins; PtdOH: Phosphatidic acid; PtdEth: Phosphatidylethanolamine.

S. Cockcroft
Department of Physiology, Rockefeller Building, University College London, London WC1 E 6JJ, UK
e-mail: S.Cockcroft@ucl.ac.uk

B. Larijani et al. (eds.), *Lipid Signaling Protocols*, DOI: 10.1007/978-1-60327-115-8_23,

23.1 Introduction

Lipid synthesis in cells is confined to specific membrane compartments (mainly the endoplasmic reticulum) and, thus, proteins have evolved that can facilitate the movement of individual lipids; these proteins are described as lipid transport (or transfer) proteins (LTPs). LTPs can be divided into different families based on both specificity for the cargo lipid and homology in amino acid sequence. The families of LTPs that can transfer specifically phosphatidylinositol are proteins that contain the PITP domain.

Phosphoinositides comprise the most interesting family of lipids where phosphatidylinositol, the parent lipid, is the source of seven phosphorylated phosphoinositides, all of which have defined functions in cells. Phosphatidylinositol transfer proteins (PITPs) were originally isolated based on their ability to transport phosphatidylinositol [1]. In the human genome, two highly related PITPs (PITPα and PITPβ) have been identified; both have been implicated in a variety of cellular functions, including signaling cascades mediated by phospholipase C and phosphoinositide 3-kinase and in membrane traffic [2, 3]. This chapter discusses methods to study the lipid binding and transport properties of PITPs using a variety of approaches. These methods can be adapted for the study of lipid transport by other LTPs.

Monitoring the lipid transfer activity of LTPs is based on two separate membrane compartments: One compartment contains a radiolabeled lipid of interest (the donor compartment), while a second compartment constitutes the acceptor compartment (Fig. 23.1). Important parameters that can influence the amount of lipid transferred are the lipid composition and the membrane curvature of both membrane compartments. Both parameters can be manipulated *in vitro*. The source of the proteins to be analyzed can be bacterially expressed recombinant proteins or crude cytosol. In addition, PITPs can be expressed in cells (e.g., COS cells) and the cytosolic fractions can be compared to analyze the lipid transfer function of the expressed proteins.

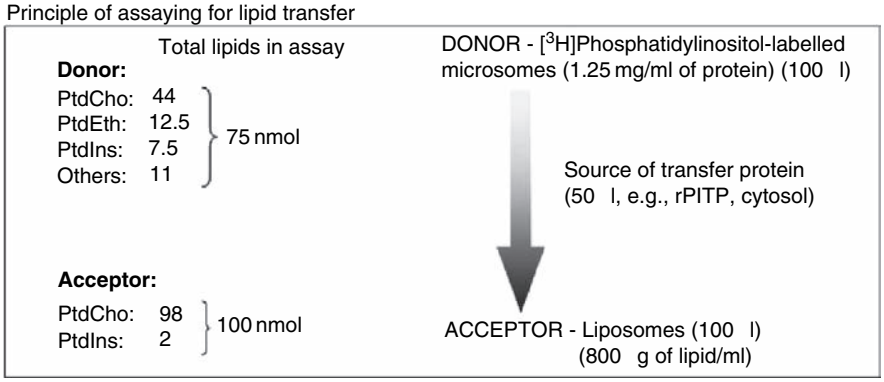

Fig. 23.1 Scheme illustrating the basic method used to measure PtdIns transfer using the microsome-liposome assay

The structures of many LTPs have been solved, and from this information a mechanism for lipid transfer has emerged. An LTP is characterized by a hydrophobic cavity that can be occupied by a single lipid [4–6]. The entrance to the cavity is closed by an amino acid sequence acting as a "lid," thus shielding the transported lipid from the aqueous phase. To gain entrance to the cavity, the "lid" swings outwards, exposing the lipid—this structural transition takes place at the membrane interface where the loading and unloading of the lipid occur. PITPα and PITPβ can bind to a single molecule of either phosphatidylinositol (PtdIns) or phosphatidylcholine (PtdCho) in their hydrophobic cavity and thus facilitate the transfer of either lipid. In addition, PITPβ can also transport sphingomyelin (SM) to a limited extent [7–9]. Whether this is physiologically relevant is not clear, as SM concentrations that are exposed to the cytosolic compartment are extremely low.

Methods to measure PtdIns transfer from a PtdIns-radiolabeled microsomal preparation or permeabilized HL60 cells (comprising the donor compartment) to chemically defined acceptor liposomes are described below. The endogenous PtdIns in the microsomal compartment can be easily labeled with [^{3}H]inositol, as the PtdIns synthase enzyme can work in a reverse fashion in the presence of manganese chloride [10]. The donor compartment is easily removed by aggregation of the proteins at pH 5, and radioactive PtdIns transferred to the liposome compartment can be measured. However, the transport protein is unlikely to discriminate the membrane compartments; therefore, transport from microsome to microsome or liposome to liposome cannot be avoided. Finally, as more of the radiolabeled lipid accumulates in the donor compartment, it too will be moved back to the microsomes or to another liposome. In practice, it is best to work under conditions where no more than 10–20% of the lipid will be transferred from the donor compartment to the acceptor compartment. This can be achieved by manipulating the time of incubation and the amount of the lipid transporter added to the system (Fig. 23.2a, b).

For measurement of PtdCho transport, chemically defined liposomes containing the radiolabeled lipid are used as the donor compartment and mitochondria as the acceptor compartment. This assay can be easily modified

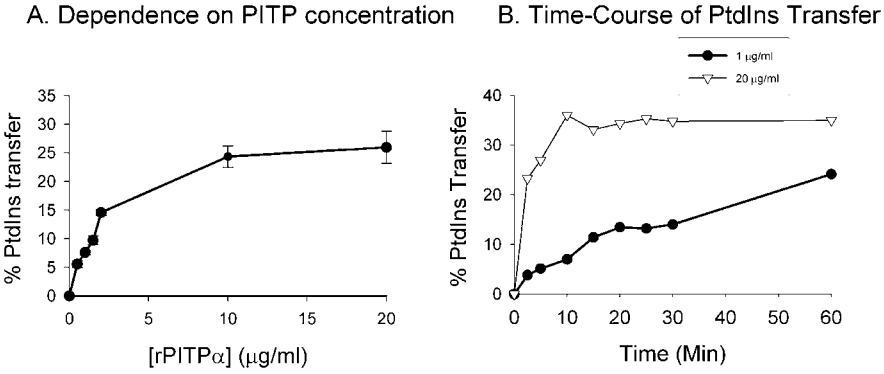

Fig. 23.2 (a) PtdIns transfer using different concentrations of recombinant PITPα. (b) Time-course of PtdIns transfer with two different concentrations of PITPα

to measure the transport of other lipids such as sphingomyelin [8]. In this case, the acceptor compartment, i.e., mitochondria, is separated from the liposomes to assess transfer; this requires more steps compared to the microsome-liposome assay. A simpler method where the PtdCho pool of the microsomes can be labeled with [^{3}H]choline is not enzymatically possible *in vitro*.

The assays for PtdIns and PtdCho transport described above are not directly comparable, and, under some circumstances, it is necessary to use the same donor and acceptor compartments to monitor the transfer activity of both lipids (*see* Note 1). With that in mind, an assay using cytosol-depleted HL60 cells as a donor compartment and liposomes as an acceptor compartment is described [5, 7]. Another parameter that can also be measured is preference for the lipids that can bind in the hydrophobic cavity of PITPs. His-tagged PITPs are added to cytosol-depleted HL60 cells and the proteins are allowed to exchange their bound lipids with the lipid of their choice from the permeabilized cells. The His-tagged proteins are purified and the lipids associated with the protein can be analyzed by TLC or mass spectrometry [5, 8, 11].

23.2 Materials

23.2.1 Assay for PtdIns or PtdCho Transfer Activity

1. PtdIns, PtdCho, phosphatidic acid (PtdOH), and phosphatidylethanolamine (PtdEth) are made as chloroform solutions at 10–20 mg/ml and stored at −20°C in a tight glass-stoppered tube (*see* Note 2).
2. Myo[2-^{3}H]inositol can be obtained from GE Healthcare (Cat. no. TRK317).
3. Sonicator (any model).
4. Rat liver microsomes with their endogenous PtdIns prelabeled with [^{3}H]inositol.
5. Buffers required for making the rat liver microsomes:

   Buffer A: 50 mM Tris-HCl, 2 mM $MnCl_2$, pH 7.4;
   Buffer B: 1 mM Tris-HCl, 2 mM inositol, pH 8.6;
   Buffer C: 10 mM-Tris-HCl, 2 mM inositol, pH 8.6.

6. Cytosol or recombinant proteins as a source of PITP.
7. SET buffer: 0.25 M sucrose, 1 mM EDTA, and 10 mM Tris-HCl, pH 7.4 (*see* Note 3).
8. Rat liver mitochondria.
9. Solution to aggregate microsomes: 0.25 M sodium acetate in 0.25 M sucrose, pH 5.

23.2.2 Assay for PtdIns or PtdCho Transfer Activity and Lipid Binding Using Permeabilized HL60 Cells

1. Streptolysin O (*see* Note 4).
2. PIPES buffer: 20 mM Na-PIPES, 137 mM NaCl, 2.7 mM KCl, 2 mM $MgCl_2$, pH 6.8.

3. Permeabilization buffer: PIPES buffer supplemented with glucose, 1 mg/ml (5.6 mM), and bovine serum albumin (0.1 mg/ml).
4. MgATP made up as a stock solution of 100 mM and kept at −20°C (*see* Note 5).
5. HL60 cells can be obtained from American Type Culture Collection (ATCC).
6. [2-^{14}C]acetate from Perkin Elmer Life Sciences and kept sterile.
7. [*Methyl*-^{3}H]choline (1 mCi/ml in ethanol) purchased from GE Healthcare (Cat. no. TRK593) and kept sterile.
8. Myo [2-^{3}H]inositol from GE Healthcare (Cat. no. TRK317) and kept sterile.
9. Sphingomyelin, [choline-methyl-^{14}C] obtained from Perkin Elmer Life Sciences.
10. Phosphatidylcholine, [choline-N-methyl-^{3}H] 1,2-dipalmitoyl purchased from GE Healthcare.
11. RPMI-1640 and Medium 199 (M199) from Sigma-Aldrich.
12. Heat-inactivated fetal calf serum (FCS) from any reliable source.
13. Penicillin/streptomycin (Sigma Cat. no. P-0906) and glutamine solution (Sigma Cat. no. G-7513).
14. HIS-Select^{TM} Nickel Affinity Gel (25 ml) (Sigma Cat. no. P 6611).
15. Spin filters and collection tubes (Thermo Fisher Scientific Inc. Pierce Spin cups - paper filter Product No. 69700).

23.3 Methods

The methods outlined in this chapter include the following:

1. preparation of [^{3}H]inositol-labeled microsomes from rat liver,
2. assay for PtdIns transfer activity using [^{3}H]inositol-labeled microsomes as a donor compartment and liposomes as an acceptor,
3. preparation of mitochondria,
4. assay for PtdCho and SM transfer activity using liposomes as donor and mitochondria as acceptor compartment *in vitro,*
5. assay for PtdIns and PtdCho transfer activity using cytosol-depleted HL60 cells as a donor compartment and liposomes as acceptor,
6. assay for PtdIns and PtdCho binding using cytosol-depleted HL60 cells as a source of lipids.

23.3.1 Preparation of [^{3}H]Inositol-Labeled Microsomes from Rat Liver

1. All manipulations are carried out on ice and solutions are maintained at 4°C unless stated otherwise.
2. Three rat livers are homogenized at 4°C in a Waring blender in 150 ml of SET buffer.

3. The homogenate is further homogenized in a motor-driven glass homogenizer with a Teflon pestle (15 strokes are sufficient).
4. The homogenate is centrifuged for 5 min at 3,000 rpm (2,000 × *g*) at 4°C to sediment unbroken cells.
5. The supernatant is retained and centrifuged for 15 min at 7,500 rpm (10,000 × *g*) at 4°C to pellet the mitochondria (*see* Note 6).
6. The supernatant is centrifuged at 100,000 × *g* for 1 h at 4°C to pellet the microsomes.
7. The microsomal pellet is resuspended in 40 ml of buffer A (e.g., 50 mM Tris-HCl, 2 mM $MnCl_2$, pH 7.4) and rehomogenized in a glass homogenizer (*see* Note 7).
8. 300 μCi of [^{3}H]inositol are added and the microsomes are incubated for 1.5 h at 37°C. The sample is then left overnight at 4°C (can be left over the weekend, if required).
9. The microsomes are centrifuged at 100,000 × *g* in an ultracentrifuge for 90 min at 4°C.
10. The pellet is resuspended in 100 ml of buffer B (e.g., 1 mM Tris-HCl, 2 mM inositol, pH 8.6).
11. After centrifugation, the microsomes are resuspended in 100 ml of buffer C (e.g., 10 mM Tris-HCl, 2 mM inositol, pH 8.6) and centrifuged at 100,000 × *g* (43 K in an ultracentrifuge) for 90 min at 4°C.
12. The microsomal pellet is resuspended in 20 ml of SET buffer and the protein concentration adjusted to 15–25 mg/ml.
13. A 10-μl aliquot is counted for radioactivity. Anticipate 50 μl to contain 10^5 dpm in PtdIns.
14. The microsomes are frozen in 0.5-ml aliquots and stored at −80°C until required.
15. Microsomes prepared from rat liver contain approximately 600 nmol phospholipids per mg protein; of this, PtdCho accounts for 350 nmol, PtdEth accounts for 100 nmol, and PtdIns accounts for 60 nmol (i.e., 10% of the total phospholipid pool) [12]. Therefore, the specific activity of PtdIns can be calculated from the amount of radioactivity present per mg of protein.

23.3.2 Assay for PtdIns Transfer Activity

The assay described is a modification of previously established assays [1, 13]. To monitor PtdIns transfer, the final assay volume is 250 μl:

100 μl of microsomes (125 μg of microsomal protein; 1.25 mg/ml);
100 μl of liposomes (100 nmol of lipids; 80 μg of lipid; 1 μmol/ml);
50 μl of material to be assayed for transfer activity.

The ratio of microsomal lipid to liposomes is 75 nmol/100 nmol, and the actual amount of PtdIns in the two membranes is 7.5 nmol (microsomes) and

2 nmol (liposomes). Thus, transfer is favorable from microsomes to liposomes initially (Fig. 23.1).

Assay procedure for analysis of 50 samples:

1. All procedures are carried out at 4°C unless stated otherwise.
2. The microsomes are diluted in 6 ml of the SET buffer to obtain a protein concentration of 1.25 mg/ml (dpm in 100 µl of microsomes should be about 50,000–100,000 dpm).
3. Liposomes (98:2; PtdCho:PtdIns) are freshly prepared by mixing stock solutions of PtdCho (100 mg/ml) and PtdIns (25 mg/ml) in a glass tube or a chloroform-resistant plastic tube. To prepare 6 ml of liposomes, add 47 µl of PtdCho (stock solution 100 mg/ml) and 4 µl of PtdIns (stock solution of PtdIns, 25 mg/ml).
4. The lipids are dried down by evaporation of the chloroform under nitrogen.
5. 6 ml of the SET buffer are added to the dried film of lipid.
6. Sonicate on low at amplitude 1, until the lipids go into solution (3 × 15 s). The solution will become slightly cloudy. (The concentration of the total lipids in the liposomes is 800 µg/ml, which comprises 784 µg of PtdCho and 16 µg of PtdIns per ml.)
7. Mix equal volumes of liposomes (6 ml) with the microsomes (6 ml).
8. Prepare Eppendorf tubes containing 50 µl of the test proteins to be assayed.
9. For measuring the background transfer, include controls that are PIPES buffer alone without any proteins.
10. Add 200 µl of the microsome-liposome mixture to the Eppendorf tubes.
11. Incubate the assay mixture at 25°C for 20 min in a water bath.
12. At the end of the incubation, transfer the tubes onto ice.
13. Add 50 µl of 0.25 M sodium acetate in 0.25 M sucrose at pH 5 to aggregate the microsomes.
14. Vortex and spin at 12,000 rpm for 15 min at 4°C to pellet the microsomes.
15. Remove 150 µl of supernatant into scintillation vials and count after adding scintillation fluid.
16. Count a 200-µl aliquot of the microsomes-liposomes mixture to determine the total amount of radioactivity added in the assay.
17. The percentage of PtdIns transfer is calculated from the total number of counts transferred from the microsomes to the liposomes in the presence of the test compound after subtraction of the background values. Since only 150 µl of the supernatant are counted out of 300 µl, this has to be taken into consideration in the calculation.

Figure 23.2a illustrates the PITP concentration dependence of PtdIns transfer, and Fig. 23.2b illustrates the time-course of PtdIns transfer. The percentage of transfer remains linear provided the concentration of PITPα is kept low. At higher concentrations of PITPα, the assay becomes nonlinear. Cytosols from any cell type can be tested for lipid transfer activity (Fig. 23.3). In this example,

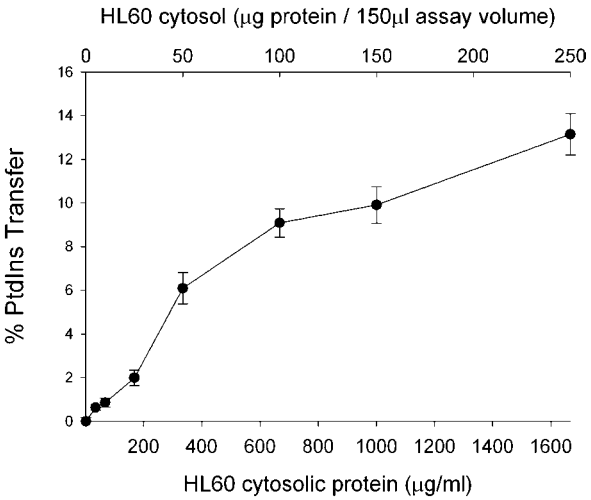

Fig. 23.3 PtdIns transfer using cytosolic fraction prepared from HL60 cells. Two separate scales are shown to illustrate the amount of protein required to be added in the assay and the concentration of cytosolic protein per ml to make comparison with the data from Fig. 23.1(b)

HL60 cytosol was titrated into the assay and because cytosol availability was restricted, the assay was modified. The final volume of the assay was 150 μl, made up of 60 μl of liposomes (60 nmol lipids per assay), 60 μl of microsomes (75 μg of protein per assay), and 30 μl of cytosol (*see* Note 8). The minimum amount of cytosolic protein added to the assay to give reliable transfer activity in the case of HL60 cytosol is 20–30 μg of protein.

23.3.3 Preparation of Mitochondria from Rat Liver

1. All manipulations are carried out on ice and solutions maintained at 4°C unless stated otherwise.
2. Three rat livers are homogenized at 4°C in a Waring blender in 150 ml of cold SET buffer.
3. The homogenate is further homogenized in a motor-driven glass homogenizer with Teflon pestle (15 strokes are sufficient).
4. The homogenate is centrifuged for 5 min at 3,000 rpm (2,000 × *g*) at 4°C to sediment unbroken cells.
5. The supernatant is retained and centrifuged for 15 min at 7,500 rpm (10,000 × *g*) at 4°C to pellet the mitochondria.
6. The mitochondrial pellet is resuspended in SET buffer (50–100 ml) and, using a glass homogenizer and Teflon pestle, the mitochondria are homogenized.
7. Centrifuge for 15 min at 7,500 rpm.
8. Repeat steps 6 and 7.
9. After this final wash, resuspend the mitochondria at 10 mg/ml (approx.) and aliquot (500 μl) in Eppendorf tubes for storage at −80°C.
10. Mitochondrial preparations are stable at −80°C for at least one year.

23.3.4 PtdCho and SM Transfer in vitro

This assay is a modification of a previously published protocol [1, 8]. To monitor PtdCho or SM transfer, liposomes radiolabeled with the appropriate lipids are incubated with mitochondria as the acceptor compartment.

The assay volume is 250 µl:

100 µl of mitochondria (1 mg of protein);
100 µl of liposomes (40 nmol lipids);
50 µl of material to be assayed for transfer activity.

23.3.4.1 Liposome Preparation for PtdCho Transfer Containing Radioactive PtdCho

1. 90 mol% PtdCho, 0.2 µCi [^{3}H]PtdCho, 10 mol PtdOH.
2. Liposomes are prepared in the SET buffer by sonication as described in steps 4–6 of Subheading 23.3.2. To obtain the above molar ratios, add 360 nmol PtdCho, and 40 nmol PtdOH per ml of liposome preparation (*see* Note 9).

23.3.4.2 Liposome Preparation for SM Transfer Containing Radioactive SM

1. 10 mol% SM, 0.2 µC [^{3}H]SM, 80 mol% PtdCho, 10 mol% PtdOH.
2. Liposomes are prepared in the SET buffer by sonication as described in steps 4–6 of Subheading 23.3.2. To obtain the above molar ratios, add 40 nmol SM, 320 nmol PtdCho, and 40 nmol PtdOH per ml of liposome preparation.
3. Assay procedure:
   a. All manipulations are carried out on ice and solutions maintained at 4°C unless stated otherwise.
   b. Samples to be analyzed are added to Eppendorf tubes in 50 µl.
   c. Equal volumes of liposomes (400 nmol /ml) are mixed with rat liver mitochondria (10 mg/ml).
   d. 200 µl of the above mixture are added to the tubes containing the 50-µl samples to be analyzed.
   e. Incubate the samples at 37°C for 30 min.
   f. The samples are transferred onto ice and the mitochondria are sedimented by centrifugation at 12,000 × *g* for 10 min at 4°C.
   g. The supernatant is carefully removed and discarded using a pipette without disturbing the mitochondrial pellet.
   h. The mitochondrial pellet is resuspended in 500 µl of the SET buffer and transferred to an Eppendorf tube containing 500 µl of 14.3% w/v sucrose.

i. Pellet the mitochondria at 12,000 × *g* for 10 min through the sucrose cushion.
j. Discard the supernatant carefully using a pipette without disturbing the mitochondrial pellet.
k. The pellet is resuspended in 50 µl of 10% SDS and vortexed vigorously. The sample is boiled for 5 min, transferred to a scintillation vial, and counted for radioactivity.
l. An aliquot of the liposomes is counted for radioactivity.
m. The percentage transfer is calculated from the total amount of counts transferred to the mitochondria from the liposomes in the presence of the test compound after subtraction of the background values.

23.3.5 Assay to Monitor Either Choline-Labeled Lipids or PtdIns Transferred from Permeabilized HL60 Cells to Liposomes

1. HL60 cells are cultured in RPMI-1640 supplemented with 12.5% heat-inactivated (v/v) fetal calf serum, 4 mM glutamine, 50 IU/ml of penicillin, and 50 µg/ml of streptomycin.
2. To monitor the transfer of choline lipids (PtdCho and SM), the HL60 cells are cultured in Medium 199 supplemented with dialyzed 12.5% heat-inactivated (v/v) fetal calf serum, 4 mM glutamine, 50 IU/ml of penicillin, 50 µg/ml of streptomycin, and 0.5 µCi/ml [^{3}H]choline in 50 ml (adequate for 40 assays) over a 48-hr period (*see* Note 10).
3. To monitor PtdIns transfer, the HL60 cells are cultured in Medium 199 supplemented with dialyzed 12.5% heat-inactivated (v/v) fetal calf serum, 4 mM glutamine, 50 IU/ml of penicillin, 50 µg/ml of streptomycin, and 1 µC/ml of [^{3}H]inositol in 50 ml (adequate for 40 assays) for 48 h.
4. 50 ml of labeled cells provide 5×10^6 HL60 cells at 80% confluence and are sufficient for 40–50 assays.
5. The HL60 cells are sedimented by centrifugation (1,200 rpm for 5 min).
6. The cell pellet is resuspended in 40 ml of the permeabilization buffer and sedimented by centrifugation (1,200 rpm for 5 min).
7. The cell pellet is resuspended in 4 ml of the permeabilization buffer.
8. To permeabilize the cells, 1 ml of a 5X concentrated cocktail containing Mg.ATP (2 mM final) and streptolysin O (0.4 IU/ml final) is added and the cells incubated for 10 min at 37°C.
9. At the end of the permeabilization, the cells are centrifuged at 3,000 rpm for 5 min at 4°C and the pellet is resuspended in 40 ml of cold permeabilization buffer.
10. The cells are centrifuged (3,000 rpm for 5 min) and resuspended in 5 ml of cold permeabilization buffer.
11. The cytosol-depleted HL60 cells (100 µl) are mixed with liposomes [100 µl–100 nmol phospholipid (98:2; PtdCho:PtdIns)] at 4°C.

12. Eppendorf tubes containing 50-µl samples to be analyzed are prepared on ice and 200 µl of the mixture containing cytosol-depleted HL60 cells and liposomes are added.
13. The samples are transferred to a water bath at 37°C and incubated for 20 min.
14. The samples are transferred back on ice and 25 µl of ice-cold 0.25 M sodium acetate in 0.25 M sucrose (pH 5) are added to aggregate the cells.
15. Samples are centrifuged at 12,000 × *g* for 10 min.
16. 150 µl of supernatant containing the liposomes are transferred into scintillation vials and counted after the addition of 3 ml of the scintillation fluid.
17. The percentage of transfer is calculated after sampling a 200-µl aliquot of the mixture of liposomes and cytosol-depleted cells and subtraction of the background reading. Since only 150 µl of the supernatant are counted out of 250 µl, this has to be taken into consideration in the calculation.

23.3.6 PtdIns and PtdCho Binding Assay in Permeabilized HL60 Cells

This method is adapted from Segui et al. [7].

1. HL60 cells are cultured in the RPMI-1640 medium supplemented with 12.5% heat-inactivated (v/v) fetal calf serum, 4 mM glutamine, 50 IU/ml of penicillin, and 50 µg/ml of streptomycin in the presence of 0.5 µCi/ml [^{14}C]acetate in 40 ml (adequate for four assays) over a 48-hr period (*see* Note 11). Per assay, 10 ml of confluent HL60 cells are required.
2. The His-tagged PITPs to be assayed are diluted to 1.2 mg/ml (100 µl per assay required) in the PIPES permeabilization buffer.
3. HL60 cells (40 ml of culture medium, ~4 × 10^7 cells) are sedimented by centrifugation (1,200 rpm for 5 min), washed twice in the permeabilization buffer, and resuspended in 4 ml of permeabilization buffer.
4. For permeabilization, add 1 ml of a cocktail consisting of streptolysin O (0.4 IU/ml) and MgATP [80 µl of MgATP from the 100 mM stock solution (2 mM final)] and incubate the cells for 10 min at 37°C.
5. The cells are diluted with 30 ml of buffer and centrifuged at 3,000 rpm (1,500 × *g*) for 5 min at room temperature to remove the leaked cytosolic proteins.
6. Discard the supernatant and resuspend the cell pellet in 1.6 ml of the permeabilization buffer (*see* Note 12).
7. Add 32 µl of MgATP from the 100 mM stock solution (2 mM final) to the permeabilized cell preparation.
8. Aliquots of 500 µl of the cytosol-depleted cell preparation are transferred to Eppendorf tubes containing the PITPs in 100 µl.

9. After 20 min at 37°C, the cells are removed by centrifugation at 1,500 × g for 5 min at 4°C.
10. The supernatant (550 µl) containing the PITPs is carefully removed and transferred to a clean Eppendorf tube.
11. The supernatant is centrifuged at 11,500 × *g* for 10 min at 4°C to remove any remaining cellular debris.
12. The supernatant (500 µl) is then removed and incubated with Nickel Affinity Gel (120 µl) in mini-spin columns (Pierce Spin Cups) for 30 min at 4°C (*see* Note 13).
13. The columns are placed on a rotating wheel to ensure optimal mixing for 30 min at 4°C.
14. The mini-spin columns are centrifuged for 5 min at 3,000 rpm.
15. The nickel agarose beads containing the captured His-tagged PITP proteins in the mini-spin columns are washed twice with 500 µl of a low-salt buffer (50 mM sodium phosphate, 300 mM NaCl, 10% glycerol, pH 6.0) followed by two washes with 500 µl of a high-salt buffer (50 mM sodium phosphate, 525 mM NaCl, 10% glycerol, pH 6.0) to remove any contaminating proteins. In each case, after centrifugation for 5 min at 3,000 rpm at 4°C, the eluate is discarded after each wash step.
16. PITPs are finally eluted from the nickel beads with 500 µl of 500 mM imidazole in a high-salt buffer into a clean collecting tube.
17. The PITPs (500 µl) are desalted using a buffer exchange column (NAP™ 5 Column, Sephadex™ G-25, GE Healthcare). Prior to use, the buffer exchange column is equilibrated in PIPES buffer by washing the column in 5 ml of the PIPES buffer.
18. Load the PITP (500 µl) onto the buffer exchange column and discard the flow-through.
19. Add 1 ml of the PIPES buffer to elute the PITP proteins into a clean 15-ml polypropylene tube (Sarstedt).
20. A 20-µl aliquot (~2 µg) of recaptured PITP is analyzed on 12% SDS-PAGE to monitor the protein recovery.
21. The 1 ml of recovered PITPs with bound lipids is extracted by adding 3.75 ml of $CHCl_3$:MeOH (1:2) followed by 1.25 ml of $CHCl_3$ and 1.25 ml of water.
22. The mixture is vortexed thoroughly, the lower organic phase is transferred into Eppendorf tubes, and the chloroform is evaporated in a Savant SpeedVac.
23. The radioactive lipids are resuspended in 50 µl of chloroform and are spotted onto Whatman silica gel 60 TLC plates that had been dessicated at 100°C for at least 1 h prior to use.
24. The TLC plates are developed using the following solvent system: $CHCl_3$:MeOH:acetic acid:water (75:45:3:1) to resolve PtdIns and PtdCho.
25. The TLC plates are dried at room temperature in a fume hood for 1–2 h to remove any trace of solvent.

26. To detect the radioactive lipids, the TLC plates are imaged using a Fuji phosphorimaging screen for 2–4 days.
27. Detection is carried out using a Fuji BAS1000 PhosphorImager.
28. Both SDS-PAGE gels and TLC plate images are quantified by densitometry using AIDA software.

Figure 23.4a provides an example demonstrating that PITPα and PITPβ bind mainly PtdIns and PtdCho from the selection of lipids that were available in the permeabilized cells. An analysis of PITPα mutants that were tested for binding properties on PtdIns and PtdCho is also shown (Fig. 23.4b). Wild-type PITPα binds both PtdIns and PtdCho. However, the mutant PITPs have lost their ability to bind to PtdIns, while their PtdCho binding ability has been retained.

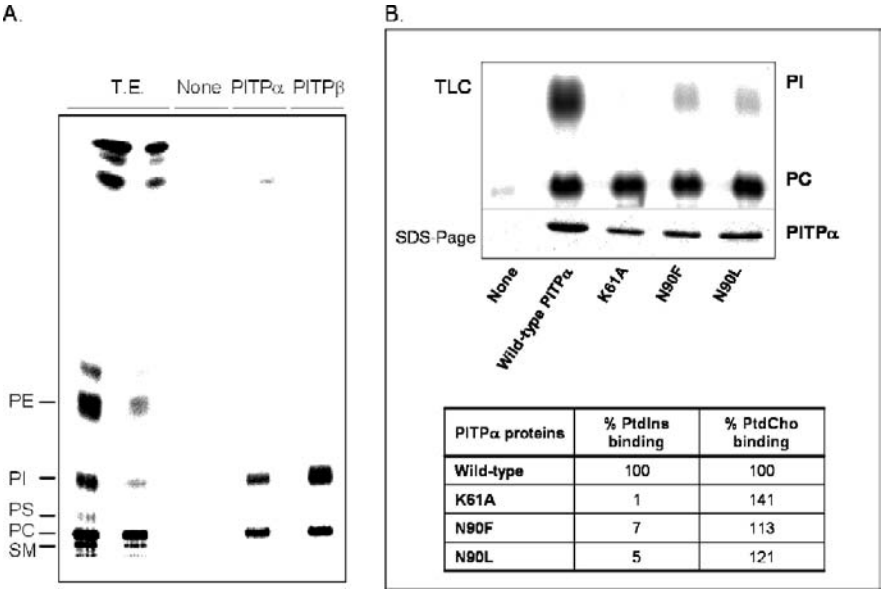

PITPα proteins	% PtdIns binding	% PtdCho binding
Wild-type	100	100
K61A	1	141
N90F	7	113
N90L	5	121

Fig. 23.4 Determination of phospholipids bound to wild-type PITPα and PITPβ and PITPα mutants K61A, N90F, and N90L. HL60 cells were radiolabeled for 48 h with [^{14}C]acetate. After permeabilization, cells were incubated in the presence of wild-type PITPα and β (a) or with wild-type PITPα, K61A, N90F, or N90L of His-tagged PITP proteins. After incubation for 20 minutes at 37°C, samples were centrifuged and the supernatants were collected. PITPα proteins were then recovered and the associated lipids were extracted and separated using TLC. (a) Specificity of lipid binding. Total extract (T.E.) illustrates the cellular lipids that are labeled. Nonetheless, PITPα and PITPβ select only PtdIns and PtdCho. Abbreviations used: PE, PtdEth; PI, PtdIns; PS, PtdSer; PC, PtdCho. (b) Identification of PITPα mutants deficient in PtdIns but not PtdCho binding. In addition to analysis by TLC (top panel), an aliquot of the recovered PITPα was also analyzed on a 12% SDS gel (bottom panel). The amount of [^{14}C]acetate-labeled PtdIns or PtdCho associated with PITPα was quantified with respect to the recovered protein (see table). Abbreviations used: PI, PtdIns; PC, PtdCho

Notes

1. For example, when comparing PITP mutants that are impaired for PtdIns or PtdCho transfer activity, using an identical donor and acceptor compartment with the same mix of lipids is preferable.
2. Lipid solutions in chloroform are prone to evaporation and the following precautions can be taken. First, the lipid solutions are always kept on ice when removed from the freezer; second, the stoppered glass is tightly sealed using Parafilm when stored in the freezer.
3. To make 100 ml of SET buffer, add 1 ml of 1 M Tris-HCl, pH 7.4, 8.56 g of sucrose (MW 342.3), and 0.0372 g of EDTA.
4. Streptolysin O can be purchased from different sources, including Sigma (Cat. no. S5265-25 KU). The lyophilized sample should be reconstituted with water, and the stock solution can be aliquoted and frozen at −80°C.
5. ATP is purchased as a disodium dihydrogen salt should be −80 not −20. To prepare a 100 mM stock solution of MgATP, dissolve 605 mg in 10 ml of a solution containing 2 ml of 1 M Tris and 1 ml of 1 M $MgCl_2$. The use of 200 mM Tris effectively results in a neutral solution (pH 7). This should be checked with a pH electrode and adjusted accordingly. Freeze-thaw of the solution is not detrimental, and 10-ml aliquots can be kept at −20°C and used repeatedly.
6. The mitochondria can be retained for use in PtdCho transfer assays. The mitochondria are resuspended in SET buffer, re-centrifuged as in step 3 to wash them, and stored in 500-µl aliquots at 20 mg/ml at −80°C.
7. $MnCl_2$ allows the exchange of inositol from PtdIns.
8. When the assay volume is reduced to 150 µl, the most important consideration is that the 60 µl of microsomes added in the assay contain sufficient counts in PtdIns for measuring the transfer. For example, if microsomes contain between 50,000–100,000 dpm present in the assay, 1% transfer is 500–1,000 dpm. A 1% tsransfer can still be monitored with a reasonable degree of confidence.
9. To convert µg phospholipid into µmol, assume that the molecular weight is 800. Therefore, 8 µg of lipid is 10 nmol.
10. [^{3}H]choline is incorporated into both PtdCho (87%) and sphingomyelin (13%).
11. Growing the cells in the presence of [^{14}C] acetate labels all the lipids to near equilibrium.
12. Because permeabilized cells do not form a tight pellet after centrifugation, care should be taken when the supernatant is discarded.
13. Mini-spin columns are prepared by adding 120 µl of Nickel Affinity Gel (agarose beads). Add 500 µl of PIPES buffer, and centrifuge for 5 min at 3,000 rpm. Repeat twice more before use.

References

1. Helmkamp GM, Jr, Harvey MS, Wirtz KWA, van Deenen LLM. Phospholipid exchange between membranes. Purification of bovine brain proteins that preferentially catalyze the transfer of phosphatidylinositol. J Biol Chem 1974;249:6382–9.
2. Cockcroft S. Phosphatidylinositol transfer proteins: A requirement in signal transduction and vesicle traffic. BioEssays 1998;20:423–32.
3. Allen-Baume V, Segui B, Cockcroft S. Current thoughts on the phosphatidylinositol transfer protein family. FEBS Lett 2002;531:74–80.
4. Yoder MD, Thomas LM, Tremblay JM, Oliver RL, Yarbrough LR, Helmkamp GM, Jr. Structure of a multifunctional protein. Mammalian phosphatidylinositol transfer protein complexed with phosphatidylcholine. J Biol Chem 2001;276:9246–52.

5. Tilley SJ, Skippen A, Murray-Rust J, Swigart P, Stewart A, Morgan CP, Cockcroft S, McDonald NQ. Structure-function analysis of human phosphatidylinositol transfer protein alpha bound to phosphatidylinositol. Structure 2004;12:317–26.
6. Schouten A, Agianian B, Westerman J, Kroon J, Wirtz KW, Gros P. Structure of apo-phosphatidylinositol transfer protein alpha provides insight into membrane association. EMBO J 2002;21:2117–21.
7. Segui B, Allen-Baume V, Cockcroft S. Phosphatidylinositol transfer protein-beta displays minimal sphingomyelin transfer activity and is not required for biosynthesis and trafficking of sphingomyelin. Biochem J 2002;366:23–34.
8. Morgan CP, Allen-Baume V, Radulovic M, Li M, Skippen AJ, Cockcroft S. Differential expression of a C-terminal splice variant of PITPβ lacking the constitutive-phosphorylated Ser262 that localises to the Golgi compartment. Biochem J 2006;398:411–21.
9. Li H, Tremblay JM, Yarbrough LR, Helmkamp GM, Jr. Both isoforms of mammalian phosphatidylinositol transfer protein are capable of binding and transporting sphingomyelin. Biochim Biophys Acta 2002;1580:67–76.
10. Holub BJ. The Mn2+-activated incorporation of inositol into molecular species of phosphatidylinositol in rat liver microsomes. Biochim Biophys Acta 1974;369:111–22.
11. Hunt AN, Skippen A, Koster G, Postle AD, Cockcroft S. Acyl chain-based molecular selectivity for HL60 cellular phosphatidylinositol and of phosphatidylcholine by phosphatidylinositol transfer protein α. Biochim Biophys Acta 2004;1686:50–60.
12. Brophy PJ, Burbach P, Nelemans SA, Westerman J, Wirtz KW, van Deenen LL. Evidence for the existence of different pools of microsomal phosphatidylinositol by the use of phosphatidylinositol-exchange protein. Biochem J 1978;174:413–20.
13. Thomas GMH, Cunningham E, Fensome A, Ball A, Totty NF, Troung O, Hsuan JJ, Cockcroft S. An essential role for phosphatidylinositol transfer protein in phospholipase C-mediated inositol lipid signalling. Cell 1993;74:919–28.

Chapter 24
In vitro Reconstitution of Activation of PLCε by Ras and Rho GTPases

Natalia Lamuño Gandarillas, Tom D. Bunney, Michelle B. Josephs, Peter Gierschik and Matilda Katan

Abstract Phosphatidylinositol-specific phospholipase C (PLC) enzymes catalyze the hydrolysis of phophatidylinositol 4,5-bisphosphate [PtdIns(4,5)P_2] to diacylglycerol (DAG) and inositol 1,4,5-triphosphate [Ins(1,4,5)P_3]. PLCε is a recently discovered isoform that has been shown to be activated by members of the Ras and Rho families of guanosine trisphosphatases (GTPases) as well as subunits of heterotrimeric G-proteins. We describe a method for expressing a truncated PLCε variant as an MBP fusion protein in *E. coli*. Subsequently, we describe the methodology necessary to reconstitute this protein with K-Ras-4B and RhoA GTPases and measure its activation.

Keywords Phospholipase C activity · reconstitution *in vitro* · phospholipase Cε · Ras · Rho · phospholipid vesicles

24.1 Introduction

The Ras superfamily of small GTPases, of which Ras oncogene proteins are the founding members, is divided into five major branches: Ras, Rho, Rab, Ran, and Arf [1]. Ras GTPases share a common regulatory mechanism acting as binary molecular switches; they cycle between an inactive GDP- and active GTP-bound conformation. The function of Ras GTPases in a specific cell signaling context is determined by the types of downstream effectors that bind to the active, GTP-bound conformation of Ras. For each of the major branches of Ras GTPases, a number of proteins have been identified as potential effectors [1]. One of the criteria in defining direct downstream effectors of Ras is the requirement that such proteins selectively bind to and/or are specifically activated by Ras in a GTP-bound conformation [2,3]. There are several experimental approaches including co-localization and co-immunoprecipitation of a small GTPase with

M. Katan
Cancer Research UK Centre for Cell and Molecular Biology, Chester Beatty Laboratories, The Institute of Cancer Research, Fulham Road, London SW3 6JB, UK
e-mail: matilda@icr.ac.uk

B. Larijani et al. (eds.), *Lipid Signaling Protocols*, DOI: 10.1007/978-1-60327-115-8_24,

a putative effector that can support the possibility that these components form complexes or that the effector is activated by the selected Ras GTPase. However, in the cellular context, it is difficult to assess whether the interaction/stimulation is direct or is mediated by other signaling components. The methodologies being developed to provide more unequivocal evidence for direct interaction, specific for RasGTP, include the reconstitution of effector activation by Ras GTPase in a cell-free system. Although quite informative as used presently, this approach needs further improvement, in particular reconstitution of components where both proteins (a small GTP-ase and an effector) are purified to homogeneity.

It has been suggested that several enzymes involved in inositol–lipid signaling could be important downstream targets of small GTP-ases from the Ras superfamily [2] The activation of phosphatidylinositol-3 kinase (PtdIns-3 K) by classical (H-, K-, and N-) Ras proteins has been well documented [4,5]. Several isoforms of phospoinositide-specific phospholipase C (PtdIns-PLC) [6,7] could also be regulated by members from the Ras and Rho branches. Examples include the activation of PLCβ2 by several Rho members (Rac1, Rac 2, Rac3, and Cdc42), PLCγ2 by Rac1, Rac 2, and Rac3, and PLCε by classical Ras proteins as well as Rho GTPases (Rho A, Rho B, and Rho C) [8–16]. The supporting evidence for these Ras-effector interactions includes data from *in vitro* reconstitution assays using enriched or purified components. The reported methods for the preparation of protein components and reconstitution protocols vary and in each case had to be adapted to a particular experimental setting. Here we describe a protocol for the reconstitution of a purified deletion variant of PLCε with preparations of K-Ras and RhoA, resulting in stimulation of PLC activity. The main steps in the purification of PLCε involve nickel-chelating chromatography, heparin Sepharose, and gel filtration. The main steps for the preparation of K-Ras and Rho involve the solubilization of baculovirus-infected sf9 membranes. The reconstitution is based on the method of Illenberger et al. [9].

24.2 Materials

24.2.1 Cells, Plasmids, Cell Culture, Baculovirus, and Protein Requirements

1. C41(DE3) *E.coli* strain (Avidis) (*see* Note 1).
2. pRare plasmid (Novagen) (*see* Note 2).
3. pIVexMBP (Roche) containing rat PLCε residues (1258-2225) cloned in-frame with the N-terminal MBP tag [MBP-rPLCε (1258-2225)].
4. 2xYT medium (produced in-house).
5. Sf9 cells (Invitrogen).

6. Sf-900 II media (Invitrogen).
7. Recombinant baculoviruses expressing Ras superfamily GTPases containing His tags or HA tags.
8. Purified MBPrPLCε enzyme stored in aliquots at –80°C (*see* Subheading 24.3.1 and Note 3).
9. Aliquots of Sf9 membranes enriched in RhoA wt or K-Ras wt proteins (*see* Subheading 24.3.2).

24.2.2 Stock Solutions

1. 1 M Tris-HCl, pH 8.0.
2. 1 M HEPES-OH, pH 7.2.
3. 5 M NaCl.
4. 1 M KCl.
5. 100 mM $CaCl_2$.
6. 500 mM imidazole.
7. 1 M dithiothreitol (DTT) (stored at –20°C).
8. 1 M Tris(2-carboxyethyl)phosphine hydrochloride (TCEP) (stored at –20°C).
9. 10 mM guanosine 5' triphospate γS (GTPγS) (stored at –80°C).
10. 10 mM guanosine 5' diphospate (GDP) (stored at –80°C).
11. 10 mM sodium deoxycholate (DOC) (stored at –20°C).
12. 10% (v/v) Triton-X-100 (Sigma, Cat no. T9284).
13. 1 M isopropyl-β-D-thio-galactopyranoside (IPTG) (stored at –20°C).
14. 50 mg/ml lysozyme (stored at –20°C).
15. 3,000 U/ml deoxyribonuclease I.
16. PBS: 1.5 mM KH_2PO_4, 8.1 mM Na_2HPO_4, 140 mM NaCl, 2.7 mM KCl.
17. L-α-phosphatidylinositol 4,5-diphosphate from bovine brain (Sigma): 1 mg/ml (MW 10982) stock solution dissolved in chloroform and stored in glass vials with Teflon-lined caps at –20°C.
18. Phosphatidylethanolamine from egg yolk (Sigma): 10 mg/ml (MW 684.0) stock in chloroform stored in glass vials with Teflon-lined caps at –20°C.
19. [^{3}H] PtdIns(4,5)P_2: Stock is as supplied by NEN PerkinElmer, i.e., 0.01 mCi/ml in methylene chloride:ethanol:water (20:10:1) aliquoted into Teflon-lined glass vials and stored at –20°C.

24.2.3 Columns for Chromatography

1. HisTrap 5-ml column (GE Healthcare).
2. HiTrap chelating 5-ml column, Ni^{2+} bound (GE Healthcare).
3. Heparin HiTrap 5-ml column (GE Healthcare).
4. Superdex 200 26/60 gel filtration column (GE Healthcare).

24.2.4 Cell Lysis and Chromatography Buffers

All buffers containing DTT or TCEP are prepared on the day of use and chilled to 4°C prior to application. All other buffers are stored at 4°C.

24.2.4.1 Buffers for MBP-rPLCε (1258-2225) Purification from *E. coli*

1. Lysis buffer: 25 mM Tris-Cl (pH 8.0), 250 mM NaCl, 10 mM imidazole, 10 mM benzamidine, 1 "Complete" protease inhibitor tablet per 50 ml of buffer.
2. Chelating chromatography buffer A: 25 mM Tris-HCl (pH 8.0), 500 mM NaCl, 10 mM imidazole, 1 mM TCEP.
3. Chelating chromatography buffer B: 25 mM Tris-HCl (pH 8.0), 500 mM NaCl, 500 mM imidazole, 1 mM TCEP.
4. Dialysis buffer: 25 mM Tris-HCl (pH 8.0), 50 mM NaCl, 1 mM TCEP.
5. Heparin Sepharose buffer A: 25 mM Tris-HCl (pH 8.0), 1 mM TCEP, 5% (v/v) glycerol.
6. Heparin Sepharose buffer B: 25 mM Tris-HCl (pH 8.0), 1 M NaCl, 1 mM TCEP, 5% (v/v) glycerol.
7. Gel filtration buffer: 25 mM Tris-HCl (pH 8.0), 50 mM NaCl, 0.5 mM EGTA, 1 mM DTT, 5% (v/v) glycerol.

24.2.4.2 Buffers for RhoA and K-Ras Purification from Baculovirus-Infected Sf9 Cells

1. Cell homogenization buffer: 20 mM Tris-HCl (pH 8.0), 100 mM NaCl, 1 mM EDTA, 1 mM DTT, 3.75 mM $MgCl_2$, 3 μM GDP, 1 "Complete" protease inhibitor tablet per 50 ml of buffer.
2. Membrane solubilization buffer: 20 mM Tris-HCl (pH 8.0), 100 mM NaCl, 1 mM EDTA, 1 mM DTT, 23 mM Na cholate, 3.75 mM $MgCl_2$, 3 μM GDP, 1 "Complete" protease inhibitor tablet per 50 ml of buffer.

24.2.4.3 Components of the Reaction Mixture for Reconstitution Experiments

PLCε is functionally reconstituted *in vitro* with RhoA and Ras GTPases in a volume of 60 μl of 50 mM HEPES/NaOH, pH 7.2, 3 mM EGTA, 70 mM KCl, 2 mM DTT, 100 μM GDP or GTPγS, 536 μM phosphatidylethanolamine, 33.4 μM PIP_2/[^{3}H] PtdIns(4,5)P_2 (185 GBq/mol), 1 mM sodium deoxycholate, and 30 nM free Ca^{2+}. The incubation volume includes the following:

1. Buffer A: 60 mM HEPES/NaOH, pH 7.2, 3.6 mM EGTA, 84 mM KCl, and 2.4 mM DTT.
2. 10 μl containing 100 ng of PLCε in buffer A.
3. 5 μl containing the GTPase in membrane solubilization buffer (*see* Subheading 24.2.4.2).
4. 10 μl of 600 μM GDP or GTPγS in buffer A (prepared from 10 mM stock solutions prepared in dd H_2O).

5. 10 µl of $CaCl_2$ in buffer A at a concentration required to adjust the concentration of free Ca^{2+} to 30 nM. The concentration is calculated using the program EqCal for Windows (Biosoft, Ferguson, MO), taking into account the concentrations of EDTA and $MgCl_2$ contained in the membrane solubilization buffer and carried over into the incubation medium, but ignoring the presence of guanine nucleotides in the incubation medium. GDP is present in the control sample instead of GTPγS to maintain an identical concentration of guanine nucleotides in all samples.
6. 5 µl of sodium deoxycholate in dd H_2O.
7. 20 µl of phospholipids micelles in buffer A.

24.3 Methods

24.3.1 Preparation of MBP-rPLCε (1258-2225)

PLCε is a multidomain protein that, ε like other phosphoinositide-specific PLC isoforms, incorporates the PH domain, EF hands, catalytic domain, and C2 domain. The unique regions of this PLC are at the N-terminus, incorporating the CDC25 domain, and at the C-terminus, which contains two RA domains (Fig. 24.1a). PLCε is the largest of all phosphoinositide-specific PLC isoforms (250 kDa), and the full-length protein can be expressed using baculovirus/insect

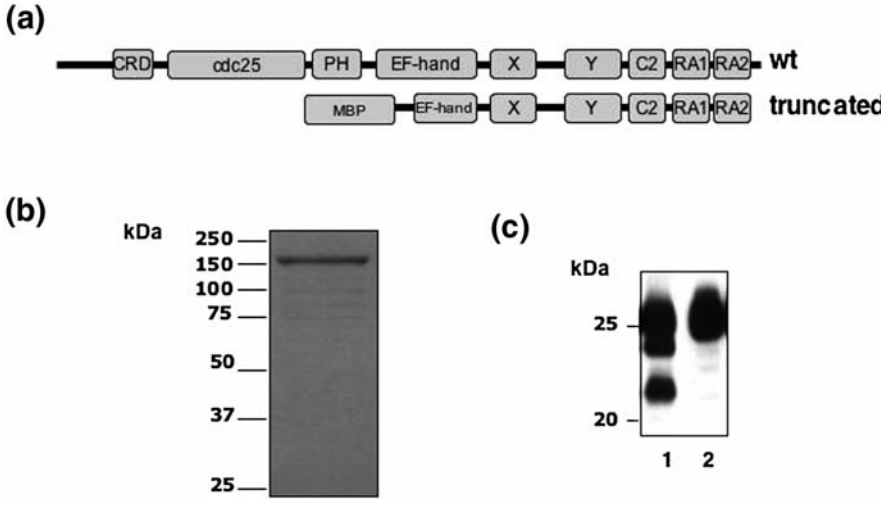

Fig. 24.1 (a) Domain organization of PLCε and the domains present in the truncated construct utilized in the reconstitution experiments. (b) 1 µg of purified MBP-rPLCε (1258-2225) as separated by SDS-PAGE and stained with Coomassie Blue. (c) 10 µg of solubilized Sf9 membranes expressing K-ras (1) or RhoA (2) were separated by SDS-PAGE and transferred to PVDF membrane. Proteins were blotted with an S-protein-HRP conjugate (Novagen) to detect the GTPases by virtue of their N-terminal S tag. Bands were visualized by ECL

cell systems, but only in small amounts [17]. The truncated version (incorporating the region from EF hands to the end of the second RA domain [15]), although still a large polypeptide (110 kDa), can be expressed in bacteria as a soluble fusion protein with MBP under specific conditions. The protein yield of this MBP-rPLCε (1258-2225) is about 0.5 mg per liter of starting bacterial culture.

The protocol described below is based on extraction of PLCε from bacterial lysate and subsequent purification using several chromatographic steps. All chromatography was carried out using an Akta Explorer 100 chromatography instrument and prepacked columns (GE Healthcare).

24.3.1.1 Expression of MBP-rPLCε (1258-2225) in *E. coli*

1. A 50-µl aliquot of chemically competent C41(DE3) cells is transformed with 10 ng of pIVexMBPrPLCε (1258-2225) and 10 ng of pRare. Cells are plated out on L-agar plates containing 50 µg/ml of ampicillin and 10 µg/ml of chloramphenicol and incubated for at least 20 h at 37°C.
2. Colonies are scraped into 2xYT medium, which was prewarmed to 37°C, containing 50 µg/ml of ampicillin and 10 µg/ml of chloramphenicol and incubated in a rotary incubator at 37°C and 250 rpm until the OD_{600} of the culture reached 0.4 (*see* Note 4).
3. The culture is cooled to 20°C and induced with the addition of 100 µM IPTG (final concentration). Cells are incubated for at least 16 h at 20°C and 250 rpm (*see* Note 5).
4. Cells are centrifuged at 4,000 × *g* and the pellet stored at –20°C until use.

24.3.1.2 Preparation of Cell Lysate

1. Each pellet derived from 1 liter of culture medium is resuspended in 25 ml of lysis buffer and incubated at 4°C for 30 min with gentle agitation.
2. 50 µl of deoxyribonuclease I and 5 ml of 10% (v/v) Triton-X-100 are added to the lysate and further incubated for 1 h at 4°C (*see* Note 6).
3. Lysate is clarified by centrifugation at 15,000 × *g* for 30 min at 4°C and used immediately for purification.

24.3.1.3 Affinity Purification with HisTrap Chromatography

1. A 5-ml HisTrap column is equilibrated with 2 column volumes of chelating chromatography buffer A.
2. The cell lysate is applied at a flow rate of 3 ml/min and the column washed with 5 column volumes of chelating chromatography buffer A.
3. Protein is eluted with a gradient to 100% chelating chromatography buffer B over 5 column volumes with all peaks collected.
4. Eluted fractions are analyzed by SDS-PAGE to locate the correct protein (molecular mass of 150 kDa). These fractions are pooled and dialyzed against 500 ml of dialysis buffer for 2 h at 4°C (*see* Note 7).

24.3.1.4 Heparin HiTrap Chromatography

1. A 5-ml heparin HiTrap column is equilibrated with 2 column volumes of heparin Sepharose buffer A.
2. The cell lysate is applied at a flow rate of 5 ml/min and the column washed with 4 column volumes of heparin Sepharose buffer A.
3. Protein is eluted with a gradient to 100% heparin Sepharose buffer B over 10 column volumes with all peaks collected.
4. Eluted fractions are analyzed by SDS-PAGE to locate the correct protein that elutes after 40% buffer B. Fractions are pooled and, if necessary, concentrated to less than 20 ml in a Vivascience Spin Concentrator (20-ml volume, 100,000-Da MWCO) (*see* Note 8).

24.3.1.5 Superdex 200 26/60 Gel Filtration Chromatography

1. Column is equilibrated in 1.5 column volumes of gel filtration buffer.
2. Sample is applied at a flow rate of 4 ml/min in a volume between 10 and 20 ml. Fractions are eluted in 1 column volume of gel filtration buffer.
3. All peaks are collected and analyzed by SDS-PAGE. The peak corresponding to monomeric MBP-rPLCε (Fig. 24.1b) is concentrated to 15 mg/ml in a Vivascience Spin Concentrator (20-ml volume, 100,000-Da MWCO) and snap-frozen in 50-μl aliquots in liquid N_2 and subsequently stored at –80°C.

24.3.2 Preparation of K-Ras-4B and RhoA from Baculovirus-Infected Sf9 Cell Membranes

Small GTP-ases are lipid-modified [18], which is important for cellular localization and also for activation of some of their effectors *in vitro* [4]. Therefore, although these small proteins (about 21 kDa) can be readily expressed in bacteria, to obtain lipid-modified proteins (that are unlike unmodified proteins attached to membranes), a suitable preparation can be made from membranes of insect or mammalian cells. Here we describe the preparation and solubilization of membranes from Sf9 cells after infection with baculoviruses encoding K-Ras-4B and RhoA.

24.3.2.1 Infection of Sf9 Cells with Virus

1. Seed 50-cm × 50-cm Corning tissue culture plates with 1.2×10^8 cells per plate. Allow to settle for 2 h at room temperature. For each virus set up three plates.
2. Remove media and add virus at an MOI of 2 in a volume of 2 ml. Incubate at room temperature for 1 h.
3. Twice during the hour of incubation, tilt the plate toward one side in order to collect all of the volume on one side of the plate, and then tilt the plate in the opposite direction.
4. After 1 h, add 60 ml of media to each plate and seal the sides of the plate with Parafilm. Incubate at 27°C for 72 h.

24.3.2.2 Cell Harvesting and Membrane Solubilization

1. Media are removed and pipetted into a 50-ml centrifuge tube. Cells on plate are scraped into 50 ml of room-temperature PBS. Media and PBS suspended cells are centrifuged at 300 × *g* for 5 min at 4°C to pellet cells. The supernatant is disposed of and cells chilled on ice.
2. Cells are resuspended in 15 ml of cell homogenization buffer and lysed by 20 strokes in a chilled cell homogenizer. Cellular debris and whole cells are pelleted by centrifugation at 300 × *g*for 10 min at 4°C.The supernatant is further centrifuged at 17,500 × *g* for 30 min at 4°C to pellet the membrane fraction.
3. Infected Sf9 membranes are solubilized in 1 ml of membrane solubilization buffer by constant stirring at 4°C. Insoluble material is removed by centrifugation at 17,5000 × *g* for 30 min at 4°C. Solubilized GTPases in the supernatant are aliquoted and snap-frozen in liquid N_2 followed by storage at –80°C. The presence of tagged GTP-ases in the membrane preparation is monitored by Western blotting, as illustrated in Fig. 24.1c.

24.3.3 Methods for Reconstitution

Studies of the regulation of PLC enzymes *in vitro* require specific conditions that have been established empirically for each pair of a given PLC isoform and a particular regulatory molecule. One of the important considerations when combining components of such systems is presentation of the substrate PtdIns(4,5)P_2, which is largely influenced by the presence of other lipids and detergents. The protocol given here, for the preparation of lipid micelles and the PLC assay, is based on Illenberger et al. [9] (Fig. 24.2).

1. Phospholipid micelles containing the PLC substrate [^{3}H] PtdIns(4,5)P_2 are prepared by evaporating a mixture of phosphatidylethanolamine, PtdIns(4,5)P_2, and [^{3}H] PtdIns(4,5)P_2 prepared from stock solutions of the individual phospholipids in chloroform under a stream of nitrogen at room temperature. To this end, this calculated volume of lipid vesicles is placed in a 10-ml Pyrex glass tube (14 × 100 mm) using a glass syringe. The mixture is dried down under nitrogen using a hose connected to the nitrogen tank from one end and to a glass Pasteur pipette mounted on a ring stand from the other. This end is lowered into the Pyrex glass containing the lipid mixture and the nitrogen flow is set on low, ensuring the formation of a uniform layer at the bottom of the tube.
2. At this point, the volume of buffer A previously calculated is added to the dried phospholipids, and the mixture is vortexed for 30 min at maximum speed at room temperature.
3. The vortexed phospholipid suspension is subsequently sonicated in a bath-type sonicator [19] for 15 min at 4°C, ensuring that the final product is an opalescent suspension.

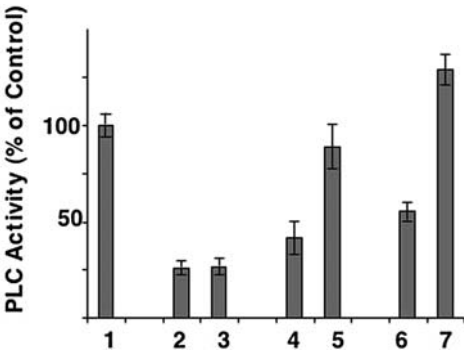

Fig. 24.2 PLC activity after incubation in standard reconstitution reaction mixture including (1) 100 ng of MBP-rPLCε (1258-2225) and activating 2.4 mM DOC and 1 mM calcium used as a control in all experiments, (2) 5 µl of membrane proteins from noninfected Sf9 cells and 100 µM GDPβS, (3) 5 µl of membrane proteins from noninfected Sf9 cells and 100 µM GTPγS, (4) 100 ng of MBP-rPLCε and 5 µl of membrane proteins from Sf9 cells infected with RhoA baculovirus in the presence of GDPβS, (5) 100 ng of MBP-rPLCε and 5 µl of membrane proteins from Sf9 cells infected with RhoA baculovirus in the presence of GTPγS, (6) 100 ng of MBP-rPLCε and 5 µl of membrane proteins from Sf9 cells infected with K-Ras-4B baculovirus in the presence of GDPβS, (7) 100 ng of MBP-rPLCε and 5 µl of membrane proteins from Sf9 cells infected with K-Ras-4B baculovirus in the presence of GTPγS

4. The phospholipase C assay is started by adding the phospholipid micelles (20 µl) to the other assay constituents (40 µl) and transferring the tubes to a water bath maintained at 30°C. The incubation is carried out for 45 min at this temperature. At this point, the reaction is terminated by the addition of 350 µl of ice-cold chloroform/methanol/concentrated HCl (100/100/0.6) followed by vortexing, transferring the tubes to an ice bath, and adding 100 µl of 1 M HCl, 5 mM EGTA.
5. After a 10-minute incubation in the ice bath, the samples are centrifuged at maximum speed (15,000 × *g*) for 1 min in a tabletop centrifuge, thus separating nonhydrolyzed radiolabeled [^{3}H] PtdIns(4,5)P_2 (lower phase) from the upper phase containing [^{3}H]inositol phosphates.
6. 200 µl of the upper phase are then added to scintillation vials filled with 4 ml of scintillation fluid. The amount of [3 H]inositol phosphates present in this volume is determined by liquid scintillation counting [19].

Acknowledgments This work is funded by a grant from Cancer Research UK.

Notes

1. The C41(DE3) strain of *E.coli* is used for the expression of the truncated MBP-rPLCε protein. In comparison to BL21(DE3), the proportion of soluble protein is higher and the bacteria grow at an increased rate.

2. The pRARE plasmid contains a chloramphenicol resistance gene and a P15A replicon. It is therefore compatible with plasmids containing ampicillin resistance and ColE1 replicons (such as pIVEXMBP).
3. Purified MBP-rPLCε is stored as 50-μl aliquots at –80°C. Once the aliquot is used, the remainder is not refrozen but disposed of.
4. The presence of both ampicillin and chloramphenicol in the bacterial broth results in slow growth. The cultures therefore need to be started early in the morning in order to allow time to reach the required OD.
5. The induction temperature of 20°C is important. We found that a few degrees to either side of 20 led to significant decreases in yield.
6. We routinely use this "gentle" lysis procedure to release soluble proteins from bacteria. It is important that the bacteria have been frozen for at least 30 minutes prior to being resuspended in the lysis buffer. We found that including a probe sonication step led to increased amounts of degradation products at the final step.
7. The dialysis step is necessary to reduce the amount of salt and imidazole in the protein sample. If the concentrations are too high, the protein will not bind to the heparin Sepharose. We found that a 2-hour incubation is sufficient.
8. Due to the presence of aggregated protein, the use of the spin concentrators can take some time.
9. The concentrations of free Ca^{2+} and sodium deoxycholate in the assay are critical determinants of the fold stimulation of phospholipases C by their regulatory proteins. We generally tend to perform the assay at the lowest possible concentration of free Ca^{2+} (e.g., 30 nM) and to compensate the low-phospholipiase C activities under this condition by using longer incubation times, higher temperature, and/or more of the PLC isoforms under investigation.

References

1. Wennerberg K, Rossman KL, Der CJ. The Ras superfamily at a glance. J Cell Sci 2005;118:843–6.
2. Downward J. Targeting RAS signalling pathways in cancer therapy. Nat Rev Cancer 2003;3:11–22.
3. Herrmann C. Ras-effector interactions: After one decade. Curr Opin Struct Biol 2003;13:122–9.
4. Suire S, Hawkins P, Stephens L. Activation of phosphoinositide3-kinase gamma by Ras. Curr Biol 2002;12:1068–75.
5. Pacold ME, Suire S, Perisic O, Lara-Gonzalez S, Davis CT, Walker EH, Hawkins PT, Stephens L, Eccleston JF, Williams RL. Crystal structure and functional analysis of Ras binding to its effector phosphoinositide 3-kinase gamma. Cell 2000;103:931–43.
6. Rebecchi MJ, Pentyala SN. Structure, function, and control of phosphoinositide-specific phospholipase C. Physiol Rev 2000;80:1291–335.
7. Rhee S-G. Regulation of phophoinositide-specific phospholipase C. Ann Rev Biochem 2001;70:281–312.
8. Illenberger D, Schwald F, Pimmer D, Binder W, Maier G, Dietrich A, Gierschik P. Stimulation of phospholipase C-beta2 by the Rho GTPases Cdc42Hs and Rac1. EMBO J 1998;17:6241–9.
9. Illenberger D, Stephan I, Gierschik P, Schwald F. Stimulation of phospholipase C-beta 2 by Rho GTPases. Methods Enzymol 2000;325:167–77.
10. Illenberger D, Walliser C, Nurnberg B, Diaz Lorente M, Gierschik P. Specificity and structural requirements of phospholipase C-beta stimulation by Rho GTPases versus G protein beta gamma dimers. J Biol Chem 2003;278:3006–14.

11. Illenberger D, Walliser C, Strobel J, Gutman O, Niv H, Gaidzik V, Kloog Y, Gierschik P, Henis YI. Rac2 regulation of phospholipase C-beta2 activity and mode of membrane interactions in intact cells. J Biol Chem 2003;278:8645–52.
12. Piechulek T, Rehlen T, Walliser C, Vatter P, Moepps B, Gierschik P. Isozyme-specific stimulation of phospholipase C-gamma2 by Rac GTPases. J Biol Chem 2005;280:38923–31.
13. Snyder JT, Singer AU, Wing MR, Harden TK, Sondek J. The pleckstrin homology domain of phospholipase C-beta2 as an effector site for Rac. J Biol Chem 2003;278:21099–104.
14. Song C, Hu CD, Masago M, Kariyai K, Yamawaki-Kataoka Y, Shibatohge M, Wu D, Satoh T, Kataoka T. Regulation of a novel human phospholipase C, PLCepsilon, through membrane targeting by Ras. J Biol Chem 2000;276:2752–7.
15. Seifert JP, Wing MR, Snyder JT, Gershburg S, Sondek J, Harden TK. RhoA activates purified phospholipase C-epsilon by a guanine nucleotide-dependent mechanism. J Biol Chem 2004;279:47992–7.
16. Wing MR, Snyder JT, Sondek J, Harden TK. Direct activation of phospholipase C-epsilon by Rho. J Biol Chem 2003;278:41253–8.
17. Ghosh M, Wang H, Kelley GG, Smrcka AV. Purification of phospholipase C beta and phospholipase C epsilon from Sf9 cells. Methods Mol Biol 2004;237:55–64.
18. Clarke S. Protein isoprenylation and methylation at carboxyl-terminal cysteine residues. Ann Rev Biochem 1992;61:355–86.
19. Gierschik P, Camps M. Stimulation of phospholipase C by G protein βγ subunits. Methods Enzymol 1994;238:181–95.

Chapter 25
Assaying Endogenous Phosphatidylinositol-4-Phosphate 5-Kinase (PIP5K) Activities

Jonathan R. Halstead, Mireille H. Snel, Sarah Meeuws, David R. Jones and Nullin Divecha

Abstract Phosphoinositides are a family of lipid second messengers interlinked by an extensive and highly regulated network of kinases and phosphatases. The modulation of phosphoinositide profiles can regulate numerous cancer-related pathways, including cell survival, cell proliferation, migration, integrin activation, and transcription. PtdIns(4,5)P_2 is at the heart of phosphoinositide signaling; its levels are controlled by enzymes that synthesize it and those that degrade it. Phosphatidylinositol-4-phosphate 5-kinases (PIP5 K) phosphorylate PtdIns4P on the 5-position and constitute the major pathway for the generation of PtdIns(4,5)P_2. We will discuss how to suppress the expression of human PIP5 Kβ using RNAi and how to measure the activity and levels of the endogenous enzyme. We describe a method to immunoprecipitate the endogenous PIP5 Kβ and to assay its activity. Western blotting with another panel of antibodies is then used to determine the levels of endogenous PIP5 Kβ in the immunoprecipitates.

Keywords Phosphoinositides · phosphatidylinositol-4-phosphate 5-kinase · RNAi suppression · enzymatic activity · PtdIns(4,5)P_2

25.1 Introduction

PtdIns(4,5)P_2 sits at a critical point of at least three different signaling pathways. It is the substrate for receptor-stimulated phospholipase C, which cleaves PtdIns(4,5)P_2 to generate water-soluble inositol 1,4,5-trisphosphate [Ins(1,4,5)P_3] and the membrane-bound neutral lipid diacylglycerol (DAG) [1]. Ins(1,4,5)P_3 is a key intracellular regulator of calcium efflux from the endoplasmic reticulum [2], while DAG is an important physiological activator of protein kinase C [3]. PtdIns(4,5)P_2 is also the substrate for phosphatidylinositol 3-kinase (PI3 K),

N. Divecha
The Inositide Laboratory, The Paterson Institute for Cancer Research,
Wilmslow Road, Manchester m20 4BX
e-mail: ndivecha@picr.man.ac.uk

B. Larijani et al. (eds.), *Lipid Signaling Protocols*, DOI: 10.1007/978-1-60327-115-8_25,

which, upon receptor activation, phosphorylates PtdIns(4,5)P_2 to generate phosphatidylinositol 3,4,5-trisphosphate [PtdIns(3,4,5)P_3] [4]. PtdIns(3,4,5)P_3 is one of the most important lipid second messengers and is able to regulate numerous cellular processes, including cell survival, proliferation, gene transcription, and membrane trafficking. Not surprisingly, the PI3 K pathway is highly upregulated in human tumors [5]. PtdIns(4,5)P_2 is also a key cofactor for the regulation of phospholipase D activity [6]. Upon receptor activation, phospholipase D cleaves a different phospholipid, phosphatidylcholine, to generate phosphatidic acid. The latter has numerous targets, including PIP5 K [7], the mammalian target of Rapamycin [8], and Raf kinase [9]. PtdIns(4,5)P_2 itself can regulate a number of cellular processes, as overexpression of PIP5 K in cells leads to dramatic changes in actin dynamics, vesicle trafficking, ion channel regulation, and inhibition of stress-induced apoptosis [10, 11]. Understanding how PIP5Ks are regulated to control the synthesis of PtdIns(4,5)P_2 is clearly of importance. Three isoforms of PIP5 K (α, β, and γ) have been shown to localize to different subcellular compartments [12]. Furthermore, they appear to perform nonredundant functions. For example, only one isoform (γ) of PIP5 K can interact with talin and can localize to focal adhesions, as this interaction site is not present in any other PIP5 K isoform. PIP5 Kα can regulate the membrane trafficking of plasma membrane receptors, while the γ isoform of PIP5 K appears to regulate a PtdIns(4,5)P_2 pool required for Ins(1,4,5)P_3 generation [13]. PIP5 Kβ appears to be involved in the regulation of a stress-sensitive pool of PtdIns(4,5)P_2 [11, 14].

In this chapter, we describe methodologies to specifically suppress the expression immunoprecipitate and measure the activity of the human PIP5 Kβ isoform.

25.2 Materials

25.2.1 Generation of Retroviruses

1. HEK293 phoenix amphotropic cells can be obtained from the Nolan laboratory (http://www.stanford.edu/group/nolan/). The cells are routinely grown in DMEM containing 10% fetal calf serum (FCS) and passaged at 70% confluence.
2. The sequence CTGCAATCATATAGGTTAA was cloned into the BglII/HindIII site in pRetro-Super to generate a PIP5 Kβ-specific targeting construct (*see* Note 1).
3. Calcium phosphate transfection: 160 mM calcium chloride. 2× HEBS buffer: 41 mM HEPES, 272 mM NaCl, 1.4 mM Na_2HPO_4, pH 7.1. These solutions should be filter-sterilized and stored at 4°C. Solutions are brought to room temperature before adding the DNA.
4. 3-ml sterile luer-lock syringes and 0.45-μm filters.

5. Cell culture-grade freezing ampules (Nunc Cat. no. 375418) for storing viral supernatants.

25.2.2 Retroviral Transduction of HeLa Cells

1. HeLa cells can be obtained from ATCC Cryostorage and are maintained in DMEM-10% FCS.
2. Polybrene A: Stock solution is made at a 1,000× strength (5 mg/ml in DMEM).
3. Puromycin A stock solution of 1 mg/ml in H_2O is filter-sterilized, aliquoted (1 ml), and stored at –20°C.

25.2.3 Immunoprecipitation of PIP5Kβ

1. Lysis buffer: 50 mM Tris-HCl, pH 8.0, 50 mM KCl, 10 mM EDTA, 1% NP40 containing freshly added 10 mM sodium fluoride, 10 mM sodium orthovanadate, and 1× Complete protease inhibitor cocktail.
2. 1 M sodium fluoride.
3. 100 mM sodium orthovanadate.
4. Complete protease inhibitor (Complete EDTA-free, Roche Cat. no. 11873580001).
5. Bio-Rad protein assay reagent (Bio-Rad Cat. no. 500-0006).
6. Anti-PIP5 Kβ antibodies can be generated against the peptide sequence SQEIVSSISQEWKDEKR (*see* Note 2).
7. Protein G-Sepharose fast flow (GE Healthcare Cat. no. 17-0618-01) is washed with the lysis buffer by repeated centrifugation and resuspended in the lysis buffer such that 50 µl yield a packed pellet volume of approximately10 µl.
8. Immunoprecipitation wash buffer (IP wash buffer): 50 mM Tris-HCl, pH 7.5, 150 mM NaCl, 5 mM EDTA, 0.1% Tween 20.
9. 2xPIPkin buffer: 100 mM Tris-HCl, pH 7.4, 20 mM $MgCl_2$, 2 mM EGTA, 140 mM KCl.
10. 10 mM Tris-HCl, pH 7.5.

25.2.4 Measurement of PIP5K Activity

1. PtdIns4P (Sichem or Echelon) adjusted to 1 µmol/ml. Synthetic commercial phosphoinositides are normally produced as ammonium salts, which are relatively insoluble in chloroform. In order to solubilize the lipids, we routinely convert them to the acidic form (*see* Note 3).
2. Phosphatidylserine (10 mM in chloroform; Sigma Cat. no. P3660).
3. Phosphatidic acid (3 mM in chloroform; Sigma).

4. Sonication water bath (*see* Note 4).
5. Shaking Eppendorf tube mixer at 30°C.
6. Stop solution: 50 ml of chloroform, 50 ml of methanol, 400 µl of Folch extract [Sigma type I Folch fraction from bovine brain (Cat. no. 030 K7063) at a stock concentration of 1 mg/ml in chloroform] can be stored at –20°C in a glass bottle.
7. 2.4 M HCl.
8. Rotary evaporation system: We use a Gyrovap GL (Howe) linked to a diaphragm pump (Divac 2.2 L) maintained in a fume hood.
9. TLC plates: Silica gel TLC plates (Merck Cat. no. 1.05721.0001) are dipped in a solution of 1% potassium oxalate, 1 mM EDTA (*see* Note 5) and then placed in an oven (110°C) for 1 h.
10. TLC developing solution: Chloroform:methanol:28% ammonia:H_2O (45:35:2:8) should be prepared fresh, placed into a TLC tank containing two pieces of Whatman 3MM paper (20 × 20 cm), and allowed to equilibrate for 1 h before plate development.

25.2.5 Western Blotting and Measurement of PIP5Kβ Protein in Immunoprecipitates

1. 4× lithium dodecylsulphate-loading buffer (Invitrogen Cat. no. NP0007).
2. 1 M dithiothreitol made in H_2O, aliquoted into 100 µl tubes, and stored at –20°C.
3. Heating block set to 73°C.
4. 4–12% gradient precast bis-tris gels (Invitrogen Cat. no. NP0322).
5. MOPS running buffer (Invitrogen Cat. no. NP0001) diluted to single strength. The 200 ml used for the upper buffer chamber contain 200 µl of antioxidant (Invitrogen Cat. no. NP0005).
6. Bio-Rad Western electrophoresis transfer tank containing 3 L of cold (4°C) buffer: 118 mM Tris, 40 mM glycine, 20% v/v methanol.
7. Nitrocellulose membranes (Schleicher and Schull, 0.45-µm pore size).
8. Ponceau S stain: 0.4% Ponceau S in 3% TCA. The solution can be stored in a glass bottle in the dark at room temperature.
9. PBS-T: 136 mM NaCl, 2.6 mM KCl, 40 mM $Na_2HPO_4 \cdot 2H_2O$, 1.7 mM KH_2PO_4, 0.1% Tween 20.
10. PBS-T-milk: PBS-T containing 5% milk powder (Nutricia or Friso).
11. The goat anti-PIP5 KβWB antibody used for Western blotting is a 1:1:1 mix of the following antibodies diluted 1:2,500 in PBS-TR-3% BSA (Santa Cruz Biotechnology Cat. nos. sc-11777, sc-11778, and sc-11779).
12. PBS-TR-3% BSA: 50 ml PBS-T containing 1 ml of Western blot blocking reagent (Roche Diagnostics Cat. no. 11921673001) and 3% BSA w/v.
13. Anti-goat-HRP (Dako).
14. SuperSignal West Dura (Pierce Biochemicals).

25.3 Methods

25.3.1 Generation of Retroviruses Encoding RNAi Targeting PIP5Kβ

1. Amphotropic HEK cells (HEK-ampho) are routinely grown in DMEM containing 10% FCS and are passaged at 70% confluency. For the generation of amphotropic virus, capable of infecting HeLa cells, the HEK-ampho cells are plated at 400,000 cells/well in a 6-well plate (day 1).
2. The HEK-ampho cells are transfected (day 2) with 5 μg of either pRetro-Super empty vector or vector containing the RNAi sequence targeting PIP5 Kβ using a calcium phosphate transfection reagent. 5 μg of DNA are diluted with 100 μl of 160 mM calcium chloride. 100 μl of 2× HEBS buffer is then added dropwise. The transfection solution is immediately added dropwise to the 2-ml medium present in each well) (*see* Note 6).
3. The cells are washed (day 3) in the morning and left until the evening, at which time the medium is replaced (2 ml) and the cells are left to grow for a further 24 h.
4. The medium (2 ml) above the cells (containing the virus) is removed (day 4) and passed through a 0.45-μm filter (*see* Note 7).
5. The virus is ready to use or can be frozen using dry ice in cell culture-grade freezing ampules and stored at –80°C.

25.3.2 Retroviral Transduction of HeLa Cells

1. HeLa cells are routinely grown in DMEM containing 10% FCS and are passaged when the cells reach approximately 80% confluency. For retroviral transduction, 100,000 cells are plated/well in a 6-well cluster plate and left overnight.
2. 2 μl of stock polybrene are added to the viral supernatant (2 ml) before the supernatant is added to the HeLa cells (after removal of the overlying medium); the cells are grown for a further 16 h.
3. The HeLa cells are washed twice with 2 ml of DMEM-10% FCS before reincubating using 2 ml of DMEM-10% FCS.
4. The next day the medium is replaced with selection medium (2 ml of DMEM-10% FCS and 2 μg/ml of puromycin) (*see* Note 8). The cells are selected over a 3–4-day period. When the cells reach confluency, they are trypsinized and seeded into 10 cm Petri dishes using selection medium. This procedure generates two cell lines, H-pRetro (HeLa containing the empty p-Retro-Super vector) and H-RNAiβ (HeLa containing the RNAi construct targeting PIP5 Kβ). Figure 25.1 indicates that the targeting construct only reduces the expression of mRNA encoding PIP5 Kβ and does not affect the level of either the α or γ isoform as determined by real-time PCR.

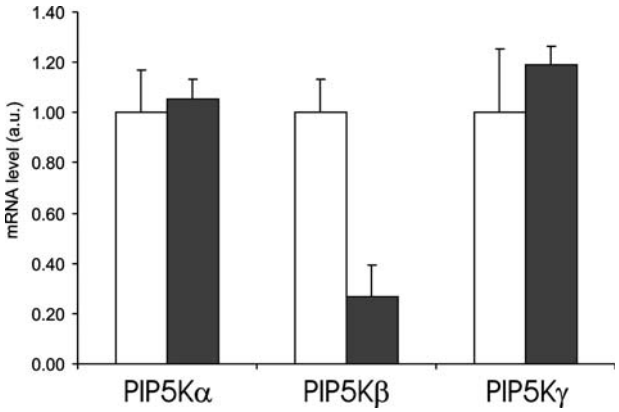

Fig. 25.1 RNA was isolated from both H-pRetro (white bars) and H-RNAiβ cells. Real-time PCR was used to assess the mRNA levels of PIP5 Kα, PIP5 Kβ, and PIP5 Kγ. As can be seen, the RNAi construct targets only the expression of PIP5 Kβ

25.3.3 Immunoprecipitation of PIP5Kβ

1. 1×10^6 H-pRetro and H-RNAiβ cells are plated separately into 10 cm Petri dishes and allowed to grow to confluency.
2. The cells are washed twice with ice-cold PBS and are lysed by the addition of 1 ml of the lysis buffer. Cell lysis is allowed to proceed for 15 min at 4°C, after which time the cells and the supernatant are collected using a cell scraper and transferred into a 1.5-ml Eppendorf tube.
3. The cell lysate is cleared by centrifugation (5 min at maximum speed in a microfuge at 4°C). The protein concentration is determined using Bio-Rad protein assay reagent (*see* Note 9).
4. 1 mg of protein is immunoprecipitated using 5 µl of either control (pre-immune serum) or anti-PIP5 Kβ specific antibody overnight at 4°C.
5. 50 µl of protein G-Sepharose solution are added to each tube followed by end-over-end rotation for 1 h at 4°C.
6. The protein G-Sepharose is pelleted by centrifugation (30 s at 8,000 rpm in a microfuge at 4°C) and the supernatant is discarded. The pellet is washed three times with IP wash buffer (1 ml each wash) by centrifugation (as above), making sure that approximately 50 µl of wash buffer are always left above the pellet each time. The pellet is then washed once with 1xPIPkin buffer (1 ml). After removal of the supernatant, the tubes are centrifuged (as above). The final 50 µl of 1xPIPkin buffer are removed using a Hamilton syringe (*see* Note 10).
7. The pelleted protein G-Sepharose is gently resuspended in 50 ml of 10 mM Tris-HCl, pH 7.5.

25.3.4 Measurement of PIP5K Activity

1. Phosphatidylserine (10 nmol × n + 1), phosphatidic acid (3 nmol × n + 1), and phosphatidylinositol 4-phosphate (1 nmol × n + 1) are mixed and dried by rotary evaporation (n = the number of samples to be assayed).
2. The dried lipid mixture is dissolved in 10 mM Tris-HCl, pH 7.5 (40 µl × n + 1), and the lipids are allowed to rehydrate for 15 min at room temperature.
3. The lipid mixture is solubilized by bath sonication (2 min at room temperature), and 40 µl are transferred into Eppendorf tubes on ice (*see* Note 4).
4. The immunoprecipitate is mixed by pipetting, and 10 µl are removed in duplicate (*see* Note 11). Each of the two replicates is mixed with the sonicated lipid solution and maintained on ice for a further 15 min.
5. Reactions are initiated by the addition of 50 µl of the 2xPIPkin buffer supplemented with 50 µM ATP and 5 µCi of [^{32}P]ATP. The samples are mixed and incubated in a shaking Eppendorf tube mixer for 10 min at 30°C.
6. The reactions are stopped by the addition of 0.5 ml of stop solution followed by 125 µl of 2.4 M HCl. The tubes are vigorously shaken and centrifuged (maximum speed in a microfuge), and the lower phase, containing the [^{32}P]PtdIns(4,5)P_2, is removed into a new 1.5-ml Eppendorf tube and dried by rotary evaporation. The upper phase, which contains the majority of free [^{32}P]ATP, is discarded.
7. [^{32}P]PtdIns(4,5)P_2 is separated from other phosphoinositides and residual free ATP by TLC. 0.5-cm pencil lines, 1 cm apart, are marked 1.5 cm above the bottom of a TLC plate. The samples are resuspended in 8 µl of chloroform:methanol (90:10) and spotted onto the pencil marks. The Eppendorf tube is washed with a further 8 µl of chloroform:methanol (90:10), and the wash is spotted on top of the original sample. The spotted samples are allowed to dry for 10 min at room temperature before development in a TLC tank containing 70 ml of TLC developing solution until the solvent front reaches 4 cm from the top of the TLC plate.
8. Quantitation of the radioactivity in [^{32}P]PtdIns(4,5)P_2 is performed using a phosphorimager (we routinely use the Fuji BAS reader) or by exposing the dried TLC plate to X-ray film, followed by scraping off the silica containing the [^{32}P]PtdIns(4,5)P_2 and quantitation by Cerenekov counting. Densitometry of the exposed X-ray film is not recommended. Figure 25.2 indicates that immunoprecipitation with the anti-PIP5 Kβ antibody yields approximately 3 times more activity than immunoprecipitation with a pre-immune serum. Importantly, the amount of PIP5 K activity immunoprecipitated with this antibody is reduced by 80% in cells that express an RNAi construct targeting PIP5 Kβ.

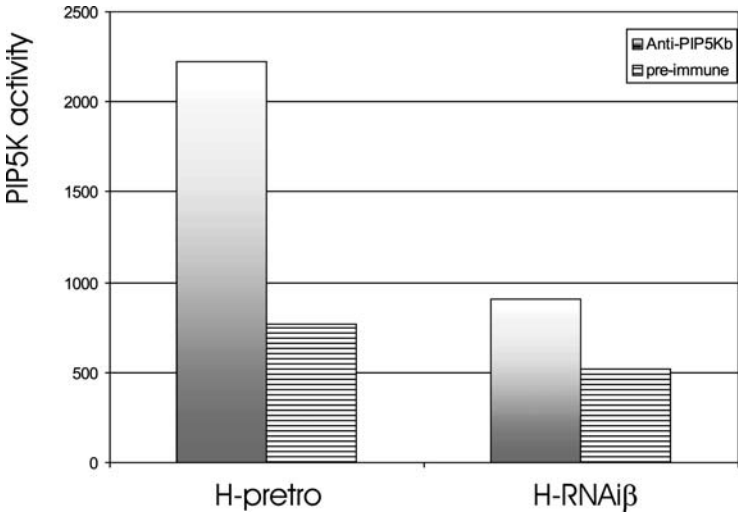

Fig. 25.2 PIP5Kβ was immunoprecipitated from lysates of H-pRetro and H-RNAiβ cells using either anti-PIP5Kβ or pre-immune serum. Three times more enzyme activity was immunoprecipitated from the H-pRetro cells using the anti-PIP5Kβ antibody compared to the pre-immune serum. Only 20% of the enzyme activity was immunoprecipitated from the H-RNAiβ cells compared to the H-pRetro cells. This is in line with the 80% decrease in mRNA found by real-time PCR

25.3.5 Western Blotting and Measurement of PIP5Kβ Protein in Immunoprecipitates

1. The immunoprecipitate is mixed by repeated pipetting and, using a yellow tip with the top 3–4 mm cut off, 20 µl are removed into a clean Eppendorf tube containing 7.5 µl of 4× lithium dodecylsulphate-loading buffer and 2.5 µl of 1 M dithiothreitol. The samples are incubated at 73°C for 10 min, after which time they are centrifuged, mixed by shaking, and recentrifuged to pellet the Sepharose (*see* Note 12).
2. 25 µl of the supernatant (containing the dissociated immunoprecipitating antibody and PIP5 Kβ) are removed and loaded onto a 4–12% gradient precast gel (Invitrogen). Electrophoresis is performed using an MOPS buffer (Invitrogen) at 180 V (constant voltage) for 60 min.
3. After electrophoresis, all proteins in the gel are transferred to a nitrocellulose membrane using a wet transfer protocol employing cold (4°C) buffer at 70 V for 90 min.
4. The nitrocellulose membrane is removed, washed once with water, and stained for 5 min with Ponceau S solution. Proteins on the membrane are destained by washing the membrane with distilled water until the red protein bands can be visualized against a white background (*see* Note 13). Total destaining of the protein bands is performed by washing the membrane with PBS-T.

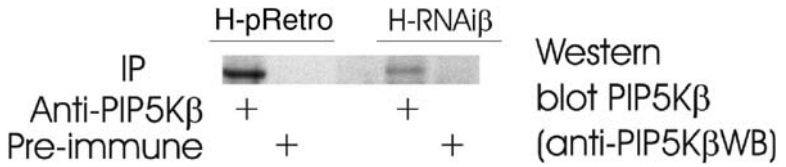

Fig. 25.3 Proteins in the immunoprecipitates described above were subjected to SDS-PAGE, transferred to nitrocellulose membranes, and immunoprobed with the mix of anti-PIP5 KβWB antibodies. The immunoprecipitations were performed using 1 mg of total protein in each case. However, approximately 70% less PIP5 Kβ was detected in lysates from the H-RNAiβ cells compared to the H-pRetro cells

5. The nitrocellulose membrane is blocked by incubation in PBS-T-milk for 30 min at room temperature, after which time the blot is washed three times with PBS-T.
6. To detect the PIP5 Kβ protein, the membrane is incubated with anti-PIP5 KβWB (diluted 1:2,500 in PBS-TR-3% BSA) overnight at 4°C (*see* Note 14).
7. The membrane is washed three times with PBS-T (10 min each) and then incubated with an antigoat polyclonal antibody conjugated to HRP (1:15,000 dilution in PBS-TR-3% BSA) for 30 min.
8. The membrane is washed three times with PBS-T (10 min each) and once with distilled water. PIP5 Kβ is then visualized using a SuperSignal chemi-illuminescence reagent. The emitted light is captured by exposing the blot to X-ray film (*see* Note 15). Figure 25.3 indicates that the anti-PIP5 KβWB antibodies specifically recognize a band of the correct molecular weight that is decreased by approximately 80% in cells that express an RNAi construct targeting the expression of PIP5 Kβ.

Acknowledgments The authors would like to acknowledge financial support from the dutch cancer society (KWF) and the Netherlands cancer institute (NKI). We would also like to thank all past and recent members of the laboratory.

Notes

1. Four different sequences targeting PIP5 Kβ were cloned and tested for their ability to suppress the expression of transfected PIP5 Kβ in HEK293 cells. The sequence indicated yielded the best results and was subsequently used to prepare the retroviruses to infect HeLa cells.
2. The peptide sequence was synthesized as a lysine tree and injected into New Zealand white rabbits. The antiserum was collected after two booster injections (separated by 1 month). Drawn blood was allowed to stand at room temperature for 5 h, after which time the clot was removed by centrifugation. The plasma was aliquoted, frozen, and stored at –20°C.
3. To convert phosphoinositides into their acidic form, the dried lipid is resuspended in 1 ml of chloroform/methanol (1:1 v/v), transferred into a 1.5-ml Eppendorf tube, and 200 µl of H_2O and 250 µl of 2.4 M HCl are added. The tube is vigorously shaken and centrifuged (maximum speed for 1 minute in an Eppendorf microfuge), and 750 µl of the upper phase are removed and discarded. The lower phase is washed with 750 µl of the theoretical

upper phase. The lower phase is removed into a new 1.5-ml Eppendorf tube. 10 µl of the lower phase are dried in a clean, high-temperature–resistant glass tube and used to measure the total amount of phospholipid phosphate [*see* Methods for the determination of the mass of nuclear PtdIns4*P*, PtdIns5*P*, and PtdIns(4,5)P_2 for this issue].

4. It is important to determine the part of the water bath that sonicates most efficiently. The easiest way to do this is to move the tube around in the water until significant vibration is felt in your fingers. The efficiency of normal water-bath sonicators varies and depends on the amount and type of solution in the bath. Recently, we have used a bath sonicator called the Bioruptor (Diagenode). This sonicates at frequencies more akin to a probe sonicator and, unlike the usual bath sonicators, provides more uniform sonication within the bath area. Furthermore, with this apparatus it is possible to sonicate six samples simultaneously.
5. Preparation of TLC dipping solution: A 1.5 L solution of 2% potassium oxalate and 2 mM EDTA in water is diluted with 1.5 L of methanol. This solution is then placed in a spare TLC tank and TLC plates are dipped in one direction (the undipped area is designated the top of the plate and should be marked with a pencil) and dried in an oven (at 110°C). The dipping solution can be stored in the TLC tank at 4°C for at least three months.
6. We normally add 0.5 µg of DNA encoding GFP-histone to assess the transfection efficiency. Other methods of transfection can be used, such as FuGENE (Roche Diagnostics). A very cheap alternative is polyethylenimine (Polysciences Inc., Polyethylenimine linear, MW 25,000, Cat. no. 23966). Polyethylenimine is dissolved in H_2O at 1 mg/ml and incubated at 55°C for 30 minutes. The solution is filter-sterilized, aliquoted (1 ml), and stored at –20°C. Once thawed, aliquots are stable at 4°C for one month. To transfect HEK293 cells, 3 µg of DNA are added to 100 µl of DMEM (without FCS), then 7 µl of PEI solution are added, and the solution is allowed to incubate at room temperature for 15 minutes. The PEI/DNA complex is then added to HEK293 cells in wells of a 6-well cluster plate in 2 ml of DMEM-10% FCS. The cells are incubated for a further 16 h, after which time the cells are treated as described above. PEI transfection can be used with a number of different cell types; however, it is useful to initially determine the DNA/PEI ratio that yields the best transfection rates (a compromise between transfection efficiency and toxicity).
7. After the removal of the viral supernatant from the HEK293 cells, another 2 ml of the medium can be added to the HEK293 cells, followed by overnight incubation to generate more viral supernatant.
8. It is advisable to empirically determine the concentration of puromycin required to kill nontransfected cells. We routinely carry out dose curves (1–20 µg/ml) and employ the lowest concentration that kills all of the nontransfected cells within two days.
9. 2.5 µl of cell lysate are added to 1 ml of protein assay reagent (Bio-Rad protein assay reagent diluted five times in MilliQ water). The samples are incubated at room temperature for 15 minutes, and the absorbance is measured at a wavelength of 595 nm. Sample amounts are quantified by comparison with a standard curve of BSA (1–25 µg).
10. It is essential to remove the final volume of wash buffer above the beads to ensure that the beads are resuspended in exactly the same volume for comparison of enzyme activity and for protein detection in Western blots.
11. In order to pipette the protein G-Sepharose beads, we normally cut off the top 3–4 mm of the end of a yellow tip. Mixing the beads is always performed by pipetting, as vortexing leads to a loss of beads on the sides of the Eppendorf tube.
12. Mixing and recentrifugation are essential to ensure that the sample buffer is homogeneous.
13. The easiest method to capture an image of the membrane is to scan it directly using a scanner linked to a computer. Photocopying is not recommended, as red does not photocopy well. A permanent stain with Ponceau S can also be generated at the end of all blotting applications. After washing the membranes extensively with PBS-T, wash once

with water and then stain for 5 minutes with Ponceau S. The membrane is then washed with water until the final desired staining is achieved. Then the membrane is placed in 10% acetic acid, 30% methanol, and 60% H_2O to permanently fix the stained membrane.

14. We have tested a number of different antibodies (including the goat anti-PIP5K antibodies used for the final Western blot) to detect PIP5K protein in cell lysates directly without the need for immunoprecipitation. However, we have been largely unsuccessful. For example, the anti-PIP5Kβ antibody from Abcam (Cat. no. ab5468) recognizes a protein band at a molecular weight of 66 kDa, but the intensity of this band does not decrease in the H-RNAiβ cells. Furthermore, the advantage of the antibodies described in our method is that the original immunoprecipitation antibody is generated in rabbits, while the Western blotting antibodies are generated in goats. This leads to a much cleaner Western blot.
15. The Western blot can be quantitated in a number of different ways. While quantitation can be performed by densitometry of the film [different exposures should be taken to ensure that the film is not saturated (overexposed)], by far the best method is to capture the chemi-illuminescent light using a CCD camera. We routinely carry this out using a system from α-Inotech. The light is captured using low-resolution/high-sensitivity settings. The advantage of the CCD camera is the large linear dynamic range of light sensitivity.
16. While we have shown that this assay can demonstrate differences in the total amounts of enzyme as a consequence of expression of an RNAi construct targeting the expression of PIP5Kβ, the entire experimental setup can be used to determine how the activity of PIP5Kβ is changed in response to various treatments such as growth factors or cellular stress.

References

1. Divecha N, Irvine RF. Phospholipid signaling. Cell 1995;80:269–78.
2. Streb H, Irvine RF, Berridge MJ, Schulz I. Release of Ca^{2+} from a nonmitochondrial intracellular store in pancreatic acinar cells by inositol-1,4,5-trisphosphate. Nature 1983;306:67–9.
3. Nishizuka Y. The role of protein kinase C in cell surface signal transduction and tumour promotion. Nature 1984;308(19–25):693–8.
4. Stephens LR, Hughes KT, Irvine RF. Pathway of phosphatidylinositol(3,4,5)-trisphosphate synthesis in activated neutrophils. Nature 1991;351:33–9.
5. Cantley LC. The phosphoinositide 3-kinase pathway. Science 2002;296:1655–7.
6. Liscovitch M, Chalifa V, Pertile P, Chen CS, Cantley LC. Novel function of phosphatidylinositol 4,5-bisphosphate as a cofactor for brain membrane phospholipase D. J Biol Chem 1994;269:21403–6.
7. Jones DR, Sanjuan MA, Merida I. Type Ialpha phosphatidylinositol 4-phosphate 5-kinase is a putative target for increased intracellular phosphatidic acid. FEBS Lett 2000;476:160–5.
8. Avila-Flores A, Santos T, Rincon E, Merida I. Modulation of the mammalian target of rapamycin pathway by diacylglycerol kinase-produced phosphatidic acid. J Biol Chem 2005;280:10091–9.
9. Andresen BT, Rizzo MA, Shome K, Romero G. The role of phosphatidic acid in the regulation of the Ras/MEK/Erk signaling cascade. FEBS Lett 2002;531:65–8.
10. Halstead JR, Jalink K, Divecha N. An emerging role for PtdIns(4,5)*P*(2)-mediated signalling in human disease. Trends Pharmacol Sci 2005;26:654–60.
11. Halstead JR, van Rheenen J, Snel MH, et al. A role for PtdIns(4,5)*P*(2) and PIP5 Kα in regulating stress-induced apoptosis. Curr Biol 2006;16(19):1850–6.

12. Santarius M, Lee CH, Anderson RA. Supervised membrane swimming: Small G-protein lifeguards regulate PIPK signalling and monitor intracellular PtdIns(4,5)P_2 pools. Biochem J 2006;398:1–13.
13. Wang YJ, Li WH, Wang J, et al. Critical role of PIP5KI{γ}87 in InsP3-mediated $Ca^{(2+)}$ signaling. J Cell Biol 2004;167:1005–10.
14. Yamamoto M, Chen MZ, Wang YJ, et al. Hypertonic stress increases phosphatidylinositol 4,5-bisphosphate levels by activating PIP5KIβ. J Biol Chem 2006;281:32630–8.

Chapter 26
Preparation of Membrane Rafts

Mark G. Waugh and J. Justin Hsuan

Abstract The concept that biological membranes contain microdomains of specialized lipid and protein composition has attracted great attention in recent years. Initially, the focus in the field was very much on the characterization of cholesterol-and sphingolipid-rich plasma membrane microdomains that were resistant to solubilization in the cold non-ionic detergent Triton X-100. Such detergent-insoluble membrane domains were of low buoyant density and could be readily purified on sucrose equilibrium density gradients. The intrinsic buoyancy of the detergent-insoluble domains gave rise to the term "lipid rafts." Cholesterol- and sphingolipid-rich rafts at the plasma membrane have been implicated in a wide range of cellular processes, including pathogen invasion, receptor signaling, and endocytosis [1]. However, work with other non-ionic detergents such as Lubrol WX and Brij-98 has revealed the existence of various raft subtypes with differing lipid compositions and proposed functions [2, 3]. More recently, there has been some focus on isolating lipid rafts from intracellular organelles, in particular membranes from the Golgi-endosomal pathway, where raft lipids have been proposed to function in processes such as the sorting of vesicular cargo [4] and the processing of amyloid precursor protein [5]. While there remains a large degree of controversy surrounding the purity, the physiological importance, and even the existence of different types of lipid rafts in intact cells, the ability to routinely purify such domains has led to significant progress in understanding the functional architecture of biological membranes. We describe a number of widely used methods to prepare rafts, based on early preparations of caveolae by density gradient ultracentrifugation [6] and immunoaffinity precipitation [7, 8].

M.G. Waugh
Centre for Molecular Cell Biology, Department of Medicine, Royal Free and University College Medical School, Hampstead, London NW3 2PF, UK
e-mail: m.waugh@medsch.ucl.ac.uk

B. Larijani et al. (eds.), *Lipid Signaling Protocols*, DOI: 10.1007/978-1-60327-115-8_26,

Keywords Lipid raft · membrane microdomain · cholesterol · sphingolipids · GPI anchor · phospholipid · cell signaling · caveolae · density gradient

Abbreviations GPI: glycosylphosphatidylinositol; PBS: Phosphate buffered saline; DL buffer: Detergent lysis buffer; BD: Beckton Dickinson; BSA: Bovine serum albumin; SDS-PAGE: sodium dodecylsulphate-polyacrylamide gel electrophoresis; PNS: postnuclear supernatant.

26.1 Introduction

This method is aimed at isolating and characterizing detergent-insoluble lipid rafts where the type of raft involved has not yet been defined, as might be the case when studying a newly identified plasma membrane-localized protein. Detergent-insoluble rafts can also contain proteins posttranslationally modified by glycosylphosphatidylinositol (GPI) anchors or saturated acyl chains, but not by prenylation.

The basic principle of the technique is to use a specific detergent to selectively solubilize nonraft regions of the membrane and to subsequently isolate the detergent-insoluble, low–buoyant density rafts by sucrose equilibrium density gradient centrifugation. At the outset, the choice of detergent and concentration to use is a key issue [9]. However, it usually is not possible to predict either of these based solely on information such as the primary structure of the protein or its subcellular localization as determined by immunofluorescence or electron microscopy. Therefore, the idea is to comprehensively test a range of different detergents, preferably in a single experiment, to establish which raft or raft subtype best defines the membrane domain to which the protein under investigation is targeted. There is no universally ideal single detergent, and results can be misleading: A given protein may be raft-associated in an intact cell (as determined by other techniques such as immunoelectron microscopy, fluorescence perturbation, or chemical cross-linking studies), but selectively solubilized from the raft by a detergent (e.g., [10, 11]); conversely, a nonraft membrane protein or proteins present in different rafts may be inherently insoluble in a detergent and thereby left apparently co-localized in isolated detergent-insoluble rafts (e.g., [12, 13]).

Given these provisos, a good starting point is to use different detergents and a nondetergent-based method to assess raft localization. Each of the following detergents has previously been used to isolate a particular type of lipid raft. The most commonly used detergents have been non-ionic detergents such as TX-100, Lubrol WX, Brij-96, and Brij-98, each of which is selective for compositionally distinct cholesterol-rich membrane rafts [9]. As an example, Lubrol WX can be used to isolate cholesterol-sphingolipid lipid rafts that contain a high molar proportion of phosphatidylcholine, which is largely absent from TX-100 rafts [14]. The detergent-free method described here for preparing lipid rafts involves fragmentation of membranes by sonication in the presence of sodium carbonate [6]. As with the detergent-based methods for raft production, rafts produced by

sonication tend to be a heterogeneous mix of low-buoyant density membrane fragments; hence, the final part of the method details a technique for immunopurifying caveolae from a carbonate-based raft preparation [7, 8].

26.2 Materials

26.2.1 Cell Homogenization and Clearing Spins

1. Phosphate buffered saline (PBS), pH 7.4, precooled on ice.
2. Detergent lysis (DL) buffer: 10 mM Tris-HCl, 1 mM EDTA, 0.5 mM EGTA, pH 7.4, and a suitable non-ionic detergent, such as 1% (v/v) TX-100, 0.5% (v/v) Lubrol WX, 0.5% (v/v) Brij-96, or 0.5% (v/v) Brij-98. Note that different detergent mixtures (e.g., [15]), the combined use of carbonate and detergent buffers (*see* Note 1), or different detergent concentrations (*see* Note 2) and/or different temperatures (*see* Note 3) can be employed to prepare different types of rafts. An alternative to the DL buffer is an alkaline carbonate lysis buffer containing 100 mM sodium carbonate. Both lysis buffers can be stored for up to a month at 4°C and, with the exception of buffers containing Brij detergents [16], must be maintained ice-cold during the preparation.
3. Complete™ protease inhibitor tablets (Roche) are added just prior to the start of the experiments at 1 tablet per 10 ml of buffer. We have found that this inhibitor cocktail is very effective in blocking proteases.
4. A loose-fitting (e.g., Wheaton B pestle) 2-ml capacity Dounce homogenizer for cell disruption.
5. Probe sonicator (e.g., Sonics and Materials Vibra-Cell™ VC 130 PB).
6. Round-bottom, polystyrene 5-ml tubes [e.g., Beckton Dickinson (BD) Falcon™ Cat. no. 32058].

26.2.2 Sucrose Equilibrium Density Gradient Ultracentrifugation

1. Sucrose solutions for use in the density gradient (*see* Notes 4 and 5): Sucrose (analytical grade) is added to 10 mM Tris-HCl, 1 mM EDTA, 0.5 mM EGTA, pH 7.4, to give final concentrations of 5%, 30%, and 80% sucrose solutions (all sucrose concentrations are w/v) that are required for the density gradient described here. These solutions are made up at room temperature and prepared just prior to use. Preparing an 80% sucrose solution in neutral buffer at room temperature can be difficult, as it is close to the solubility limit. One way of dissolving the sucrose is to add 16 g of sucrose to a 50-ml conical tube (e.g., BD Falcon™ Cat. no. 352098). Add the Tris buffer until just short of the 20-ml mark on the tube. Place the tube on its side and roll on a rotating platform until the sucrose has dissolved, and then adjust to 20 ml. This method allows the sucrose to dissolve using a bigger

surface area and is much more effective for preparing high-concentration sucrose solutions than, for example, rotation on a mixing wheel.
2. 12-ml ultracentrifuge tubes (e.g., Beckman Coulter Ultra-Clear™ polycarbonate Cat. no. 344059).
3. Ultracentrifuge and swing-out rotor able to sustain 175,000 × *g* at 4°C (e.g., Beckman Coulter Optima™ LE80-K and SW41Ti, respectively).
4. Refractometer (optional): A variety of models can be used (e.g., Leica AR200).
5. Protein assay reagent (optional): BCA (bicinchoninic acid) Protein Assay Reagent (Pierce Biotechnology).
6. Antibodies for Western blotting (*see* step 4 of Subheading 26.2.3).

26.2.3 Immunoaffinity Purification of Caveolae

1. Sheep antirabbit IgG-coated M280 magnetic Dynabeads and an MPC®-S magnetic particle concentrator (Dynal).
2. PBS, pH 7.4, precooled on ice.
3. Bovine serum albumin (BSA) fraction V (Sigma).
4. Antibodies: We use a rabbit anti-caveolin antiserum (BD Biosciences Cat. no. 610060) for immunoprecipitations (*see* Note 6) and anti-caveolin monoclonal antibody C060 for Western blots (BD Biosciences Cat. no. 610058). Anti-flotillin antibodies (e.g., BD Biosciences Cat. no. 610821) can be used in Western blots to identify non-caveolar rafts [17]. Anti-transferrin receptor antibodies (e.g., BD Biosciences Cat. no. 612125) are commonly used in Western blots to identify the nonraft plasma membrane fraction. To identify other nonraft membranes (*see* Note 7), we use anti-calnexin antiserum (Stressgen) to detect endoplasmic reticulum membranes, anti-syntaxin 6 monoclonal antibody (BD Biosciences Cat. no. 610636) to detect TGN-derived rafts, and anti-EEA1 monoclonal antibody (BD Biosciences Cat. no. 610457) to detect the early endosomes [18].

26.3 Methods

26.3.1 Cell Homogenization and Clearing Spins

1. Cells are grown on 100-mm culture dishes. We routinely use two confluent plates of fibroblasts or epithelial cells for each raft preparation, but up to four plates can be combined per ultracentrifugation tube. The addition of larger quantities of starting material can compromise separation in the density gradient. However, it is possible to greatly scale up preparations by first making postnuclear supernatants and then pelleting total cell membranes, which can be pooled as a starting material for raft preparations (*see* Note 8).
2. Wash the cells twice in ice-cold PBS buffer. It is important to remove as much of the cell culture medium as possible, as residual serum proteins in particular

can complicate subsequent proteomic analyses of lipid rafts. Tilting the cell culture dish on its side while keeping it on ice can aid in draining off residual culture medium prior to aspiration. These washing steps can be usefully speeded up by setting up a bench-top vacuum aspirator. When using more than one plate, cell culture dishes should be transferred quickly to a tray of ice following removal from the incubator and only removed immediately prior to washing and solubilization. This is to minimize disruption to the cell membrane architecture arising from acute environmental changes.

3. As soon as the last PBS wash is complete, 2 ml of ice-cold DL buffer or 2 ml of 100 mM sodium carbonate should be added. In experiments where profiling lipids is an aim, it is useful to include commercially available phospholipase C inhibitors such as U73122 (10 μM; Calbiochem) and general lipid phosphatase inhibitors such as okadaic acid (1 μM; Calbiochem) to minimize lipid degradation. To ensure that the entire cell monolayer is covered in DL buffer, it maybe necessary to gently agitate the dish. It is important to keep the cell culture dish on ice throughout this entire process. Where more than one plate of cells is employed, we recommend that DL or carbonate buffer is added to one dish at a time and transferred sequentially from plate to plate so as to limit the volume to 2 ml. This allows starting samples to be concentrated without any concomitant increase in the volume of material added to the gradient.
4. After 1 min in the DL buffer, the cell lysate is removed from the dish by scraping with a disposable plastic cell scraper (Fisher). Again, tilting the dish on one end ensures that all the cell lysate can drain down toward one area on the dish so that as much of the original 2 ml of lysate buffer as possible can be collected. The cell lysate is now transferred to a 2-ml loose-fitting Dounce homogenizer that has been prechilled on ice. To ensure complete cell disruption, the lysate is subjected to homogenization by 10 strokes of the homogenizer. To avoid foaming of the detergent, it is best not to carry out this step too vigorously.
5. For carbonate-based preparations, there is an additional sonication step at this point. The carbonate-treated cell lysate (2 ml) is transferred to a 5-ml polystyrene round-bottomed tube. As these lysates tend to be very viscous and sticky, use a Pasteur pipette to transfer cell lysates to the round-bottomed tubes. The high viscosity is due to nuclear lysis and is a particular problem when larger amounts of cells are used. The tube is then set in a 200-ml plastic beaker half-filled with ice. The cell homogenate is sonicated by six 5-s blasts at an amplitude of 60, or the equivalent on other apparatus. The probe should be placed approximately halfway down the tube in the middle of the cell lysate to minimize foaming. The viscosity of the solution decreases very noticeably after sonication.

26.3.2 Sucrose Equilibrium Density Gradient Ultracentrifugation

1. The cell homogenate is pipetted into the bottom of a 12-ml ultracentrifuge tube. The volume is adjusted to 2 ml and then an equal volume of

80% sucrose is added. It can be difficult to pipette the very viscous 80% sucrose solution. One technique that is useful to get around this is the so-called reverse displacement pipetting technique. Using a standard positive-displacement pipette, the required volume is set and then the plunger is depressed maximally to dispel all the air present. The pipette tip is then placed in the dense solution and the plunger very slowly released so that a volume of liquid greater than that actually required is drawn up into the pipette tip. Finally, the plunger is slowly depressed until it meets its first resistance or stop point: The ensuing volume of liquid expelled should match the amount indicated on the dial. The two solutions are then mixed thoroughly by pipetting up and down several times to give a final concentration of 40% sucrose in a 4-ml volume. This forms the bottom sucrose density layer in the ultracentrifuge tube.

2. 4 ml of 30% sucrose solution are now layered on top using a 1-ml pipette. This has to be done slowly in order to avoid mixing with the 40% layer. We tend to add the 30% solution drop by drop down the side of the ultracentrifuge tube and close to and following the meniscus as it rises.
3. Finally, 4 ml of 5% sucrose are added and the tube is topped up with 5% sucrose to within a couple of millimeters of the rim. It is important to do this because even a 5-mm gap can result in the tube collapsing in on itself during ultracentrifugation. Performing this step next to the centrifuge will reduce the chance of spilling or disturbing the layers.
4. The tube is then carefully placed in a swing-out rotor and centrifuged overnight (or for at least 4 h) at 4°C at 175,000 × *g*.
5. After centrifugation, the swing-out buckets are carefully removed from the rotor. Sometimes the ultracentrifuge tubes can be difficult to remove from the buckets. This may be due to a small amount of trapped moisture between the tube and the bucket that allows a partial vacuum to be generated as the tube is raised. Passive warming to room temperature sometimes allows the tube to be recovered more easily. Tubes are placed in an ice bucket and allowed to stand vertically before fractions are removed. At this stage it may be possible to visualize a turbid white or opaque membrane band located between the 5% and 30% sucrose layers that contains the detergent-insoluble, low-buoyant density rafts.
6. To harvest gradient fractions, we use a 1-ml pipette to slowly decant off 12 1-ml fractions beginning at the top of the sucrose gradient. As the volume of the tubes tends to be slightly greater than 1 ml, the 12th fraction tends to have a volume greater than 1 ml. There is often a detergent-insoluble pellet at the bottom of the tube which can be harvested. This pellet can be resuspended by scraping with a pipette tip in 1 ml of Tris-HCl buffer followed by repeated pipetting to disperse the pellet. For very stubborn pellets, we recommend adding the buffer and then sonicating with three 5-s bursts with the probe sonicator set at an amplitude of 60. If low temperature is not a critical factor at this stage of the experiment, this process can be aided by solubilizing in warm (e.g., 37°C) DL buffer.

7. At this point it is often useful to verify the density profile in the gradients. This can be easily done using a refractometer, which measures the refractive index of aqueous solutions—a property that increases with increasing solute concentration. Handheld refractometers are easy to operate and allow a rapid determination of the density profile of the gradient.
8. Another common property to measure at this stage is the protein content of each fraction. For detergent-based preparations, this can be problematic as the commonly used Bradford assay is often inaccurate when sucrose (>10%) or detergent [e.g., >0.125% (v/v) TX-100] is present. However, there are some commercially available protein assay kits that are more resistant to detergent and sucrose: For example, the BCA kit from Pierce tolerates TX-100 to 5% (v/v) and sucrose to 40%. Often there is very little protein measurable in the buoyant raft fraction compared with the dense fractions where the vast majority of the cellular protein is to be found. Another commonly used method, albeit only qualitative, is to separate samples by sodium dodecylsulphate-polyacrylamide gel electrophoresis (SDS-PAGE) followed by either Coomassie staining or silver staining to visualize the protein distribution in different gradient fractions.
9. Validation of the lipid raft preparation (*see* Note 7): It is important to confirm that the membrane fraction containing lipid rafts contains markers reported in the literature. Western blotting can be used to confirm the presence of caveolin and flotillin. Conversely, Western blotting should also be used to demonstrate the absence of established nonraft markers such as the transferrin receptor and clathrin.
10. Where the subsequent analysis of fractions is not sensitive to degradation, such as in determinations of lipid and protein composition, we tend to split gradient fractions into aliquots for storage at −70°C. Gradient fractions stored in this way appear to be stable for several years. For protein analysis by SDS-PAGE, we immediately treat samples with an equal volume of 2× SDS-PAGE sample buffer. Avoid boiling the samples, as experience has shown that raft-associated, palmitoylated proteins can aggregate when boiled and are poorly resolved by subsequent gel electrophoresis.

26.3.3 Immunoaffinity Purification of Caveolae

As mentioned earlier, lipid rafts prepared using density gradient centrifugation of either detergent- or carbonate-based cell lysates are very likely to be heterogeneous. This heterogeneity may arise from rafts that have similar biophysical properties and therefore co-localize in the sucrose gradient but originate from distinct cellular localizations. As an example, it is well established that TX-100–resistant rafts can originate from both Golgi and plasma membranes. Therefore, where possible, it is useful to include a final raft-immunoaffinity

step in order to purify the raft subpopulation of interest. The method here describes the immunoaffinity isolation of caveolar rafts from a carbonate-based preparation using a magnetic bead separation system. Similar methodologies have been successfully used for other rafts (*see* Note 6).

1. In order to remove the storage buffer added by the manufacturer, first gently vortex the vial containing the superparamagnetic polystyrene M280 sheep antirabbit immunoglobulin Dynabeads for about 3 s—this is necessary as the beads tend to settle in storage. Remove 100 µl of the bead suspension to a 1.5-ml Eppendorf tube containing 900 µl of PBS buffer and place in the magnetic particle concentrator. The brown Dynabeads will be attracted to the wall of the test tube adjacent to the magnet and can be visualized as a brown streak. This process of harvesting the Dynabeads is usually complete within 2 min. The Dynabead storage buffer is then removed by pipetting. The beads are resuspended by removing the slide-out magnet while keeping the tube in place and then washed in 1 ml of PBS. The tube is capped, removed from the magnetic isolator, inverted a couple of times, and replaced with the magnet in order to remove the beads from suspension. After pipetting off the PBS, the process is repeated.
2. Nonspecific binding is a very big problem in these types of isolations and may arise from the intrinsic affinity of the membranes for hydrophobic surfaces of the beads. However, substitution with other separation matrices such as protein A-Sepharose (GE Healthcare) works less well due to even higher levels of nonspecific binding. In order to reduce nonspecific binding in subsequent steps, the Dynabeads are pre-incubated with 0.1% (w/v) BSA in PBS. Once suspended in the BSA solution, the tubes are rotated for 1 h. Temperature is not critical at this stage; we have found similar results when the washing and blocking were performed at room temperature.
3. The preblocked beads are now divided into two 0.5-ml aliquots. One aliquot will be used to isolate caveolae, while the second will be used to control for nonspecific binding. 1 µl of rabbit anti-caveolin antiserum is added to the first aliquot and 1 µl of PBS to the second. Both tubes are rotated at 4°C for 1 h, before the beads are harvested using the magnet and washed twice as described for the initial buffer exchange with 1 ml of ice-cold 0.1% (w/v) BSA in PBS. The blocked beads are resuspended in 100 µl of 0.1% (w/v) BSA in PBS.
4. 200 µl of the low-buoyant density raft preparation are added to 800 µl of 0.1% (w/v) BSA in PBS and gently mixed by inverting the tube several times. This sample is then divided into four 250-µl aliquots in fresh tubes. This allows for duplicate immunoaffinity isolation and control tubes. For the immunoaffinity isolation, 10 µl of the anti-caveolin antibody-coated Dynabeads are added to sample tubes and 10 µl of uncoated Dynabeads to control tubes. The tubes are then rotated for 1 h at 4°C.
5. The tubes are placed against the magnet and the resultant bead-free supernatant is pipetted off. Supernatants can be kept to study non-caveolar rafts

and can either be stored at 4°C for immediate use or be frozen at ≤−20°C for several months.

6. The control and anti-caveolin bead fractions are now washed at least five times in 0.1% (w/v) BSA in PBS. It is important not to allow the pipette tip to touch the magnetic side of the Eppendorf tubes during these wash steps, as this can dislodge the beads and return them to the wash buffer where they may be subsequently lost through the pipetting. At the end of this procedure, the anti-caveolin beads should be decorated with intact caveolin-rich vesicles that can be stored as described in the previous step.

Acknowledgments We gratefully acknowledge the generous support of the Wellcome Trust and the Wolfson Foundation.

Notes

1. Phosphatidylinositol and the principal mammalian phosphoinositide kinase—the type II phosphatidylinositol 4-kinase—are present in carbonate rafts but not in TX-100 rafts, indicating that both the enzyme and its substrate are stripped out by treatment with TX-100. We have found that the addition of 10 mM β-octylglucoside and 4 mM deoxycholate to a standard carbonate lysis buffer preserves the phosphatidylinositol and phosphatidylinositol 4-kinase content of the carbonate rafts but solubilizes other components of carbonate rafts, such as caveolin and EGF receptors [19, 20]. These β-octylglucoside-deoxycholate-insoluble rafts may provide a useful subset of rafts suitable for studying membrane compartmentalization.
2. In the method described, we suggest that an initial experiment should be designed around using the most commonly used detergent concentrations in the literature. However, for weakly raft-associated proteins, these concentrations may be too high and lead to their exclusion from the isolated lipid raft preparation and hence the misleading conclusion that they are not raft-associated. A classic example is the FcεRI immunoglobulin receptor, which localizes to rafts prepared using lysis at low TX-100 concentrations (0.05%) but is lost at the standard 1% concentration [21]. Therefore, if, on the first round of analysis, a protein appears not be raft-associated, it may be worthwhile repeating the experiment with reduced concentrations of detergent (≥ critical micelle concentration) in order to detect weaker raft interactions. A particular concern in using this approach is that very low detergent concentrations may be ineffective in solubilizing nonraft regions of the membrane. One way of testing for the effectiveness of solubilization is to Western blot the resultant fractions for accepted nonraft plasma membrane markers such as the transferrin receptor or clathrin.
3. For the majority of the detergent-based raft isolation procedures in the literature, it is essential to use detergent solutions on ice or at 4°C, because these same detergents can solubilize rafts at higher temperatures. This has led to the criticism that rapid cooling itself could lead to the generation of artifacts. An exception is the polyoxyethylene ether detergent Brij-98, which can be used to isolate lipid rafts at the physiological temperature of 37°C [16].
4. The sucrose density gradient described here comprises three distinct steps in sucrose concentration. Although limited in resolution, in certain experiments a continuous gradient of sucrose may be able to provide a more subtle analysis of rafting, for example by revealing raft populations of different density [22].

5. The methods described here use sucrose solutions to form the density gradient. However, alternative methods have been developed using gradients formed by iodinoxal (OptiPrep™) and Nycodenz® [8, 23]. In the former method, which was designed specifically to purify cell surface caveolae in a detergent-free neutral buffer, a plasma membrane–enriched fraction is prepared using a Percoll™ gradient prior to sonication. In contrast, the latter method employs various detergents to isolate rafts from total cell lysates.
6. It has been notoriously difficult to isolate rafts by immunoaffinity purification, and this has been reported for only a few types. In general, only very poor clearance of the target antigen (~1–2%) can be attained. The exceptions include caveolae (*see* Subheading 26.3.3), rafts containing the GPI-anchored raft proteins Thy-1 and prion protein PrP [15], and rafts containing sucrase isomaltase [24]. The anti-caveolin antiserum recommended here (BD Biosciences Cat. no. 610060) was termed Transduction Laboratories Cat. no. C13630 in many previous publications. If an unproven antibody is to be used for immunopurification, it must be optimized for use (see, for example, the approaches taken by Oh and Schnitzer [8] and Madore et al. [15]), and many that we have tried work well against detergent-solubilized target proteins but not at all well using intact rafts.
7. Lipid rafts are not exclusive to the plasma membrane: Detergent-insoluble membranes have also been found in intracellular membranes, including secretory vesicles, endosomes, and the *trans*-Golgi network [4]. Furthermore, several different proteins that move between raft and nonraft regions of one or more subcellular membranes can either transiently [25] or progressively [10] associate with rafts. This presents a problem when using total cell lysates to isolate rafts, as such techniques will not readily differentiate among rafts originating from different subcellular sites, all of which are likely to float to the same region on density gradients. To get around this problem, it is useful to carry out a round of subcellular fractionation prior to membrane fragmentation and raft isolation in order to determine the subcellular distribution of the protein of interest and then to subsequently prepare rafts from specific cell membranes or organelles that contain the protein of interest. The most straightforward approach is to first prepare a postnuclear supernatant of the cell line in question (*see* Note 8). The postnuclear supernatant is then layered on a discontinuous sucrose gradient consisting of 2 ml of each of the following: 60% sucrose, 50% sucrose, 40% sucrose, 30% sucrose, 20% sucrose. An equilibrium density gradient separation is then produced by overnight centrifugation at 100,000 × *g*. Gradient fractions are harvested as before and probed with antibodies against the protein(s) of interest by Western blotting. The subcellular distribution of target proteins can then be assessed by correlating with tandem blots for organelle marker proteins (*see* Subheading 26.2.3). Note, however, that care needs to be taken with some commonly used markers, such as LAMP-1, that have radically different distributions in different cell types; in addition, it is essential to verify organelle localization using fluorescence or electron microscopy.
8. Allow washed cells to osmotically swell for 1 minute by adding 20 ml of ice-cold Tris-HCl, pH 7.4. Aspirate and harvest by scraping cells into 10 ml of ice-cold homogenization buffer containing protease inhibitors. Homogenize the cells in a loose-fitting Dounce homogenizer. Ten strokes are usually sufficient. Spin out nuclei by centrifugation at 4°C for 10 minutes at 1,000 × *g*. The resulting supernatant—termed the "postnuclear supernatant" (PNS)— is then transferred to a 12-ml polycarbonate ultracentrifugation tube and spun at least for 1 h at 100,000 × *g*. This results in a pellet composed of all the nonnuclear cell membranes that can be used immediately for cell fractionation and raft isolation, or they can be stored for up to several years at −70°C without compromising the sample. Before use, pelleted membranes are resuspended by the addition of the raft-preparation buffer of choice (e.g., 2 ml of DL buffer). In some instances, it may be necessary to sonicate with a probe sonicator to ensure that the pellet is fully dispersed. Where multiple pellets are to be pooled, the same buffer volume can be used to solubilize several pellets, in this way increasing the amount of starting membrane

that is onto the gradient without increasing the starting volume. Another advantage of this technique is that it reduces the complexity of the starting material loaded onto the density gradient by removing large amounts of cytosolic and nucleus-associated protein.

References

1. Simons K, Ikonen E. Functional rafts in cell membranes. Nature 1997;387:569–72.
2. Pike LJ. Lipid rafts: Heterogeneity on the high seas. Biochem J 2004;378:281–92.
3. Pike LJ. Rafts defined: a report on the Keystone Symposium on Lipid Rafts and Cell Function. J Lipid Res 2006;47(7):1597–8.
4. Helms JB, Zurzolo C. Lipids as targeting signals: Lipid rafts and intracellular trafficking. Traffic 2004;5:247–54.
5. Cordy JM, Hooper NM, Turner AJ. The involvement of lipid rafts in Alzheimer's disease. Mol Membr Biol 2006;23:111–22.
6. Song SK, Li S, Okamoto T, Quilliam LA, Sargiacomo M, Lisanti MP. Co-purification and direct interaction of Ras with caveolin, an integral membrane protein of caveolae microdomains. Detergent-free purification of caveolae microdomains. J Biol Chem 1996;271:9690–7.
7. Stan RV, Roberts WG, Predescu D, Ihida K, Saucan L, Ghitescu L, Palade GE. Immunoisolation and partial characterization of endothelial plasmalemmal vesicles (caveolae). Mol Biol Cell 1997;8:595–605.
8. Oh P, Schnitzer JE. Immunoisolation of caveolae with high affinity antibody binding to the oligomeric caveolin cage. Toward understanding the basis of purification. J Biol Chem 1999;274:23144–54.
9. Chamberlain LH. Detergents as tools for the purification and classification of lipid rafts. FEBS Lett 2004;559:1–5.
10. Roper K, Corbeil D, Huttner WB. Retention of prominin in microvilli reveals distinct cholesterol-based lipid micro-domains in the apical plasma membrane. Nat Cell Biol 2000;2:582–92.
11. Holm K, Weclewicz K, Hewson R, Suomalainen M. Human immunodeficiency virus type 1 assembly and lipid rafts: Pr55(gag) associates with membrane domains that are largely resistant to Brij98 but sensitive to Triton X-100. J Virol 2003;77:4805–17.
12. Mayor S, Maxfield FR. Insolubility and redistribution of GPI-anchored proteins at the cell surface after detergent treatment. Mol Biol Cell 1995;6:929–44.
13. Wilson BS, Steinberg SL, Liederman K, Pfeiffer JR, Surviladze Z, Zhang J, Samelson LE, Yang LH, Kotula PG, Oliver JM. Markers for detergent-resistant lipid rafts occupy distinct and dynamic domains in native membranes. Mol Biol Cell 2004;15:2580–92.
14. Drobnik W, Borsukova H, Bottcher A, Pfeiffer A, Liebisch G, Schutz GJ, Schindler H, Schmitz G. Apo AI/ABCA1-dependent and HDL3-mediated lipid efflux from compositionally distinct cholesterol-based microdomains. Traffic 2002;3:268–78.
15. Madore N, Smith KL, Graham CH, Jen A, Brady K, Hall S, Morris R. Functionally different GPI proteins are organized in different domains on the neuronal surface. EMBO J 1999;18:6917–26.
16. Drevot P, Langlet C, Guo XJ, Bernard AM, Colard O, Chauvin JP, Lasserre R, He HT. TCR signal initiation machinery is pre-assembled and activated in a subset of membrane rafts. EMBO J 2002;21:1899–908.
17. Morrow IC, Parton RG. Flotillins and the PHB domain protein family: Rafts, worms and anaesthetics. Traffic 2005;6:725–40.
18. Waugh MG, Minogue S, Anderson JS, Balinger A, Blumenkrantz D, Calnan DP, Cramer R, Hsuan JJ. Localization of a highly active pool of type II phosphatidylinositol 4-kinase in a p97/valosin-containing-protein-rich fraction of the endoplasmic reticulum. Biochem J 2003;373:57–63.

19. Minogue S, Anderson JS, Waugh MG, dos Santos M, Corless S, Cramer R, Hsuan JJ. Cloning of a human type II phosphatidylinositol 4-kinase reveals a novel lipid kinase family. J Biol Chem 2001;276:16635–40.
20. Waugh MG, Lawson D, Hsuan JJ. Epidermal growth factor receptor activation is localized within low-buoyant density, non-caveolar membrane domains. Biochem J 1999;337:591–7.
21. Field KA, Holowka D, Baird B. Fc epsilon RI-mediated recruitment of p53/56lyn to detergent-resistant membrane domains accompanies cellular signaling. Proc Natl Acad Sci. USA 1995;92:9201–5.
22. Parkin ET, Turner AJ, Hooper NM. Isolation and characterization of two distinct low-density, Triton-insoluble, complexes from porcine lung membranes. Biochem J 1996;319:887–96.
23. Naslavsky N, Stein R, Yanai A, Friedlander G, Taraboulos A. Characterization of detergent-insoluble complexes containing the cellular prion protein and its scrapie isoform. J Biol Chem 1997;272:6324–31.
24. Heine M, Cramm-Behrens CI, Ansari A, Chu HP, Ryazanov AG, Naim HY, Jacob R. Alpha-kinase 1, a new component in apical protein transport. J Biol Chem 2005;280:25637–43.
25. Vainio S, Heino S, Mansson JE, Fredman P, Kuismanen E, Vaarala O, Ikonen E. Dynamic association of human insulin receptor with lipid rafts in cells lacking caveolae. EMBO Rep 2002;3:95–100.

Index

Color Plates

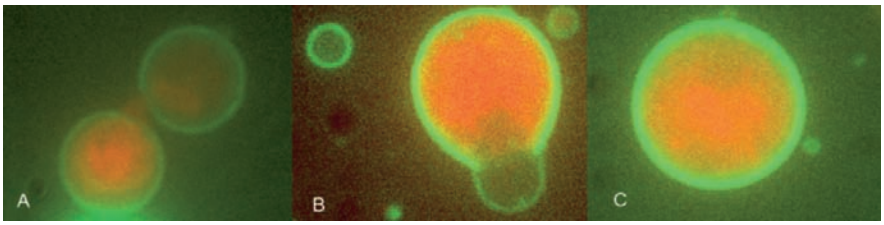

Color Plate 1. 85:10:5 mol% DOPtdCho/DOPtdEth/PtdInsP_2 vesicles, membrane labeled with DOPtdEth-NBD and PLC-delta 1 PH domain. (*See* complete caption and discussion on p. 136)

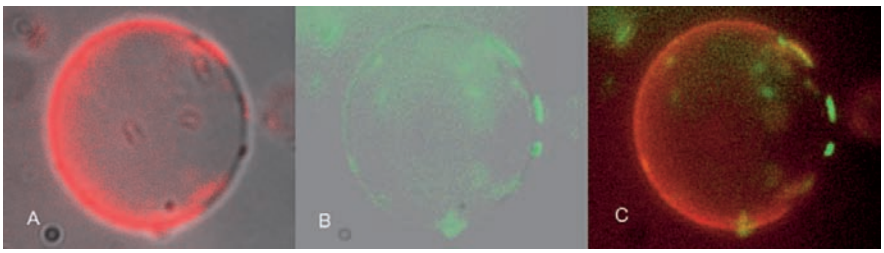

Color Plate 2. (a) 45/40/5/10 mol% DOPtdCho/SM/Chol/PtdInsP_2 vesicles, liquid-disordered membrane labeled with DOPtdEth-NBD with brightfield image. (*See* complete caption and discussion on p. 137)

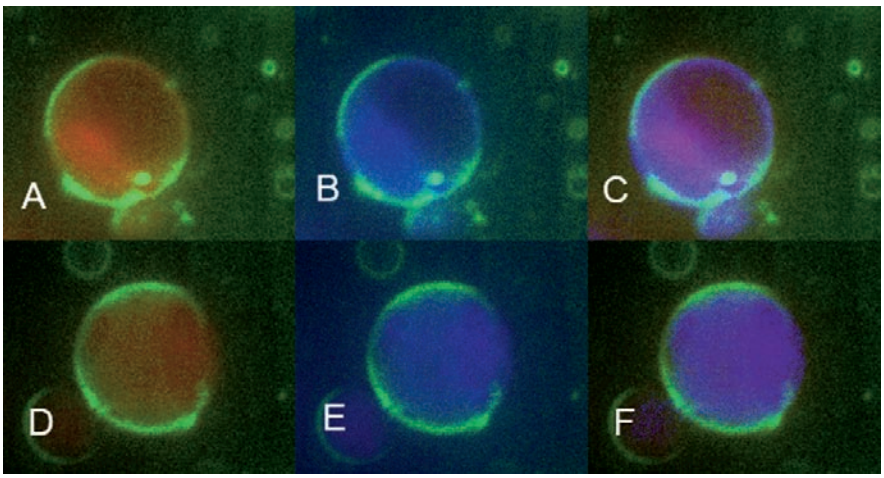

Color Plate 3. (a) and (d) 55/15/5/25 DOPtdCho/SM/Chol/PtdInsP_2 vesicles, liquid-disordered membrane labeled with DOPtdEth-NBD with PLC-delta 1 PH domain. (*See* complete caption and discussion on p. 137)

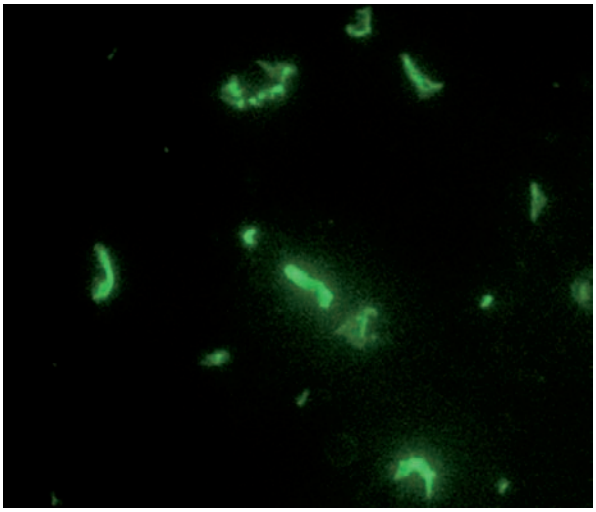

Color Plate 4. PH domain fibrils formed without BSA in imaging solution. (*See* complete caption and discussion on p. 144)

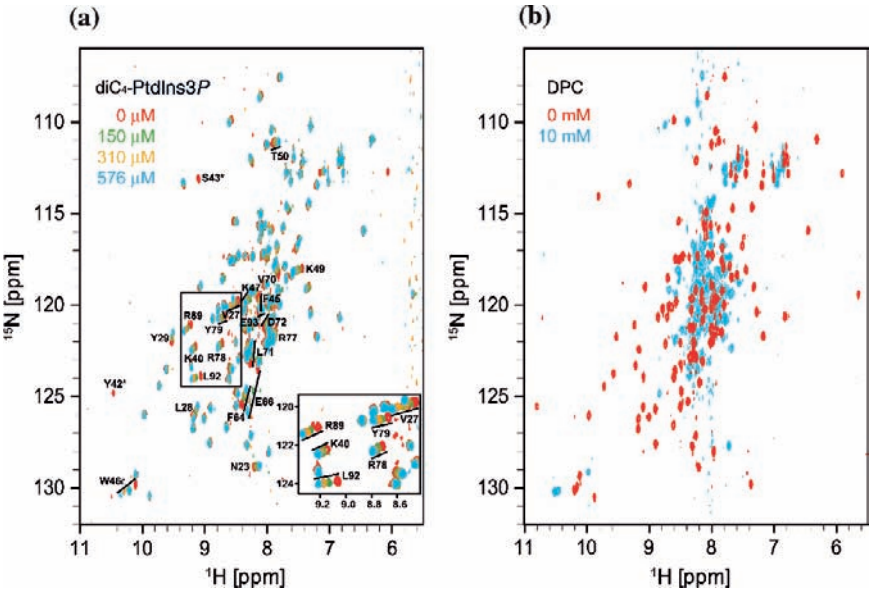

Color Plate 5. NMR spectra were recorded at 25°C on Varian INOVA 800-MHz spectrometer. (*See* complete caption and discussion on p. 301)

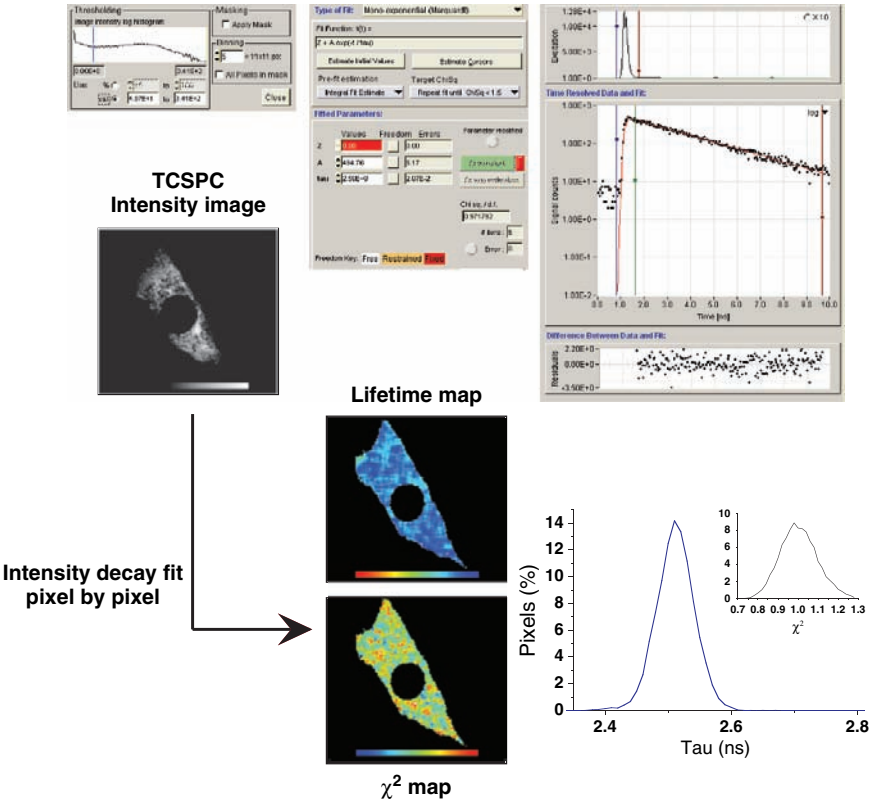

Color Plate 6. Converting TCSPC intensity image in a fluorescence lifetime map. (*See* complete caption and discussion on p. 320)

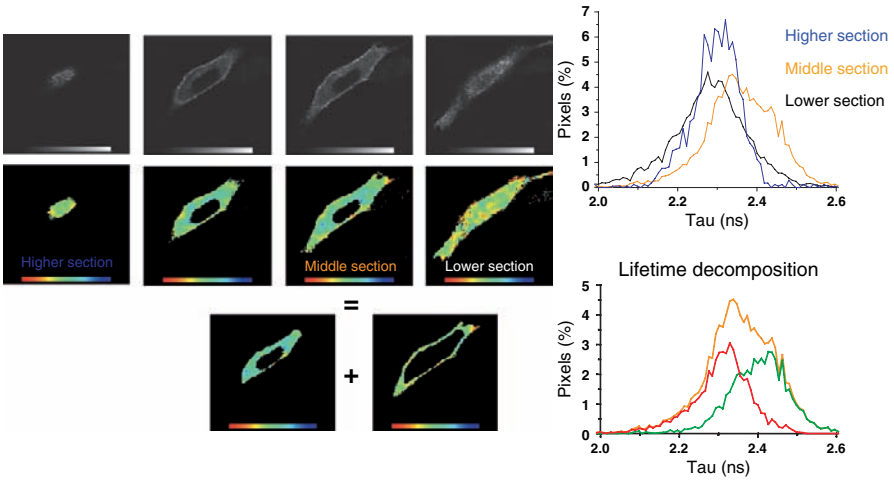

Color Plate 7. Acquiring a Z stack. (*See* complete caption and discussion on p. 321)

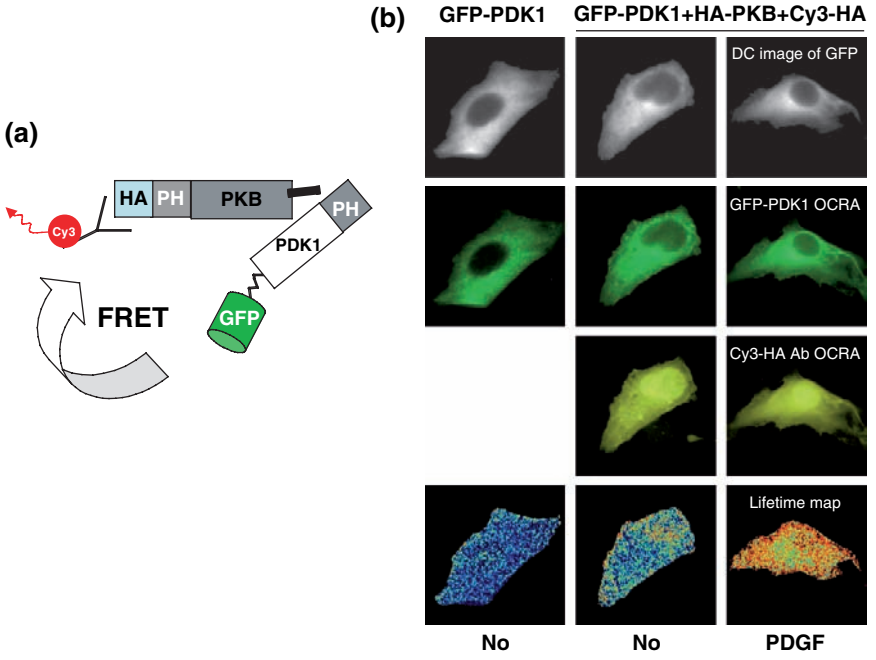

Color Plate 8. GFP-PDK1/RFP-PKB interaction determined by frequency-domain FLIM. (*See* complete caption and discussion on p. 327)

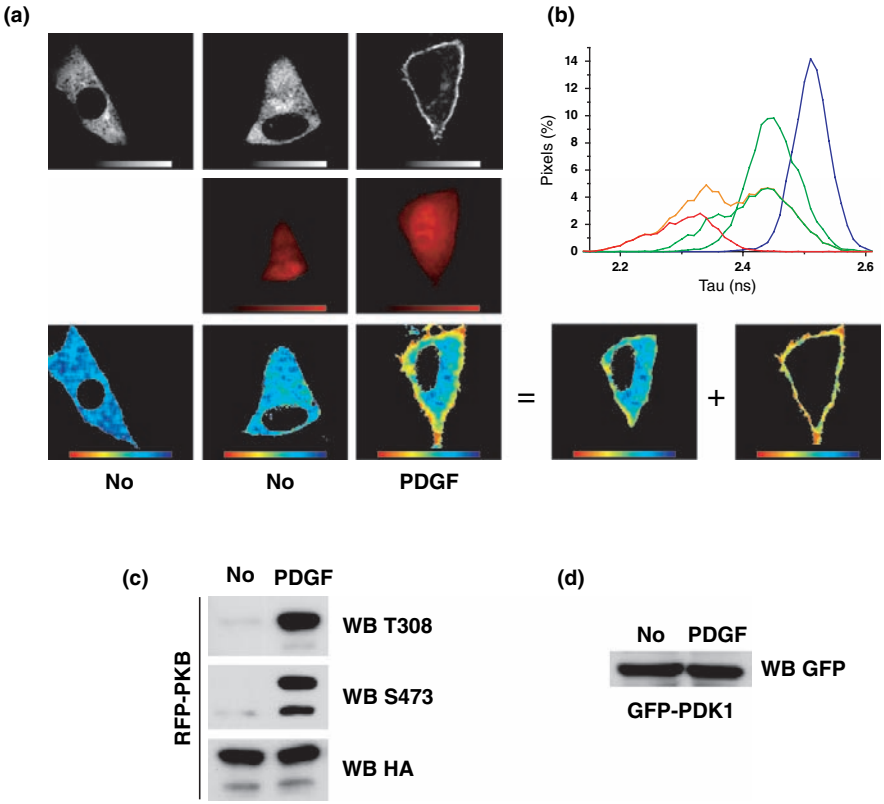

Color Plate 9. GFP-PDK1/RFP-PKB interaction determined by time-domain FLIM. (*See* complete caption and discussion on p. 328)

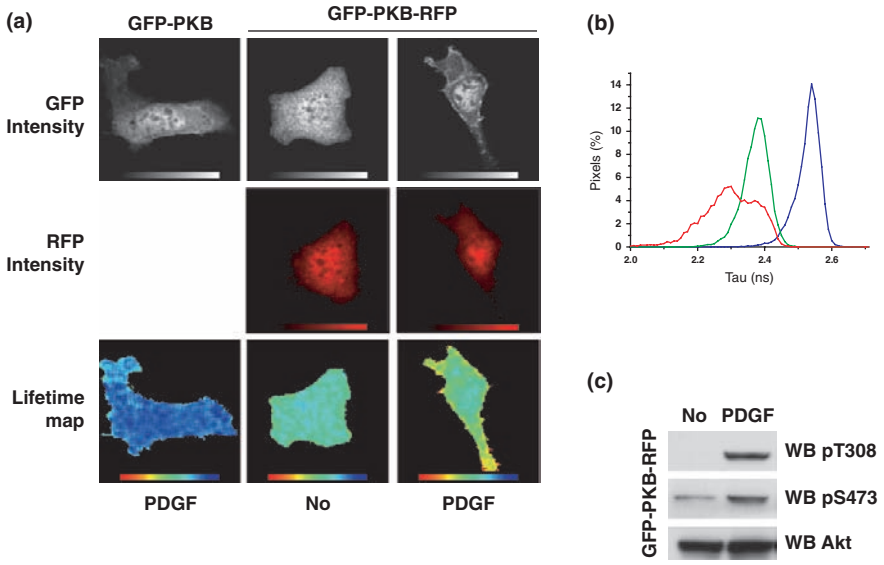

Color Plate 10. Change in conformation of GFP-PKB-RFP monitored by time-domain FLIM. (*See* complete caption and discussion on p. 332)

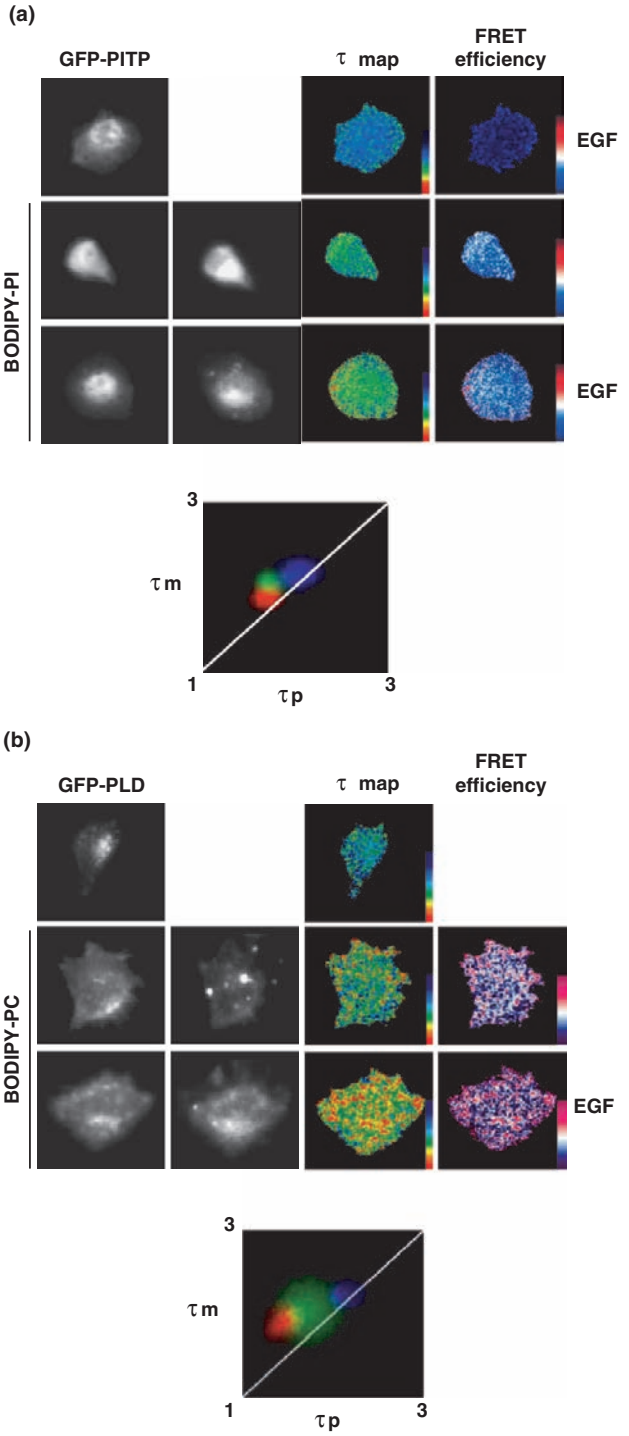

Color Plate 11. GFP-PITP/BODIPY-PtdIns and GFP-PLD/BODIPY-PtdCho interactions monitored by frequency-domain FLIM. (*See* complete caption and discussion on p. 334)

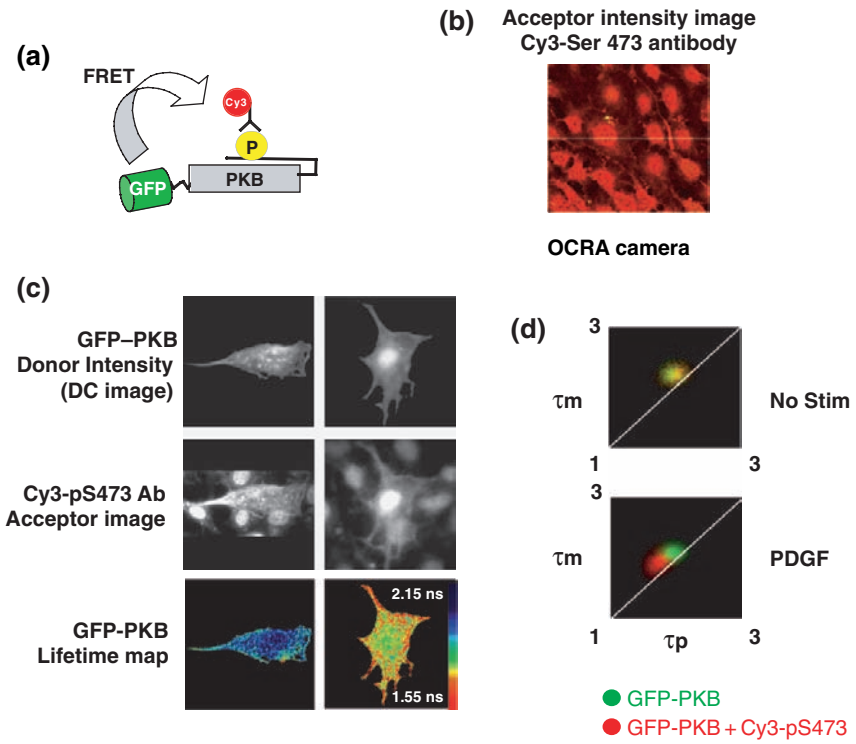

Color Plate 12. Monitoring *in situ* GFP-PKB phosphorylation. (*See* complete caption and discussion on p. 338)